# *Chimie*



**Thematic Issue / *Numéro thématique***
Biocatalysis and Synthesis /
*La biocatalyse en synthèse*

**Guest Editor / *Rédactrice en chef invitée***
Juliette Martin

# Comptes Rendus
## Chimie

**Objective of the journal**

*Comptes Rendus Chimie* is an international peer-reviewed electronic journal, covering all areas of chemistry.

It publishes special issues, original research articles, review articles, accounts, historical perspectives, pedagogical texts or conference proceedings, of unlimited length, in English or in French and in as flexible a format as necessary (figures, associated data, etc.).

*Comptes Rendus Chimie* has been published since 2020 with the centre Mersenne pour l'édition scientifique ouverte (Mersenne Center for open scientific publishing), according to a virtuous Diamond Open Access policy, free for authors (no author processing charges nor publishing fees) as well as for readers (immediate and permanent open access).

**About the journal**

*Comptes Rendus Chimie* is published exclusively in electronic format.

All information on the journal, as well as the full text of all articles, is available on its website at: https://comptes-rendus.academie-sciences.fr/chimie/.

**Author enquiries**

For any inquiries about submitting a manuscript, please refer to the journal's website: https://comptes-rendus.academie-sciences.fr/chimie/.

**Contact**

Académie des sciences
23 quai de Conti
75006 Paris (France)
cr-chimie@academie-sciences.fr

# Contents / *Sommaire*

*Page numbers below refer to the top-of-the-page pagination in this document*
*which compiles articles published individually with a different pagination*
*(retained on the top left and top right of each article).*

Biocatalysis and Synthesis

# Guest Editor



**Juliette Martin**

**Juliette Martin** graduated her doctorate in organic chemistry at the University of Caen (France), in the field of organocatalysis and asymmetric synthesis under the supervision of Pr. Marie-Claire Lasne. She then followed an Industrial Post-doctoral fellowship at Zeneca Life Science Molecules in UK in homogeneous and heterogeneous catalysis. Integrated into the R&D department, she focused on developing new technology platforms in chemo- and bio-catalysis at Avecia – CDMO (Contract Development Manufacturing Organization) in Huddersfield (UK). Besides, she co-wrote a chapter in « Asymmetric Catalysis on Industrial Scale », Wiley-VCH. She also involved through the UK national organization "Innovative Manufacture Initiative" for investigating new technical tools to speed up efficiency through R&D projects.

Back to France, she had several R&D process development positions within PPG-Sipsy (now Zach System) and PCAS (now SEQENS). She was appointed R&D Manager on one of the industrial site at PCAS (now SEQENS) focusing on process development of some key technologies, including polymers for controlled drug release and was Head of Biocatalysis for Pharmaceutical Synthesis. She was then appointed CEO of Protéus (a protein science company integrated since 2017 in SEQENS).

Today, she values 25 years' experience in the field of synthetic chemistry and industrial biocatalysis to leverage R&D network and bridge scientific communication gap between various area of chemistry and business. Juliette is author and co-author of more than 20 scientific articles. She currently holds the position of Scientific Communication Manager at SEQENS – an integrated global leader in pharmaceutical solutions & specialty ingredients, 16 manufacturing sites, 9 countries, 9 R&D Centers, +300 research scientists & experts.

Biocatalysis and Synthesis

# Foreword

**Juliette Martin**

**Biocatalysis at the heart of synthetic chemistry.**

In synthetic chemistry, biocatalysis offers a technical solution for designing routes to produce simple to complex molecules. Considering the significant advances in the field of biotechnologies over the past two decades, the access to new ways of conducting chemical transformations and the emergence of numerous new enzymes have occurred. The landscape of attractive retrosynthetic disconnections to selectively build new bonds and design fundamentally new syntheses of (complex) molecular structures has significantly expanded. Moreover, enzymes are easy to handle and can operate in water-organic solvent mixtures or even without water. Ultimately, integrating enzymatic approaches may enlarge alternative routes and potential shortcuts.

The conciseness, environmental friendliness, and atom economy of synthetic methods have become important aspects of synthetic chemistry. Undeniably, biocatalysis aligns well with green and sustainable chemistry principles, offering efficient, economical, and low-waste alternatives over some traditional chemical synthesis. As a result, enzyme-driven processes have gained much more attention for the production of ever-increasing molecular complexity across numerous industries.

Enzyme-catalyzed chemistries involve using biocatalysts, such as enzymes soluble or immobilized or whole cells. This method, also known as biotransformation, leverages the precise selectivity of enzymes, making it valuable in industrial applications. The stability and productivity of biocatalysts for commercial applications have already been well-demonstrated.

The science behind the enzyme from discovery, design to its production require a broad range of competencies, such as biochemistry, molecular biology, microbiology, protein engineering, bioinformatics, fermentation processes, bioengineering, computer science, material science. Their respective contribution has accelerated the ability to discover and engineer novel enzyme classes to build natural and unnatural molecules and will continue to expand.

In this dynamic field, the work contribution of academic researchers, start-ups and industry scientists have brought significant advances leading to innovative approaches and broaden the scope of synthetic methods and strategies. Overall, the synergy through fruitful collaborations and cross-fertilization of multiple competencies have never been so impactful for also translating the findings into commercial applications. Ultimately, we all share the same goal which is problem solving.

In this Special Issue, in which I have been honored to act as Guest Editor, I would like to thank all the authors and co-authors for their willingness to share their work and expertise covering very diverse areas of this fascinating discipline. It comprises fourteen mini reviews, articulated around three main topics briefly presented below.

**Tools for enzyme optimization (articles 1–3):**

In some cases, to match specific performance requirements, biocatalysts may need increased enzyme stability, catalytic efficiency, selectivity, and substrate scope. New strategies and tools such as protein engineering based on DNA recombination may be required to enhance the characteristics of natural enzymes to reach such high efficiency requirements.

Along with computational tools, comprehensive understanding of the protein structure and dynamics in terms of molecular details or exploring the biodiversity are strategies that can significantly enhance the performance of enzymes. From an analytical point of view, to measure enzymatic activities, innovative methods are also being developed, especially when extensive studies through experimental tests are required and can be challenging.

**Enzyme-catalyzed reactions (articles 4–9):**

This edition covers a broad range of biotransformations, including oxidation, reduction, amination, amidation, nucleosides synthesis. New strategies such as multi-catalysis has emerged to enhance the scope of synthetic protocols, including enzymatic cascade reactions, and hybrid catalysis by merging bio- and chemo-catalysis. Despite challenges that need to be addressed with respect to compatibility issues and catalyst reactivity ordering, recent studies show promising solutions.

**Enzyme-based processes (articles 10–14):**

Some pharmaceutical companies have been pioneers in the use and acceptance of biocatalysis for the unique properties that enzymes can deliver. Complemented by remarkable progress in bioprocess engineering, reaction engineering, or exploring new devices for continuous flow systems, process chemists are just beginning to take full advantage of the specificity with which enzymes react.

To tackle some limitations, innovative approaches exhibiting enzyme stability, activity and potentially reusability are being developed. These techniques include reactor design, enzyme immobilization, continuous flow process. These approaches are promising for the wide spread of industrial enzyme usage and ultimately reducing the production cost.

Within all chemistry disciplines, biocatalysis is only being slowly adopted, especially due to a lack of familiarity, some misconceptions and practical experience. Its awareness should be enhanced. Enzymatic catalysis is a mature technology and yet the full potential of this technology is to be unlocked, especially for reactions that are highly underexplored in enzyme catalysis or not yet known to the enzyme universe. This should encourage more chemists to take further ownership and expand applications in contemporary chemistry.

We hope that this special issue will be a source of inspiration for readers. There is a huge avenue for exploiting biocatalysis in synthetic chemistry!

Juliette Martin
SEQENS, Nîmes, France
juliette.martin@seqens.com

ACADÉMIE
DES SCIENCES
INSTITUT DE FRANCE

Review article

# Harnessing native enzyme diversity for biocatalysis

**Célestin Gamonet** [®],[a]**, Anne Zaparucha** [®],[a] **and Carine Vergne-Vaxelaire** [®],[*],[a]

[a] Génomique Métabolique, Genoscope, Institut François Jacob, CEA, CNRS, Univ
Evry, Université Paris-Saclay, 91057 Evry, France

*E-mails:* celestin.gamonet@genoscope.cns.fr (C. Gamonet),
anne.zaparucha@genoscope.cns.fr (A. Zaparucha), carine.vergne@genoscope.cns.fr
(C. Vergne-Vaxelaire)

**Abstract.** The use of enzymes for synthetic purposes typically relies on well-known or commercially available proteins, valued for their established properties. However, these enzymes may not always be ideal for specific reactions, prompting researchers to explore the vast diversity of enzymes within biodiversity. Genome and metagenome mining offers a rich reservoir of sequences, revealing novel enzymes with enhanced properties such as thermostability and substrate specificity, which are crucial for industrial applications. Advances in large-scale sequencing have exponentially increased available protein sequences, with over 2.4 billion reported in 2023 compared to 123 million in 2018.

Despite its potential, enzyme discovery from metagenomic data remains challenging due to the immense volume of sequences. This necessitates innovative computational tools and bioinformatics workflows to streamline the identification of biocatalysts. Bioinformatics plays a pivotal role in predicting enzyme functions, analyzing protein superfamilies, and selecting key enzymes via biosynthetic gene clusters. Integration of artificial intelligence (AI) further enhances enzyme discovery and retrosynthetic pathway design, enabling the customization of enzymes for specific applications.

Case studies from our laboratory illustrate the efficiency of genome mining and bioinformatics in discovering enzymes complementary to known ones, modifying metabolic reactions, and identifying novel scaffolds. These methods have expanded the diversity of enzymes available for synthesis, underscoring the importance of synergizing bioinformatics with biocatalysis to harness biodiversity and develop a versatile enzymatic toolbox.

**Keywords.** Sequence-driven enzyme discovery, Biodiversity, Biocatalysts, Nitrilase, Dioxygenase, CoA ligases, Amine dehydrogenase.

## 1. Introduction

The application of enzymes for synthetic purposes usually relies on a restricted set of proteins, commonly known by the biocatalytic community or even commercially available ones. The knowledge of their features (substrate scope, activity, stability, structure...) reassures researchers, who tend to use them by default or for convenience. However, these properties may not always be the most suitable for specific reactions (or cascade reactions). Every organism has its own arsenal of enzymes which, from a synthetic application point of view, constitutes a truly diverse reservoir of sequences and structures. It is up to us to make the most of it, to offer an enzymatic toolbox of great diversity. When required, each enzyme can be adapted to a targeted reaction, which may be very different from that for which it has naturally evolved, by engineering or directed evolution. So genome mining for enzyme discovery

---

*Corresponding author

is still of interest and must not be opposed to protein engineering. As mentioned by NGuyen et al., "a treasure trove of enzyme chemistry awaits to be uncovered" [1]. As a matter of fact, the number of available sequences increases daily, thanks in particular to the development of large-scale sequencing projects for marine and terrestrial biodiversity. The number of available protein sequences has increased more than 20-fold in the last 6 years, with more than 2.4 billion reported in 2023 compared to approximately 123 million in 2018 [2,3]. According to some reports, metagenome mining has a high success rate (99%) in identifying diverse genes encoding for novel enzymes, which are crucial for biocatalytic applications [4]. Sequences coding for characterized protein homologs and many of unknown functions are added to (meta)genomic databases, already rich in proteins that can be used for synthesis [5]. The quest for other biocatalysts among biodiversity is important to enlarge the spectrum of substrates and reactions but is not restricted to this aspect [6]. For industrial applications, enzyme stability is an essential parameter. Recent studies have reported the discovery of unique enzymes, especially in the "hidden sequence space" by metagenomic mining, which exhibit enhanced properties (e.g., thermostability, substrate specificity), making them valuable for various industrial applications, including pharmaceutical ones. The impact of metagenomics on biocatalysis is undeniable [7,8].

However the prospection for enzymes with enhanced catalytic properties and specific features is not straightforward. Discovering enzymes within the extensive array of available metagenomic data is a significant challenge, requiring the development of innovative computational and functional screening tools. The integration of bioinformatics into biocatalysis facilitates a more systematic approach to the discovery and design of novel biocatalysts. Biocatalysis and bioinformatics must work in synergy to optimize the identification of enzymes of interest within biodiversity and minimize the number of candidates to be screened. Bioinformatics tools enable the identification of enzyme functions and the prediction of their properties, mainly from sequence-based and function-based screening and modeling [9,10]. The analysis of protein superfamilies allows the rational selection and design of enzymes with improved catalytic properties, focusing

on sequence–function relationships and catalytic residues, including their conformational variation [11,12]. Identification and analysis of biosynthetic gene clusters is also a powerful approach to select key enzymes [13]. Furthermore, the entire biocatalytic process, from enzyme discovery to the design of the retrosynthetic pathway, is increasingly being enhanced and streamlined through the integration of deep neural networks and artificial intelligence (AI). All our knowledge of enzyme natural diversity helps in parallel the development of hybrid generative AI methods, so that we can progressively customize the dream enzyme for each application [14].

Here, we present case studies from our laboratory illustrating the potential outcomes of genome mining approaches and the input of bioinformatic workflows in their efficiency to: (1) identify enzymes complementary to those already characterized; (2) leverage known enzyme mechanisms to modify natural reactions; (3) discover entirely new enzyme scaffolds for a specific transformation. The results in terms of diversity in sequences, structures and synthesis potential are described. Without going into detail, we present in each case the (meta)genome mining method used to select candidate enzymes within biodiversity.

## 2. Genome mining to expand biocatalytic properties within established enzyme families

### 2.1. *Example with the nitrilase activity*

Exploring the biodiversity for native enzymes is an efficient way to broaden the scope of already known or even commercially available biocatalysts [15]. It worked especially well for nitrilases (EC 3.5.5), enzymes enabling the hydrolysis of nitriles into their corresponding carboxylic acids. This biotransformation has been studied for years due to the benefits it provides over the chemical transformation [16]. In 2012, when we started this project, characterized nitrilases were still scarce, especially for regio- and stereospecific applications. We applied a genome mining approach to identify new nitrilases within biodiversity and proposed three preparative scale reactions for applications of this expanded enzymatic toolbox [17].

In our process, exploring enzyme diversity first requires the careful selection of experimentally
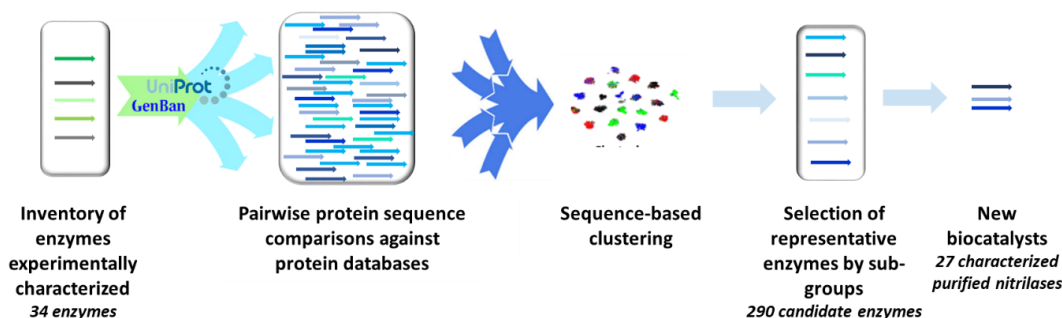
**Figure 1.** Pipeline for the selection of candidate enzymes by sequence-driven approach within the FunDivEx platform. Source: Figure adapted from Zaparucha et al. [15].

validated enzymes of diverse sequences to recover the greatest possible diversity. We selected 34 reference nitrilases, based on their activity toward various nitriles and, noteworthily, without taking into account their annotation or their organism of origin. The corresponding protein sequences were used to fish out prokaryotic enzymes in the UniprotKB database using a basic local alignment search tool (BLAST) sequence alignment [18]. Only sequences presenting over 30% identity on more than 80% of their length were kept. We then classified the sequences on the basis of 80% sequence identity in order to have isofunctional clusters. By choosing a few representatives per cluster, or just one, we ensured that we covered the biodiversity being explored while minimizing the number of proteins to be screened. The representatives were chosen based on genome availability in the Genoscope strain collection (700 prokaryotic species) and in an in-house wastewater treatment plant metagenomic collection of sequences ("Cloaca maxima"), alongside nucleic sequence features like guanine-cytosine content. DNA was purchased for cluster representatives that were unavailable in the internal collection. This workflow, integrated within the FunDivEx platform, is automated. The pipeline resulted in the identification of 290 candidate nitrilases, mostly annotated as hydrolases or carbon-nitrogen hydrolases. After overexpression in *Escherichia coli* (*E. coli*) BL21(DE3) cells, we obtained 163 candidate proteins, each tagged with a hexahistidine tag to simplify subsequent purification (Figure 1).

The 163 candidates were screened against 25 nitrile substrates grouped into six categories by chemical properties (saturated, unsaturated, arylaceto-, α-hydroxylated, β-hydroxylated, and β-aminated) using a sensitive UV-spectrophotometric assay. This assay, adapted here for the first time for nitrilase activity screening, leverages glutamate dehydrogenase (GDH) to catalyze a non-limiting reaction with release of ammonia ($NH_3$), enabling kinetic measurement through NADH consumption monitored at 340 nm, which correlates with initial $NH_3$ concentration and thus with nitrilase activity. We identified 125 nitrilases with varying activity levels across the substrates; while some exhibited substrate specificity, most were promiscuous, efficiently hydrolyzing nitriles with aromatic groups (77%), saturated nitriles (60%), and unsaturated nitriles (50%). Notably, NIT93 from *Lysinibacillus sphaericus* (UniProtKB: B1HZZ4) and NIT278 from *Syntrophobacter fumaroxidans* (UniProtKB: A0LKP2) were active across all six substrate groups, displaying marked substrate promiscuity. The top 37 nitrilases were subsequently purified and reassessed, yielding 27 enzymes with activity spanning nearly the entire substrate range, except for 3-aminopentanenitrile.

As shown in Figure 2, the selection of homologs with less than 40% sequence identity resulted in nitrilases active on a structurally diverse set of nitriles, capturing enzymatic diversity around the reference sequences. It's interesting to note that most candidates have more than 50% amino acid similarity with the reference enzymes (Figure 2B), with over 75% of the top 27 nitrilases presenting 30–40% sequence identity, underscoring the advantage of genome mining across a broad sequence landscape to identify homologs down to 30% identity. Of the newly identified nitrilases, nearly 60% showed less than 40% identity to any of the 34 previously characterized prokaryotic
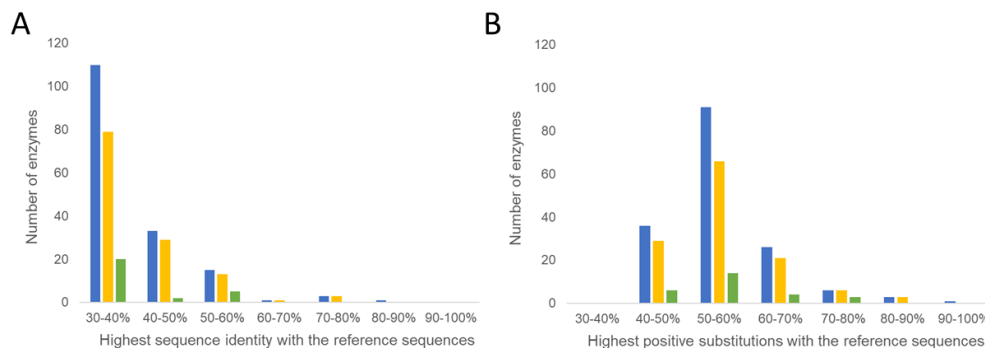
**Figure 2.** Distribution of the nitrilase collection based on their sequence identity with the best sequence hits in the reference set. For the analysis, we used (A) the percent sequence identity; or (B) the percent positive substitutions, i.e., amino acids that are either identical or have similar properties based on the BLOSUM62 scores. Blue bars correspond to the 163 candidate enzymes, yellow bars to the 125 screening hits, and green bars to the 27 validated enzymes with the best activities.

nitrilases, thus expanding the available catalog of nitrilases for synthetic biocatalysis.

The screening revealed several enzymes with significant activity, forming a versatile toolkit of catalytic options. We used this toolbox to identify enzymes active toward specific synthons. We focused on enzymes exhibiting activity toward the generic substrate structurally related to targeted synthons in a second screening round on these more functionalized molecules frequently used in chemical synthesis. This approach yielded promising results: NIT28 from *Sphingomonas wittichii* (UniParc ID: UPI0000E98FFB), NIT278 from *Syntrophobacter fumaroxidans* (UniProtKB ID: A0LKP2), and NIT158 from *Sphingomonas wittichii* (UniParc ID: UPI0000E990F3) successfully converted 3-cyano-2-phenylpropanoate (**1**), 3-oxocyclopentanecarbonitrile (**2**), and iminodiacetonitrile (**3**) into (*R*)-3-methoxycarbonyl-3-phenylbutanoic acid (**4**) (*ee* = 46 ± 2%), (*S*)-3-oxocyclopentanecarboxylic acid (**5**) (*ee* = 48 ± 2%), and the monoacid 2-[(cyanomethyl)amino]acetic acid (**6**), respectively, with moderate to high yields, demonstrating substantial biocatalytic potential (Figure 3).

Through genome mining, we have been able to identify new nitrilases with a substrate range complementary to the initial reference set. Further analysis highlighted the distinct characteristics of these enzymes, such as their pH and solvent tolerance, along with their thermoactivity profiles. This work demonstrates that screening diverse representative enzymes across structurally varied substrates builds an enzyme toolbox that can be leveraged for further, more targeted applications in synthesis.

## 2.2. *Example with the α-ketoacid-dependent dioxygenase activity*

Another example employing this strategy is our exploration of α-ketoacid-dependent oxygenases (αKAOs), enzymes primarily known for catalyzing hydroxylation. We concentrated on bacterial αKAOs involved in hydroxylating side chains of free amino acids or peptide-bound amino acids in non-ribosomal peptide synthesis pathways. Hydroxylated amino acids are valuable chiral building blocks widely used in synthetic chemistry. Except for the production of hydroxyprolines which found applications in pharmaceutical and feed industries, the broader industrial use of αKAOs in biocatalytic processes remains limited, likely due to insufficient efficiency and a lack of comprehensive understanding of this enzyme family's full potential. To address this gap, we undertook a genome-mining approach to identify new native dioxygenases with activity toward free amino acids and structurally related compounds.

A collection of candidate αKAOs was generated from an initial set of eleven experimentally validated enzymes. Using the established workflow described above, we obtained 274 candidate sequences after
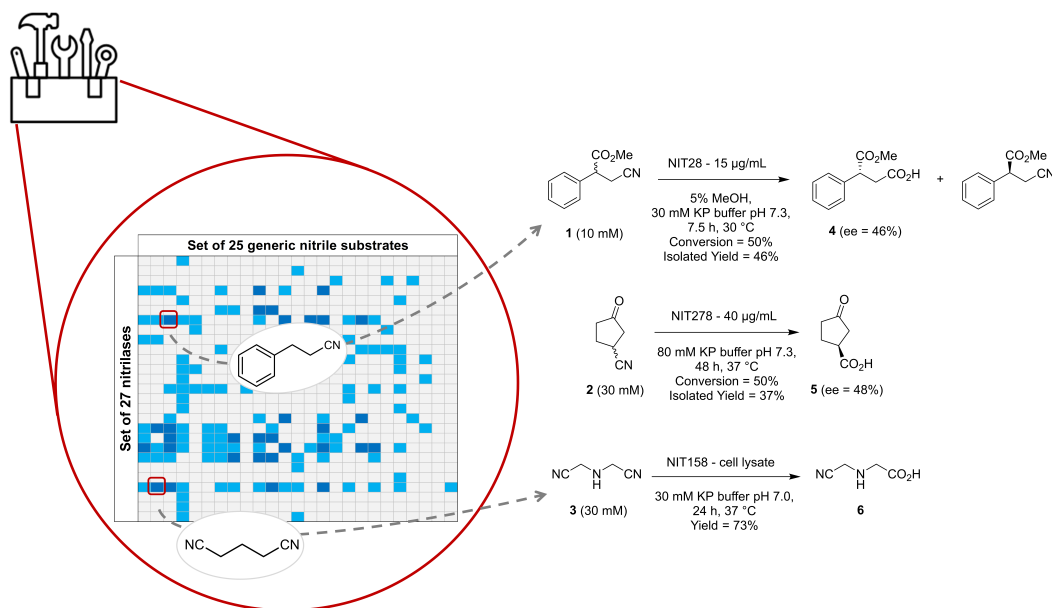
**Figure 3.** Genome-mined nitrilase toolbox for preparative scale hydrolysis of functionalized nitriles. The imbedded table illustrates results obtained with the set of purified enzymes where navy blue squares indicate high activities (more than 1 mM converted in 4 h) and light blue squares moderate activity (less than 1 mM converted in 4 h). Source: Figure adapted from Vergne-Vaxelaire et al. [17].

clustering. To expand the collection, we also included homologs containing InterPro motifs associated with the target activity (proline hydroxylase—IPR007803 and clavaminate synthase-like (CSL)—IPR014503), thus adding 56 enzymes representative of clusters with 80% identity or more. This brought the total to 331 candidates, of which 131 were successfully cloned with a His-tag and expressed in *E. coli* as previously described [19].

For a project aiming to capture the full diversity of biocatalysts for a specific transformation, it is essential to choose the substrates to encompass a wide range of chemical reactivities and structural constraints, minimizing the risk of overlooking potential activities.

To streamline the process, the fourty-six chosen substrates were organized into twelve pools. Each pool contained known substrates from the reference set and derivative targets, including non-natural amino acids, as well as amine and keto derivatives with aliphatic or aromatic chains, and aliphatic sulfates.

Dioxygenase activity was monitored using the GDH assay mentioned above, this time quantify-

ing residual α-ketoglutarate, the αKAO cosubstrate. Enzyme hits were purified and tested on individual substrates, with product quantification by HPLC or GC-MS. This screening led to the identification of previously uncharacterized enzymes active on both known and novel substrates. Notably, three enzymes exhibited activity on ʟ-lysine (**7**), with either C3 regioselectivity (KDO1 from *Catenulispora acidiphila*, UniProtKB ID: C7QJ42) or C4 regioselectivity (KDO2 from *Chitinophaga pinensis*, UniProtKB ID: C7PLM6; KDO3 from *Flavobacterium johnsoniae*, UniProtKB ID: A5FF23), and on ʟ-ornithine (ODO from *Catenulispora acidiphila*, UniProtKB ID: C7Q942). Interestingly, KDO2 and KDO3 were the first αKAOs observed with C4 regioselectivity on a polar amino acid like lysine, later supplemented by homologs KDO4 and KDO5 (UniProtKB ID: G8T8D0 and UniProtKB ID: J3BZS6). Further study of ODO and KDO1,2,3 confirmed their total regio- and stereoselectivities. ODO achieved up to 68 and 50% conversion of ʟ-ornithine and ʟ-arginine into (3*S*)-3-hydroxy-ʟ-ornithine and (3*S*)-3-hydroxy-ʟ-arginine, respectively. KDO1 and KDO2,3 fully converted ʟ-lysine **7** into (3*S*)-3-hydroxy-ʟ-lysine (**8**)
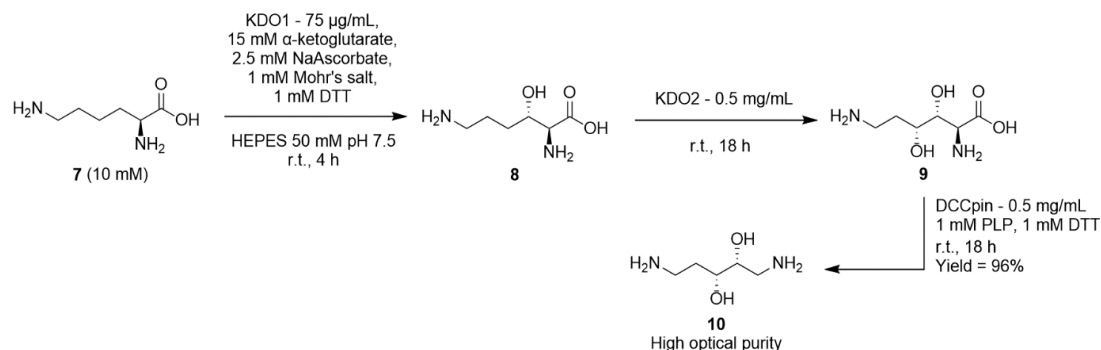
**Figure 4.** Preparative-scale dioxygenase-decarboxylase enzyme cascade yielding (2*R*,3*R*)-1,5-diaminopentane-2,3-diol (**10**) from L-lysine **7**.

and (4*R*)-4-hydroxy-L-lysine, respectively. Moreover, sequential hydroxylation of L-lysine by KDO1 and KDO3 yielded (3*R*,4*R*)-3,4-dihydroxy-L-lysine (**9**), which was further transformed into the lactone (3*R*,4*R*,5*R*)-3-amino-5-(2-aminoethyl)-4-hydroxyoxolan-2-one, an interesting chiral scaffold for synthesis.

By coupling KDOs with PLP-dependent decarboxylases, we designed straightforward synthesis of chiral hydroxy amines from amino acids through two- or three-step one-pot cascade reactions. The decarboxylases were selected based on their genomic context and native substrates, specifically targeting metabolic diamines such as cadaverine. Notably, combining KDO1, KDO2, and DCC$_{pin}$ (a decarboxylase from *Chitinophaga pinensis*, UniProtKB ID: C7PLM7, genomic context of KDO2) in a three-step, one-pot synthesis led to the production of (2*R*,3*R*)-1,5-diaminopentane-2,3-diol (**10**) with high optical purity and 96% yield, starting from L-lysine **7** (Figure 4).

To understand the enzyme selectivity, we performed a structural and computational analysis of the enzymes. Sequence similarity network (SSN) analysis, which clusters closely related proteins, revealed that KDO2-5 homologs form a distinct group, clearly separate from other CSL dioxygenases, including KDO1 [20]. This classification aligns well with experimental findings (Figure 5A). Through genome mining, we have begun to identify and define subfamilies within this enzyme family, although many remain experimentally uncharacterized or potentially misannotated. This underscores the importance of combining in vitro screening with bioinfor-

matic analysis to comprehensively map and harness enzymatic diversity.

Combining sequence diversity to active site structural diversity is a key strategy to build solid hypotheses regarding enzyme mechanism, substrate selectivity, and regio- and stereoselectivity. In this regard, we further explored the diversity of the family via structural studies using the active site modeling and clustering (ASMC) method, thanks to the resolution of the crystal structures of KDO1 and KDO5 in complex with their ligands [22]. It clearly enables us to visualize the high amino acid conservation within some groups of this hierarchical tree of the family, key residues hypothesized from the solved structures. In this way, the C4 regioselectivity was explained by the presence of an arginine in a specific spatial position responsible for a salt bridge with the carboxylate group of the L-lysine substrate, and not found in C3-regioselective enzymes like KDO1 classified in another ASMC group (Figure 5B). A subpocket was also identified as responsible for the substrate specificity in the CSL family, stabilizing either hydrophobic or positively or negatively charged amino acid substrates depending on its surface charge and hydrophobicity. Extensive characterizations like that are especially useful to feed back into the genome mining process. Indeed, we can now look further into dioxygenases using genome mining reinforced with structure-based searches to look for new KDOs.

These two examples highlight the potential of genome-driven biodiversity screening, ranging from numerous hits for enzyme families with wide substrate promiscuity, such as nitrilases, to a more restricted set of hits for enzyme families tested against
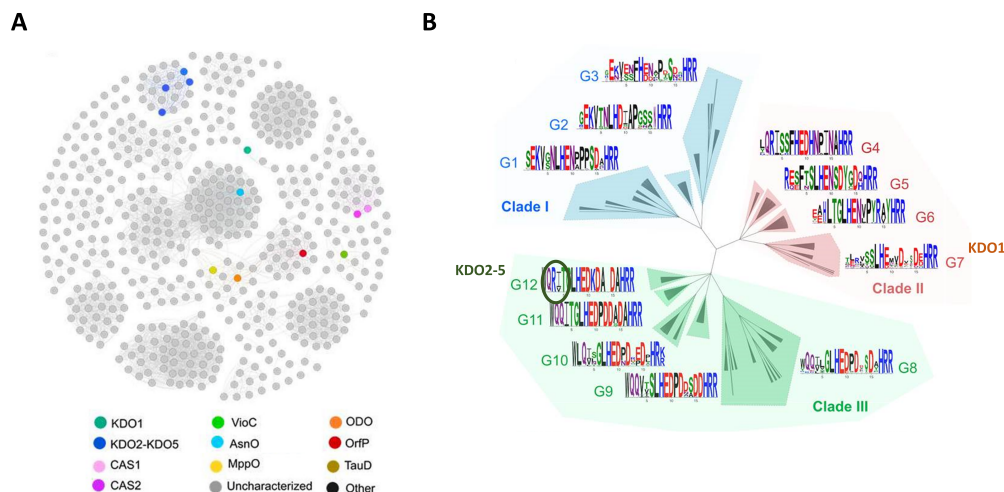
**Figure 5.** Sequence and active site-structural diversity of the clavaminate synthase-like (CSL) family. (A) Sequence similarity network (SSN) of the CSL family (IPR014503) from the αKAOs superfamily. Nodes represent proteins and edges are the links between those proteins that have at least 50% sequence identity. Experimental data retrieved from Swissprot is mapped on the SSN with KDO1 colored in emerald green, KDO2-5 in dark blue and ODO in orange. The network was made with the EFI-EST tool and visualized with Gephi [21]. (B) Active site modeling and clustering (ASMC) hierarchical tree of the CSL family, encompassing 523 proteins grouped into three main clades (I, II, III). For each ASMC group (G1 to G12), a linear projection of the three-dimensional superposition of modeled and crystallographically resolved active sites is provided, via sequence logos illustrating residue conservation within each active site pocket of the ASMC group. A conserved arginine residue, specific to G12, which clusters the KDO2-5 homologs, is highlighted with a green circle marker. Source: Figure adapted from Bastard et al. [20] under Creative Commons Attribution 4.0 International License.

specific substrates and exhibiting high specificity. As databases of enzyme sequences, including many uncharacterized entries, continue to expand, genome mining emerges as an indispensable tool for uncovering this latent potential. It delivers crucial findings that enhance our understanding of sequence diversity and enrich the repertoire of biocatalysts available for biotransformations in synthetic chemistry.

## 3. Genome mining to divert an enzyme activity toward an un-natural synthetic reaction: a use case with coenzyme A (CoA) ligases

The transformations catalyzed by native enzymes can inspire new synthetic strategies for desirable chemical steps. One approach involves partially leveraging a native enzyme system to benefit from only the mechanistic steps useful for the targeted transformation. A notable example, reported in 2017, is the synthesis of amides using carboxylic acid

reductases (CARs), which naturally catalyze the reduction of carboxylic acids to aldehydes. This reaction proceeds through a sequence involving the formation of acyl adenylate and enzyme-thioester intermediates, followed by an NADPH-dependent reduction to aldehyde. By adding a free amine to the reaction mixture, these intermediates can instead be intercepted by this nucleophile, producing amides rather than aldehydes [23]. Further enzyme engineering allowed the optimization of this promising method for enzymatic amide synthesis [24].

Following the same philosophy, we aimed to utilize other members of the adenylate-forming enzyme superfamily to achieve efficient amide synthesis. Amides are crucial precursors for fine chemical and pharmaceutical production [26]. By coupling bacterial coenzyme A (CoA) ligases, for the activation of carboxylic acids, with amines, we developed a chemoenzymatic route for diverse amides [27]. CoA ligases typically catalyze the ATP-dependent
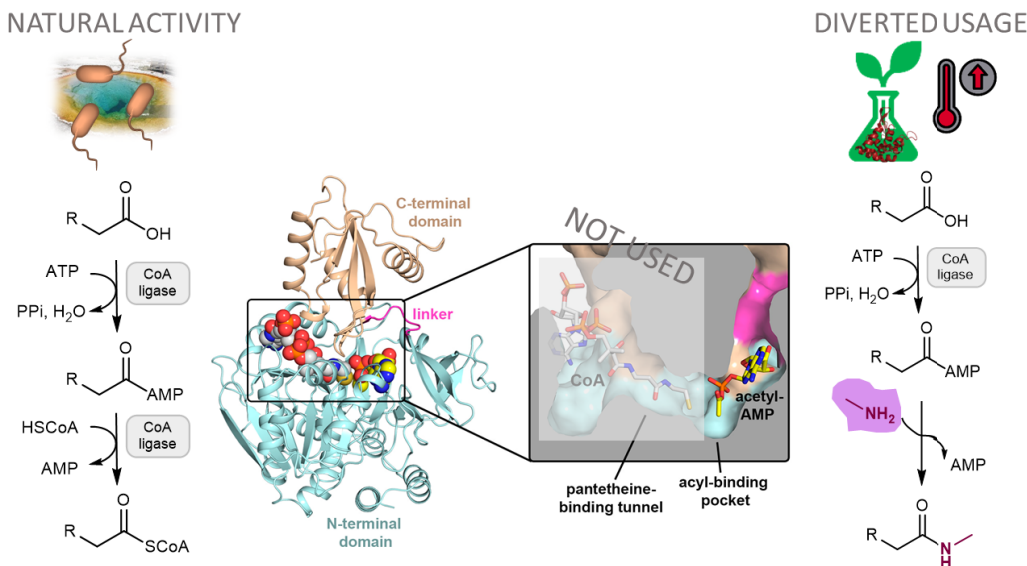
**Figure 6.** Synthesis of *N*-methylalkylamides by biocatalysis with CoA ligases diverted from their ATP-dependent acyl-CoA thioesterification natural activity. Source: Figure adapted from Capra et al. [25] under the CC-BY license.

acyl/aroyl-CoA thioester formation from carboxylic acids in two steps: adenylation with ATP followed by thioesterification in the presence of CoA. To enhance process efficiency, we made the adenylate intermediate the direct target of amine addition, avoiding the costly use of CoA for thioesterification. To drive the nucleophilic attack, we increased the reaction temperature to 60 °C. We selected CoA ligases from thermophilic organisms to ensure stability at this temperature (Figure 6). This approach offers significant advantages over the conventional chemical synthesis of amides, which typically relies on activating carboxylic acids with reagents of low atom economy, such as carbodiimides, oxalyl or thionyl chlorides, or 1,1′-carbonyldiimidazole [28].

As a proof of concept, we focused on synthesizing *N*-methylbutyramide (**12**) from butyric acid (**11**) [27]. Based on literature, we selected carboxylic acid CoA ligases (ACLs) reported as active on small carboxylic acids and expressed by thermophilic organisms: *Ms*ACL (UniProtKB ID: A4YDT1) and *Msed*ACL2 (UniProtKB ID: A4YDR9) from *Metallosphaera sedula*, *Gthe*ACL (UniProtKB ID: A4INB3) from *Geobacillus thermodenitrificans*, and *Stok*ACL (UniProtKB ID: Q973W5) from *Sulfolobus tokodaii*. To address ATP costs, an enzymatic ATP regener-

ation system was implemented, using a thermally stable polyphosphate kinase 2 (class III) to convert the released AMP directly to ATP, with polyphosphate (PolyP$_n$) as the phosphate donor. After 24 h at 65 °C in MOPS buffer (pH 8.5), with 0.02 mg/mL *DgeoPPK2-III* from *Deinococcus geothermalis* (UniProtKB ID: Q1W43), 0.002 mg/mL *PhPPase* from *Pyrococcus horikoshii* (UniProtKB ID: O59570), 5 mM butyric acid, 0.5 mM ATP, and 50 equiv. of methylamine, the conversion rate to *N*-methylbutyrylamide reached 55 to over 99% across all four CoA ligases.

Interestingly, *Ms*ACL also accepts a range of carboxylic acids, primarily short, linear ones, but activity was also observed with 5-oxo-hexanoic acid. Activity levels with propionic to pentanoic acids (761–1514 mU/mg of purified enzyme) exceeded those for phenyl derivatives (e.g., 3-phenylpropanoic acid) or longer chains (e.g., decanoic acid). Notably, *Gthe*ACL demonstrated the highest activity (3.2 U/mg for butyric and pentanoic acid), although its substrate scope was narrower, with no activity detected for decanoic acid or 3-phenylpropanoic acid. A preparative 10 mL-scale reaction using a reduced methylamine quantity (10 equiv.) and 10 mM butyric acid confirmed the feasibility of this approach for synthetic applications (Figure 7) [27].
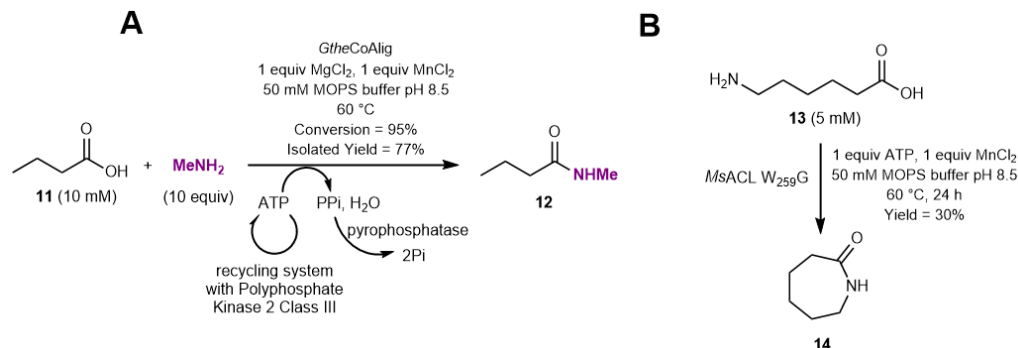
**Figure 7.** Preparative biocatalytic synthesis of (A) *N*-methylbutyramide (**12**) by the thermophilic CoA ligase from *Geobacillus thermodenitrificans* and (B) seven-membered lactam **14** from 6-aminohexanoic acid (**13**) by the *Ms*ACL (CoA ligase from *Metallosphaera sedula*) enzyme variant.

As with CARs, one of the advantages of this approach is the diversity of amides that can be obtained, since attack by the nucleophilic amine is not catalyzed by the enzyme. A priori, all amines or other nucleophiles are considered, the limitation remaining their nucleophilicity and solubility under CoA ligase reaction conditions. As the critical step from a sustainability and energetic point of view is the acid activation step and not the addition of the amine, this strategy constitutes an alternative to conventional chemistry. Recently, this advantage was harnessed in the hybrid synthesis of 5-aminomethyl-2-furancarboxylic acid (AMFC)-derived amides from alcohols, combining supported gold nanoparticles with these CoA ligases [29]. It is worth noting that another promising biocatalytic approach for amide synthesis involves catalysis by amide bond synthetases, a rare subclass within the ANL superfamily, which also includes carboxylic acid-CoA ligase [30]. In this case, the enzyme catalyzes the entire transformation [31].

Building on these successful results, we further diverted the native reaction by looking for CoA ligases active on ω-amino acids to enable intramolecular lactam formation [25]. Lactams are valuable compounds, particularly as precursors to polymers like ε-caprolactam, essential for nylon production. Such enzymes would catalyze the formation of ω-amino acyl adenylates which, for five- to seven-membered chains, could then undergo spontaneous intramolecular aminolysis of the phosphoester bond. This reaction would lead to the formation of five- to seven-membered lactams, specifically

γ-butyrolactam, δ-valerolactam, and ε-caprolactam **14**, respectively. To do so, we improved the acyl-binding pockets of the promiscuous propionate-CoA ligase *Ms*ACL, also reported to be active toward the ω-functionalized substrate 4-hydroxybutyric acid, by structure-guided protein engineering [32]. The thermoactivity and stability of this enzyme is all the more important for the desired intramolecular aminolysis reaction step. The three-dimensional structure of *Ms*ACL in a thioesterification state with bound acetyl-AMP and CoA was determined in collaboration with the University of Groningen, providing insight into the key residues shaping the acyl-binding pocket. Structure analysis, supplemented with docking and mutant design, revealed the interest of mutating the position W259 in *Ms*ACL located at the "pocket floor" into a smaller residue to generate a deeper pocket suitable for ω-amino acid stabilization. Docking experiments of the intermediates 5-aminopentanoyl-AMP and 6-aminohexanoyl-AMP into the W259G mutated pocket resulted in low energy binding poses with formation of hydrogen bonds and van der Waals interactions with neighboring residues (V238 and F350), not obtained in the wild-type enzyme. Combined with mutations at these latter positions to enhance interactions with the ω-amino group of the substrate, purified mutants generated by directed mutagenesis and expression in *E. coli* were tested for the formation of six- and seven-membered lactams. The variant W259G/V238T/F350V gave rise to the highest analytical yield in δ-valerolactam (26%), while none of the tested double or triple mutants provided higher

yield in ε-caprolactam **14** than the W259G variant (30%). For the formation of γ-butyrolactam from 4-aminobutyric acid, the best analytical yield was obtained with the wild-type enzyme (63% yield) as expected from the in silico analysis. It is worth noting that the main beneficial mutation W259G also induced significantly higher activity for the intermolecular amide formation with various longer carboxylic acids up to eleven-carbon chain length.

This example highlights the benefit of drawing inspiration from nature by repurposing its natural functions to support advancements in the chemical industry, with the understanding that revisiting Nature often provides further insights. For lactam-forming CoA ligases, ongoing efforts are focused on identifying candidates within biodiversity using the genomic approach outlined in Section 2.1, complemented by insights gained from X-ray structural data and protein engineering of *Ms*ACL.

## 4. Genome mining for identification of a new family of biocatalysts: a use case with amine dehydrogenases (AmDHs)

In some cases, for a given biocatalyzed transformation, no naturally occurring enzymes capable of catalyzing the reaction are known; only engineered enzymes derived from those catalyzing different reactions can be reported in the literature. This was the case in 2015 for the reductive amination of carbonyl compounds to synthesize optically active amines, where NAD(P)-dependent enzymes from *Streptomyces virginiae* were documented, but their corresponding protein sequences had not been identified. Given the potential of this biocatalytic route as an alternative to conventional reductive amination for optically active amine synthesis, we sought to identify this activity across biological diversity. However, the selection of reference protein sequences to find homologs proved more complex than for previously studied activities (see above), as no sequences for this specific activity were available. To address this, we mined metabolic databases to identify reactions that convert ketones to amines using ammonia and NAD(P)H, specifically excluding α/β-amino acid dehydrogenases from our search criteria. Homologous sequences of (2*R*,4*S*)-2,4-diaminopentanoate dehydrogenase (2,4-DAPDH), found in ornithine-fermenting bacteria, were selected via the FunDivEx platform using the previously described pipeline [33]. The selected hits, heterologously produced in *E. coli*, including AmDH4 and others, were active toward the native substrate lacking an amino group at the α-position but retaining the necessary carboxylic acid (i.e., 4-oxopentanoic acid). These hits were used in a subsequent iteration, ultimately leading to the discovery of the first gene sequences encoding native AmDHs that catalyze amination of ketones without requiring any carboxylic acid group (specifically, *Cfus*AmDH and *Msme*AmDH). Interestingly, these sequences were evolutionarily distinct from both engineered AmDHs (eng-AmDHs) and imine reductases (IREDs), including reductive aminases (RedAms), other NAD(P)-dependent enzymes that typically utilize primary amines rather than ammonia. The sequence space for this novel activity was further explored through a sequence similarity network constructed from 5313 protein homologs of AmDH4, *Cfus*AmDH, and *Msme*AmDH, limited to sequences found in the UniProtKB database and an in-house metagenomic dataset [34].

A search limited to the closest homologs of previously identified native AmDHs (nat-AmDHs) in metagenomic databases specific to marine environments (OM-RGC and MATOUv1) and human microbiomes (Integrated Gene Catalog) confirmed the presence of this activity across multiple biomes [35]. Recently, we proposed an innovative approach leveraging advances in bioinformatics to gain a more detailed understanding of the entire family across biodiversity. This involved an extensive in silico screening of billions of sequences, covering a substantial portion of publicly available metagenomic data [36]. We designed an efficient bioinformatic workflow to capture remote homologs—proteins with similar structures and functions that exhibit low sequence similarity and are challenging to detect using traditional sequence-to-sequence or sequence-to-profile methods. This approach involved screening Hidden Markov Models (HMMs) profiles of an expanded nat-AmDH family against HMM profiles of NAD(P)-dependent enzymes built within a vast dataset of 2.6 billion sequences from ten genomic and metagenomic sequence databases (2020 update). While this strategy has been applied within the metabolic biology community to annotate proteins with unknown functions, it has yet to be widely adopted in the biocatalysis research community. This approach
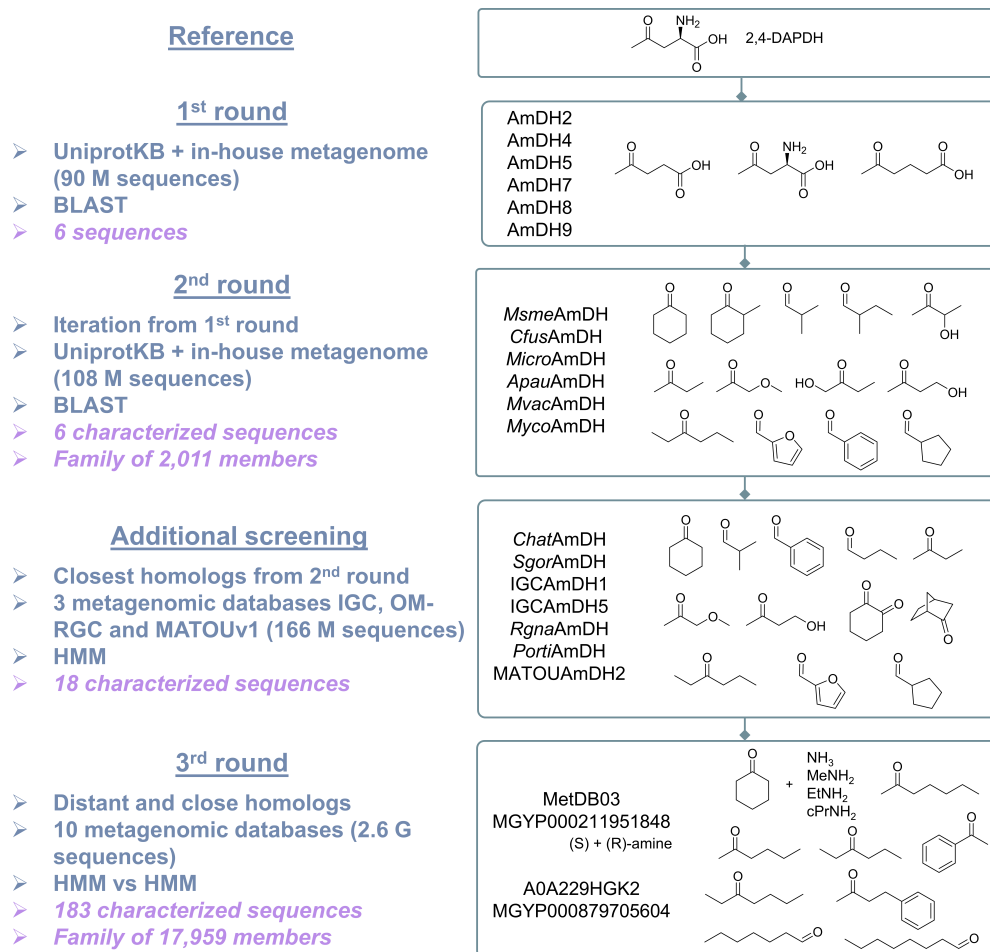
**Figure 8.** Different screenings carried out to identify native amine dehydrogenases (nat-AmDHs). Substrates of some characterized enzymes are drawn (list not exhaustive).

expanded the nat-AmDH family from 2011 to 17,959 sequences, with no additional phylogenetic or structural groups identified, indicating that we captured the full enzymatic diversity for this transformation within biodiversity. Notably, we combined this extensive in silico enzyme capture with in vitro experiments to validate the function of selected representatives and to uncover nat-AmDHs with previously unreported substrate scopes. The previously straightforward search within the UniProtKB database revealed (*S*)-stereoselective nat-AmDHs active on carbonyl compounds limited to short aliphatic aldehydes and methyl ketones (five carbon atoms or less), favoring ammonia over primary amines. In contrast, this large-scale metagenomic screen-

ing identified members active on bulkier carbonyls and ethyl ketones, capable of utilizing methylamine, cyclopropylamine, and displaying increased (*R*)-selectivity, along with close homologs of previously identified nat-AmDHs (Figure 8).

With the crystallographic structures of AmDH4, *Cfus*AmDH, *Msme*AmDH, and MATOUAmDH2, we conducted further analysis using the Active Site Modeling and Clustering (ASMC) method [34,37]. This resulted in a hierarchical tree for the nat-AmDH family, organized into five groups (G1–G5) based on active site residue patterns and frequency. Groups G3 and G4 include AmDHs like *Msme*AmDH and its homologs, which are active on simple ketones and aldehydes, while the more distant G2 contains
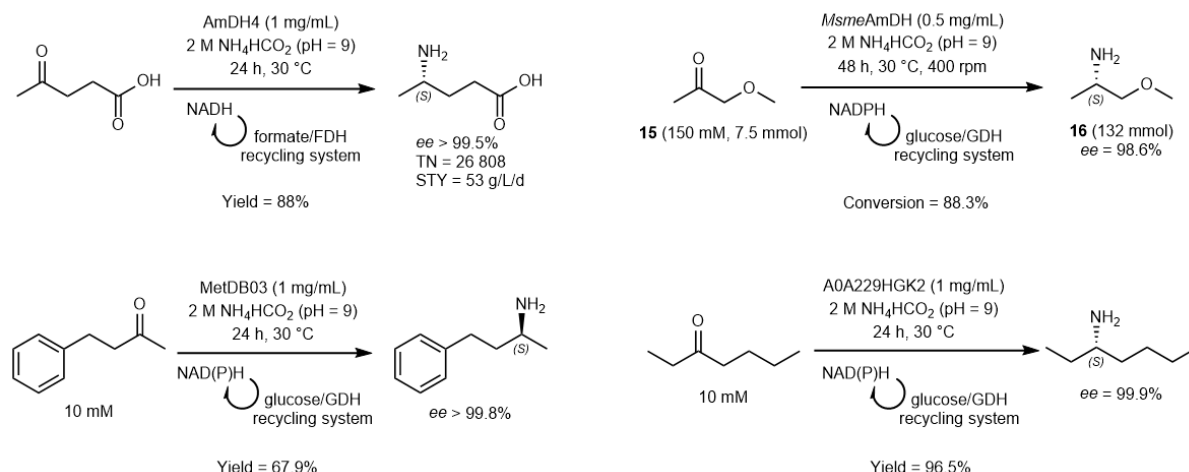
**Figure 9.** Example of biocatalytic reactions performed with native amine dehydrogenases (nat-AmDHs). FDH = formate dehydrogenase, GDH = glucose dehydrogenase; TN = Turnover Number; STY = Space Time Yield.

AmDH4-type enzymes, active on γ-keto acids and 2,4-diaminopentanoate. It should be noted that the reductive amination activity of G3–G4 members toward the substrates tested may not be the metabolic function that has yet to be elucidated. Enzymes in G1 and G5 remain functionally undefined. This classification provides a valuable tool for identifying unusual members by visualizing both conserved and divergent residues at specific 3D positions within the active site. Coupled with docking experiments, this method allows clearer differentiation of active sites suited to more hindered or uniquely functionalized substrates.

Notably, understanding the diversity of residues at specific spatial positions is invaluable to design active site variants. Considering naturally occurring diversity enables the prediction of impactful, viable mutations within the protein context, enhancing the efficiency of protein engineering efforts. This approach has proven beneficial in our work on *Cfus*AmDH and nine additional nat-AmDHs, where biodiversity mining and protein engineering guided the development of variants capable of catalyzing the amination of sterically hindered *n*-alkyl aldehydes and *n*-alkyl ketones from C6 to C9 [38].

Some members of this family were further examined for enzyme kinetics, stability, and biocatalytic potential. Their $k_{cat}$ values ranged from 0.1 to 10 s$^{-1}$, with $K_M$ values for carbonyl compounds between 0.5

and 100 mM. Similar to eng-AmDHs, the $K_M$ for NH$_3$ was high (100–400 mM), while the preferred nicotinamide cofactor had a $K_M$ between 10 and 50 μM [34,35]. Although each characterized AmDH showed a cofactor preference, most favored NADP; however, certain substrate/enzyme couples displayed preference for NAD. Structural analysis pinpointed key residues responsible for this specificity [36]. Interestingly, some nat-AmDHs functioned efficiently as ketoreductases in the absence of an ammonia source; they exhibited minimal activity in the reverse reaction for alcohol or amine oxidation [39]. Stability studies included assessments of thermal tolerance and buffer compatibility. For instance, AmDH4 from *Petrotoga mobilis*, a thermophilic bacterium, proved exceptionally stable with a half-life of 65 h at 60 °C and retained 90% of its initial activity after 14 days at 30 °C [33].

Regarding conversion yields and productivity when a cofactor recycling system was implemented, moderate to high conversions were obtained with high enantiomeric excess of the resulting amines (*ee* from 98 to over 99.9%) for most of them. In the case of 1-methoxypropan-2-one (**15**), a semi-preparative synthesis at 7.5 mmol scale (150 mM) was performed with 0.5 mg/mL of *Msme*AmDH to access, with 88.3% yield and 98.6% *ee*, to the (*S*)-MOIPA **16**, a key chiral element within the Outlook® herbicide (BASF) (Figure 9) [40].
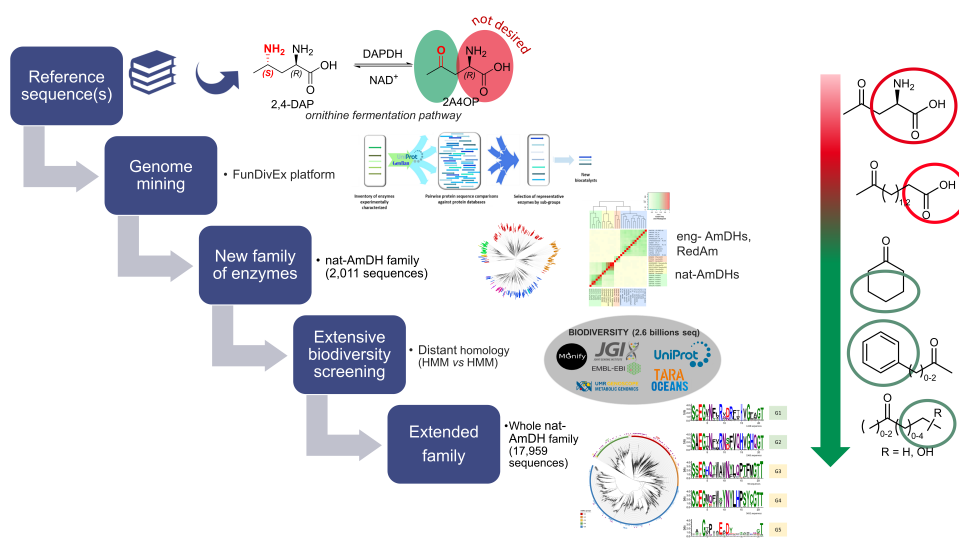
**Figure 10.** Iterative strategy to decipher a new group of enzymes for biocatalysis. Example with the identification of the native amine dehydrogenase (nat-AmDH) family. Source: Figure adapted from Zaparucha et al. [15], Mayol et al. [34], Caparco et al. [35], and Elisee et al. [36], the last under Creative Commons Attribution 4.0 International License.

The kinetics as well as the stability and biocatalytic potential can now be improved by protein engineering and/or directed evolution, these enzymes still being native ones heterologously overexpressed in *E. coli*. The success of some preliminary site-directed mutations carried out on some of them to modify their substrate range makes us confident that modification of these enzymes will lead to soluble and effective enzymes.

This iterative strategy for identifying new enzyme groups suitable for biocatalysis is highly effective and broadly applicable to other enzyme families that remain underexplored in biocatalysis (Figure 10). Searching for distant homologs within the vast pool of publicly available metagenomic databases is a key approach for efficiently and comprehensively exploring what Nature offers for biocatalytic applications, as demonstrated in this study with the exploration of reductive amination activity.

## 5. Conclusion and perspectives

Through these examples, we highlight the benefits of genome mining for expanding the enzyme toolbox for synthetic applications. Analyzing sequence diversity provides a crucial foundation, supporting not only targeted searches within existing and upcoming metagenomic datasets, but also the engineering of customized enzymes tailored to specific industrial needs. This approach is bolstered by a broad array of emerging methods for generating mutant libraries, allowing researchers to explore sequence diversity beyond what Nature alone offers [41]. Biocatalysis is increasingly driven by advanced bioinformatics workflows, which are essential for addressing the demands of sustainable chemistry with speed and precision. Machine learning and artificial intelligence are becoming pivotal in analyzing sequence diversity and predicting protein structures [42–44]. When integrated with innovations in automation and high-throughput screening, these technologies significantly enhance our capacity to discover, modify, and design enzymes with tailored functions.

Although labor-intensive, harnessing native enzyme diversity for biocatalysis is essential and promises significant long-term benefits, especially with the implementation of robust databases and standardized data practices. Initiatives like RHEA, EnzChemRED, EnzymeML, SABIO-RK must operate within a user-friendly findable, accessible, interoperable, reusable (FAIR) environment to encourage widespread adoption [45–49]. By integrating these tools into research workflows, the full potential of genome mining for synthetic applications can

be unlocked, driving significant advancements in biocatalysis.

## Declaration of interests

## Funding

## Acknowledgements

## References

[1]   D. T. Nguyen, D. A. Mitchell and W. A. van der Donk, "Genome mining for new enzyme chemistry", *ACS Catal.* **14** (2024), no. 7, pp. 4536–4553.

[2]   L. Richardson, B. Allen, G. Baldi, et al., "MGnify: the microbiome sequence data analysis resource in 2023", *Nucleic Acids Res.* **51** (2023), no. D1, pp. D753–D759.

[3]   M. Steinegger and J. Söding, "Clustering huge protein sequence sets in linear time", *Nat. Commun.* **9** (2018), no. 1, article no. 2542.

[4]   T. Ahmad, R. S. Singh, G. Gupta, A. Sharma and B. Kaur, "Chapter 15 - Metagenomics in the search for industrial enzymes", in *Advances in Enzyme Technology* (R. S. Singh, R. R. Singhania, A. Pandey and C. Larroche, eds.), Elsevier: Amsterdam, 2019, pp. 419–451.

[5]   T. Patel, H. G. Chaudhari, V. Prajapati, S. Patel, V. Mehta and N. Soni, "A brief account on enzyme mining using metagenomic approach", *Front. Syst. Biol.* **2** (2022), article no. 1046230.

[6]   A. Rodríguez Benítez and A. R. H. Narayan, "Frontiers in biocatalysis: profiling function across sequence space", *ACS Central Sci.* **5** (2019), no. 11, pp. 1747–1749.

[7]   B. N. Hogg, C. Schnepel, J. D. Finnigan, S. J. Charnock, M. A. Hayes and N. J. Turner, "The impact of metagenomics on biocatalysis", *Angew. Chem. Int. Ed.* **63** (2024), no. 21, article no. e202402316.

[8]   R. Buller, S. Lutz, R. J. Kazlauskas, R. Snajdrova, J. C. Moore and U. T. Bornscheuer, "From nature to industry: Harnessing enzymes for biocatalysis", *Science* **382** (2023), no. 6673, article no. eadh8615.

[9]   S. L. Robinson, J. Piel and S. Sunagawa, "A roadmap for metagenomic enzyme discovery", *Nat. Prod. Rep.* **38** (2021), no. 11, pp. 1994–2023.

[10]  R. Wohlgemuth, "Biocatalysis - key enabling tools from biocatalytic one-step and multi-step reactions to biocatalytic total synthesis", *New Biotechnol.* **60** (2020), pp. 113–123.

[11]  I. G. Riziotis, A. J. M. Ribeiro, N. Borkakoti and J. M. Thornton, "Conformational variation in enzyme catalysis: A structural study on catalytic residues", *J. Mol. Biol.* **7** (2022), no. 434, article no. 167517.

[12]  F. L. Sirota, S. Maurer-Stroh, Z. Li, F. Eisenhaber and B. Eisenhaber, "Functional classification of super-large families of enzymes based on substrate binding pocket residues for biocatalysis and enzyme engineering applications", *Front. Bioeng. Biotechnol.* **9** (2021), article no. 701120.

[13]  V. Libis, N. Antonovsky, M. Zhang, et al., "Uncovering the biosynthetic potential of rare metagenomic DNA using co-occurrence network analysis of targeted sequences", *Nat. Commun.* **10** (2019), no. 1, article no. 3848.

[14]  D. Dessaux, S. Buchet, L. Barthe, et al., "Designing symmetrical multi-component proteins using a hybrid generative AI approach", preprint, bioRxiv, 2024. Online at https://doi.org/10.1101/2024.06.13.598662.

[15]  A. Zaparucha, V. de Berardinis and C. Vaxelaire-Vergne, "Chapter 1. Genome mining for enzyme discovery", in *Modern Biocatalysis: Advances Towards Synthetic Biological Systems* (G. Williams and M. Hall, eds.), The Royal Society of Chemistry: Cambridge, 2018, pp. 1–27.

[16]  J.-D. Shen, X. Cai, Z.-Q. Liu and Y.-G. Zheng, "Nitrilase: a promising biocatalyst in industrial applications for green chemistry", *Crit. Rev. Biotechnol.* **41** (2021), no. 1, pp. 72–93.

[17]  C. Vergne-Vaxelaire, F. Bordier, A. Fossey, et al., "Nitrilase activity screening on structurally diverse substrates: providing biocatalytic tools for organic synthesis", *Adv. Synth. Catal.* **355** (2013), no. 9, pp. 1763–1779.

[18]  J. Ye, S. McGinnis and T. L. Madden, "BLAST: improvements for better sequence analysis", *Nucleic Acids Res.* **34** (2006), no. suppl_2, W6–W9.

[19]  D. Baud, P.-L. Saaidi, A. Monfleur, et al., "Synthesis of Mono- and dihydroxylated amino acids with new $\alpha$-ketoglutarate-dependent dioxygenases: biocatalytic oxidation of C–H bonds", *ChemCatChem* **6** (2014), no. 10, pp. 3012–3017.

[20]  K. Bastard, T. Isabet, E. A. Stura, P. Legrand and A. Zaparucha, "Structural studies based on two lysine dioxygenases with distinct regioselectivity brings insights into enzyme specificity within the clavaminate synthase-like family", *Sci. Rep.* **8** (2018), no. 1, article no. 16587.

[21]  J. A. Gerlt, J. T. Bouvier, D. B. Davidson, H. J. Imker, B. Sadkhin, D. R. Slater and K. L. Whalen, "Enzyme function initiative-enzyme similarity tool (EFI-EST): A web tool for generating protein sequence similarity networks", *Biochim. Biophys. Acta* **1854** (2015), no. 8, pp. 1019–1037.

[22] R. C. de Melo-Minardi, K. Bastard and F. Artiguenave, "Identification of subfamily-specific sites based on active sites modeling and clustering", *Bioinformatics* **26** (2010), no. 24, pp. 3075–3082.

[23] A. J. L. Wood, N. J. Weise, J. D. Frampton, et al., "Adenylation activity of carboxylic acid reductases enables the synthesis of amides", *Angew. Chem. Int. Ed.* **46** (2017), no. 56, pp. 14498–14501.

[24] C. Schnepel, L. R. Pérez, Y. Yu, et al., "Thioester-mediated biocatalytic amide bond synthesis with in situ thiol recycling", *Nat. Catal.* **6** (2023), no. 1, pp. 89–99.

[25] N. Capra, C. Lelièvre, O. Touré, A. Fossey-Jouenne, C. Vergne-Vaxelaire, D. B. Janssen, A.-M. W. H. Thunnissen and A. Zaparucha, "Adapting an acyl CoA ligase from *Metallosphaera sedula* for lactam formation by structure-guided protein engineering", *Front. Catal.* **4** (2024), article no. 1360129.

[26] M. Winnacker and B. Rieger, "Biobased polyamides: recent advances in basic and applied research", *Macromol. Rapid Commun.* **37** (2016), no. 17, pp. 1391–1413.

[27] C. M. Lelièvre, M. Balandras, J.-L. Petit, C. Vergne-Vaxelaire and A. Zaparucha, "ATP regeneration system in chemoenzymatic amide bond formation with thermophilic CoA ligase", *ChemCatChem* **4** (2020), no. 12, pp. 1184–1189.

[28] J. R. Dunetz, J. Magano and G. A. Weisenburger, "Large-scale applications of amide coupling reagents for the synthesis of pharmaceuticals", *Org. Proc. Res. Dev.* **20** (2016), no. 2, pp. 140–177.

[29] L. Bisel, A. Fossey-Jouenne, R. Martin, et al., "Hybrid synthesis of AMFC-derived amides using supported gold nanoparticles and acyl-coenzyme A ligases", preprint, ChemRxiv, 2024. Online at https://doi.org/10.26434/chemrxiv-2024-2d7wr.

[30] M. Winn, M. Rowlinson, F. Wang, L. Bering, D. Francis, C. Levy and J. Micklefield, "Discovery, characterization and engineering of ligases for amide synthesis", *Nature* **593** (2021), no. 7859, pp. 391–398.

[31] Q. Tang, M. Petchey, B. Rowlinson, T. J. Burden, I. J. S. Fairlamb and G. Grogan, "Broad spectrum enantioselective amide bond synthetase from streptoalloteichus hindustanus", *ACS Catal.* **2** (2024), no. 14, pp. 1021–1029.

[32] A. B. Hawkins, M. W. W. Adams and R. M. Kelly, "Conversion of 4-hydroxybutyrate to acetyl coenzyme A and its anapleurosis in the *Metallosphaera sedula* 3-hydroxypropionate/4-hydroxybutyrate carbon fixation pathway", *Appl. Environ. Microbiol.* **80** (2014), no. 8, pp. 2536–2545.

[33] O. Mayol, S. David, E. Darii, et al., "Asymmetric reductive amination by a wild-type amine dehydrogenase from the thermophilic bacteria *Petrotoga mobilis*", *Catal. Sci. Technol.* **6** (2016), no. 20, pp. 7421–7428.

[34] O. Mayol, K. Bastard, L. Beloti, et al., "A family of native amine dehydrogenases for the asymmetric reductive amination of ketones", *Nat. Catal.* **2** (2019), pp. 324–333.

[35] A. A. Caparco, E. Pelletier, J. L. Petit, et al., "Metagenomic mining for amine dehydrogenase discovery", *Adv. Syn. Catal.* **362** (2020), no. 12, pp. 2427–2436.

[36] E. Elisee, L. Ducrot, R. Meheust, et al., "A refined picture of the native amine dehydrogenase family revealed by extensive biodiversity screening", *Nat. Commun.* **15** (2024), no. 1, article no. 4933.

[37] M. Bennett, L. Ducrot, C. Vergne-Vaxelaire and G. Grogan, "Structure and mutation of the native amine dehydrogenase MATOUAmDH2", *ChemBiochem* **23** (2022), no. 10, article no. e202200136.

[38] L. Ducrot, M. Bennett, G. André-Leroux, et al., "Expanding the substrate scope of native amine dehydrogenases through in silico structural exploration and targeted protein engineering", *ChemCatChem* **14** (2022), no. 22, article no. e202200880.

[39] A. Fossey-Jouenne, L. Ducrot, E. P. J. Jongkind, E. Elisée, A. Zaparucha, G. Grogan, C. E. Paul and C. Vergne-Vaxelaire, "Native amine dehydrogenases can catalyze the direct reduction of carbonyl compounds to alcohols in the absence of ammonia", *Front. Catal.* **3** (2023), article no. 1105948.

[40] L. Ducrot, M. Bennett, A. A. Caparco, J. A. Champion, A. S. Bommarius, A. Zaparucha, G. Grogan and C. Vergne-Vaxelaire, "Biocatalytic reductive amination by native amine dehydrogenases to access short chiral alkyl amines and amino alcohols", *Front. Catal.* **1** (2021), article no. 781284.

[41] L. Alejaldre, J. N. Pelletier and D. Quaglia, "Methods for enzyme library creation: Which one will you choose?: A guide for novices and experts to introduce genetic diversity", *Bioessays* **43** (2021), no. 8, article no. e2100052.

[42] P. S. Sampaio and P. Fernandes, "Machine learning: a suitable method for biocatalysis", *Catalysts* **13** (2023), no. 6, article no. 961.

[43] B. Markus, C. G. Christian, K. Andreas, K. Arkadij, L. Stefan, O. Gustav, S. Elina and S. Radka, "Accelerating biocatalysis discovery with machine learning: a paradigm shift in enzyme engineering, discovery, and design", *ACS Catal.* **13** (2023), no. 21, pp. 14454–14469.

[44] S. Goldman, R. Das, K. K. Yang and C. W. Coley, "Machine learning modeling of family wide enzyme-substrate specificity screens", *PLoS Comput. Biol.* **18** (2022), no. 2, article no. e1009853.

[45] P.-T. Lai, E. Coudert, L. Aimo, et al., "EnzChemRED, a rich enzyme chemistry relation extraction dataset", *Sci. Data* **11** (2024), no. 1, article no. 982.

[46] A. S. Behr, J. Surkamp, E. Abbaspour, M. Häußler, S. Lütz, J. Pleiss, N. Kockmann and K. Rosenthal, "Fluent integration of laboratory data into biocatalytic process simulation using EnzymeML, DWSIM, and Ontologies", *Processes* **12** (2024), no. 3, article no. 597.

[47] S. Lauterbach, H. Dienhart, J. Range, et al., "EnzymeML: seamless data flow and modeling of enzymatic data", *Nat. Methods* **20** (2023), no. 3, pp. 400–402.

[48] U. Wittig, M. Rey, A. Weidemann, R. Kania and W. Müller, "SABIO-RK: an updated resource for manually curated biochemical reaction kinetics", *Nucleic Acids Res.* **46** (2018), no. D1, pp. D656–D660.

[49] A. Morgat, K. Axelsen, T. Lombardot, et al., "Updates in Rhea–a manually curated resource of biochemical reactions", *Nucleic Acids Res.* **43** (2015), no. D1, pp. D459–D464.

ACADÉMIE
DES SCIENCES
INSTITUT DE FRANCE

Review article

# Shortest Path Map correlation-based tool for capturing functionally relevant allosteric networks and its application in enzyme design

**Esther Pruna Cortada** [®], [a] **and Sílvia Osuna** [®], [*, a, b]

[a] Institut de Química Computacional i Catàlisi and Departament de Química, Universitat de Girona, Parc R+i Univ. Girona, Ed. Monturiol, c/ Emili Grahit 91, 17003 Girona, Spain

[b] ICREA, Pg. Lluís Companys 23, 08010 Barcelona, Spain

*E-mail:* silvia.osuna@udg.edu (S. Osuna)

**Abstract.** The impact of distal mutations on enzyme design is analogous to the allosteric regulation effect observed in effector binding or substrate transport within heterocomplexes. Building on this analogy, we employed molecular dynamics simulations to estimate the conformational landscape of enzymes and developed the Shortest Path Map (SPM) tool. This tool identifies key conformationally relevant positions that regulate enzymatic function. In this review, we highlight various applications of the SPM method in its use as a tool for investigating the effects of distal mutations on the conformational landscape, characterizing allosteric regulation, and rationally designing enzymes. A brief description of the method is provided together with several examples reported over the years (from us and other labs) in which the SPM method has been successfully applied.

**Keywords.** Molecular dynamics simulations, Correlation-based tools, Enzyme design, Shortest Path Map, Allostery.

*Manuscript received 13 November 2024, revised 14 February 2025, accepted 26 February 2025.*

## 1. Introduction

Enzyme design seeks to develop biocatalysts with improved "à la carte" characteristics by altering the amino acid sequences of natural enzymes or generating new sequences and tertiary structures. The interest in enzyme design and engineering stems from the unique potential benefits of these catalysts, such as their ability to work efficiently under mild biological conditions while achieving exceptional efficiency, selectivity, and specificity. Enzyme design is intellectually stimulating, serving as a stringent test of our understanding of enzyme stability, folding, evolution, and catalysis.

The process of enzyme design, whether starting from a natural or computationally generated scaffold, involves selecting specific residues for mutation, creating new variants, and applying screening methods to evaluate the desired properties [1]. There are two primary approaches that can be effectively combined: rational design [2–4] and directed evolution (DE) [5–7]. Rational design focuses on predetermined key residues, identified through the analysis of multiple sequence alignments (MSAs), structural evaluation of active sites, substrate-binding tunnels, reaction mechanisms, and key intermediates formed during the reaction, using techniques like quantum mechanics, molecular mechanics, molecular dynamics (MD), and Monte Carlo simulations [3,8]. Rational methods typically target as mutation hotspots active site residues [9,10] or those involved in the bottleneck regions of tunnels, using tools like CAVER, AQUA-DUCT, and HotSpot Wizard [8,11,12]. Inspired by

---

*Corresponding author

the deep-learning (DL) AF2 approach [13–15], recognized with the 2024 Noble Prize in Chemistry, many DL techniques have been recently developed for generating new protein sequences and scaffolds, which then are further refined using sequence design methods such as ProteinMPNN [16–22]. All these different designs generated by means of traditional methods or DL can also be further improved with DE. Recognized with the 2018 Nobel Prize in Chemistry, DE traditionally utilized random mutagenesis but has advanced to integrate bioinformatics [23–28], rational methods [29,30], sequence analysis [31,32], NMR data [33], and high-throughput screening [34], often guided by machine-learning models [35,36]. The DE approach is particularly powerful for improving low-activity computational enzyme designs [37–39] and enhancing side activities [40,41]. Numerous lab-engineered enzymes have been developed over the years, contributing to drug production, biotherapeutics, and fragrance production [42].

One key advantage of DE is its ability to introduce mutations across the entire protein unlike traditional rational design strategies, which often focus on the active site or substrate tunnels for helping substrate binding/product release and/or altering the water content [8,43]. The DE studies have shown significant activity increases through mutations distant from the active site, which are difficult to predict computationally [6,44–46]. This has been observed in various enzyme families, where in many cases mutations occur around 15 Å from the active site [44]. Intriguingly, the impact of mutations on the enzyme turnover ($k_{cat}$) is not directly correlated to their proximity to the active site, which contrasts with the more deterministic role of active site mutations in specificity [6]. Such regulation of the enzyme catalytic activity by means of distal mutations suggests that allostery (i.e., regulation of catalytic activity by effector and/or protein binding) plays a key role in many proteins [47]. Molecular dynamics simulations have explained how such mutations influence enzyme conformational dynamics and enhance catalytic activity by altering the network of non-covalent interactions [46,48], thus regulating the flexibility of dynamical elements such as loops or lids gating the active site access [40,49,50]. Although computational models can rationalize these changes, predicting which distal mutations will affect activity remains challenging [46,48,51]. The insights gained

from DE about the role of distal mutations regulating enzymatic function could help develop computational approaches for designing efficient enzymes with natural-like functionality [44].

The influence of distal mutations in enzyme design parallels the allosteric regulation seen in effector binding or substrate transport within heterocomplexes. These mutations can shift the conformational landscape of the enzyme, favoring a subset of conformations that enhance catalysis. Recognizing this similarity, we explored the application of MD simulations for estimating the enzymes' conformational landscape and extracting key conformationally relevant positions for their use in enzyme design [2,48]. We developed the Shortest Path Map (SPM) tool [52], which constructs a graph based on mean distances and correlation values between residues as determined from MD simulations. Unlike previous allosteric studies that identified regions of importance [53], the SPM method identifies specific residue pairs that significantly influence enzyme dynamics (Figure 1). This precise identification of key residues is valuable in enzyme design, enabling the creation of targeted libraries for mutagenesis.

## 2. SPM tool

The SPM builds a graph based on mean distances and correlation values computed from MD simulations, following a strategy similar to the protocol used by Sethi et al. [53]. For each protein residue, a node is created centered on the carbon alpha atom. The next step is to establish edges between node pairs. An edge is formed between pairs of nodes whose $C_\alpha$ atoms remain within 6 Å of each other throughout the MD simulation. The edge distance is then derived from the calculated correlation values, which represent the information transfer along that edge. Residue pairs with higher correlation values (closer to 1 or −1) have shorter edge distances while less correlated pairs (values closer to 0) have longer edge distances. This approach results in a graph with nodes and edges reflecting residue proximity and correlation, which is then simplified as illustrated in Figure 1.

Unlike previous allosteric studies that focus on identifying communities within the first complex graph generated, we compute the shortest path lengths. The SPM identifies which edges of the graph
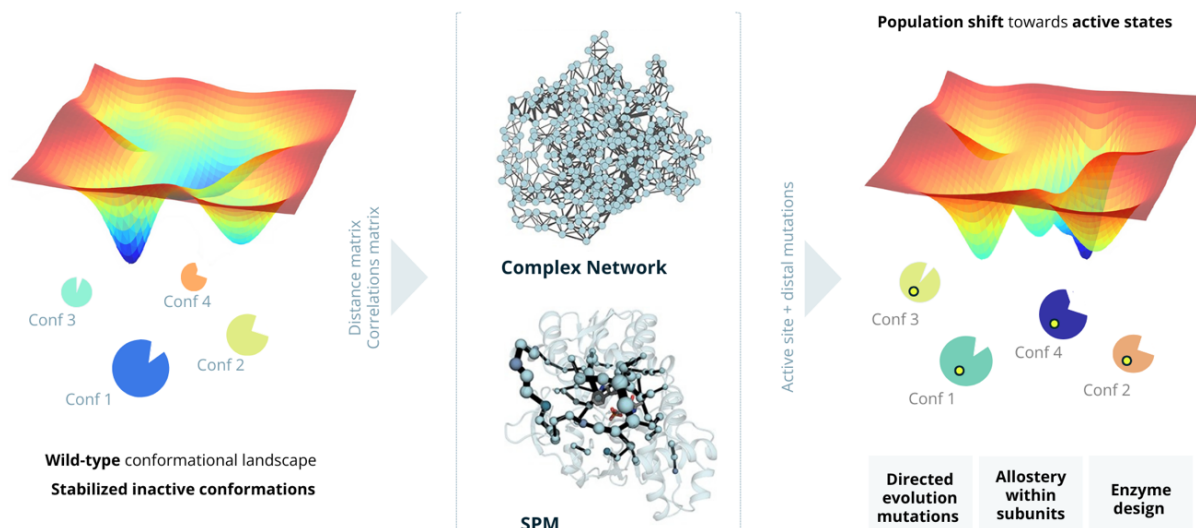
**Figure 1.** Computational enzyme design based on inducing a population shift on the enzyme conformational landscape towards active states by using the SPM method. Left: The wild-type enzyme conformational landscape features multiple stable states, which are predominantly catalytically inactive (labeled Conf 1, Conf 2, Conf 3, and Conf 4). This represents the enzyme conformational heterogeneity, but the enzyme presents poor catalytic efficiency as active states are poorly populated. Center: By computing the distance and the correlation matrices from the multiple replica MD simulations, the first complex graph network is generated, which is further simplified to obtain the SPM network. SPM identifies potential mutational hotspots that can influence the global conformational landscape and induce a shift in the population distribution towards catalytically active states. Right: By introducing targeted mutations at both active and distal sites, the conformational landscape is reshaped to favor catalytically active states. This approach has a wide range of applications, including directed evolution mutation identification (Section 2.1), elucidation and optimization of allosteric pathways (Section 2.2), and finally, rational enzyme design (Section 2.3).

are the shortest (i.e., most correlated) and most frequently used when passing through all the protein residues. After normalizing all edges, only those with the highest contribution are depicted and visualized in the 3D structure. The key advantage of the SPM is that it directly pinpoints critical residues rather than broad regions, making it especially valuable for enzyme design by enabling the construction of small libraries of hotspot positions.

The SPM has proven effective in identifying mutation spots, either within the active site or at distal locations targeted by DE. It has also been applied for elucidating the allosteric regulation existing in multimeric protein structures and more recently for enzyme design. The following sections discuss several cases where SPM has been applied: (1) identification of DE mutation hotspots, (2) rationalization of

allosterically relevant residues, and (3) for enzyme design.

## 2.1. *SPM captures DE mutations*

The DE approach has become an invaluable strategy in enzyme design engineering, enabling the discovery of enzymes with improved or novel functionalities through iterative rounds of mutation and selection [5–7]. The key advantage of DE is its ability to identify beneficial mutations across the entire protein, which are often difficult to predict computationally, but it lacks mechanistic insights into how the identified mutations affect enzyme dynamics and conformational changes. Computational models can rationalize DE mutations, but the challenge persists in the prediction of these key mutations.

The SPM's predictive capabilities have been validated in several key case studies, where it successfully identified mutations that mirrored those obtained through DE. For instance, in the case of mechanistically complex **retro-aldolase (RA) enzymes**, DE introduced multiple mutations scattered throughout the enzyme, which drastically increased its catalytic activity towards the abiological aldol substrate methodol [23,45,48]. The SPM tool could predict most of the mutational hotspots observed in the experimentally evolved enzymes. Specifically, the SPM identified seven of the thirteen mutations introduced by DE while four others were located at adjacent positions and only two were more than six positions away in the sequence (Figure 2a). Of note is that designed RAs are $(\beta\alpha)_8$-barrel enzymes, which is a fold shared by many enzymes suggesting that the application of the SPM tool might be quite broad. A similar result was observed in the complex homodimeric **monoamine oxidase from *Aspergillus niger* (MAO-N)** [49,54,55], where DE was employed to increase catalytic activity towards chiral amines and broaden the enzyme's substrate scope [56]. Five positions were introduced by DE for obtaining the MAO-N D5 evolved variant [57]. The key DE mutations include one active site mutation, one mutation at the entrance tunnel, and three additional distant mutations up to 18–19 Å away from the active site, all of them, despite being computationally challenging to predict, identified by the SPM tool or located at adjacent positions (Figure 2d). The computational evaluation of the conformational changes induced by these mutations by means of Markov state models indicated major changes in beta-hairpin conformation between wild-type and D5 variants. Additionally, the SPM applied to D5 contains the DE positions for generating D9 and D11 variants [57]. This agreement between computational predictions and experimental outcomes underscores the SPM's effectiveness in identifying functionally relevant distal positions and highlights its ability to predict key residues regulating enzyme activity by analyzing the conformational dynamics of the starting enzyme [44].

The SPM tool was also employed by the Mulholland Laboratory to analyze shifts in dynamical networks within the transition-state (TS) ensemble along the DE of a computationally designed **Kemp eliminase**, which catalyzes a proton abstraction from carbon by a base [58]. An SPM analysis of the closed states uncovered a dynamical network that connected the active site to more distal regions of the protein, which indicates fine-tuning of its dynamics by remote mutations (Figure 2c). Mutations such as Q211G and L184F, introduced during DE, were also identified by SPM as key contributors to this network, facilitating the global response of the enzyme scaffold to the TS. Mutation Q211G increased flexibility, fine-tuning the dynamic response while L184F enhanced packing by tightening the interactions between neighboring solvent-exposed loops, further stabilizing the TS. These mutations were essential in reducing the structural fluctuations in the TS ensemble, thereby improving catalytic preorganization.

Another striking example of SPM's utility to identify the mutations introduced by DE comes from work on the heterocomplex **tryptophan synthase from *Pyrococcus furiosus* (*Pf*TrpS)**. The TrpB complex, a subunit of the tryptophan synthase complex (TrpS), was subjected to DE to create an efficient stand-alone enzyme variant independent of the alpha subunit (TrpA) with improved catalytic activity [59,60]. The evolved variant, *Pf*TrpB-0B2, contained six distal mutations that restored the enzyme's ability to access essential conformational states in the absence of its TrpA protein binding partner [61,62] (Figure 2b). Two of the distal mutations, P12L and E17G, introduced by DE are located near the TrpA–TrpB interface. Another mutation, F247S, is found in a known tunnel while T292S is situated in one of the loops close to the essential COMM domain that covers the active site where the pyridoxal phosphate cofactor is located. Additionally, two more mutations, I68V and T321A, are present in more remote regions of the enzyme. Of the six mutations in *Pf*TrpB-0B2, the first two were directly predicted by SPM and three were making persistent non-covalent interactions with SPM-identified positions. Mutation T292S, which significantly enhanced enzyme activity, modulated COMM domain closure via interactions with D300, supporting SPM predictions. The only residue not captured by the SPM is T321, which is considered to play a minor role in COMM domain conformational dynamics. The comparison of the free energy landscapes between the wild type and the evolved *Pf*TrpB-0B2 indicated that these distal mutations recovered the conformational heterogeneity observed for the wild type when forming complexes with TrpA [61]. This study highlights the
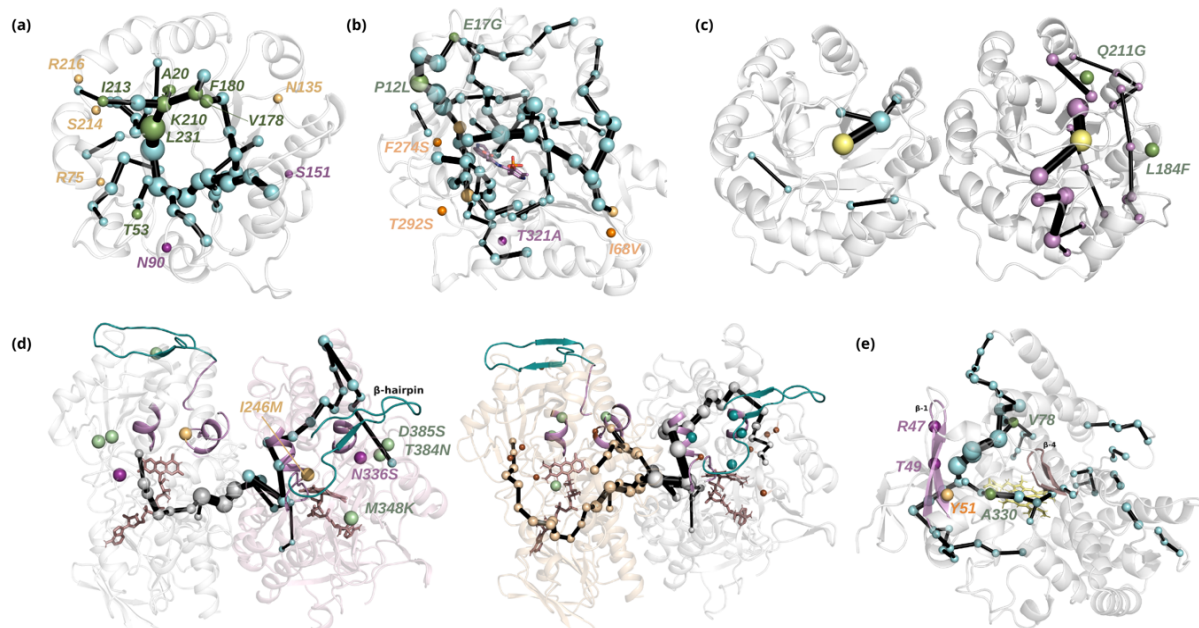
**Figure 2.** Some examples of the application of the SPM method for capturing DE mutations. (a) SPM is applied to retro-aldolase enzyme. Of the thirteen mutations introduced by DE, seven were directly identified by SPM (green) with an additional four located at adjacent positions (yellow). Only two mutations (purple) were positioned more than six residues away in sequence. (b) Six distal mutations in *Pf*TrpB were introduced by DE to generate a stand-alone *Pf*TrpB-0B2 variant. Of these, five mutations were identified by SPM: two directly captured by SPM (green) and three adjacent to SPM-identified positions (orange). The only distal mutation not captured by SPM is shown in purple. (c) The SPM in 1A53-2 (left) and 1A53-2.5 (right) depicts the interaction network centered on the transition state and extending to the closed state of the protein. The two mutations found by DE are directly involved in the SPM. (d) Right: The five mutations in MAON-WT identified by DE to generate MAON-D5 evolved variant are shown as spheres. The key DE mutations include one active site mutation (purple), one mutation at the entrance tunnel (yellow), and three additional distant mutations (green). Left: The DE mutations on MAON-D5 towards MAON-D9 variant are also captured by SPM and are shown in dark green while previous mutations are shown in brown. The beta-hairpin structure is highlighted in teal, and the entrance loop is represented in violet in both images. The FAD cofactors are depicted as sticks in dark violet. (e) The SPM pathway of the CYP450 enzyme included the previously identified DE mutations V78 and A330 (green). SPM also depicts the long-distance connection between beta-sheet 1 (purple) and beta-sheet 4 (light violet). The key mutation Y51I, identified by SPM as an adjacent position, is shown in yellow.

potential of the SPM in identifying key residues for improving enzyme function, offering a powerful tool for targeting allosterically regulated systems.

The SPM was also applied to study the epistatic effects and conformational dynamics in the stepwise evolution of a **cytochrome P450-BM3 monooxygenase** engineered for regioselective and stereoselective hydroxylation of a steroid [63]. The previously identified DE mutations V78 and A330 were

successfully included in the SPM pathway of the parent enzyme (Figure 2e). Additionally, combinatorial saturation mutagenesis revealed that the mutant R47I/T49I/Y51I/F87A exhibited improved activity compared to the wild type, achieving 94% 2β-selectivity and 67% substrate conversion. Computational analysis showed that while mutations R47I and T49I alone did not affect selectivity, the Y51I mutation shifted substrate orientation, increasing

2β-selectivity. The SPM successfully identified the Y51 position providing the key residue responsible for both activity and selectivity. Furthermore, the SPM pathway detected a long-distance communication network between β4 and β1, involving positions R47, T49, and Y51.

These selected examples show that the SPM method is a valuable computational tool for capturing the conformational effects of mutations introduced by DE. By pinpointing key residues and pathways that regulate conformational transitions, the SPM can be, in principle, used to enhance the efficiency of enzyme engineering efforts by predicting conformationally relevant positions not strictly located at the active site. The successful application of the SPM in enzymes like RA, monoamine oxidase, tryptophan synthase, Kemp eliminase, and cytochrome P450 illustrates its potential to complement and rationalize DE approaches, accelerating the development of enzymes with optimized functionalities through a deeper understanding of their conformational landscapes.

## 2.2. *SPM identifies allosteric pathways*

Allosteric regulation is a fundamental process in which distant residues within a protein communicate to regulate its activity. This long-range communication allows proteins to respond to various signals, adjusting their function accordingly. Understanding the specific pathways through which allosteric signals travel is crucial to enzyme design and for understanding how mutations alter protein function. The SPM has proven effective in mapping allosteric pathways in key proteins, offering insights into how mutations can alter their regulation and function. For instance, the SPM was applied to 5 μs atomistic MD simulations of the **K-Ras4B protein** embedded in a phospholipid membrane to investigate its allosteric regulation [64]. Allosteric regulation in K-Ras, particularly the oncogenic K-Ras4B, is key to its function in cellular signaling. K-Ras switches between an active GTP-bound state and an inactive GDP-bound state with allosteric changes in key regions of the G domain (switches I and II), enabling effector recruitment and signal transduction. Mutations, especially in Gly12 and Gly13, can disrupt this regulation, locking K-Ras in an active state and driving cancer progression [64]. The SPM

identified a prominent allosteric pathway starting at the hypervariable region (HVR), a near-membrane region that might be receiving allosteric messages and transferring them to the major hub, located on helix α5, loop α3–β5, and the N-terminus of sheet β5 (Figure 3a). Branching out to key areas in the G domain, the allosteric route extends to regions crucial to K-Ras function, including the P-loop, Thr58, and Ala59 on switch II and Thr35 on switch I. The analysis of the allosteric communication existing in K-Ras4B was also assessed by means of other measures: distance fluctuation analysis [65,66], anisotropic thermal diffusion [67], and dynamical non-equilibrium simulations [68], which provided complementary information on how allostery is transmitted when hydrolyzing GTP [64]. The SPM therefore provided useful insights into K-Ras allostery that help in identifying potential allosteric sites for therapeutic targeting, advancing drug design efforts for this protein.

In a recent study, the allosteric regulation mechanism of the human mitochondrial heat shock protein (**Hsp60**), which is responsible for controlling proteostasis, is elucidated using the SPM tool [69]. This study examines the effect of V72I point mutation, linked to hereditary spastic paraplegia SPG13, which is characterized by progressive weakness and spasticity of the lower limbs. An SPM analysis was performed on MD simulations of both the wild-type (M WT) and mutant (M V72I) Hsp60 monomers (Figure 3b). The results indicate that the extensive interdomain allosteric communication present in the wild-type monomer is entirely disrupted in the V72I mutant, leading to decreased efficiency in communication across the intermediate domain, which contains the critical catalytic residue Asp 397. By mapping the allosteric network in the Hsp60 monomer, this work offers valuable insights into the pathogenic effects of the V72I mutation, demonstrating how specific distal mutations can alter protein function and contribute to disease and highlighting the potential applicability of SPM in rationalizing allosterically regulated mechanisms.

Imidazole glycerol phosphate synthase (IGPS) enzyme has been a model for studying allosteric regulation [70–72]. The enzyme IGPS consists of two subunits, HisH and HisF, with HisH catalyzing glutamine hydrolysis and HisF delivering ammonia through an internal tunnel. Bound 30 Å from the
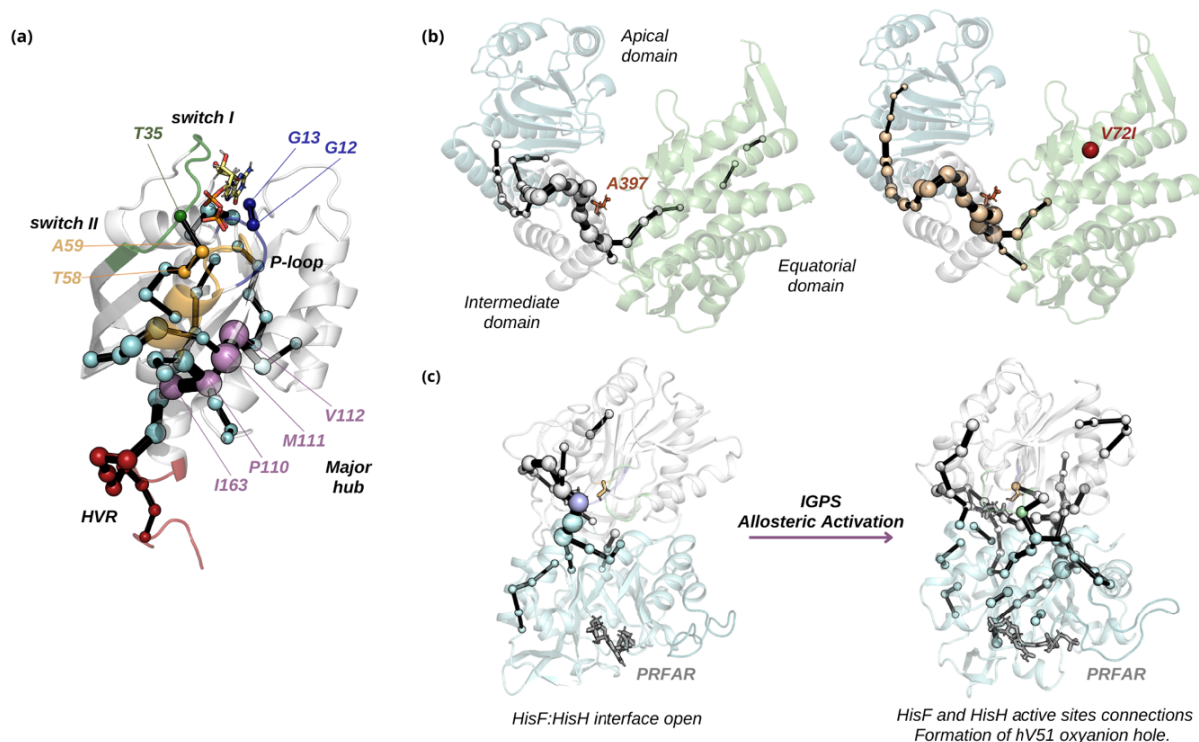
**Figure 3.** Some examples of the application of the SPM method for identifying allosteric networks. (a) K-Ras4B: SPM reveals the allosteric network connecting the membrane-embedded HVR region (dark red) to the central hub (violet), which extends to switch II (orange) and further connects to switch I (green). Notably, the critical mutations Gly12 and Gly13 in the P-loop (blue) are also captured by SPM. (b) Hsp60: The allosteric network links the equatorial domain (wheat), intermediate domain (white), and apical domain (dark red). Introducing the V72I mutation disrupts this network, disrupting the communication between the equatorial domain and the active site, represented by residue A397 in dark orange. (c) IGPS: SPM analysis shows the progression of IGPS from the open HisH–HisF interface to an allosterically active state, where multiple pathways connect HisF and HisH active sites, facilitating the formation of the hV51 oxyanion hole.

HisH active site, PRFAR acts as an allosteric effector, enhancing glutaminase activity by 4500-fold [73]. In this case, a time-evolution Shortest Path Map (te-SPM) analysis is applied to MD simulations, specifically by examining accelerated MD simulations in 600 ns time intervals, uncovering the progression of allosteric activation [74] (Figure 3c). Initially, correlated motions are limited to the HisH subunit and the HisF–HisH interface. However, as the te-SPM analysis progresses, it reveals concerted motions that are activated upon productive closure of the HisF–HisH interface, extending throughout the entire HisF subunit, the interdomain region, and the HisH active site, leading to the formation of the hV51

oxyanion hole. This dynamic process aligns with µs–ms motions observed by NMR and suggests that IGPS allosteric activation follows a "violin model" of dynamics-based allostery, similar to what is found in some protein kinases [75]. The truncated SPM approach for the time-evolution analysis can be also used to decipher the molecular basis of allosteric mechanisms in related allosterically regulated enzymes.

All the provided examples support the idea that the SPM tool is a useful strategy for uncovering the intricate mechanisms of allosteric regulation in proteins by identifying critical pathways of residue communication. So far, the SPM has offered deep insights

into how proteins modulate their functions and how mutations can disrupt this regulation. Therefore, the SPM serves as a promising tool for rational design of targeted therapeutics and enzyme engineering.

## 2.3. *Conformationally driven enzyme design with SPM*

The application of the SPM in different unrelated enzymes demonstrates that analyzing an enzyme conformational ensemble can pinpoint key positions that significantly impact its conformational dynamics. Notably, the SPM identifies positions throughout the enzyme, not just in the active site, allowing for the prediction of distal mutations. This suggests a strategy for conformationally driven enzyme design involving the reconstruction of the enzyme conformational landscape, detection of critical positions using the SPM, and identification of the specific amino acid substitution for each mutation through experimental or computational methods.

We engineered a **stand-alone functional TrpB** by combining the SPM with ancestral sequence reconstruction (ASR) [76]. Interestingly, ASR revealed that the last bacterial common ancestor (LBCA) is allosterically inhibited by TrpA, thus presenting high stand-alone activity [77,78]. Over the course of evolution, this inhibition shifted towards allosteric activation; specifically ANC3 TrpS is the first ancestral enzyme displaying allosteric activation by TrpA. By coupling SPM and sequence conservation analysis between LBCA and ANC3 TrpB, six key positions were rationally identified, leading to the SPM6 variant, which achieved a sevenfold increase in catalytic activity [76] (Figure 4a). This improvement of activity obtained by the experimental testing of a few (<5) variants was similar to that obtained after multiple rounds of DE in *Pf*TrpB that required the generation and screening of more than 3000 variants [59]. Two additional variants were developed that further validate the approach: SPM3, based on ANC2 TrpB, involved three mutations; SPM8, derived from an additional SPM analysis of ANC3 TrpS instead of TrpB, added two allosterically relevant positions [76]. While SPM8 achieved similar catalytic improvement to SPM6, SPM3 showed a smaller enhancement, which was expected from the reduced number of mutations. An additional comparison of SPM with MSA revealed the complementarity of the

two methods, as they identified distinct mutation sites with only one shared residue mutation between them [76].

In another recent study also focused on a tryptophan synthase, the SPM tool was employed to enhance the **stand-alone activity of Zea mays TrpA (*Zm*TrpA)** by identifying key conformationally relevant positions [79] (Figure 4b). Unlike TrpB, where a shift in allosteric regulation was observed along its phylogenetic tree, LBCA TrpA was already allosterically activated by TrpB [77,78]. This made more difficult the identification of positions for stand-alone activity using traditional methods like MSA. However, the structurally similar stand-alone enzyme *Zm*BX1 [80] from the secondary metabolism of maize served as a model for designing an enhanced TrpA variant [79].

The initial approach involved engineering the *Zm*TrpA to the *Zm*TrpA-L6Bx1 variant by switching the L6 loop with the L6 found in ZmBX1 [80], as L6 closed conformation observed in *Zm*BX1 was reported to be crucial to TrpA stand-alone activity [79]. This resulted in a significant increase in catalytic turnover ($k_{cat}$) but at the expense of increasing $K_M$, indicating the need for additional improvements to achieve better catalytic efficiency [80]. To further enhance the stand-alone activity of *Zm*TrpA, the SPM method was applied to identify key conformationally relevant positions by comparing the intramolecular pathways of *Zm*TrpA-L6BX1 and *Zm*BX1 at the catalytically activated state. The motivation for specifically targeting the IGP-bound catalytically activated state was the experimental observation that the conformational transition to achieve the catalytically active state is rate-determining [81]. By comparing the generated SPM for the starting *Zm*TrpA-L6BX1 scaffold and *Zm*BX1, a subset of non-conserved SPM-identified positions was selected for mutation, leading to the *Zm*TrpA-SPM4-L6BX1 variant, which exhibits a 178-fold improvement in catalytic efficiency towards IGP cleavage [79]. With this study, the power of SPM in identifying both active site and distal mutations to boost stand-alone activity is highlighted and paves the way for enzyme design in those enzymatic systems where conformational change is rate-limiting.

The SPM tool was also successfully applied to predict mutations that converted **hydroxynitrile lyase (HbHNL)** from the rubber tree into an
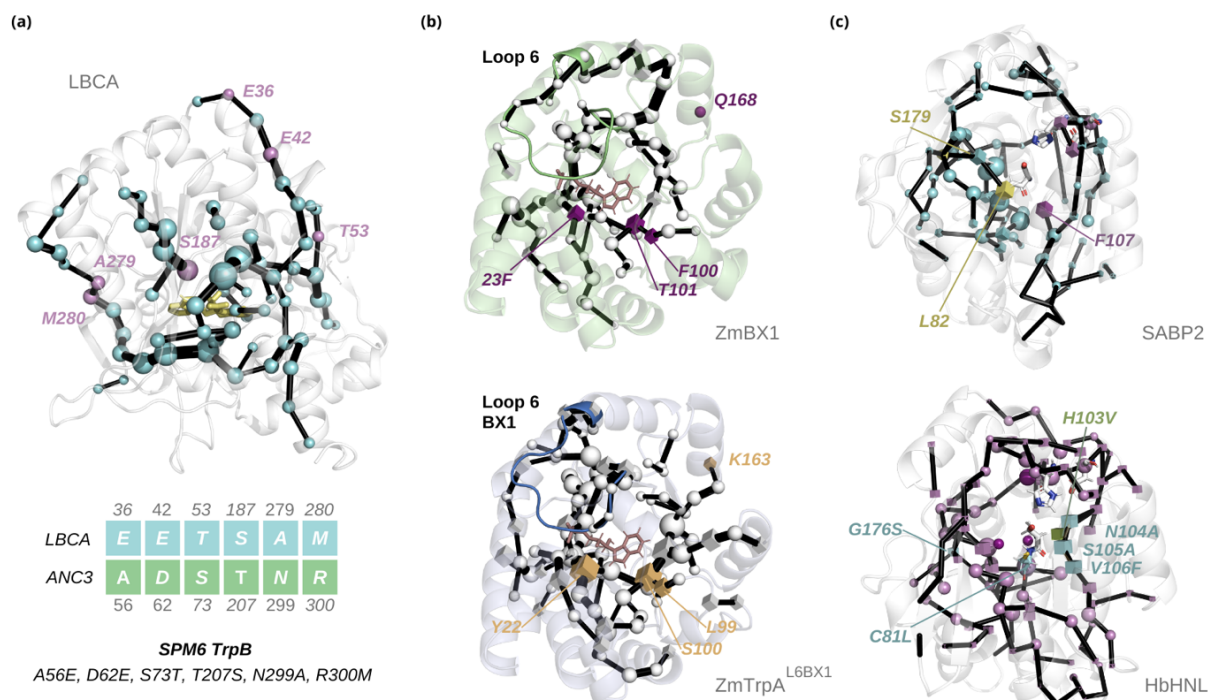
**Figure 4.** Some examples of the application of the SPM method for rational enzyme design. (a) Designing stand-alone TrpB variants based on the ancestral ANC3-TrpB scaffold: SPM identifies a set of conformationally relevant positions in LBCA-TrpB (violet), which after sequence analysis conservation with ANC3-TrpB residues led to the SPM6 TrpB design exhibiting a sevenfold increase in catalytic activity with respect to ANC3 WT. (b) Designing stand-alone TrpA enzymes: the comparison of the SPM graphs computed considering IGP-bound catalytically activated states of the stand-alone ZmBX1 (top) and ZmTrpA-L6BX1 (bottom) allowed the generation of the ZmTrpA-SPM4-L6BX1 variant. The selected positions mutated are shown in purple for ZmBX1 and in yellow for ZmTrpA-L6BX1. ZmTrpA-SPM4-L6BX1 presents a 178-fold higher stand-alone catalytic efficiency compared to ZmTrpA. (c) Designing efficient esterases from hydroxynitrile lyases: the introduction of the three obvious active site mutations for providing an oxyanion hole pocket to *Hb*HNL and one additional stabilization mutation yielded HNL3V, which shows poor esterase activity. The SPM analysis applied to the reference SABP2 esterase (top) and HNL3V (bottom) is depicted, with spheres indicating residues shared between both proteins and cubes marking differing residues. Four/five SPM positions were selected for mutagenesis, yielding HNL7 and HNL8 that both exhibit a 300-fold enhancement in esterase catalytic activity as compared to *Hb*HNL. The incorporation of evolutionary information into SPM provided HNL7T, which displays a 1450-fold increase in catalytic efficiency, thus surpassing that of the SABP2 esterase taken as reference.

efficient esterase by comparison with tobacco **esterase (SABP2)** [82] (Figure 4c). Both enzymes are present in the $\alpha, \beta$-hydrolase fold and despite the fact that they share the same catalytic Ser–His–Asp triad, they exhibit very different forms of reactivity. Initial efforts to engineer *Hb*HNL into an esterase produced the HNL3V variant, which focused on the

three obvious active site mutations (T11G, E79H, K236M) to introduce the oxyanion hole residues and to replace the polar site by a hydrophobic site as observed in SABP2. However, these three obvious mutations only showed limited esterase activity. To further enhance the esterase activity, SPM analysis of HNL3V, a stabilized version of HNL3 for experimental

purposes, and SABP2 revealed five additional positions outside the active site, which were connected to the catalytic residues and could potentially affect the oxyanion hole and the catalytic Asp preorganization. By replacing these positions with those from SABP2, the HNL6V, HNL7V, and HNL8V variants were created, enhancing esterase activity by 300-fold. The SPM-guided mutations targeted correlated movements essential for catalysis by removing unwanted movements in HNL3V and adding the missing ones from SABP2. To this end, the residues in HNL3V were replaced with the corresponding ones from SABP2. Notably, most of the engineered mutations were outside the active site, demonstrating the ability of the SPM to identify distal residues contributing to catalytic function.

The combination of SPM analysis with an MSA of esterases resulted in the identification of the most effective variant, HNL7TV. Among the mutations tested, the N104A substitution produced the largest increase in turnover rate ($k_{cat}$). However, sequence alignment revealed that most esterases naturally have a threonine at this position rather than an alanine. Introducing the N104T substitution led to the best overall variant with approximately twice the catalytic efficiency ($k_{cat}/K_M$) of SABP2, thus increasing the esterase catalytic efficiency of the starting *Hb*HNL scaffold by 1450-fold. Despite this impressive improvement, the turnover rate ($k_{cat}$) of HNL7TV remained 13-fold lower than SABP2, indicating a need for further refinement. Nevertheless, the dramatic increase in catalytic efficiency demonstrated the ability of the SPM to predict which residues outside the active site contribute to catalytic activity [82].

## 3. Conclusions

Recognizing the high similarity between allosteric processes and the effect exerted by distal active site mutations on the enzyme catalytic activity, we hypothesized that the computational identification of allosteric networks could bring interesting insights into enzymatic function and design [44]. To that end, we developed the SPM method [44,52], which identifies a set of conformationally relevant positions based on the application of graph theory to the distance and correlation matrices computed from MD data. Over the years, we (and others) have applied the SPM to identify conformationally relevant

positions and compared those with residues mutated in DE experiments [2,44,48,58,63]. Interestingly, in many different enzyme classes and families, the application of SPM has revealed that some of the DE mutations are introduced in conformationally relevant sites, thus suggesting its potential application for enzyme design.

The SPM has also been used for elucidating the intricate mechanisms of allosteric regulation in different enzymatic and protein systems [64,69,74]. The SPM allosteric networks identify critical pathways of residues, some of which are experimentally known to have a large effect on enzyme/protein regulation. We have also tested the applicability of SPM, especially if combined with ASR and/or MSA, to rationally design new improved enzymes with enhancements in catalytic efficiency that range from 7- to 1450-fold [76,79,82]. Altogether these examples show the potential of the SPM method for understanding the effect of distal mutations into the enzyme conformational dynamics and how they affect enzymatic function. More importantly, integrating SPM with other computational techniques such as MSA and ASR corresponds to a successful approach for rational enzyme design.

## Declaration of interests

The authors do not work for, advise, own shares in, or receive funds from any organization that could benefit from this article, and have declared no affiliations other than their research organizations.

## References

[1]   E. L. Bell, W. Finnigan, S. P. France, et al., "Biocatalysis", *Nat. Rev. Meth. Primers* **1** (2021), article no. 46.

[2]   M. A. Maria-Solano, E. Serrano-Hervás, A. Romero-Rivera, J. Iglesias-Fernández and S. Osuna, "Role of conformational dynamics in the evolution of novel enzyme function", *Chem. Commun.* **54** (2018), pp. 6622–6634.

[3]   A. Romero-Rivera, M. Garcia-Borràs and S. Osuna, "Computational tools for the evaluation of laboratory-engineered biocatalysts", *Chem. Commun.* **53** (2017), pp. 284–297.

[4]   J. Damborsky and J. Brezovsky, "Computational tools for designing and engineering enzymes", *Curr. Opin. Chem. Biol.* **19** (2014), pp. 8–16.

[5]   F. H. Arnold, "The nature of chemical innovation: new enzymes by evolution", *Quart. Rev. Biophys.* **48** (2015), pp. 404–410.

[6] A. Currin, N. Swainston, P. J. Day and D. B. Kell, "Synthetic biology for the directed evolution of protein biocatalysts: navigating sequence space intelligently", *Chem. Soc. Rev.* **44** (2015), pp. 1172–1239.

[7] Y. Wang, P. Xue, M. Cao, T. Yu, S. T. Lane and H. Zhao, "Directed evolution: methodologies and applications", *Chem. Rev.* **121** (2021), pp. 12384–12444.

[8] C. E. Sequeiros-Borja, B. Surpeta and J. Brezovsky, "Recent advances in user-friendly computational tools to engineer protein function", *Brief. Bioinform.* **22** (2020), article no. baa150.

[9] J. J. Ruiz-Pernía, K. Świderek, J. Bertran, V. Moliner and I. Tuñón, "Electrostatics as a guiding principle in understanding and designing enzymes", *J. Chem. Theory Comput.* **20** (2024), pp. 1783–1795.

[10] C. Jerves, R. P. P. Neves, S. L. da Silva, M. J. Ramos and P. A. Fernandes, "Rate-enhancing PETase mutations determined through DFT/MM molecular dynamics simulations", *New J. Chem.* **48** (2024), pp. 45–54.

[11] J. Stourac, O. Vavra, P. Kokkonen, J. Filipovic, G. Pinto, J. Brezovsky, J. Damborsky and D. Bednar, "Caver Web 1.0: identification of tunnels and channels in proteins and analysis of ligand transport", *Nucleic Acids Res.* **47** (2019), W414–W422.

[12] L. Sumbalova, J. Stourac, T. Martinek, D. Bednar and J. Damborsky, "HotSpot Wizard 3.0: web server for automated design of mutations and smart libraries based on sequence input information", *Nucleic Acids Res.* **46** (2018), W356–W362.

[13] A. W. Senior, R. Evans, J. Jumper, et al., "Improved protein structure prediction using potentials from deep learning", *Nature* **577** (2020), pp. 706–710.

[14] A. Ourmazd, K. Moffat and E. E. Lattman, "Structural biology is solved — now what?", *Nat. Meth.* **19** (2022), pp. 24–26.

[15] J. Jumper, R. Evans, A. Pritzel, et al., "Highly accurate protein structure prediction with AlphaFold", *Nature* **596** (2021), pp. 583–589.

[16] S. Ovchinnikov and P.-S. Huang, "Structure-based protein design with deep learning", *Curr. Opin. Chem. Biol.* **65** (2021), pp. 136–144.

[17] W. Gao, S. P. Mahajan, J. Sulam and J. J. Gray, "Deep learning in protein structural modeling and design", *Patterns* **1** (2020), article no. 100142.

[18] Y. Ming, W. Wang, R. Yin, M. Zeng, L. Tang, S. Tang and M. Li, "A review of enzyme design in catalytic stability by artificial intelligence", *Brief. Bioinform.* **24** (2023), pp. 1–19.

[19] A. Lauko, S. J. Pellock, I. Anischanka, et al., "Computational design of serine hydrolases", *Science* **0** (2025), article no. eadu2454.

[20] P. Notin, N. Rollins, Y. Gal, C. Sander and D. Marks, "Machine learning for functional protein design", *Nat. Biotechnol.* **42** (2024), pp. 216–228.

[21] J. Dauparas, I. Anishchenko, N. Bennett, et al., "Robust deep learning-based protein sequence design using ProteinMPNN", *Science* **378** (2022), pp. 49–56.

[22] B. I. M. Wicky, L. F. Milles, A. Courbet, et al., "Hallucinating symmetric protein assemblies", *Science* **378** (2022), pp. 56–61.

[23] L. Jiang, E. A. Althoff, F. R. Clemente, et al., "De novo computational design of retro-aldol enzymes", *Science* **319** (2008), pp. 1387–1391.

[24] D. Rothlisberger, O. Khersonsky, A. M. Wollacott, et al., "Kemp elimination catalysts by computational enzyme design", *Nature* **453** (2008), pp. 190–195.

[25] J. B. Siegel, A. Zanghellini, H. M. Lovick, et al., "Computational design of an enzyme catalyst for a stereoselective bimolecular Diels–Alder reaction", *Science* **329** (2010), pp. 309–313.

[26] R. Kourist, H. Jochens, S. Bartsch, et al., "The α/β-hydrolase fold 3DM database (ABHDB) as a tool for protein engineering", *ChemBioChem* **11** (2010), pp. 1635–1643.

[27] R. K. Kuipers, H.-J. Joosten, W. J. H. van Berkel, et al., "3DM: systematic analysis of heterogeneous superfamily data to discover protein functionalities", *Proteins: Struct. Funct. Bioinform.* **78** (2010), pp. 2101–2113.

[28] R. K. P. Kuipers, H.-J. Joosten, E. Verwiel, et al., "Correlated mutation analyses on super-family alignments reveal functionally important residues", *Proteins: Struct. Funct. Bioinform.* **76** (2009), pp. 608–616.

[29] R. Blomberg, H. Kries, D. M. Pinkas, P. R. E. Mittl, M. G. Grütter, H. K. Privett, S. L. Mayo and D. Hilvert, "Precision is essential for efficient catalysis in an evolved Kemp eliminase", *Nature* **503** (2013), pp. 418–421.

[30] M. Pavlova, M. Klvana, Z. Prokop, et al., "Redesigning dehalogenase access tunnels as a strategy for degrading an anthropogenic substrate", *Nat. Chem. Biol.* **5** (2009), pp. 727–733.

[31] T. A. Addington, R. W. Mertz, J. B. Siegel, et al., "Prediction and ranking of mutations required for functional interconversion of enzymes", *J. Mol. Biol.* **425** (2013), pp. 1378–1389.

[32] A. Pavelka, E. Chovancova and J. Damborsky, "HotSpot Wizard: a web server for identification of hot spots in protein engineering", *Nucleic Acids Res.* **37** (2009), W376–W383.

[33] S. Bhattacharya, E. G. Margheritis, K. Takahashi, et al., "NMR-guided directed evolution", *Nature* **610** (2022), pp. 389–393.

[34] H. Xiao, Z. Bao and H. Zhao, "High throughput screening and selection methods for directed enzyme evolution", *Ind. Eng. Chem. Res.* **54** (2015), pp. 4011–4020.

[35] K. K. Yang, Z. Wu and F. H. Arnold, "Machine-learning-guided directed evolution for protein engineering", *Nat. Methods* **16** (2019), pp. 687–694.

[36] S. Mazurenko, Z. Prokop and J. Damborsky, "Machine learning in enzyme engineering", *ACS Catal.* **10** (2020), pp. 1210–1223.

[37] P. A. Romero and F. H. Arnold, "Exploring protein fitness landscapes by directed evolution", *Nat. Rev. Mol. Cell Biol.* **10** (2009), pp. 866–876.

[38] C. Jaeckel, P. Kast and D. Hilvert, "Protein design by directed evolution", *Annu. Rev. Biophys.* **37** (2008), pp. 153–173.

[39] H. Renata, Z. J. Wang and F. H. Arnold, "Expanding the enzyme universe: accessing non-natural reactions by mechanism-guided directed evolution", *Angew. Chem. Int. Ed.* **54** (2015), pp. 3351–3367.

[40]  E. Campbell, M. Kaltenbach, G. J. Correy, et al., "The role of protein dynamics in the evolution of new enzyme function", *Nat. Chem. Biol.* **12** (2016), pp. 944–950.

[41]  R. B. Leveson-Gower, C. Mayer and G. Roelfes, "The importance of catalytic promiscuity for enzyme design and evolution", *Nat. Rev. Chem.* **3** (2019), pp. 687–705.

[42]  R. Buller, S. Lutz, R. J. Kazlauskas, R. Snajdrova, J. C. Moore and U. T. Bornscheuer, "From nature to industry: harnessing enzymes for biocatalysis", *Science* **382** (2023), article no. eadh8615.

[43]  A. Gora, J. Brezovsky and J. Damborsky, "Gates of enzymes", *Chem. Rev.* **113** (2013), pp. 5871–5923.

[44]  S. Osuna, "The challenge of predicting distal active site mutations in computational enzyme design", *WIREs Comput. Mol. Sci.* **11** (2021), article no. e1502.

[45]  R. Obexer, A. Godina, X. Garrabou, P. R. E. Mittl, D. Baker, A. D. Griffiths and D. Hilvert, "Emergence of a catalytic tetrad during evolution of a highly active artificial aldolase", *Nat. Chem.* **9** (2017), pp. 50–56.

[46]  G. Jiménez-Osés, S. Osuna, X. Gao, et al., "The role of distant mutations and allosteric regulation on LovD active site dynamics", *Nat. Chem. Biol.* **10** (2014), pp. 431–436.

[47]  K. Gunasekaran, B. Ma and R. Nussinov, "Is allostery an intrinsic property of all dynamic proteins?", *Proteins: Struct. Funct. Bioinform.* **57** (2004), pp. 433–443.

[48]  A. Romero-Rivera, M. Garcia-Borràs and S. Osuna, "Role of conformational dynamics in the evolution of retro-aldolase activity", *ACS Catal.* **7** (2017), pp. 8524–8532.

[49]  C. Curado-Carballada, F. Feixas, J. Iglesias-Fernández and S. Osuna, "Hidden conformations in Aspergillus niger monoamine oxidase are key for catalytic efficiency", *Angew. Chem. Int. Ed.* **58** (2019), pp. 3097–3101.

[50]  D. Petrović, V. A. Risso, S. C. L. Kamerlin and J. M. Sanchez-Ruiz, "Conformational dynamics and enzyme evolution", *J. R. Soc. Interface* **15** (2018), article no. 20180330.

[51]  P. Campitelli, T. Modi, S. Kumar and S. B. Ozkan, "The role of conformational dynamics and allostery in modulating protein evolution", *Annu. Rev. Biophys.* **49** (2020), pp. 267–288.

[52]  G. Casadevall, J. Casadevall, C. Duran and S. Osuna, "The shortest path method (SPM) webserver for computational enzyme design", *Protein Eng. Des. Select.* **37** (2024), article no. gzae005.

[53]  A. Sethi, J. Eargle, A. A. Black and Z. Luthey-Schulten, "Dynamical networks in tRNA:protein complexes", *Proc. Natl. Acad. Sci. USA* **106** (2009), pp. 6620–6625.

[54]  V. F. Batista, J. L. Galman, D. C. G. A. Pinto, A. M. S. Silva and N. J. Turner, "Monoamine oxidase: tunable activity for amine resolution and functionalization", *ACS Catal.* **8** (2018), pp. 11889–11907.

[55]  F. Zhao, D. Masci, S. Ferla, et al., "Monoamine oxidase (MAO-N) biocatalyzed synthesis of indoles from indolines prepared via photocatalytic cyclization/arylative dearomatization", *ACS Catal.* **10** (2020), pp. 6414–6421.

[56]  R. Carr, M. Alexeeva, A. Enright, T. S. C. Eve, M. J. Dawson and N. J. Turner, "Directed evolution of an amine oxidase possessing both broad substrate specificity and high enantioselectivity", *Angew. Chem. Int. Ed.* **42** (2003), pp. 4807–4810.

[57]  D. Ghislieri, A. P. Green, M. Pontini, S. C. Willies, I. Rowles, A. Frank, G. Grogan and N. J. Turner, "Engineering an enantioselective amine oxidase for the synthesis of pharmaceutical building blocks and alkaloid natural products", *J. Am. Chem. Soc.* **135** (2013), pp. 10863–10869.

[58]  H. A. Bunzel, J. L. R. Anderson, D. Hilvert, V. L. Arcus, M. W. van der Kamp and A. J. Mulholland, "Evolution of dynamical networks enhances catalysis in a designer enzyme", *Nat. Chem.* **13** (2021), pp. 1017–1022.

[59]  A. R. Buller, S. Brinkmann-Chen, D. K. Romney, M. Herger, J. Murciano-Calles and F. H. Arnold, "Directed evolution of the tryptophan synthase β-subunit for stand-alone function recapitulates allosteric activation", *Proc. Natl. Acad. Sci. USA* **112** (2015), pp. 14599–14604.

[60]  E. Watkins-Dulaney, S. Straathof and F. Arnold, "Tryptophan synthase: biocatalyst extraordinaire", *ChemBioChem* **22** (2021), pp. 5–16.

[61]  M. A. Maria-Solano, J. Iglesias-Fernández and S. Osuna, "Deciphering the allosterically driven conformational ensemble in tryptophan synthase evolution", *J. Am. Chem. Soc.* **141** (2019), pp. 13049–13056.

[62]  A. R. Buller, P. van Roye, J. K. B. Cahn, R. A. Scheele, M. Herger and F. H. Arnold, "Directed evolution mimics allosteric activation by stepwise tuning of the conformational ensemble", *J. Am. Chem. Soc.* **140** (2018), pp. 7256–7266.

[63]  C. G. Acevedo-Rocha, A. Li, L. D'Amore, et al., "Pervasive cooperative mutational effects on multiple catalytic enzyme traits emerge via long-range conformational dynamics", *Nat. Commun.* **12** (2021), article no. 1621.

[64]  M. Castelli, F. Marchetti, S. Osuna, A. S. F. Oliveira, A. J. Mulholland, S. A. Serapian and G. Colombo, "Decrypting allostery in membrane-bound K-Ras4B using complementary in silico approaches based on unbiased molecular dynamics simulations", *J. Am. Chem. Soc.* **146** (2024), pp. 901–919.

[65]  A. Triveri, C. Sanchez-Martin, L. Torielli, et al., "Protein allostery and ligand design: computational design meets experiments to discover Novel chemical probes", *J. Mol. Biol.* **434** (2022), article no. 167468.

[66]  M. Castelli, K. Bhattacharya, E. Abboud, S. A. Serapian, D. Picard and G. Colombo, "Phosphorylation of the Hsp90 Co-Chaperone Hop changes its conformational dynamics and biological function", *J. Mol. Biol.* **435** (2023), article no. 167931.

[67]  N. Ota and D. A. Agard, "Intramolecular signaling pathways revealed by modeling anisotropic thermal diffusion", *J. Mol. Biol.* **351** (2005), pp. 345–354.

[68]  A. S. F. Oliveira, G. Ciccotti, S. Haider and A. J. Mulholland, "Dynamical nonequilibrium molecular dynamics reveals the structural basis for allostery and signal propagation in biomolecular systems", *Eur. Phys. J. B* **94** (2021), article no. 144.

[69]  L. Torielli, F. Guarra, H. Shao, J. E. Gestwicki, S. A. Serapian and G. Colombo, "How a pathogenic mutation impairs Hsp60 functional dynamics from monomeric to fully assembled states", preprint, bioRxiv, 2024, 2024.09.09.611948.

[70] S. Beismann-Driemeyer and R. Sterner, "Imidazole glycerol phosphate synthase from thermotoga maritima: quaternary structure, steady-state kinetics, and reaction mechanism of the bienzyme complex", *J. Biol. Chem.* **276** (2001), pp. 20387–20396.

[71] I. Rivalta, G. P. Lisi, N.-S. Snoeberger, G. Manley, J. P. Loria and V. S. Batista, "Allosteric communication disrupted by a small molecule binding to the imidazole glycerol phosphate synthase protein–protein interface", *Biochemistry* **55** (2016), pp. 6484–6494.

[72] B. Reisinger, J. Sperl, A. Holinski, et al., "Evidence for the existence of elaborate enzyme complexes in the Paleoarchean era", *J. Am. Chem. Soc.* **136** (2014), pp. 122–129.

[73] G. P. Lisi, K. W. East, V. S. Batista and J. P. Loria, "Altering the allosteric pathway in IGPS suppresses millisecond motions and catalytic activity", *Proc. Natl. Acad. Sci. USA* **114** (2017), E3414–E3423.

[74] C. Calvó-Tusell, M. A. Maria-Solano, S. Osuna and F. Feixas, "Time evolution of the millisecond allosteric activation of imidazole glycerol phosphate synthase", *J. Am. Chem. Soc.* **144** (2022), pp. 7146–7159.

[75] L. G. Ahuja, S. S. Taylor and A. P. Kornev, "Tuning the "violin" of protein kinases: the role of dynamics-based allostery", *IUBMB Life* **71** (2019), pp. 685–696.

[76] M. A. Maria-Solano, T. Kinateder, J. Iglesias-Fernández, R. Sterner and S. Osuna, "In silico identification and experimental validation of distal activity-enhancing mutations in tryptophan synthase", *ACS Catal.* **11** (2021), pp. 13733–13743.

[77] M. Schupfner, K. Straub, F. Busch, R. Merkl and R. Sterner, "Analysis of allosteric communication in a multienzyme complex by ancestral sequence reconstruction", *Proc. Natl. Acad. Sci. USA* **117** (2020), pp. 346–354.

[78] F. Busch, C. Rajendran, K. Heyn, S. Schlee, R. Merkl and R. Sterner, "Ancestral tryptophan synthase reveals functional sophistication of primordial enzyme complexes", *Cell Chem. Biol.* **23** (2016), pp. 709–715.

[79] C. Duran, T. Kinateder, C. Hiefinger, R. Sterner and S. Osuna, "Altering active site loop dynamics enhances standalone activity of tryptophan synthase alpha-subunit", *ACS Catal.* **14** (2024), pp. 16986–16995.

[80] M. Schupfner, F. Busch, V. H. Wysocki and R. Sterner, "Generation of a stand-alone tryptophan synthase α-subunit by mimicking an evolutionary blueprint", *ChemBioChem* **20** (2019), pp. 2747–2751.

[81] V. Kulik, E. Hartmann, M. Weyand, M. Frey, A. Gierl, D. Niks, M. F. Dunn and I. Schlichting, "On the structural basis of the catalytic mechanism and the regulation of the alpha subunit of tryptophan synthase from Salmonella typhimurium and BX1 from maize, Two evolutionarily related enzymes", *J. Mol. Biol.* **352** (2005), pp. 608–620.

[82] G. Casadevall, C. Pierce, B. Guan, et al., "Designing efficient enzymes: eight predicted mutations convert a hydroxynitrile lyase into an efficient esterase", preprint, bioRxiv, 2023, 2023.2008.2023.554512.

ACADÉMIE
DES SCIENCES
INSTITUT DE FRANCE

Review article

# Screen-printed carbon electrodes as a tool for the discovery and the characterization of new enzymes active on lignocellulosic biomass

**Marjorie Ochs** [ORCID],*,[a] **and Bastien Doumèche** [ORCID],[a]

[a] Institut de Chimie et Biochimie Moléculaires et Supramoléculaires, ICBMS UMR 5246 CNRS, Université de Lyon, Université Lyon 1, CNRS, INSA Lyon, CPE Lyon, 1 rue Victor Grignard, 69622 Villeurbanne Cedex, France

*E-mail:* marjorie.ochs@univ-lyon1.fr (M. Ochs)

**Abstract.** The development of efficient biocatalysts requires the detection and quantification of proven enzymatic activities on natural substrates. Electrochemical methods are particularly suitable for monitoring redox enzymatic activities when the substrates or products are electroactive species. These methods also have the advantage of being fast, sensitive and suited to heterogeneous environments. In this context, screen-printed carbon electrodes are particularly interesting because of their flexibility and low cost.

This article outlines the potential of screen-printed electrodes in the identification and characterization of new enzymes involved in the depolymerization of lignocellulosic biomass. The first part describes the interest and the fabrication of screen-printed carbon electrodes (SPCEs), with particular emphasis on the use of paper as a support for screen printing. The following sections describe examples of applications of screen-printed electrodes for the detection of small aromatic compounds and for screening peroxidase activities, in particular their use for the characterization of a catalase peroxidase. Finally, the article opens the way for the use of paper-based SPCEs to develop a biomimetic plant cell wall, that can be applied for the detection of lytic polysaccharide monooxygenases (LPMO) and ligninase activities.

**Keywords.** Screen-printed carbon electrodes, Paper-based electrodes, Ligninase, Lytic polysaccharide monooxygenase, Oxidase, Detection of aromatic and hydroxycinnamic compounds.

**Note.** This article is written at the invitation of the editorial committee.

*Manuscript received 23 November 2024, revised 17 March 2025, accepted 20 May 2025.*

## 1. Introduction

Lignocellulosic biomass (LCB), the main component of the plant cell wall, is obtained from plant biomass like wood, herbaceous plants, coproducts and wastes from agro-industries. LCB appears to be the best promising alternative to fossil carbon due to its sustainability and abundance on Earth. Lignocellulosic biomass is rich in cellulose, a polymer composed of linear glucose chains; hemicelluloses, branched heteropolymers composed of hexoses and pentoses; and lignin, an amorphous polymer composed of three structural units, H (*p*-hydroxyphenyl), G (guaiacyl), and S (syringyl), resulting from the condensation of three phenylpropane monomers: coumaryl, coniferyl, and sinapyl alcohols [1]. The composition and amounts of polysaccharides and lignins greatly vary between different plant species, yielding heterogeneous structures of the LCB. Until now, polysaccharides have been the main fraction of interest in biomass biorefinery processes while lignin valorization needs further research efforts. Specific

---

*Corresponding author

and selective fractionation of LCB, including lignin and derivatives, would enable these compounds to be used in a rational and sustainable way. Enzymatic fractionation makes it possible, by catalyzing specific bond cleavage under mild and low-energy reaction conditions. In Nature, the enzymatic depolymerization of LCB is efficiently carried out by bacteria, white- and brown-rot fungi that decompose wood [2–4].

However, to date, no biotechnological system has been shown to be sufficiently efficient to allow their use at industrial scale. The low efficiency and stability of the biocatalysts used is the main limitation of lignin valorization. Thus, the identification of efficient and stable ligninolytic enzymes still presents a technological challenge. Ligninolytic enzymes are oxidoreductases and include mainly laccases, peroxidases (versatile peroxidases (VP), dye decolorizing peroxidases (DyP), lignin peroxidases (LiP) and manganese peroxidases (MnP)) [5–7]. Furthermore, the enzymatic fractionation and upgrade of LCB and lignins is improved by the action of auxiliary enzymes operating in synergy with the cellulolytic, hemicellulolytic and ligninolytic enzymes. Among them, oxidases generate hydrogen peroxide, oxygenases convert dioxygen or hydrogen peroxide into water, and reductases as well as dehydrogenases reduce radicals.

Oxidoreductases involved in lignin degradation are usually identified and characterized by methods based on the light absorption properties of lignin-like monomers like guaiacol, pyrogallol, sinapic acid, synthetic dimers models like guaiacyl glycerol-$\beta$-guaiacyl ether (GGE), veratryl glycerol-$\beta$-guaiacyl ether (VGE) or other synthetic redox substrates like syringaldazine or azino-bis(3-ethylbenzothiazoline-6-sulfonic acid) (ABTS) [3,8–11]. These methods require clear and uniform media to perform accurate enzyme activity measurements. As a result, the activities monitored by these methods do not account for the enzyme interactions with water-insoluble lignin polymers. Furthermore, evaluating the impact of enzymes on polymeric lignin substrates requires analytical methods like liquid or gas chromatography combined with mass spectrometry, nuclear magnetic resonance [9,10,12]. The challenging evaluation of ligninolytic activities and their effect on native and technical lignins prevents the discovery of new efficient ligninolytic enzymes.

Electrochemical methods are particularly adapted to monitor redox enzymatic activities when substrates or products are electroactive species. They also show the advantages of being rapid, sensitive, adapted to heterogeneous media and do not require expensive apparatus. Species to be measured could be oxidized or reduced at the electrode resulting in current densities representative of their concentration. Consequently, electrochemical methods have the potential to circumvent the current lack of convenient methods for the characterization of ligninolytic and auxiliary enzymes active on polymers.

Among all electrode configurations, screen-printed electrodes (SPEs) are of particular interest due to their flexibility and low cost. This article outlines the potential of SPEs in identifying and characterizing novel enzymes involved in the depolymerization of lignocellulosic biomass. Firstly, the choice of screen-printed carbon electrodes (SPCEs) and paper-based electrodes is presented; secondly, an example of the application of SPCEs for the detection of small aromatic compounds and for the screening of peroxidase activities is outlined. Thirdly, the use of paper-based electrodes for the detection of LMPO activity, classified as an auxiliary activity in the carbohydrate active enzymes (CAZy) database (http://www.cazy.org/) [13], is demonstrated. Finally, the use of paper-based SPEs as a biomimetic substrate for the detection of depolymerizing ligninase activity will be presented.

## 2. Screen-printed electrodes and paper-based electrodes

In analytical sciences, electrochemical detection is commonly used because it could be conducted in nearly all media (organic or aqueous media). This detection is not influenced by media transparency compared to optical methods (UV–vis spectroscopy, fluorescence) and the number of configurations is nearly infinite from a classical three-electrode system (work, reference, counter electrodes) in mL reactors to microelectrodes for in vivo sensing. In the field of biosensors, SPEs are usually preferred because of their commercial availability, because they are single-use, a requirement for diagnosis and because the geometry of the electrode or its composition (gold, silver, carbon) could be easily adapted to the need [14,15]. Moreover, screen printing is a mature
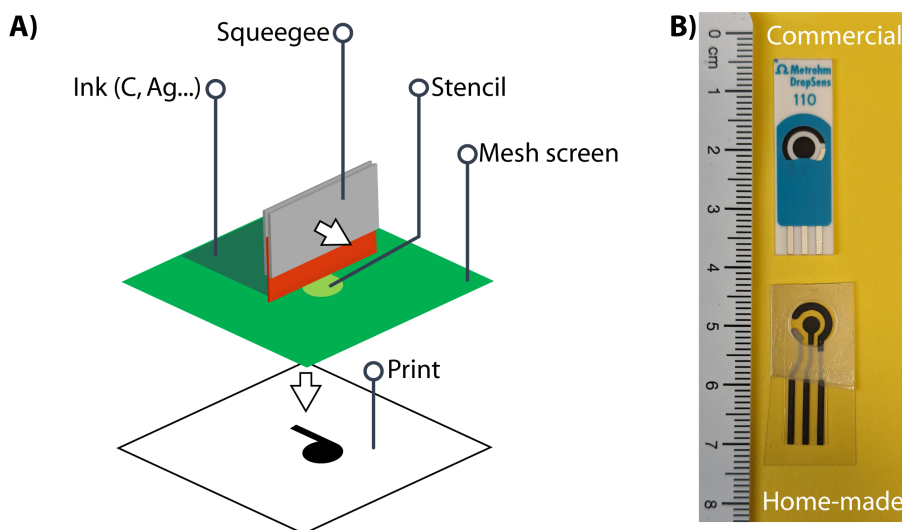
**Figure 1.** (A) Scheme illustrating the principle of screen printing and (B) commercial and home-made screen-printed electrodes.

technology allowing mass production. The principle of screen printing is rather simple (Figure 1): a stencil is prepared by photolithography to obtain the electrode motif (permeable) on a mesh screen (impermeable). The substrate on which the electrodes are to be printed is plated below the mesh screen. The substrate could be plastic, paper, ceramics, printed-circuit board (PCB), fabric, or any material that could be obtained in a two-dimensional format. The electrode material provided as an ink or paste is applied on the top of the mesh screen and forced to pass through the stencil by a squeegee. The stencil-shaped ink is recovered on the substrate that is further cured at medium-to-high temperature to obtain a solid electrode. The inks and pastes are composed of the electrode's conductive material (graphite particle, gold, silver, indium thin oxide) and a polymeric binder that ensure the stability of the electrode after curing, both dissolved in a solvent that evaporates during curing. The inks could also be doped with electrochemical mediators or nanomaterials, the most common being Prussian blue particles, carbon nanotubes, and gold nanoparticles.

Since the key publication of Whitesides et al. in 2007 with paper [16], cellulosic material has been proposed as a substrate for SPEs. Since then, several reviews on the subject have been published [17–19]. The advantages of using paper, particularly absorbing paper such as Whatman #1 are nu-

merous: (1) it is truly disposable by incineration whereas plastic is not, (2) paper and cellulosic material could be produced everywhere in the world at low cost, (3) paper technology is one of the most ancient in the world with numerous types of paper available, (4) the printing (or drawing) technologies on paper are also mature including inkjet, laser, and wax printing among others, (5) it is biocompatible and biodegradable (without considering the electrode material) and (6) the porosity of paper allows to design hydrophilic microfluidic channels together with the chromatographic (separation) properties of the cellulosic material. Whatman #1 paper for instance should be seen as a tridimensional porous material with interconnected cellulose microfibrils suitable for chemical modification close to the electrode but far enough to prevent passivation.

## 3. Application of SPCEs for the detection of small aromatic compounds and screening of peroxidase activities

### 3.1. *SPCEs used for the detection of aromatic and phenylpropanoid compounds*

Screen-printed electrodes (SPEs) are widely used for analytical purposes. Commercial electrodes offer the advantage of regular shapes, composition, and are ready to use, while home-made SPEs allow
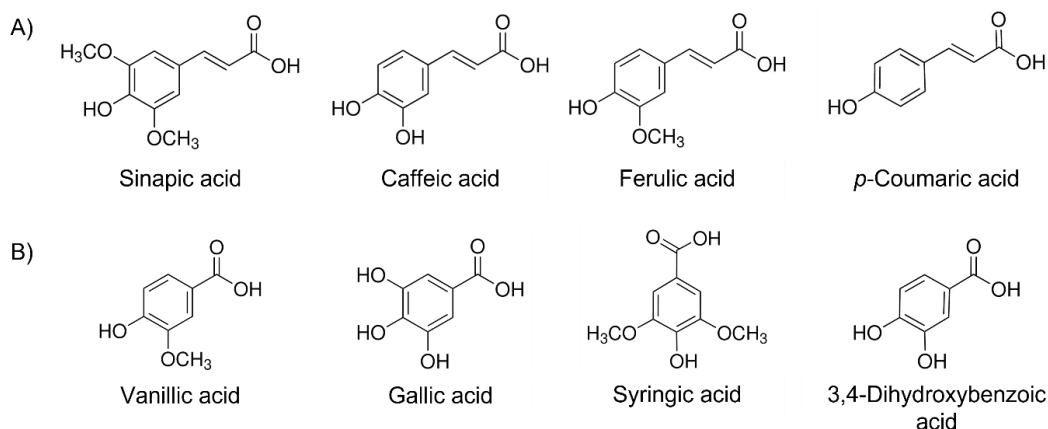
**Figure 2.** Structures of some (A) hydoxycinnamic acids and (B) hydroxyphenolic acids.

customizations, such as designing the shape of the electrodes, choosing the material substrate for the screen-printing, or adapting the composition of the inks. One of the common modifications of SPCEs is the functionalization of the carbon working electrode in order to form nanostructures at the electrode surface. For example, SPCEs modified by deposition of thin layers containing bismuth, gold, silver, multi-walled carbon nanotubes (MWCNs) or carbon nanofibers (CNFs) are used for the detection and the quantification of heavy metals in water, beverages, food, and biologic samples [20]. Metabolites (e.g., glucose, ascorbic acid, uric acid), drugs (furaltadone, dopamine methotrexate, erythromycin metronidazole, estrogens), phenolic and polyphenolic compounds (bisphenol A, caffeic acid, tannins, catechins, flavonoids, etc.) are also usually detected by using layered SPEs [21]. These modifications are known to increase sensitivity, enabling lower detection thresholds and broader detection ranges.

Hydroxycinnamic acids (Figure 2A) and hydroxyphenolic acids (Figure 2B) are small aromatic and electroactive compounds, allowing their detection by electrochemical methods. Caffeic acid is the most frequently analyzed hydroxycinnamic acid due to its favorable electrochemical response and its prevalence as a common antioxidant in food and beverages. Its detection and quantification can be achieved through the use of SPCEs, with or without electrode modifications, including the deposition of CNFs or MWCNs. Additionally, SPCEs can be modified with several other materials, including catechin (CT) decorated with gold nanoparticles (AuNP-CT)

or tungsten disulfide supported by carbon black (SPE-CB-WS2/CT), cobalt(II,III) or cerium(IV) oxides nanoparticles ($Co_3O_4$/SPCE; $CeO_2$ NPs), Graphene Oxide (GO), and reduced Graphene Oxide (rGO) itself decorated with gold (Au@rGO) [22–28]. These modifications enhance the quantification of hydroxycinnamic acids (Table 1). The linear range for the detection of hydroxycinnamic acids, using non-functionalized SPCEs, is comprised between 0.42 and 13.9 µM for caffeic acid between 26 and 515 µM for ferulic acid [29,30]. Functionalization of the working electrode allows broadening the linear range and quantifying higher concentrations, up to 2 mM and 1 mM for caffeic and ferulic acids, respectively [23,28]. Moreover, the modification of the carbon electrode decreases the oxidation potential, compared to non-modified carbon electrodes, improving the specificity of the electrode. This allows the detection and quantification of caffeic acid in a mixture containing ferulic and gallic acids, or sinapic, p-coumaric acids, present in red wine, rapeseed oil, or phyto-homeopathic tablets [22–24].

Additionally, caffeic acid oxidation leads to the formation of electroactive dimers and contributes to the modification of the electrode surface. Furthermore, caffeic acid can also react with other electroactive compounds through its quinine equivalent [31].

## 3.2. *Application of SPCEs to the screening of peroxidase substrates*

In a recent work, the electrochemical properties of hydroxycinnamic and hydroxybenzoic acids are used

**Table 1.** Electrochemical detection of hydroxycinnamic acids and gallic acid using SPCEs.

| Compound | Method | Electrode modifications[1] | pH | Linear range (μM) | Ref. |
|---|---|---|---|---|---|
| | CV | None (Dropsens 110) | <2 | 0.4–13.9 | [29] |
| | CV | CNF (Dropsens 110) | | 0.8–1000 | [22] |
| | CV | Au@rGO (EcoBioServices) | 7 | 0.5–100 | [25] |
| | CV | rGO (EcoBioServices) | 7 | 0.5–100 | [25] |
| Caffeic acid | CV | MWCNT (homemade SPEs) | <2 | 2.0–50 | [26] |
| | CV | $CeO_2$ NPs (Dropsens 110) | 7.4 | 50–200 | [24] |
| | DPV | $Co_3O_4$ (-) | 7 | 0.2–272 | [27] |
| | DPV | rGO (-) | 7 | 0.2–2100 | [28] |
| | DPV | CB-WS$_2$/AuNP-CT (EcoBioServices) | 7 | 0.4–112.5 | [23] |
| Ferulic acid | CV | None (paperbased homemade SPCE) | 5 | 26–515 | [30] |
| | CV | CNF (Dropsens 110) | | 0.8–1000 | [22] |
| Sinapic acid | DPV | CB-WS2/AuNP-CT (EcoBioServices) | 7 | 0.7–125.0 | [23] |
| *p*-Coumaric acid | DPV | CB-WS2/AuNP-CT (EcoBioServices) | 7 | 1.4–93.7 | [23] |
| Gallic acid | CV | $CeO_2$ NPs (Dropsens 110) | 7.4 | 2–20 | [24] |

CV: cyclic voltammetry; DPV: differential pulsed voltammetry; CNF: carbon nanofibers; rGO: reduced graphene oxide; MWCNT: multi-walled carbon nanotubes; $CeO_2$ NPs: cerium oxide nanoparticles; $Co_3O_4$: cobalt oxide; CB-WS$_2$/AuNP-CT: tungsten disulfide supported by carbon black/catechin decorated with gold nanoparticles. [1]Commercial or homemade SPCEs are indicated.

to develop the first electrochemical screening assay for the detection of ligninase activity [32]. The assay is applied to identify small phenolic molecules derived from lignin as substrates of a newly discovered bifunctional bacterial catalase–peroxidase. Peroxidase activity consists in the oxidation of a substrate in the presence of $H_2O_2$ as electron acceptors. Peroxidases are often expressed by microorganisms when they are fed with lignin-rich substrates. Furthermore, hydroxycinnamic and hydroxybenzoic acids have been identified as peroxidase substrates, which suggests that these activities contribute to the depolymerization of lignin. Additionally, it has been reported that catalase–peroxidases assist the main lignin-degrading enzymes and further oxidize dimers or monomers after the depolymerization of the lignin macromolecule [4].

The strategy of the screening assay developed in this study is based on the use of lignin-derived aromatic substrates as electron donors. The potential of hydroxycinnamic and hydroxyphenolic acids, including 3,4-dihydroxybenzoic, sinapic, vanillic, syringic, *o*-coumaric, caffeic, and *p*-coumaric acids as substrates is investigated. These acids are selected

based on their proven ability to generate anodic current at +800 mV vs Ag|AgCl. The oxidation of these aromatics substrates by the enzyme was monitored by intermittent pulsed amperometry (IPA) on 96-SPCE plates (Figure 3). An oxidation overpotential of +800 mV vs Ag|AgCl is applied to detect electroactive species and to quantify the substrate depletion after 4 h incubation in the presence of the enzyme. The results obtained by the electrochemical method are consistent with those obtained by spectrophotometric methods using azino-bis(3-ethylbenzothiazoline-6-sulfonic acid) (ABTS) and $Mn^{2+}$ as the positive controls and veratryl alcohol as the negative one.

The results show that the electrochemical SPCE-based screening is applicable to detect the peroxidase activity. It also evidences that the catalase–peroxidase from the bacteria *Thermobacillus xylanilyticus* is able to oxidize 3,4-dihydroxybenzoic (3,4-DHB), sinapic, vanillic, syringic, *o*-coumaric, caffeic, and *p*-coumaric acids, whose current densities differ significantly (>10%) in the presence of enzyme, compared to the standard reaction without enzyme (Table 2).

**Table 2.** Monomers oxidized by the catalase–peroxidase from Thermobacillus xylanilyticus ($Tx$CP) and screened by intermittent pulsed amperometry (adapted from [32]).

| Compound | Current density (μA·cm$^{-2}$) | | Variation (%) of the current density |
|---|---|---|---|
| | Without $Tx$CP | With $Tx$CP | |
| Caffeic acid | $417 \pm 18$ | $620 \pm 103$ | 49 |
| 3,4-DHB acid | $498 \pm 62$ | $348 \pm 52$ | 30 |
| Vanillic acid | $90 \pm 7$ | $51 \pm 5$ | 44 |
| Ferulic acid | $50 \pm 7$ | $62 \pm 9$ | 23 |
| Syringic acid | $42 \pm 5$ | $24 \pm 4$ | 42 |
| Sinapic acid | $331 \pm 40$ | $168 \pm 22$ | 49 |
| $o$-coumaric | $68 \pm 9$ | $28 \pm 7$ | 59 |
| $p$-coumaric | $61 \pm 2$ | $101 \pm 16$ | 65 |
| MnCl$_2$ | $455 \pm 27$ | $321 \pm 19$ | 30 |
| ABTS | $289 \pm 48$ | $205 \pm 15$ | 29 |
| Veratryl alcohol | $22 \pm 4$ | $20 \pm 1$ | <10 (non significant) |
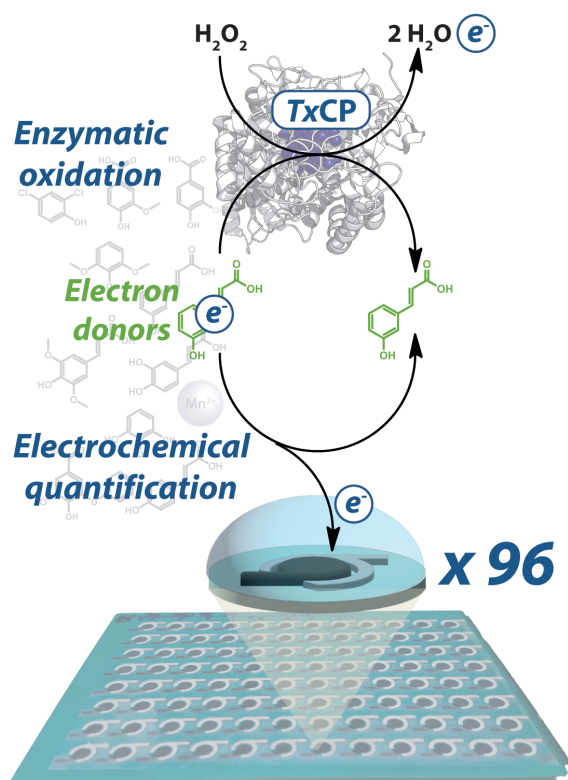


**Figure 3.** Strategy applied for the screening of small lignin-derived compounds as substrates of a catalase–peroxidase ($Tx$CP) using SPCEs (adapted from [32]).

## 4. Paper-based SPCEs applied to the measurement of LPMO activities

### 4.1. *Consumption of ascorbic acid by LPMO activity monitored by electrochemical methods*

Lytic polysaccharide monooxygenases (LPMO, EC 1.14.99.53-56) are copper-dependent oxidative enzymes catalyzing the depolymerization of polysaccharides or oligosaccharides in the presence of an oxidant and an electron donor. The oxidation of C1 and/or C4 carbon of the glycosidic backbone, causing the cleavage of the glycosidic bonds, results from a monooxygenase activity in the presence of oxygen or from a peroxygenase activity in the presence of hydrogen peroxide (Equations (1) and (2), respectively) [33–36]. In the absence of a glycosidic substrate, an oxidase activity is also observed (Equation (3)) [37].
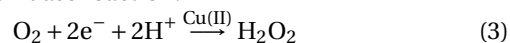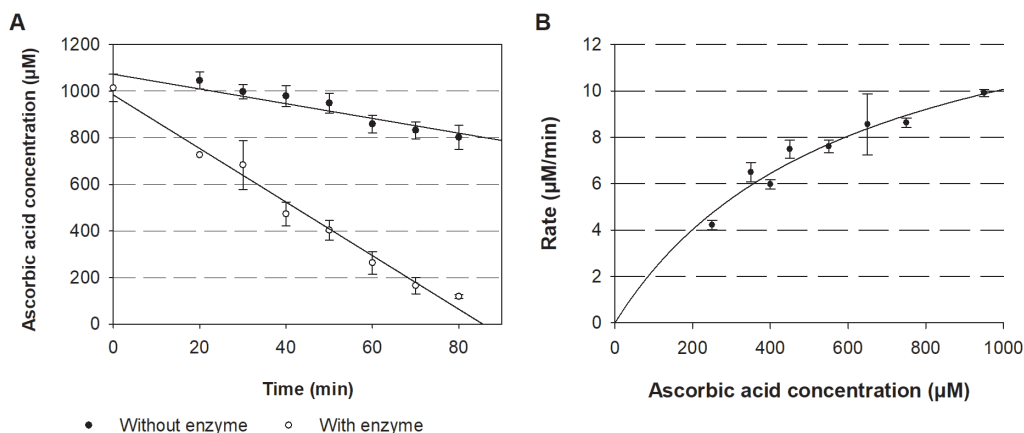
Monooxygenase reaction:

$$R–H + O_2 + 2e^- + 2H^+ \xrightarrow{\text{Cu(II)}} R–OH + H_2O \quad (1)$$

Peroxygenase reaction:

$$R–H + H_2O_2 \xrightarrow{\text{Cu(I)}} R–OH + H_2O \quad (2)$$

Oxidase reaction:

$$O_2 + 2e^- + 2H^+ \xrightarrow{\text{Cu(II)}} H_2O_2 \quad (3)$$
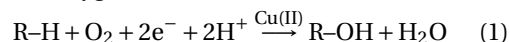
As LPMOs are three-substrate enzymes (oxidant, electron donor, and glycosidic substrate), the measurement of their activity is delicate. Most of
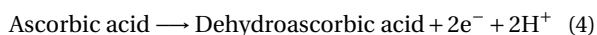
**Figure 4.** (A) Kinetics of ascorbic acid consumption and (B) Michaelis–Menten plots corresponding to ascorbic acid consumption rates by *Nc*LPMO9C. Reactions are performed in the presence of 1 µM *Nc*LPMO9C, ascorbic acid (1 mM for (A), 250–1000 µM for (B)), microcrystalline cellulose 1% (w/v) in sodium phosphate buffer (20 mM, pH 6) incubated at 45 °C ($n \geq 3$).

the published studies focus on the quantification and identification of some short-length oligosaccharide products using liquid chromatography and/or mass spectrometry [38–45]. Recently, a method was developed to measure the peroxygenase activity using a rotating disc electrode selective to hydrogen peroxide through the presence of Prussian blue as the electrocatalyst [46]. This method is adapted to fundamental studies of the enzymatic reaction, but is less adapted to screen applicative conditions in complex media.

As explained in 1 and 2, SPCEs are adapted to the needs of high-throughput screening. In this context, we developed an electrochemical method to measure the initial rates of the oxygenase reaction (equally monooxygenase and peroxygenase reactions) catalyzed by LPMOs. The method is based on the direct detection by IPA of the remaining electron donor, without further chemical derivation or separation steps. Ascorbic acid (1 mM) is used as the electron donor (Equation (4)) in reactions containing a suspension of microcrystalline cellulose 1% (w/v) and LPMO9C isolated from *Neurospora crassa* (*Nc*LPMO9C). The reactions are performed in test tubes at 45 °C, with regular sampling. The remaining ascorbic acid is quantified at +0.6 V vs Ag|AgCl by IPA onto SPCEs.

Detection of ascorbic acid:

$$\text{Ascorbic acid} \longrightarrow \text{Dehydroascorbic acid} + 2e^- + 2H^+ \quad (4)$$

The consumption of ascorbic acid by LPMOs was linear over at least 70 min (Figure 4A). The decrease of the signal, due to ascorbic acid oxidation at 45 °C, was less than 20% in 70 min. In the same time, around 80% of the ascorbic acid disappeared in the presence of LPMO, leading to a specific activity of 196 nmol·min$^{-1}$·mg$^{-1}$. Apparent kinetic constants for ascorbic acid with microcrystalline cellulose as co-substrate obtained from Michaelis–Menten plots are $K_{\text{m}}^{\text{App}} = 601 \pm 166$ µM and $k_{\text{cat}}^{\text{App}} = 16.1 \pm 2.3$ min$^{-1}$ (Figure 4B).

These results highlight that the direct measurement of ascorbic acid consumption by electrochemistry appears to be a suitable alternative to spectrophotometric methods for the measurement of oxygenase LPMO activities.

### 4.2. *Evaluation of filter paper instead of microcrystalline cellulose as substrate for the electrochemical detection of LPMO activity*

The interest in LPMO is increasing since it has been proposed that some are active on recalcitrant cellulose and, therefore could play a key role in the enzymatic deconstruction of lignocellulosic biomass. Indeed, these enzymes are supposed to reduce the crystallinity of cellulose and operate synergistically with glycoside hydrolases that are active on amorphous cellulose [39,47–49].

**Table 3.** Electrochemical characteristics of the electron donors measured using carbon screen-printed electrodes in acetate buffer (50 mM, pH 5).

| Electron donor | Oxidation potential (V vs Ag/AgCl) | Reduction potential (V vs Ag/AgCl) | Sensitivity at +0.8 V vs Ag/AgCl ($\mu A \cdot cm^{-2} \cdot \mu M^{-1}$) |
|---|---|---|---|
| Ascorbic acid | +0.46 | n.d. | 0.467[*] |
| Caffeic acid | +0.5 | 0 | 0.796 |
| 3,4-DHB acid | +0.65 | 0 | 0.498 |
| Syringic acid | +0.7 | n.d. | 0.243 |

[*]At +0.6 V vs Ag/AgCl for ascorbic acid; n.d.: not detected.

The three-substrates LPMO is ideal for the development of original screening methods for depolymerizing enzymatic activities including paper-based SPCE as substrate. Indeed, Whatman paper made of cellulose can constitute the polymeric substrate for the reaction. Paper-based electrodes present interesting properties that could be exploited for a screening method. In this context, we investigated the possibility of measuring LPMO activity using Whatman paper instead of microcrystalline cellulose as the substrate for *Nc*LPMO.

The rate of ascorbic acid consumption using 1% (w/v) of both cellulosic substrates was measured by IPA with different enzyme concentrations at 45 °C. No significant differences between Whatman paper and microcrystalline cellulose substrates were observed regarding ascorbic acid consumption rates ($15.7 \pm 2.2$ min$^{-1}$ and $18.6 \pm 3.5$ min$^{-1}$, respectively). This opens the way for paper-based SPCEs as a screening tool to detect LPMO activity.

## 4.3. *Screening of electron donor using SPCEs*

LPMOs, notably *Nc*LPMO9C, oxidize lignin-derived electroactive species obtained from biomass pretreatments [50]. However, due to the molecular complexity of the crude liquid lignin fraction obtained after lignocellulosic biomass pretreatment, structural analogs of lignin monomers are used instead of real samples. Therefore, *Nc*LPMO9C's ability to oxidize three putative electron donors (caffeic, 3,4-DHB, and syringic acids) was investigated. Cyclic voltammetry of these aromatic acids showed oxidation peaks between +0.46 and +0.7 V vs Ag|AgCl in sodium acetate buffer (50 mM, pH 5) (Table 3). The reduction potential of caffeic acid

and 3,4-dihydroxybenzoic acid is +0 V vs Ag|AgCl, whereas the oxidation of syringic acid is irreversible. In order to quantify simultaneously the remaining substrate after 2 h of enzymatic reaction, an overpotential of +0.8 V vs Ag|AgCl was applied on the SPCE.

In the absence of *Nc*LPMO9C, the current density did not evolve after 2 h at 45 °C for caffeic and 3,4-DHB acids (946 $\mu A \cdot cm^{-2}$ and 539 $\mu A \cdot cm^{-2}$, respectively) while it strongly decreased from 390 $\mu A \cdot cm^{-2}$ to 82 $\mu A \cdot cm^{-2}$ for syringic acid, meaning it is unstable in these conditions. The sensitivities were also different for the electron donors (0.243 $\mu A \cdot cm^{-2} \cdot \mu M^{-1}$ for syringic acid, 0.498 $\mu A \cdot cm^{-2} \cdot \mu M^{-1}$ for 3,4-dihydroxybenzoic acid, and 0.796 $\mu A \cdot cm^{-2} \cdot \mu M^{-1}$ for caffeic acid) (Table 3).

When *Nc*LPMO9C (1 $\mu$M) was incubated with ascorbic acid and Whatman paper (1% w/v) for 2 h, the current density was in the background showing the full conversion of ascorbic acid. When caffeic, 3,4-DHB or syringic acids were used as substrates, the current densities decreased by 60, 56 and 54%, respectively (Figure 5), confirming that these compounds are electron donors for *Nc*LPMO9C. This also suggests some guidelines regarding the redox potential of the electron donor, as it appears that species having an oxidation potential up to +0.7 V vs Ag|AgCl could supply electrons to *Nc*LPMO9C. The role of these compounds as electron donor for LPMOs was also recently shown by following the apparition of oxidized oligosaccharide using HPLC [40]. While this transformation requires a 20-hour incubation followed by HPLC analysis, only two hours are necessary with our electrochemical method to identify electron donors as well as to estimate the enzymatic conversion rate (5 $\mu M \cdot min^{-1}$).
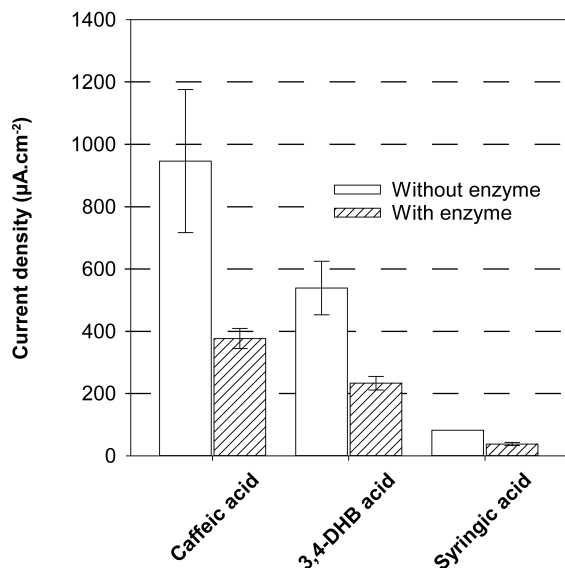
**Figure 5.** Activity of *Nc*LPMO9C 1 μM using several electron donors: caffeic acid, 3,4-dihydroxybenzoic acid, and syringic acid. Reactions are performed with Whatman paper as cellulosic substrate 1% (w/v), electron donor 1 mM and incubation for 2 h at 45 °C. Current density is measured by intermittent pulsed amperometry at a fixed potential of +0.8 V vs Ag|AgCl.

Using IPA, up to 96 independent samples could be measured at a time using a given potential in 1 min [51–53]. The thermolability of some electron donors is pointed out, but in this work, all reactions were performed at 45 °C (optimal temperature of LPMOs). However, as the duration of analysis is short and the sensitivity of the method is high, the reactions could also be performed at room temperature. This enables rapidly identification of the electron donor and carbohydrate substrate for one or more LPMOs, as well as acquisition of kinetic parameters.

### 4.4. *Important remarks*

Studying and measuring LPMO activities is challenging because three substrates are involved and because several mechanisms are proposed. The methods currently applied to monitor the reaction are based on the quantification of the glycosidic products after hours of incubation, which is time-consuming and not representative of the early stage of the reaction. In this work, we present the development of a general electrochemical method based on monitoring electron donor consumption by LPMOs, with reduced analysis time for fast characterization of LPMO oxygenase activity.

The reaction rates of *Nc*LPMO9C were determined as well as apparent Michaelis–Menten constant for ascorbic acid in less than 1 h. The values obtained are in agreement with published ones. Activities were equivalent, either using the cellulosic substrate (microcrystalline cellulose) or Whatman paper, confirming the possibility of using paper-based SPCEs directly as substrate. Therefore, this electrochemical method is found to be suitable to identify electron donors for LPMOs. This is a proof-of-concept highlighting that electrochemical electron donor detection can be used for fast monitoring of LPMO oxygenase activity using natural substrates, i.e., without the use of chromophores or fluorophores. Moreover, the possibility of acquiring a large amount of data using IPA together with 96 SPEs open the way to electrochemical high-throughput screening assays for LPMOs.

### 5. Paper-based SPCE as a biomimetic substrate for the detection of lignin depolymerizing enzymes

Lignin, a hydrophobic and amorphous heteropolymer, mainly composed of phenyl propanoid units, is one of the three polymers (with cellulose and hemicellulose) composing the secondary plant cell wall and the lignocellulosic biomass. As lignin constitutes up to 40% of the plant cell wall, it is considered to be the most abundant biobased source of aromatic compounds such as vanillin, syringaldehyde, acetovanillone, ferulic acid or vinyl guaiacol [4,55].

The conversion of lignin into smaller aromatic molecules of interest is challenging owing to its structural heterogeneity. Enzymatic depolymerization of lignin is a promising approach [56]. However, the characterization of new ligninolytic enzymes is challenging due to the lack of relevant methods. Electrochemical measurements are ideal for measuring redox reactions. This non-optical method can measure different substances in a few minutes, meaning that electrochemical methods may be useful to measure ligninolytic processes more easily. In recent years,
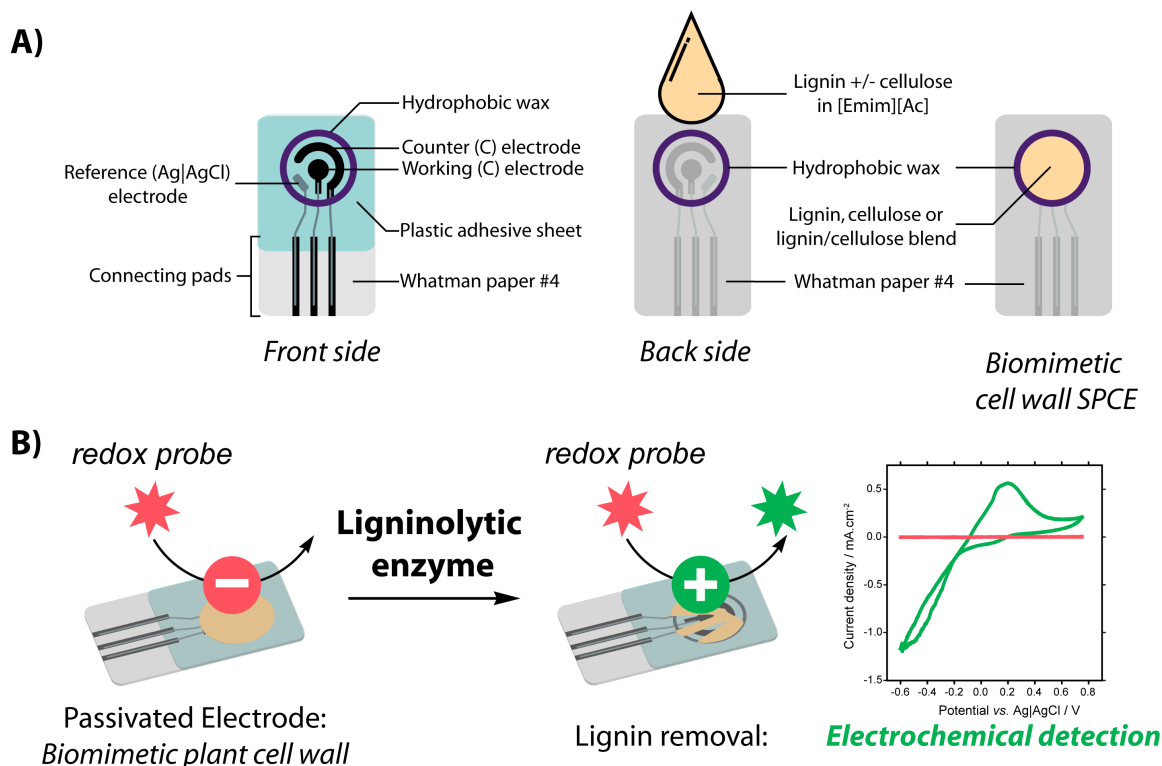
**Figure 6.** (A) Scheme of the biomimetic SPCE configuration and preparation: First a wax circle is printed on filter paper (diameter = 6 mm); secondly, on the front side, carbon and Ag|AgCl inks are screenprinted. Then, lignin (blended with cellulose) is deposited on the back side of the paper electrode. (B) Detection of ligninase activity is made possible by recovering the signal corresponding to a redox probe by cyclic voltammetry after action of the enzyme (green line) (adapted from [54]).

paper-based electrodes have emerged as tools in the field of bioelectrochemistry. This is due to a number of factors, including their ease of use, biodegradability, and straightforward fabrication [17,57,58]. In a recent work, we described the development of a new methodology using paper-based SPCEs to characterize the activities of ligninolytic enzymes [54].

The strategy relies on the preparation of an integrated substrate/detection system composed of a "biomimetic" plant cell wall on the back side of a paper-based SPCE (Figure 6A). The polymeric substrate is formed by cellulosic material from Whatman paper and by lignin coated around the cellulose microfibrils after ionic liquid-assisted precipitation. Characterization of the substrate/electrode by profilometry and electronic microscopy showed that lignin is homogeneously deposited as nanoparticles around the cellulosic fibers (Figure 7A, B). These

nanoparticles are not only deposited at the surface but deeply penetrate into the paper, mimicking polymer organization in the plant cell wall where lignin acts as a matrix engulfing cellulose and hemicellulose. Electrochemical characterization of the substrate/electrode highlighted that, when deposited in sufficient amount, the coated lignin constitutes an electrical insulator, preventing access to the electrode by soluble compounds (e.g., a redox probe). Depolymerization of this biomimetic plant cell wall by the ligninolytic enzyme catalase–peroxidase from *Thermobacillus xylanilyticus* (*Tx*CP) is evidenced by the recovery of the $Fe(CN)_6^{3-/4-}$ redox signal by cyclic voltammetry (Figure 6B). Detection of the probe is correlated with physical modification of the fibers as observed by SEM. Indeed, aggregates coating the fibers are no more observed and fibers are strongly degraded after incubation with *Tx*CP (Figure 7C),
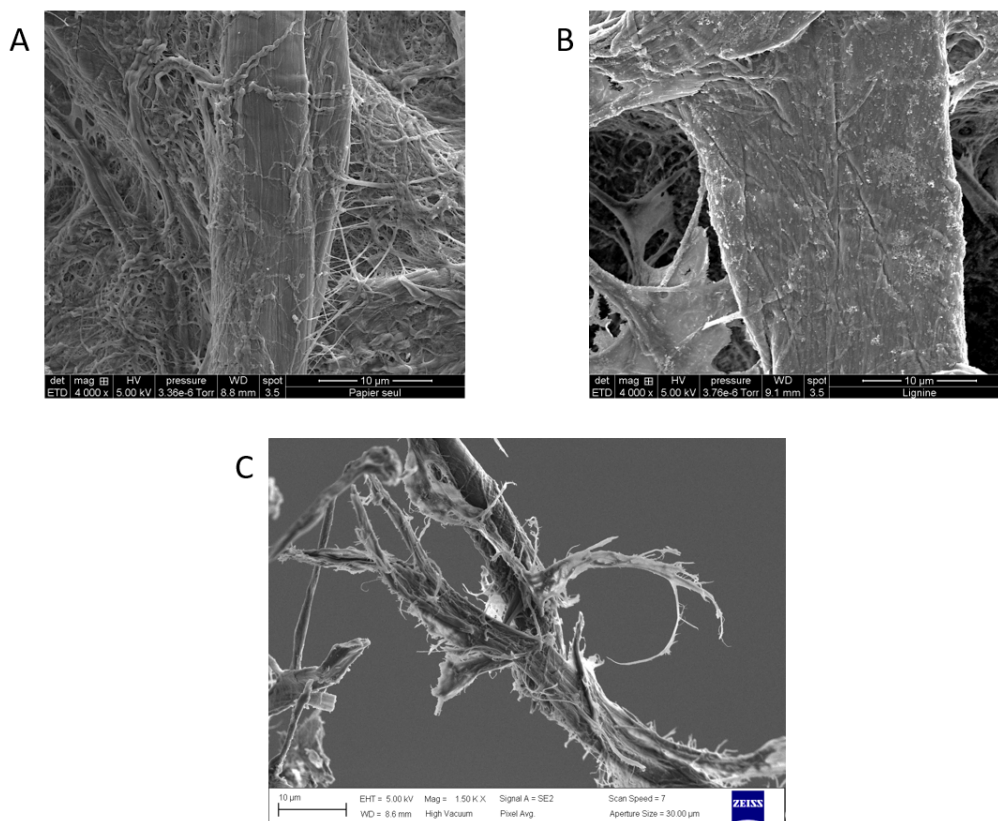
**Figure 7.** SEM analysis showing (A) cellulose fibers at the back side of bare paper-based electrodes, (B) biomimetic substrate-electrodes impregnated with lignin showing nanoparticles coating the cellulose fibers, (C) biomimetic substrate-electrodes impregnated with lignin after incubation with catalase–peroxidase, showing degraded cellulose fibers (adapted from [54]).

indicating that the insulating barrier formed by the coated lignin is weakened by the enzyme-catalyzed reaction.

These results highlight the interest of developing paper-based SPCEs to detect ligninolytic activity and could be used for rapid screening of efficient ligninolytic enzymes. This method could be further improved for the electrochemical detection of products during oxidative depolymerization of lignin. Such a strategy could help solve the technological challenge of rapidly identifying robust biocatalysts with ligninolytic activities.

## 6. Conclusion

The discovery of new enzymes active on plant wall polymers is a major challenge for the development of biochemical routes for the valorization of lignocellulosic biomass and co-products from agricultural activities. Electrochemical methods involving screen-printed carbon electrodes have shown their interest in detecting, characterizing and quantifying small compounds, and consequently in screening for enzymatic activities associated with these compounds. For example, the detection of small aromatic compounds, such as hydroxycinnamic and hydroxyphenolic acids, potentially derived from lignin depolymerization, enables the detection of peroxidase or lytic polysaccharide monooxygenase activities by cyclic voltammetry or intermittent pulsed amperometry. Modifying or functionalizing the electrodes could improve the detection of compounds of interest, thus refining the determination of the enzymatic activities. The use of paper as

support for screen-printed carbon electrodes adds another dimension for screening, in particular for cellulose-active enzymes such as lytic polysaccharide monooxygenases. In this configuration, a certain proximity between the enzyme, its cellulosic substrate and the electrode used for detection was achieved. This proximity can help to overcome substrate accessibility issues encountered in heterogeneous media. Paper-based electrodes allow exploiting the three-dimensional structure of paper to design biomimetic substrates of the plant wall, involving several types of interlocking polymers. Finally, the possibility of custom-designing the shape of the electrodes, and in particular of miniaturizing the systems, notably to work in 96-electrode format, opens the way to a wealth of potentialities in the context of high-throughput screening of enzymatic activity and reaction conditions.

## Declaration of interests

The authors do not work for, advise, own shares in, or receive funds from any organization that could benefit from this article, and have declared no affiliations other than their research organizations.

## Acknowledgements

## References

[1]  F. N. U. Asina, I. Brzonova, E. Kozliak, A. Kubátová and Y. Ji, "Microbial treatment of industrial lignin: Successes, problems and challenges", *Renew. Sustain. Energy Rev.* **77** (2017), pp. 1179–1205.

[2]  N. Kamimura, K. Takahashi, K. Mori, T. Araki, M. Fujita, Y. Higuchi and E. Masai, "Bacterial catabolism of lignin-derived aromatics: new findings in a recent decade: update on bacterial lignin catabolism", *Environ. Microbiol. Rep.* **9** (2017), pp. 679–705.

[3]  R. S. Granja-Travez, R. C. Wilkinson, G. F. Persinoti, F. M. Squina, V. Fülöp and T. D. H. Bugg, "Structural and functional characterisation of multi-copper oxidase CueO from lignin-degrading bacterium Ochrobactrum sp. reveal its activity towards lignin model compounds and lignosulfonate", *FEBS J.* **285** (2018), pp. 1684–1700.

[4]  P. S. Chauhan, "Role of various bacterial enzymes in complete depolymerization of lignin: a review", *Biocatal. Agric. Biotechnol.* **23** (2020), article no. 101498.

[5]  C. Crestini, F. Melone and R. Saladino, "Novel multienzyme oxidative biocatalyst for lignin bioprocessing", *Bioorg. Med. Chem.* **19** (2011), pp. 5071–5078.

[6]  N. Kamimura, S. Sakamoto, N. Mitsuda, E. Masai and S. Kajita, "Advances in microbial lignin degradation and its applications", *Curr. Opin. Biotechnol.* **56** (2019), pp. 179–186.

[7]  B. Tsegaye, C. Balomajumder and P. Roy, "Microbial delignification and hydrolysis of lignocellulosic biomass to enhance biofuel production: an overview and future prospect", *Bull. Natl. Res. Cent.* **43** (2019), pp. 1–16.

[8]  M. Ahmad, J. N. Roberts, E. M. Hardiman, R. Singh, L. D. Eltis and T. D. H. Bugg, "Identification of DypB from *Rhodococcus jostii* RHA1 as a lignin peroxidase", *Biochemistry* **50** (2011), pp. 5096–5107.

[9]  E. Liu, F. Segato, R. A. Prade and M. R. Wilkins, "Exploring lignin depolymerization by a bi-enzyme system containing aryl alcohol oxidase and lignin peroxidase in aqueous biocompatible ionic liquids", *Bioresour. Technol.* **338** (2021), article no. 125564.

[10]  D. J. Levy-Booth, L. E. Navas, M. M. Fetherolf, L. Y. Liu, T. Dalhuisen, S. Renneckar, L. D. Eltis and W. W. Mohn, "Discovery of lignin-transforming bacteria and enzymes in thermophilic environments using stable isotope probing", *ISME J.* **16** (2022), pp. 1–13.

[11]  D. Tavares, A. C. Sousa and M. P. Robalo, "Engineering a bacterial DyP-type peroxidase for enhanced oxidation of lignin-related phenolics at alkaline pH", *ACS Catal.* **7** (2017), pp. 3454–3465.

[12]  J. Dillies, C. Vivien, M. Chevalier, A. Rulence, G. Châtaigné, C. Flahaut, V. Senez and R. Froidevaux, "Enzymatic depolymerization of industrial lignins by laccase-mediator systems in 1,4-dioxane/water", *Biotechnol. Appl. Biochem.* **67** (2020), pp. 774–782.

[13]  E. Drula, M.-L. Garron, S. Dogan, V. Lombard, B. Henrissat and N. Terrapon, "The carbohydrate-active enzyme database: functions and literature", *Nucleic Acids Res.* **50** (2022), pp. D571–D577.

[14]  R. D. Crapnell and C. E. Banks, "Electroanalytical overview: screen-printed electrochemical sensing platforms", *ChemElectroChem* **11** (2024), article no. e202400370.

[15]  C. E. Banks, C. W. Foster and R. O. Kadara, *Screen-Printing Electrochemical Architectures*, Springer: Cham, 2016.

[16]  A. W. Martinez, S. T. Phillips, M. J. Butte and G. M. Whitesides, "Patterned paper as a platform for inexpensive, low-volume, portable bioassays", *Angew. Chem. Int. Ed.* **46** (2007), pp. 1318–1320.

[17]  C. Desmet, C. A. Marquette, L. J. Blum and B. Doumèche, "Paper electrodes for bioelectrochemistry: Biosensors and biofuel cells", *Biosens. Bioelectron.* **76** (2016), pp. 145–163.

[18]  N. Colozza, V. Caratelli, D. Moscone and F. Arduini, "Origami paper-based electrochemical (bio)sensors: state of the art and perspective", *Biosensors* **11** (2021), article no. 328.

[19]  E. Noviana, C. P. Mccord, K. M. Clark, I. Jang and C. S. Henry, "Electrochemical paper-based devices: sensing approaches and progress toward practical applications", *Lab. Chip.* **20** (2019), pp. 9–34.

[20] A. Rubino and R. Queirós, "Electrochemical determination of heavy metal ions applying screen-printed electrodes based sensors. A review on water and environmental samples analysis", *Talanta Open.* **7** (2023), article no. 100203.

[21] A. Garcí-Miranda Ferrari, S. J. Rowley-Neale and C. E. Banks, "Screen-printed electrodes: transitioning the laboratory in-to-the field", *Talanta Open.* **3** (2021), article no. 100032.

[22] A. V. Bounegru and C. Apetrei, "Simultaneous determination of caffeic acid and ferulic acid using a carbon nanofiber-based screen-printed sensor", *Sensors* **22** (2022), article no. 4689.

[23] F. Della Pelle, D. Rojas, F. Silveri, G. Ferraro, E. Fratini, A. Scroccarello, A. Escarpa and D. Compagnone, "Class-selective voltammetric determination of hydroxycinnamic acids structural analogs using a WS2/catechin-capped AuNPs/carbon black–based nanocomposite sensor", *Microchim. Acta* **187** (2020), article no. 296.

[24] V. Andrei, E. Sharpe, A. Vasilescu and S. Andreescu, "A single use electrochemical sensor based on biomimetic nanoceria for the detection of wine antioxidants", *Talanta* **156–157** (2016), pp. 112–118.

[25] A. Scroccarello, R. A. Lvarez-Diduk, F. D. Pelle, C. De Carvalho Castro E Silva, A. Idili, C. Parolo, D. Compagnone and A. Merkoç, "One-step laser nanostructuration of reduced graphene oxide films embedding metal nanoparticles for sensing applications", *ACS Sens.* **14** (2024), pp. 598–609.

[26] D. A. G. Araújo, J. R. Camargo, L. A. Pradela-Filho, A. P. Lima, R. A. A. Muñoz, R. M. Takeuchi, B. C. Janegitz and A. L. Santos, "A lab-made screen-printed electrode as a platform to study the effect of the size and functionalization of carbon nanotubes on the voltammetric determination of caffeic acid", *Microchem. J.* **158** (2020), article no. 105297.

[27] S. Ramki, P. Balasubramanian, S. M. Chen, T. W. Chen, T. W. Tseng and B. S. Lou, "Voltammetric determination of caffeic acid using $Co_3O_4$ microballs modified screen printed carbon electrode", *Int. J. Electrochem. Sci.* **13** (2018), pp. 1241–1249.

[28] M. Velmurugan, P. Balasubramanian and S. M. Chen, "Determination of caffeic acid in wine samples based on the electrochemical reduction of graphene oxide modified screen printed carbon electrode", *Int. J. Electrochem. Sci.* **12** (2017), pp. 4173–4182.

[29] E. Fernández, L. Vidal and A. Canals, "Rapid determination of hydrophilic phenols in olive oil by vortex-assisted reversed-phase dispersive liquid-liquid microextraction and screen-printed carbon electrodes", *Talanta* **181** (2018), pp. 44–51.

[30] Y. Yao and C. Zhang, "A novel one-step fabricated, droplet-based electrochemical sensor for facile biochemical assays", *Sensors* **16** (2016), pp. 5–15.

[31] A. V. T. Le, Y. L. Su and S. H. Cheng, "A novel electrochemical assay for aspartame determination via nucleophilic reactions with caffeic acid ortho-quinone", *Electrochim. Acta* **300** (2019), pp. 67–76.

[32] I. Fall, Q. Czerwiec, S. Abdellaoui, B. Doumèche, M. Ochs, C. Rémond and H. Rakotoarivonina, "A thermostable bacterial catalase-peroxidase oxidizes phenolic compounds derived from lignins", *Appl. Microbiol. Biotechnol.* **107** (2023), pp. 201–217.

[33] B. Bissaro, Å. K. Røhr, G. Müller, et al., "Oxidative cleavage of polysaccharides by monocopper enzymes depends on $H_2O_2$", *Nat. Chem. Biol.* **13** (2017), pp. 1123–1128.

[34] S. Kuusk, B. Bissaro, P. Kuusk, Z. Forsberg, V. G. H. Eijsink, M. Sørlie and P. Väljamäe, "Kinetics of $H_2O_2$-driven degradation of chitin by a bacterial lytic polysaccharide monooxygenase", *J. Biol. Chem.* **293** (2018), pp. 523–531.

[35] P. H. Walton and G. J. Davies, "On the catalytic mechanisms of lytic polysaccharide monooxygenases", *Curr. Opin. Chem. Biol.* **31** (2016), pp. 195–207.

[36] T. Tandrup, K. E. H. Frandsen, K. S. Johansen, J.-G. Berrin and L. Lo Leggio, "Recent insights into lytic polysaccharide monooxygenases (LPMOs)", *Biochem. Soc. Trans.* **46** (2018), pp. 1431–1447.

[37] R. Kittl, D. Kracher, D. Burgstaller, D. Haltrich and R. Ludwig, "Production of four *Neurospora crassa* lytic polysaccharide monooxygenases in *Pichia pastoris* monitored by a fluorimetric assay", *Biotechnol. Biofuels,* **5** (2012), pp. 1–14.

[38] J. S. M. Loose, Z. Forsberg, D. Kracher, S. Scheiblbrandner, R. Ludwig, V. G. H. Eijsink and G. Vaaje-Kolstad, "Activation of bacterial lytic polysaccharide monooxygenases with cellobiose dehydrogenase", *Prot. Sci.* **25** (2016), pp. 2175–2186.

[39] B. Westereng, M. T. Arntzen, F. L. Aachmann, A. Várnai, V. G. H. Eijsink and J. W. Agger, "Simultaneous analysis of C1 and C4 oxidized oligosaccharides, the products of lytic polysaccharide monooxygenases acting on cellulose", *J. Chromatogr. A* **1445** (2016), pp. 46–54.

[40] M. Frommhagen, S. K. Mutte, A. H. Westphal, et al., "Boosting LPMO-driven lignocellulose degradation by polyphenol oxidase-activated lignin building blocks", *Biotechnol. Biofuels* **10** (2017), pp. 1–16.

[41] M. Frommhagen, S. Sforza, A. H. Westphal, et al., "Discovery of the combined oxidative cleavage of plant xylan and cellulose by a new fungal polysaccharide monooxygenase", *Biotechnol. Biofuels* **8** (2015), pp. 1–12.

[42] M. A. S. Kadowaki, A. Várnai, J.-K. Jameson, et al., "Functional characterization of a lytic polysaccharide monooxygenase from the thermophilic fungus *Myceliophthora thermophila*", *PLoS One* **13** (2018), pp. 1–16.

[43] S. Ladevèze, M. Haon, A. Villares, B. Cathala, S. Grisel, I. Herpoël-Gimbert, B. Henrissat and J.-G. Berrin, "The yeast *Geotrichum candidum* encodes functional lytic polysaccharide monooxygenases", *Biotechnol. Biofuels* **10** (2017), pp. 1–11.

[44] J. S. M. Loose, Z. Forsberg, M. W. Fraaije, V. G. H. Eijsink and G. Vaaje-Kolstad, "A rapid quantitative activity assay shows that the *Vibrio cholerae* colonization factor GbpA is an active lytic polysaccharide monooxygenase", *FEBS Lett.* **588** (2014), pp. 3435–3440.

[45] B. Westereng, J. W. Agger, S. J. Horn, G. Vaaje-Kolstad, F. L. Aachmann, Y. H. Stenstrøm and V. G. H. Eijsink, "Efficient separation of oxidized cello-oligosaccharides generated by cellulose degrading lytic polysaccharide monooxygenases", *J. Chromatogr. A* **1271** (2013), pp. 144–152.

[46]  L. Schwaiger, F. Csarman, H. Chang, O. Golten, V. G. H. Ei-jsink and R. Ludwig, "Electrochemical monitoring of het-erogeneous peroxygenase reactions unravels LPMO kinet-ics", *ACS Catal.* **14** (2024), pp. 1205–1219.

[47]  S. S. Ghatge, A. A. Telke, T. R. Waghmode, Y. Lee, K.-W. W. Lee, D.-B. B. Oh, H.-D. D. Shin and S.-W. W. Kim, "Mul-tifunctional cellulolytic auxiliary activity protein HcAA10-2 from *Hahella chejuensis* enhances enzymatic hydroly-sis of crystalline cellulose", *Appl. Microbiol. Biotechnol.* **99** (2015), pp. 3041–3055.

[48]  S. Horn, G. Vaaje-Kolstad, B. Westereng and V. G. Eijsink, "Novel enzymes for the degradation of cellulose", *Biotech-nol. Biofuels* **5** (2012), pp. 1–12.

[49]  B. Song, B. Li, X. Wang, et al., "Real-time imaging reveals that lytic polysaccharide monooxygenase promotes cellu-lase activity by increasing cellulose accessibility", *Biotech-nol. Biofuels* **11** (2018), pp. 1–11.

[50]  M. N. Muraleedharan, D. Zouraris, A. Karantonis, E. Topakas, M. Sandgren, U. Rova, P. Christakopoulos and A. Karnaouri, "Effect of lignin fractions isolated from differ-ent biomass sources on cellulose oxidation by fungal lytic polysaccharide monooxygenases", *Biotechnol. Biofuels* **11** (2018), pp. 1–15.

[51]  S. Abdellaoui, M. Bekhouche, A. Noiriel, R. Henkens, C. Bonaventura, L. J. Blum and B. Doumèche, "Rapid electro-chemical screening of NAD-dependent dehydrogenases in a 96-well format", *Chem. Commun.* **49** (2013), pp. 5781–5783.

[52]  C. Aymard, C. Bonaventura, R. Henkens, C. Mousty, L. Hecquet, F. Charmantray, L. J. Blum and B. Doumeche, "High-throughput electrochemical screening assay for free and Immobilized oxidases: electrochemilumines-cence and intermittent pulse amperometry", *ChemElec-troChem* **4** (2017), pp. 957–966.

[53]  C. M. G. Aymard et al., "Innovative electrochemical screen-ing allows to identify new transketolase inhibitors", *Anal. Chem.* **90** (2018), pp. 9241–9248.

[54]  I. Fall, B. Doumèche, S. Abdellaoui, C. Rémond, H. Rako-toarivonina and M. Ochs, "Paper-based electrodes as a tool for detecting ligninolytic enzymatic activities", *Bioelectro-chemistry* **156** (2024), article no. 108609.

[55]  R. Nadányi, A. Ház, A. Lisý, M. Jablonský, I. Šurina, V. Majová and A. Baco, "Lignin modifications, applications, and possible market prices", *Energies* **15** (2022), article no. 6520.

[56]  T. D. H. Bugg and R. Rahmanpour, "Enzymatic conversion of lignin into renewable chemicals", *Curr. Opin. Chem. Biol.* **29** (2015), pp. 10–17.

[57]  X. Wu, M. Zhang, T. Song, H. Mou, Z. Xiang and H. Qi, "Highly durable flexible paper electrode with a dual fiber matrix structure for high-performance supercapacitors", *ACS Appl. Mater. Interfaces* **12** (2020), pp. 13096–13106.

[58]  H. Manisha, J. Sonia, S. Shashikiran, S. Yuvarajan, P. D. Rekha and K. Sudhakara Prasad, "Computer numeri-cal control-printed paper electrodes for electrochemi-cal detection of Pseudomonas aeruginosa virulence fac-tor pyocyanin", *Electrochem. Commun.* **137** (2022), article no. 107259.

ACADÉMIE
DES SCIENCES
INSTITUT DE FRANCE

Review article

# Extending the toolbox for enzymatic carboligation: synthesis of α-hydroxyketones catalyzed by thermostable transketolase from *Geobacillus stearothermophilus*

**Franck Charmantray** [®],[a] **and Laurence Hecquet** [®],[*],[a]

[a] Université Clermont Auvergne, CNRS, Clermont Auvergne INP, Institut de Chimie de Clermont-Ferrand (ICCF), F-63000 Clermont-Ferrand, France

*E-mail:* laurence.hecquet@uca.fr (L. Hecquet)

**Abstract.** Enzymatic carbon–carbon (C–C) bond formation represents an efficient asymmetric alternative for the preparation of multifunctional products. This paper presents an overview of the advances made by engineering a thermostable thiamine-dependent carboligase, transketolase from *Geobacillus stearothermophilus* (TK$_{gst}$), for the synthesis of various α-hydroxyketones (aliphatic, hydroxylated, and aromatic). While TKs in cells exclusively transfer a ketol unit from a ketose phosphate to an aldose phosphate Cn leading to a Cn+2 ketose phosphate yielding a reversible reaction, the results reported in this paper showed the wide range of non-phosphorylated substrates accepted by the selected TK$_{gst}$ variants, particularly towards α-ketoacids used as nucleophiles, render the reaction irreversible due to the release of carbon dioxide. To enhance TK$_{gst}$ activity towards the targeted nucleophiles, analogues of pyruvate, and electrophiles such as aliphatic, polyhydroxylated, and aromatic aldehydes, the best variants were selected from libraries created by rational design. As the main hurdle for biocatalytic application is the instability/cost of α-ketoacids, one-pot strategies were performed for in situ generation of α-ketoacids from corresponding amino acids with transaminase or amino acid oxidase. A novel promising promiscuous TK$_{gst}$ reaction based on selective cross-acyloin condensation of two aldehydes, one playing the role of the nucleophile in place of the α-ketoacid and the other aldehyde acting as an electrophile, was also investigated. This original TK$_{gst}$ catalyzed reaction provides atom economy while avoiding carbon dioxide release and achieving similar efficiency compared to the usual pathway.

**Keywords.** Biocatalysis, Thiamine-dependent enzyme, C–C bond formation, Transketolase, Mutagenesis, α-hydroxyketones.

## 1. Introduction

The creation of carbon–carbon (C–C) bonds with tight control of chemo-, regio-, and stereoselectivity is the key reaction to construct the carbon framework of organic molecules [1,2]. Consequently, sophisticated methods for asymmetric synthesis as well as protection/deprotection strategies have to be considered together with eco-friendly conditions. In this context, enzymatic biocatalytic C–C coupling

---

*Corresponding author

represents an efficient (asymmetric) alternative for the preparation of multifunctional products [3–5]. In the last few decades, several carboligases have been reported, each of them leading to a specific functional group or motif such as aldolases, Pictet–Spenglerases, oxidases, prenyltransferases, squalene/hopene cyclases, engineered hemoproteins, and thiamine diphosphate (ThDP) dependent enzymes. The last group is recognized as a powerful tool for the preparation by C–C bond formation of enantiopure $\alpha$-hydroxyketones [6–9], a structural motif present in a wide range of highly valuable compounds such as pharmaceuticals [10–15], flavors [16], sweetners [17,18], surfactants [19], and important synthetic intermediates for the preparation of diols or aminoalcohols.

ThDP-dependent enzymes display the formation of a C–C bond between two carbonylated compounds (aldehyde or ketone) according to a common mechanism involving activated ThDP **I** (Figure 1) to produce a highly reactive intermediate (**III)** via polarity reversal (umpolung reaction) characterized by two mesomeric forms (carbanion–enamine). The carbanion subsequently attacks the carbonyl group of a more electrophile (acceptor) substrate, leading to the formation of a C–C bond (**IV**) and to the release of the product (Figure 2). The stereocontrol of the new asymmetric carbon depends on the type of ThDP enzyme and the structure of substrates.

Among ThDP enzymes, transketolase (TK, EC 2.2.1.1) has been largely studied and used for the synthesis of various enantiopure $\alpha$-hydroxyketones considering its large scope of substrates. TKs are ubiquitous enzymes found in the cytoplasm of animal, plant, and microbial cells and in vivo catalyze the reversible transfer of a two-carbon ketol unit from D-xylulose 5-phosphate to D-ribose 5-phosphate or D-erythrose-4-phosphate to generate D-sedoheptulose-7-phosphate or D-fructose-6-phosphate and D-glyceraldehyde-3-phosphate (Figure 3).

With TK providing a link between the glycolysis and pentose phosphate pathway, this enzyme plays a key role in metabolic regulation in all living cells [20]. Particularly in humans, TK has been reported to be involved in neurodegenerative diseases Wernicke–Korsakoff syndrome and Alzheimer's disease, and diabetes and cancers [21–23].

The first in vitro biocatalytic applications of this enzyme were described by Whitesides et al. in 1992 [24]. The reaction becomes more generally useful for synthetic purposes by using hydroxypyruvic acid (HPA) as a C2-ketol group donor, rendering the reaction almost irreversible due to the concomitant release of carbon dioxide as a by-product (Figure 4). The lithium salt of HPA is preferred as it is the commercially available cheaper form of this compound, and its synthesis is also described [25].

Wild-type transketolases from spinach, *S. cerevisiae*, and *E. coli* were first used for the synthesis of $\alpha$-hydroxyketones mostly polyhydroxylated such as natural and unnatural ketoses and analogues obtained from Li-HPA as donors and preferentially ($R$)-hydroxylated aldehydes as acceptors [26–32]. To extend the substrate spectra, the engineering of TKs by mutagenesis was developed together with appropriate screening assays providing efficient variants towards new $\alpha$-ketoacids as donors (analogues of pyruvate) and aldehydes as acceptors (polyhydroxylated or not, arylated), leading to enantiopure $\alpha$-hydroxyketones [33–35].

Another criterion to make biocatalytic applications more competitive is related to the thermostability of enzymes. Indeed, from the industrial point of view, enzymatic processes at elevated temperature offer many advantages such as higher reaction rate, improved solubility of organic substrates, and higher tolerance towards non-conventional media. In addition, for improvement by mutagenesis, thermostable enzymes also display better resistance against protein destabilizing factors [36]. For these reasons, this paper presents an overview of the advances obtained with a thermostable transketolase from *Geobacillus stearothermophilus* (TK_{gst}) for the synthesis of various $\alpha$-hydroxyketones in the context of other thermostable TKs having been isolated and used in biocatalysis but at a faster rate [37,38].
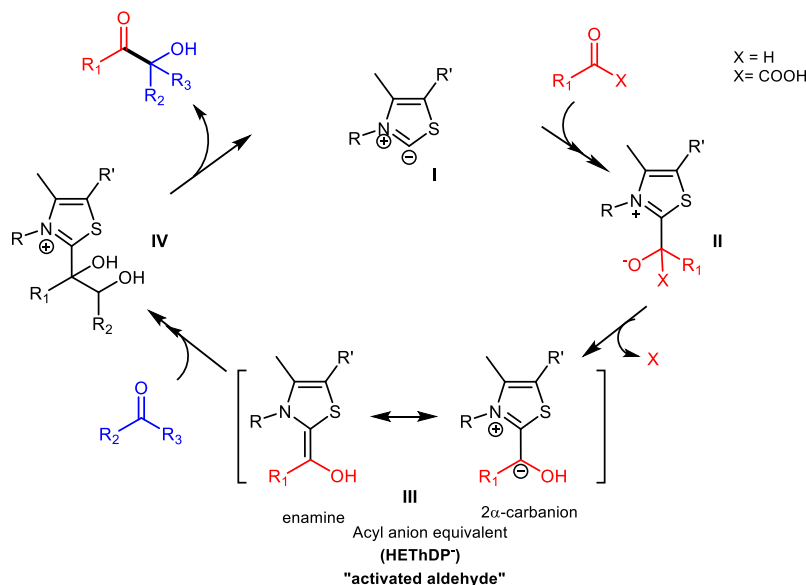
## 2. Results and discussion
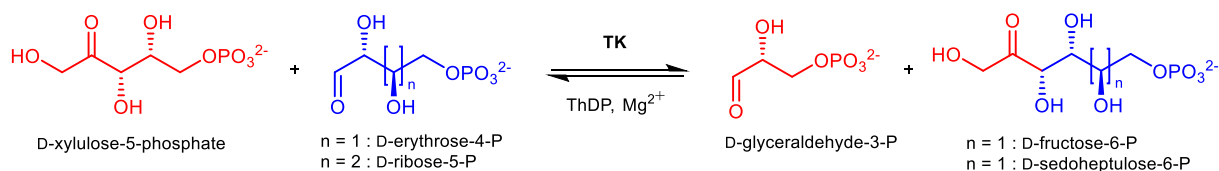
### 2.1. *Production of TK_{gst}*

We have chosen *Geobacillus stearothermophilus* (formerly *Bacillus stearothermophilus*) as a potential source of a thermally stable TK enzyme [39]. This Gram-positive thermophilic bacterium is widely distributed in soil, hot springs, and ocean sediments, and grows in the temperature range of 30–758 °C. Many heat-stable enzymes, such as xylanase [40],
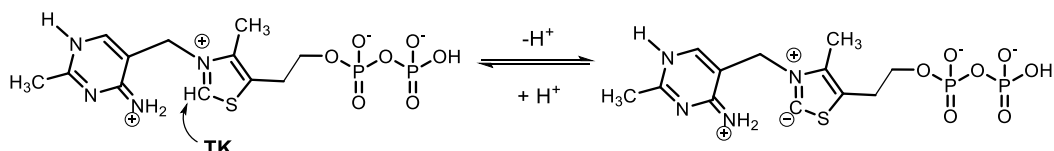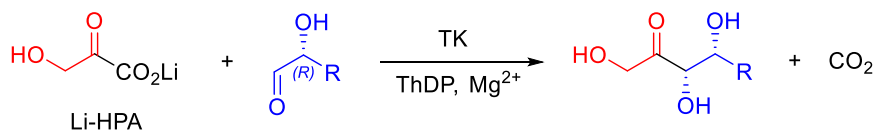
**Figure 1.** Activation of thiamine diphosphate.



**Figure 2.** Catalytic cycle of ThDP-dependent carboligases.



D-xylulose-5-phosphate

n = 1 : D-erythrose-4-P
n = 2 : D-ribose-5-P

D-glyceraldehyde-3-P

n = 1 : D-fructose-6-P
n = 1 : D-sedoheptulose-6-P

**Figure 3.** In vivo transketolase reaction.



Li-HPA

**Figure 4.** Irreversible reaction catalyzed by TKs in the presence of HPA.

L-arabinose isomerase [41], glycosidases [42], and α-amylases [43], have been isolated from this thermophilic bacterium. Before our discovery in 2013 in collaboration with de Berardinis et al. [39], no complete genome sequence was available in public databases for any *G. stearothermophilus* strain and no transketolase enzyme had hitherto been described. TK$_{gst}$ was expressed with a His6-tag at the N-terminus in *E. coli* BL21(DE3) and was purified using immobilized metal affinity chromatography.

The expressed fusion proteins were applied to a Ni$^{2+}$ chelating affinity column for purification. By this procedure, 160 mg each of the purified enzymes TK$_{gst}$ (0.6 U·mg$^{-1}$) were effectively obtained from the cells grown in 1 L culture (5 g·L$^{-1}$ of wet cells). We note that the enzyme can be lyophilized, producing a powder easy to use for chemists and enabling preservation over several months without loss of activity. TK$_{gst}$ also showed higher tolerance over time compared to other mesophilic TKs towards high-percentage cosolvents (up to 50%) such as DMF and ionic liquids such as BMIMCl, which is a useful property when substrates are not water soluble [44].

## 2.2. *Thermostability of TK$_{gst}$*

As is characteristic of a microorganism, TK$_{gst}$ has an optimum temperature range of 60–70 °C, leading to an improvement of up to 10-fold when compared to the activity measured at 20 °C. TK$_{gst}$ retained 100% activity for 1 week at 50 °C and 3 days at 70 °C, and its activity decreased rapidly at 75 °C (half-life was about 15 min) [39]. The thermostability of TK$_{gst}$ was much higher than that of other characterized TKs from microbial sources commonly used in biocatalysis such as TK$_{sce}$ having an half-life of 35 min at 50 °C with immediate activity loss at 70 °C or TK$_{eco}$ more resistant (100% activity recovery at 50 °C for 90 min) but completely vanishing during 5 min exposure at 70 °C.

Given the TK$_{gst}$ thermostability, an alternative purification procedure by heat shock treatment at 65 °C for 45 min enabled an easy and rapid purification method, yielding 132 mg of purified enzyme from the cells grown in 1 L of culture [39].

## 2.3. *Immobilization of transketolase from Geobacillus stearothermophilus*

From an industrial point of view, the reusability of an enzyme is also a crucial point. For that reason, we investigated different supports for TK$_{gst}$ immobilization. First in collaboration with Forano et al., we showed that layered double hydroxides gave efficient adsorption/entrapment of TK$_{gst}$ with almost total immobilization, recovery of initial activity, and reusability over six cycles without loss of activity [44,45]. The strategy is cheap, rapid, and eco-friendly. More recently in collaboration with Szymanska et al., TK$_{gst}$ was covalently immobilized on

silica monolithic pellets. This strategy allowed performing the reaction in a basket-type reactor [46].

## 2.4. *Substrate scope of wild-type TK$_{gst}$*

### 2.4.1. *Substrate scope of wild-type TK$_{gst}$ towards donor and acceptor substrates*

As indicated before, the major advance for biocatalytic applications of TKs including TK$_{gst}$ was the use of HPA, rendering the reaction almost irreversible due to the release of carbon dioxide (Figure 5). We showed later that pyruvate can be accepted as a donor substrate by TK$_{gst}$ but with lower activity compared to HPA.

As expected, knowing the high homology of the TK active sites, we observed that the TK$_{gst}$ acceptor substrate spectrum in the presence of HPA as the donor was very similar to those of TK$_{sce}$ and TK$_{eco}$ already described (Figure 6).

TK$_{gst}$ showed high activity towards short-chain (2$R$) α-hydroxylated aldehydes (C2–C4). A significant decrease in TK$_{gst}$ activity was observed with aldehydes displaying a long carbon chain length (C5–C6) or without a hydroxyl group at the α or β position or hydrophobic and aromatic aldehydes.

In contrast with other described microbial TKs, TK$_{gst}$ showed significant activities towards (2$S$)-hydroxylated aldehydes with three and four carbon atoms [47] such as L-glyceraldehyde, L-lactaldehyde, L-erythrose, and D-threose. This is particularly interesting because these aldehydes can lead to the production of rare, high-value ketoses. However, the TK$_{gst}$ activities were much lower than those determined with their (2$R$) epimers (approximately 20 and 30 times lower in the case of lactaldehyde and glyceraldehyde, respectively). TK$_{gst}$ being thermostable, studies conducted at 60 °C showed an improvement in activities by a factor 4 to 5 towards C3 (L-glyceraldehyde and L-lactaldehyde) and C4 aldoses (L-erythrose and D-threose) compared to results obtained at 25 °C (Figure 7). These analytical results were significant because the activities measured at high temperatures were comparable to those obtained in the presence of their (2$R$) analogues at 25 °C.

Considering all these results, the improvement and broadening of the TK$_{gst}$ substrate scope particularly towards other α-ketoacids as donors and long carbon chain aldoses and hydrophobic and
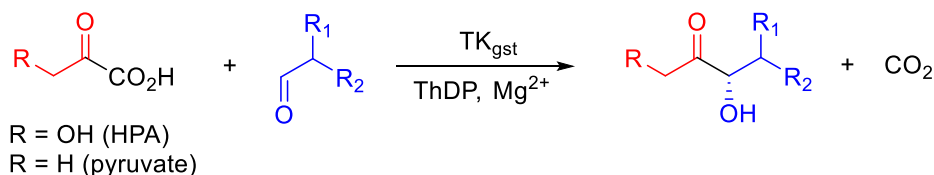
**Figure 5.** Irreversible reaction catalyzed by $TK_{gst}$ in the presence of $\alpha$-ketoacid.
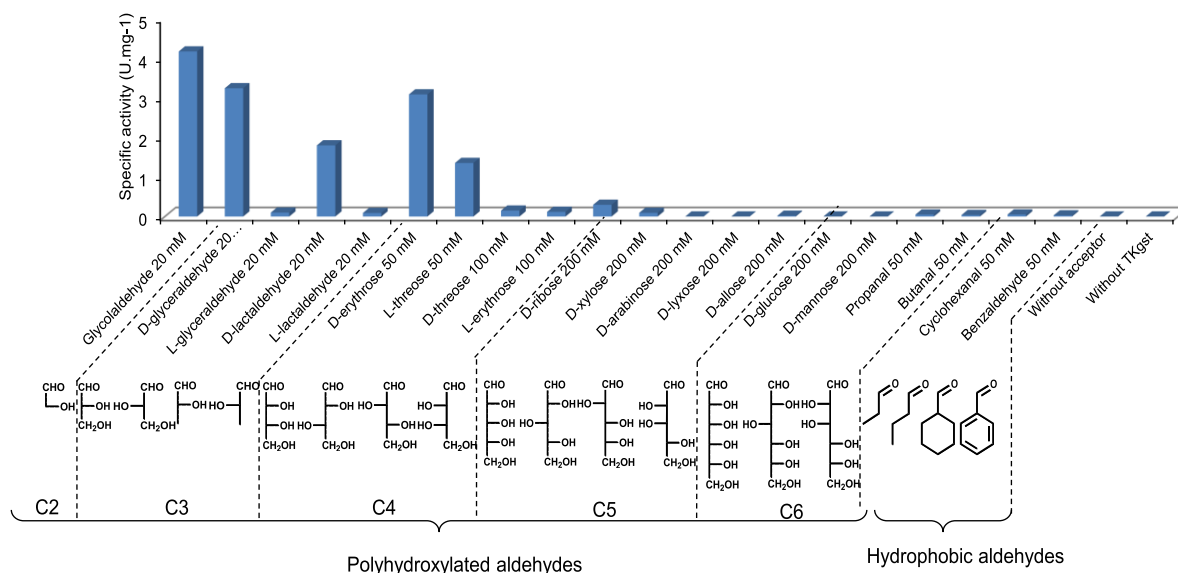


**Figure 6.** Specific activities of $TK_{gst}$ towards a panel of acceptor aldehydes (20–200 mM) were determined in the presence of Li-HPA at 25 °C.
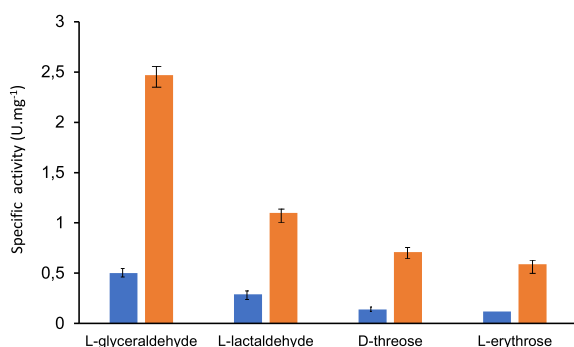


**Figure 7.** Specific activity of $TK_{gst}$ with (2*S*)-hydroxylated aldehydes and C3 (L-glyceraldehyde, L-lactaldehyde) and C4 aldoses (L-erythrose, D-threose) in the presence of Li-HPA at ■ 25 °C and ■ 60 °C.

aromatic aldehydes as acceptors was investigated by mutagenesis strategies.

## 2.5. *Improvement and modification of $TK_{gst}$ properties*

### 2.5.1. *Strategies for generating $TK_{gst}$ variant libraries*

The strategies were based on the analysis of the active site to determine the key positions that should be mutated to improve $TK_{gst}$ activity towards the targeted substrates. The 3D structure of $TK_{gst}$ with its cofactors was recently determined showing as for the other TKs a dimeric enzyme with each monomer containing an identical active site [48]. However, as this structure was not yet available for the studies presented here, a model of active $TK_{gst}$ [49] was constructed by homology with TK from *Bacillus anthracis* ($TK_{ban}$) using a template already crystallized (PDB entry 3M49) belonging to the same microorganism species and having 74% identity. This model was validated by comparison with the 3D structure of $TK_{gst}$.
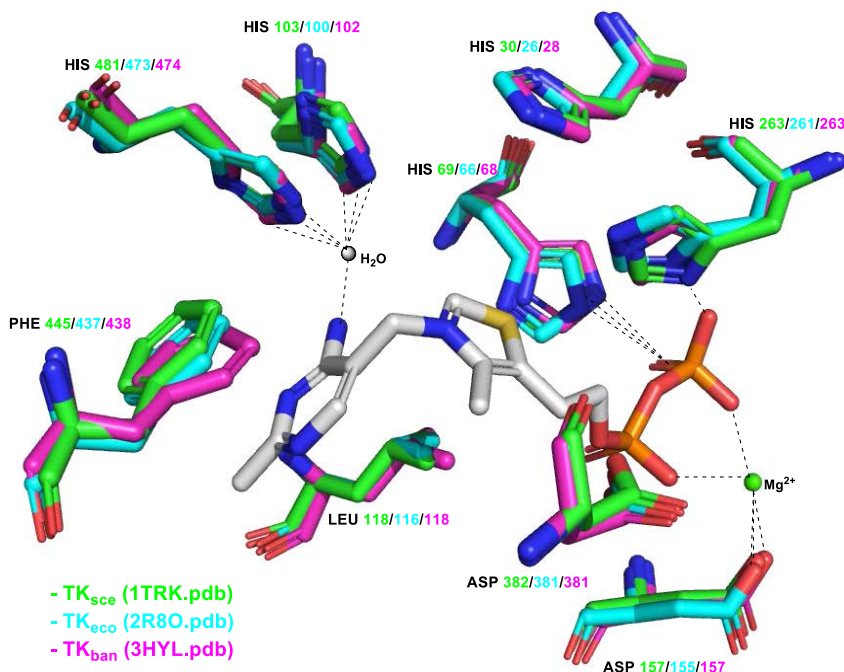
**Figure 8.** Comparison of ThDP binding motifs of TK$_{sce}$ (green 1TRK.pdb), TK$_{eco}$ (cyan 2R8O.pdb), and TK$_{ban}$ (violet 3HYL.pdb).

It can be noted a high homology with the active sites of the other TK sources used in biocatalysis such as TK$_{eco}$ and TK$_{yeast}$ and also with the active sites of all other microbial TKs. The superimposition of TK$_{eco}$, TK$_{sce}$, and TK$_{ban}$ active sites shows the same residues with a similar position to ThDP and divalent cation Mg$^{2+}$ (Figure 8).

After the identification of the targeted residues, each targeted amino acid of the wild-type sequence was replaced by the other 19 amino acids by site saturation mutagenesis (SSM) [50]. Different types of degenerate codons can be used such as NNS and NDT. In NNS, "N" stands for any nucleotide (A, T, G, or C) and "S" stands for G or C. NNS can encode 32 possible codons ($4 \times 4 \times 2 = 32$) including 20 codons for all amino acids plus 12 additional codons that encode some amino acids multiple times or encode stop codons. Alternative codons "NDT" [51] were designed to completely avoid stop codons while encoding several representative amino acids in each category: anionic, cationic, aliphatic, hydrophobic, hydrophilic, and aromatic. These "NDT" codons provide functional diversity without redundancy while reducing the number of enzyme

variants compared to NNS and consequently the screening efforts. When more than two positions were investigated, NDT strategy was preferred in the studies presented here to reduce the size of the libraries.

### 2.5.2. *Screening assays*

The principle of the generic assay developed in liquid or solid phase was based on the TK-catalyzed decarboxylation of $\alpha$-ketoacid and the release of carbon dioxide, inducing the variation in pH of the reaction medium monitored by a pH indicator. Indeed, during the reaction catalyzed by TK in the presence of $\alpha$-ketoacid as the donor, a proton is consumed in each cycle, which releases an equivalent of HCO$_3^-$ bicarbonate ions, leading to a pH increase in the reaction medium (Figure 9).

The bicarbonate ion is the dissociated form of carbonic acid (H$_2$CO$_3$) and is involved in a dynamic equilibrium of dissociation in water. This leads to a basification of the solution due to the partial formation of hydroxide ion raising the pH of the medium, which is approximately 7.5. Based on this pH variation in reaction medium, we first developed
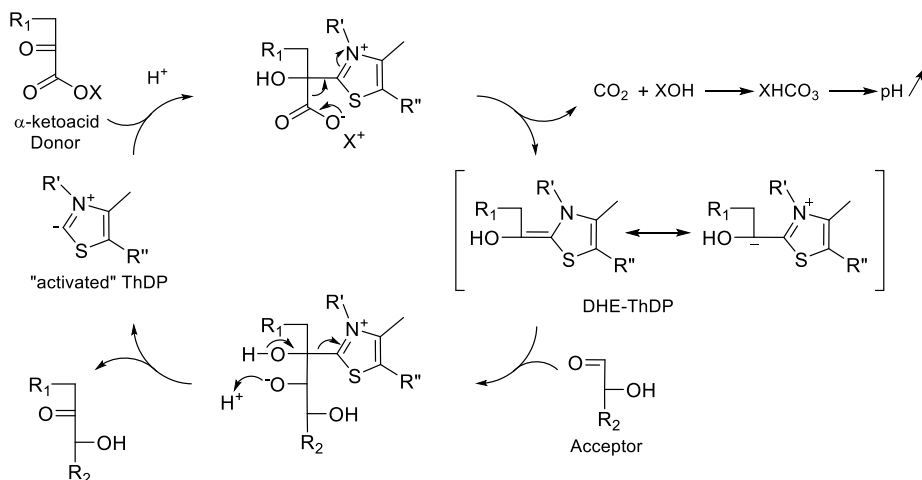
**Figure 9.** Catalytic cycle of TK in the presence of Li-HPA.

in collaboration with Fessner et al. a colorimetric screening assay in the liquid phase with purified variants [52]. More recently, the same principle was applied to a semi-solid phase, allowing the direct detection of clones expressing active TK$_{gst}$ variants [53].

For the qualitative liquid screening assay [52], upon release of carbon dioxide from $\alpha$-ketoacid, the pH increase in the reaction mixture can be determined photometrically by the color change of phenol red. This pH indicator was selected for its p$K_a$ of 7.4 and its turning zone (6.8 < pH < 8.2) being compatible with the optimal pH of the reaction catalyzed by TK, which is approximately 7.5 [54]. Phenol red changes from bright yellow at acidic pH to bright pink at basic pH, allowing easy visualization of the progress of the reaction (Figure 10). In addition, phenol red in its deprotonated form has a high molar absorption coefficient: $\varepsilon = 56{,}000\,M^{-1}{\cdot}cm^{-1}$ at $\lambda_{max} = 557$ nm, detected by spectrophotometry with high sensitivity. At low buffer concentration (2 mM of triethanolamine, pH 7.5), this generic, cheap, rapid method allowed continuous monitoring for quantitative determination of kinetic parameters [52].

The qualitative solid phase assay procedure [53] was based on the strategies already developed with other enzymes by Turner et al. [55] and Bornscheuer et al. [56], allowing one to detect the color variation directly in clones expressing the targeted variant. In our case, the pH indicator used to detect the variation in the reaction medium was bromothymol blue offering higher contrast than phenol red described previously in the liquid phase. The libraries of clones expressing TK$_{gst}$ variants were first cultured on Petri dishes and transferred on a nitrocellulose membrane, which was placed on a semi-solid medium containing the substrates, cofactors, and a pH indicator bromothymol blue. The colonies became blue if TK variants were active towards the substrates (Figure 11).

### 2.5.3. *Extension of TK$_{gst}$ substrate spectra*

**Enhancement of TK$_{gst}$ activity towards (2$S$ or 2$R$) $\alpha$-hydroxyaldehydes (C3–C6) as acceptors with Li-HPA as donor.** Due to their scarcity in nature and complex synthesis, natural and unnatural ketoses particularly with long carbon chains have not been widely assayed for their potential properties on different biological targets, but recent studies have started considering these forgotten compounds. For these reasons, the improvement of TK$_{gst}$ towards the appropriate substrates for obtaining such ketoses and analogues with different types of stereochemistry is of great interest.

Our strategy was based on the analysis of the wild-type TK$_{gst}$ active site with the physiological acceptor substrate D-erythrose-4-phosphate (Figure 12). We applied SSM to key positions in direct interaction of this substrate depending on the structure of the novel targeted aldehyde as the substrate.
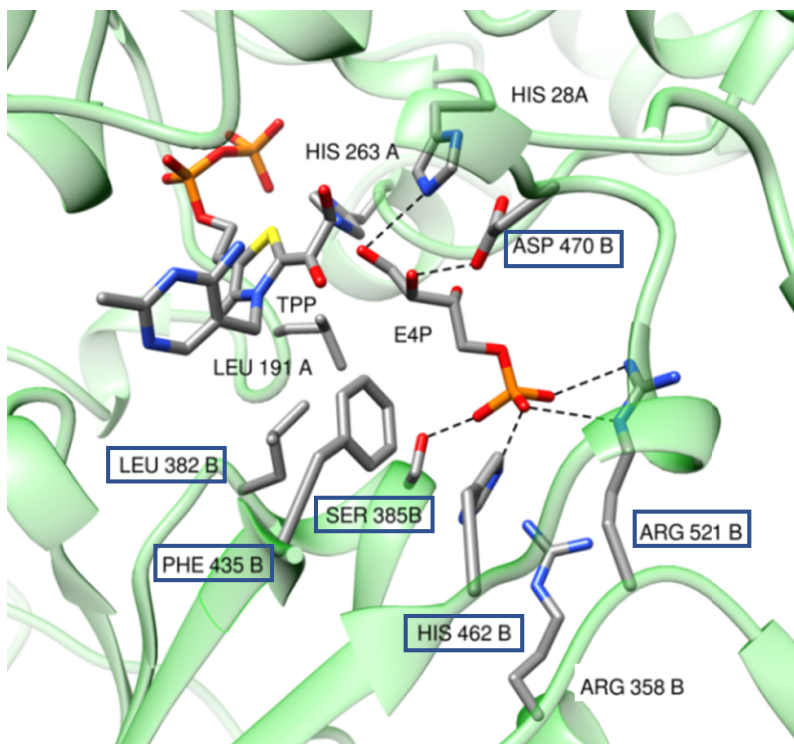
Some examples of ketoses obtained with specific variants selected from TK$_{gst}$ libraries are presented in Table 1.
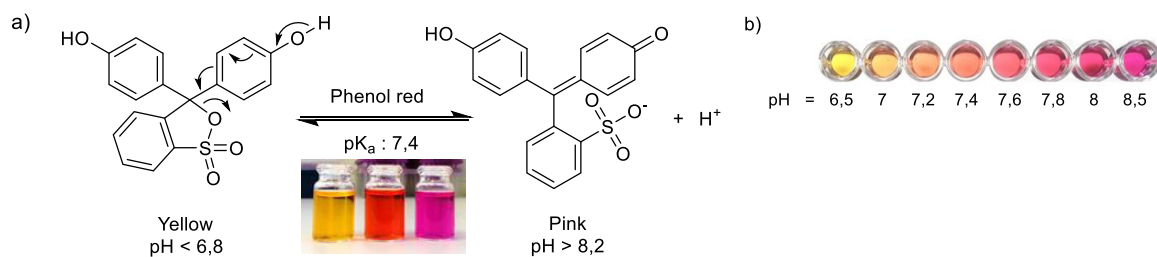
**Figure 10.** TK pH-metric activity test based on the use of phenol red as the colored indicator.
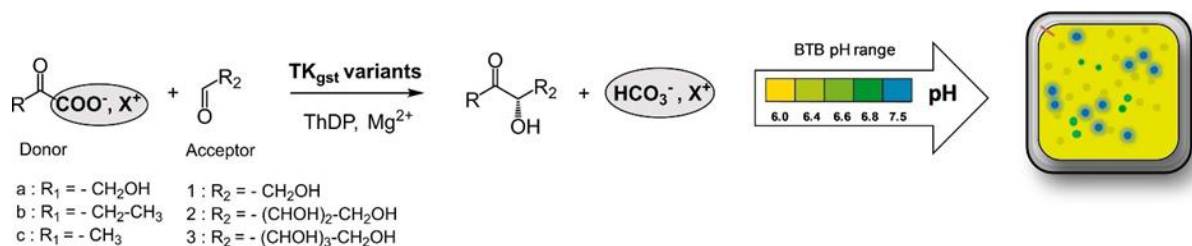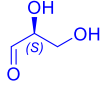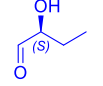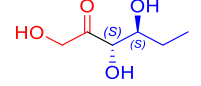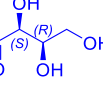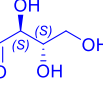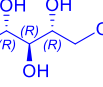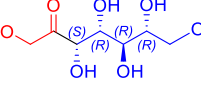


**Figure 11.** pH-metric activity test based on semi-solid medium containing bromothymol blue as the colored indicator.



**Figure 12.** Model of wild-type TK$_{gst}$ based on the X-ray crystal structure of TK$_{ban}$ (PDB entry 3M49) with the physiological acceptor substrate D-erythrose-4-phosphate (E4P).

**Table 1.** Synthesis of ketoses (C5–C8) from aldoses (C3–C6) in the presence of the most efficient $TK_{gst}$ variants

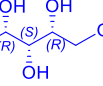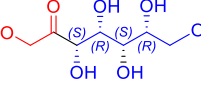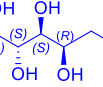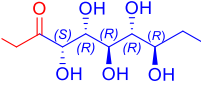| $C_n$ aldose acceptors | $C_{n+2}$ ketose product | $TK_{gst}$ variant | Reaction progress (%) | Reaction time | Isolated yield (%) | de (%) |
|---|---|---|---|---|---|---|
|  L-glyceraldehyde C3 |  L-ribulose C5 | L382D/D470S | 98 | 24 h | 63 | >95 |
|  L-lactaldehyde C3 |  5-deoxy-L-ribulose C5 | L382D/D470S | 98 | 24 h | 55 | >95 |
|  D-threose C4 |  D-tagatose C6 | L382F/F435Y | >95 | 48 h | 62 | >95 |
|  L-erythrose C4 |  L-psicose C6 | L382F/F435Y | >95 | 72 h | 84 | >95 |
|  D-ribose C5 |  D-*altro*-heptulose C7 | H462N/R521Y | >95 | 32 h | 67 | >95 |
|  D-xylose C5 |  D-*ido*-heptulose C7 | H462N/R521Y | >95 | 96 h | 59 | >95 |
|  D-allose C6 |  D-*glycero*-D-*altro*-octulose C8 | S385D/H462S/R521V | 93 | 7 days | 70 | >95 |

As we reported that wild-type $TK_{gst}$ tolerates at 60 °C (2*S*)-hydroxylated aldehyde as an acceptor substrate contrary to the other TKs [48], we first investigated extending these activities towards short carbon chain aldehydes (C3) such as (2*S*)-lactaldehyde and (2*S*)-glyceraldehyde through SSM at two key positions: D470, which interacts with the C2(*R*) hydroxyl group of the physiological erythrose-4-phosphate (DE4P) in the wild-type enzyme, and L382, located at the opposite side of the C2 aldehyde (Figure 12). The best variant, L382D/D470S, increased activity by factors 4 and 5 towards (2*S*)-lactaldehyde and (2*S*)-glyceraldehyde, respectively, forming the corresponding products 5-deoxy-L-ribulose and L-ribulose with 63% and 55% isolated yields, respectively.

Based on these first results, a second generation of $TK_{gst}$ variants was investigated to extend $TK_{gst}$ activity towards longer carbon chain aldoses (C3–C6) by targeting four other positions S385, F435, H462, and R521 near, or by direct interaction with, the phosphate group of the physiological acceptor substrate D-E4P (Figure 12) [57,58]. Three efficient $TK_{gst}$ variants were identified following the screening of $TK_{gst}$ variant libraries. The L382F/F435Y variant showed an improvement by factors 3.7 and 4 compared to the wild-type $TK_{gst}$ towards the (2S)-tetroses D-threose and L-erythrose, respectively, producing the corresponding Cn+2 ketoses D-tagatose and L-psicose, respectively. The double variant H462N/R521Y demonstrated an increase in conversion by factors 3.5 and 4 towards the pentoses D-ribose and D-xylose compared to the wild-type enzyme, forming D-*altro*- and D-*ido*-heptulose, respectively, with 67% and 59% yields. The triple variant S385D/H462S/R521V allowed the synthesis of D-*glycero*-D-*altro*-octulose from D-allose while this was impossible with wild-type $TK_{gst}$.

In conclusion, the aldoses (C3–C6) were almost totally converted into the expected ketose products with good to excellent isolated yields (62%–80%) and in reasonable reaction time (24 h–72 h) except the hexose D-allose requiring 7 days of reaction time with the double variant H462S/R521V. Globally, the mutations of variants on targeted positions near the phosphate group of the physiological substrate gave higher or de novo conversions compared to the wild-type enzyme. In addition, all compounds were obtained with excellent diastereoselectivities,

one stereoisomer being obtained by in situ nuclear magnetic resonance (NMR) analysis of the reaction mixture. In all cases, the (*S*)-configuration of the C3 ketose product was confirmed by NMR spectrum comparison with the already described product.

Among the ketoses listed in Table 1, some of them have been already described for their valuable biological properties. Hexoses include D-tagatose, which is a sweetener and antidiabetic compound [17,18], and L-psicose, which is used for the synthesis of L-fructose, a precursor of an inhibitor of glucosidases [59,60]. The heptulose D-*altro*-heptulose is a marker of sugar metabolism disorders such as cystinosis [61,62]. The D-*ido*-heptulose has been reported to be a precursor of valiolamine and *N*-substituted derivatives, glucosidase inhibitors useful for the treatment of hyperglycemic symptoms [63]. Among octuloses, D-*glycero*-D-*altro*-octulose has been identified in the plant *Spinacia oleracea*, and its (5*S*)-epimer D-*glycero*-D-*ido*-octulose, which is very abundant in *Craterostigma plantagineum*, has been described as a plant antioxidant involved in desiccation tolerance and could be a potential reactive oxygen species scavenger with applications in nutrition and healthcare [64–66]. Recent studies have also shown the essential role of octuloses in the metabolism of parasites such as *Trypanosoma* and various *Leishmania* species, opening the way for potential octulose analogue-based inhibitors to treat the diseases caused by these parasites [67].

**Enhancement of $TK_{gst}$ activity towards aromatic aldehydes with Li-HPA as donor.** In collaboration with the Fessner group, we investigated novel electrophiles ortho-, meta-, and para-substituted nitrosoarenes, which had not been previously investigated with TKs [68,69]. These substrates led to the formation of corresponding aromatic hydroxamic acids, which have a wide range of medical applications (antifungal, antibacterial, antioxidant, anti-inflammatory) due to their chelating properties (Table 2) [70,71].

A key aspect of these reactions was the formation of a carbon–nitrogen bond instead of the typical carbon–carbon bond formed by TKs with other aldehydes as electrophiles. The $TK_{gst}$ variant L382N/D470S (positions previously identified for improved activity towards hydrophobic aldehydes)

**Table 2.** Panel of nitroarenes (ortho-, meta-, and para-substituted) used as acceptor substrates for TK$_{gst}$ variant in the presence of Li-HPA to obtain the corresponding hydroxamic acids

| Aromatic group (X)[a,b] | Acyl group (R) | Yield (%) |
|---|---|---|
| H | $CH_2OH$ | 41/50 |
| 4-Br | $CH_2OH$ | 28/54 |
| 4-Cl | $CH_2OH$ | 41 |
| 3-Cl | $CH_2OH$ | 20 |
| 3,4-Cl$_2$ | $CH_2OH$ | 10 |
| 4-CH$_3$ | $CH_2OH$ | 49 |
| 3-CH$_3$ | $CH_2OH$ | 29 |
| 4-Cl, 3-CH$_3$ | $CH_2OH$ | 37 |
| 3-Cl, 4-CH$_3$ | $CH_2OH$ | 32 |
| 4-CF$_3$ | $CH_2OH$ | 9 |
| 3-CF$_3$ | $CH_2OH$ | 17 |
| 4-N(Me)$_2$ | $CH_2OH$ | 0 |
| H | $CH_3$ | 5 |

[a] Substituent position relative to the nitroso group.

[b] DMSO as cosolvent for X=H and 4-Br and acetone as cosolvent for the other aromatic group.

exhibited the highest activity towards these substrates, with a sevenfold increase in activity compared to wild-type TK$_{gst}$. The replacement of aspartate at position 470 with serine, a non-charged but polar amino acid, seems to enhance interaction during the carboligation step. This mutation had been described in a previous study with non-hydroxylated acceptor substrates [72]. Additionally, this variant has a melting temperature ($T_m$) of 73.9 °C (compared to 75.5 °C for wild-type TK$_{gst}$) and remains highly stable in the presence of cosolvents, retaining 80% to 100% residual activity in DMF, acetone, and acetonitrile.

**Enhancement of TK$_{gst}$ activity towards novel hydrophobic $\alpha$-ketoacids as donors and different aldehydes as acceptors.** In 2017, a challenging work developed jointly with Fessner et al. was conducted to expand the donor substrate spectrum of TK$_{gst}$ to $\alpha$-ketoacids with hydrophobic side chains, which had not previously been considered for TKs [72]. The selection of key positions in the active site was

guided by a structural study based on the model of TK$_{gst}$ with HPA as the donor substrate, constructed from the crystal structure of TK$_{ban}$ (Figure 13).

The active site residues interacting with the hydroxyl group of HPA, namely H68, H102, G116, and H474, were targeted. After screening libraries created by the SSM technique at positions H102 and H474, the variant H102L/H474S showed relative rate increases by factors of 4.4–32 with pyruvate, 2-oxobutyrate, and 3-methyl-2-oxobutyrate (Figure 14).

In position His474, it seems to be essential to preserve a hydrogen bond with the carbonyl group, which was attained by the replacement by serine, providing a slightly reduced size. The replacement of His102 by a non-polar leucine residue not only provided extra space but also improved the binding of the hydrophobic alkyl chain of the substrate in the otherwise initially highly polar active site of wild-type TK$_{gst}$. The best variants using glycolaldehyde as the acceptor were H102L with pyruvate giving a 6-fold increase, H102L/474S with 2-oxobutyrate giving a 30-fold increase, and H102T with 3-methyl-2-oxobutyrate giving a 11.4-fold increase while wild-type TK$_{gst}$ produced any activity with 2-oxobutyrate and 3-methyl-2-oxobutyrate and slight activity with pyruvate (Figure 16). We note that the H102T activity towards pyruvate reached 80% of that obtained with 1-deoxy-D-xylulose-5-phosphate-synthase (DXS$_{eco}$) when using pyruvate as the physiological substrate.

These results offered interesting prospects for the combination of these new donors with hydroxylated or non-hydroxylated aldehydes as acceptors.

**Enhancement of TK$_{gst}$ activity towards hydrophobic $\alpha$-ketoacid as donors and hydrophobic aldehyde as acceptors.** The hydrophobic donors particularly 2-oxobutyrate were investigated with hydrophobic aldehyde as acceptors to produce the corresponding unsymmetrical $\alpha$-hydroxyketones (acyloins), which are valuable as flavors or non-ionic surfactants when compounds display long carbon chains (Figure 15) [16,19].

New TK$_{gst}$ variants were created by combining the most beneficial mutations identified previously with hydrophobic donors (H102L/H474S) with those identified earlier for hydrophobic aldehydes (F435I) [73]. The triple variant H102L/H474S/F435I
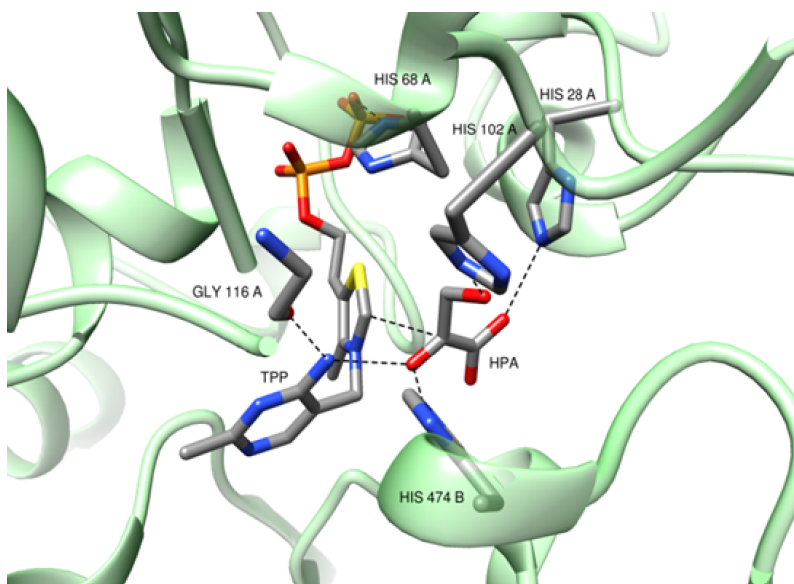
**Figure 13.** Model of wild-type TK$_{gst}$ based on the X-ray crystal structure of TK$_{ban}$ (PDB entry 3M49) with hydroxypyruvate (HPA) as donor. The model was built using Modeller 9.14 and Chimera.
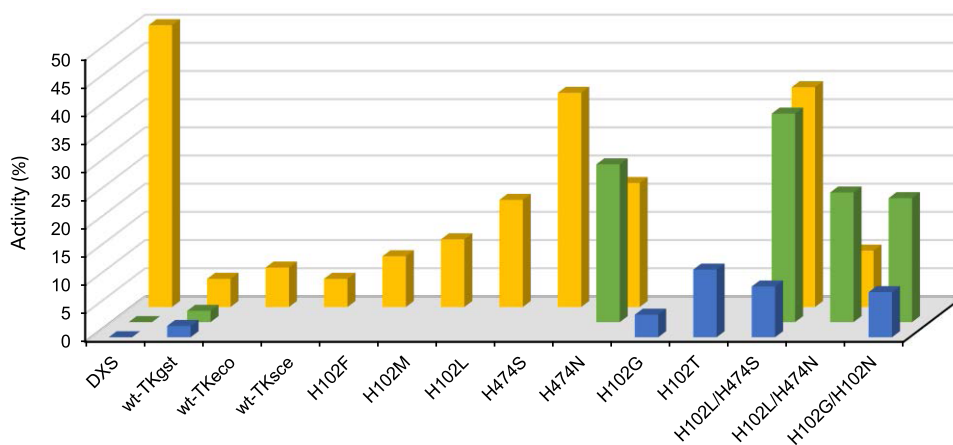


**Figure 14.** Activity of TK$_{gst}$ variants ($k_{cat}$) with glycolaldehyde as acceptor against non-natural nucleophile substrates relative to wt-1-deoxy-D-xylulose-5-phosphate-synthase (DXS$_{eco}$), wt-TK$_{gst}$, and wt-TK$_{eco}$ (■ pyruvate ■ 2-oxobutanoate ■ 3-methyl-2-oxobutanoate).

was able to transfer the acyl group from 2-oxobutyrate to aliphatic aldehydes, enabling the synthesis of the corresponding monohydroxylated α-hydroxyketones (C3–C7) while except with propanal, any activity of the wild-type TK$_{gst}$ was observed with the longer carbon chain aldehydes. Even if the yields and enantiomeric excess (ee) were globally lower than those obtained with HPA, the products obtained with oxobutyrate as the donor are not easy to obtain with other enzymatic or chemical routes and were isolated and purified with accepted yields except for C8 (Table 3) [74].
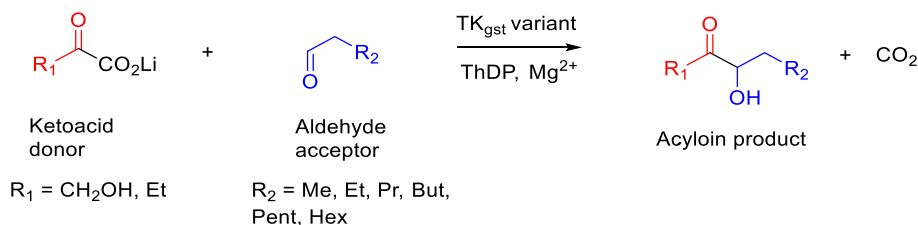
**Figure 15.** Synthesis of monohydroxylated $\alpha$-hydroxyketones from hydrophobic $\alpha$-ketoacid as donors and hydrophobic aldehyde as acceptors.
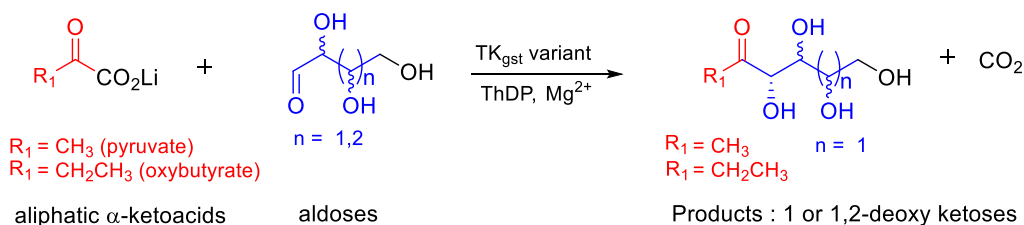


**Figure 16.** Synthesis of 1- and 1,2-deoxy-ketoses from aliphatic $\alpha$-ketoacids combined with aldoses (C4–C5).

**Table 3.** Combination of hydrophobic donor ketoacids and aldehydes for the synthesis of monohydroxylated $\alpha$-hydroxyketones in the presence of the triple variant H102L/H474S/F435I

| Ketoacid donor | Aldehyde acceptor | TK$_{gst}$ variant | Fold increase for TK$_{gst}$ wt | Reaction time (h) | Isolated yield (%) | ee (%) |
|---|---|---|---|---|---|---|
| HPA $R_1 = -CH_2OH$ | $R_2 = Me$ | L382F | 4 | 24 | 56 | 94 |
| | $R_2 = Et$ | L382F | 6 | 24 | 43 | 99 |
| | $R_2 = Pr$ | L382F | 0.5 | 24 | 44 | 99 |
| | $R_2 = But$ | L382F | 2 | 24 | 41 | 98 |
| | $R_2 = Pent$ | L382F | $\infty$ | 24 | 21 | 87 |
| | $R_2 = Hex$ | L382F | 6 | 24 | 7 | 91 |
| Oxobutyrate $R_1 = -Et$ | $R_2 = Me$ | H102L/H474S/F435I | 20 | 24 | 25 | 12 |
| | $R_2 = Et$ | H102L/H474S/F435I | $\infty$ | 24 | 47 | 6 |
| | $R_2 = But$ | H102L/H474S/F435I | $\infty$ | 24 | 20 | 31 |
| | $R_2 = Pent$ | H102L/H474S/F435I | $\infty$ | 24 | 25 | 33 |
| | $R_2 = Hex$ | H102L/H474S/F435I | $\infty$ | 24 | <5 | nd |
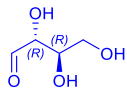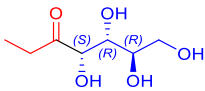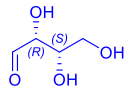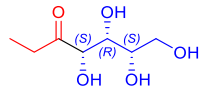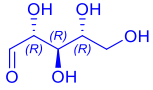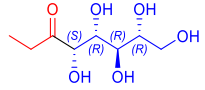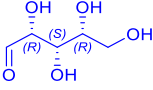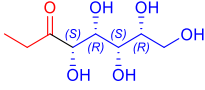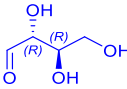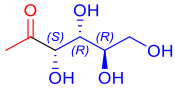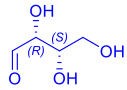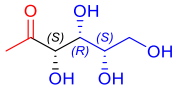
nd = not determined.

**Enhancement of TK$_{gst}$ activity towards hydrophobic $\alpha$-ketoacid as donors and hydroxylated aldehyde as acceptors.** The objective was to produce 1- or 1,2-deoxy-ketoses when using pyruvate or 2-oxobutyrate, respectively, as donors appropriately polyhydroxylated with increased carbon chain length aldoses such as two tetroses (D-erythrose (C4) and L-

threose (C4)) and two pentoses (D-ribose (C5) and D-xylose (C5)) (Figure 16, Table 4) [75,76].

Among the previous TK$_{gst}$ variants, we combined the best mutations identified earlier, H102L and H474S, for hydrophobic $\alpha$-ketoacids (pyruvate and oxobutyrate) with a new mutation on L118I, which is involved in the stabilization of the thiazolium cycle

**Table 4.** Synthesis of 1- and 1,2-deoxy-ketoses at 50 °C using $TK_{gst}$ variants in the presence of 2-oxobutyrate and pyruvate as donors and aldoses as acceptors (D-erythrose, L-threose, D-ribose, D-xylose)

| Donor | Acceptor | Product | Time (h) | $TK_{gst}$ variant | $TK_{gst}$ (mg/mL) | In situ yield[a] (%) | Isolated yield (%)[a,b] |
|---|---|---|---|---|---|---|---|
| R₁ = Et Oxobutyrate | D-erythrose | 1,2-deoxy-D-*arabino*-hept-3-ulose | 24 | H102L/L118I | 0.5 | 85 | 71 |
| | L-threose | 1,2-deoxy-D-*ido*-hept-3-ulose | 6 | H102L/L118/H474S | 0.5 | 89 | 86 |
| | D-ribose | 1,2-deoxy-D-*altro*-oct-3-ulose | 72 | H102L/L118I | 3 | 68 | 68 |
| | D-xylose | 1,2-deoxy-D-*ido*-oct-3-ulose | 48 | H102L/L118I | 3 | 82 | 61 |
| R₁ = Me Pyruvate | D-erythrose | 1-deoxy-D-fructose | 24 | H102L/L118/H474S | 1 | 74 | 68 |
| | L-threose | 1-deoxy-L-sorbose | 24 | H102L/L118/H474S | 1 | 81 | 60 |

[a] Reactions were carried out with $TK_{gst}$ (0.5–3 mg), ThDP (0.1 mM), $MgCl_2$ (1 mM), donors (50–60 mM), and $\alpha$-hydroxyaldehydes (50 mM) at pH 7 and 50 °C.

[b] Determined by in situ ^{1}H NMR analysis.

of ThDP and which could also stabilize the aliphatic donor substrates when histidine replaced isoleucine by interacting with an appropriate longer carbon chain residue.

Even if the use of higher enzyme quantities was required when using pentoses as acceptors, both donors 2-oxobutyrate and pyruvate formed the expected 1,2-deoxy-hexoses or 1,2-heptuloses and 1-deoxyhexoses, respectively, in pure form (one stereoisomer was identified in the reaction mixture by NMR) with good to excellent isolated yields. Some of them have been already described as

displaying interesting properties; for example, 1-deoxy-D-fructose is a potential metabolic inhibitor and antimetabolite.

## 2.6. *Multienzymatic synthesis strategies involving TKs*

We applied the strategy of cascade reaction for in situ generation of $TK_{gst}$ donor and acceptor substrates, which were unstable or costly or not commercially available. To compete with the productivity of traditional methods, the use of two or even more enzymes in cascade can considerably improve the efficiency of a multistage synthesis by obviating the isolation of intermediates, thus saving time, resources, reagents, and energy while reducing waste [77,78]. Cascade reactions can be performed along a simultaneous one-pot strategy when all the enzyme requirements are compatible. To meet limitations, such as substrate/product/reagent inhibition or incompatibility of reaction conditions (pH, temperature), a telescoped, sequential one-pot procedure can be used.

Knowing that Li-HPA was obtained from toxic bromopyruvate with modest yields [20] and its instability at higher temperatures than 25 °C [25,47], a different strategy for HPA in situ generation was investigated. We first reported a procedure with L-α-transaminase from *Thermosinus carboxydivorans* ($TA_{tca}$) able to produce HPA from L-serine, developed in collaboration with de Berardinis et al. (Figure 17) [54].

This is the first example of TA–TK coupling at high temperature cited in the literature. The $TA_{tca}$ being thermostable, it could be coupled in a "one-pot" at 60 °C with the thermostable $TK_{gst}$. This approach was applied to the synthesis of rare L-*erythro*-ketoses (3*S*, 4*S*) in the presence of (2*S*)-aldehydes for which $TK_{gst}$ has low activity at 20 °C. The reaction products were obtained in good to excellent yields (51%–98%) with no accumulation of HPA in the medium and complete conversion of L-serine.

Ward et al. has since discovered more efficient thermostable TAs within metagenomic libraries [37] from *Thermobifida fusca* ($TA_{tfu}$) and *Geobacillus stearothermophilus* ($TA_{gst}$), which showed opposite stereoselectivities. The two thermostable TAs retain approximately 70% of their activity after 24 h of incubation at 60 °C. They were selected to generate HPA from a racemic mixture of serine.

Based on our bi-enzymatic cascade reaction, an additional third enzymatic step was investigated to generate (2*S*)-aldehydes such as L-glyceraldehyde, D-threose, and L-erythrose in collaboration with Clapes et al. [79] The precursors of α-hydroxylated aldehydes (2*S*) are glycolaldehyde and formaldehyde, which are inexpensive and achiral in the presence D-fructose-6-phosphate aldolase from *E. coli* ($FSA_{eco}$) (Figure 18).

The simultaneous coupling of $FSA_{eco}$ and $TK_{gst}$ in a one-pot was not possible since glycolaldehyde and formaldehyde would react directly with HPA in the presence of $TK_{gst}$ to form L-erythrulose and DHA, respectively. Therefore, a sequential process was developed in which the α-hydroxylated (2*S*) aldehyde is produced in the first step catalyzed by $FSA_{eco}$ and then used in solution without intermediate purification as the acceptor substrate of $TK_{gst}$. The synthesis of the corresponding L-*erythro*-ketoses (3*S*, 4*S*) was carried out from HPA also in situ generated from L-serine in the presence of the thermostable $TA_{tca}$ described previously. The simultaneous coupling of $TA_{tca}$ and $TK_{gst}$ makes it possible to carry out the synthesis at 60 °C and thus to increase the low affinity of $TK_{gst}$ for (2*S*)-hydroxylated aldehydes.

This process made possible the synthesis of three rare ketoses (3*S*, 4*S*)—L-ribulose from L-glyceraldehyde, D-tagatose from D-threose, and L-psicose from L-erythrose—which are compounds with high added value, with diastereomeric excess (de) greater than 95% and product isolated yields of 53, 55, and 49%, respectively.

The main disadvantage of these TA strategies for HPA generation is the release of alanine as the by-product, which is not in favor of atom economy. Another enzymatic strategy avoiding the use of cosubstrate has been considered via serine, allowing the oxidation of the amine function by a microbial amino acid oxidase (AAO, EC 1.4.3.3) in the presence of $O_2$ and catalase (EC 1.11.1.6) to dismutate the hydrogen peroxide formed during the oxidation stage. We turned to $DAAO_{rg}$ [80], already reported by Pollegioni et al. [81,82], to accept the polar amino acid D-serine with higher specific activity compared to DAAO from pig kidney. But $DAAO_{rg}$ has never been investigated for producing α-ketoacid HPA from D-serine, especially at the preparative scale. In a sequential reaction, we also investigated producing D-serine in collaboration with Protéus by
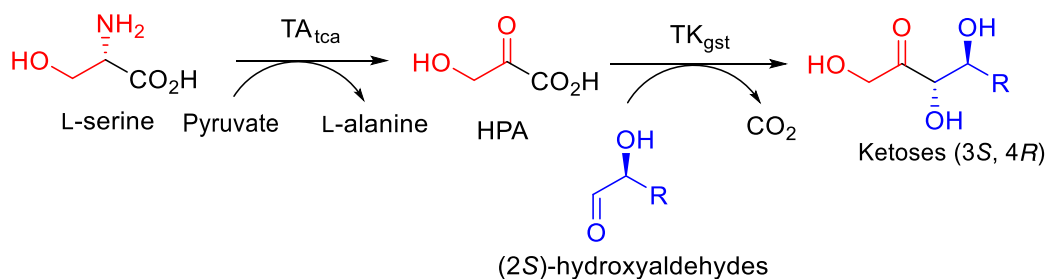
**Figure 17.** In situ generation of HPA catalyzed by $TA_{tca}$ coupled with $TK_{gst}$ for the synthesis of ($3S$, $4S$) ketoses.
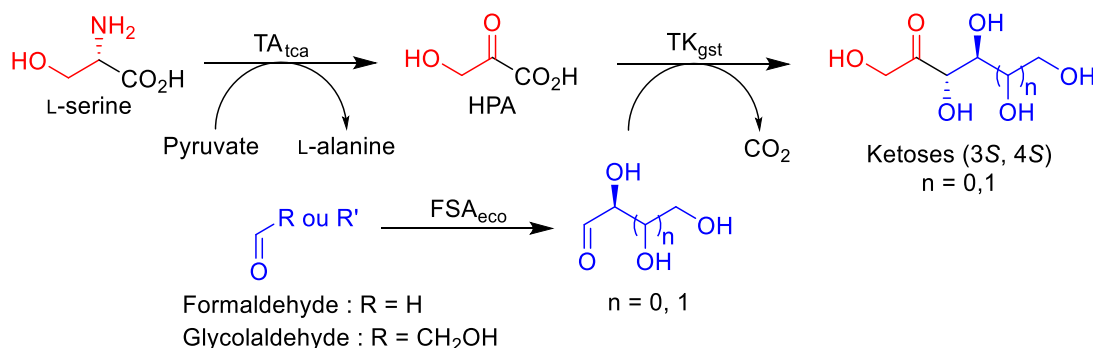


**Figure 18.** In situ generation of aldehydes ($2S$) with $FSA_{eco}$ and HPA with $TA_{tca}$ coupled with $TK_{gst}$ in a one-pot sequential cascade.

Seqens from achiral glycine and formaldehyde as precursors with *E. coli* cells expressing threonine aldolase [83]. After total conversion of the substrate, the crude extract containing D-serine was used as the precursor of HPA (Figure 19).

In parallel, we discovered in collaboration with Prozomix a thermostable DAAO4536 from metagenomic library screening not applicable for producing HPA but pyruvate and oxobutyrate from D-alanine and D-homoalanine, respectively (Figure 21) [74].

Finally, DAAO$_{rg}$ (or DAAO4536) was coupled with the $TK_{gst}$ variant in a one-pot, two-step simultaneous or sequential cascade sequence with different aldehydes (hydrophobic or polyhydroxylated with increased carbon chain length) as $TK_{gst}$ acceptor substrates introduced into the reaction mixture at the same concentration as D-amino acids. A complete conversion of all substrates was observed, and targeted compounds were recovered with high enantio- and diastereoselectivities. These approaches appeared particularly appropriate for expensive, unstable, and commercially unavailable *a*-ketoacid synthesis.

### 2.7. *Promiscuous cross-acyloin condensation reaction catalyzed by $TK_{gst}$*

Previous studies conducted with propanal showed that the variant H102L/L118I/H474S was capable of catalyzing the self-acyloin condensation of propanal to yield propioin (Figure 20) [84].

According to these results, a possible mechanism for the acyloin condensation reaction was investigated in the presence of two aldehydes as $TK_{gst}$ substrates by in silico studies using H102L/L118I/H474G(S) $TK_{gst}$ variant active site models [85]. The presence of leucine in place of histidine in the 102 position (H102L) may contribute to the stabilization of the first aldehyde molecule in the active site. Then, an attack of ThDP carbanion **I** on the carbonyl of the first molecule of aldehyde acting as a nucleophile followed by a proton transfer of **I–B** via a water molecule to His263 led to acylThDP carbanion **II** (Figure 21). In the last step, acylThDP carbanion **II** attacked the carbonyl group of the second aldehyde molecule acting as the electrophile to form the acyloin product. In this
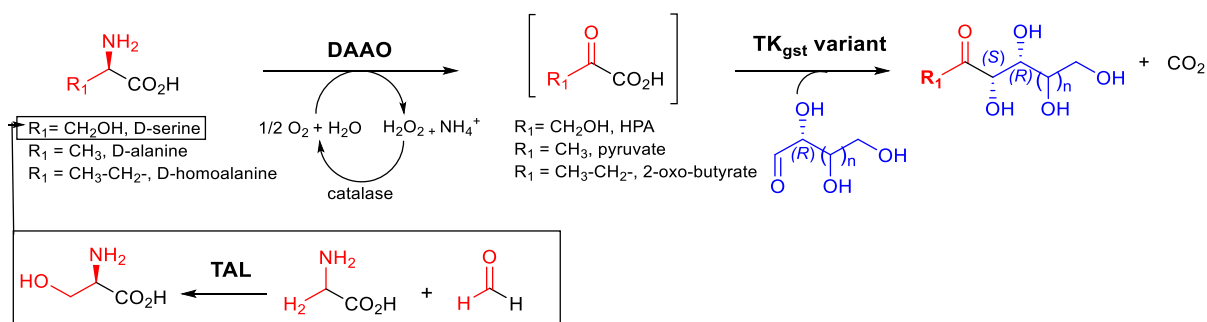
**Figure 19.** In situ generation of α-ketoacids from DAAO (DAAO$_{rg}$ for HPA and DAAO4536 for pyruvate and oxobutyrate) coupled with TK$_{gst}$ for the synthesis of ketoses and analogues.
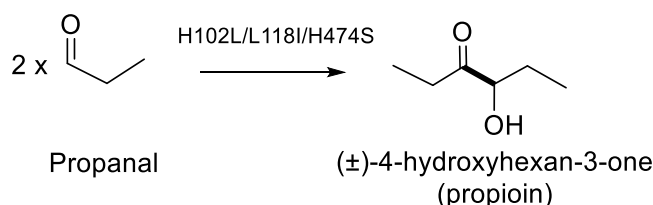


**Figure 20.** Self-condensation of two propanal molecules giving (±)-4-hydroxyhexan-3-one (propioin) catalyzed by TK$_{gst}$ variant H102L/L118I/H474S.
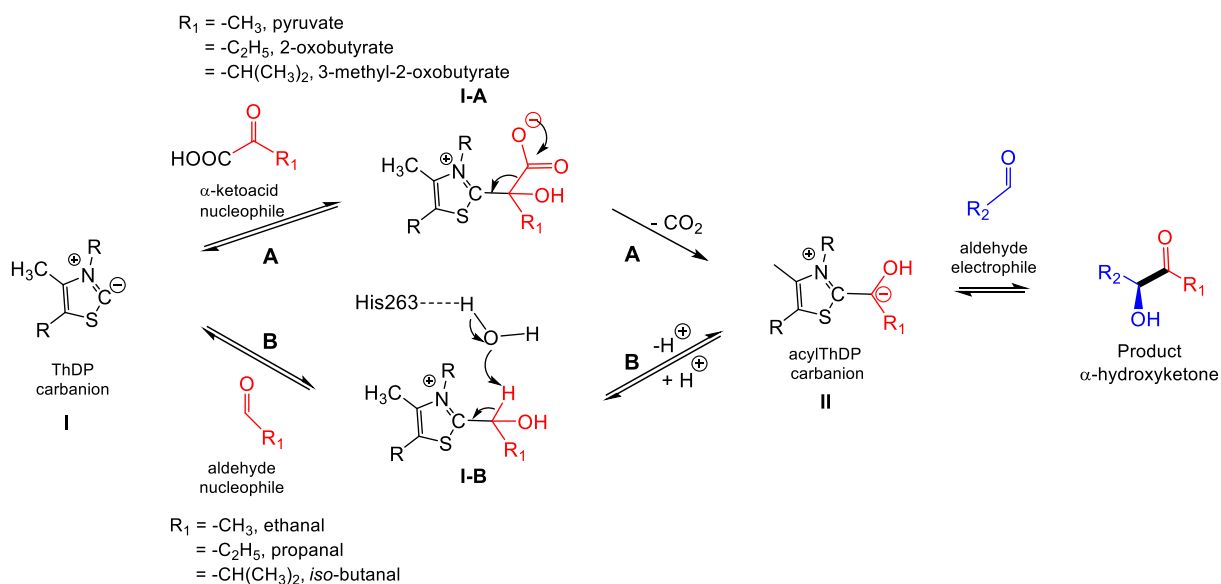


**Figure 21.** Proposed mechanism for acyloin condensation according to pathway B compared to pathway A giving the common α-hydroxy-β-(polyhydroxy)alkylthiamine diphosphate (acylThDP) carbanion **II** generated from aliphatic α-ketoacids (pathway A) or from corresponding aliphatic aldehydes (pathway B).
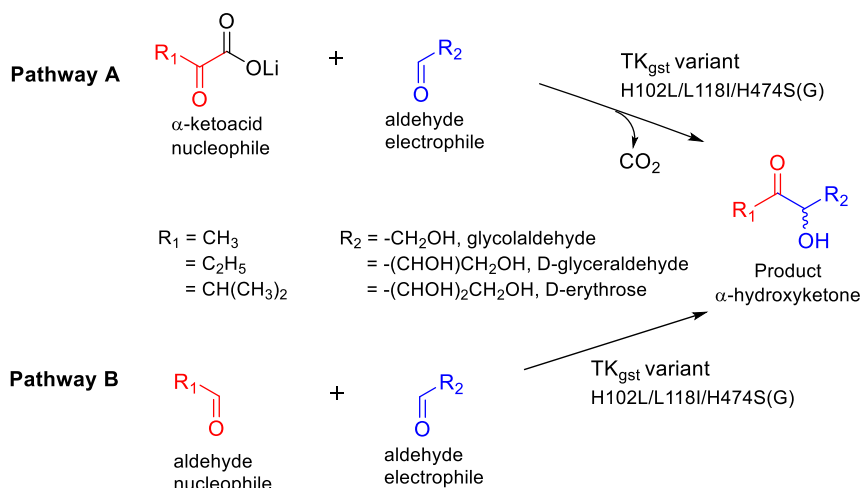
**Figure 22.** Synthesis of $\alpha$-hydroxyketones catalyzed by $TK_{gst}$ variants from two possible nucleophiles, aliphatic $\alpha$-ketoacids (pyruvate, 2-oxobutyrate, 3-methyl-2-oxobutyrate; pathway A) and the corresponding aliphatic aldehydes (propanal, butanal, iso-butanal; pathway B) in the presence of hydroxylated aldehydes as electrophiles.

mechanism, the aldehyde acting as the nucleophile can replace the corresponding acyl group of corresponding $\alpha$-ketoacids but avoids decarboxylation and the release of carbon dioxide. We proved that both pathways led to the same acylThDP carbanion **II** and products [85].

To extend this reaction to the more challenging cross-acyloin condensation, we used three aldehydes' (ethanal, propanal, and *iso*-butanal) analogues of $\alpha$-ketoacids (pyruvate, 2-oxobutyrate, and 3-methylbutyrate used previously) combined with hydroxylated aldehydes (C2–C4; glycolaldehyde, D-glyceraldehyde, and D-erythrose) in the presence of $TK_{gst}$ variants H102L/L118I/H474S(G) identified earlier (Figure 22) [85].

For each synthesis with stoichiometric amounts of both different aldehydes (Table 5), the in situ analysis of the reaction medium by NMR showed the formation of only one $\alpha$-hydroxyketone, highlighting the selectivity of the variants. Indeed, the uncontrolled cross-acyloin condensation can lead to four products. All $\alpha$-hydroxyketones were obtained with good isolated yields comparable to those obtained by pathway A from the carboxylation of $\alpha$-ketoacids (Table 5) [85].
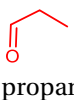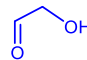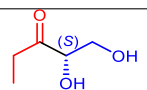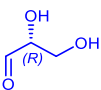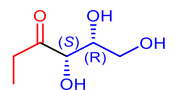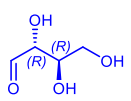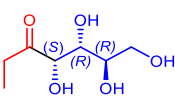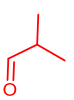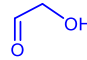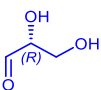
The formation of the targeted $\alpha$-hydroxyketones by cross-acyloin condensation offers the great advantage of ensuring atom economy by avoiding the

release of carbon dioxide generated by the decarboxylation of $\alpha$-ketoacids. This novel enzymatic acyloin condensation reaction catalyzed by TK should broaden the synthetic toolkit for creating unsymmetrical $\alpha$-hydroxyketones and enhance the efficiency of previous enzymatic and chemical approaches in terms of mass metrics.

## 3. Conclusion

Wild-type TKs in cells exclusively transfer a ketol unit from a ketose phosphate to an aldose phosphate Cn leading to a Cn+2 ketose phosphate by a reversible reaction. The results reported in this paper showed that $TK_{gst}$ engineering allowed the synthesis of a wide range of non-phosphorylated $\alpha$-hydroxyketones (aliphatic, hydroxylated, or aromatic) in one step with excellent yields and stereoselectivities. The noteworthy evolvability of thermostable $TK_{gst}$ was mostly based on its robust 3D structure against destabilizing mutagenesis factors. The best variants selected from libraries created by rational design based on active site analysis enhanced the wild-type $TK_{gst}$ towards targeted nucleophiles, analogues of pyruvate, coupled with electrophiles such as aliphatic, increased carbon chain length polyhydroxylated, and aromatic aldehydes. An essential tool to select the best variants was the development of a

**Table 5.** Synthesis of $\alpha$-hydroxyketones using $TK_{gst}$ variants in the presence of ethanal, propanal, and iso-butanal as nucleophiles (50 mM) and hydroxylated aldehydes (glycolaldehyde, D-glyceraldehyde, D-erythrose) as electrophiles (50 mM). Reactions were performed at 37 °C in phosphate buffer (50 mM) at pH 7.0

| Donor | Acceptor | Product | Time (h) | $TK_{gst}$ variant | In situ yield (%)[a] | Isolated yield (%) | de[b] (%) |
|---|---|---|---|---|---|---|---|
| propanal | glycolaldehyde | | 72 | H102L/L118I/ H474G | 80 | 50 | 69 (S) |
| | D-glyceraldehyde | | 72 | H102L/L118I/ H474S | 48 | 31 | >95 |
| | D-erythrose | | 48 | H102L/L118I/ H474S | 75 | 50 | >95 |
| Iso-butanal | glycolaldehyde | | 72 | H102L/L118I/ H474G | 82 | 60 | 34 (S) |
| | D-glyceraldehyde | | 48 | H102L/L118I/ H474S | 39 | 31 | >95 |

[a] Determined by in situ $^1$H NMR using TSP-$d_4$ as an internal standard and calculated based on in situ product formation.

[b] Determined by chiral GC-MS analysis after derivatization.

generic rapid and cheap pH-shift-based screening assay applied in the liquid or solid phase. The latter enabled visual detection of clones expressing active $TK_{gst}$ by their specific coloration.

The best efficient $TK_{gst}$ variants were first used to catalyze the usual TK reaction from the $\alpha$-ketoacid and aldehyde as the nucleophile and electrophile, respectively. As the main hurdle for biocatalytic application is the instability/cost of $\alpha$-ketoacids, one-pot strategies were investigated for in situ generation of $\alpha$-ketoacids from corresponding L- or D-amino acids with L-transaminase or D-amino acid oxidase. The novel promising approach was based on a promiscuous $TK_{gst}$ reaction, allowing selective cross-acyloin condensation of two aldehydes, one playing the role of the nucleophile in place of $\alpha$-ketoacid and the other aldehyde acting as the electrophile. This original $TK_{gst}$ catalyzed reaction provides atom economy while avoiding carbon dioxide release and achieving similar efficiency compared to the commonly used pathway.

## Declaration of interests

The authors do not work for, advise, own shares in, or receive funds from any organization that could

benefit from this article, and have declared no affiliations other than their research organizations.

## References

[1]   S. Van de Vyver and Y. Roman-Leshkov, *Angew. Chem., Int. Ed.* **54** (2015), pp. 12554–12561.

[2]   S. H. Cho, J. Y. Kim, J. Kwak and S. Chang, *Chem. Soc. Rev.* **40** (2011), pp. 5068–5083.

[3]   K. Faber, W. D. Fessner and N. J. Turner, *Biocatalysis in Organic Synthesis*, Science of Synthesis, Georg Thieme: Stuttgart, 2015.

[4]   N. G. Schmidt, E. Eger and W. Kroutil, *ACS Catal.* **6** (2016), pp. 4286–4311.

[5]   Y. F. Miao, M. Rahimi, E. M. Geertsema and G. J. Poelarends, *Curr. Opin. Chem. Biol.* **25** (2015), pp. 115–123.

[6]   M. Müller, G. A. Sprenger and M. Pohl, *Curr. Opin. Chem. Biol.* **17** (2013), pp. 261–270.

[7]   H. C. Hailes, D. Rother, M. Müller, R. Westphal, J. M. Ward, J. Pleiss, C. Vogel and M. Pohl, *FEBS J.* **280** (2013), pp. 6374–6394.

[8]   M. Müller, D. Gocke and M. Pohl, *FEBS J.* **276** (2009), pp. 2894–2904.

[9]   M. Pohl, G. A. Sprenger and M. Muller, *Curr. Opin. Biotechnol.* **15** (2004), pp. 335–342.

[10]  T. Tanaka, M. Kawase and S. Tani, *Bioorg. Med. Chem.* **12** (2004), pp. 501–505.

[11]  O. B. Wallace, D. W. Smith, M. S. Deshpande, C. Polson and K. M. Felsenstein, *Bioorg. Med. Chem. Lett.* **13** (2003), pp. 1203–1206.

[12]  S. Fürmeier and J. O. Metzger, *Eur. J. Org. Chem.* **5** (2003), pp. 885–893.

[13]  M. Godino-Ojer, M. Shamzhy, J. Čejka and E. Pérez-Mayoral, *Catal. Today* **345** (2020), pp. 258–266.

[14]  B. M. Santoyo, C. González-Romero, O. Merino, R. Martínez-Palou, A. Fuentes-Benites, H. A. Jiménez-Vázquez, F. Delgado and J. Tamariz, *Eur. J. Org.Chem.* **15** (2009), pp. 2505–2518.

[15]  P. Hoyos, J.-V. Sinisterra, F. Molinari, A. R. Alcántara and P. Domínguez de María, *Acc. Chem. Res.* **43** (2010), pp. 288–299.

[16]  F. Neuser, H. Zorn and R. G. Berger, *J. Agric. Food Chem.* **48** (2000), pp. 6191–6195.

[17]  M. Ensor, A. B. Banfield, R. R. Smith, J. Williams and R. A. Lodder, *J. Endocrinol. Diabetes Obes.* **3** (2015), pp. 1–12.

[18]  J. P. Manisha, C. A. Rekha, T. P. Arti, R. D. Samir and H. P. Darshan, *Enzyme Microb. Technol.* **97** (2017), pp. 27–33.

[19]  B. Zhu, D. Belmessieri, J. F. Ontiveros, J.-M. Aubry, G.-R. Chen, N. Duguet and M. Lemaire, *ACS Sustain. Chem. Eng.* **6** (2018), pp. 2630–2640.

[20]  B. L. Horecker, *J. Biol. Chem.* **277** (2002), pp. 47965–47971.

[21]  J. Zhao and C. J. Zhong, *Neurosci. Bull.* **25** (2009), pp. 94–99.

[22]  Z. Shi, Y. Tang, K. Li and Q. Tumour, *Biol.* **36** (2015), pp. 8519–8529.

[23]  X. Zheng and H. Li, *Biochem. Biophys. Res. Commun.* **503** (2018), pp. 572–579.

[24]  Y. Kobori, D. C. Myles and G. M. Whitesides, *J. Org. Chem.* **57** (1992), pp. 5899–5907.

[25]  F. Dickens and D. H. Williamson, *Biochem. J.* **68** (1958), pp. 74–81.

[26]  T. Ziegler, A. Straub and F. Effenberger, *Angew. Chem. Int. Ed. Engl.* **100** (1998), pp. 737–738.

[27]  L. Hecquet, J. Bolte and C. Demuynck, *Tetrahedron* **52** (1999), pp. 8223–8232.

[28]  F. T. Zimmermann, A. Schneider, U. Schörken, G. A. Sprenger and W.-D. Fessner, *Tetrahedron: Asymmetry* **10** (1999), pp. 1643–1646.

[29]  N. J. Turner, *Curr. Opin. Biotechnol.* **11** (2001), pp. 527–531.

[30]  F. Charmantray, V. Helaine, B. Legeret and L. Hecquet, *J. Mol. Catal. B: Enzym.* **57** (2009), pp. 6–9.

[31]  A. Ranoux, S. K. Karmee, J. Jin, A. Bhaduri, A. Caiazzo, I. W. Arends and U. Hanefeld, *ChemBioChem* **13** (2012), pp. 1921–1931.

[32]  S. R. Marsden, L. Gjonaj, S. J. Eustace and U. Hanefeld, *ChemCatChem* **9** (2017), pp. 1808–1814.

[33]  J. L. Galman, D. Steadmann, S. Bacon, P. Morris, M. E. B. Smith, J. Ward, P. A. Dalby and H. C. Hailes, *Chem. Commun.* **46** (2010), pp. 7608–7610.

[34]  A. Cázares, J. L. Galman, M. E. Crago Smith, J. Strafford, L. Ríos-Solís, G. L. Lye, P. A. Dalby and H. C. Hailes, *Org. Biomol. Chem.* **8** (2010), pp. 1301–1130.

[35]  F. Subrizi, M. Cárdenas-Fernández, G. J. Lye, J. M. Ward, P. A. Dalby, T. D. Sheppard and H. C. Hailes, *Green Chem.* **18** (2016), pp. 3158–3165.

[36]  J. D. Bloom, S. T. Labthavikul, C. R. Otey and F. H. Arnold, *Proc. Natl. Acad. Sci. USA* **103** (2006), pp. 5869–5874.

[37]  M. Bawn, F. Subrizi, G. J. Lye, T. D. Sheppard, H. C. Hailes and J. M. Ward, *Enzyme Microb. Technol.* **116** (2018), pp. 16–22.

[38] P. James, M. N. Isupov, S. A. De Rose, C. Sayer, I. S. Cole and J. A. Littlechild, *Front. Microbiol.* **11** (2020), article no. 592353.

[39] J. Abdoul Zabar, I. Sorel, V. Hélaine, et al., *Adv. Synth. Catal.* **355** (2013), pp. 116–128.

[40] G. Garg, S. S. Dhiman, R. Mahajan, A. Kaur and J. Sharma, *J. Biotechnol.* **1** (2011), pp. 58–64.

[41] L. Cheng, W. Mu, B. Jiang, W. Xu, W. Zhang, T. Zhang, B. Jiang and W. Mu, *Trends Food Sci. Technol.* **78** (2018), pp. 25–33.

[42] S. Ferdjani, M. Ionita, B. Roy, M. Dion, Z. Djeghaba, C. Rabiller and C. Tellier, *Biotechnol. Lett.* **3** (2011), pp. 1215–1219.

[43] W. Cuevas, D. A. Estell, S. H. Hadi, et al., US patent, PCT/US2009/046034, 2009.

[44] G. Ali, T. Moreau, C. Forano, C. Mousty, V. Prevot, F. Charmantray and L. Hecquet, *ChemCatChem* **7** (2015), pp. 3163–3170.

[45] O. Pascu, S. Marre, B. Cacciuttolo, G. Ali, L. Hecquet, M. Pucheault, V. Prevot and C. Aymonier, *ChemNanoMat* **3** (2017), pp. 614–619.

[46] D. Swietochowska, A. Łochowicz, N. Ocal, L. Pollegioni, F. Charmantray, L. Hecquet and K. Szymanska, *Catalysts* **13** (2023), article no. 95.

[47] M. Lorillière, *Ingénierie de la transcétolase de Geobacillus stearothermophilus : nouvelles stratégies pour la synthèse enzymatique de cetoses rares*, 2017. Chimie organique. Université Clermont Auvergne [2017–2020], Français. ffNNT : 2017CLFAC080ff. fftel-01818066f.

[48] C. Leogrande, F. Rabe von Pappenheim and K. Tittmann, *Crystal Structure of Transketolase from Geobacillus stearothermophilus*, PDB, 2023.

[49] J. Abdoul Zabar, M. Lorillière, D. Yi, L. Nauton, F. Charmantray, V. Hélaine, W.-D. Fessner and L. Hecquet, *Adv. Synth. Catal.* **357** (2015), pp. 1715–1720.

[50] M. Reetz, *ChemBioChem* **23** (2022), article no. e202200049.

[51] A. E. Firth and W. M. Patrick, *Bioinformatics* **21** (2005), pp. 3314–3315.

[52] D. Yi, T. Saravanan, T. Devamani, J. Abdoul-Zabar, F. Charmantray, V. Helaine, L. Hecquet and W.-D. Fessner, *ChemBioChem* **13** (2012), pp. 2290–2300.

[53] N. Ocal, A. Lagarde, F. Charmantray and L. Hecquet, *ChemBioChem* **22** (2021), pp. 2814–2820.

[54] M. Lorillière, M. De Sous, F. Bruna, et al., *Green Chem.* **19** (2017), pp. 425–435.

[55] S. C. Willies, J. L. Galman and N. J. Turner, *Phil. Trans. R. Soc. A.* **374** (2016), article no. 20150084.

[56] I. Martin, V. Weiß, C. Pavlidis, M. H. Vickers and U. T. Bornscheuer, *Anal. Chem.* **86** (2014), pp. 118847–118853.

[57] M. Lorillière, R. Dumoulin, M. L'Enfant, et al., *ACS Catal.* **9** (2019), pp. 4754–4763.

[58] G. Arbia, M. Joly, L. Nauton, C. Leogrande, K. Tittmann, F. Charmantray and L. Hecquet, *ChemSusChem* (2024), article no. e202401834.

[59] K. Leang, I. Sultana, G. Takada and K. A. Izumori, *J. Biosci. Bioeng.* **95** (2003), pp. 310–312.

[60] H. Itoh and K. Izumori, *J. Ferment. Bioeng.* **81** (1996), pp. 351–353.

[61] M. M. Wamelink, E. A. Struys, E. E. W. Jansen, et al., *Mol. Genet. Metab.* **102** (2011), pp. 339–342.

[62] M. M. C. Wamelink, E. A. Struys, V. Valayannopoulos, M. Gonzales, J.-M. Saudubray and C. Jakobs, *Prenat. Diagn.* **5** (2008), pp. 460–462.

[63] S. Horii, H. Fukase, T. Matsuo, Y. Kameda, N. Asano and K. Matsui, *J. Med. Chem.* **6** (1986), pp. 1038–1046.

[64] E. P. Carpenter, A. R. Hawkins, J. W. Frost and K. A. Brown, *Nature* **394** (1998), pp. 299–302.

[65] K. Brilisauer, J. Rapp, P. Rath, et al., *Nat. Commun.* **10** (2019), article no. 545.

[66] Q. Zhang and D. Bartels, *Funct. Plant. Biol.* **43** (2017), pp. 684–694.

[67] J. Kovářová and M. P. Barrett, *Trends Parasitol.* **32** (2016), pp. 622–634.

[68] I. Fúster Fernández, L. Hecquet and W.-D. Fessner, *Adv. Synth. Catal.* **364** (2022), pp. 612–621.

[69] T. Saravanan, M.-L. Reif, D. Yi, M. Lorillière, F. Charmantray, L. Hecquet and W.-D. Fessner, *Green Chem.* **19** (2017), pp. 481–489.

[70] R. Cood, *Coord. Chem. Rev.* **252** (2008), pp. 1387–1408.

[71] E. Muri, M. Nieto, R. Sindelar and J. Williamson, *Curr. Med. Chem.* **17** (2002), pp. 1631–1653.

[72] T. Saravanan, S. Junker, M. Kickstein, et al., *Angew. Chem. Int. Ed.* **56** (2017), pp. 5358–5362.

[73] D. Yi, T. Saravanan, T. Devamani, F. Charmantray, L. Hecquet and W.-D. Fessner, *Chem. Commun.* **51** (2015), pp. 480–483.

[74] H. Casajus, A. Lagarde, M. Leremboure, et al., *ChemCatChem* **12** (2020), pp. 5772–5779.

[75] N. Ocal, G. Arbia, A. Lagarde, M. Joly, S. Gittings, K. M. Graham, F. Charmantray and L. Hecquet, *Adv. Synth. Catal.* **365** (2022), pp. 78–87.

[76] C. Zhou, T. Saravanan, M. Lorillière, D. Wei, F. Charmantray, L. Hecquet, W.-D. Fessner and D. Yi, *ChemBioChem* **18** (2017), pp. 455–459.

[77] J. H. Schrittwieser, S. Velikogne, M. Hall and W. Kroutil, *Chem. Rev.* **118** (2018), pp. 270–348.

[78] J. M. Sperl and V. Sieber, *ACS Catal.* **8** (2018), pp. 2385–2396.

[79] M. Lorillière, C. Guérard-Hélaine, V. Hélaine, et al., *ChemCatChem* **12** (2020), pp. 812–817.

[80] M. L'Enfant, F. Bruna, M. Lorillière, N. Ocal, W.-D. Fessner, L. Pollegioni, F. Charmantray and L. Hecquet, *Adv. Synth. Catal.* **361** (2019), pp. 2550–2558.

[81] L. Pollegioni, K. Diederichs, G. Molla, S. Umhau, W. Welte, S. Ghisla and M. S. Pilone, *J. Mol. Biol.* **324** (2002), pp. 535–546.

[82] L. Pollegioni, S. Iametti, D. Fessas, L. Caldinelli, L. Piubelli., A. Barbiroli, M. S. Pilone and F. Bonomi, *Protein Sci.* **12** (2003), pp. 1018–1029.

[83] N. Ocal, M. L'enfant, F. Charmantray, L. Pollegioni, J. Martin, P. Auffray, J. Collin and L. Hecquet, *Org. Process Res. Dev.* **24** (2020), pp. 769–775.

[84] H. Casajus, A. Lagarde, L. Nauton, et al., *ACS Catal.* **12** (2022), pp. 3566–3576.

[85] G. Arbia, C. Gadona, H. Casajus, L. Nauton, F. Charmantray and L. Hecquet, *Green Chem.* **26** (2024), pp. 7320–7330.

ACADÉMIE
DES SCIENCES
INSTITUT DE FRANCE

Research article

# Regioselective hydration of geraniol by *Escherichia coli* fumarases in whole-cell biotransformations

**Natalie Härterich** [#,a]**, Philip Horz** [#,a]**, Yingtong Fan** [a]**, Benjamin Aberle** [⊙,a,b] **and Bernhard Hauer** [⊙,∗,a,b]

[a] Institute of Biochemistry and Technical Biochemistry, Department of Technical Biochemistry, University of Stuttgart, 70569 Stuttgart, Germany

[b] Microbiology and Biotechnology at the Institute of Molecular Physiology, Johannes Gutenberg University Mainz, 55128 Mainz, Germany

*E-mail:* hauerber@uni-mainz.de (B. Hauer)

**Abstract.** The regioselective hydration of carbon–carbon double bonds to generate alcohols is a fundamental reaction in synthetic organic chemistry, offering pathways to valuable secondary and tertiary alcohols. Biocatalysis using hydratase enzymes, which add water to a double bond, provides a selective and sustainable alternative to traditional chemical methods. This study investigates the potential of *Escherichia coli* to hydrate the monoterpene geraniol in whole-cell biotransformation systems. Through a targeted knockout approach using the Keio collection, fumarases were identified as key contributors to geraniol hydration. Overexpression studies further revealed that FumA and FumB overexpression substantially enhanced geraniol hydration activity at the terminal alkene, suggesting promiscuity towards this non-native substrate. This result indicates an expanded substrate scope of class I fumarases beyond their established role in fumarate metabolism. By establishing a link between geraniol hydration and specific genes, we aim to extend the enzymatic toolbox for monoterpene transformations. Utilizing the inherent regioselectivity and atom economy of fumarases, the potential of fumarases as efficient biocatalysts in terpene modification could open new avenues to advance applications in green chemistry and biocatalysis.

**Keywords.** Fumarase, Hydratase, Water addition, Geraniol, Terpenes, Alkenes.

**Funding.** German Federal Ministry of Education and Research (BMBF) (grant number 031B1343A).

**Note.** This article is submitted at the invitation of the editorial committee (Juliette Martin).

*Manuscript received 13 December 2024, revised 22 March 2025, accepted 23 May 2025.*

## 1. Introduction

The chemical synthesis of alcohols remains a long-standing challenge. In addition to the time-consuming and sometimes costly preparation of the partially toxic transition metal catalysts, harmful by-products can be produced, or the reaction is dependent on multiple reaction steps (protective group chemistry), harsh reaction conditions and often does not reach the desired selectivity for chiral products [1–4]. These challenges evoke a sustained interest to explore additional or new approaches. Nature provides an ideal template, offering not only sustainable reaction conditions but also remarkable selectivity often provided by enzymes. The atom-economical, biocatalytic addition of water to alkenes offers an environmentally friendly alternative to the harsh reaction conditions of organic chemistry. Hydratases belong to the enzyme class of hydro-lyases (EC 4.2.1.X) and enable uncomplicated access to secondary and tertiary alcohols, thus opening up new possibilities for their synthesis [5].

---

[#]Contributed equally

[∗]Corresponding author

The enzymes are categorized into two groups based on their mechanism, the first group comprises hydratases that hydrate conjugated C=C double bonds in $\alpha,\beta$-unsaturated carbonyl compounds by a nucleophilic Michael addition. The second group catalyzes the addition of water to non-activated C=C double bonds by an electrophilic addition [6,7].

The second group of enzymes is present, for example, in the metabolism of terpenes, where hydratases are involved in the conversion of terpenes by hydrating specific C=C double bonds, thereby forming tertiary alcohols with high selectivity. A prominent example is that of carotenoid hydratases, which catalyze the hydration of terminal prenyl units. Based on their function and their natural substrates, these hydratases are divided into two distinct evolutionary groups, the CrtC superfamily and the CruF family. Both acyclic (e.g., lycopene) and monocyclic (e.g., $\gamma$-carotene) carotenoid substrates can be converted to their corresponding hydroxy compounds (Figure S1). An interesting representative example of this enzyme group is the membrane-bound CrtC from *Rubrivivax gelatinosus*, which can convert the $C_{40}$ carotenoid lycopene in a regioselective manner to hydroxylycopene and 1,1-dihydroxylycopene and can therefore catalyze both single and double hydration [8–10]. In addition to the hydration of carotenoids, hydratases such as kievitone hydratase and phaseollidine hydratase have been demonstrated to convert isoflavonoids, including kievitone, xanthohumol, and phaseollidine, to their corresponding hydroxy derivatives (Figure 1) [7,11,12]. In addition to very large terpenes, short-chain monoterpenes such as limonene can also be modified by hydratases. Hydrations of limonene have already been observed in yeasts and bacteria, but mostly in whole cell preparations, which means that isolated enzyme studies are rare. An exceptional case is the membrane-bound $\alpha$-terpineol dehydratase from *Pseudomonas gladioli*, which was isolated in 1992 [13]. Although the enzyme was classified as a dehydratase, its natural function was shown to be the hydration of limonene to $\alpha$-terpineol. The only published work on the heterologous expression of a limonene hydratase is by Chang et al. who expressed a limonene hydratase (LIH) from *Geobacillus stearothermophilus* in *E. coli* and converted limonene to terpineol [14,15]. Another interesting case is the bifunctional enzyme linalool dehydratase isomerase (LinD). This enzyme

catalyzes the hydration of myrcene to (*S*)-linalool and its further isomerization to geraniol, as well as the respective reverse reactions, with the formation of myrcene from geraniol being the thermodynamically preferred process [16]. In addition to natural substrates, shortened and extended linalool derivatives could also be converted [16–20].

One of the most frequently used enzymes for the conversion of non-activated C=C double bonds can be found in the cofactor-dependent fatty acid hydratases (FAHs). They catalyze the regioselective addition of water to C=C double bonds of unsaturated fatty acids to form the corresponding hydroxy fatty acids [10,19]. FAHs have attracted a lot of attention mainly due to their wide distribution in food-safe microorganisms such as *Lactobacillus* [21]. The oleate hydratase from *Elizabethkingia meningoseptica*, discovered in 1962, is the most extensively studied FAH. This enzyme catalyzes the conversion of oleic acid to 10-hydroxystearic acid. The enzyme requires flavin adenine dinucleotide (FAD) as a cofactor, but its redox state does not change during the reaction. Enzyme engineering has already opened up a broad substrate spectrum with different FAHs. Fatty acids with different chain lengths ($C_{11}$–$C_{22}$) or numbers of double bonds (up to 6) as well as oleic acid derivatives with different head groups could be converted [21–25]. In addition, shorter, non-activated alkenes ($C_5$–$C_{10}$) were also converted to the corresponding secondary alcohol using a carboxylic acid dummy substrate [26–28]. Furthermore, the acceptance of alkynes, internal alkenes, substituted alkenes, and styrene derivatives was demonstrated with this dummy substrate [26,27].

Fumarases, also known as fumarate hydratases, are enzymes catalyzing the reversible hydration of fumarate to malate, a reaction central to the citric acid cycle and ubiquitous across all kingdoms of life (Figure 2A) [29]. Prominent examples include the porcine fumarase, the *Saccharomyces cerevisiae* fumarase, and the three fumarases from *Escherichia coli* (FumA, FumB, and FumC). Fumarases are categorized into two classes: class I, dimeric enzymes that contain a 4Fe–4S cluster, and class II, comprising tetrameric, thermostable, cofactor-free enzymes that are well studied due to their robustness [30–32]. Fumarases are known for their exceptional stereoselectivity, and a narrow substrate scope [33,34]. From an early stage, halogenated derivatives of fumarate,
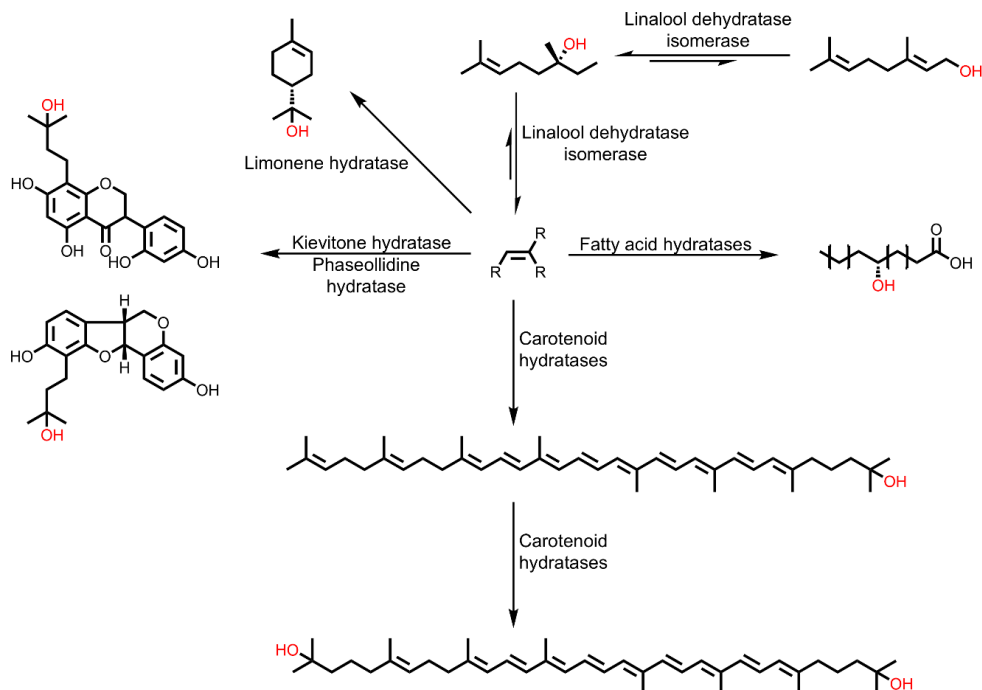
**Figure 1.** Overview of different hydratases adding water to C=C double bonds of different terpenes, terpenoids and fatty acids following the Markovnikov-rule (electrophilic addition).

such as fluorofumarate and chlorofumarate, have been demonstrated to be accepted by class II fumarases, such as the porcine fumarase, which served as an early model enzyme (Figure 2) [35,36]. In the case of FumA from *E. coli*, a member of class I fumarases, reports from 1994 state that fluorofumarate is a promiscuous substrate for hydration [37]. Moreover, it was demonstrated that a C≡C triple bond can be accepted by both fumarase classes in the hydration of acetylene dicarboxylate to oxalacetate [35]. It was also shown that the epoxide L-*trans*-2,3-epoxysuccinate can be transformed to a diol [38].

Among the fumarases of *E. coli*, FumA and FumB are class I enzymes that share 90% sequence homology [39]. FumC is a class II fumarase, like the fumarases found in eukaryotic organisms, and is therefore structurally very different from FumA and FumB [31]. The expression of the three fumarases in *E. coli* varies with oxygen availability, carbon source, and growth conditions [37,40]. While FumA predominantly mediates fumarate hydration under most conditions, FumB expression is elevated under anaerobic conditions, possibly due to its high affinity for (*S*)-malate. FumC is thought to compen-
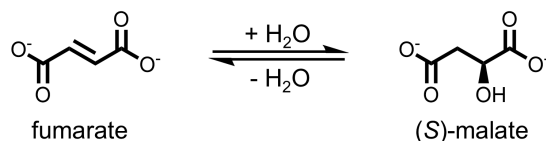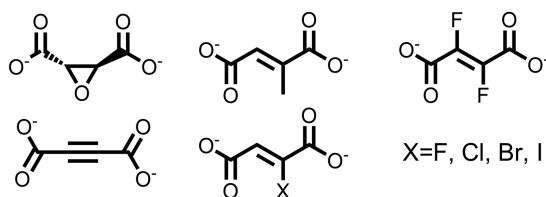


**Figure 2.** (A) Fumarases catalyze the reversible hydration of fumarate to (*S*)-malate. (B) The substrate scope reported for fumarases is limited to structures very close to fumarate and malate.

sate for the limitations of FumA and FumB during iron limitation, superoxide radical accumulation, or

elevated temperatures [30,37,40]. Notably, FumA and FumB, despite being class I fumarases, demonstrate catalytic efficiencies that are comparable to those of the class II fumarases, which are typically faster than class I [37].

Industrially, fumarases have been utilized since the 1970s for the production of (*S*)-malate. Processes employing immobilized *Brevibacterium flavum* cells and whole-cell *Corynebacterium glutamicum* have demonstrated large-scale production capabilities, reaching outputs of up to 2000 tons annually [41].

For the hydration of small dicarboxylic acids, fumarases are well-established enzymes valued for their stability and industrial utility. On the other hand, large terpene substrates are converted by, for example, carotenoid and kievitone hydratases. Internal alkenes in fatty acids can be hydrated with high selectivity and efficiency by FAHs. From a synthetic point of view, there is still a gap for a more general enzyme platform for the isoprene moiety in smaller molecules and for enzymes that can selectively add water to linear monoterpenes. Although the hydration of sesquiterpenes and geraniol has been observed in several studies utilizing fungal fermentations, these activities have yet to be attributed to specific genes or enzyme sequences [42–45]. This study revisits the catalytic potential of fumarases, proposing greater versatility regarding the substrate scope than was previously anticipated, and a potential to address the current gap in the hydration of monoterpenes.

## 2. Results and discussion

The hydration of geraniol was observed in *E. coli* strains ITB94, BL21(DE3), and BW25113 with and without a vector system, indicating that endogenous *E. coli* enzymes catalyze the reaction. The hydration does not occur spontaneously, as verified by buffer control experiments. This observation initiated an investigation to identify the specific gene responsible for this activity. To achieve this, we utilized the Keio collection, a comprehensive library of single-gene deletions in *E. coli* K-12 BW25113 [46]. From the library of 3985 strains, we selected strains lacking a gene annotated as hydratase-encoding (according to ecocyc.org) and tested 42 individual knockout strains. These strains were screened using a 96-deep-well plate assay coupled with GC-FID analysis. The

main product of the reaction was identified through a preparative-scale reaction (see Section 4.4), followed by isolation and characterization using NMR (Figures S4 and S5). By this approach, the strain lacking the enzyme responsible for the hydration activity should be identified.

Screening the selected hydratase candidates revealed varying levels of the hydration product across the knockout strains, with the notable exception of three strains: those lacking a gene for one of the three fumarases (Δ*fumA*, Δ*fumB*, Δ*fumC*; Figure 3). In these knockouts, the hydration product was entirely absent, strongly suggesting that fumarase enzymes are responsible for the observed hydration of geraniol.

Given the complete loss of product formation in Δ*fumA*, Δ*fumB* and Δ*fumC* strains, we further investigated the activity of each fumarase gene individually by overexpressing them in *E. coli* ITB94, the strain in which the hydration activity was first discovered. For this purpose, three pDHE1650 plasmids were constructed, each harboring a gene encoding for one of the fumarases (FumA, FumB or FumC). The overexpression was confirmed in whole cells (Figure S3). Given that the strain ITB94 still contains all three fumarase genes within its genome, a background conversion was expected and observed using an empty vector control (pDHE1650 without gene insert). To optimize the reaction conditions for clear differentiation between background and overexpressed enzyme activity, experiments were conducted with 50 mg/mL cell concentration, 10 mM substrate concentration, and a reaction time of 24 h. Under these conditions, the influence of the enzymes on geraniol conversion was clearly detectable, as background activity remained sufficiently low while significant hydration activity was observed for the overexpressed enzymes. The hydration of geraniol at the terminal alkene position was considerably increased by the overexpression of FumA (17-fold) and FumB (22-fold), in comparison to the empty vector control (Figure 4). In contrast, overexpression of FumC did not noticeably alter geraniol hydration activity. Besides the terminal hydration product, we also detected an internal hydration product. Overexpression of FumA and FumB also enhanced the formation of the internal hydration product by 2.4-fold and 4.5-fold, respectively (Figure 4). With FumC overexpression, no internal hydration product was detected.
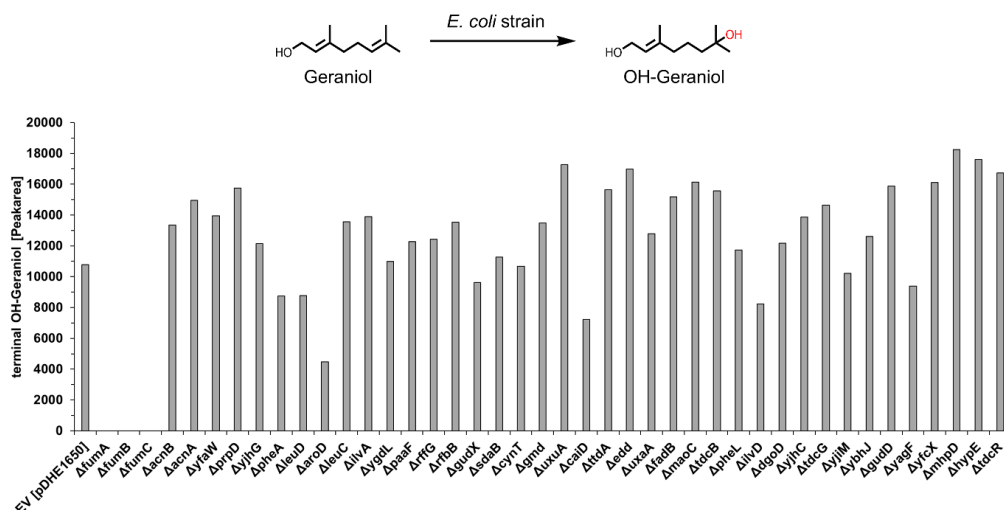
**Figure 3.** Screening of various knockout strains from the *E. coli* Keio collection to identify hydratases responsible for the conversion of geraniol. The hydration activity of different *E. coli* strains, lacking genes annotated as hydratases, was measured using 96-deep-well screening (1 mM substrate, 1% DMSO (v/v), 30 °C, 24 h, 300 rpm, extraction with 500 μL cyclohexane/ethylacetate 1:1).
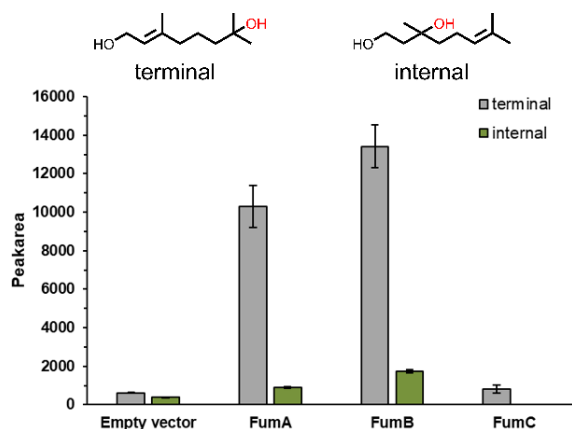


**Figure 4.** Formation of the terminal (grey) and internal (green) hydration products of geraniol with *E. coli* whole cells overexpressing one of the three fumarases (FumA, FumB, FumC) analyzed by GC-FID (10 mM substrate, 1% DMSO (v/v), 30 °C, 24 h, 300 rpm, extraction with 500 μL cyclohexane/ethylacetate 1:1). The values shown are average values from triplicates, the error bars show the standard deviation.

FumA and FumB catalyze the hydration of geraniol to a similar extent, while FumC does not demonstrate promiscuity with geraniol under the tested conditions. The similar behavior of FumA and FumB in geraniol hydration aligns with previous findings that these enzymes catalyze the fumarase reaction with nearly identical kinetic parameters [37,47]. This is also reasonable in view of the fact that they share 90% sequence similarity [39]. Notably, FumA and FumB exhibited regioselectivity for terminal hydration, with FumA achieving an 11.3-fold higher formation of the terminal hydration product and FumB a 7.8-fold higher formation of the terminal product. Slight differences between FumA and FumB have been reported before for certain substrates, such as D-tartrate, which may reflect their physiological specialization, with FumA being more relevant under aerobic and FumB under anaerobic conditions [40].

In addition to the hydration of geraniol, the reduction of geraniol to citronellol was also observed during the experiments. Among the overexpressed fumarases, cells overexpressing FumB showed an increase in geraniol reduction, while overexpression of FumA had little effect, and overexpression of FumC resulted in decreased citronellol formation (Figure S2). These results, especially those with FumC, suggest an indirect link between fumarase overexpression and geraniol reduction, emphasizing the interconnected nature of metabolic networks.

Further investigation into the specific enzymes responsible for this reduction, similar to the study presented here, could elucidate the underlying mechanisms and expand our understanding of the metabolic context surrounding these reactions.

## 3. Conclusion

Our findings demonstrate that *E. coli* fumarases might exhibit a broader substrate promiscuity than previously recognized. The hydration of the terpenoid geraniol, observed with overexpression of FumA and FumB, suggests an extension of the substrate range for these enzymes, which are considered highly specific for fumarate and only a few derivatives [33,34]. While the hydration of geraniol has been previously reported using the marine fungus *Hypocrea* sp. MFAac46-2 in a three-day fermentation [42], our study represents the first direct linkage of this activity to specific genes and their enzyme sequences. The unexpected substrate conversion by these class I fumarases, despite their more thermolabile and oxygen-sensitive nature compared to class II fumarases, may encourage a reconsideration of class I fumarases as valuable tools in biocatalysis. Furthermore, this discovery suggests that fumarases may contribute to side reactions involving terpenes and alkenes in fermentative processes. To the best of our knowledge, fumarases have not been tested for activity towards terpenes before. And since fumarases are very fast-acting enzymes on their natural substrates ($k_{cat}$ of 3100 s$^{-1}$) [37], the assay times used were often in the range of seconds and minutes, which may be a reason why much slower promiscuous reactions are not detected. The possibility of using fumarases in terpene hydration and related reactions highlights their potential as highly efficient biocatalysts, which are particularly valued for their 100% atom economy—a key attribute in sustainable chemical processes. These results underscore the promise of hydratases and fumarases as versatile tools and encourage deeper exploration of their applications in biocatalysis and green chemistry.

## 4. Experimental section

### 4.1. *Materials*

All chemicals and solvents were purchased from different suppliers (Alfa Aesar, Carl Roth GmbH, Enamine, Macherey-Nagel, Merck, Sigma-Aldrich, Thermo Fisher, VWR) without further purification. Phusion High-Fidelity DNA Polymerase and DpnI were purchased from New England Biolabs.

### 4.2. *Screening of Keio collection (knockout strains)*

#### 4.2.1. *Expression*

The investigation of the Keio Collection took place in 96-deep-well plates (DWPs). Therefore, overnight cultures were prepared in 96-DWPs by inoculating 1 mL of lysogeny broth (LB) medium containing 30 µg/mL kanamycin (knockouts) or 150 µg/mL ampicillin (empty vector) per well, with glycerol stocks of the knockout variants and empty vector controls. The plates were incubated at 37 °C and 300 rpm for 16 h in an orbital shaker. The main cultures in 96-DWPs were set up using TB-media containing either 30 µg/mL kanamycin (knockouts) or 150 µg/mL ampicillin (empty vector), inoculated with 1% overnight culture, and incubated for 24 h at 37 °C and 300 rpm in the orbital shaker. After 24 h of incubation, the plates were centrifuged at 4000 g for 20 min at 4 °C, and the harvested cells were immediately used for biotransformation experiments.

#### 4.2.2. *Biotransformation (screening)*

For biotransformations, the fresh cells were resuspended in 495 µL KPi-buffer (50 mM, pH 7.0) and 5 µL of geraniol substrate stock (100 mM substrate in DMSO; final concentration 1 mM) were added and incubated for 24 h at 30 °C and 300 rpm. The reactions were stopped by adding 500 µL of cyclohexane/ethylacetate 1:1. Extraction took place by shaking and inverting with subsequent phase separation by centrifugation at 4000 g for 10 min at room temperature. Finally, 200 µL of the organic phase was transferred into autosampler glass vials with inlets for GC-FID analysis.

### 4.3. *Cloning and biotransformations of fumarases*

#### 4.3.1. *Cloning of FumA, FumB and FumC in pDHE1650 vector*

The genes for the fumarase types FumA, FumB and FumC were successfully integrated into the

pDHE1650 vector using Gibson Assembly [48]. For PCR, the standard protocol of Phusion® High Fidelity Polymerase was used. The PCR products were digested using *Dpn*I (1 μL *Dpn*I for 25 μL PCR product, 4 h at 37 °C), purified and transformed via heat shock into *E. coli* XL1-Blue and after sequencing into ITB94 (derivate of commercial strain TG1, with L-rhamnose-isomerase knockout and two unspecific ADH—Δ*yahK* and Δ*yjgB*—knockouts).

### 4.3.2. *Expression*

Single colonies were inoculated in 5 mL overnight cultures (LB-medium with ampicillin 150 μg/mL) and incubated at 37 °C and 180 rpm. Main cultures were set up using terrific broth (TB) medium containing 150 μg/mL ampicillin and 0.5 g/L L-rhamnose (500 mL medium in 2 L Erlenmeyer flasks), inoculated with 1% overnight culture and incubated at 30 °C and 180 rpm for 24 h. Cells were harvested at 10,000 g for 30 min at 4 °C and immediately used for biotransformation experiments.

### 4.3.3. *Biotransformation*

To investigate the functionality and differences in fumarase biotransformation, experiments were conducted after expression of the cells at a 500 μL scale in 2 mL glass vials. The experimental setup included 495 μL of 50 mg/mL whole-cell suspension (FumA, B, C, or empty vector, in 50 mM NaPi, pH 7.4) mixed with 5 μL of geraniol stock (1 M in DMSO, final substrate concentration: 10 mM). The buffer control was prepared with 495 μL NaPi (50 mM, pH 7.4) and 5 μL of geraniol stock (final concentration 10 mM, in DMSO). Each reaction was performed in triplicates and incubated at 30 °C for 24 h with shaking at 300 rpm. The reaction mixtures were extracted with 500 μL of cyclohexane/ethylacetate 1:1, vortexed, and centrifuged at 4000 g at rt for 5 min. Subsequently, 200 μL of the organic phase was transferred into autosampler glass vials with inlets for further GC analysis.

### 4.4. *Semi-preparative biotransformation*

Semi-preparative biotransformations took place in 100 mL shot flasks with 100 mL of reaction volume. Therefore, cells with empty vector were cultivated as described in Section 4.3. Fresh harvested cells were resuspended in KPi-buffer (50 mM, pH 7.0) to a cell concentration of 40 $mg_{cww}$/mL and 10 mM substrate (geraniol) was added. The biotransformation was incubated for 5d at 30 °C at 200 rpm in an orbital shaker. The reaction was stopped by extracting three times with cyclohexane/ethylacetate 1:1 (in total 1 L solvent) and the pooled organic phase was concentrated in vacuo. The crude product was then dissolved in $CH_2Cl_2$ and purified by column chromatography on silica gel 60M 0.04–0.063 mm and with cyclohexane/ethylacetate 8:1 as the eluent. The determination of the product structures was achieved by NMR (additional figures in the SI).

### 4.4.1. *Terminal hydrated OH-geraniol*

Isolated product: 97.4 mg of yellow clear oil (56% isolated yield):

$^1$H NMR (500 MHz, CDCl₃) $\delta$ = 5.13 (t, $^3J_{H,H}$ = 7.1 Hz, 1H), 4.12 (d, $^3J_{H,H}$ = 7.1 Hz, 2H), 1.69 (s, 3H), 1.25 (s, 6H) ppm.

$^{13}$C NMR (125 MHz, CDCl₃) $\delta$ = 132.1, 124.2, 74.0, 59.9, 42.4, 41.7, 29.7 (2C), 21.1, 17.7 ppm.

The NMR data obtained are consistent with previously reported values [49].

### 4.4.2. *Internal hydrated OH-geraniol*

Isolated product: 6.47 mg of yellow clear oil (3.7% isolated yield):

$^1$H NMR (500 MHz, CDCl₃) $\delta$ = 5.12 (t, $^3J_{H,H}$ = 7.0 Hz, 1H), 3.96 (m, 2H), 2.05 (m, 2H), 1.83 (ddd, $^3J_{H,H}$ = 14.3, 7.0, 5.0 Hz, 1H), 1.69 (s, 4H), 1.63 (s, 3H), 1.54 (m, 2H), 1.26 (s, 3H) ppm.

$^{13}$C NMR (125 MHz, CDCl₃) $\delta$ = 132.6, 124.1, 71.3, 61.3, 42.2, 39.7, 26.9, 25.7, 22.7, 17.7 ppm.

The NMR data obtained are consistent with previously reported values [50].

### 4.5. *Gas chromatography*

To analyze the products from biotransformations, gas chromatography (GC) was used. Analysis was performed on a Shimadzu GC2010 instrument using a ZB-5 column (Zebron-Phenomenex, 30 m × 0.25 mm, 0.25 μm film) and hydrogen as carrier gas. The GC was equipped with a flame ionization detector (FID) set to 335 °C. Injections of 1 μL injection volume were performed with an inlet temperature of 260 °C in split mode (split 1:10). The oven temperature started at 110 °C with a gradient of 10 °C per min up to 300 °C, holding the end temperature for 1 min.

## Declaration of interests

## Funding

## Acknowledgements

## Supplementary data

Supporting information for this article is available on the journal's website under https://doi.org/10.5802/crchim.407 or from the author.

## References

[1] C. Wuensch, J. Gross, G. Steinkellner, K. Gruber, S. M. Glueck and K. Faber, "Asymmetric enzymatic hydration of hydroxystyrene derivatives", *Angew. Chem. Int. Ed.* **52** (2013), pp. 2293–2297.

[2] S. J. Geier, C. M. Vogels, J. A. Melanson and S. A. Westcott, "The transition metal-catalysed hydroboration reaction", *Chem. Soc. Rev.* **51** (2022), pp. 8877–8922.

[3] F. Zhang and Q. H. Fan, "Synthesis and application of bulky phosphoramidites: highly effective monophosphorus ligands for asymmetric hydrosilylation of styrenes", *Org. Biomol. Chem.* **7** (2009), pp. 4470–4474.

[4] M. Beller, J. Seayad, A. Tillack and H. Jiao, "Catalytic Markovnikov and anti-Markovnikov functionalization of alkenes and alkynes: recent developments and trends", *Angew. Chem. Int. Ed.* **43** (2004), pp. 3368–3398.

[5] H. Gröger, "Hydroxy functionalization of non-activated C-H and C=C bonds: new perspectives for the synthesis of alcohols through biocatalytic processes", *Angew. Chem. Int. Ed.* **53** (2014), pp. 3067–3069.

[6] G. Jones, "The Markovnikov rule", *J. Chem. Educ.* **38** (1961), article no. 297.

[7] B. S. Chen, L. G. Otten and U. Hanefeld, "Stereochemistry of enzymatic water addition to C=C bonds", *Biotechnol. Adv.* **33** (2015), pp. 526–546.

[8] A. Hiseni, I. W. C. E. Arends and L. G. Otten, "Biochemical characterization of the carotenoid 1,2-hydratases (CrtC) from Rubrivivax gelatinosus and Thiocapsa roseopersicina", *Appl. Microbiol. Biotechnol.* **91** (2011), pp. 1029–1036.

[9] A. Hiseni, L. G. Otten and I. W. C. E. Arends, "Identification of catalytically important residues of the carotenoid 1,2-hydratases from Rubrivivax gelatinosus and Thiocapsa roseopersicina", *Appl. Microbiol. Biotechnol.* **100** (2016), pp. 1275–1284.

[10] A. Hiseni, I. W. C. E. Arends and L. G. Otten, "New cofactor-independent hydration biocatalysts: structural, biochemical, and biocatalytic characteristics of carotenoid and oleate hydratases", *ChemCatChem* **7** (2015), pp. 29–37.

[11] P. J. Kuhn and D. A. Smith, "Isolation from Fusarium solani f. sp. phaseoli of an enzymic system responsible for kievitone and phaseollidin detoxification", *Physiol. Plant Pathol.* **14** (1979), pp. 179–190.

[12] C. S. Turbek, D. A. Smith and C. L. Schardl, "An extracellular enzyme from Fusarium solani f. sp. phaseoli which catalyses hydration of the isoflavonoid phytoalexin, phaseollidin", *FEMS Microbiol. Lett.* **94** (1992), pp. 187–190.

[13] K. R. Cadwallader, R. J. Braddock and M. E. Parish, "Isolation of α-terpineol dehydratase from Pseudomonas gladioli", *J. Food Sci.* **57** (1992), pp. 241–244.

[14] M. Engleder and H. Pichler, "On the current role of hydratases in biocatalysis", *Appl. Microbiol. Biotechnol.* **102** (2018), pp. 5841–5858.

[15] H. C. Chang, D. A. Gage and P. J. Oriel, "Cloning and expression of a limonene degradation pathway from Bacillus stearothermophilus in Escherichia coli", *J. Food Sci.* **60** (1995), pp. 551–553.

[16] B. M. Nestl, C. Geinitz, S. Popa, et al., "Structural and functional insights into asymmetric enzymatic dehydration of alkenols", *Nat. Chem. Biol.* **13** (2017), pp. 275–281.

[17] D. Brodkorb, M. Gottschall, R. Marmulla, F. Lüddeke and J. Harder, "Linalool dehydratase-isomerase, a bifunctional enzyme in the anaerobic degradation of monoterpenes", *J. Biol. Chem.* **285** (2010), pp. 30436–30442.

[18] X. Wang, J. Wang, X. Zhang, J. Zhang, Y. Zhou, F. Wang and X. Li, "Efficient myrcene production using linalool dehydratase isomerase and rational biochemical process in Escherichia coli", *J. Biotechnol.* **371–372** (2023), pp. 33–40.

[19] R. M. Demming, M. P. Fischer, J. Schmid and B. Hauer, "(De)hydratases—recent developments and future perspectives", *Curr. Opin. Chem. Biol.* **43** (2018), pp. 43–50.

[20] S. Weidenweber, R. Marmulla, U. Ermler and J. Harder, "X-ray structure of linalool dehydratase/isomerase from Castellaniella defragrans reveals enzymatic alkene synthesis", *FEBS Lett.* **590** (2016), pp. 1375–1383.

[21] A. Hirata, S. Kishino, S. B. Park, M. Takeuchi, N. Kitamura and J. Ogawa, "A novel unsaturated fatty acid hydratase toward C16 to C22 fatty acids from Lactobacillus acidophilus", *J. Lipid Res.* **56** (2015), pp. 1340–1350.

[22] J. Schmid, L. Steiner, S. Fademrecht, K. Pleiss, K. B. Otte and B. Hauer, "Biocatalytic study of novel oleate hydratases", *J. Mol. Catal. B Enzym.* **133** (2016), S243–S249.

[23] M. Engleder, G. A. Strohmeier, H. Weber, et al., "Evolving the promiscuity of Elizabethkingia meningoseptica oleate

hydratase for the regio- and stereoselective hydration of oleic acid derivatives", *Angew. Chem. Int. Ed.* **58** (2019), pp. 7480–7484.

[24] B. E. Eser, M. Poborsky, R. Dai, et al., "Rational engineering of hydratase from Lactobacillus acidophilus reveals critical residues directing substrate specificity and regioselectivity", *ChemBioChem* **21** (2020), pp. 550–563.

[25] L. E. Bevers, M. W. H. Pinkse, P. D. E. M. Verhaert and W. R. Hagen, "Oleate hydratase catalyzes the hydration of a nonactivated carbon–carbon bond", *J. Bacteriol.* **191** (2009), pp. 5010–5012.

[26] M. Gajdoš, J. Wagner, F. Ospina, A. Köhler, M. K. M. Engqvist and S. C. Hammer, "Chiral alcohols from alkenes and water: directed evolution of a styrene hydratase", *Angew. Chem. Int. Ed.* **62** (2023), article no. e202215093.

[27] R. M. Demming, S. C. Hammer, B. M. Nestl, S. Gergel, S. Fademrecht, J. Pleiss and B. Hauer, "Asymmetric enzymatic hydration of unactivated, aliphatic alkenes", *Angew. Chem.* **131** (2019), pp. 179–183.

[28] Y. R. Zhao, J. Q. Zhang, Y. C. He, et al., "Asymmetric enzymatic hydration of unactivated terminal alkenes by two promiscuous oleate hydratases mined from marine metagenome", *Mol. Catal.* **546** (2023), article no. 113249.

[29] R. M. Bock and R. A. Alberty, "Studies of the enzyme fumarase. I. Kinetics and equilibrium", *J. Am. Chem. Soc.* **75** (1953), pp. 1921–1925.

[30] S. A. Woods, S. D. Schwartzbach and J. R. Guest, "Two biochemically distinct classes of fumarase in Escherichia coli", *Biochim. Biophys. Acta (BBA)/Protein Struct. Mol.* **954** (1988), pp. 14–26.

[31] T. M. Weaver, D. G. Levitt, M. I. Donnelly, P. P. Wilkens Stevens and L. J. Banaszak, "The multisubunit active site of fumarase c from Escherichia coli", *Nat. Struct. Biol.* **2** (1995), pp. 654–662.

[32] A. Bellur, S. Das, V. Jayaraman, et al., "Revisiting the burden borne by fumarase: enzymatic hydration of an olefin", *Biochemistry* **62** (2023), pp. 476–493.

[33] K. Faber, *Biotransformations in Organic Chemistry*, Springer: Berlin, Heidelberg, 2004.

[34] J. Jin and U. Hanefeld, "The selective addition of water to C=C bonds; enzymes are the best chemists", *Chem. Commun.* **47** (2011), pp. 2502–2510.

[35] J. W. Teipel, G. M. Hass and R. L. Hill, "The substrate specificity of fumarase", *J. Biol. Chem.* **243** (1968), pp. 5684–5694.

[36] M. A. Findeis and G. M. Whitesides, "Fumarase-catalyzed synthesis of L-threo-Chloromalic acid and its conversion to 2-deoxy-D-ribose and D-erythro-Sphingosine", *J. Org. Chem.* **52** (1987), pp. 2838–2848.

[37] D. H. Flint, "Initial kinetic and mechanistic characterization of escherichia coli fumarase A", *Arch. Biochem. Biophys.* **311** (1994), pp. 509–516.

[38] F. Albright and G. J. Schroepfer, "L-trans-2,3-epoxysuccinate. A new substrate for fumarase", *Biochem. Biophys. Res. Commun.* **40** (1970), pp. 661–666.

[39] P. J. Bell, S. C. Andrews, M. N. Sivak and J. R. Guest, "Nucleotide sequence of the FNR-regulated fumarase gene (fumB) of Escherichia coli K-12", *J. Bacteriol.* **171** (1989), pp. 3494–3503.

[40] C. P. Tseng, C. C. Yu, H. H. Lin, C. Y. Chang and J. T. Kuo, "Oxygen- and growth rate-dependent regulation of Escherichia coli fumarase (FumA, FumB, and FumC) activity", *J. Bacteriol.* **183** (2001), pp. 461–467.

[41] L. Andreas, S. Karsten and W. Christian, *Industrial Biotransformations*, Wiley-VCH Verlag GmbH & Co. KGaA: Weinheim, 2006.

[42] A. S. Leutou, G. Yang, V. N. Nenkep, et al., "Microbial transformation of a monoterpene, geraniol, by the marine-derived fungus Hypocrea sp.", *J. Microbiol. Biotechnol.* **19** (2009), pp. 1150–1152.

[43] W. Abraham and H. Arfmann, "Addition of water to acyclic terpenoids by Fusarium solani", *Appl. Microbiol. Biotechnol.* **297** (1989), pp. 295–298.

[44] W. R. Abraham, "Microbial formation of caparrapidiol and derivatives from trans-nerolidol", *World J. Microbiol. Biotechnol.* **9** (1993), pp. 319–322.

[45] M. Miyazawa, H. Nankai and H. Kameoka, "Biotransformations of acyclic terpenoids, (±)-cis-nerolidol and nerylacetone, by plant pathogenic fungus, Glomerella cingulata", *Phytochemistry* **40** (1995), pp. 1133–1137.

[46] T. Baba, T. Ara, M. Hasegawa, et al., "Construction of Escherichia coli K-12 in-frame, single-gene knockout mutants: the Keio collection", *Mol. Syst. Biol.* **2** (2006), article no. 2006.0008.

[47] B. M. A. van Vugt-Lussenburg, L. van der Weel, W. R. Hagen and P. L. Hagedoorn, "Biochemical similarities and differences between the catalytic [4Fe-4S] cluster containing fumarases FumA and FumB from Escherichia coli", *PLoS ONE* **8** (2013), pp. 1–7.

[48] D. G. Gibson, L. Young, R. Y. Chuang, J. C. Venter, C. A. Hutchison and H. O. Smith, "Enzymatic assembly of DNA molecules up to several hundred kilobases", *Nat. Methods* **6** (2009), pp. 343–345.

[49] T. Kametani, K. Suzuki, H. Kurobe and H. Nemoto, "A new selenium-assisted cyclization—a biogenetic-type synthesis of Safranal", *Chem. Pharm. Bull.* **29** (1981), pp. 105–109.

[50] H. Knapp, M. Straubinger, S. Fornari, N. Oka, N. Watanabe and P. Winterhalter, "(S)-3,7-dimethyl-5-octene-1,7-diol and related oxygenated monoterpenoids from petals of Rosa damascena mill", *J. Agric. Food Chem.* **46** (1998), pp. 1966–1970.

ACADÉMIE
DES SCIENCES
INSTITUT DE FRANCE

Research article

# From characterization to biocatalytic application of two peroxygenases from *Collariella virescens* and *Daldinia caldariorum*

**Angelique Pothuizen** [#],[a], **Rosalie I. Wouters** [#],[a], **Hugo Brasselet** [a], **Thomas Hilberath** [a], **Yinqi Wu** [a] and **Frank Hollmann** [©],[*],[a]

[a] Department of Biotechnology, Delft University of Technology, Van der Maasweg 9, 2629 HX Delft, The Netherlands

*E-mail:* f.hollmann@tudelft.nl (F. Hollmann)

**Abstract.** Peroxygenases are promising biocatalysts for selective oxyfunctionalization reactions including hydroxylation, epoxidation, and sulfoxidation. In this study, we explore the activity of two recently reported peroxygenases from *Collariella virescens* (*Cvi*UPO) and *Daldinia caldariorum* (*Dca*UPO) in a range of synthetically relevant transformations. Both enzymes were heterologously expressed in *Escherichia coli* and tested for various oxidative reactions. *Dca*UPO generally demonstrated higher activity compared to *Cvi*UPO across several substrates, showing significant conversions in alcohol and arene oxidations as well as enantioselective epoxidations of styrene derivatives. Notably, the enzymes exhibited complementary selectivities in several reactions including allylic hydroxylation and benzylic oxidation. These results broaden the substrate scope of *Cvi*UPO and *Dca*UPO and highlight their potential for industrial applications. However, challenges with enzyme expression in *E. coli* remain, necessitating future work on alternative expression systems such as *Pichia pastoris* to improve yields.

## 1. Introduction

Selective oxyfunctionalization, that is, the regio- and enantioselective insertion of an oxygen atom into (nonactivated) C–H bonds still represents one of the major challenges for organic synthesis. Among the biocatalytic methods (striking by their high selectivity), peroxygenase-catalyzed oxyfunctionalization reactions have been receiving particular interest [1–3]. Particularly, heme-containing enzymes catalyze

a broad range of synthetically relevant oxyfunctionalization reactions. The catalytically active species in these enzymes is the so-called Compound I (CpdI, a highly reactive oxyferryl heme species). Compared to P450 monooxygenase-catalyzed oxyfunctionalization reactions [4], peroxygenases are marked by their simplicity owing to the following reason. Instead of relying on complex and weak electron transport chains to generate CpdI via reductive activation of $O_2$ as in the case of P450 monooxygenases, unspecific peroxygenases (UPOs) form CpdI directly from $H_2O_2$ (Scheme 1).

The enormous synthetic potential of UPOs is exemplified by their outstanding performance in terms of total turnover numbers [5,6] and productivity

[#]Contributed equally

[*]Corresponding author
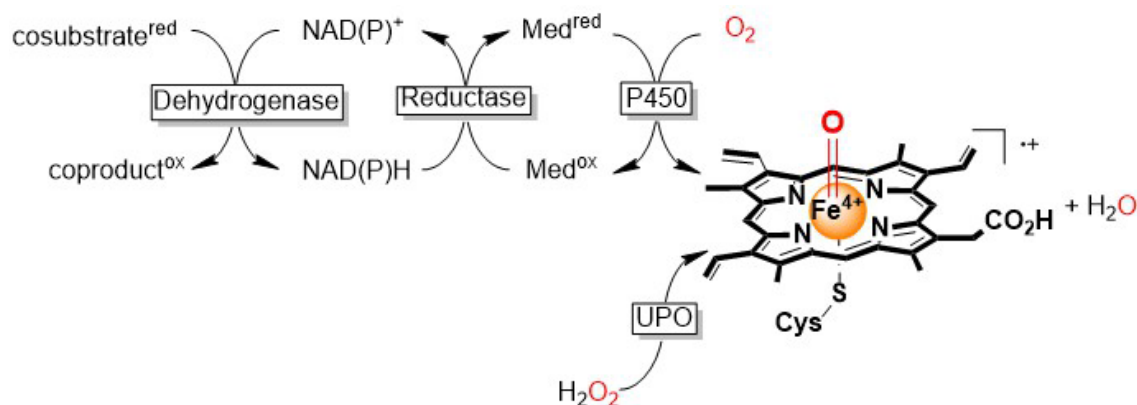
**Scheme 1.** Comparison of Compound I (CpdI) formation in the case of P450 monooxygenases and peroxygenases (UPOs).

achievable [7]. Frequently, UPOs outperform their P450 monooxygenase counterparts [8].

However, one current drawback of UPOs is the rather narrow substrate scope, which can be assigned to the yet low number of practical UPOs and UPO-mutants reported so far [9–15]. Hence, broadening the scope of UPOs available is mandatory to address this limitation.

Recently, two new UPOs from the ascomycetes *Collariella virescens* (*Cvi*UPO) and *Daldinia caldariorum* (*Dca*UPO) have been reported for the oxyfunctionalization of fatty acids [16–22]. Both enzymes have been expressed in *Escherichia coli* and preliminarily evaluated for alkane hydroxylation. Though alkane hydroxylation (e.g., on renewable fatty acids) is of tremendous interest for the synthesis of polyester precursors, it represents only a fraction of chemically relevant oxyfunctionalization reactions.

We therefore set out to further explore the scope of *Cvi*UPO and *Dca*UPO for more oxyfunctionalization reactions.

## 2. Materials and methods

### 2.1. *Expression of UPO genes in E. coli*

The pET-28a plasmids containing gene sequences for the UPOs from *C. virescens* or *D. caldariorum* (SI 1) were transformed into chemically competent *E. coli* BL21 (DE3). Recombinant *E. coli* strains were grown in autoinduction media (12 g·L$^{-1}$ peptone, 24 g·L$^{-1}$ yeast extract, 15 mg·L$^{-1}$ glucose, 220 mg·L$^{-1}$ lactose,

6.3 g·L$^{-1}$ glycerol, 90 mM KPi buffer, pH 7.0) for 4 days at 16 °C and 140 rpm [23]. Production cultures were inoculated to an optical density at 600 nm (OD$_{600}$) of 0.05 from overnight precultures. When the cells reached an OD$_{600}$ of 0.5, 5-aminolevulinic acid (5-Ala) and FeSO$_4$ were added to final concentrations of 500 μM and 0.1 M, respectively.

### 2.2. *Preparation of crude cell extract*

After cultivation, cells were harvested by centrifuging at 17,500× $g$ for 30 min at 4 °C. The supernatant was discarded, and the remaining cell pellets were washed with 50 mM phosphate buffer (pH 7.0). The remaining cells were resuspended in the same buffer at a concentration of 50 g/L after which the cells were disrupted during three consecutive cycles using a CF1 Cell Disruptor from Constant Systems at 1.5 kbar. The remaining solution after cell disruption was spun down for 30 min at 36,635× $g$ and 4 °C. The supernatant containing the enzymes was stored at −20 °C until further use.

### 2.3. *ABTS activity assays*

To determine the peroxidase activity of the UPOs, a photometric assay using 2,2′-azinobis-(3-ethylbenzothiazoline-6-sulfonic acid) (ABTS) as the substrate was performed. Citric acid buffer of 850 μL 100 mM (pH 4.4) was mixed with 50 μL 10 mM ABTS and 50 μL CFE (diluted if necessary). The reaction was started with the addition of 2 mM H$_2$O$_2$

**Table 1.** ABTS activity determination of *E. coli* cell extracts

| Enzyme | *E. coli* BL21 empty vector | *Dca*UPO | *Cvi*UPO |
|---|---|---|---|
| Activity (U·mg$^{-1}$) | 0.006 ± 0.0004 | 0.034 ± 0.002 | 0.662 ± 0.167 |

(final concentration). The increase in absorption at 420 nm was tracked for 90 s in a Cary 60 UV–Vis Spectrophotometer (Agilent Technologies). The linear slope between 20 and 80 s was used to calculate the volumetric activity (U·ml$^{-1}$) using the extinction coefficient for ABTS ($\varepsilon_{420} = 36.0$ mM$^{-1}$·cm$^{-1}$). 1 U is defined as the amount of enzyme required to convert 1 µmol substrate in 1 min under assay conditions.

## 2.4. *CO-difference spectra*

The amount of UPO present in the CFE was determined using CO-difference spectra. 950 µL of the enzyme was diluted in 50 mM phosphate buffer (pH 7). A baseline spectrum was recorded between 400 and 500 nm, after which the sample was shortly exposed to CO. Next, 50 µL of 1 M Na$_2$S$_2$O$_4$ was added and the difference spectrum between 400 and 500 nm was recorded. Per sample, 10 spectra with 30 s intervals were recorded to obtain the maximum difference spectra. Measurements were carried out in duplicate. The UPO concentration was calculated using the difference in absorption at 490 nm and the maximum absorption value at 446 nm (*Dca*UPO) and 442 nm (*Cvi*UPO). Because the extinction coefficients for these enzymes are so far unknown, the general P450 extinction coefficient in CO-difference spectra of 91 mM$^{-1}$·cm$^{-1}$ was used [24].

## 2.5. *Substrate screening assays*

Substrate screening was performed under the same reaction conditions with a total reaction volume of 500 µL. Reactions were performed in 50 mM phosphate buffer (pH 7) with 1 µM UPO and 5 mM of the substrate in 10 vol% ACN using a feeding rate of 2 mM H$_2$O$_2$ per hour. As the negative control, CFE of *E. coli* transformed with an empty vector containing no peroxygenase gene was used. Reactions were continued for 3 h at 25 °C and 600 rpm in an Eppendorf Thermomixer. Reaction mixtures were analyzed using gas chromatography (GC); detailed GC protocols can be found in supplementary information (SI 2).

## 3. Results and discussion

### 3.1. *Cloning and expression of CviUPO and DcaUPO*

*Dca*UPO and *Cvi*UPO were produced in recombinant *E. coli* BL21 (DE3) containing the respective pET28a-expression plasmids. Typically cells were cultivated in Studier's autoinduction medium [23] for 4 days at 16 °C and 140 rpm. After cultivation, *E. coli* cells were harvested and disrupted resulting in crude cell extract containing the UPOs of interest. An SDS-PAGE analysis revealed that both genes were overexpressed upon induction but mostly yielded the desired UPOs as an insoluble fraction (Figure 1).

Nevertheless, correct folding of the UPOs in the soluble lysate was confirmed though recording of CO-difference spectra, showing the characteristic shift of the Soret peak from 420 to 442 (*Cvi*UPO) and 446 nm (*Dca*UPO) when CO is bound to the reduced heme cofactor (Figure 2). Based on the abundance of the 450 nm peak, we estimated the UPO titers to be 8.4 mg·L$^{-1}$ and 5.8 mg·L$^{-1}$ for *Cvi*UPO and *Dca*UPO, respectively.

Soluble production of the UPOs was further confirmed by measuring the peroxidase activity. The peroxidase activity of the produced UPOs was tested with an ABTS assay using crude cell extract (Table 1).

### 3.2. *Oxidation reactions*

Having *Cvi*UPO and *Dca*UPO in hand, we investigated their applicability for several chemical transformations of interest. Among them, we investigated C–H bond hydroxylation reactions, alcohol oxidations, epoxidation reactions, and sulfoxidation reactions.

#### 3.2.1. *Oxidation of alcohols*

A selection of primary and secondary alcohols was subjected to *Cvi*UPO- and *Dca*UPO-catalyzed conversion. Already, the semi-quantitative screening revealed some interesting observations (Figure 3). First, *Dca*UPO generally was more active than
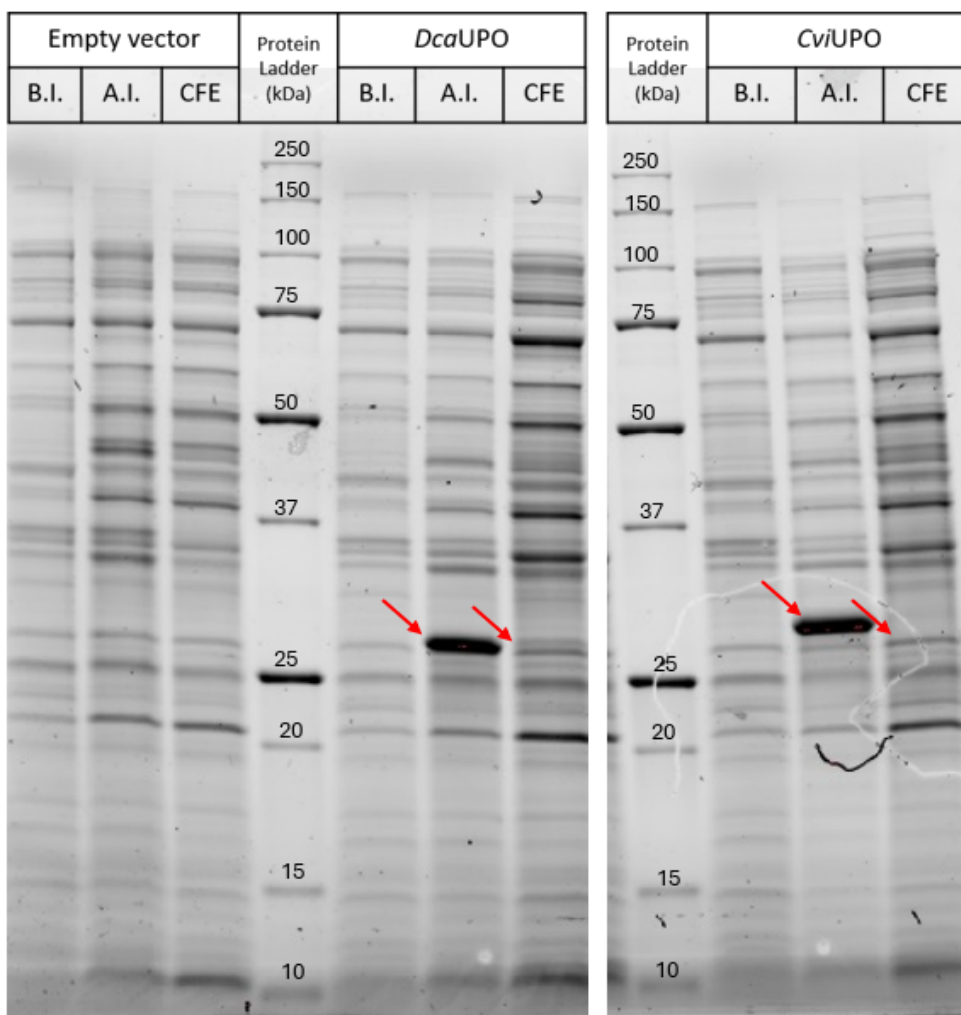
**Figure 1.** SDS-PAGE analysis of the *E. coli* production of *Dca*UPO and *Cvi*UPO. Lanes marked with B.I. and A.I. are whole-cell SDS samples before and after induction of protein expression, respectively. CFE samples show proteins in the supernatant after cell disruption. CFE SDS samples have been normalized to a protein concentration of 1 mg/mL based on BC assay. The Bio-Rad Precision Plus Protein™ Unstained Protein Standards ladder was used for size reference.

*Cvi*UPO. Second, both enzymes exhibited a clear preference for secondary alcohols over primary alcohols. The latter observation is in line with the lower C–H bond dissociation energy of secondary alcohols compared to primary alcohols. Rhododendrol was not converted by any of the UPOs, possibly due to steric hindrance.
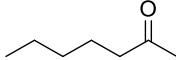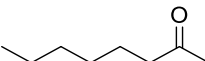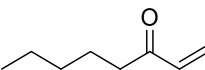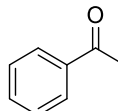
The transformations of 2-heptanol, 2-octanol, oct-1-en-3-ol, and 1-phenyl ethanol were analyzed in more detail based on calibration curves with authentic standards (Table 2). Chiral GC analysis of

the *Dca*UPO-catalyzed oxidation reactions showed that both enantiomers of, for example, 2-octanol or 1-phenyl ethanol were converted at roughly the same rate with a slight preference for the (*R*)-enantiomers (SI 3).

### 3.2.2. *Oxidation of arenes*

Next, a range of substituted arenes were evaluated (Figure 4). Like the oxidation of alcohols, *Dca*UPO generally exhibited a significantly higher activity as compared to *Cvi*UPO. Toluene was not converted

**Table 2.** Quantitative analysis of some alcohol oxidations catalyzed by *Dca*UPO and *Cvi*UPO

| Product[a] | UPO | Concentration [mM][a] | TN (UPO)[b] |
|---|---|---|---|
| 2-heptanone | *Dca*UPO | 1.42 | 1417 |
| | *Cvi*UPO | 0.36 | 358 |
| 2-octanone | *Dca*UPO | 1.43 | 1425 |
| | *Cvi*UPO | 0.44 | 437 |
| oct-1-en-3-one | *Dca*UPO | 0.9 | 899 |
| acetophenone | *Dca*UPO | 0.62 | 618 |
| | *Cvi*UPO | 0.24 | 243 |

[a] Based on authentic standards; [b] TN = $c$(product) $\times$ $c$(UPO)$^{-1}$.
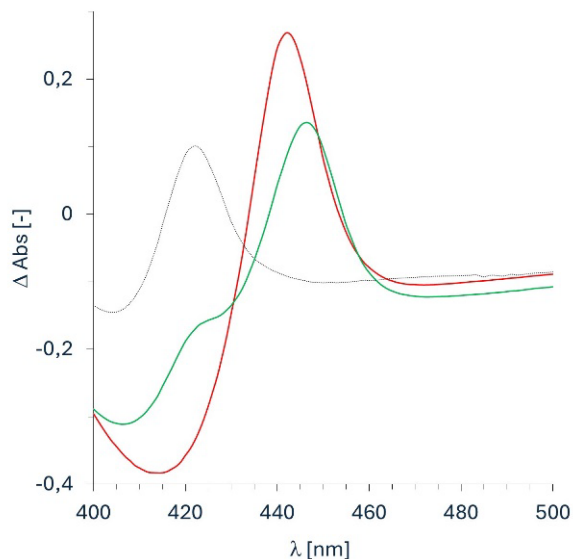


**Figure 2.** CO-difference spectra of *E. coli* cell crude extracts expressing *Cvi*UPO (—, red) and *Dca*UPO (—, green) compared to the negative control (empty vector, ⋯).

by either UPO whereas ethyl benzene, 4-phenyl-2-butanone (containing elongated alkyl substituents), and pseudocumene (1,2,4-trimethyl benzene) as well as p-cymene (4-isopropyl toluene) and thymol (2-isopropyl-5-methylphenol or 3-hydroxy p-cymene) were converted at least by *Dca*UPO.

*Dca*UPO-catalyzed conversion of ethyl benzene yielded (*R*)-1-phenyl ethanol in very modest enantiomeric excess (ee) of 55%. Furthermore, some overoxidation to acetophenone was observed. With toluene, no apparent transformation was observed, which may be explained by the higher C–H bond strength of benzylic CH$_3$ group compared to the benzylic CH$_2$ group in the case of ethyl benzene. Interestingly, however, pseudocumene (1,3,4-trimethyl benzene) was converted comparably well. Possibly the electron-donating effect of the additional CH$_3$ groups already sufficed to activate the CH$_3$ group converted. Preliminary GC- and GC/MS data suggest selective CH$_3$ hydroxylation (SI). Future, preparative-scale transformations will yield sufficient amounts for more detailed structure elucidation. *p*-Cymene, containing a highly activated tertiary C–H group, however, was almost not converted. Possibly steric effects impeding the interaction of the bulky CH(CH$_3$)$_2$ with CpdI dominated the electronic activation.

Thymol was accepted by both UPOs with a notable difference with respect to selectivity; while the
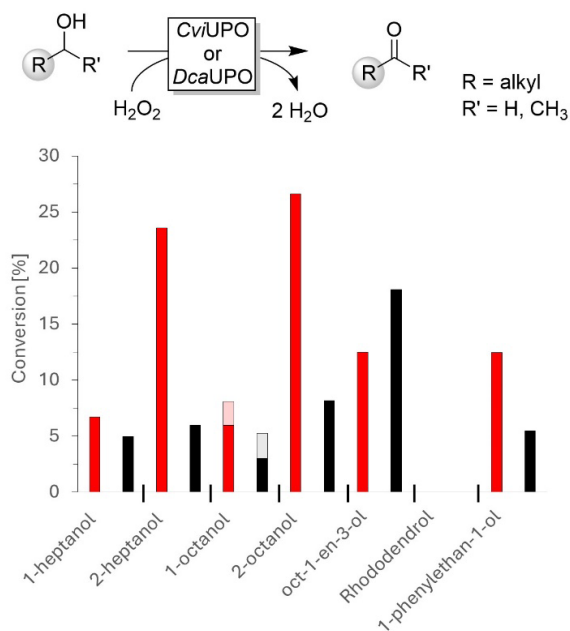
**Figure 3.** Substrate screening of selected alcohols using *Dca*UPO (red) and *Cvi*UPO (black). Conditions: $c$(UPO) = 1 µM, $c$(substrate) = 5 mM, buffer: 50 mM NaPi buffer, pH = 7.0, containing 10% ($v/v$) of acetonitrile. $H_2O_2$ addition: 2 mM per hour (from 100 mM stock). $T$ = 25 °C, orbital shaking at 600 rpm, reaction time = 3 h. Red/black: estimated conversion into the envisaged carbonyl product (aldehyde or ketone), light red/gray: yet undefined side product.



**Figure 4.** Substrate screening of some substituted arenes using *Dca*UPO (top) and *Cvi*UPO (bottom). Conditions: $c$(UPO) = 1 µM, $c$(substrate) = 5 mM, buffer: 50 mM NaPi buffer, pH = 7.0, containing 10% ($v/v$) of acetonitrile. $H_2O_2$ addition: 2 mM per hour (from 100 mM stock). $T$ = 25 °C, orbital shaking at 600 rpm, reaction time = 3 h. Blue: estimated conversion into the envisaged carbonyl product (aldehyde or ketone), red: yet undefined side product.

*Dca*UPO-catalyzed transformation was apparently highly selective, with *Cvi*UPO at least four different products were observed. The occurrence of multiple products may be attributed to the peroxidase activity of UPOs with activated arenes such as phenols resulting in radical-coupling products [19–21]. We therefore compared the *Dca*UPO-catalyzed conversion of thymol in the presence and absence of ascorbic acid, a well-established radical scavenger (Figure 5). Indeed, the product spectrum completely changed; GC-MS analysis suggested thymoquinone being the main product in the absence of ascorbic acid and the corresponding thymohydroquinone.

Interestingly, 4-phenyl-2-butanone was converted by *Dca*UPO while in the case of structurally related rhododendrol, no conversion was detectable. It is

also interesting to note that three different products were observed exhibiting M+ peaks of 164, 146, and 106. This may be rationalized by assuming that
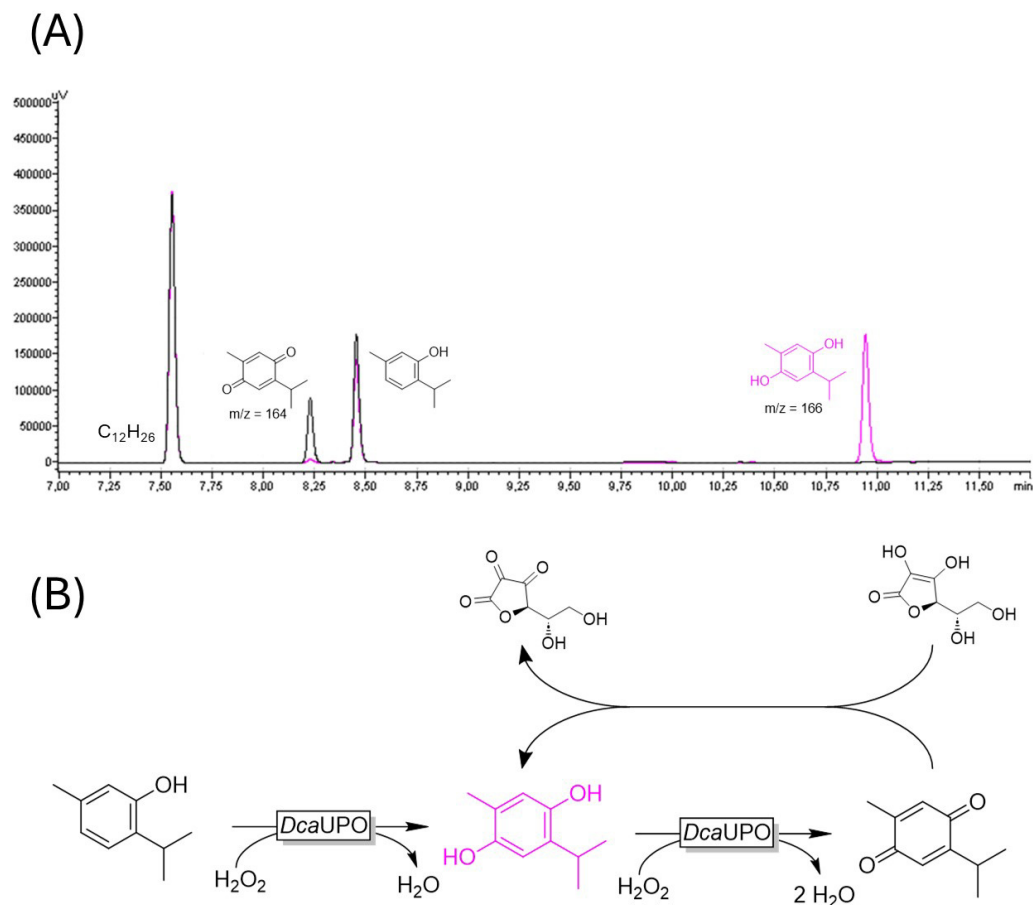
**Figure 5.** (A) GC chromatograms of thymol without the addition of ascorbic acid (black) and with the addition of 20 mM ascorbic acid (pink). (B) Suggested reaction pathway.

*Dca*UPO catalyzed the benzylic hydroxylation of the starting material (resulting in the main product with a putative molar mass of 164 g·mol$^{-1}$). The latter may spontaneously undergo either dehydration (yielding the product with a putative molar mass of 146 g·mol$^{-1}$) or a retro-aldol reaction resulting in benzaldehyde ($M_W$ = 106 g·mol$^{-1}$ and acetone, which under current analytical conditions was not detectable) (Scheme 2).

### 3.2.3. *Epoxidation reactions*

Next to hydroxylation reactions, epoxidations are of significant interest for organic synthesis. Therefore, we evaluated the activity of *Dca*UPO and *Cvi*UPO with some styrene derivatives (Figure 6).

First, the activity difference between *Dca*UPO and *Cvi*UPO was not as pronounced as for the transformations discussed before. The enantiose-lectivity of the epoxidation reactions was highly dependent on the alkene substitution pattern. Styrene oxide was obtained with rather low (*S*)-selectivity (24 and 34% ee) with *Dca*UPO and *Cvi*UPO, respectively. In contrast, epoxides obtained from α-methyl styrene were essentially optically pure. Interestingly, *Dca*UPO yielded the (*R*)-enantiomer whereas *Cvi*UPO produced the (*S*)-enantiomer exclusively. Moreover, in the case of *cis*-β-methyl styrene both enzymes were enantiocomplementary albeit again with rather low enantioselectivities. Expectedly, the epoxides obtained from *trans*-β-methyl styrene were enantiomeric to those obtained from the *cis*-starting material, again with poor enantioselec-tivity. It is worth noting that with *trans*-β-methyl styrene, the main products observed with *Cvi*UPO
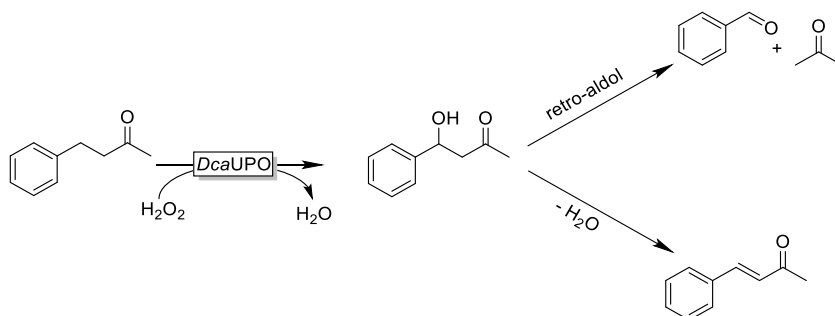
**Scheme 2.** Hypothesized benzylic hydroxylation of 4-phenyl-2-butanone followed by (spontaneous) dehydration and/or retro-aldol reaction.
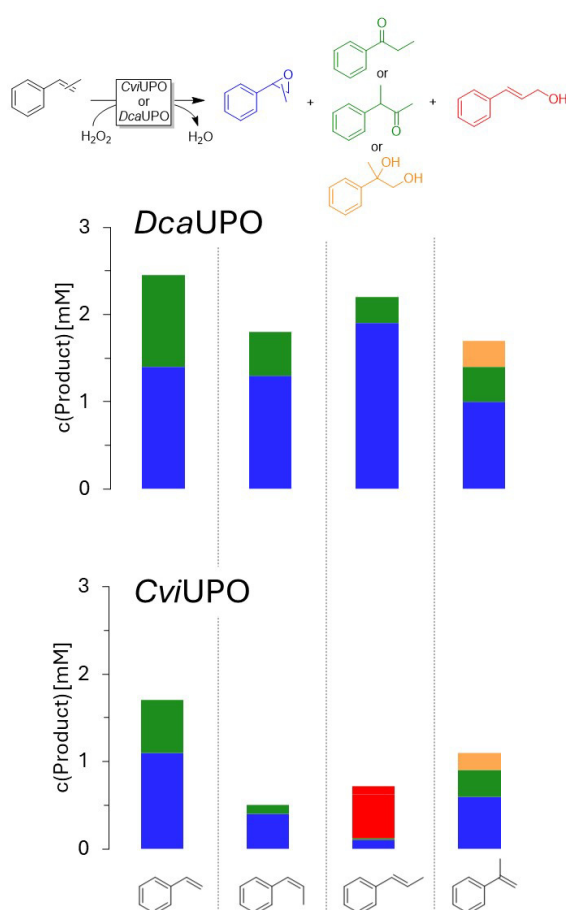


**Figure 6.** Product distribution of the *Dca*UPO- and *Cvi*UPO-catalyzed epoxidation of some styrene derivatives. Conditions: [UPO] = 1 μM, [substrate] = 5 mM, buffer: 50 mM NaPi buffer, pH = 7, containing 10% (*v*/*v*) of acetonitrile. $H_2O_2$ addition: 2 mM per hour (from 100 mM stock). *T* = 25 °C, orbital shaking at 600 rpm, reaction time = 3 h.

were allylic hydroxylation products (alcohol and aldehyde).

Terpenes such as limonene, α-pinene, and β-ionone were converted at low selectivity (Figure 7). One notable exception was the rather selective hydroxylation of β-ionone to the 4-hydroxy product.

### 3.2.4. *Sulfoxidation reactions*

Finally, we evaluated (*p*-Me-)thioanisole as the substrate for sulfoxidation (Figure 8). Both UPOs exhibited significant activity but were not completely selective for the sulfoxide products as in both cases sulfone formation was also observable.

## 4. Conclusions

In conclusion, with this contribution we have broadened the known substrate scope of *Cvi*UPO and *Dca*UPO. In addition to the previously reported ω-1 hydroxylation activity, both enzymes are also capable of other typical peroxygenase reactions. Some reactivities such as the formation of β-hydroxy ketones and selective allylic hydroxylation, however, stand out from the regular portfolio and certainly deserve further investigation and rationalization. Currently, the poor performance of the *E. coli* based expression system presents the major hurdle en route to further investigation and upscaling. Our focus in further investigations will be on producing these enzymes via *Pichia pastoris* based expression systems.

## Declaration of interests

The authors do not work for, advise, own shares in, or receive funds from any organization that could
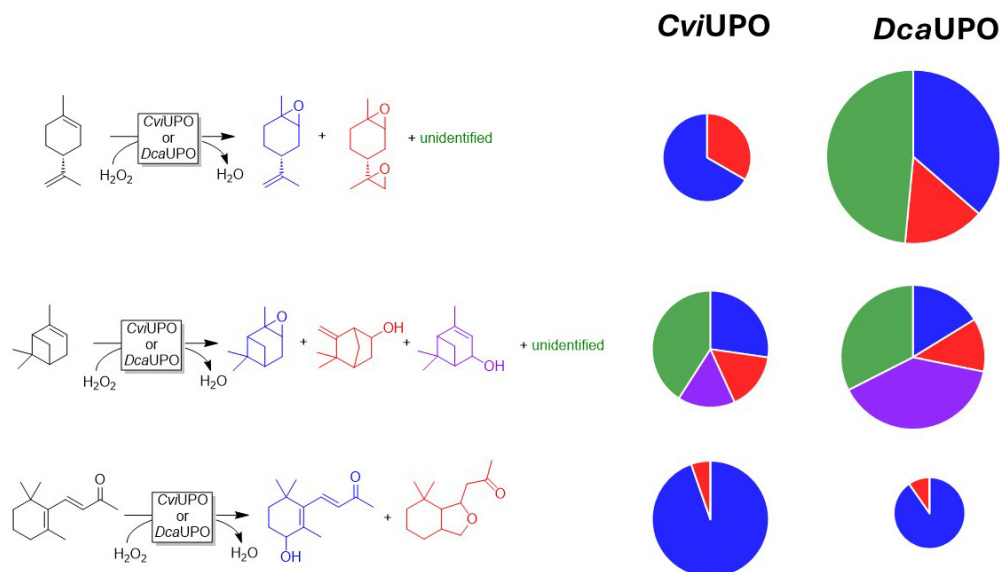
**Figure 7.** Selection of terpene hydroxylation reactions catalyzed by *Dca*UPO and *Cvi*UPO. Conditions: [UPO] = 1 μM, [substrate] = 5 mM, $H_2O_2$ feeding rate = 2 mM·h$^{-1}$, performed in phosphate buffer (50 mM, pH = 7, NaPO$_4$) with 10% ($v/v$) acetonitrile for 3 h (25 °C, 600 rpm).



|          |          |            |             |
|----------|----------|------------|-------------|
| R = H    | *Cvi*UPO | 4.5 ± 0.3  | n.d.        |
|          | *Dca*UPO | 3.9 ± 0.1  | 0.2 ± 0.01  |
| R = CH$_3$ | *Cvi*UPO | 5 ± 0.1    | 0.8 ± 0.2   |
|          | *Dca*UPO | 3.7 ± 0.2  | < 0.1       |
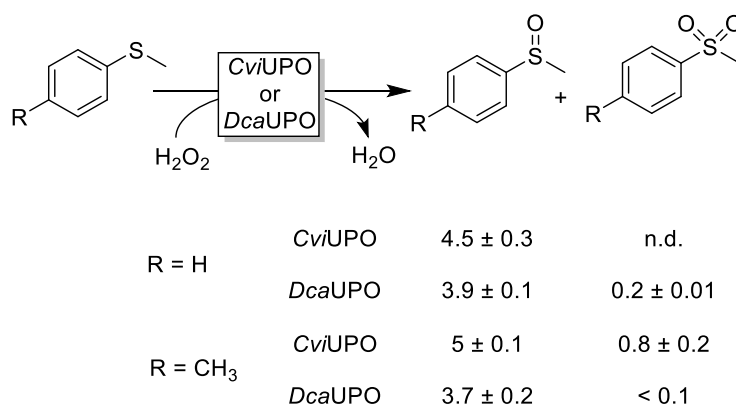
**Figure 8.** Sulfoxidation of *p*-methylthioanisole. Reaction conditions: [UPO] = 1 μM, [substrate] = 5 mM, $H_2O_2$ feeding rate of 2 mM·h$^{-1}$, performed in phosphate buffer (50 mM, pH = 7, NaPO$_4$) with 10% ($v/v$) acetonitrile for 3 h (25 °C, 600 rpm). Unfortunately, our current analytical setup does not permit baseline separation of sulfoxide enantiomers, which is why no information about the optical purity of the sulfoxide can be given.

## Supplementary data

Supporting information for this article is available on the journal's website under https://doi.org/10.5802/crchim.375 or from the author.

# References

[1] M. Hobisch, D. Holtmann, P. G. de Santos, M. Alcalde, F. Hollmann and S. Kara, *Biotechnol. Adv.* **51** (2021), article no. 107615.

[2] D. T. Monterrey, A. Menés-Rubio, M. Keser, D. Gonzalez-Perez and M. Alcalde, *Curr. Opin. Green Sustain. Chem.* **41** (2023), article no. 100786.

[3] A. Beltrán-Nogal, I. Sánchez-Moreno, D. Méndez-Sánchez, P. Gómez de Santos, F. Hollmann and M. Alcalde, *Curr. Opin. Struct. Biol.* **73** (2022), article no. 102342.

[4] R. Bernhardt and V. B. Urlacher, *Appl. Microbiol. Biotechnol.* **98** (2014), pp. 6185–6203.

[5] N. Teetz, S. Lang, A. Liese and D. Holtmann, *Chem. Cat. Chem.* **16** (2024), article no. e202400908.

[6] L.-E. Meyer, B. Fogtmann Hauge, T. Müller Kvorning, P. De Santis and S. Kara, *Catal. Sci. Technol.* **12** (2022), pp. 6473–6485.

[7] T. Hilberath, R. van Oosten, J. Victoria, H. Brasselet, M. Alcalde, J. M. Woodley and F. Hollmann, *Org. Proc. Res. Dev.* **27** (2023), pp. 1384–1389.

[8] X. Xu, T. Hilberath and F. Hollmann, *Curr. Opin. Green Sustain. Chem.* **39** (2023), article no. 100745.

[9] J. Münch, N. Dietz, S. Barber-Zucker, F. Seifert, S. Matschi, P. Püllmann, S. J. Fleishman and M. J. Weissenborn, *ACS Catal.* **14** (2024), pp. 4738–4748.

[10] J. Münch, J. Soler, N. Hünecke, D. Homann, M. Garcia-Borràs and M. J. Weissenborn, *ACS Catal.* **13** (2023), pp. 8963–8972.

[11] A. Knorrscheidt, J. Soler, N. Hünecke, P. Püllmann, M. Garcia-Borràs and M. J. Weissenborn, *Catal. Sci. Technol.* **11** (2021), pp. 6058–6064.

[12] K. Ebner, L. J. Pfeifenberger, C. Rinnofner, V. Schusterbauer, A. Glieder and M. Winkler, *Catalysts* **13** (2023), article no. 206.

[13] P. Püllmann and M. J. Weissenborn, *ACS Synth. Biol.* **10** (2021), pp. 1360–1372.

[14] A. Knorrscheidt, J. Soler, N. Hünecke, P. Püllmann, M. Garcia-Borràs and M. J. Weissenborn, *ACS Catal.* **11** (2021), pp. 7327–7338.

[15] P. Gomez de Santos, I. Mateljak, M. D. Hoang, S. J. Fleishman, F. Hollmann and M. Alcalde, *J. Am. Chem. Soc.* **145** (2023), pp. 3443–3453.

[16] D. Linde, E. Santillana, E. Fernández-Fueyo, A. González-Benjumea, J. Carro, A. Gutiérrez, A. T. Martínez and A. Romero, *Antioxidants* **11** (2022), article no. 891.

[17] E. D. Babot, C. Aranda, J. Kiebist, K. Scheibner, R. Ullrich, M. Hofrichter, A. T. Martínez and A. Gutiérrez, *Antioxidants* **11** (2022), article no. 522.

[18] A. González-Benjumea, G. Marques, O. M. Herold-Majumdar, J. Kiebist, K. Scheibner, J. C. del Río, A. T. Martínez and A. Gutiérrez, *Front. Bioeng. Biotechnol.* **8** (2021), article no. 605854.

[19] A. González-Benjumea, D. Linde, J. Carro, R. Ullrich, M. Hofrichter, A. T. Martínez and A. Gutiérrez, *Antioxidants* **10** (2021), article no. 1888.

[20] D. Linde, A. Olmedo, A. González-Benjumea, et al., *Appl. Environ. Microbiol.* **86** (2020), article no. e02899-19.

[21] A. Gonzalez-Benjumea, J. Carro, C. Renau-Minguez, D. Linde, E. Fernandez-Fueyo, A. Gutierrez and A. T. Martinez, *Catal. Sci. Technol.* **10** (2020), pp. 717–725.

[22] T. Li, R. Jin, B. Wu, D. Lan, Y. Ma and Y. Wang, *Chin. Chem. Lett.* **35** (2024), article no. 108701.

[23] F. W. Studier, *Prot. Express. Purif.* **41** (2005), pp. 207–234.

[24] T. Omura and R. Sato, *J. Biol. Chem.* **239** (1964), pp. 2370–2378.

ACADÉMIE
DES SCIENCES
INSTITUT DE FRANCE

Review article

# Hybrid catalysis: an efficient tool for biomass valorization and for the production of new building blocks in chemistry

**Sara Arteche Echeverría** [®],[a],[b], **Rénato Froidevaux** [®],[c], **Sarah Gaborieau** [a],
**Anne Zaparucha** [®],[d] **and Egon Heuson** [®],[*],[a]

[a] Univ. Lille, CNRS, Centrale Lille, Univ. Artois, UMR 8181-UCCS-Unité de Catalyse et Chimie du Solide, F-59000 Lille, France

[b] Early Development Chemistry, Sanofi, 1 impasse des Ateliers, 94400 Vitry-sur-Seine Cedex, France

[c] UMR Transfrontalière BioEcoAgro No 1158, Univ. Lille, INRAE, Univ. Liège, UPJV, JUNIA, Univ. Artois, Univ. Littoral Côte d'Opale, Institut Charles Viollette, 59655 Villeneuve d'Ascq, France

[d] Génomique Métabolique, Genoscope, Institut François Jacob, CEA, CNRS, Univ Evry, Université Paris-Saclay, Evry, France

*E-mail:* egon.heuson@centralelille.fr (E. Heuson)

**Abstract.** The unsustainable exploitation of finite natural resources, such as oil reserves, has accelerated resource depletion and harmed biodiversity, with projections indicating the exhaustion of oil reserves by mid-century. This pressing issue highlights the necessity for sustainable consumption and production models. Chemistry has responded by adopting Green Chemistry principles, emphasizing renewable and alternative raw materials over fossil-based ones. Biomass, particularly from unexploited wastes, stands out as a renewable carbon source, but its complex composition creates challenges for chemical transformations. Catalysis is critical in addressing these issues. While traditional chemical catalysts struggle with the intricate mixtures in biomass, biological catalysts, like enzymes, excel in processing such substrates due to their natural specificity and efficiency. However, enzymes face limitations from biomass inhibitors, such as plant-derived defense molecules. Innovative catalytic systems are needed to selectively target specific molecules and mitigate inhibitors. A promising solution lies in hybrid catalysis, which combines biological and chemical catalysts to leverage their complementary strengths. Indeed, hybrid systems enable multi-steps reactions with higher yields, equilibrium shifts, and inhibitor removals, promoting the synthesis of new molecules from challenging substrates. Over the past decade, hybrid catalysis has expanded thanks to its potential to transform biomass into valuable compounds. By integrating the robustness of chemical catalysts with the selectivity of biological ones, hybrid catalysis aligns with sustainability objectives, offering a pathway to more efficient and innovative chemical transformations. This emerging technology can play a pivotal role in sustainable development and industrial innovation, especially when it comes to biorefineries.

**Keywords.** Hybrid catalysis, Biomass, Platform molecules, Enzymes, Chemical catalysts, Green Chemistry.

**Funding.** ANRT (CIFRE 2024/0663), French National Research Agency (ANR) (ANR-11EQPX-0037).

*Manuscript received 5 December 2024, revised 16 March 2025, accepted 2 April 2025.*

[*] Corresponding author

# 1. Hybrid catalysis for biomass valorization

The exploitation of limited natural resources such as oil reserves has damaged nature and biodiversity for the last decades [1], leading to an accelerated exhaustion of these resources. It is estimated that natural oil reserves will be consumed by the second half of the century if the current average exploitation is maintained [2]. With this in mind, it is necessary to adopt sustainable consumption and production models [3]. In order to achieve this objective, chemistry is shifting toward more sustainable practices, notably following the Green Chemistry principles proposed by Anastas and Warner at the end of the twentieth century, which include the use of alternative and renewable prime material sources rather than limited fossil fuels [4,5]. Hence why, biomass, largely available in unexploited waste, stands out as a highly potential alternative for a new carbon source, especially as it is renewable [6]. Due to its complex composition, biomass presents significant challenges as a substrate for chemical transformations. Catalysis, therefore, has a pivotal role in addressing these challenges. However, conventional catalysts, initially designed for transforming purified products are ill-suited for handling complex mixtures [7]. Biological catalysts such as enzymes, on the contrary, are far more effective with these types of substrates. Indeed, many organisms already use enzymes to break down, depolymerize, and/or transform biomass molecules [8]. For example, cell-wall degrading enzymes (CWDE) are used by bacteria and fungi to feed on lignocellulose, or enzymes of the hydrolase family that are specific for degrading certain triglycerides and fatty acids in the case of vegetable or animal oils. Nevertheless, the use of biocatalysts remains a challenge at present, again due to the complexity of biomass sources which may contain a large number of inhibitors, including molecules produced by plants themselves to defend against pathogen enzymes. Thus, to incorporate biomass as a starting material, innovative catalysts capable of targeting only specific molecules in complex mixtures and that could alleviate the issue of the presence of inhibitors, need to be developed. Rather than working on the development of new, more robust, and more specific catalysts, an alternative solution could be to combine existing catalysts with complementary skills. A smart design leveraging the synergistic potential of catalysts of different
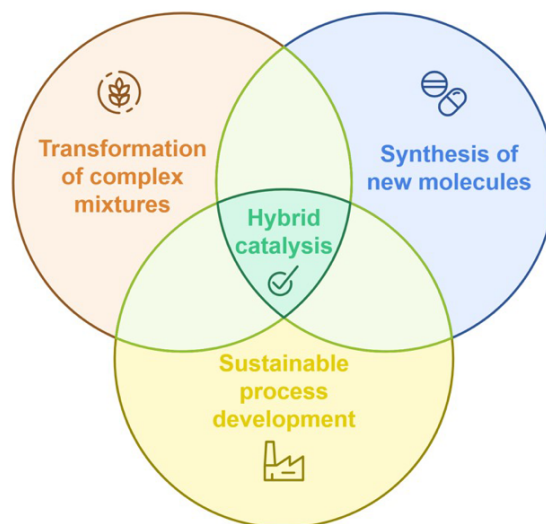


**Figure 1.** Main fields of application of hybrid catalysis (enhancement of sustainable development by reducing atom economy, energetic and economic cost; transformation of complex mixtures through the complementary selectivities of the combined catalysts).

natures—biological and non-biological—could significantly enhance chemical transformations. This approach holds particular promise for optimizing existing chemical processes, which often face limitations preventing their maturity and scalability at industrial levels. For illustration, in the case of high energy consumption for heating, where combination of catalysts logically allows to reduce the overall energetic cost by heating just one reactor [9]. Furthermore, such combined orthogonal processes could pave the way for entirely new families of molecules with valuable properties, by enabling the coupling of reactions that are otherwise difficult to conciliate. More specifically, the integration of chemical and biological catalysts could harness their complementarity and/or orthogonality for selectivity. This synergy may result in multi-step catalytic systems with high yields, driven by reaction equilibrium shifts and, in certain cases, the removal of inhibitors either inherent to the biomass or generated during the reaction. This innovative catalytic approach, which has gained significant attention over the past decade [10], is commonly referred to as "hybrid catalysis" (Figure 1).

Usually, the term "hybrid catalysis" refers to the combination of chemical and biological catalysis.

This combination illustrates the main criteria followed when designing a hybrid catalytic system: joining catalysis whose properties, but also limitations, are very distinct. Although hybrid catalysis can technically be composed of as many types and numbers of catalytic stages as desired, to our knowledge, examples with more than two of them are rarely found currently. The first example of a hybrid catalytic system for biomass valorization was reported in 1980 by Makkee et al., where D-glucose was transformed into D-mannitol through the combination of a biocatalytic isomerization and a chemocatalytic hydrogenation [11]. It is important to note that although the starting molecule, D-glucose, was biosourced, there was no question of biomass valorization when this study was carried out. Moreover, although the value of combining these two types of catalysts was demonstrated, particularly in a one-pot reaction, there was no real interest, at that stage, for the treatment of complex mixtures. Regardless of its ingenuity, this first approach only allowed obtaining 46% of D-mannitol, whereas 92% of D-glucose was converted into D-fructose. To improve the efficiency of the system, the process was later optimized by the same authors by combining the same biocatalytic isomerization of D-glucose to D-fructose as seen before with heterogeneous copper-based catalyst supported on silica (Figure 2). The key characteristic of this metallic catalyst is its substrate specificity, as it prefers interacting with D-fructose, and therefore here offers a solution to selectively act on one single substrate in a mixture of isomers, reflected in the increased D-mannitol yield (66%) [12].

These pioneer works were a milestone in the design of new catalytic systems and led to the exploration of new combinations of chemo- and biocatalysts to enhance new reaction pathways with uncommon, and sometimes unexpensive, starting materials. Biomass has emerged as an excellent candidate to employ hybrid catalysis for several reasons. One reason is that biomass is largely composed of low energy chemical bonds (e.g., esters, amides, sometimes ethers with higher energy bonds) [14], it makes biomass suitable for reactions with enzymes under mild conditions, unlike fossil fuel-based chemicals, almost exclusively composed of carbon and hydrogen [15]. The second reason is that, biomass provides a wide variety of molecules that are hardly discriminated against by chemical catalysts due to

their often low selectivity, leading to the formation of complex product mixtures. In this instance, while offering access to a large number of starting structures, the use of biomass as a starting material also calls for selectivity, potentially offered by enzymes, in order to limit downstream processing steps. Additionally, this complex nature also means that pretreatment systems are needed to avoid potentially toxic or undesirable species, or simply to make the desired starting substrates available, especially in cases where a single product is targeted. For instance, in lignocellulosic biomass, it is mostly cellulose that is converted [16]. The possibility of exploding the entire lignocellulose matrix in a single combined process (with the catalytic valorization steps included directly afterwards), would therefore be advantageous both in terms of atom economy and access to a wider range of new biosourced molecules. Hybrid catalysis could be very helpful in coupling the single-molecule valorization step with a pretreatment one, using a more robust and less specific catalyst, for example.

Indeed, to better understand all the potential of hybrid catalysis, the main attributes and resulting complementarities should be considered when combining catalysts (Figure 3). Biocatalysis, is characterized by its high chemo-, regio- and stereoselectivity [17]. These properties are provided by the tridimensional structure of enzymes, which can selectively host the substrates in their active sites, usually depending on how well they can sterically and electronically interact with each other [13]. This high selectivity is of great interest in the pharmaceutical industry since it can lead to enantiopure compounds [18]. Besides, biocatalytic systems can be conducted in a reaction cascade system, which provides an interesting set of chemical tools and reactions in the same pot, leading to especially high energy- and atom-saving processes [17].

As an example, Merck recently developed a new biocatalytic cascade system for the synthesis of molnupiravir by combining five different enzymes, allowing not only the production of the target antiviral, but also the regeneration of the phosphate needed in the reaction on an industrial scale [19]. This system shortens the previous reported chemical synthesis from ten to only three steps and increases the yield from approximately 10% to 70%. Despite the interesting possibilities of such elegant biocatalytic cascades, the limited stability and high
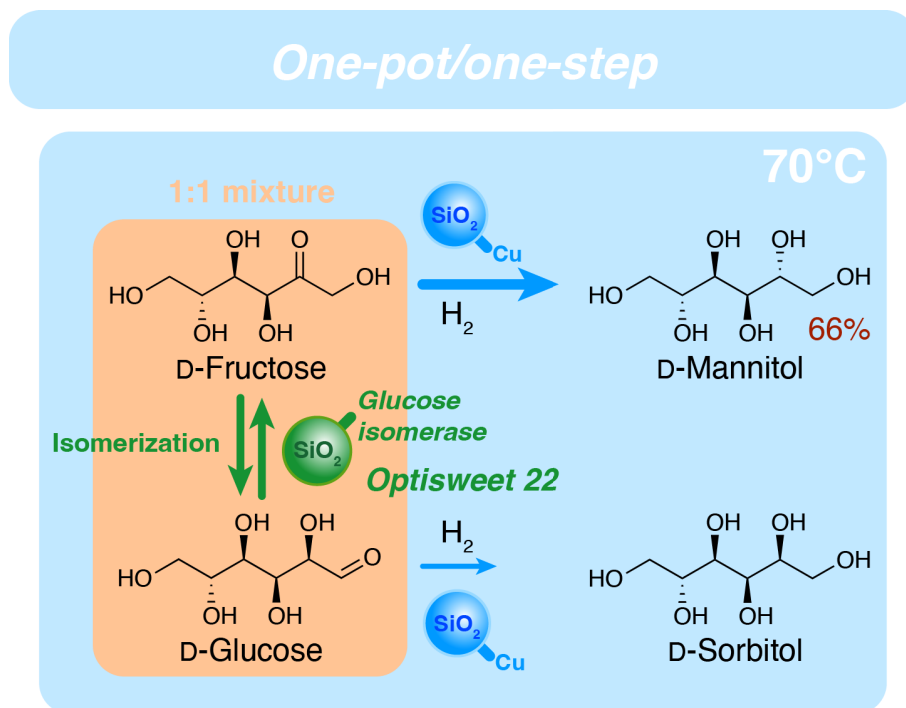
**Figure 2.** One-pot/one-step hybrid process designed by Makkee et al. where a biocatalytic isomerization accesses D-fructose from D-glucose, preferred substrate by a copper catalyst for its subsequent hydrogenation into D-mannitol. Redrawn from Heuson et al. [13].
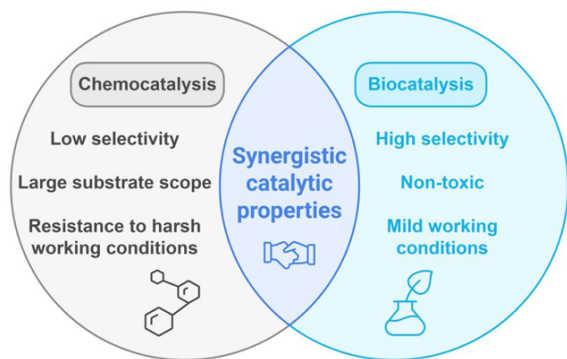


**Figure 3.** Complimentary catalytic properties of chemo- and biocatalysis, leading to the synergistic properties of hybrid catalysis.

price of enzymes become a bottleneck in their incorporation on an industrial scale [20]. Meanwhile, heterogeneous chemocatalysts can enhance the recovery of the catalysts from the reaction mixture, as well as providing good stability under harsh working conditions, making them more suitable for industrial

applications [21]. Regarding their properties, they are mostly related to their electronic structure [13], while leading to lower selectivity due to a very limited steric control of the catalytic center, makes them very versatile and consequently very well suited for complex mixtures. In addition, chemocatalysts tolerate better the exposition to toxic molecules and can then be interesting candidates for "depolluting" reaction media from inhibitors, to which biocatalysts are particularly sensitive and therefore vulnerable [22]. This potential use is perfectly demonstrated by Smeets et al. [23], who were able to design a zeolite-based multifunctional material, for the conversion of allylic alcohol into glycidol, employing the toxic and in situ produced hydrogen peroxide. Here, the TS-1 zeolite was able to both host the concerned enzyme, e.g., glucose oxidase, and simultaneously act as an inorganic catalyst. This hybrid material therefore allowed the production and removal, in the same process, of a substrate that can also be a potential inhibitor. Since the substrate here employed is glucose, this approach could be extended to biomass-containing

mixtures, usually rich in polysaccharides. However, these approaches are not yet widespread. Another example of product protection and/or inhibitor removal is the recent development of nonionic surfactants by Novartis [24], capable of hosting water nonsoluble compounds, which could be either the product of the reaction, a chemocatalyst or any other potentially harmful species for the biocatalyst, allowing, at last, the biocatalyst to be protected from them. In addition, as it will be illustrated later in this article, it is also possible to design new types of reactors offering access to a more spatially isolated compartmentalization system while still offering the possibility for molecules to circulate from one compartment to another, using a liquid or solid permeable membrane. In essence, compartmentalization techniques that could behave as decontamination strategies enhance the cohabitat of chemo- and biocatalysts, or avoid inhibition phenomena, and are here again very interesting for biomass valorization. Therefore, chemo- and biocatalysis should no longer be considered as incompatible but rather complimentary. Their unique properties can overcome their respective limitations, making them capable of addressing the afore-mentioned challenging fields of biomass valorization and new compound synthesis.

However, the number of hybrid processes designed to directly run on biomass is still limited. In the case of lignocellulose, the few systems available are mainly aimed at the synthesis of furfural and its derivatives, which can be obtained by the dehydration of the sugars present in it. Mainly derived from hemicellulose, furfural is indeed considered as one of the top 30 platform chemicals [25], as it provides access to many derivatives with very different applications in polymer, pharmaceutical or food industries. Nonetheless, direct and efficient furfural synthesis from untreated biomass remains, again, mostly undeveloped, especially when it comes to generating its functionalized derivatives such as 5-hydroxymethylfurfural (HMF), furandicarboxylic acid (FDCA), or even furfurylamines like 5-aminomethyl-2-furancarboxylic acid (AMFC). Indeed, the processes to reach these compounds typically need tedious separation steps and control of the reactivity of the aldehyde moiety of furfural, which has been found to be particularly unstable since it can undergo multiple reactions (acetalization, acylation, aldolization, amination, halogenation or redox reactions, among others) [25,26]. Therefore, such high reactivity not only does it make furfural a good platform molecule, but also a particularly excellent precursor for the above cited molecules. However, it also complexifies its related processes and storage, requiring fully integrated systems where furfural is present, ideally, only present in transient form before being converted into a more stable molecule. In this context, advances in hybrid catalysis have offered several solutions for the direct conversion of lignocellulosic biomass into furfural and its derivatives that otherwise would be difficultly accessible by conventional catalysis. A good example illustrating this upgrading of lignocellulosic biomass is the work of He et al. [27–31]. These authors first developed a one-pot/three-step process involving the initial acidic depolymerization of various biomass sources (chestnut shell, corncob, sorghum stems, rice straw or even bamboo shoot shells), into sugars, typically D-xylose. In a second step, a tin-based catalyst was used to convert the sugar into furfural, which was finally selectively employed in a third step by different biocatalysts (e.g., reductases, alcohol dehydrogenases, transaminases) to branch a whole range of chemical groups leading to higher value-added products (e.g., alcohols, carboxylic acids, amines). More recently, the authors have improved their process by combining the first two steps, where cellulose and hemicellulose are directly chemocatalytically converted into furfural, which can then be transformed, in a second step, by the selected biocatalyst (Figure 4). In the case of furfurylamine production, a transaminase was employed for example, either as the isolated enzyme or as a whole cell system [32,33]. Different variants of the process have been designed, employing a similar variety of biomass sources, adjusting it to the desired products. In most of them, a biobased carrier (rice stalk, nutshell, etc.) was employed for the preparation of the concerned heterogeneous tin catalyst. The similar composition of the carrier and the lignocellulosic substrates improves their interactions, mainly due to their similar hydrophobicity and therefore favored adsorption on the surface. In addition, the catalyst supported on rice stalk showed 592-, 17- and more than 2-fold larger specific surface area, pore volume and pore size, respectively, compared to the previously employed material, which might increase the substrate load and therefore provide higher catalytic performance. The reaction media
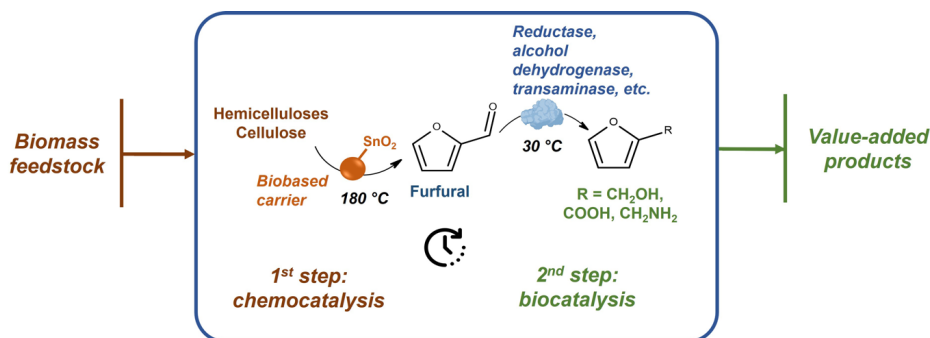
**Figure 4.** General one-pot/two-steps hybrid approach for different biomass conversion (e.g., corncob, rice stalk) into value-added furfural derivatives by combining a tin-based heterogeneous catalyst supported on a biobased carrier and a biocatalyst.

appears as biphasic systems, like in the case of the preparation of furfurylamine, which was performed in a toluene/water solution, working at 170 °C and 35 °C for the chemocatalytic and biocatalytic step, respectively. The authors highlight the utility of this arrangement as it allows the avoidance of the possible inhibition of the biocatalyst by furfural, as it proved to be toxic at high concentrations [32]. The use of toluene might be a drawback when scaling up, and therefore greener alternatives should be explored. This one-pot/two-steps system has been further explored by adding oxalic acid as the cocatalyst in the first step, followed by the biocatalytic step by using whole cells in deep eutectic solvent (ethylamine/hydrochloride/glycine/water) [33]. The motivation behind this approach was again to tackle several problems related to furfural (e.g., low solubility in water, degradation or cross-polymerization) by enhancing its extraction while keeping the above-mentioned energetic advantages of working in one single reactor. Here, adding an organic acid provides a partial pretreatment of the mixture, adding valuable properties to the hybrid system beyond the catalysis itself and demonstrating flexibility and polyvalency.

Overall, these examples demonstrate particularly well the versatility of the combination of two catalysts of different nature, once the common coupling conditions are defined. Typically, the authors were able to combine a broad number of different biocatalysts with the same chemical catalyst under similar conditions, giving them access to a complete range of molecules, while simplifying the development of

the associated processes. The potential of combining a relatively universal chemical catalyst acting first on the biomass, with variable polymer compositions from different sources, was highlighted. The same intermediate, in this case furfural, can then be transformed by different enzymes.

Such versatility enabled by hybrid catalysis was also reflected in the work of Zhang et al. [34], who managed to functionalize asymmetric C–H bonds on a wide alkane substrate scope through a photo-biocatalytic hybrid one-pot/two-steps reaction system. In the first stage, sulfonate anthraquinone was employed for the photo-oxidation of different alkanes (cyclohexane and toluene derivatives, mainly) to ketones, which were subsequently converted, in a second biocatalytic stage, to different functional groups (carboxylic acids, amines, alcohol cyanides and esters) by an enzyme (e.g., transaminase, reductase, lyase) (Figure 5). Although the incompatibility of both catalytic steps imposed a two-step manner way of working, a single aqueous phase at 30 °C could be employed for the whole reaction, notably thanks to the sulfonate group present in the photo-organocatalyst, which favors the latter soluble in water. As a result, the green character of the process is favored as it does not require undesired and often toxic organic solvents. Another remarkable aspect relies on the fact that this coupled catalytic system not only accepts a broad substrate scope, comprising in this case of 14 different substrates, but also leads to the formation of a large and often chiral range of products. Hybrid catalysis provides, again, one single process applicable to numerous substrates that leads
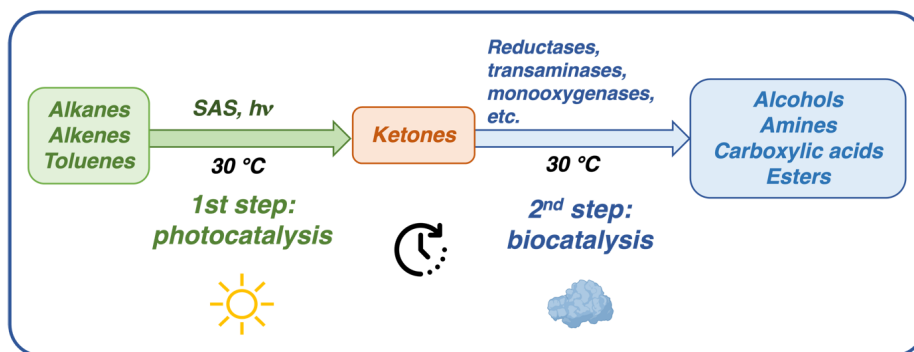
**Figure 5.** Photobiocatalytic one-pot/two-steps hybrid approach for C–H functionalization of different alkanes, alkenes and toluene derivatives. The system combines sodium anthraquinone sulfonate (SAS) as a photo-organocatalyst with various enzyme families, in aqueous medium at 30 °C. Redrawn from Zhang et al. [34].

to many different products of higher value, notably enantiomerically enriched. This last aspect illustrates, indeed, the additional complementarity of the catalysts, with the association of a nonstereoselective step with a highly stereoselective one, allowing to reach a wider product range in a relatively simple approach.

Additionally, the catalytic singularity of hybrid technologies can also give rise to unexplored reaction pathways in organic chemistry, allowing new and often structurally rich products to be reached. The synthetic potential of hybrid catalysis relies on the conjunction of the numerous reactions enhanced by chemocatalysts (e.g., metal-catalyzed cross-couplings, organocatalytic asymmetric synthesis, oxidoreductions) and the high selectivity of biocatalysts, resulting, for instance, in the delicate creation of new stereogenic centers. Among the most targeted chemical structures by synthetic chemists, special attention has been drawn to nitrogen-containing structures, as they are often found in building blocks used to access pharmaceutical compounds [17]. As an example, a *N*-acetyl-ᴅ-glucosamine-derived chiral alcohol was prepared by Hao et al. employing a chemobiocatalytic approach in a stereo- and especially chemoselective manner [35]. The process combined tyrosine hydrochloride for the dehydration of *N*-acetyl-ᴅ-glucosamine at 160 °C, and a carbonyl reductase for the asymmetric reduction of a ketone at 30 °C (Figure 6).

Compared to the previous processes, where the intermediate is purified, the one-pot/two-steps hybrid catalysis led to an increase in the enantiomeric excess of the furane derivative from 91% to over 99%. In addition, the 99% of the *E* factor (6025) is related to solvent waste from product purification, which again highlights the sustainable character of this one-pot transformation. Nine different substrates were obtained in good to excellent yields, showing the versatility of the system to reach multiple high value-added building blocks from inexpensive chitin. Overall, this work reinforces the potential of valorizing inexpensive biomass through hybrid catalysis to access new compounds with high enantiopurity and to reduce the environmental impact. Another interesting example in the framework of stereo-controlled synthesis is the recent work of Gastaldi et al. [36], who prepared, from achiral alkynes, chiral polyhydroxylated a rare analog of monosaccharides through a one-pot/two-steps process at 60 °C. A gold N-heterocyclic carbene, responsible for the hydration of the alkyne to the corresponding ketone, was combined with an aldolase, which enhanced the formation of a C–C bond in the presence of an aldehyde and led to two new stereogenic centers. A family of five different chiral monosaccharides were formed in excellent yields, all of them being high value-added products with potential applications in food and pharmaceutical industries. As in the previous example, the reaction was performed as a one-pot/two-steps, due to the different temperatures and pH working ranges of the catalysts, 60 °C and pH 3 for the chemocatalytic step, and room temperature and pH 7 for biocatalytic one, respectively.
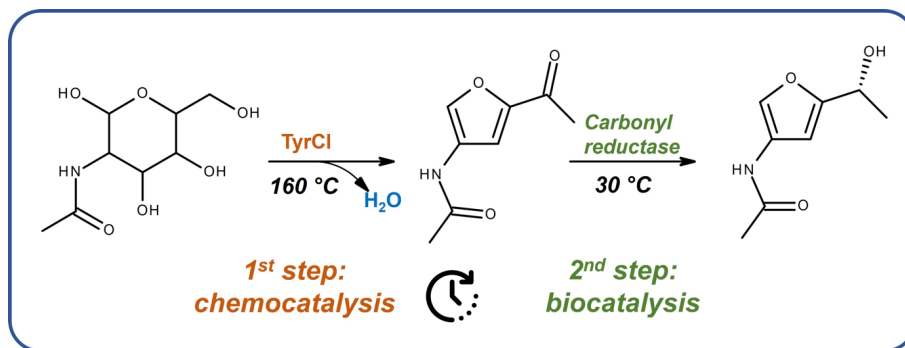
**Figure 6.** One-pot/two-steps process for the asymmetric synthesis of acetamido-5-(hydroxyethyl)furan that combines a chemocatalytic dehydration with tyrosine chloride (TyrCl) as catalyst and biocatalytic reduction of *N*-acetyl-ᴅ-glucosamine. Redrawn from Hao et al. [35].

Striving to reach a one-step process, an attempt to increase the pH of the chemocatalytic step was done, which unfortunately derived in a quick decrease of the ketone production. In addition to the synthesis of new products, the hybrid process again shows a major advantage in terms of atom economy, as it presents a fourfold lower value of *E* factor (0.5) with respect to the previous conventional synthesis, and also helps avoiding the isolation of the freshly formed hydroxyacetone, which is particularly unstable given its tendency to polymerize and/or undergo aldol condensation [37]. With the same hydration step and further alkyne transformations, Li et al. have very recently reported the hybrid regioselective conversion of alkynes to chiral alcohols also using a gold catalyst [38]. Similarly to the previous example, the reaction occurs in a one-pot/two-steps manner and combines the chemocatalytic hydration step with the biocatalytic reduction of the intermediate ketone to a chiral alcohol by using a carbonic anhydrase. Again, a step differentiation was required so the pH could be increased from acidic to alkaline (pH 8) and so the temperature could be decreased from 65 °C to room temperature, which contributed to the energy and atom efficiency by not requiring any separation or exogeneous energy-demanding process for the second step. This process afforded a wide scope of differently substituted chiral alcohols with excellent enantioselectivities (>99%) and good to excellent yields (most of products obtained in between 60% and 90% yield). Most remarkably, within this work, the same authors have developed two other parallel hybrid systems for the synthesis of chiral alcohols that allow the enlargement of the

substrate scope to alkanes and alkenes [38]. When alkanes were employed as starting materials, a photocatalytic oxidation followed by a biocatalytic reduction was achieved, while in the case of alkenes, a metal-catalyzed oxidation was performed, followed by a biocatalytic reduction. Therefore, Li et al. was able to design three hybrid reactions to produce chiral alcohols from nonfunctionalized alkanes, alkenes, and alkynes, which widely enlarged the substrate scope and led to a notable increase in the final value of the obtained products (Figure 7). In all cases, the one-pot/two-steps setup was maintained to avoid incompatibility issues, mainly related to pH, temperature, or light-exposure working conditions.

Among these approaches, the photobiocatalytic one is particularly interesting from a sustainable perspective, as it allows the use of visible light as an energy source. This case echoes the above-mentioned work of Zhang et al. [34], which already showed the potential of photocatalysts to oxidize C–H bonds to carbonyls for their potential transformation by biocatalysts. Expanding this reactivity presents therefore huge potential as different chemical functions can be obtained from alkanes, which could also be extrapolated to biomass-derived substrates, such as fatty acids or lignin derivatives.

All these studies can be seen as great proof of concept regarding the advantages that can be provided by hybrid catalysis in organic chemistry. Firstly, it affords the possibility to combine catalysts in one single reactor instead of sequential systems, and therefore reducing significantly the energetic and economic cost of the process. Secondly, as it is frequent for one-pot systems, the isolation of intermediates
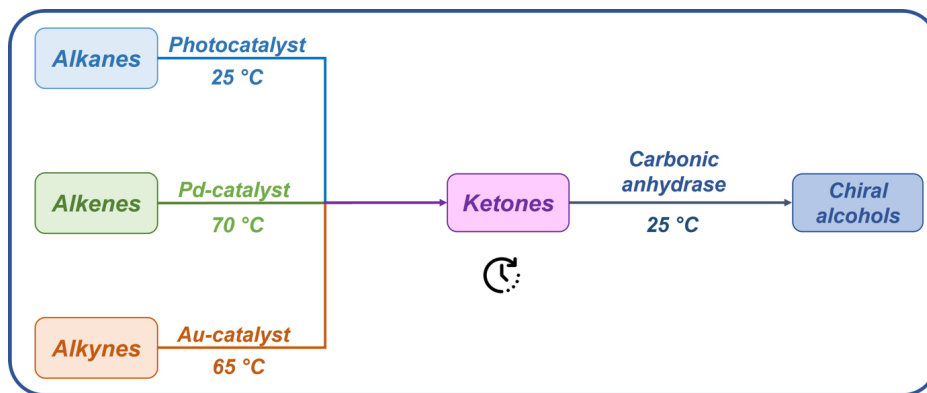
**Figure 7.** Three parallel one-pot/two-steps hybrid approaches for synthesis of chiral alcohols depending on starting from alkanes, alkenes and alkynes, respectively. Redrawn from Li et al. [38].

is not necessary. This leads to more efficient atom use, as evidenced in the afore-mentioned *E* factor values, it results in safer processes because reactive species are rapidly transformed, minimizing uncontrolled side-reactions and undesired byproducts. Over these technical aspects, the synthetic potential should be highlighted. In all the reported works, innovative reactional approaches were highly stereoselective. Particularly interesting for the pharmaceutical industry, hybrid catalysis can therefore provide high value-added structures in a relatively convenient and economic way. Other hybrid processes, which will be detailed in the next part of this work, alternatively focus more on introducing highly reactive and functionalizable chemical groups on building blocks to access new platform molecules. Whatever the final objective, hybrid catalysis could be the key to unlocking numerous simplified, and more importantly, efficient synthetic strategies, especially for future biorefineries.

Beyond all the above-mentioned synthetic and industrial interests, technical adaptability of hybrid catalysis with the reaction should also be mentioned. The main aspects to consider are the catalysts involved, their allocation in the reactors and the sequence of the reaction steps. The choice of the catalysts depends on the nature of the reaction, the requirements of the process and the energy source. The most relevant hybrid approaches for biomass conversion were recently classified by Heuson and Dibenedetto based on the nature of the biocatalysts involved, and the way they were combined [13]. But, as a final illustration of both the complexity and ad-

vantages of hybrid catalysis, we finally propose to detail the constraints that can govern the combination of catalysts of different natures and operating conditions through a series of examples we recently developed around the conversion of glucose into new platform molecules, which notably involve the development of a completely new type of reactor specifically designed to overcome the inhibition of the catalysts involved in the transformation.

## 2. Application: from glucose to furfurylamides through hybrid processes

In line with the advantages that we have detailed previously for hybrid catalysis, we have developed several approaches to exploit two main advantages: the design of more economical processes and the discovery of completely new synthetic routes to access new families of molecules. We will illustrate these two aspects through the conversion of glucose into HMF, a process that has already been implemented but which we have tried to improve in a hybrid way. Then through the production of furfurylamines, and then of furfurylamides again through a hybrid route, families of molecules with interesting potential yet to be identified.

### 2.1. *From D-glucose to 5-hydroxymethylfurfural through a two-pots/one-step system*

As we have already seen from several examples cited above, one D-glucose-derived platform molecule that is at the heart of all concerns

is 5-hydroxymethylfurfural (HMF) [39]. Indeed, HMF can be further valorized by different reactions, including hydrogenation, which leads to 2,5-dimethylfuran (2,5-DMF) [40], a promising fuel additive, or to a precursor to terephthalic acid by a dehydrative Diels–Alder reaction with ethylene to form *p*-xylene, followed by an oxidation [41,42]. Alternatively, HMF oxidation can also yield 2,5-furandicarboxylic acid (FDCA), a biosourced alternative to terephthalic acid with significant potential for polyester plastic production [43,44]. However, D-glucose, despite its abundance, is not the preferred substrate for efficient HMF production compared to the more reactive and costly D-fructose. This preference is due to the fact that fructose, with its fructofuranose tautomer, dehydrates to a furanic ring with lower energy barriers than D-glucose [45]. Therefore, isomerizing D-glucose into D-fructose is a crucial step that cannot be bypassed. One solution for this additional step could be an enzymatic D-glucose isomerization, which is already widely used in industrial production of high-fructose corn syrup (HFCS) [46]. This enzymatic reaction remains the method of choice due to its high efficiency and moderate cost. Although this process requires, high-purity D-glucose, specialized buffers and multiple ion-exchange resins to remove metallic impurities in food-grade HFCS, it is still favored over chemical isomerization, despite renewed interest in the latter [47–50]. The enzymatic process, however, is limited by its thermodynamic equilibrium ($K_{eq} \approx 1$), restricting D-glucose conversion [51,52]. While this equilibrium is not an issue for HFCS production (which tolerates D-glucose/D-fructose mixtures), it is less than ideal in the case of HMF production as the remaining D-glucose cannot be converted into the final product. One solution is then to shift the isomerization equilibrium by directly coupling the first reaction with D-fructose dehydration, as the latter is irreversible. Nevertheless, this requirement introduces challenges, as catalyst compatibility between the isomerization system and the dehydration system remains problematic. However, Huang et al. proposed a very interesting one-pot/two-steps hybrid process combining a thermophilic glucose isomerase immobilized on aminopropyl-functionalized mesoporous silica (FMS) with a heterogeneous Brønsted acid catalyst (propylsulfonic-FMS-SO$_3$H) in a THF/H$_2$O (4/1 v/v) solvent mixture [53]. But, although iso-

merization with the enzyme at 363 K achieved a promising 61% D-fructose yield, subsequent dehydration required a higher temperature (403 K), which only led to a HMF 30% yield, and more importantly, caused complete denaturation of the glucose isomerase. Overall, these results highlight the difficulty of integrating these processes together.

As an alternative to what has been proposed, we thought it would be interesting to turn to an alternative two-pot/one-step process for this particular situation, as the separation of the reactions could allow different reaction conditions (pH, temperature, etc.) when run in parallel, while still benefitting from the possibility of continuously consuming D-fructose. Indeed, strategies have already been adopted to combine enzymatic isomerization of D-glucose to D-fructose and chemical dehydration. These approaches involve the separation of bio- and chemo-catalysis and D-fructose transportation between the aqueous phase for isomerization and an organic phase for subsequent reactivity. Huang et al. first introduced this concept by adding sodium tetraborate to the aqueous isomerization medium, forming a fructoboronate complex through interaction with D-fructose [54]. This complex was then transported to a separate organic phase with the aid of a cationic quaternary ammonium salt, enhancing D-glucose conversion by shifting the isomerization equilibrium toward D-fructose. The dehydration of D-fructose in the organic phase led to an increase in HMF yield to 63%, compared to 28% without borate addition, and by improving the conversion of glucose from 53 to 88%. However, the selectivity of the complexation between D-glucose and D-fructose was suboptimal, which was later addressed by Delidovich et al., who optimized the chemical nature of the boronate species [55]. A global process exploiting this concept for D-glucose to HMF production has concomitantly been proposed by Alipour [56]. Therein, D-fructose is complexed with phenylboronic acid and transferred to an organic phase, which is then separated and brought into contact with an acidic ionic liquid phase to release free D-fructose. The D-fructose-rich ionic liquid is subsequently used for dehydration to HMF in a biphasic medium, with HMF being back-extracted into a final low boiling point organic phase. This method relies on four distinct media and intermediate phase separations which consequently limits its industrial potential.
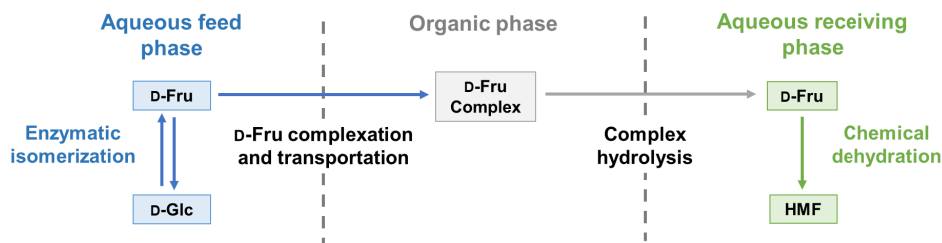
**Figure 8.** General principle of the hybrid "two-pot/one-step" simultaneous process applied to the transformation of D-glucose to HMF (D-Glc = D-glucose, D-Fru = D-fructose, HMF = 5-hydroxymethylfurfural).

Inspired by these sequential steps, we therefore sought to propose a more streamlined and integrated approach that reduces the number of steps and avoids the use of costly and difficult-to-recover ionic liquids. It would be composed of the following steps: (1) isomerization of D-glucose in a first aqueous phase at neutral or slightly basic pH, compatible with the enzyme; (2) complexation of the D-fructose produced with an arylboronic acid, allowing its solubilization from the first aqueous phase into a second, organic "transport" phase; (3) hydrolysis of the complex at the interface of a second, acidic pH aqueous "receiving" phase; in which (4) the D-fructose is dehydrated to HMF using an acid catalyst. This concept is illustrated in Figure 8.

Through a first study [57], we optimized the various parameters related to each of the steps independently, starting with the isomerization step with glucose isomerase. For this, we studied a temperature range from 323 K to 363 K and tried to find the optimum pH between 4.5 and 9. These parameters were applied to a commercially available immobilized glucose isomerase (Sweetzyme® IT Extra, D-xylose ketol-isomerase), to make the process as scalable as possible. As a result, we observed that the enzyme exhibited maximum activity around pH 7.5, at a temperature of 343 K. As the extraction of D-fructose by formation of a complex [D-fructose–boronic acid]$^-$ is favored if the pH of the aqueous solution containing D-fructose is larger than the p$K_a$ of boronic acid and the p$K_a$ of the main boronic acids are lower than 8.5, we chose pH 8. This condition allows us to overcome the p$K_a$-related lock of the selected boronic acid to transport D-fructose to the organic phase while maintaining a relative activity of more than 80% of the enzyme. Under these conditions, a final yield of 55% in D-fructose

isomerization could be obtained. We then turned our attention to optimizing the D-fructose extraction from the aqueous "giving" phase to the organic "transport" phase. For the latter, methylisobutylketone (MIBK) was selected over other solvents like methyl-*tert*-amyl ether and dimethyl carbonate based on solubility, toxicity, and boiling point. Despite similar D-fructose extraction yields, MIBK's higher boiling point (117 vs. 86 °C for methyl-*tert*-amyl ether) made it more suitable for chemical catalysis at 80–90 °C. Then, inspired by a previous study [58], we chose the couple lipophilic arylboronic acid (carrier) along with a quaternary ammonium salt (Aliquat336®) as a phase transfer agent for D-fructose extraction into the MIBK. At the chosen pH conditions (pH 8), aryl boronic acid ArB(OH)$_2$ is actually present under its hydroxylated anionic form, as a tetrahedral aryltrihydroxyborate ArB(OH)$_3{}^-$ [59]. At the interface between the aqueous and organic phases, D-fructose further reacts with the arylborate to form a tetrahedral fructoboronate ester. The fructoboronate complex then forms an intimate ion pair with Aliquat336®, which enables its transportation to the organic phase [60]. We then studied the influence of the boronic acid structure to optimize the kinetics and maximize the selectivity of D-fructose complexation/transportation. Seven arylboronic acids, which differ through the electronic properties of their substituents and thus by the p$K_a$, were screened in the complexation with D-fructose: 3,4-dichlorophenylboronic acid (3,4-DCPBA), 3,5-dichlorophenylboronic acid (3,5-DCPBA), 2,4-dichlorophenylboronic acid (2,4-DCPBA), 2,3-dichlorophenylboronic acid (2,3-DCPBA), 4-*tert*-butylphenylboronic acid (4-TBPBA), and 4-(trifluoromethyl)phenylboronic acid (4-TFMPBA). With an excellent extraction yield and

rate (46.5% and 1.48 μmol/min, respectively) under our conditions, 3,4-DCPBA was chosen as the aryl boronic acid for the continuation of our studies. The 3,4-DCPBA/Aliquat336® molar ratio was then studied, again with a view to maximizing extraction speed and yield. The best yield was obtained with a 1/2 ratio, as the increase in Aliquat336® concentration meant that no more D-fructose could be extracted above it. Keeping a molar ratio of aryl boronic acid/Aliquat336® equal to 1/2 and at fixed initial D-fructose amount, both 3,4-DCPBA and Aliquat336® concentrations were then varied. From this screening, we found that the D-fructose/3,4-DCPBA/Aliquat336® ratio of 1/1/2 (with D-fructose used at 100 mM) was the most effective, even though the extraction yield could not be further improved compared to previously obtained results. The release of D-fructose into the aqueous "receiving" phase was also studied as a function of its pH. By changing the pH from 8 to 1, the release yield was increased from 20% to 100%, and over 91% at pH 5. We concluded that, as expected, the pH of the recipient phase should be as low as possible. Finally, the optimal conditions for D-fructose dehydration to HMF were studied at different temperatures, as for the isomerization, along with different catalyst-to-D-fructose mass ratios. For this study we chose, as an alternative to a strong homogeneous acid that cannot be recycled in processes, a commercially available acidic resin containing strong sulfonic groups. This resin, indeed, facilitates a potential reusability and recyclability of the catalyst. In addition, this reduces the risk of using and heating strong acids in liquid form. A temperature of 80 °C was found to be the most effective with this catalyst. At this temperature, no humins were detected, avoiding significant resin browning observed at 90 °C.

In the formerly optimized conditions, a sequential process was tested. The first step involved simultaneous D-glucose isomerization and D-fructose transport by using a fructoboronate complex. This was followed by the hydrolysis of the complex, releasing D-fructose into the aqueous receiving phase. Finally, the third step dehydrated the released D-fructose to HMF using the sulfonic resin. All these steps were performed one after the other, the organic phase being first isolated, before being put in contact with the aqueous "receiving" phase, without the chemocatalyst, the latter being added in a third time. As
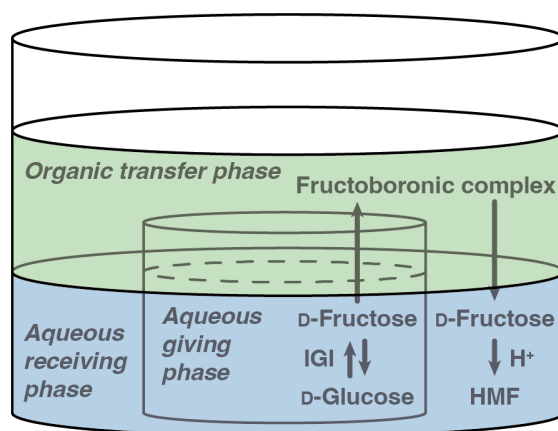


**Figure 9.** Illustration of the combined process for the conversion of D-glucose to HMF using a triphasic system, combining an immobilized glucose isomerase (IGI) and an acidic catalyst. Redrawn from Gimbernat et al. [57].

a result, only 57% of D-fructose (based on 100% of potential D-glucose to be converted) was extracted from the "giving" phase, followed by a release of 63% of the extracted D-fructose into the "receiving" phase, and 20% of this extracted D-fructose could be dehydrated into the final product, leading to a very small overall HMF yield of 5%. However, as each phase is decoupled from the previous/subsequent one, this sequential approach benefits little from the shift in the isomerization equilibrium. The latter is only pulled by the D-fructose extraction to the organic phase, which also has its own equilibrium. Not so surprisingly, low yield was obtained. Logically, we then attempted to couple the three phases and the two catalytic stages, into a single, very simple system, as described in Figure 9.

As a result, the isomerization of D-glucose was achieved with a 70% yield. Half of the produced D-fructose was successfully transported to the "receiving" phase, leading to 35% of D-glucose transformed to D-fructose available for further dehydration in the acidic phase, as for the sequential process. Therefore, it is with no surprise that we again obtained a very low HMF final yield of 4%. Despite showcasing the potential of such a chemoenzymatic catalysis cascade for direct HMF production from D-glucose, our process was clearly limited by additional
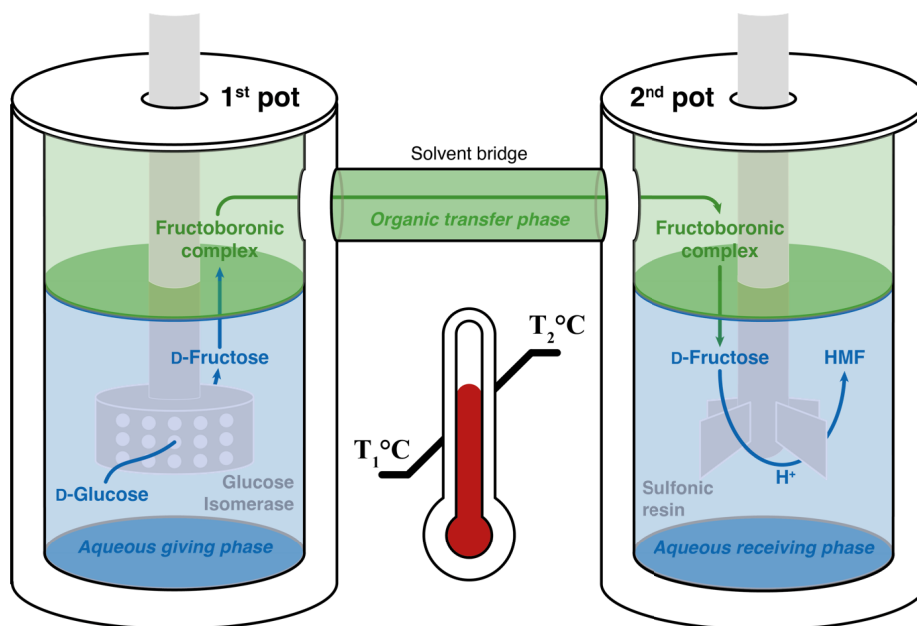
**Figure 10.** H-type reactor concept for HMF production from D-glucose in a two-pot/one-step hybrid process combining a glucose isomerase and a sulfonic resin in three different phases. Redrawn from Heuson et al. [13].

factors, the most preeminent one being probably insufficient phase agitation.

This consequently led us to rethink completely the architecture of the reactor, toward a more complex, but also more efficient system to promote the continuous extraction of D-fructose toward the receiving phase. In order to propose radically different reaction conditions between the two aqueous phases (donor and recipient), while maximizing diffusion of the D-fructose formed from one to the other, we switched to a rather unusual "H"-type reactor topology (Figure 10) [61]. This reactor incorporates all the stages previously tested, but this time with two separate compartments that can be independently thermostated, linked by a bridge for circulation of the organic transfer phase. With this new reactor at our disposal, we repeated the tests with the different combined phases we had previously carried out, but unfortunately did not observe the increase in D-fructose transfer we hoped. Conversely, we observed a strong accumulation of the fructoboronic complex in the organic phase of the first pot. Given the small diameter of the solvent bridge, we concluded that the main limitation was the lack of circulation of the organic phase between the two pots. Therefore, we

added a fin with baffles in the opposite direction in both compartments, allowing the flow of the organic phase created by the rotation of the two stirring systems to be redirected, so that the organic phase could circulate freely from one compartment to the other. This improvement enabled us to increase the rate of D-fructose release into the receiving aqueous phase by a factor of three. However, in order to further improve the process, we optimized a number of additional parameters. Firstly, we observed that, as previously mentioned, a pH difference between the two aqueous phases was important to enable efficient continuous extraction of D-fructose from the donor to the recipient phase. This is because, at basic pH, the fructoboronic complex can form and dissolve in the organic phase, which can then be hydrolyzed in the receiving phase at a more acidic pH, and the greater the pH difference, the more the equilibrium of the two dissolutions is exceeded in the receiving phase. However, following the introduction of the fin with baffles, we observed that the pH of the two phases tended to equilibrate, with the organic phase partially transferring protons from one phase to the other, helped by the new MIBK circulation, albeit rather slowly. We therefore investigated the

possibility of buffering the two aqueous solutions in an attempt to slow down or even eliminate this phenomenon. To this end, we used a buffer at three different concentrations in each phase, to see whether the buffer strength also had a predominant role in this limitation, while maintaining a pH difference of 5.5 between the phases (pH 8.5 and 3 for the donor and recipient phases, respectively). As a result, with a sufficient buffer concentration (500 mM), we were able to limit the fall in pH difference to a value of 3.5 over 6 h of reactions, which showed promise for the efficiency of the hybrid reaction. Obviously, this efficiency decreases with decreasing buffer concentration. It should be noted that this type of strategy is obviously not transferable to a larger scale, and it would then be preferable to set up active pH control in each of the bases by adding base and acid respectively, or even to envisage a continuous system directly for the aqueous phases, with the organic bridge remaining static, to dilute the pH variation, while still maximizing the effects of equilibrium displacement.

In parallel, we also restudied the concentration ratio of D-fructose/3,4-DCPBA, and determined that with this new system a new ratio of 1/0.25 was now more efficient (while maintaining the 3,4-DCPBA/Aliquat336® ratio at 1/2) for D-fructose extraction, while allowing a considerable reduction in the amount of 3,4-DCPBA and Aliquat336® used, which represents another advantage of the new reactor. With these latest optimizations in hand, we tested the new complete hybrid process for HMF production on a scale of 100 mM initial D-glucose. For this experiment, a temperature of 70 °C was set in the first pot (enzymatic isomerization step) while 80 °C was set in the second pot (chemical dehydration step), and isomerization, extraction and dehydration efficiencies were then followed over 32 h. At the end of the reaction, the isomerization, D-fructose extraction and HMF production yields reached 79%, 97%, and 31%, respectively. The extraction yield obtained thus demonstrates the efficiency of our new process and its associated optimized parameters for D-fructose transportation between the two aqueous phases, while the isomerization yield clearly highlighted an equilibrium shift as expected. The carbon balance in both aqueous phases was found to be equivalent to 90% in D-glucose, D-fructose and HMF, proving the efficiency of the release process. The only

step that was really limiting here was therefore the dehydration, with a final yield of only 30.9% in the desired product. Although this is on a par with the best attempts previously described, such as that of Huang et al. [53], it seems crucial to now turn our attention to optimizing the dehydration step, probably by choosing a better catalyst than the sulfonic resin, or perhaps by considering a better process control so as to be able to further lower the pH and increase, if possible, the temperature of the second pot, while keeping humins formation as low as possible.

Nonetheless, this first proof-of-concept clearly highlights the effectiveness of the hybrid catalysis concept in obtaining molecules of interest more efficiently, in this case the transformation of D-glucose, that can easily be obtained from biomass, into the highly valuable HMF, under mild conditions. More precisely, it shows how the combination of different catalytic steps within the same system can greatly help shift the equilibrium of reactions that are normally highly reversible. Interestingly enough, it would also be possible to apply this process with the H-shape reactor and organic membrane to an unrefined D-glucose source, typically a lignocellulosic biomass extract, insofar as the MIBK could prevent or, at least, limit the diffusion of polar species that could poison the chemical catalyst toward the phase where dehydration takes place. If we take the concept a step further, why not consider direct cellulose and hemicelluloses depolymerization using an enzymatic cascade in the donor phase, insofar as the first stage takes place under conditions that are entirely compatible with the action of cell wall degrading enzymes. But more than just a synthesis proof-of-concept, this approach, with all the process-level optimization that it required, illustrates how different combinations of catalysts, in one-pot/two-steps or two-pots/one-step systems, can enable radically different catalytic functionalities to be accessed, and offer specific advantages in each case. This makes the combination of these processes highly complementary and interesting.

## 2.2. *One-pot conversion of 5-hydroxymethyl-furfural into 5-aminomethyl-2-furan-carboxylic acid*

As described above, HMF is a very interesting platform molecule as it can be transformed into a variety

of value-added building blocks [62–64], including monomers useful for the production of biobased polymers such as 2,5-dihydroxymethylfuran (DHMF), 2,5-dicarboxaldehydefuran (DCAF), 5-hydroxymethyl-2-furancarboxylic acid (HFCA) and 2,5-furandicarboxylic acid (FDCA), thanks to a wide range of innovative catalytic pathways [65–67]. The conversion of HMF to FDCA, for example, has been the subject of intensive research in recent decades, and numerous approaches have been reported [67–69]. Noble-metal-based chemical catalysts demonstrate high efficiency in HMF oxidation, with supported noble metal nanoparticles exhibiting exceptional catalytic performance in liquid-phase oxidation under both alkaline and acidic conditions [70–76]. Moreover, enzymes were also applied. One of the earliest studies on biological oxidation of HMF was conducted by Koopman et al., who identified a novel HMF oxidoreductase from *Cupriavidus basilensis* HMF14. By introducing the *hmfH* gene into *Pseudomonas putida* S12, a whole-cell biocatalyst was created. This system produced 30.1 g/L of FDCA from HMF in fed-batch experiments, using glycerol as the carbon source, with an impressive yield of 97% [77]. For their part, Dijkman et al. utilized an HMF oxidase, expressed in *E. coli*, for a four-step oxidation of HMF to FDCA. This FAD-dependent enzyme led over 95% conversion of HMF within 24 h at 25 °C, in an aqueous phosphate buffer solution (pH 7) [78]. Still with the same objective, Carro et al. combined an aryl-alcohol oxidase (AAO) with an unspecific peroxygenase (UPO), both from *Agrocybe aegerita* in a cascade reaction [79]. AAO reduced $O_2$ to generate $H_2O_2$, while enabling stepwise oxidation of HMF to DFF (2,5-diformylfuran) and FFCA (5-formylfuran-2-carboxylic acid). However, as AAO could not oxidize the carbonyl groups in FFCA directly, the authors combined it with the UPO to perform the conversion of FFCA into FDCA using $H_2O_2$, generated during the first step, to produce FDCA with a 91% yield after 116 h [80]. Finally, and although examples are rare, a few hybrid attempts have also been made. Liu and coworkers applied an immobilized laccase on magnetic nanoparticles with TEMPO as a chemomediator, obtaining a FDCA yield of 90.2% in 96 h at 35 °C [81]. What all these examples have in common is that they carry out only one reaction type, i.e., oxidation (alcohol to carbonyl and then carbonyl to acid). Obviously, it is much

more complex to get catalysts to cohabit when the types of functionalization reactions sought are different, or even in some cases opposed, as is the case for oxidations and reductions. Nonetheless, with the same mindset, furfurylamines have been identified as valuable precursors for biobased polymers such as polyamides, polyimides, polyaspartimides, polyureas, polyhydroxyurethanes, polyimines, and polyenamines. Their monomers can be conveniently synthesized from biosourced furfural derivatives, further supporting their potential in sustainable material development [82]. These compounds also have several applications including the preparation of benzoxazine derivatives for flame-retardant resins [83,84] and, after conversion to difurfuryl diisocyanates, the replacement of petroleum-based diphenylmethane diisocyanate in polyurethane systems [85,86]. Furfurylamines are typically synthesized through the reductive amination of the carbonyl group in the furfural structure under mild conditions with inexpensive reagents [87]. However, such processes often require the use of protecting groups, numerous chemical steps, and toxic reductive agents [87,88]. It is worth mentioning that the reduction combined with the potential oxidation of HMF's hydroxyl groups, to obtain the corresponding $\omega$-amino aldehyde or acid, is obviously particularly challenging. To circumvent these issues, several chemocatalytic pathways have been recently developed [87–92]. However, these are not ideal for the synthesis of furfurylamines derived from HMF, owing to the sensitivity of the furan ring to reductive conditions and the tendency of these compounds to form secondary and tertiary amines [65–67,93]. An efficient alternative to perform amination of HMF derivatives is the use of transaminases, their primary catalytic function being the nonreductive amination (transfer of an amine) of carbonyl groups in water at low temperatures [34]. Recently, several $\omega$-transaminases were employed for the synthesis of several furfurylamines from HMF derivatives [93,94]. Dunbabin et al. reported yields up to 92% for the aminated products, starting from different HMF and furfural derivatives. Among them, they achieved the synthesis of 5-hydroxymethylfurfurylamine (HMFA), 5-aminomethyl-2-furancarboxaldehyde (AMFA), furan-2,5-diyldimethanamine (FDMA), and the 5-aminomethyl-2-furancarboxylic acid (AMFC). However, in the case of AMFC, they performed the
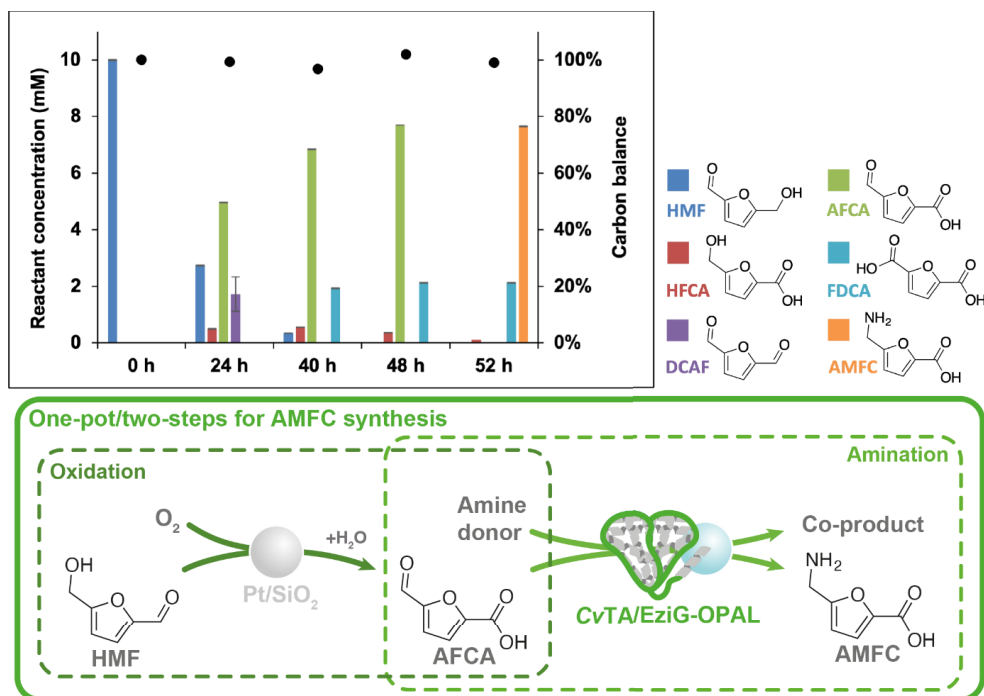
synthesis directly on 5-aldehyde-2-furancarboxylic acid (AFCA) instead of HMF, as the only amine that can be directly produced from HMF, in a single step with one catalyst, is HMFA, the other furfurylamines requiring a coupled oxidation step, whether before or after the amination. It is precisely here that hybrid catalysis can be of great interest by proposing the combination of an oxidation catalyst with a transaminase, as has already been done for other applications we described earlier, to gain access to other more complex derivatives of HMF-derived furfurylamines. We have paid particular attention to the synthesis of AMFC, as it is a promising building block for polymer synthesis. Being an ω-amino acid, it can be used to produce unnatural peptides such as cyclopeptides [95,96], but could more generally be integrated in aromatic polyamides. Thus, we attempted to develop the combination of an oxidative metal chemocatalyst and a transaminase for the direct synthesis of AMFC from HMF.

To achieve this synthesis, we took full advantage of the high-throughput screening capabilities of the REALCAT platform in Lille, enabling us to select the best catalysts, both for the chemical catalyst and the enzyme, from a panel of catalysts of different natures, particularly regarding supported metal nanoparticles. Indeed, depending on the metal used and the properties of the support, the selectivity of the catalyst is particularly different, which can lead to the production of undesirable byproducts. In a parallel study, for example, we demonstrated that under certain conditions, several of our supported metal catalysts were capable of performing oxidative deamination of furfurylamines [97], which is obviously problematic in the context of AMFC synthesis, since the latter is then converted back into purely oxygenated derivatives. Another challenge was to find a chemical catalyst capable of operating at a relatively neutral pH, since this is generally the optimum pH for transaminases. Indeed, many supported noble metal nanoparticle catalysts are more active at more basic pH, which is typically the case with gold nanoparticles, for example [36]. After screening 15 catalysts containing nanoparticles of gold, palladium, platinum, ruthenium and even some bimetals, immobilized on different types of supports, metal oxides for the majority of them, we were able to demonstrate that one of the combinations, namely platinum immobilized on silica, was able to carry out the oxidation of HMF to AFCA (the ω-aldehyde acid derivative) directly using the oxygen present in the headspace gas phase of the reaction. This catalyst proved highly effective at pH 8 and at 60 °C, enabling a 100% substrate conversion in less than 24 h. Notably, this temperature could in theory also allow for the use of different transaminases, several of which have already been described as thermostable [98]. A negative aspect of this catalyst, however, was its lack of selectivity for the oxidation of the alcohol or aldehyde function of the substrate. Indeed, when oxidation step takes place before the amination step, apart from the desired intermediate (AFCA), a byproduct from the complete oxidation of the two functions to the acid (FDCA) is also found. Despite the previously mentioned interest of FDCA and the possibility of directly incorporating it into polymerization matrices, its formation naturally limits the obtainable yield of AMFC. Therefore, the use of this catalyst should ideally take place sequentially to the amination, which would avoid the adoption of a one-pot/one-step system. In our process, this represented the main limitation since at the time of the study, we still did not have any thermostable transaminases capable of carrying out the amination of AFCA, and therefore had to introduce the enzyme into the reaction medium in a second step, once the reaction had returned to room temperature. Nonetheless, we could employ one of the transaminases classically described in the literature for furfural amination, e.g., *Chromobacterium violaceum*. Notably, we had immobilized it beforehand on silica too, in order to enhance its removal from the medium by simple filtration like for the chemical catalyst, simplifying the posttreatment of the process. As a final result, by using two different amine donors, methylbenzylamine and isopropylamine, which are formed through transamination of the thermodynamically stable acetophenone and the easily removable acetone product, respectively shifting the reaction equilibrium. Following this approach, we reached a process leading to a 77% yield in AMFC in 52 h and with FDCA as the only byproduct (Figure 11).

Interestingly, this process has paved the way for other attempts by various research groups. We should mention the one from Giri and coworkers [100], who recently reported a robust transaminase from *Shimia marina* (SMTA) that enables the scalable amination of HMF to biobased

**Figure 11.** One-pot/two-steps hybrid synthesis of 5-aminomethyl-2-furancarboxylic acid (AMFC) combining an oxidation step catalyzed by platinum nanoparticles immobilized on silica leading to the formation of an intermediate 5-aldehyde-2-furancarboxylic acid (AFCA), which is then aminated by the immobilized *Cv*TA transaminase in a second step in the same reaction medium. Redrawn from Lancien et al. [99].

furfurylamines with high activity and broad substrate specificity. In their case, they succeeded in developing a similar cascade reaction, only enzymatically, coupling an aldehyde reductase from *Synechocystis* sp. PCC 6906 (SAHR), in a one-pot/two-steps system, nearly yielding a quantitative production of AMFC in 30 h. However, as the authors themselves acknowledged, obtaining the AFCA intermediate by a purely enzymatic route generally requires the use of several consecutive oxidases (two in their case) as well as the regeneration of expensive cofactors (which involve an additional catalase and horseradish peroxidase in their process), which drastically increases the complexity and the cost of the system, and consequently, limits the industrial application of this approach. This demonstrates, again, the potential of hybrid catalysis, particularly when chemical catalysts are used to replace the costliest steps of cofactor regeneration and inhibitor suppression (e.g., $H_2O_2$).

### 2.3. *Taking the concept a step further: one-pot/two-steps hybrid production of furfurylamides from AMFC*

Recently, willing to take the concept a step further, we sought to directly convert AMFC into a new family of molecules. More precisely, we wanted to take advantage of the polyfunctional character of AMFC, and even more precisely of the presence of two ionizable functions, one of them positively (amine) and the other one negatively (carboxylic acid), to try to produce amphiphilic molecules with different properties, by attaching a fatty chain to one of these two functions. Among the many types of new bonds that can be formed on these two functions to introduce a fatty chain, one of them seemed particularly promising, as it could potentially be applied to both functionalities of the molecule: the creation of an amide bond from a fatty alcohol or acid. This type of bond also seemed relevant because of its rigidity

and resistance to hydrolysis, guaranteeing a certain stability of the produced compound. More generally speaking, the synthesis of amides is one of the most important transformations in agrochemical, pharmaceutical and polymer industries [101,102]. In recent decades, there has been growing interest in amide-producing processes after the ACS Green Chemistry Institute pointed out the need for more sustainable approaches to amide production as a key research area for a more environmentally friendly chemistry [103]. The most common approach for producing amides is the nucleophilic addition of an amine to an activated carboxylic acid. However, the activating agents involved in these reactions often lead to the generation of waste and hazardous byproducts [104,105]. It should be noted, however, that many enzymes are also capable of forming amide bonds, such as hydrolases (e.g., lipases, esterases, and acylases), nitriles hydratases, and transglutaminases that have already been used at an industrial scale under milder conditions compared to the traditional organic synthesis routes [106]. It is worth mentioning that other and much less exploited classes of enzymes are also available to form these bonds, notably acyl-coenzyme A ligases (ACLs) [107,108]. ACLs catalyze ATP-dependent formation of acyl-CoA thioesters from carboxylic acids in a two-step reaction: (1) formation of adenylate derivative from carboxylic acid and ATP and (2) nucleophilic attack of coenzyme A (HSCoA) [109]. Diversion of the native reaction by adding an extra amine nucleophile in absence of HSCoA leads to the formation of amides [110–112]. One of the main advantages of this reaction, unlike the use of hydrolases for example, is that the amine used for nucleophilic substitution, responsible for the formation of the final amide bond, is not taken over by the enzyme at all, since the substitution takes place spontaneously thanks to the intrinsic reactivity of the adenylate intermediate. Thus, virtually any amine could be used, substituted by an infinite number of substituents, as long as it is sufficiently nucleophilic to attack the adenylate, implying that the products formed could therefore be highly chemomodulated. Using these enzymes, it would therefore be possible to either; (1) activate the AMFC acid and transform it into an amide by attacking a free amine in the medium; or (2) consider using AMFC as a nucleophilic amine, by activating another carboxylic acid,

which might also be derived from biomass. In either case, if the other reagent contains a fatty chain, it is possible to obtain a relatively apolar AMFC derivative, but one which retains a polar head, ionizable in acidic or basic media depending on the strategy chosen. When the amide is formed from the carboxylic acid of AMFC, it should be noted that it would also be possible to form a quaternary ammonium at its free amino group, leading to a charged molecule. In any case, to our knowledge, none of these molecule families has ever been reported, which makes them a very promising subject for study. Having at our disposal a library of ACLs produced from previous work, we verified that AMFC was indeed a substrate for one of the ACLs. Unfortunately, none of the eight enzymes we tested, which had shown the most promise in previous assays (activity, stability, etc.), showed activity toward AMFC, as these enzymes tend to accept aliphatic substrates with different chain lengths. This stopped, for now, the acid functionalization pathway for AMFC, and we therefore turned our attention to the possibility of using the latter as a nucleophilic amine. Still seeking to branch out into a variety of fatty chains, and given the estimated substrate selectivity of our enzymes, we then screened our library on fatty mono- and diacids, ranging from four to ten carbon atoms. It should be noted that we did include in the panel some aromatic substrates whose ring was distant from the carboxylic acid. Different selectivity was observed for short and long chains depending on the enzyme (Figure 12). Considering the possibility of using these enzymes in hybrid processes, we carried out the assays at 60 °C, a temperature which had proved interesting in our previous study with the chemical catalysts tested. One particular TsACL displayed a broad substrate range, being very active toward all the tested monocarboxylic acids excepted the decanoic acid and revealed to be almost the only ACL accepting a diacid (e.g., succinic acid). Thus, we can consider that the production of AMFC dimers linked by a fatty chain enables to obtain two polar heads instead of just one on the same molecule. It should also be noted that these screenings were carried out directly with AMFC as the nucleophilic amine, which gives an indication of the yields, even though the assays were carried out on an analytical scale. Also, looking more specifically at TsACL, yields between 53% and 71% for aliphatic acids and 39% for succinic acid, respectively, can be obtained, which is

already an excellent result in itself. However, determined to go one step further by proposing the use of a wider range of substrates, we were interested to see if we could couple these enzymes with oxidative catalysts, similar to those we had previously developed. This time, however, fatty alcohols would directly be used instead of fatty acids, given the higher stability of the alcohols for storage purposes rather than the acids. The idea was then to carry out a first oxidation step, once again using immobilized metal nanoparticles to transform a fatty alcohol into the corresponding acid, then to make the ACL act on the formed acid to enable it to be attacked by AMFC, in a one-pot process (Figure 12).

To bring this concept to fruition, a screening of chemical catalysts, assisted by the REALCAT platform's robots, was carried out to confirm their ability to oxidize alcohols into their corresponding acid, under conditions compatible with those of the enzymes. To this end, the reaction was performed at 60 °C and a family of gold nanoparticles immobilized on a variety of supports with acidic, basic or neutral properties tested. As expected, nanoparticles immobilized on the basic support, and more particularly on calcium oxide (CaO), proved the most active, with a total conversion in less than 24 h, and perfect selectivity for the desired acid. These assays were first carried out on butanol, and then extended to the evaluation of the activity measurement for the best catalyst (Au/CaO) to the alcohol panel corresponding to the acids accepted by TsACL. Here, the catalyst demonstrated an equivalent activity on all substrates, with total conversion to the desired aliphatic acids, as well as to 1,4-butanediol leading to succinic acid. This highlights the highly versatile nature of this new catalyst, making it an ideal candidate for our hybrid system. On the other hand, recycling tests of this catalyst led to leach out observation, with the basic sites gradually being eliminated, leading to its gradual deactivation. This effect was first observed, albeit more slowly, in water, and then much more rapidly when using a buffer to prepare the combination of the two catalysts. We screened different buffers potentially compatible with ACLs (MOPS, TRIS and CAPS) at different pH values ranging from 8 to 11, and it was observed that the catalyst activity was greater at more basic pHs, as well as the recycling activity. Surprisingly, it was also observed that TRIS and CAPS were strongly degraded by the catalyst, although the

degradation products have not yet been identified. In the end, it was the 100 mM MOPS buffer that provided the best catalyst activity, with around 80% conversion in 24 h for pH 8 and 9. We also took advantage of this assay to test the activity of the catalyst in the presence of $MgCl_2$ and $MnCl_2$, two cofactors of the enzyme, knowing that the enzyme can use both quite indifferently. It was found that the activity of the chemical catalyst was surprisingly greatly diminished in the presence of $Mn^{2+}$, whereas the $Mg^{2+}$ ion did not allow us to see any significant difference. Having demonstrated the activity of the catalyst in a buffered medium, the coupling of our two catalysts could be achieved. A first assay was carried out on butanol as substrate, which was first converted to butanoic acid, then acidified to give 5-(butyramidomethyl)furan-2-carboxylic acid by introducing TsACL, with AMFC and ATP in the medium in a second step. Under the previously optimized conditions, a 65% yield of the desired product was obtained in 48 h, with alcohol-to-acid conversion always quantitative, the limiting step being the enzymatic amide formation, although the obtained yield is in line with the one from the enzyme screening. We then extended our one-pot/two-steps process to other alcohols and obtained the corresponding amides in similar yields to butanol for pentanol and hexanol, and lower yields (26%) for octanol, perhaps due to alcohol solubility issues, the latter having been slightly less oxidized (88% in acid formation) than the shorter-chain alcohols by the chemical catalyst. Interestingly, we also managed to perform the hybrid cascade on 1,4-butanediol, with a modest 24% yield. Nevertheless, the presence of two products was confirmed by NMR as mono- and disubstituted succinic acid, with a preference for the second one (16% yield vs. 8% for the monosubstituted). This creates opportunities for additional valorization pathways and applications for AMFC. To sum up, this tandem heterogeneous enzymatic catalysis, performed under mild aqueous conditions, marks a significant advancement through the integration of gold nanoparticles and enzymes within a one-pot reaction. Concretely, it represents the first association of an ACL with a chemocatalyst, showing how such strategies can offer access to valuable amides. A limitation of the present process though, is the use of large excess of ATP, but this could be easily circumvented by setting up an ATP regeneration system previously reported in the use of ACL
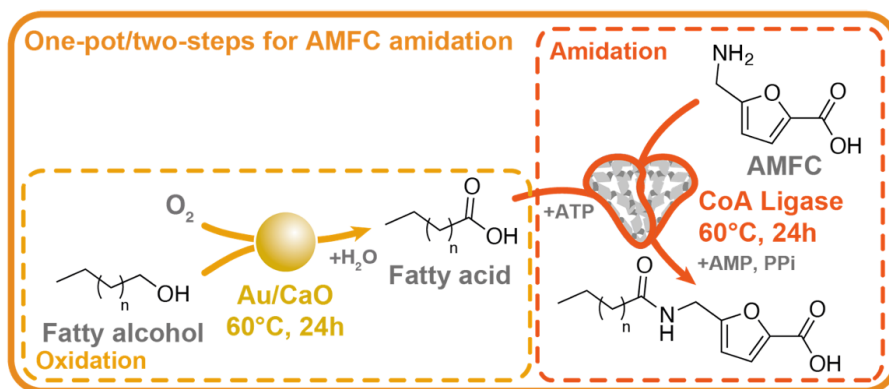
**Figure 12.** General scheme for the synthesis of AMFC-based amides through the implementation of a one-pot/two-steps process combining supported gold nanoparticles as oxidative chemocatalyst and a CoA ligase as biocatalyst. Redrawn from Bisel et al. [113].

enzymes [114]. Another avenue for improvement is the implementation of a fully integrated process in a single step, ideally using catalyst compartmentalization techniques to limit their direct interaction. This aspect might be crucial as, after trying to set up the one-pot/one-step hybrid system, the chemical catalyst seemed to be poisoned by enzyme—its oxidation capacity falling to zero as soon as the enzyme was introduced into the medium. Indeed, it is not a concept detailed in the present article but the production of "multicatalytic hybrid materials" combining the active centers of the catalysts in a finely compartmentalized manner, represents one of the major promises of hybrid process. As already mentioned in several previous reviews, these new materials could represent an excellent solution for avoiding cross-poisoning, while maximizing the synergistic effects of the catalysts, and simplifying processes [115]. In the meantime, a two-pot/one-step system could also be considered, especially as the molecules generated here have probably a different partition coefficient with respect to an organic transfer phase, depending on their oxidation state and level of functionalization.

## 3. Conclusion

In conclusion, through these three examples, as well as with the important work accomplished by the community in hybrid catalysis over the last decade, we have tried to show that the combination of catalysts of different natures, and more particularly

chemical and biological ones, could be highly relevant for the valorization of biosourced molecules. Indeed, the aforementioned recent developments in hybrid catalysis have shown the possibility of directly transforming untreated biomass materials into value-added products. In this field, the production of furfural is one of the most targeted molecules found in the literature; as many of its derivatives can have potential applications in different industries (pharmaceuticals, polymers, food, for instance). It is worth mentioning that the developed systems are not only simple in terms of substrate and product treatment, notably without needing any additional pretreatment or intermediate isolation and purification steps, but also more efficient in terms of atom and energy economy, thanks to a one-pot set-up. In parallel, research in hybrid catalysis has also enhanced the exploration of new synthetic pathways. As a result, structurally rich molecules, often chiral and therefore interesting to access pharmaceutical molecules, can now be accessed through such approaches. The wide substrate scopes and the subsequent obtainment of a range of products show the versatility of hybrid approaches, which from a future industrial application perspective, could be very interesting. All these aspects are reflected on the presented application, showing the whole workflow to develop a series of hybrid approaches where biosourced D-glucose is converted into HMF, then to AMFC, a furfurylamine, and then to amphiphilic furfurylamides that were never produced to the best of our knowledge. Still, despite this high

potential, catalyst combination remains very limited due to their cross-poisoning or incompatibility between reaction conditions. Smart processes, based on innovative chemical engineering, can nonetheless help overcome these limitations with new equipment (two-pot/one-step process), or in the ideal situation, tailor-made compartmentalized hybrid materials. Among all, hybrid catalysis stands as a highly interdisciplinary and emerging subject, which will increasingly require close collaboration between different scientific fields, notably chemistry and biology, while also keeping an engineering perspective to enhance further efficient applications.

## Declaration of interests

The authors do not work for, advise, own shares in, or receive funds from any organization that could benefit from this article, and have declared no affiliations other than their research organizations.

## Acknowledgments

## References

[1] H. O. Pörtner, R. J. Scholes, A. Arneth, et al., "Overcoming the coupled climate and biodiversity crises and their societal impacts", *Science* **380** (2023), article no. eabl4881.

[2] M. Saleem, "Possibility of utilizing agriculture biomass as a renewable and sustainable future energy source", *Heliyon* **8** (2022), article no. e08905.

[3] Y. Queneau and B. Han, "Biomass: renewable carbon resource for chemical and energy industry", *Innovation* **3** (2022), article no. 100184.

[4] R. A. Sheldon, "Green chemistry and biocatalysis: engineering a sustainable future", *Catal. Today* **431** (2024), article no. 114571.

[5] P. T. Anastas and J. C. Warner, "Principles of green chemistry", in *Green Chemistry: Theory and Practice*, Oxford Academic: Oxford, 2000, pp. 29–56. Online edition, October 31, 2023.

[6] T. Kalak, "Potential use of industrial biomass waste as a sustainable energy source in the future", *Energies* **16** (2023), article no. 1783.

[7] A. Bayu, A. Abudula and G. Guan, "Reaction pathways and selectivity in chemo-catalytic conversion of biomass-derived carbohydrates to high-value chemicals: a review", *Fuel Process. Technol.* **196** (2019), article no. 106162.

[8] P. Nargotra, V. Sharma, Y.-C. Lee, et al., "Microbial lignocellulolytic enzymes for the effective valorization of lignocellulosic biomass: a review", *Catalysts* **13** (2022), article no. 83.

[9] E. Heuson and F. Dumeignil, "The various levels of integration of chemo- and bio-catalysis towards hybrid catalysis", *Catal. Sci. Technol.* **10** (2020), pp. 7082–7100.

[10] C. Gastaldi, A. Gautier, C. Forano, V. Hélaine and C. Guérard-Hélaine, "Hybrid catalysis in concurrent mode: how to make catalysts and biocatalysts compatible?", *ChemCatChem* **16** (2024), article no. e202301703.

[11] M. Makkee, A. P. G. Kieboom, H. van Bekkum and J. A. Roels, "Combined action of enzyme and metal catalyst, applied to the preparation of D-mannitol", *J. Chem. Soc. Chem. Commun.* (1980), pp. 930–931.

[12] M. Makkee, A. P. G. Kieboom and H. van Bekkum, "Combined action of an enzyme and a metal catalyst on the conversion of d-glucose/d-fructose mixtures into d-mannitol", *Carbohydr. Res.* **138** (1985), pp. 237–245.

[13] E. Heuson and A. Dibenedetto, "15 Hybrid catalysis: bridging two worlds for greener chemicals and energy production", in *Biorefinery: From Biomass to Chemicals and Fuels* (M. Aresta, A. Dibenedetto and F. Dumeignil, eds.), De Gruyter: Berlin, 2022, pp. 493–536. Online at https://www.degruyter.com/document/doi/10.1515/9783110705386-016/html (accessed on January 4, 2022).

[14] F. H. Isikgor and C. Remzi Becer, "Lignocellulosic biomass: a sustainable platform for the production of bio-based chemicals and polymers", *Polym. Chem.* **6** (2015), pp. 4497–4559.

[15] İ. Yıldız, *Comprehensive Energy Systems*, Elseveier: Oxford, 2018, pp. 521–567. ISBN 9780128149256.

[16] Z. Chen, Y. Wang, H. Cheng and H. Zhou, "Integrated chemo- and biocatalytic processes: a new fashion toward renewable chemicals production from lignocellulosic biomass", *J. Chem. Technol. Biotechnol.* **98** (2022), pp. 331–345.

[17] A. I. Benítez-Mateos, D. Roura Padrosa and F. Paradisi, "Multistep enzyme cascades as a route towards green and sustainable pharmaceutical syntheses", *Nat. Chem.* **14** (2022), pp. 489–499.

[18] S. P. France, R. D. Lewis and C. A. Martinez, "The evolving nature of biocatalysis in pharmaceutical research and development", *JACS Au* **3** (2023), pp. 715–735.

[19] J. A. McIntosh, T. Benkovics, S. M. Silverman, et al., "Engineered ribosyl-1-kinase enables concise synthesis of

molnupiravir, an antiviral for COVID-19", *ACS Cent. Sci.* **7** (2021), pp. 1980–1985.

[20] S. Wu, R. Snajdrova, J. C. Moore, K. Baldenius and U. T. Bornscheuer, "Biocatalysis: enzymatic synthesis for industrial applications", *Angew. Chem. Int. Ed.* **60** (2021), pp. 88–119.

[21] M. Abdelgaid and G. Mpourmpakis, "Structure–activity relationships in lewis acid–base heterogeneous catalysis", *ACS Catal.* **12** (2022), pp. 4268–4289.

[22] I. P. Rosinha Grundtvig, S. Heintz, U. Krühne, K. V. Gernaey, P. Adlercreutz, J. D. Hayler, A. S. Wells and J. M. Woodley, "Screening of organic solvents for bioprocesses using aqueous-organic two-phase systems", *Biotechnol. Adv.* **36** (2018), pp. 1801–1814.

[23] V. Smeets, W. Baaziz, O. Ersen, E. M. Gaigneaux, C. Boissière, C. Sanchez and D. P. Debecker, "Hollow zeolite microspheres as a nest for enzymes: a new route to hybrid heterogeneous catalysts†", *Chem. Sci.* **11** (2019), pp. 954–961.

[24] H. Gröger, F. Gallou and B. H. Lipshutz, "Where chemocatalysis meets biocatalysis: in water", *Chem. Rev.* **123** (2023), pp. 5262–5296.

[25] P. P. Upare, R. E. Clarence, H. Shin and B. G. Park, "An overview on production of lignocellulose-derived platform chemicals such as 5-hydroxymethyl furfural, furfural, protocatechuic acid", *Processes* **11** (2023), article no. 2912.

[26] X. Yue and Y. Queneau, "5-hydroxymethylfurfural and furfural chemistry toward biobased surfactants", *ChemSusChem* **15** (2022), article no. e202102660.

[27] J. Di, C. Ma, J. Qian, X. Liao, B. Peng and Y. He, "Chemoenzymatic synthesis of furfuralcohol from chestnut shell hydrolysate by a sequential acid-catalyzed dehydration under microwave and Escherichia coli CCZU-Y10 whole-cells conversion", *Bioresour. Technol.* **262** (2018), pp. 52–58.

[28] D. Yang, C. Ma, B. Peng, J. Xu and Y. He, "Synthesis of furoic acid from biomass via tandem pretreatment and biocatalysis", *Ind. Crop. Prod.* **153** (2020), article no. 112580.

[29] L.-Z. Qin and Y. He, "Chemoenzymatic synthesis of furfuryl alcohol from biomass in tandem reaction system", *Appl. Biochem. Biotechnol.* **190** (2019), pp. 1289–1303.

[30] Y. Huang, X. Liao, Y. Deng and Y. He, "Co-catalysis of corncob with dilute formic acid plus solid acid $SO4^{2-}$/SnO2-montmorillonite under the microwave for enhancing the biosynthesis of furfuralcohol", *Catal. Commun.* **120** (2019), pp. 38–41.

[31] X.-X. Xue, C.-L. Ma, J.-H. Di, X.-Y. Huo and Y. He, "One-pot chemo-enzymatic conversion of D-xylose to furfuralcohol by sequential dehydration with oxalic acid plus tin-based solid acid and bioreduction with whole-cells", *Bioresour. Technol.* **268** (2018), pp. 292–299.

[32] L. Zhu, J. Di, Q. Li, Y.-C. He and C. Ma, "Enhanced conversion of corncob into furfurylamine via chemoenzymatic cascade catalysis in a toluene–water medium", *J. Mol. Liq.* **380** (2023), article no. 121741.

[33] W. He, Y.-C. He and J. Ye, "Efficient synthesis of furfurylamine from biomass via a hybrid strategy in an EaCl:Gly–

water medium", *Front. Bioeng. Biotechnol.* **11** (2023), article no. 1144787.

[34] W. Zhang, E. F. Fueyo, F. Hollmann, L. L. Martin, M. Pesic, R. Wardenga, M. Hoehne and S. Schmidt, "Combining photo-organo redox- and enzyme catalysis facilitates asymmetric C–H bond functionalization", *Eur. J. Org. Chem.* **2019** (2019), pp. 80–84.

[35] Y.-C. Hao, M.-H. Zong, Q. Chen and N. Li, "Engineering carbonyl reductase for one-pot chemobiocatalytic enantioselective synthesis of a value-added N-containing chiral alcohol from N-acetyl-D-glucosamine", *Green Chem.* **25** (2023), pp. 5051–5058.

[36] C. Gastaldi, G. Mekhloufi, C. Forano, A. Gautier and C. Guérard-Hélaine, "Mixing chemo- and biocatalysis for rare monosaccharide production by combining aldolase and N-heterocyclic carbene gold catalysts", *Green Chem.* **36** (2022), article no. 10.1039.D2GC00667G.

[37] J. N. Chheda and J. A. Dumesic, "An overview of dehydration, aldol-condensation and hydrogenation processes for production of liquid alkanes from biomass-derived carbohydrates", *Catal. Today* **123** (2007), pp. 59–70.

[38] Z. Li, Z. Wan, W. Wang, L. Chen and P. Ji, "Chemoenzymatic sequential catalysis with carbonic anhydrase for the synthesis of chiral alcohols from alkanes, alkenes, and alkynes", *ACS Catal.* **14** (2024), pp. 8786–8793.

[39] R.-J. van Putten, J. C. van der Waal, E. de Jong, C. B. Rasrendra, H. J. Heeres and J. G. de Vries, "Hydroxymethylfurfural, a versatile platform chemical made from renewable resources", *Chem. Rev.* **113** (2013), pp. 1499–1597.

[40] M. Moliner, Y. Román-Leshkov and M. E. Davis, "Tin-containing zeolites are highly active catalysts for the isomerization of glucose in water", *Proc. Natl. Acad. Sci. USA* **107** (2010), pp. 6164–6168.

[41] J. J. Pacheco and M. E. Davis, "Synthesis of terephthalic acid via Diels-Alder reactions with ethylene and oxidized variants of 5-hydroxymethylfurfural", *Proc. Natl. Acad. Sci. USA* **111** (2014), pp. 8363–8367.

[42] Z. Lin, V. Nikolakis and M. Ierapetritou, "Alternative Approaches for p-xylene production from starch: techno-economic analysis", *Ind. Eng. Chem. Res.* **53** (2014), pp. 10688–10699.

[43] E. de Jong, M. A. Dam, L. Sipos and G. J. M. Gruter, *Biobased Monomers, Polymers, and Materials*, ACS Symposium Series, American Chemical Society: Washington, DC, 2012, pp. 1–13. ISBN13: 9780841227675.

[44] A. Boisen, T. B. Christensen, W. Fu, et al., "Process integration for the conversion of glucose to 2,5-furandicarboxylic acid", *Chem. Eng. Res. Des.* **87** (2009), pp. 1318–1327.

[45] G. R. Akien, L. Qi and I. T. Horváth, "Molecular mapping of the acid catalysed dehydration of fructose", *Chem. Commun.* **48** (2012), pp. 5850–5852.

[46] K. Parker, M. Salas and V. Nwosu, "High fructose corn syrup: Production, uses and public health concerns", *Biotechnol. Mol. Biol. Rev.* **5** (2011), pp. 71–78.

[47] H. Li, A. Riisager, S. Saravanamurugan, A. Pandey, R. S. Sangwan, S. Yang and R. Luque, "Carbon-increasing catalytic strategies for upgrading biomass into energy-

intensive fuels and chemicals", *ACS Catal.* **8** (2018), pp. 148–187.

[48] V. Choudhary, A. B. Pinar, R. F. Lobo, D. G. Vlachos and S. I. Sandler, "Comparison of homogeneous and heterogeneous catalysts for glucose-to-fructose isomerization in aqueous media", *ChemSusChem* **6** (2013), pp. 2369–2376.

[49] A. A. Marianou, C. M. Michailof, A. Pineda, E. F. Iliopoulou, K. S. Triantafyllidis and A. A. Lappas, "Glucose to fructose isomerization in aqueous media over homogeneous and heterogeneous catalysts", *ChemCatChem* **8** (2016), pp. 1100–1110.

[50] I. Delidovich and R. Palkovits, "Catalytic isomerization of biomass-derived aldoses: a review", *ChemSusChem* **9** (2016), pp. 542–542.

[51] M. Demerdash and R. M. Attia, "Equilibrium kinetics of D-glucose to D-fructose isomerization catalyzed by glucose isomerase enzyme from streptomyces phaeochromogenus", *Zentralbl. Mikrobiol.* **147** (1992), pp. 297–303.

[52] Y. Takasaki, "Kinetic and equilibrium studies on d-mannose-d-fructose isomerization catalyzed by mannose isomerase from streptomyces aerocolorigenes", *Agric. Biol. Chem.* **31** (2014), pp. 435–440.

[53] H. Huang, C. A. Denard, R. Alamillo, A. J. Crisci, Y. Miao, J. A. Dumesic, S. L. Scott and H. Zhao, "Tandem catalytic conversion of glucose to 5-hydroxymethylfurfural with an immobilized enzyme and a solid acid", *ACS Catal.* **4** (2014), pp. 2165–2168.

[54] R. Huang, W. Qi, R. Su and Z. He, "Integrating enzymatic and acid catalysis to convert glucose into 5-hydroxymethylfurfural", *Chem. Commun.* **46** (2009), pp. 1115–1117.

[55] I. Delidovich and R. Palkovits, "Catalytic versus stoichiometric reagents as a key concept for green chemistry", *Green Chem.* **18** (2016), pp. 590–593.

[56] S. Alipour, "High yield 5-(hydroxymethyl)furfural production from biomass sugars under facile reaction conditions: a hybrid enzyme- and chemo-catalytic technology", *Green Chem.* **18** (2016), pp. 4990–4998.

[57] A. Gimbernat, M. Guehl, N. Lopes Ferreira, et al., "From a sequential chemo-enzymatic approach to a continuous process for HMF production from glucose", *Catalysts* **8** (2018), article no. 335.

[58] M. J. Karpa, P. J. Duggan, G. J. Griffin and S. J. Freudigmann, "Competitive transport of reducing sugars through a lipophilic membrane facilitated by aryl boron acids", *Tetrahedron* **53** (1997), pp. 3669–3678.

[59] P. R. Westmark, S. J. Gardiner and B. D. Smith, "Selective monosaccharide transport through lipid bilayers using boronic acid carriers", *J. Am. Chem. Soc.* **118** (1996), pp. 11093–11100.

[60] T. Shinbo, K. Nishimura, T. Yamaguchi and M. Sugiura, "Uphill transport of monosaccharides across an organic liquid membrane", *J. Chem. Soc. Chem. Commun.* (1986), pp. 349–351.

[61] A. Gimbernat, E. Heuson, F. Dumeignil, D. Delcroix, J.-S. Girardon and R. Froidevaux, "Reactor development for a one-step hybrid catalytic conversion of D-glucose to HMF", *ChemCatChem* **16** (2024), article no. e202300713.

[62] A. A. Rosatella, S. P. Simeonov, R. F. M. Frade and C. A. M. Afonso, "5-Hydroxymethylfurfural (HMF) as a building block platform: Biological properties, synthesis and synthetic applications", *Green Chem.* **13** (2011), pp. 754–793.

[63] W. Fan, C. Verrier, Y. Queneau and F. Popowycz, "5-hydroxymethylfurfural (HMF) in organic synthesis: a review of its recent applications towards fine chemicals", *Curr. Org. Synth.* **16** (2019), pp. 583–614.

[64] L. Hu, L. Lin, Z. Wu, S. Zhou and S. Liu, "Recent advances in catalytic transformation of biomass-derived 5-hydroxymethylfurfural into the innovative fuels and chemicals", *Renew. Sustain. Energy Rev.* **74** (2017), pp. 230–257.

[65] L. Hu, A. He, X. Liu, J. Xia, J. Xu, S. Zhou and J. Xu, "Biocatalytic transformation of 5-hydroxymethylfurfural into high-value derivatives: recent advances and future aspects", *ACS Sustain. Chem. Eng.* **6** (2018), pp. 15915–15935.

[66] B. Hočevar, M. Grilc and B. Likozar, "Aqueous dehydration, hydrogenation, and hydrodeoxygenation reactions of bio-based mucic acid over Ni, NiMo, Pt, Rh, and Ru on neutral or acidic catalyst supports", *Catalysts* **9** (2019), article no. 286.

[67] M. Mojca Cajnko, U. Novak, M. Grilc and B. Likozar, "Enzymatic conversion reactions of 5-hydroxymethylfurfural (HMF) to bio-based 2,5-diformylfuran (DFF) and 2,5-furandicarboxylic acid (FDCA) with air: mechanisms, pathways and synthesis selectivity", *Biotechnol. Biofuels* **13** (2020), article no. 66.

[68] R. Wojcieszak and I. Itabaiana, "Engineering the future: perspectives in the 2,5-furandicarboxylic acid synthesis", *Catal. Today* **354** (2020), pp. 211–217.

[69] F. Drault, Y. Snoussi, S. Paul, I. Itabaiana and R. Wojcieszak, "Recent advances in carboxylation of furoic acid into 2,5-furandicarboxylic acid: pathways towards bio-based polymers", *ChemSusChem* **13** (2020), pp. 5164–5172.

[70] C. P. Ferraz, N. J. S. Costa, E. Teixeira-Neto, et al., "5-hydroxymethylfurfural and furfural base-free oxidation over AuPd embedded bimetallic nanoparticles", *Catalysts* **10** (2020), article no. 75.

[71] A. Roselli, Y. Carvalho, F. Dumeignil, F. Cavani, S. Paul and R. Wojcieszak, "Liquid phase furfural oxidation under uncontrolled ph in batch and flow conditions: the role of in situ formed base", *Catalysts* **10** (2020), article no. 73.

[72] J. Sha, S. Paul, F. Dumeignil and R. Wojcieszak, "Au-based bimetallic catalysts: how the synergy between two metals affects their catalytic activity", *RSC Adv.* **9** (2019), pp. 29888–29901.

[73] C. P. Ferraz, A. G. M. Da Silva, T. Silva Rodrigues, P. H. C. Camargo, S. Paul and R. Wojcieszak, "Furfural oxidation on gold supported on $MnO_2$: influence of the support structure on the catalytic performances", *Appl. Sci.* **8** (2018), article no. 1246.

[74] C. P. Ferraz, M. Zieliński, M. Pietrowski, S. Heyte, F. Dumeignil, L. M. Rossi and R. Wojcieszak, "Influence of support basic sites in green oxidation of biobased substrates using au-promoted catalysts", *ACS Sustain. Chem. Eng.* **6** (2018), pp. 16332–16340.

[75]   S. Chen, C. Ciotonea, K. De Oliveira Vigier, F. Jérôme, R. Wojcieszak, F. Dumeignil, E. Marceau and S. Royer, "Hydroconversion of 5-hydroxymethylfurfural to 2,5-dimethylfuran and 2,5-dimethyltetrahydrofuran over non-promoted Ni/SBA-15", *ChemCatChem* **12** (2020), pp. 2050–2059.

[76]   N. Capece, A. Sadier, C. P. Ferraz, et al., "Aerobic oxidation of 1,6-hexanediol to adipic acid over Au-based catalysts: the role of basic supports", *Catal. Sci. Technol.* **10** (2020), pp. 2644–2651.

[77]   F. Koopman, N. Wierckx, J. H. de Winde and H. J. Ruijssenaars, "Efficient whole-cell biotransformation of 5-(hydroxymethyl)furfural into FDCA, 2,5-furandicarboxylic acid", *Bioresour. Technol.* **101** (2010), pp. 6291–6296.

[78]   W. P. Dijkman, D. E. Groothuis and M. W. Fraaije, "Enzyme-catalyzed oxidation of 5-hydroxymethylfurfural to furan-2,5-dicarboxylic acid", *Angew. Chem.* **126** (2014), pp. 6633–6636.

[79]   J. Carro, P. Ferreira, L. Rodríguez, et al., "5-hydroxymethylfurfural conversion by fungal aryl-alcohol oxidase and unspecific peroxygenase", *FEBS J.* **282** (2015), pp. 3218–3229.

[80]   J. Carro, P. Ferreira, L. Rodríguez, et al., "5-hydroxymethylfurfural conversion by fungal aryl-alcohol oxidase and unspecific peroxygenase", *FEBS J.* **282** (2015), pp. 3218–3229.

[81]   K.-F. Wang, C.-l. Liu, K.-y. Sui, C. Guo and C.-Z. Liu, "Efficient catalytic oxidation of 5-hydroxymethylfurfural to 2,5-furandicarboxylic acid by magnetic laccase catalyst", *ChemBioChem* **19** (2018), pp. 654–659.

[82]   V. Froidevaux, C. Negrell, S. Caillol, J.-P. Pascault and B. Boutevin, "Biobased amines: from synthesis to polymers; present and future", *Chem. Rev.* **116** (2016), pp. 14181–14224.

[83]   K. Krishnamoorthy, D. Subramani, N. Eeda and A. Muthukaruppan, "Development and characterization of fully bio-based polybenzoxazine-silica hybrid composites for low-k and flame-retardant applications", *Polym. Adv. Technol.* **30** (2019), pp. 1856–1864.

[84]   X. Chen, J. Wang, S. Huo, S. Yang, B. Zhang and H. Cai, "Preparation of flame-retardant cyanate ester with low dielectric constants and dissipation factors modified with novel phosphorus-contained Schiff base", *J. Therm. Anal. Calorim.* **135** (2019), pp. 3153–3164.

[85]   J. L. Cawse, J. L. Stanford and R. H. Still, "Polymers from renewable sources, 1. Diamines and diisocyanates containing difurylalkane moieties", *Die Makromolekulare Chemie* **185** (1984), pp. 697–707.

[86]   M. S. Holfinger, A. H. Conner, D. R. Holm and C. G. Hill, "Synthesis of difurfuryl diamines by the acidic condensation of furfurylamine with aldehydes and their mechanism of formation", *J. Org. Chem.* **60** (1995), pp. 1595–1598.

[87]   M. Chatterjee, T. Ishizaka and H. Kawanami, "Reductive amination of furfural to furfurylamine using aqueous ammonia solution and molecular hydrogen: an environmentally friendly approach", *Green Chem.* **18** (2015), pp. 487–496.

[88]   G. Chieffi, M. Braun and D. Esposito, "Continuous reductive amination of biomass-derived molecules over carbonized filter paper-supported FeNi alloy", *ChemSusChem* **8** (2015), pp. 3590–3594.

[89]   S. Jiang, C. Ma, E. Muller, M. Pera-Titus, F. Jérôme and K. De Oliveira Vigier, "Selective synthesis of THF-derived amines from biomass-derived carbonyl compounds", *ACS Catal.* **9** (2019), pp. 8893–8902.

[90]   X. Wang, W. Chen, Z. Li, X. Zeng, X. Tang, Y. Sun, T. Lei and L. Lin, "Synthesis of bis(amino)furans from biomass based 5-hydroxymethyl furfural", *J. Energy Chem.* **27** (2018), pp. 209–214.

[91]   D. Chandra, Y. Inoue, M. Sasase, M. Kitano, A. Bhaumik, K. Kamata, H. Hosono and M. Hara, "A high performance catalyst of shape-specific ruthenium nanoparticles for production of primary amines by reductive amination of carbonyl compounds", *Chem. Sci.* **9** (2018), pp. 5949–5956.

[92]   Z. Xu, P. Yan, W. Xu, S. Jia, Z. Xia, B. Chung and Z. Conrad Zhang, "Direct reductive amination of 5-hydroxymethylfurfural with primary/secondary amines via Ru-complex catalyzed hydrogenation", *RSC Adv.* **4** (2014), pp. 59083–59087.

[93]   A. Dunbabin, F. Subrizi, J. M. Ward, T. D. Sheppard and H. C. Hailes, "Furfurylamines from biomass: transaminase catalysed upgrading of furfurals", *Green Chem.* **19** (2016), pp. 397–404.

[94]   A. Petri, G. Masia and O. Piccolo, "Biocatalytic conversion of 5-hydroxymethylfurfural: Synthesis of 2,5-bis(hydroxymethyl)furan and 5-(hydroxymethyl)furfurylamine", *Catal. Commun.* **114** (2018), pp. 15–18.

[95]   M. Sharma, P. Kumar, H. Singh and T. K. Chakraborty, "Preferential cyclotrimerization of 5-(aminomethyl)-2-furancarboxylic acid (AMFC): electrostatic and orbital interactions studies", *J. Mol. Struct.: THEOCHEM* **764** (2006), pp. 109–115.

[96]   T. K. Chakraborty, S. Tapadar and S. Kiran Kumar, "Cyclic trimer of 5-(aminomethyl)-2-furancarboxylic acid as a novel synthetic receptor for carboxylate recognition", *Tetrahedron Lett.* **43** (2002), pp. 1317–1320.

[97]   A. Lancien, E. Heuson, F. Dumeignil, I. Itabaiana, R. Froidevaux and R. Wojcieszak, "Pt nanoparticles with enhanced deaminase-like activity: example of oxidative deamination of 5-hydroxymethylfurfurylamine and glutamic acid", *ChemNanoMat* **8** (2022), article no. e202200062.

[98]   M. Cárdenas-Fernández, O. Sinclair and J. M. Ward, "Novel transaminases from thermophiles: from discovery to application", *Microb. Biotechnol.* **15** (2021), pp. 305–317.

[99]   A. Lancien, R. Wojcieszak, E. Cuvelier, et al., "Hybrid conversion of 5-hydroxymethylfurfural to 5-aminomethyl-2-furancarboxylic acid: toward new bio-sourced polymers", *ChemCatChem* **13** (2021), pp. 247–259.

[100]  P. Giri, S. Lim, T. P. Khobragade, et al., "Biocatalysis enables the scalable conversion of biobased furans into various furfurylamines", *Nat. Commun.* **15** (2024), article no. 6371.

[101] Y. Jiang and K. Loos, "Enzymatic synthesis of biobased polyesters and polyamides", *Polymers* **8** (2016), article no. 243.

[102] J. Pitzer and K. Steiner, "Amides in nature and biocatalysis", *J. Biotechnol.* **235** (2016), pp. 32–46.

[103] D. J. C. Constable, P. J. Dunn, J. D. Hayler, et al., "Key green chemistry research areas—a perspective from pharmaceutical manufacturers", *Green Chem.* **9** (2007), pp. 411–420.

[104] R. M. Lanigan and T. D. Sheppard, "Recent developments in amide synthesis: direct amidation of carboxylic acids and transamidation reactions", *Eur. J. Org. Chem.* **2013** (2013), pp. 7453–7465.

[105] V. R. Pattabiraman and J. W. Bode, "Rethinking amide bond synthesis", *Nature* **480** (2011), pp. 471–479.

[106] B. M. Dorr and D. E. Fuerst, "Enzymatic amidation for industrial applications", *Curr. Opin. Chem. Biol.* **43** (2018), pp. 127–133.

[107] A. J. L. Wood, N. J. Weise, J. D. Frampton, et al., "Adenylation activity of carboxylic acid reductases enables the synthesis of amides", *Angew. Chem.* **129** (2017), pp. 14690–14693.

[108] M. Petchey, A. Cuetos, B. Rowlinson, et al., "The broad aryl acid specificity of the amide bond synthetase McbA suggests potential for the biocatalytic synthesis of amides", *Angew. Chem. Int. Ed.* **57** (2018), pp. 11584–11588.

[109] H. K. Philpott, P. J. Thomas, D. Tew, D. E. Fuerst and S. L. Lovelock, "A versatile biosynthetic approach to amide bond formation", *Green Chem.* **20** (2018), pp. 3426–3431.

[110] N. Capra, C. Lelièvre, O. Touré, et al., "Adapting an acyl CoA ligase from Metallosphaera sedula for lactam formation by structure-guided protein engineering", *Front. Catal.* **4** (2024), article no. 1360129.

[111] T. Abe, Y. Hashimoto, H. Hosaka, K. Tomita-Yokotani and M. Kobayashi, "Discovery of amide (Peptide) bond synthetic activity in Acyl-CoA synthetase*", *J. Biol. Chem.* **283** (2008), pp. 11312–11321.

[112] J. Zhang, E. Kao, G. Wang, E. E. K. Baidoo, M. Chen and J. D. Keasling, "Metabolic engineering of escherichia coli for the biosynthesis of 2-pyrrolidone", *Metab. Eng. Commun.* **3** (2016), pp. 1–7.

[113] L. Bisel, A. Fossey-Jouenne, R. Martin, et al., "Hybrid synthesis of AMFC-derived amides using supported gold nanoparticles and acyl-coenzyme a ligases", 2024. Online at https://doi.org/10.26434/chemrxiv-2024-2d7wr.

[114] C. M. Lelièvre, M. Balandras, J.-L. Petit, C. Vergne-Vaxelaire and A. Zaparucha, "ATP regeneration system in chemoenzymatic amide bond formation with thermophilic CoA ligase", *ChemCatChem* **12** (2020), pp. 1184–1189.

[115] E. Heuson, R. Froidevaux, I. Itabaiana, R. Wojcieszak, M. Capron and F. Dumeignil, "Optimisation of catalysts coupling in multi-catalytic hybrid materials: perspectives for the next revolution in catalysis", *Green Chem.* **23** (2021), pp. 1942–1954.

Review article

# Biocatalysis, a great toolbox for the upgrading of biomass

**Louis Michel Marie Mouterde** ®,*,#,*a* **and Florent Allais** ®,*,#,*a*

*a* URD Agro-Biotechnologies Industrielles (ABI), CEBB, AgroParisTech, 51110, Pomacle, France

*E-mails:* Louis.mouterde@agroparistech.fr (L. M. M. Mouterde), florent.allais@agroparistech.fr (F. Allais)

**Abstract.** The development and application of biocatalysis have evolved significantly, from the classical use of commercial enzymes to the production, modification and implementation of non-commercially available enzymes, driving advancements in sustainable bioprocesses for bio-based chemical and material production. We have focused on combining chemistry, biocatalysis and process intensification, to create efficient (chemo)enzymatic routes capable of transforming renewable raw materials into valuable industrial products. The portfolio of biocatalysts has been expanded through the integration of biocatalysis and green chemistry principles, facilitating innovative, eco-friendly alternatives to traditional petrochemical processes and supporting the transition towards a circular bioeconomy.

**Keywords.** Green chemistry, Biocatalysis, Molecular biology, Enzymes, Biomass, Bio-based molecules.

**Funding.** Région Grand Est, Conseil Départemental de la Marne, Grand Reims.

*Manuscript received 13 November 2024, revised 6 March 2025, accepted 20 May 2025.*

## 1. Introduction

URD ABI (Agro-Industrial Biotechnologies Research and Development Unit) [1], a research unit within AgroParisTech [2], is located in the European Center for Biotechnology and Bioeconomy (CEBB) at the heart of the Pomacle–Bazancourt biorefinery [3]. URD ABI drives innovation and its transfer to industrialization, covering the Technology Readiness Level (TRL) scale from 1 to 4. More precisely, URD ABI aims to transform plant and agricultural materials, as well as agro-industrial by-products, into sustainable industrial solutions, aligning with both the bioeconomy concept and several of the United Nations Sustainable Development Goals (UNSDG) [4].

One pillar of URD ABI, biocatalysis has been at the heart of many flagship projects since the unit

was founded. Initially limited to the use of commercial enzymes and liquid fermentation, URD ABI's expertise in the field of biotechnology has rapidly expanded to molecular biology, and enzymology.

In this mini-review, we will use a few examples to illustrate how biocatalysis has evolved within URD ABI and how it is now positioned as a major asset in the development of sustainable access routes to molecules and materials with (very) high added value.

## 2. Discussion

### 2.1. *Episode 1: First steps in biocatalysis*

Initially, biocatalysis activities at URD ABI were limited to the use of commercially available enzymes. To stand out from the stiff competition in this field, we focused on the use of lipases and laccases for the valorization of phenolic molecules, e.g., *p*-hydroxycinnamic acids and the corresponding

---

*Corresponding authors

#Contributed equally
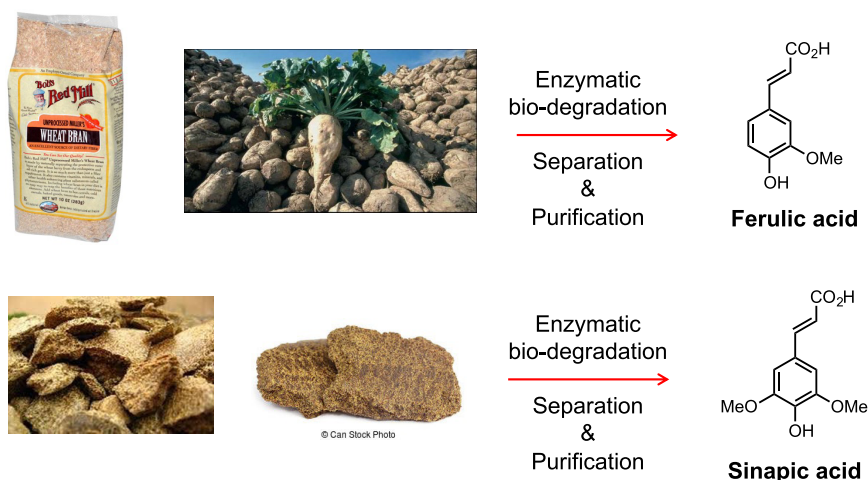
**Scheme 1.** Esterase-mediated production of ferulic acid and sinapic acid from wheat bran and sugar beet pulp, and mustard and rapeseed cakes, respectively.
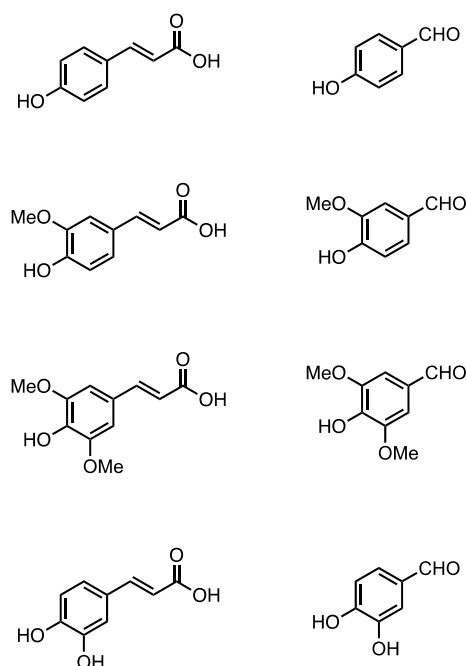


**Figure 1.** Naturally occurring *p*-hydroxy-cinnamic acids and corresponding benzalde-hydes.

benzaldehydes (Figure 1), which until then had remained relatively unexplored.

At first, the project focused on the production of new bis- and tris-phenolic molecules to replace bisphenol A, a petrochemical criticized for its toxicity (endocrine disruption) and allergenicity. Starting directly from the *p*-hydroxycinnamic acids that can be readily obtained from local biomasses (ferulic acid in wheat bran and sinapic acid in rapeseed meal or mustard bran) through commercially available esterase-mediated hydrolysis (Scheme 1) [5–7], we have developed and optimized two chemo-enzymatic synthetic routes leading to a new family of bis/trisphenols and syringaresinol, respectively (Figure 2).

The synthesis of ferulic-acid-based bis- and trisphenols and sinapic-acid-based bisphenol are based on a one-pot two-step Fisher esterification reaction and pallado-catalyzed hydrogenation of ferulic or sinapic acids, followed by transesterification of the resulting saturated ester by diols (1,3-propanediol, 1,4-butanediol, isosorbide) and triol (glycerol) by using *Candida antarctica* type B lipase immobilized on polystyrene beads (aka Novozyme 435, CAL-B) (Scheme 2) [8].

Coupled with a membrane purification process [9], this solvent-free biocatalysis, carried out under reduced pressure, enables the production of bis- and trisphenols with high yields (90–95%) and purity (98%), and has been validated on a kilogram scale. It is noteworthy to mention that this strategy has also been successfully applied to the production of bisphenol amides [10].

**Ferulic acid derivatives**



**Sinapic acid derivative**
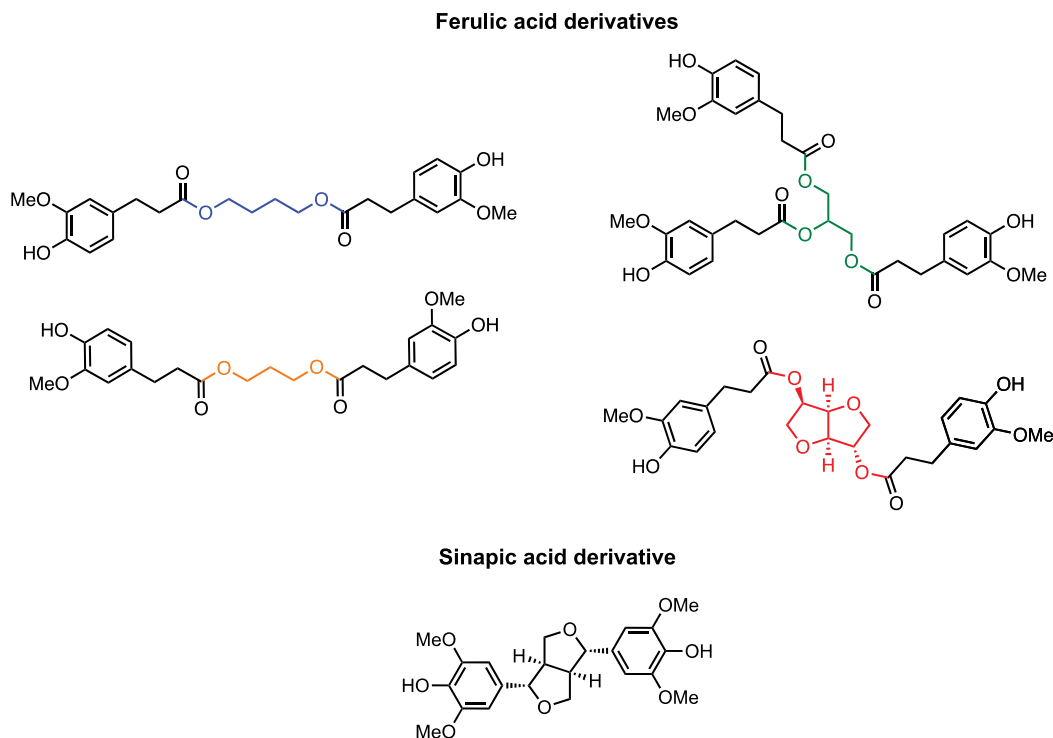


**Figure 2.** Ferulic-acid-based bis- and trisphenols and sinapic-acid-derived syringaresinol.

The second chemo-enzymatic synthetic route developed is based on a strategy fairly similar to the previous one. Sinapic acid was esterified and then reduced by DIBAL-H to afford the corresponding allyl alcohol. The latter was then subjected to a laccase from *Trametes versicolor*, in a buffer solution, to obtain syringaresinol in 93% yield (Scheme 3) [11]. It is important to note here that the high selectivity of the reaction—obtained by using a design of experiment—allows the almost exclusive production of syringaresinol (β–β dimer) and the absence of the β-O-4 dimer, which is generally the major product of this reaction.

As the original aim was to propose biosourced, non-toxic alternatives to bisphenol A, the study of the toxicity of the aforementioned compounds was realized in collaboration with INSERM Montpellier and showed that they did not exhibit any activity, regardless of their concentration (Figure 3) [12].

Moreover, possessing free phenol moieties, all compounds exhibit valuable antioxidant activities, both in solution or in plastics [13,14]. Interestingly, the antioxidant activity was further enhanced through a highly selective laccase-mediated

oligomerization of ferulic-acid-based bisphenols (Scheme 4) [15].

Subsequently, in collaboration with INRAE, Rensselaer Polytechnic Institute, and ICGM, we demonstrated that, of all the phenolic compounds developed, syringaresinol led to epoxy-amine resins with thermo-mechanical properties similar to those of bisphenol A-based ones [16], whereas the bisphenolic esters provided degradable epoxy-amine resins [12,17]. It is worth mentioning that these bisphenols were also used as monomers for the production of bio-based non-isocyanate polyurethanes (NIPUs) [18,19]. High added-value applications have been developed from these molecules. For example, butane-1,4-diyl bis(3-(4-hydroxy-3-methoxyphenyl) propanoate) (BDF), the bisphenol derived from ferulic acid and 1,4-butanediol, has been used to develop (i) new polylactic acid (PLA)/BDF blends with shape-memory elastomer properties [20,21], (ii) self-healing materials [22], and (iii) reversible adhesives [23].

More recently, still in the field of phenolic compounds, biocatalysis has been put to good use in a project dedicated to the production of naturally
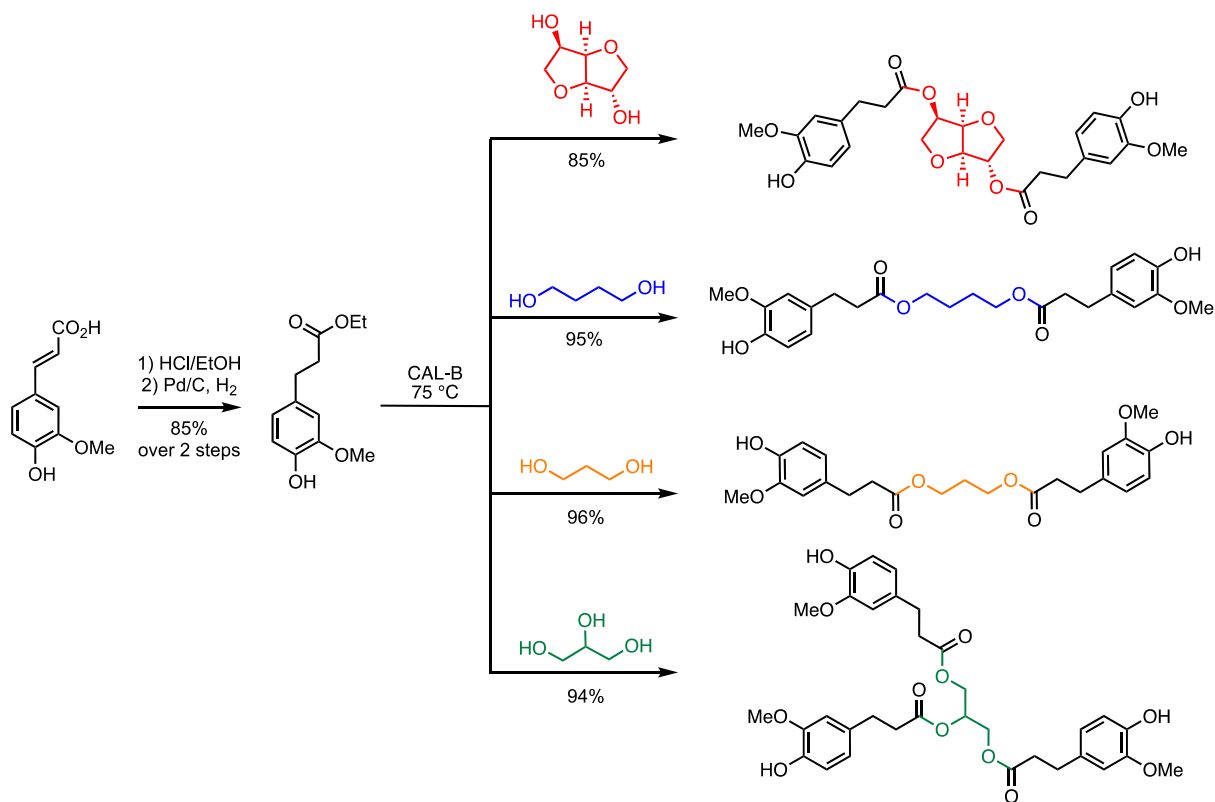
**Scheme 2.** Chemo-enzymatic synthesis of ferulic-acid-derived bis- and trisphenolic esters.
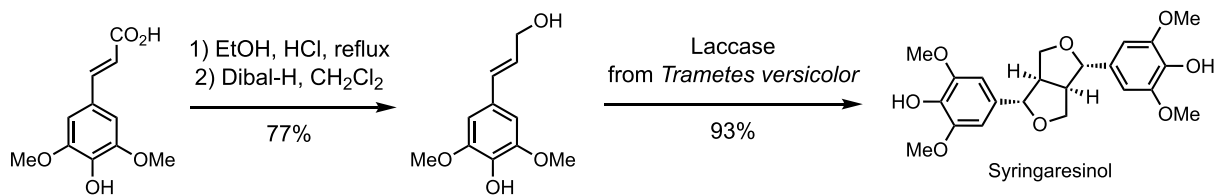


**Scheme 3.** Chemo-enzymatic synthesis of syringaresinol from sinapic acid.

occurring sinapoyl malate (Scheme 5), which is proving a multifunctional phenolic compound with UV-filtering, antioxidant and anti-tyrosinase properties for the cosmetics and biocontrol sectors [24].

Although highly active, sinapoyl malate was difficult to formulate due to the *p*-hydroxycinnamic acid ester core and the two acid moieties. To overcome this problem, one solution was to add hydrophobic moieties to the two malic esters. However, such a selective (trans)esterification of these malic acids/esters, without affecting the α,β-unsaturated

ester, was not conceivable by purely chemical means. Fortunately, by exploiting the inability of CAL-B to transesterify *p*-hydroxycinnamic acids, we were able to graft the fatty chains in a completely regioselective manner to produce new and more easily formulated analogs (Scheme 6) [25].

CAL-B has also been used for the valorization of levoglucosenone (LGO), a chiral molecule with high added value obtained through the pyrolysis of cellulose [26]. Because of its chirality, α,β-unsaturated ketone and ketal, LGO is an ideal
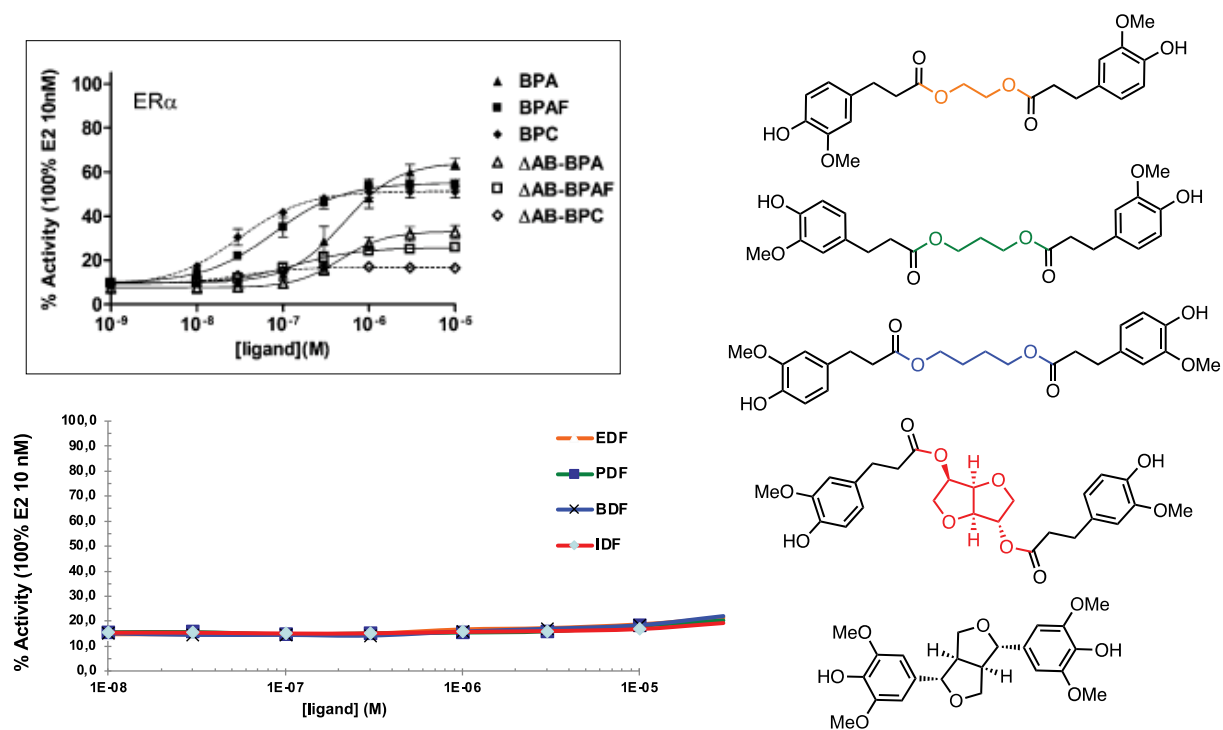
**Figure 3.** Endocrine disruption activity of bisphenol A and bio-based bis- and trisphenols.



$M_n$ up to 10 kDa
$285 < T_d\ (5\%) < 340\ ^{\circ}$C
$30 < T_g < 95\ ^{\circ}$C
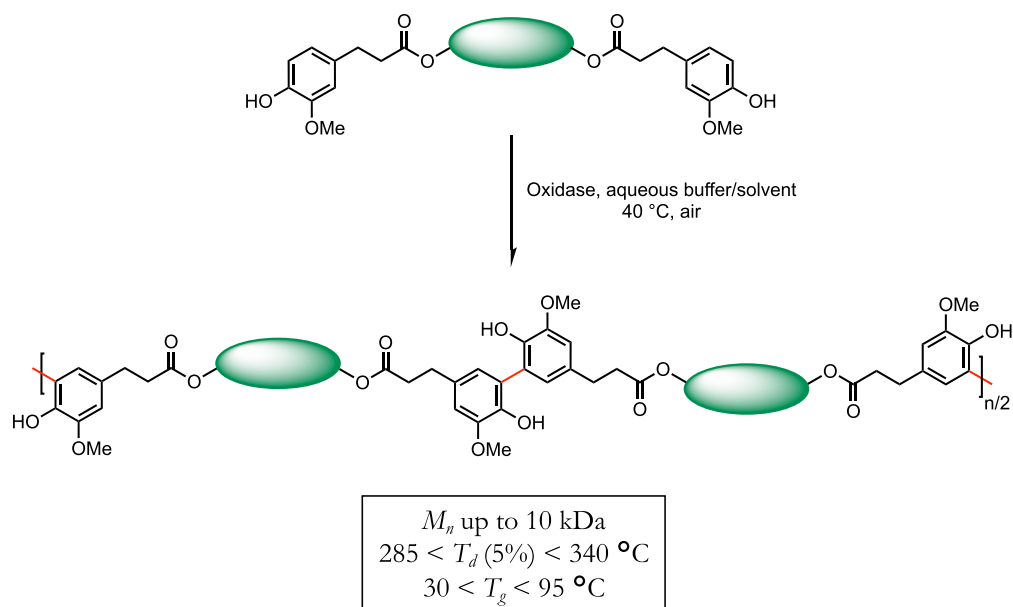
**Scheme 4.** Laccase-mediated regioselective oligomerization of bisphenols.
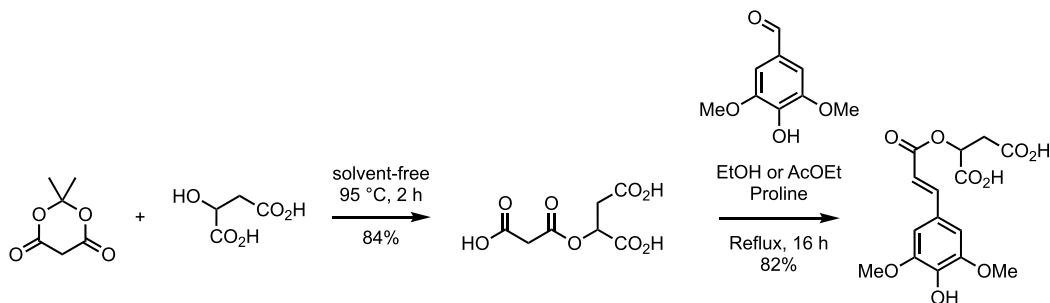
**Scheme 5.** Sustainable three-step synthesis of sinapoyl malate.
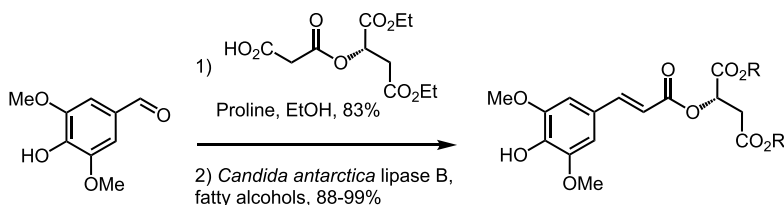


**Scheme 6.** Lipase-mediated regioselective transesterification toward fatty esters of sinapoyl malate.
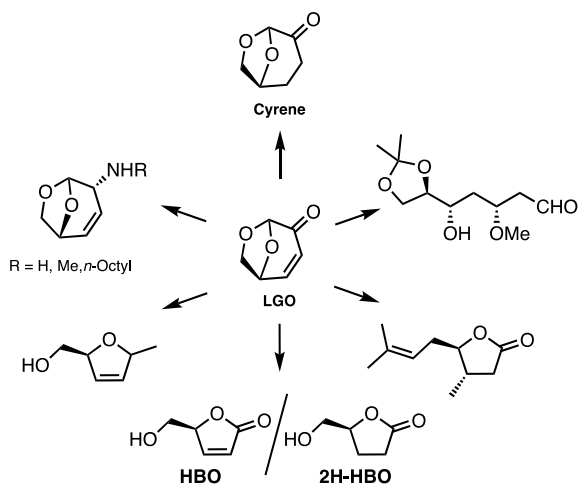


**Scheme 7.** LGO, a valuable chiral chemical platform.



Koseki's procedure: a) MCPBA or AcOOH, Me$_2$S, 48 h, rt
c) MeOH, HCl, 45 °C, overnight
Paris' procedure:    b) metal-zeolite, H$_2$O$_2$, 100 °C, 4 to 48 h
d) Amberlyst-15, rt

**Scheme 8.** Hazardous and toxic chemical synthetic routes toward LGO.

These chiral butyrolactone/butenolide can be used to produce drugs [27], aromas [28], polymers [29,30] etc. Until the URD ABI studied its production from LGO, HBO was obtained by Baeyer-Villiger oxidation of LGO, either in the presence of peracids [31] or in the presence of zeolites [32] (Scheme 8). In both cases, although effective in terms of yield, these two chemical processes are nevertheless dangerous and toxic for humans as well as for the environment due to the use of toxic and/or explosive reagents and toxic solvents.

To overcome these limitations, we designed and optimized a sustainable alternative chemical pathway based on the use of CAL-B and hydrogen

platform molecule for organic chemists. Among the many chiral molecules that can be synthesized from LGO, (*S*)-γ-hydroxymethyl-α,β-butenolide (HBO) and its reduced derivative ((*S*)-γ-hydroxymethyl-γ-butyrolactone, 2H-HBO) are probably the ones that open up the widest range of possibilities (Scheme 7).

**Scheme 9.** Lipase-mediated Baeyer-Villiger oxidation of unsaturated and saturated LGO into HBO and 2H-HBO, respectively.
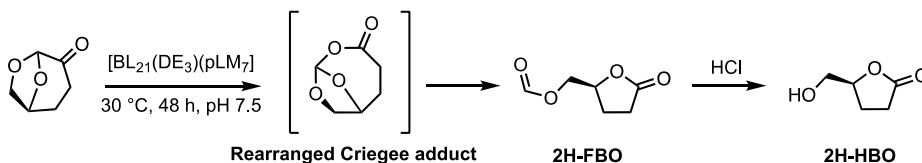


**Scheme 10.** Bioconversion of Cyrene™ into 2H-HBO.

peroxide in ethyl acetate (AcOEt) to produce in situ peracetic acid, which oxidizes LGO to HBO in high yields without the need for harsh oxidizing agents in large excess or hazardous petroleum-based organic solvents (Scheme 9) [33]. It is noteworthy to mention that, to recycle CAL-B, HEPES buffer can be used.

As the above examples show, the implementation of biocatalytic reactions using commercially available enzymes has been a key element in the strategy of URD ABI for the production of high added-value molecules and materials using sustainable processes. However, due to the relatively limited number of enzymes on the market, the high potential of biocatalysis could not be fully exploited within URD ABI. Aware of these limitations, it was decided to acquire the capacity to produce enzymes on site and thus go even further in terms of innovation.

### 2.2. *Episode 2: Fully harnessing the potential of molecular biology and biocatalysis*

With these new capacities, and in collaboration with the University of Florida, we first explored another biocatalytic strategy for the conversion of LGO into HBO via cyclohexanone monooxygenase (CHMO). This strategy has the advantage of (i) using oxygen from air as oxidative species and therefore significantly improving the system in terms of safety compared to $H_2O_2$ and, (ii) not implementing organic

solvent such as AcOEt. However, the use of the CHMO collection from Stewart Lab did not lead to positive results and no activity was observed. However, using Cyrene™ as substrate allowed us to observe the formation of 2H-HBO. We then explored the biodiversity using the basic local alignment search tool (BLAST) and the DNA sequence coding for the CHMO from *Acinetobacter* sp. NCIB 9871 as the parent sequence in an attempt to find new CHMOs. A hit from *Pseudomonas aeruginosa* strain Pa1242 was identified with a query cover and identity percentage of 97 and 67%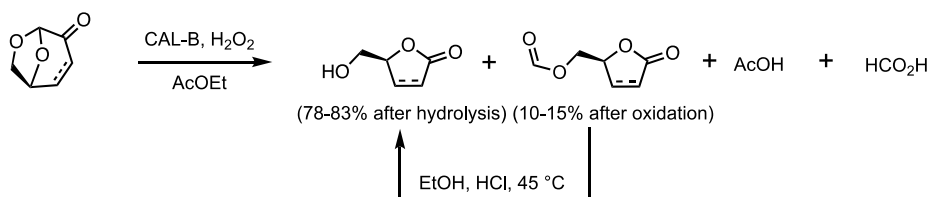 respectively. As CHMOs are NADPH-dependent, a quite expensive cofactor, we further implemented the system in whole cells to take advantage of the cells' capacity to regenerate NADPH by themselves (Scheme 10). Doing so allowed us to reach a concentration of 20 g/L (160 mM) over 48 h or a consumption rate of $401 \pm 36$ mg/L/h [34,35].

As it was previously discussed in this review, it is possible to access aromas from LGO, such as the flavoring agent dairy lactone (butter, peach, or fruity aroma depending on the concentration used) [28,36]. The transfer from a classical organic step toward a biocatalytic one is of particular interest in such a pathway. Indeed, naturality is progressively becoming a requested standard for almost all industries nowadays and it is particularly the case for the food industry. The implementation of a classical organic synthesis step in a pathway causes the natural character of the targeted molecule to be lost. With this
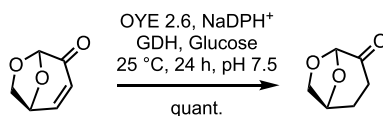
**Scheme 11.** Biocatalytic transformation of LGO into Cyrene™.
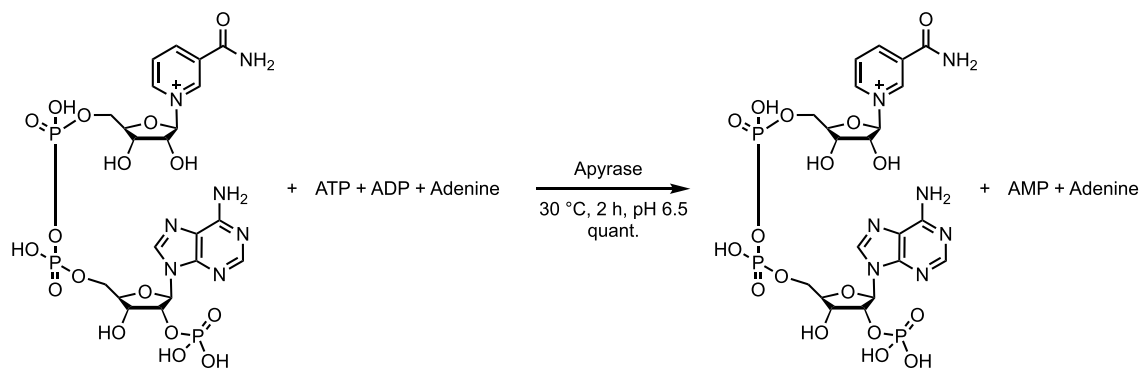


**Scheme 12.** Simplification of the reaction medium using apyrase.

first proof of feasibility, we decided to go further in trying to substitute each step by a biocatalytic system in order to access natural dairy lactone. Therefore, we explored the possibility of transforming LGO into Cyrene™ by old yellow enzymes (OYEs) as it could add a second biocatalytic step toward dairy lactone and provide Cyrene™ through a method that does not use transition metals such as palladium. Indeed, some industries that could use Cyrene™ as substitute for DMSO, DMF or NMP are required to have very small traces of transition metal, parts per billion, and a biocatalytic pathway would be able to provide such a grade. The OYE 2.6 from *Pichia stipitis* was chosen as it displayed the best activity from the set of OYEs tested [37,38]. Contrary to the transformation of Cyrene™ into 2H-HBO, the whole-cell strategy for scaling up the process could not be applied because of the high toxicity of LGO toward cells. Therefore, a regeneration system of NADPH has been implemented using glucose dehydrogenase and glucose as the sacrificial agent. The process was scaled up to five liters with a final concentration of 250 mM (Scheme 11).

Although the system was proven to be efficient, its cost remains relatively high, mostly due to the use of NADP⁺, which represents more than 70% of raw material cost. Therefore, we looked into a strategy that could allow us to reduce the production cost. We identified that the purification steps of NADP⁺ production represents the majority of the cost as it is usually performed through ion exchange chromatography followed by a desalting step using activated charcoal. In order to overcome such drawbacks, we developed and patented a membrane filtration strategy that allows purifying high molecular weight adenosine-based cofactors in a 3-to-1 process that enables (i) purifying, (ii) desalting, and (iii) recycling the by-products. The proof of feasibility was made on coenzyme A, FAD, NAD, and NADP⁺ [39,40]. In the case of NADP⁺, we added a final step involving an apyrase from potatoes in order to simplify the profile of by-products (Scheme 12), allowing us to reach higher purity and productivity [41].

Another approach investigated to mitigate coenzyme-associated expenses was the immobilization of the coenzymes on cellulose nanocrystals (CNCs). We used ATP as a case study and were able to graft it by a click chemistry approach onto CNCs. We then used the resulting material in a biocatalysis involving a pantothenate kinase from *E. coli* for the production of pantethine diphosphate and showed that the biocatalysis was occurring as observed when using *free* ATP (Scheme 13). It must be noted that both mono and dephosphorylated products were
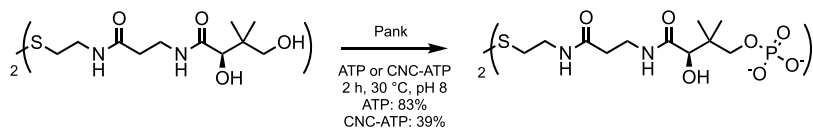
**Scheme 13.** Biocatalytic production of pantethine diphosphate using CNC-ATP.

observed. Such results open up real perspectives for cofactor immobilization [42].

Unlocking the access to coenzymes is crucial for biocatalysis as it can give access to a very large variety of biocatalytic activities.

## 3. Conclusion

By integrating chemistry and biocatalysis, a powerful approach has been implemented for developing sustainable processes aimed at producing bio-based chemicals and materials. This interdisciplinary synergy leverages the precision of chemical methods alongside the selectivity and eco-friendliness of biological catalysts, such as enzymes and microorganisms. Biocatalysts enable highly specific transformations under mild reaction conditions, often reducing energy requirements and minimizing the need for toxic solvents or harsh chemicals. When combined with advanced chemical methods, biocatalysis can enhance reaction efficiency, yield, and selectivity, opening new pathways for the valorization of renewable biomass into high-value chemicals, polymers, and advanced materials. Key advancements in enzyme engineering, metabolic pathway optimization, and hybrid chemo-enzymatic processes have expanded the repertoire of bio-based products that can be produced sustainably, offering promising alternatives to petrochemical-derived products. This combined approach supports circular economy principles by using renewable feedstocks and designing biodegradable end-products, ultimately reducing environmental impact and reliance on limited resources.

## Declaration of interests

The authors do not work for, advise, own shares in, or receive funds from any organization that could benefit from this article, and have declared no affiliations other than their research organizations.

## References

[1] Online at https://urd-abi-agroparistech.com/Home/. (accessed November 14, 2024).

[2] Online at https://agroparistech.fr/en. (accessed November 14, 2024).

[3] F. Allais, H. Lescieux-Katir and J.-M. Chauvet, "The continuous evolution of the Bazancourt–Pomacle site rooted in the commitment and vision of pioneering farmers. When reality shapes the biorefinery concept", *EFB Bioeco. J.* **1** (2021), article no. 100007.

[4] Online at https://sdgs.un.org/goals. (accessed November 14, 2024).

[5] S. Dupoiron, M.-L. Lameloise, M. Bedu, et al., "Recovering ferulic acid from wheat bran enzymatic hydrolysate by a novel and non-thermal process associating weak anion-exchange and electrodialysis", *Sep. Pur. Technol.* **200** (2018), pp. 75–83.

[6] J. M. B. Domingo, A. R. S. Teixeira, S. Dupoiron, F. Allais and M.-L. Lameloise, "Simultaneous recovery of ferulic acid and sugars from wheat bran enzymatic hydrolysate by diananofiltration", *Sep. Pur. Technol.* **242** (2020), article no. 116755.

[7] V. Reungoat, M. Chadni, L. M. M. Mouterde, F. Brunissen, F. Allais, H. Ducatel and I. Ioannou, "Liquid–liquid extraction of sinapic acid from a mustard seed by-product using a hollow fiber membrane contactor", *Sep. Purif. Technol.* **331** (2024), article no. 126615.

[8] F. Pion, A. F. Reano, P.-H. Ducrot and F. Allais, "Chemo-enzymatic preparation of new bio-based bis- and trisphenols: new versatile building blocks for polymer chemistry", *RSC Adv.* **3** (2013), pp. 8988–8997.

[9] A. R. S. Teixeira, G. Willig, J. Couvreur, A. L. Flourat, A. A. M. Peru, P. Ferchaud, H. Ducatel and F. Allais, "From bench scale to kilolab production of renewable ferulic acid-based bisphenols: optimisation and evaluation of different purification approaches towards technical feasibility and process environmental sustainability", *React. Chem. Eng.* **2** (2017), pp. 406–419.

[10] F. Pion, *L'acide férulique, un synthon naturel pour la préparation de nouveaux polymères aromatiques*, Thesis dissertation, AgroParisTech, 2014.

[11] A. S. Jaufurally, A. R. S. Teixeira, L. Hollande, F. Allais and P.-H. Ducrot, "Optimization of the laccase-catalyzed synthesis of (±)-syringaresinol and study of its thermal and antiradical activities", *ChemistrySelect* **1** (2016), pp. 5165–5171.

[12] A. Maiorana, A. F. Reano, R. Centore, P. Balaguer, M. Grimaldi, F. Allais and R. A. Gross, "Structure property relationships of biobased *n*-alkyl bisferulate epoxy resins", *Green Chem.* **18** (2016), pp. 4961–4973.

[13] A. F. Reano, J. Chérubin, A. M. M. Peru, Q. Wang, T. Clément, S. Domenek and F. Allais, "Structure–activity relationships and structural design optimization of a series of *p*-hydroxycinnamic acids-based bis- and trisphenols as novel sustainable antiradical/antioxidant additives", *ACS Sustain. Chem. Eng.* **3** (2015), pp. 3486–3496.

[14] A. F. Reano, S. Domenek, M. Pernes, J. Beaugrand and F. Allais, "Ferulic acid-based bis/trisphenols as renewable antioxidants for polypropylene and poly(butylene succinate)", *ACS Sustain. Chem. Eng.* **4** (2015), pp. 6562–6571.

[15] A. F. Reano, F. Pion, S. Domenek, P.-H. Ducrot and F. Allais, "Chemo-enzymatic preparation and characterization of renewable oligomers with bisguaiacol moieties: promising sustainable antiradical/antioxidant additives", *Green Chem.* **18** (2016), pp. 3334–3345.

[16] M. Janvier, L. Hollande, A. S. Jaufurally, et al., "Syringaresinol: a renewable and safer alternative to bisphenol A for epoxy-amine resins", *ChemSusChem* **4** (2017), pp. 738–746.

[17] R. Ménard, S. Caillol and F. Allais, "Ferulic acid-based renewable esters and amides-containing epoxy thermosets from wheat bran and beetroot pulp: Chemo-enzymatic synthesis and thermo-mechanical properties characterization", *Ind. Crop. Prod.* **95** (2016), pp. 83–95.

[18] M. Janvier, P.-H. Ducrot and F. Allais, "Isocyanate-free synthesis and characterization of renewable poly(hydroxy)urethanes from syringaresinol", *ACS Sustain. Chem. Eng.* **5** (2017), pp. 8648–8656.

[19] R. Ménard, S. Caillol and F. Allais, "Chemo-enzymatic synthesis and characterization of renewable thermoplastic and thermoset isocyanate-free poly(hydroxy)urethanes from ferulic acid derivatives", *ACS Sustain. Chem. Eng.* **5** (2017), pp. 1446–1456.

[20] A. Gallos, J.-M. Crowet, L. Michely, et al., "Blending ferulic acid derivatives and polylactic acid into biobased and transparent elastomeric materials with shape memory properties", *Biomacromolecules* **22** (2021), pp. 1568–1578.

[21] V. S. Raghuwanshi, A. Gallos, D. J. Mendoza, M. Lin, F. Allais and G. Garnier, "Nanocrystallisation and self-assembly of biosourced ferulic acid derivative in polylactic acid elastomeric blends", *J. Colloid Interf. Sci.* **606** (2021), pp. 1842–1851.

[22] P. Sinah Roy, M. M. Mention, M. A. P. Turner, F. Brunissen, V. G. Stavros, G. Garnier, F. Allais and K. Saito, "Bio-based photo-reversible self-healing polymer designed from lignin", *Green Chem.* **23** (2021), pp. 10050–10061.

[23] P. Sinah Roy, M. M. Mention, A. F. Patti, G. Garnier, F. Allais and K. Saito, "Photo-responsive lignin fragment-based polymers as switchable adhesives", *Polym. Chem.* **14** (2023), pp. 913–924.

[24] C. Peyrot, M. M. Mention, R. Fournier, F. Brunissen, J. Couvreur, P. Balaguer and F. Allais, "Expeditious and sustainable two-step synthesis of sinapoyl-L-malate and analogues: towards non-endocrine disruptive bio-based and water-soluble bioactive compounds", *Green Chem.* **22** (2020), pp. 6510–6518.

[25] B. Rioux, L. M. M. Mouterde, J. Alarcan, et al., "An expeditive and green chemo-enzymatic route to diester sinapoyl-L-malate analogues: sustainable bioinspired and biosourced UV filters and molecular heaters", *Chem. Sci.* **14** (2023), pp. 13962–13978.

[26] G. R. Court, C. H. Lawrence, W. D. Raverty and A. J. Duncan, US patent, US9505985, November 29, 2016.

[27] A. L. Flourat, A. Haudrechy, F. Allais and J.-H. Renault, "(*S*)-γ-hydroxymethyl-α,β-butenolide, a valuable chiral synthon: syntheses, reactivity, and applications", *Org. Process. Res. Dev.* **24** (2020), pp. 615–636.

[28] A. Peru, A. L. Flourat, C. Gunawan, W. D. Raverty, M. Jevric, B. Greatrex and F. Allais, "Chemo-enzymatic synthesis of chiral epoxides ethyl and methyl (*S*)-3-(Oxiran-2-yl)propanoates from renewable levoglucosenone: an access to enantiopure (*S*)-dairy lactone", *Molecules* **21** (2016), article no. 988.

[29] F. Diot-Néant, E. Radoster, S. Miller and F. Allais, "Chemo-enzymatic synthesis and free radical polymerization of renewable acrylate monomers from cellulose-based lactones", *ACS Sustain. Chem. Eng.* **6** (2018), pp. 17284–17293.

[30] L. Pezzana, S. Fadlallah, G. Giri, C. Archimbaud, I. Roppolo, F. Allais and M. Sangermano, "DLP 3D printing of levoglucosenone-based monomers: exploiting thiol-ene chemistry for bio-based polymeric resins", *ChemSusChem* **17** (2024), article no. e202301828.

[31] K. Koseki, T. Ebata, H. Kawakami, et al., Method of preparing (S)-γ-hydroxymethyl-α,β-butenolide, US patent, US49947585, February 19, 1991.

[32] C. Paris, M. Moliner and A. Corma, "Metal-containing zeolites as efficient catalysts for the transformation of highly valuable chiral biomass-derived products", *Green Chem.* **15** (2013), pp. 2101–2109.

[33] A. L. Flourat, A. A. M. Peru, A. R. S. Teixeira, F. Brunissen and F. Allais, "Chemo-enzymatic synthesis of key intermediates (*S*)-γ-hydroxymethyl-α,β-butenolide and (*S*)-γ-hydroxymethyl-γ-butyrolactone *via* lipase-mediated Baeyer–Villiger oxidation of levoglucosenone", *Green Chem.* **17** (2015), pp. 404–412.

[34] L. M. M. Mouterde, J. Couvreur, M. M. J. Langlait, F. Brunois and F. Allais, "Identification and expression of a CHMO from the *Pseudomonas aeruginosa* strain Pa1242: application to the bioconversion of Cyrene™ into a key precursor (*S*)-γ-hydroxymethyl-butyrolactone", *Green chem.* **23** (2021), pp. 2694–2702.

[35] F. Allais, J. D. Stewart and L. M. M. Mouterde, Biocatalytic method for producing 2H-HBO and β-substituted analogues from LGO using a cyclohexanone monooxygenase, FR patent, PCT/FR2019/052677, 2019.

[36] F. Allais, A. Flourat, A. Peru, B. Greatrex, W. D. Raverty and A. Duncan, Method for synthesizing a precursor of a single dairy-lactone isomer, WO patent, WO2016162646A1, 2016.

[37] L. M. M. Mouterde, F. Allais and J. D. Stewart, "Enzymatic reduction of levoglucosenone by an alkene reductase (OYE 2.6): a sustainable metal- and dihydrogen-free access to the bio-based solvent Cyrene®", *Green Chem.* **20** (2018), no. 24, pp. 5528–5532.

[38] F. Allais, J. D. Stewart and L. M. M. Mouterde, Materials and methods for alkene reduction of levoglucosenone by an alkene reducatase, WO patent, WO2018183706, 2018.

[39] L. M. M. Mouterde, G. Willig, M. M. J. Langlait, F. Brunois, M. Chadni and F. Allais, "Unlocking the access to oxidized coenzyme A via a single-step green membrane-based purification", *Sci. Rep.* **12** (2022), article no. 12991.

[40] L. M. M. Mouterde, F. Allais and G. Willig, Method for purifying high molecular weight adenosine-based coenzymes by tangential diafiltration, WO patent, WO2021005314, 2021.

[41] C. Bourgery, G. Willig, F. Allais and L. M. M. Mouterde, "Combining the power of biocatalysis and membrane-based purification to access NADP$^+$", *ACS Sust. Chem. Eng.* **11** (2023), no. 12, pp. 4662–4669.

[42] C. Bourgery, D. J. Mendoza, G. Garnier, L. M. M. Mouterde and F. Allais, "Immobilization of adenosine derivatives onto cellulose nanocrystals via click chemistry for biocatalysis applications", *ACS Appl. Mater. Interfaces* **16** (2024), no. 9, pp. 11315–11323.

ACADÉMIE
DES SCIENCES
INSTITUT DE FRANCE

Review article

# Nucleoside chemistry: a challenge best tackled together

**Sarah Westarp** [●],[a], **Peter Neubauer** [●],[a] **and Anke Kurreck** [●],[*],[b]

[a] Chair of Bioprocess Engineering, Institute of Biotechnology, Faculty III Process Sciences, Technische Universität Berlin, Ackerstrasse 76, 13355 Berlin, Germany

[b] BioNukleo GmbH, Ackerstrasse 76, 13355 Berlin, Germany

*E-mails:* s.westarp@tu-berlin.de (S. Westarp), peter.neubauer@tu-berlin.de
(P. Neubauer), anke.kurreck@bionukleo.com (A. Kurreck)

**Abstract.** Nucleoside analogues (NAs) are among the most successful small-molecule classes in the fight against cancer and viral infections. Their importance has recently been further underlined by the approval of sofosbuvir for the treatment of hepatitis C virus infections and by developments related to the corona pandemic. In view of the enormous interest from the academic world and the pharmaceutical industry, a variety of chemical and enzymatic synthesis routes have been developed since the first approval of an NA. The selective chemical synthesis of β-anomeric NAs through chemical *N*-glycosylation remains a challenging and, sometimes, a prohibitively expensive process, thus limiting the available chemical space. In response, full enzymatic cascades for the synthesis of NAs have been developed since the discovery of suitable biocatalysts. Despite significant success, particularly due to advances in enzyme engineering, constraints persist due to a limited substrate scope of the available biocatalysts. This mini-review aims to address both the challenges and potential of chemical and biocatalytic approaches in NA synthesis. It also illustrates how a combined strategy could substantially enhance synthesis efficiency as demonstrated by a few existing examples. Thus the authors hope to encourage scientists from both domains to join their efforts to drive innovative solutions in this field.

**Keywords.** Nucleoside synthesis, Biocatalysis, Chemoenzymatic synthesis, *N*-glycosylation, Nucleoside analogue.

**Note.** This article was submitted upon invitation by the guest editor Juliette Martin.

*Manuscript received 28 November 2024, revised 14 February 2025, accepted 21 February 2025.*

## 1. Introduction

Nucleoside analogues (NAs) are highly significant pharmaceutical agents. Their relevance is based on the biological functions of their natural counterparts (Scheme 1a) as building blocks of nucleic acids or as regulators of gene expression, mRNA translation, and cell signaling. The main fields of application of nucleoside drugs are the treatment of cancer and viral infections [1,2]. The desired activity is achieved by alteration of the canonical nucleoside scaffold and its functional groups (Scheme 1b). The resulting β-NAs inhibit key enzymes such as methyltransferases, deaminases, and polymerases, thereby preventing infection or curing diseases. Additionally, the application of NAs has been approved for the treatment of the autoimmune disease multiple sclerosis [3], and some NAs even exhibit antibiotic properties [4,5].

Given the significance of NAs as therapeutic agents, various chemical, biocatalytic, and chemoenzymatic methods have been developed (Schemes 2

*Corresponding author

## a) canonical nucleosides (examples)



purine
e.g. adenosine

pyrimidine
e.g. thymidine
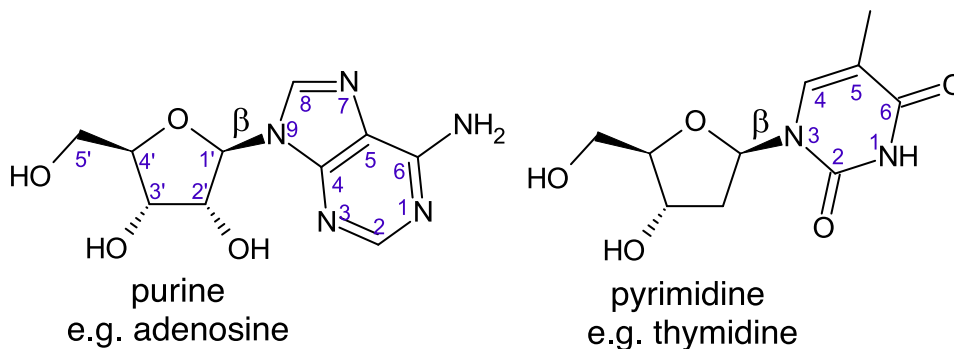
## b) nucleoside analogues
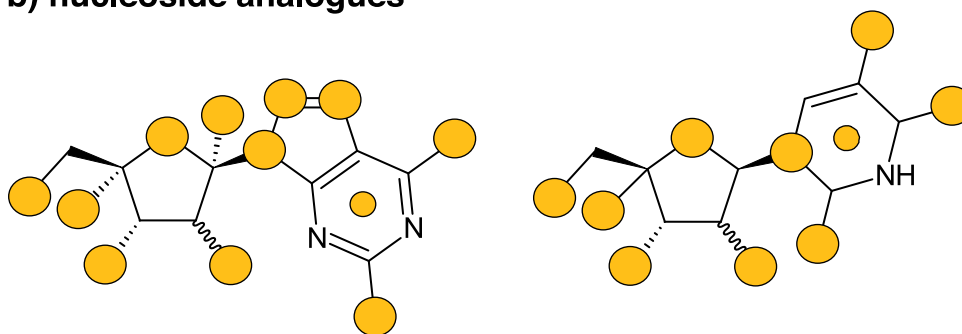


**Scheme 1.** Nucleoside scaffolds: (a) canonical nucleosides and (b) nucleoside analogues. Numbering convention (blue numbers) and reported modification sites (yellow circles). Yellow circles within nucleobases signify modifications of the core structure such as heteroatom position or incomplete rings.

and 3). In this mini-review, chemical synthesis refers to processes that do not involve biocatalysts (enzymes) in contrast to biocatalytic synthesis. Chemoenzymatic synthesis, on the other hand, denotes methods that combine both chemical and enzymatic strategies. These terms specifically refer to the individual reaction steps or corresponding cascade reactions under consideration. If the synthesis of starting materials were included in this discussion, the enzymatic production of NAs would always be classified as a chemoenzymatic approach since the precursor building blocks are typically derived from synthetic sources.

Chemical synthesis is the gold standard in NA production. Recently, this has been impressively demonstrated by Kothapalli and colleagues in their comprehensive review on synthetic routes for NAs with antiviral activity [10]. Chemical synthesis routes were described for all the 14 compounds investigated

while a biocatalytic route was only outlined for one compound, namely islatravir [11]. This highlights the significant potential of synthetic chemistry and explains the number of approaches available for NA synthesis.

Since the discovery of nucleoside phosphorylases [12], biochemists have focused on enzymatic processes for NA production to overcome the limitations of chemical methods. The identification of additional suitable biocatalysts for NA synthesis has broadened the scope of enzymatic methods, and the production of a wide range of NAs has been reported. The field has experienced a revival driven by the demand for sustainable manufacturing processes and the challenges posed by the COVID-19 pandemic [7,11].

*N*-Glycosylation is a key step in nucleoside (bio)chemistry, facilitating the formation of β-nucleosides from a sugar synthon and a nucleobase.

*Vorbrüggen glycosylation*



$$\text{(eq. 1)}$$

R: Ac, Bz, etc

*Glycosyl halides*



$$\text{(eq. 2)}$$

Hoffer's chloro-sugar
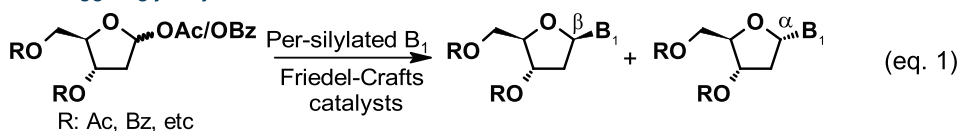
(N7- and N9-purine nucleosides)

*Glycosyl-orthoesters*



$$\text{(eq. 3)}$$

*N*-glycosylation

Substrate → Product

*transglycosylation*



$$\text{(eq. 4)}$$

2'-deoxynucleoside 1     ribosyl-NDT intermediate     2'-deoxynucleoside 2



$$\text{(eq. 5)}$$

nucleoside 1     a-pentose-1-phosphate     nucleoside 2

R (ribosyl- or arabinosyl) : H, OH

*direct glycosylation*



$$\text{(eq. 6)}$$

$\alpha$-pentose-1-phosphate     nucleoside 2
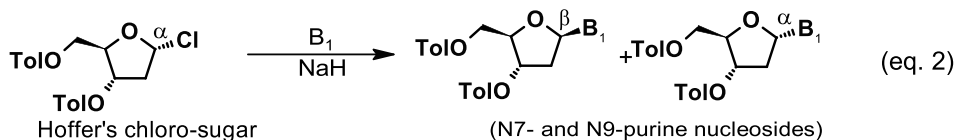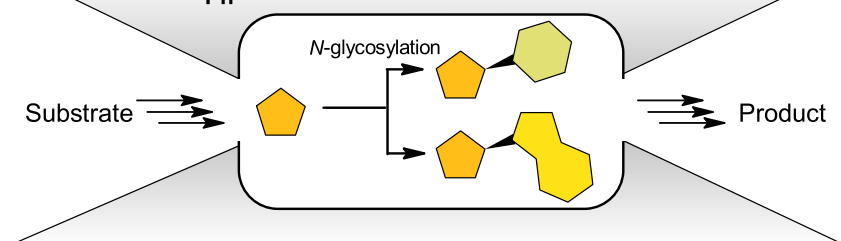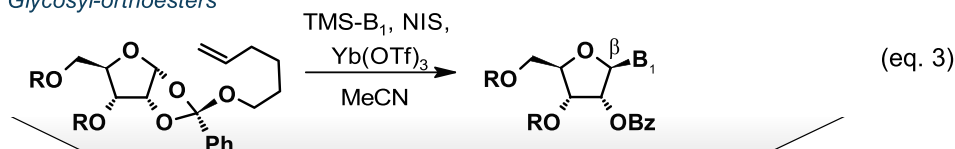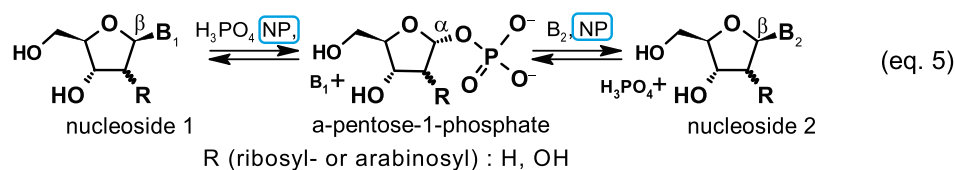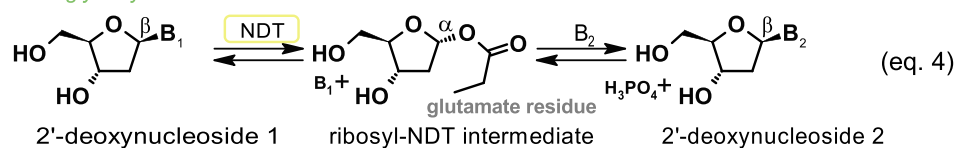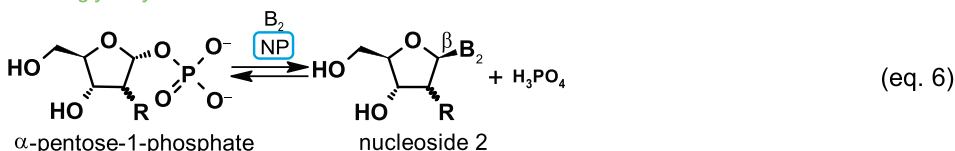
**Scheme 2.** *N*-glycosylation as a key step in nucleoside analogue synthesis. Chemical glycosylation reactions are adapted from [6]. $B_1$—nucleobase 1 and $B_2$—nucleobase 2. Nucleobases typically have either a purine or a pyrimidine scaffold.     NP, nucleoside phosphorylase;    NDT, nucleoside $2'$-deoxyribosyltransferase.

In synthetic chemistry, over time, three core strategies for the *N*-glycosylation step have been developed. The Vorbrüggen glycosylation is frequently used but is known to produce nucleosides with poor $\alpha/\beta$ anomeric purity, particularly for $2'$-deoxynucleosides, and exhibits low regioselectivity

a) Molnupuravir Synthesis by McIntosh et. al.
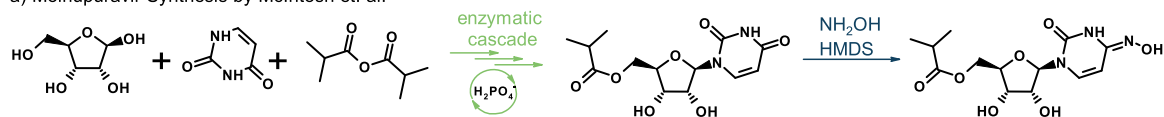


b) 4'-thio-5-ethynyluridine Synthesis by Westarp et. al.
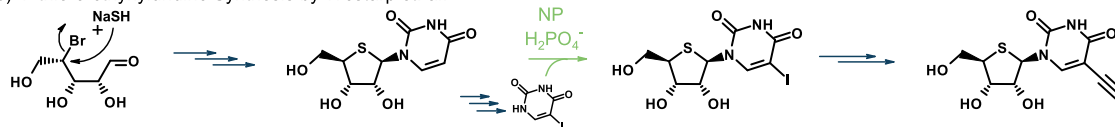


c) MK-1454 Synthesis by Benkovics et. al.
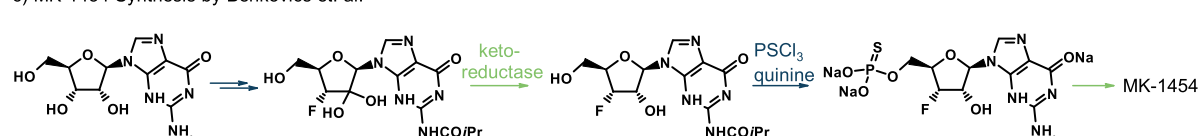


**Scheme 3.** Chemoenzymatic workflows. (a) Chemoenzymatic cascade reaction towards molnupuravir [7]. (b) Biocatalytic base diversification of synthetic 4′-thiouridine and subsequent ethynylation via a Sonogashira cross-coupling reaction [8]. (c) Section of the synthesis route to the cyclic dinucleotide MK-1454 [9]. NP, nucleoside phosphorylase.

for purine nucleosides (Scheme 2, Equation (1)). To address these challenges, several alternative synthesis methods have been introduced as reviewed by Wang and colleagues [6]. Some of these approaches, such as gold-catalyzed *N*-glycosylation with ester or ortho ester ribosyl donors or the use of halide leaving groups, offer good regio- and stereoselectivity, even for 2′-deoxyribosides [6,13] (Scheme 2, Equations (2) and (3)). To meet the ongoing demand for novel NAs to be synthesized and evaluated as potential drugs, numerous specialized synthesis routes have been developed over time [14,15]. For example, intramolecular ring formation represents an alternative strategy and was first described by Hager and Liotta in 1991 [16]. It involves the formation of the *N*-glycosidic bond prior to ring closure. This method provides greater control over the stereochemical configuration of the *N*-glycosidic bond and offers more versatility compared to the aforementioned *N*-glycosylation reactions. More recent efforts have focused on developing protecting-group-free synthesis routes [17].

All reported biocatalytic *N*-glycosylation reactions are either transglycosylation or direct glycosylation reactions (Scheme 2, Equations (4)–(6)). These reactions utilize enzymes from nucleotide salvage pathways and are anomer-specific. Two enzyme classes have been identified as efficient biocatalysts for the synthesis of β-nucleosides:

nucleoside phosphorylases and nucleoside 2′-deoxyribosyltransferases [18–20]. Recent advancements include one-pot nucleobase diversification of unconventional sugar modifications, such as 4′-methylated nucleosides [21] and 4′-thionucleosides [8], using nucleoside phosphorylases as well as a comprehensive characterization of the substrate scope of *Ll*NDT-2 [22]. To enhance the competitiveness of biocatalysis compared to synthetic chemistry, several strategies have been explored to (i) improve solubility, (ii) address thermodynamic limitations, and (iii) broaden the range of substrates. For instance, employing thermostable enzyme variants enables reactions at temperatures up to 90 °C and the use of solvents, which can significantly increase substrate concentration [23–25]. Thermodynamic limitations can be overcome through direct glycosylation [26,27] and the removal of released phosphate using enzymes like sucrose phosphorylase and pyruvate oxidase [7,11]. Additionally, enzyme engineering presents a promising approach to broaden the substrate range of biocatalysts [7,11,28].

This review provides an overview of advantages and drawbacks of purely chemical and biocatalytic synthesis routes. Regarding chemoenzymatic approaches, solutions are presented that overcome still existing challenges of both synthetic chemistry and biocatalysis, showcasing the advantages
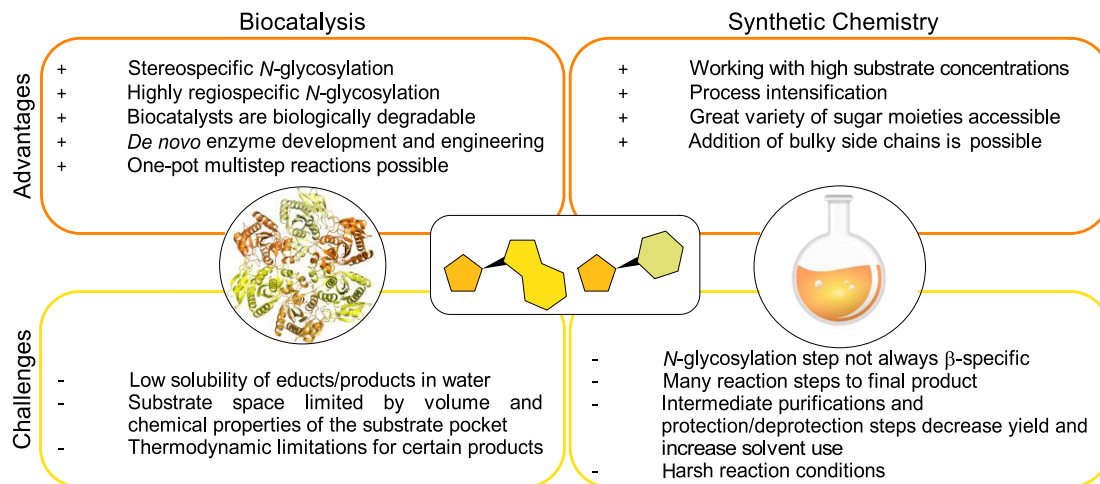
**Figure 1.** Strengths and drawbacks of chemical and biocatalytic synthesis routes.

of combining both methods. By presenting the key strategies of NA synthesis, the authors aim to inspire researchers from both disciplines to collaborate to harness the full potential of this integrated approach. Hopefully, this will help address the existing challenges in NA synthesis and pave the way for more efficient production methods.

## 2. Strengths and weaknesses of synthetic chemistry and biocatalysis

The success of synthetic chemistry in NA synthesis can be attributed to several key advantages: the wide availability of sugar synthons, the ability to work with high substrate loads, and the tolerance for diverse and often extensive modifications (Figure 1). Disregarding factors such as yield, efficiency, and sustainability, synthetic chemistry offers the flexibility to develop a process for virtually any NA. However, despite its established dominance, chemical synthesis routes for NAs still show several drawbacks, including the requirement for harsh reaction conditions, multiple protection and deprotection steps, and challenges with regard to regioselectivity and stereoselectivity. These factors often result in complex multistep procedures, which in sum decrease overall process efficiency [29].

In contrast, biocatalytic synthesis routes are highly regio- and stereoselective, enabling efficient one-pot cascade reactions under mild reaction conditions. De novo enzyme development and enzyme

engineering now also allow the synthesis of highly modified compounds. However, despite significant advancements, biocatalytic production still faces challenges, such as the limited tolerance for large substituents and certain thermodynamic constraints (Figure 1).

## 3. Chemoenzymatic approaches for NA synthesis

In the literature on nucleoside chemistry, only a few chemoenzymatic synthesis routes have been described so far. Most of the reported methods primarily focus on biocatalytic endgame reactions, utilizing either nucleoside phosphorylases or nucleoside 2′-deoxyribosyltransferases. This section aims to highlight three recent cascade synthesis strategies for NAs, each designed to leverage the complementary strengths of both chemical and enzymatic methods. Two examples illustrate biocatalytic reactions that have been coupled with a chemical reaction step, and one example demonstrates a chemical synthesis that incorporates a biocatalytic step.

One impressive chemoenzymatic cascade reaction is the synthesis of molnupuravir, which was reported by McIntosh and colleagues. After the C5-acylation of ribose by *Candida antarctica* lipase B, ribosyl-1-phosphate was formed using engineered 5-(*S*)-methylthioribose kinase and *N*-glycosylation was realized by engineered uridine phosphorylase

(Scheme 3a) [7]. The reaction was driven by a sophisticated ATP regeneration system based on pyruvate oxidase and acetate kinase. The last reaction step required the interconversion of the amidic carbonyl in the uracil ring to the corresponding oxime and was performed using synthetic chemistry. It was necessary to follow this regime as uridine phosphorylase does not accept cytidine derivatives as substrates. Hence, this approach duly shows how to overcome substrate limitations of the biocatalyst by implementing a chemical step.

The second example is work from our own group: starting from commercially available ribose, where $1'$-OAc-$4'$-thioribose was initially obtained in seven synthetic steps. From there, Pummerer-type glycosylation yielded $\beta$-$4'$-thiouridine with good selectivity [30,31]. We employed thermostable nucleoside phosphorylase to convert $4'$-thiouridine, for example, to $4'$-thio-5-iodouridine with 82% yield. For this, 4 equiv of base was applied in the transglycosylation reaction. After purification by semi-preparative HPLC, a Pd-catalyzed Sonogashira cross-coupling reaction gave $4'$-thio-5-ethynyluridine in quantitative yields (Scheme 3b). A final synthetic step was necessary since 5-ethynyluridine is thermodynamically unfavored with respect to most other nucleosides and therefore hard to access by nucleoside phosphorylase catalyzed transglycosylation. In the same publication, we demonstrated the versatility of this enzymatic platform by synthesizing a range of other halogenated purine and pyrimidine nucleosides [8].

The third example is the synthesis of nucleotide analogue MK-1454 reported by Benkovic and colleagues. In this process, engineered $\alpha$-ketoreductase is used in between chemical transformations to ensure the correct anomeric configuration of the $2'$-hydroxy group from a $2'$-ketonucleoside intermediate. This approach exhibited superior diastereoselectivity compared to several traditional catalysts explored by the authors [9] (Scheme 3c).

The limited number of examples of chemoenzymatic synthesis routes can likely be attributed to the highly specialized environments in which chemists and biochemists typically work. A 2023 survey by Gallou et al. examined how decision-makers in the chemical industry perceive biocatalysis. The findings revealed that they tend to rely more on the strengths of their own discipline to solve problems rather than seeking solutions from other fields. Interestingly, however, most participants in the survey recognized the potential of biocatalysis [32]. This raises the question of how to facilitate the development of new chemoenzymatic synthesis methods. If approached effectively, nucleoside chemistry could greatly benefit from the complementary strengths of both fields (Figure 1).

## 4. Conclusion

The most recent reviews on nucleoside chemistry and sugar synthesis primarily focus on the achievements and challenges within synthetic chemistry [14,33]. Even though Wang et al. and Cosgrove and Miller acknowledge the potential of biocatalysts and highlight their respective strengths, they still predominantly emphasize chemical approaches [6,34]. We believe that integrating both strategies is key to overcoming the most pressing challenges since biocatalytic synthesis can address some of the limitations inherent in chemical synthesis and vice versa.

## CRediT author contributions

SW, AK: Conceptualization. SW: Methodology, Formal Analysis, Investigation, Resources, Data Curation, Writing—Original Draft. SW, AK, PN: Writing—Review & Editing. SW: Visualization. AK: Supervision. PN: Project Administration, Funding Acquisition.

## Declaration of interest

Anke Kurreck is CEO of BioNukleo GmbH, Peter Neubauer is a member of the advisory board. The authors declare no conflict of interest.

## Acknowledgment

## References

[1]  V. E. Kataev and B. F. Garifullin, "Antiviral nucleoside analogs", *Chem. Heterocycl. Compd.* **57** (2021), pp. 326–341.

[2]  T. Manna, S. Maji, M. Maity, B. Debnath, S. Panda, S. Alam Khan, R. Nath and M. J. Akhtar, "Anticancer potential and structure activity studies of purine and pyrimidine derivatives: an updated review", *Mol. Divers.* **29** (2024), pp. 817–848.

[3]  R. Cortese, G. Testa, F. Assogna and N. De Stefano, "Magnetic resonance imaging evidence supporting the efficacy of cladribine tablets in the treatment of relapsing-remitting multiple sclerosis", *CNS Drugs* **38** (2024), pp. 267–279.

[4]  J. M. Thomson and I. L. Lamont, "Nucleoside analogues as antibacterial agents", *Front. Microbiol.* **10** (2019), article no. 952.

[5]  J. Motter, C. M. M. Benckendorff, S. Westarp, P. Sunde-Brown, P. Neubauer, A. Kurreck and G. J. Miller, "Purine nucleoside antibiotics: recent synthetic advances harnessing chemistry and biology", *Nat. Prod. Rep.* **41** (2024), pp. 873–884.

[6]  H.-J. Wang, Y.-Y. Zhong, Y.-C. Xiao and F.-E. Chen, "Chemical and chemoenzymatic stereoselective synthesis of $\beta$-nucleosides and their analogues", *Org. Chem. Front.* **9** (2022), pp. 1719–1741.

[7]  J. A. McIntosh, T. Benkovics, S. M. Silverman, et al., "Engineered Ribosyl-1-Kinase enables concise synthesis of molnupiravir, an antiviral for COVID-19", *ACS Cent. Sci.* **7** (2021), pp. 1980–1985.

[8]  S. Westarp, C. M. M. Benckendorff, J. Motter, et al., "Biocatalytic nucleobase diversification of 4′-thionucleosides and application of derived 5′-ethynyl-4′-thiouridine for RNA synthesis detection", *Angew. Chem. Int. Ed.* **63** (2024), article no. e202405040.

[9]  T. Benkovics, F. Peng, E. M. Phillips, et al., "Diverse catalytic reactions for the stereoselective synthesis of cyclic dinucleotide MK-1454", *J. Am. Chem. Soc.* **144** (2022), pp. 5855–5863.

[10]  Y. Kothapalli, R. A. Jones, C. K. Chu and U. S. Singh, "Synthesis of fluorinated nucleosides/nucleotides and their antiviral properties", *Molecules* **29** (2024), article no. 2390.

[11]  M. A. Huffman, A. Fryszkowska, O. Alvizo, et al., "Design of an in vitro biocatalytic cascade for the manufacture of islatravir", *Science* **366** (2019), pp. 1255–1259.

[12]  H. M. Kalckar, "Enzymatic synthesis of a nucleoside", *J. Biol. Chem.* **158** (1945), pp. 723–724.

[13]  R. Liu, Y. Chen, J. Zheng, L. Zhang, T. Xu, P. Xu and Y. Yang, "Synthesis of nucleosides and deoxynucleosides via gold(I)-catalyzed *N*-glycosylation of glycosyl (*Z*)-ynenoates", *Org. Lett.* **24** (2022), pp. 9479–9484.

[14]  D. G. Rajapaksha, S. Mondal, J. W. Wang and M. W. Meanwell, "A guide for the synthesis of key nucleoside scaffolds in drug discovery", *Med. Chem. Res.* **32** (2023), pp. 1315–1333.

[15]  M. Guinan, C. Benckendorff, M. Smith and G. J. Miller, "Recent advances in the chemical synthesis and evaluation of anticancer nucleoside analogues", *Molecules* **25** (2020), article no. 2050.

[16]  M. W. Hager and D. C. Liotta, "Cyclization protocols for controlling the glycosidic stereochemistry of nucleosides. Application to the synthesis of the antiviral agent 3′-azido-3′-deoxythymidine (AZT)", *J. Am. Chem. Soc.* **113** (1991), pp. 5117–5119.

[17]  A. Michael Downey and M. Hocek, "Strategies toward protecting group-free glycosylation through selective activation of the anomeric center", *Beilstein J. Org. Chem.* **13** (2017), pp. 1239–1279.

[18]  S. Kamel, H. Yehia, P. Neubauer and A. Wagner, "Enzymatic synthesis of nucleoside analogues by nucleoside phosphorylases", in *Enzymatic and Chemical Synthesis of Nucleic Acid Derivatives*, 1st edition (J. Fernández-Lucas, ed.), Wiley: Hoboken, NJ, 2019, pp. 1–28.

[19]  H. Yehia, S. Kamel, K. Paulick, P. Neubauer and A. Wagner, "Substrate spectra of nucleoside phosphorylases and their potential in the production of pharmaceutically active compounds", *Curr. Pharm. Des.* **23** (2018), pp. 6913–6935.

[20]  M. A. Konkina, M. S. Drenichev, D. I. Nasyrova, Y. B. Porozov and C. S. Alexeev, "Studies on enzymatic transglycosylation catalyzed by bacterial nucleoside deoxyribosyltransferase II and Nucleoside phosphorylase for the synthesis of pyrimidine 2′-deoxyribonucleosides containing modified heterocyclic base", *Sustain. Chem. Pharm.* **32** (2023), article no. 101011.

[21]  F. Kaspar, M. Seeger, S. Westarp, et al., "Diversification of 4′-methylated nucleosides by nucleoside phosphorylases", *ACS Catal.* **11** (2021), pp. 10830–10835.

[22]  A. Salihovic, A. Ascham, A. Taladriz-Sender, et al., "Gram-scale enzymatic synthesis of 2′-deoxyribonucleoside analogues using nucleoside transglycosylase-2", *Chem. Sci.* **15** (2024), pp. 15399–15407.

[23]  S. Kamel, I. Thiele, P. Neubauer and A. Wagner, "Thermophilic nucleoside phosphorylases: their properties, characteristics and applications", *Biochim. Biophys. Acta (BBA) - Proteins Proteom.* **1868** (2020), article no. 140304.

[24]  J. Del Arco, P. A. Sánchez-Murcia, J. Miguel Mancheño, F. Gago and J. Fernández-Lucas, "Characterization of an atypical, thermostable, organic solvent- and acid-tolerant 2′-deoxyribosyltransferase from chroococcidiopsis thermalis", *Appl. Microbiol. Biotechnol.* **102** (2018), pp. 6947–6957.

[25]  J. Fernández-Lucas, A. Fresco-Taboada, I. De La Mata and M. Arroyo, "One-step enzymatic synthesis of nucleosides from low water-soluble purine bases in non-conventional media", *Bioresource Technol.* **115** (2012), pp. 63–69.

[26]  F. Kaspar, R. T. Giessmann, K. F. Hellendahl, P. Neubauer, A. Wagner and M. Gimpel, "General principles for yield optimization of nucleoside phosphorylase-catalyzed transglycosylations", *ChemBioChem* **21** (2020), pp. 1428–1432.

[27]  J. Motter, S. Westarp, J. Barsig, et al., "A deamination-driven biocatalytic cascade for the synthesis of ribose-1-phosphate", *Green Chem.* **26** (2024), pp. 11600–11607.

[28]  M. Willmott, W. Finnigan, W. R. Birmingham, et al., "An engineered aldolase enables the biocatalytic synthesis of 2′-functionalized nucleoside analogues", *Nat. Synth.* **4** (2024), pp. 156–166.

[29]  F. Kaspar, M. R. L. Stone, P. Neubauer and A. Kurreck, "Route efficiency assessment and review of the synthesis of $\beta$-nucleosides via *N*-glycosylation of nucleobases", *Green Chem.* **23** (2021), pp. 37–50.

[30]   C. M. M. Benckendorff, Y. S. Sanghvi and G. J. Miller, "Preparation of a 4′-thiouridine building-block for solid-phase oligonucleotide synthesis", *Curr. Protoc.* **3** (2023), article no. e878.

[31]   M. Guinan, N. Huang, C. S. Hawes, M. A. Lima, M. Smith and G. J. Miller, "Chemical synthesis of 4′-thio and 4′-sulfinyl pyrimidine nucleoside analogues", *Org. Biomol. Chem.* **20** (2022), pp. 1401–1406.

[32]   F. Gallou, H. Gröger and B. H. Lipshutz, "Status check: biocatalysis, its use with and without chemocatalysis. How does the fine chemical industry view this area?", *Green Chem.* **25** (2023), pp. 6092–6107.

[33]   C. Maria and A. P. Rauter, "Nucleoside analogues: *N*-glycosylation methodologies, synthesis of antiviral and antitumor drugs and potential against drug-resistant bacteria and Alzheimer's disease", *Carbohydr. Res.* **532** (2023), article no. 108889.

[34]   S. C. Cosgrove and G. J. Miller, "Advances in biocatalytic and chemoenzymatic synthesis of nucleoside analogues", *Expert Opin. Drug Discov.* **17** (2022), pp. 355–364.

ACADÉMIE
DES SCIENCES
INSTITUT DE FRANCE

Research article

# Innovative carrier materials for advancing enzyme immobilization in industrial biocatalysis

**Quentin Hanniet** [©],[a,b]**, Coline Mateos** [a]**, Ludivine Onillon** [a]**, Awilda Maccow** [a]**,
Thierry Gefflaut** [©],[c]**, Mélanie Hall** [d]**, Tamara Reiter** [©],[d]**, Mélanie Bordeaux** [©],[e]**,
Nicolas Brun** [©],[a,b] **and Jullien Drone** [*],[a,b]

[a] ICGM, Univ. Montpellier, CNRS, ENSCM, Montpellier, France

[b] CarboZym SAS, Cap Alpha, 3 avenue de l'Europe - 34830 Clapiers, France

[c] Université Clermont Auvergne, Clermont-Auvergne INP, CNRS, Institut de Chimie de Clermont-Ferrand, 63000 Clermont-Ferrand, France

[d] Institute of Chemistry, University of Graz, Heinrichstrasse 28, 8010 Graz, Austria

[e] Fundacion Nicafrance, Finca La Cumplida, Matagalpa, Nicaragua

*E-mail:* jullien.drone@enscm.fr (J. Drone)

**Abstract.** Industrial biotechnology stands at a turning point. While enzymes have long promised green, efficient catalysis, their widespread adoption has been held back by practical limitations. In this work, we introduce an innovative family of sustainable carrier materials that redefine enzyme immobilization. These materials are synthesized via a controlled solvothermal process, using renewable sources of sugars and polyphenols to create an interconnected porous structure with tunable surface chemistry. This design enables strong enzyme binding through mechanisms such as metal complexation, hydrophobic interactions, and hydrogen bonding, offering high loading capacities and exceptional operational stability. Developed with sustainability at their core, these materials set new standards for both performance and environmental responsibility, bridging the gap between laboratory research and industrial applications in biocatalysis.

## 1. Introduction

Enzyme immobilization has emerged as a powerful technique to enhance enzyme stability, reusability, and efficiency [1]. It represents a crucial technological advancement in industrial biotechnology, bridging the gap between the remarkable catalytic properties of enzymes and the practical demands of industrial processes. This strategy, which has evolved significantly since its first documented use in 1916 [2], has become instrumental in various industrial sectors and continues to shape the future of sustainable chemical manufacturing.

The industrial application of enzymes spans numerous sectors, demonstrating their versatility and importance in modern manufacturing processes. Key industries utilizing enzymatic processes include food processing [3], textile manufacturing [4], biodiesel production [5], biosensors [6], paper making [7], cosmetics [3], therapeutic molecules [8] and, but not limited to, chemical synthesis [9].

---

*Corresponding author

To understand the scale of enzyme utilization in industry, consider that glucose production alone involves the conversion of $10^9$ tons of corn starch annually using soluble amylases. Similarly, the glucose isomerase process handles the conversion of $10^7$ tons of glucose per year to make high-fructose corn syrup, highlighting the massive scale of these operations [1]. From the economical standpoint, the global enzyme market was valued at USD 14.0 billion in 2024 and is projected to reach USD 20.4 billion by 2029, recording a Compound Annual Growth Rate (CAGR) of 7.8% [10].

However, their successful implementation is often hindered by several inherent limitations. One major challenge is their operational instability. Enzymes are susceptible to denaturation under the harsh conditions prevalent in many industrial processes, such as extreme temperatures and pH fluctuations. Their natural structures may not withstand prolonged operational periods, leading to a decline in catalytic activity. Furthermore, the recovery of free enzymes, which act as homogeneous catalysts, presents a significant hurdle. Being water-soluble, they cannot be easily separated from the reaction mixture. Traditional recovery methods, like membrane processes, are often costly and inefficient, making continuous processing difficult. Another challenge arises from the tendency of enzymes to aggregate, particularly in hydrophobic environments or near their isoelectric point. This aggregation limits diffusion and reduces accessibility to active sites, ultimately decreasing overall activity [11].

Enzyme immobilization technology presents a compelling solution to the challenges associated with the use of free enzymes in industrial processes [12]. By anchoring enzymes onto a solid support, immobilization confers several key advantages.

Firstly, it transforms enzymes from homogeneous to heterogeneous catalysts, enabling straightforward recovery through simple filtration or centrifugation techniques. This eliminates the need for costly and inefficient downstream processing methods, significantly reducing overall process costs and improving efficiency.

Furthermore, immobilization significantly enhances enzyme stability [13]. The immobilized enzymes exhibit greater resistance to harsh environmental conditions, such as temperature fluc-

tuations and pH changes. This is translated to an extended operational lifetime and a broader range of applicable reaction conditions.

Moreover, immobilized enzymes are ideally suited for continuous flow operations, allowing for seamless integration into packed or fluidized bed reactors. This improved process control enables more precise regulation of reaction parameters and enhances overall system efficiency [14,15]. The choice of support material plays a crucial role in the immobilization process, affecting the properties of the resulting biocatalytic system [16]. A wide range of materials, including inorganic, organic, hybrid, and composite supports, have been explored for enzyme immobilization [16,17]. Additionally, agroindustrial wastes have shown potential as cost effective and environmentally friendly carriers for enzyme immobilization, coconut fiber being a preferred option [18,19].

While enzyme immobilization offers numerous benefits, the field still faces certain challenges that limit its widespread adoption since no single method is universally applicable. One key hurdle lies in the complexity and time-consuming nature of immobilization protocols [20]. Current methods often require lengthy procedures, sometimes extending up to 48 h, involving the use of hazardous chemicals such as glutaraldehyde and can result in variable protein loading capacities, hindering efficient enzyme utilization. Moreover, the recycling potential of immobilized enzymes may turn out to be limited, requiring frequent replacement and contributing to increased the operational costs.

Another challenge stems from the intrinsic limitations of support materials. Many carriers currently used are expensive and/or rely on oil-based materials, raising concerns about sustainability [21].

Furthermore, the performance of immobilized enzymes is often dependent on the specific carrier used, leading to inconsistent results. Enzyme activity retention can vary significantly, and protein loading capacity remains limited, typically reaching around 5% or 50 mg of enzyme per gram of carrier [22].

These limitations highlight the need for continued research and development to optimize immobilization techniques and develop more efficient, versatile and sustainable solutions.
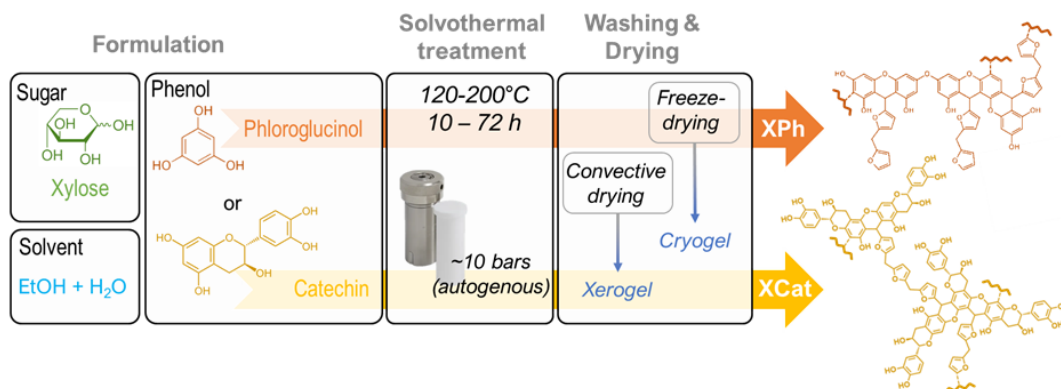
**Figure 1.** Description of XPh and XCat CarboZym support synthesis and chemical structure.

## 2. The CarboZym technology: a game changer

At CarboZym SAS[1], a multidisciplinary team of researchers in chemistry, bioprocess engineering, and biocatalysis collaborates to make enzyme-powered biomanufacturing both accessible and cost-effective and to pave the way for a more sustainable future by streamlining enzyme integration in processes.

### 2.1. *Underlying principle*

The CarboZym technology, which we will call "CarboZym", marks a significant advancement in biocatalysis by patenting a biosourced, universally adaptable porous support for enzyme immobilization [23,24]. This innovative support, derived from renewable precursors such as sugars (xylose, glucose, fructose) and phenols (phloroglucinol, catechin), leverages polycondensation mechanisms and intermolecular reactions [25]. Unique characteristics of this material include an interconnected porous structure and adjustable surface chemistry [26], enabling various types of interactions with enzymes. Relying on green chemistry principles and biodegradable raw materials, this technology meets sustainability requirements while minimizing carbon footprint, notably by revalorizing bio-waste rich in phenolic compounds (such as condensed tannins).

### 2.2. *Material synthesis and properties*

The preparation of the CarboZym support material involves a controlled synthesis process in an autoclave under solvothermal, subcritical conditions (Figure 1). The process begins with dissolving the precursors, namely a sugar and a phenol, in a water–ethanol mixture. Under solvothermal conditions, the sugars undergo dehydration: xylose is converted to furfural, while glucose and fructose generate 5-(hydroxymethyl)furfural (HMF). These heterocyclic aldehydes then quickly react with phenols such as phloroglucinol or catechin (at positions 2, 4, 6 of the aromatic ring) via intermolecular dehydration and electrophilic aromatic substitution mechanisms [25].

Initially, polymerization occurs between active sites of the phenols and the dehydrated sugars, forming oligomers that gradually assemble into three-dimensional networks through successive steps of nucleation, particle growth, and agglomeration. Within the autoclave, these steps promote the formation of a gel with interconnected pores (ranging from microporosity (<2 nm) to macroporosity (a few micrometers)) filled with liquid. This structure mimics sol–gel processes but is influenced by the composition of the precursors and the applied solvothermal conditions.

The precursor solution solidifies during the reaction in the autoclave, enabling the material to be shaped into various forms by placing a mold in the autoclave (see Figure S1.a for a macroscopic view of the shaped material). Alternatively, the material can be reduced to a powder after post-drying milling for applications in fluidized systems.

---

[1]CarboZym SAS, a CNRS spin-off established in November 2024, has set itself the mission to transform chemical manufacturing through the power of enzymes.

Following gel formation, two crucial steps are required to replace the interstitial liquid with air or another gas: solvent exchange through intensive washing, and drying [27]. The choice of solvent and drying method (supercritical drying, freeze drying or air drying) can significantly affect the final material properties:

(i) Supercritical drying is the method of choice as it yields aerogels with full preservation of the original pore texture of the wet gel. It is usually performed with carbon dioxide that presents moderate critical point temperature and pressure (31.1 °C at 1072 psi). When performed correctly, supercritical drying can largely preserve the material's textural properties.

(ii) Freeze-drying produces cryogels and involves solvent exchange with water or water–alcohol mixtures, freezing and ice sublimation at low pressure (to the range of a few millibars). However, ice crystal growth during the freezing stage can induce large distortion of the porous structure and a drastic loss of porosity [25].

(iii) Convective or evaporative air-drying is a much more delicate method to use, since drying occurs by direct solvent evaporation and the gel is therefore subject to high capillary forces. It yields xerogels that often display slightly different yet functional characteristics [27].

This step allows the creation of materials with BET (Brunauer–Emmett–Teller theory)-equivalent specific surface areas ranging from 200 to 900 $m^2$/g and pore volumes between 0.2 and 2 $cm^3$/g, with adjustable pore sizes between 20 and 70 nm, depending on the synthesis conditions (Figure S1.b shows adsorption and desorption isotherms of XCat and XPh materials, and Figure S1.c illustrates their BJH (Barrett–Joyner–Halenda Model) pore distribution).

## 2.3. *Technology description*

The flexibility of CarboZym material synthesis offers optimization possibilities tailored to industrial needs. For instance, by selecting catechin as the phenol and xylose as the sugar, the final material (designated XCat) retains unaltered catechol functions, allowing chelation with metal ions (see chemical structure in Figure 1). This option enables binding of His-tagged proteins to the material through metal complex formation [28,29]. In the presence of an ion such as nickel, cobalt, or iron, these catechol groups form stable bonds with His-tagged enzymes, ensuring robust fixation and precise enzyme orientation on the support (Figure 2b). This binding also facilitates enzyme recycling by simply washing out the bound enzyme under mild conditions that disrupt the His–Nickel interaction, by using imidazole, which is essential for continuous-flow or industrial processes where the catalytic lifespan of the enzyme is crucial.

The CarboZym material also exhibits compatibility with non-His-tag enzymes, which interact through weak bonds such as hydrophobic interactions or hydrogen bons, enabled by functional groups present on the porous surface. Thus, an XPh-type material (derived from xylose and phloroglucinol, Figure 1) would be suitable for non-His-tagged proteins as it is more likely to interact with a protein via hydrophobic interactions given its less oxygen-rich surface chemistry compared to XCat. The material's adaptability in terms of surface and chemistry makes it compatible with a wide range of enzymes, rendering this technology potentially universal.

The enzymatic immobilization protocol is simplified compared to conventional methods (such as cross-linking, entrapment, covalent attachment) (Figure 2a), where the enzyme self-confines directly within the material meso- and macroporosity via physisorption and/or chemisorption. At the molecular scale (Figure 2b), the immobilization of His-tagged enzymes appears to occur through metal complexation with catechol groups in XCat gels, while non-His-tag enzymes bind to the material through electrostatic interactions (via lysine, histidine, or arginine residues), van der Waals forces, π–π stacking and/or hydrophobic interactions (e.g., between proline residue and polyphenol ring) [30–32].

The sugars and phenols used in the synthesis of CarboZym supports enhance its biosourced aspect. Catechin, for example, is a monomer of condensed tannins, demonstrating the feasibility of using biowaste containing these compounds to design the gel. Revalorizing this waste (such as wood or seed extracts) in the material's production not only reduces environmental impact but also allows for sustainable and economical precursor sourcing [33,34].
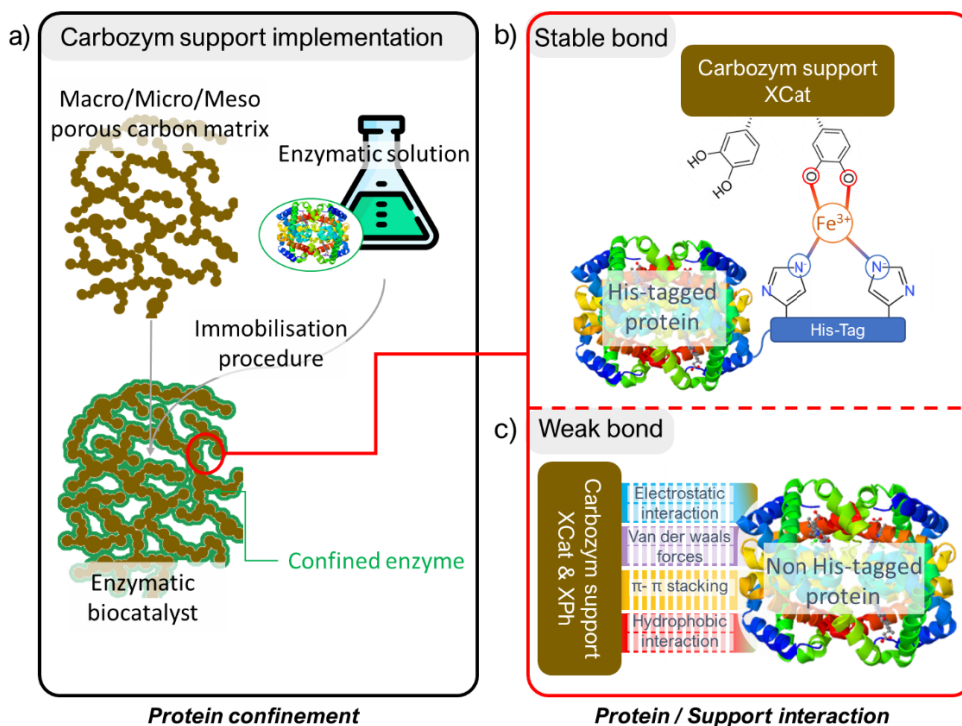
**Figure 2.** (a) Protein confinement in the CarboZym support; (b) Protein bonding through formation of a stable XCat–$Fe^{3+}$–histidine complex; (c) Weak bonding of protein through electrostatic interaction, Van der Waals forces, $\pi$–$\pi$ stacking and/or hydrophobic interaction.

## 2.4. *Green chemistry and industrial relevance*

From an industrial standpoint, enzyme immobilization on CarboZym carrier material offers several major advantages over the use of free enzyme use. First, with the ability to immobilize up to 50 wt% of enzyme on the CarboZym material enables reusability, significantly lowering the cost per usage cycle. Moreover, this technology allows enzyme utilization in continuous mode, meeting the growing industrial demand for flow optimization. However, technical challenges remain in enzyme immobilization, such as activity loss due to diffusion limitations or demanding attachment conditions.

CarboZym addresses limitations of traditional immobilization technologies. The binding process is fast and spontaneous, without requiring costly activation steps. The material's interconnected pores enhance mass transfer, minimizing activity losses from diffusion constraints. Additionally, enzyme reuse is assured, making this approach compatible with moderately active enzymes, thereby avoiding costly enzyme engineering optimizations. Finally,

the biosourced nature and green chemistry principles underlying this technology strengthen its positioning in sustainable industrial applications.

## 3. Illustrative case studies

### 3.1. *Tailoring Candida antarctica lipase B (CALB) performance through surface chemistry*

Lipases are enzymes that catalyze the hydrolysis of ester bonds in lipid molecules [35]. Their natural function is the breakdown of fats, but they are also widely used in synthetic processes such as esterification and transesterification, especially in non-aqueous environments [36,37]. These enzymes are favored in biocatalysis because of their broad substrate specificity, regioselectivity, and stereoselectivity, making them valuable tools in the pharmaceutical, food, and chemical industries. Lipases work at the interface between aqueous and organic phases, and their activity is often enhanced by this interfacial activation. One of the most prominent lipases
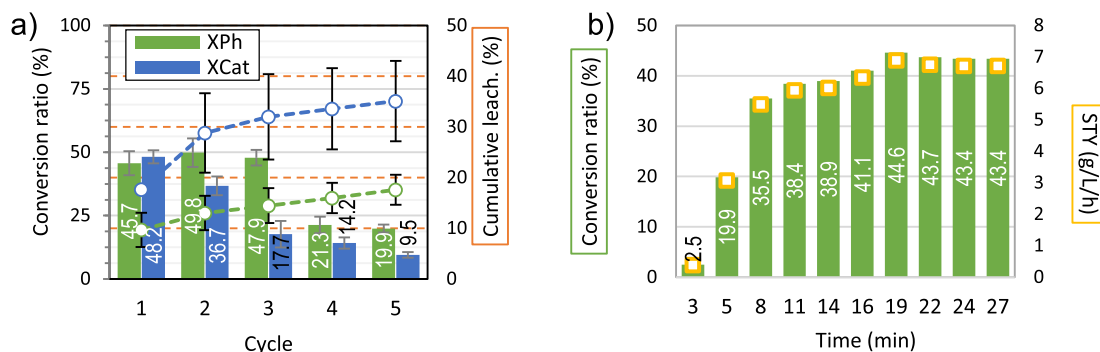
**Figure 3.** Results for immobilized CALB (a) Batch mode: conversion ratio and cumulative leaching for XPh and XCat support ([*buffer*: 20 mM Tris-HCl + 1 wt% genapol; pH 7] [*immobilization conditions*: 10 mg XCat or XPh support—10% (w/w) protein loading—800 rpm; 4 °C]; [*reaction conditions*: 15 mM pNPB—25 °C]); (b) Continuous mode: conversion ratio and STY ([*buffer*: same as batch mode] [*immobilization conditions*: 65 mg support—10% (w/w) protein loading—0.1 ml/min; 4 °C]; [*reaction conditions*: same as batch mode; circulation mode—5 mM p-NPB—13.3 ml at 0.5 ml/min—5 cycles]).

in industrial applications is *Candida antarctica* lipase B (CALB). This enzyme stands out due to its high stereoselectivity and substrate flexibility, making it a key player in asymmetric synthesis, particularly for secondary alcohols. CALB's robust catalytic performance under various conditions, including in organic solvents, at wide temperature and pH range, contributes to its broad use in reactions such as polymerization, hydrolysis, and esterification.

Despite its numerous benefits, CALB's cost can be a significantly limiting factor for large-scale industrial applications. To address this, immobilization of CALB is often employed to enable enzyme reuse and thus lower the overall production cost. However, the commercial version of CALB, such as Novozyme 435, is already immobilized on a resin. Despite its widespread use, one of the challenges associated with this preparation is leaching—the gradual loss of enzyme from the support during reactions. This leaching can diminish the enzyme's activity over time, reducing the expected cost savings from immobilization [38].

The immobilization of CALB was carried out on two versions of CarboZym support to form biocatalysts *i*-CALB-XCat and *i*-CALB-XPh. Such biocatalysts were implemented in the hydrolysis of p-nitrophenyl butyrate (pNPB) as a model reaction (see Figure 3 caption and supporting information for more detailed protocol). Conversion ratio and cumulative leaching on 5 cycles associated are displayed on Figure 3 for both biocatalysts. In both cases, the enzyme is still active after 5 cycles but their

remaining activity is different, averaging 20 and 44% for *i*-CALB-XCat and *i*-CALB-XPh, respectively. One explanation probably is linked to the fact that the cumulative leaching over 5 cycles is almost 2 times greater for XCat than for XPh support. According to these observations, XPh support is a more suitable material for CALB immobilization as it is more difficult to remove the enzyme from the material probably due to a stronger interaction. Our hypothesis here is that the CALB interacts with the carbon-based support through hydrophobic interactions which are stronger with XPh than XCat.

The *i*-CALB-XPh biocatalyst was then implemented in a fluidized bed continuous flow system (see Supplementary Information) to prove the implementation of CarboZym technology in such industry-approved reactors. In continuous mode, the substrate solution was flowed (without re-circulation) through the thermostatted column at 0.5 ml/min with negligible protein loss and achieving space–time yields (STY) close to 7 $g·L^{-1}·h^{-1}$ (for the p-NPB hydrolysis). These results demonstrate significant progress toward achieving the industry-standard metrics required to ensure process viability [39].

## 3.2. *GsOYE-catalyzed reduction of 2-cyclohexenone to cyclohexanone*

Ene-reductases (EREDs) are a class of oxidoreductase enzymes that catalyze the asymmetric reduction of activated alkenes to saturated products, typically
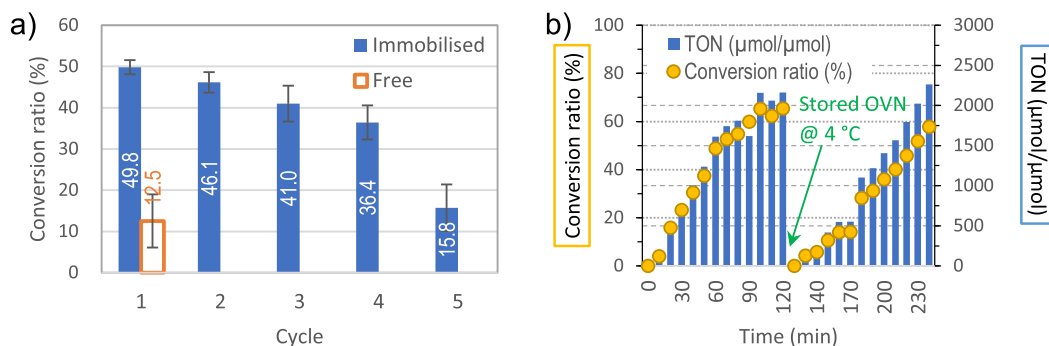
**Figure 4.** Results for immobilized *Gs*OYE. (a) Batch mode: conversion ratio and cumulative leaching ([*buffer*: 200 mM Tris-HCl + 50 mM NaCl + 2 vol% DMSO; pH 7.5] [*immobilization conditions*: 25 mg Fe-XCat support—10% (w/w) protein loading—800 rpm; 4 °C]; [*reaction conditions*: 50 mM cyclohexenone—75 mM NADH—30 °C]); (b) Continuous mode: conversion ratio and STY ([*buffer*: same asbatch mode] [*immobilization conditions*: 50 mg Fe-XCat support—10% (w/w) protein loading—0.1 ml/min; 4 °C]; [*reaction conditions*: same as batch mode; recirculation mode—120 ml at 1 ml/min—5 cycles]).

using nicotinamide cofactors such as NAD(P)H as electron donors. Among the ene-reductases, the old yellow enzyme (OYE) family is one of the most well-studied and widely applied groups. OYE enzymes are flavin mononucleotide (FMN)-dependent oxidoreductases known for their ability to catalyze the reduction of a wide variety of α,β-unsaturated carbonyl compounds, including ketones, aldehydes, and nitroalkenes [40,41]. OYE enzymes exhibit broad substrate specificity and high stereoselectivity can be obtained, making them valuable for applications in asymmetric synthesis. One notable application is the reduction of cyclohexenone to cyclohexanone, a key reaction in the synthesis of fine chemicals and pharmaceutical intermediates. In this reaction, the α,β-unsaturated bond in cyclohexenone is reduced to the corresponding cyclohexanone with excellent stereoselectivity, highlighting the utility of ene-reductases for producing optically pure compounds. The versatility and stability of OYE enzymes, coupled with their ability to perform reductions under mild conditions, have made them a focal point in efforts to develop greener and more sustainable chemical processes. Ongoing research and enzyme engineering have expanded the substrate scope and improved the efficiency of OYEs, making them a powerful tool for modern synthetic applications [42].

The *Gs*OYE is a newly identified ene-reductase from *Galdieria sulphuraria* alga [41]. It features properties that fulfill the specifications required for industrial applications, such as high catalytic activity and robustness (thermostability, wide range pH optimum, cosolvent tolerance) as well as high-yield production/purification.

*Gs*OYE was expressed in *E. coli* with an N-terminal His-tag. Fe-XCat CarboZym support was then chosen to immobilize the protein via coordination with iron bound to XCat material. Such *i*-*Gs*OYE-Fe-XCat biocatalyst was implemented to catalyze the reduction of cyclohexenone to cyclohexanone (see Figure 4 and Supplementary Information for protocol details). As described in Figure 4a, the biocatalyst was used in batch mode and displays a conversion ratio ~3.5 times higher than the free enzyme from cycle 1 onwards. It suggests that the enzyme activity can be enhanced upon immobilization. This may be caused by the fact that the immobilized state promotes a more catalytically favored conformation compared to its free form. Reuse of *i*-*Gs*OYE-Fe-XCat biocatalyst showed that the enzyme can remain active over five cycles (with a mean remaining activity around 32%) resulting in a Total Turnover Number (TTN) of $5868 \pm 758$ compared with $860 \pm 338$ for the free enzyme.

Continuous mode operation was also tested, where the reaction mixture was recirculated through a packed column filled with *i*-*Gs*OYE-Fe-XCat (Figure 4b). Over the course of two hours, *Gs*OYE consistently reduced cyclohexenone, with steadily increasing conversion rate and TON. It was also shown that after stopping the process and storing it overnight at 4 °C, the continuous reaction can be restarted and
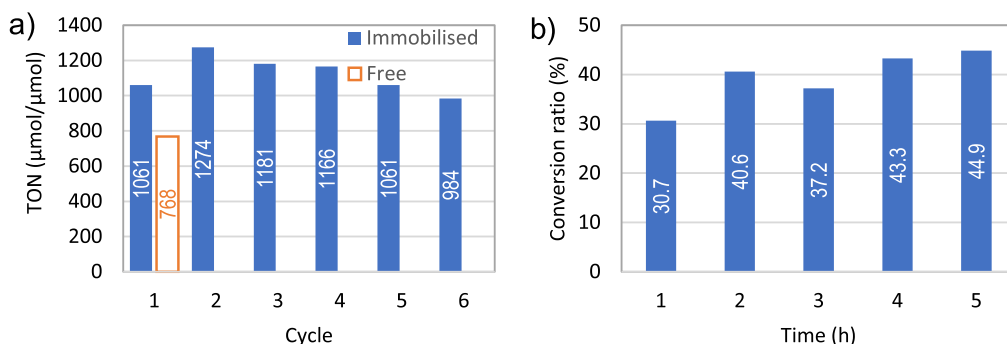
**Figure 5.** Results for immobilized B9L0N2. (a) Batch mode: conversion ratio and cumulative leaching ([*buffer*: 50 mM Tris-HCl + 300 mM NaCl + 10 wt% glycerol; pH 7.5] [*immobilization conditions*: 25 mg Fe-XCat support—10% (w/w) protein loading—800 rpm; 4 °C]; [*reaction conditions*: 25 mM pyruvate, 25 mM racemic α-methylbenzylamine, 0.1 mM PLP—25 °C]); (b) Continuous mode: conversion ratio ([*buffer*: same as batch mode] [*immobilization conditions*: 70 mg Fe-XCat support—5% (w/w) protein loading—0.1 ml/min; 4 °C]; [*reaction conditions*: same as batch mode; circulation mode—0.1 ml/min— 5 hours]).

regained an efficiency similar to that before storage. The low leaching and robust activity under continuous conditions position this system as an effective biocatalyst for scalable processes. It should also be noted that the leaching measured in batch and continuous mode remains very low (<1%), probably thanks to the stable binding provided by the support/His-tag interaction.

### 3.3. *Immobilized transaminase for efficient pyruvate conversion*

Transaminases (TAs) are widely recognized for their role in catalyzing the transfer of amino groups from amine donors to acceptor molecules, such as ketones or aldehydes, facilitating the formation of valuable chiral amines [43]. These enzymes are particularly attractive for green chemistry applications in industries such as pharmaceuticals and agrochemicals, where they are employed for the synthesis of enantiopure compounds [44,45]. The demand for such biocatalysts is driven by their high selectivity, operational stability, and ability to operate under mild conditions, reducing the need for toxic chemicals and harsh environments. One example is the transaminase from *Thermomicrobium roseum* (UniProt accession number B9L0N2), classified as an ω-transaminase. This class of transaminases typically operates with both primary amines and ketones, which makes them versatile tools in biotransformations. These enzymes belong to

a family of enzymes dependent on pyridoxal-5′-phosphate (PLP) as a cofactor [46]. PLP plays a critical role in the catalytic mechanism, acting as an intermediate carrier of the amino group during the transamination process. B9L0N2 demonstrates excellent activity in the asymmetric synthesis of a variety of chiral amines. This enzyme shows high efficiency in catalyzing the conversion of substrates like pyruvate and racemic amines, making it a valuable tool in producing pharmaceutical intermediates [47].

The advantages of using B9L0N2 include its ability to perform reactions under mild conditions and with minimal by-products, as well as its compatibility with continuous processing, which enhances its potential industrial applications. Its robustness, combined with low substrate inhibition and tolerance to organic solvents, makes it highly versatile for use in different biotechnological settings.

Similarly to *Gs*OYE, B9L0N2 was immobilized on Fe-XCat support to form a *i*-B9L0N2-Fe-XCat biocatalyst through $Fe^{3+}$/His-tag coordination. The transamination of pyruvate in the presence of racemic α-methylbenzylamine was chosen as a model reaction to evaluate the efficiency of such a biocatalyst both in batch and continuous mode. The results of these assays are displayed on Figures 5a and 5b, respectively.

The batch test results demonstrate that the enzyme activity remains highly stable across six consecutive cycles, with a relative residual activity of

approximately 92% from the first to the sixth cycle. Under these conditions, the cumulative turnover number over these cycles is increased by a factor of about 8.75 compared to the enzyme in its free form, indicating that immobilizing B9L0N2 can reduce enzyme-related costs proportionally. Given the robust stability of the immobilized biocatalyst, this factor has the potential to be enhanced further by extending the number of cycles, underscoring the practicality of utilizing CarboZym technology for this application.

Additionally, performance in continuous mode (without recirculation) showed similarly high stability, with a consistent conversion rate maintained over a five-hour period. Importantly, minimal enzyme leaching was observed in both batch and continuous setups (<1%), supporting the durability of the immobilization. These findings demonstrate, as a proof of concept, that CarboZym technology offers significant benefits for the industrial application of transaminases like B9L0N2, enabling efficient and cost-effective biocatalysis.

## 4. Future prospects and industry applications

### 4.1. *Enzyme co-immobilization: mimicking nature's metabolic efficiency*

Enzyme co-immobilization represents a sophisticated approach that bridges the gap between nature's complex metabolic networks and industrial requirements [48,49]. This strategy involves the immobilization of multiple enzymes onto a single support material. It allows running enzymatic cascades into one-pot reaction systems creating an artificial microenvironment where sequential enzymatic transformations can occur efficiently within a single reaction vessel. By mimicking the intricate choreography of natural metabolic pathways, this strategy offers a powerful solution to the limitations of traditional single-enzyme approaches.

#### 4.1.1. *Fundamental principles and advantages*

In living cells, metabolic pathways operate through precisely organized spatial arrangements of enzymes. This natural organization enables rapid substrate channeling, where intermediates are efficiently transferred between consecutive enzymes [50]. Enzyme co-immobilization seeks to recreate this efficiency in artificial systems by positioning multiple enzymes on a single support material, eliminating the need for intermediate isolation or purification [51].

Traditional single-enzyme approaches face significant limitations when handling complex multistep reactions. Each enzymatic step typically requires separate reaction vessels, leading to increased complexity, cost, and logistical challenges. Moreover, intermediates produced in one step may degrade before being utilized in subsequent reactions, resulting in reduced yields and increased purification demands [52].

Co-immobilization elegantly addresses these challenges by creating a concentrated microenvironment where enzymes work in concert. The close proximity of enzymes facilitates direct transfer of intermediates, minimizing diffusion limitations and byproduct formation. This spatial arrangement promotes faster reaction rates and shields enzymes from harsh conditions, enhancing their operational stability and lifespan [53].

#### 4.1.2. *Design and technical considerations*

Successfully implementing enzyme co-immobilization requires careful attention to multiple factors. The choice of support material is crucial, as it must provide sufficient surface area and appropriate chemical functionality while maintaining individual enzyme activities. The material should offer mechanical stability and enable efficient mass transfer of substrates and products.

Several strategies have emerged for enzyme co-immobilization, each with distinct advantages. Entrapment within porous matrices, such as alginate beads or hydrogels, offers a simple and cost-effective approach but may face diffusion limitations [54]. Covalent attachment through chemical bonds provides stable immobilization and precise control over enzyme positioning but requires careful selection of coupling chemistry to preserve activity [55].

Physical adsorption relies on non-covalent interactions like hydrogen bonding and electrostatic forces, offering a gentler alternative that better preserves enzyme activity and allows for enzyme replacement when needed [21]. Surface modification techniques enable precise control over enzyme orientation and density through the creation of specific binding sites on the support material.

The ratio of different enzymes in the co-immobilized system requires careful optimization to prevent bottlenecks and ensure smooth reaction progression [56]. Unlike natural systems with tightly regulated enzyme expression, artificial systems need balanced enzyme activities to match sequential reaction rates.

### 4.1.3. *Applications across industries*

The versatility of enzyme co-immobilization has led to its adoption across various sectors. In pharmaceutical production, co-immobilized enzymes enable the synthesis of complex drug molecules with high selectivity and purity, including the production of chiral intermediates and the biotransformation of drug precursors [57]. The food and beverage industry utilizes this technology for producing modified sweeteners, flavorings, and other additives, while also enabling the bioconversion of food waste into valuable products [58]. In the biofuel sector, co-immobilized enzyme systems show promise in converting complex biomass into useful products, particularly in the degradation of cellulosic materials and the production of biodiesel from vegetable oils [59]. Environmental applications include bioremediation of contaminated soils and water, degradation of toxic pollutants, and the production of bioplastics from renewable resources [60].

### 4.1.4. *Current challenges and limitations*

Despite its potential, enzyme co-immobilization faces several challenges. The complexity of optimizing multiple parameters simultaneously makes system design and implementation demanding. Mass transfer limitations become more significant in co-immobilized enzymes, requiring careful consideration of substrate and product diffusion through the support material [61].

The stability of these systems can be compromised if any single enzyme in the cascade fails, potentially necessitating complete system replacement. Economic viability often depends on achieving sufficient operational stability and reusability to justify the initial investment in expensive support materials and complex immobilization procedures [62].

### 4.1.5. *Future perspectives and innovations*

The future of enzyme co-immobilization lies in developing more sophisticated systems that better mimic natural metabolic pathways. An elegant study by Korman et al. designed a homogeneous system comprising 27 enzymes for the conversion of glucose into monoterpenes such as limonene, pinene and sabinene with high yields [63]. Co-immobilization of this entire synthetic biochemistry platform would probably improve its stability and the total turnover numbers reached paving the way to challenge cell-based systems.

Advanced materials science and nanotechnology could offer promising solutions for creating structured support materials with precise control over enzyme positioning [64].

The field continues to evolve through computational modeling and artificial intelligence, which could accelerate system optimization by predicting optimal enzyme arrangements and ratios [65]. As our understanding of enzyme interactions and immobilization techniques advances, co-immobilized systems will likely play an increasingly important role in enabling sustainable and efficient production processes across diverse industries [66].

The versatility of CarboZym's immobilization carriers was shown to be an asset to successfully perform the simultaneous co-immobilization of up to six different enzymes on the same carrier. We are currently demonstrating this concept with a simplified enzymatic cascade allowing the access to terpenoids starting from isopentenol [67–70]. The six overexpressed and purified enzymes were mixed, and XPh was added to co-immobilize them. This immobilized preparation successfully catalyzed the conversion of isopentenol to limonene, demonstrating the successful co-immobilization of the six enzymes and their catalytic capabilities. This promising study is currently being investigated by CarboZym and a proof of concept will be published in the near future.

## 4.2. *Enzymatic cofactor recycling*

Enzymatic cofactor recycling represents a crucial aspect of industrial biocatalysis, particularly for reactions involving nicotinamide cofactors (NADH/NADPH) and adenosine triphosphate (ATP) [71,72]. These essential molecules serve as electron carriers and energy sources in numerous biochemical transformations, but their high cost and stoichiometric consumption pose significant challenges for industrial applications.

This overview examines the importance of cofactor recycling systems, their implementation strategies, and their integration with enzyme immobilization technologies.

### 4.2.1. *Fundamental principles*

Nicotinamide cofactors play vital roles in oxidation–reduction reactions, serving as electron carriers in numerous enzymatic transformations. NAD(P)H acts as a reducing agent in many valuable synthetic processes, including the production of chiral alcohols, amino acids, and other fine chemicals [73]. ATP, on the other hand, functions as an energy carrier, driving thermodynamically unfavorable reactions and enabling phosphorylation processes essential for many biotransformations [74].

The economic feasibility of enzymatic processes heavily depends on efficient cofactor recycling systems. Without recycling, the stoichiometric use of these expensive cofactors would make most industrial applications prohibitively expensive. For instance, the cost of NADH and NADPH can represent a significant portion of the overall process costs. Similarly, ATP's high cost and inherent instability necessitate efficient regeneration systems for practical applications [75].

### 4.2.2. *Technical approaches to cofactor recycling*

**NAD(P)H recycling.** Several strategies have been developed for NAD(P)H regeneration, each with distinct advantages [71]. The enzyme-coupled approach employs secondary enzymes such as formate dehydrogenase, glucose dehydrogenase, or alcohol dehydrogenase to regenerate the reduced cofactor. These systems typically use inexpensive sacrificial substrates like formate, glucose, or isopropanol to drive the regeneration of NAD(P)H.

Substrate-coupled recycling represents an elegant alternative where a single enzyme catalyzes both the main reaction and cofactor regeneration. This approach simplifies the reaction system but requires careful optimization to balance the main reaction and regeneration rates.

**ATP recycling.** ATP regeneration systems often utilize phosphoryl transfer enzymes such as acetate kinase or pyruvate kinase, coupled with high-energy phosphate donors like acetyl phosphate or phosphoenolpyruvate. These systems can achieve multiple recycling cycles, though their efficiency is typically lower than NAD(P)H regeneration systems due to ATP's complex chemistry and stability issues [71].

### 4.2.3. *Integration with enzyme immobilization*

The combination of cofactor recycling with enzyme immobilization technologies offers promising solutions for industrial applications [76]. Co-immobilization of main and recycling enzymes can create efficient microenvironments where cofactors are rapidly regenerated and reused. This spatial organization mimics natural metabolic pathways and can significantly enhance the overall process efficiency [77].

Various strategies have been developed for immobilizing both enzymes and cofactors. Cofactor tethering involves the chemical modification of cofactors to enable their attachment to support materials, while maintaining their catalytic function. This approach can reduce cofactor loss but may affect the kinetics of enzymatic reactions due to diffusion limitations [78].

### 4.2.4. *Applications and industrial impact*

Cofactor recycling systems have enabled numerous industrial applications. In the pharmaceutical industry, NAD(P)H-dependent reactions are crucial for the synthesis of chiral alcohols and amines which are key building blocks for many active pharmaceutical ingredients. The integration of efficient recycling systems has made these processes economically viable at industrial scales [79].

ATP-dependent processes find applications in the production of phosphorylated compounds, including nucleotides and sugar phosphates. These molecules serve as important intermediates in various biochemical pathways and have applications in both pharmaceutical and food industries.

The combination of cofactor recycling with enzyme immobilization has led to the development of continuous flow processes, where immobilized enzyme systems can operate for extended periods with minimal cofactor loss. These systems offer improved productivity and reduced operational costs compared to batch processes [80].

### 4.2.5. *Current challenges*

Despite significant progress, several challenges remain in the field of cofactor recycling. The stability of

cofactors under industrial conditions remains a concern, particularly for ATP, which is susceptible to hydrolysis. The development of more stable cofactor analogs or protective strategies represents an active area of research [81,82]. Mass transfer limitations in immobilized systems can affect the efficiency of cofactor recycling, particularly when multiple enzymes and cofactors are involved. The design of carrier materials with optimal porosity and surface chemistry is crucial for addressing these limitations [83].

### 4.2.6. *Future perspectives*

The successful conversion of isopentenol into limonene with six co-immobilized enzymes (see Section 4.1.5) also exemplifies the recycling of ATP. Indeed isopentenol is successively phosphorylated into isopentenyl phosphate (IP) and isopentenyl diphosphate (IPP) involving the concomitant consumption of two molecules of ATP yielding $2 \times$ ADP. In this case, ATP regeneration is catalyzed by an acetate kinase (one of the six co-immobilized enzymes) using acetyl phosphate as a phosphate donor [8].

The continued development of innovative solutions that address current limitations while maintaining economic viability will shape the future of this field, enabling more sustainable and efficient production processes across various industries.

## 4.3. *Scaling up hydrothermal carbonization: from laboratory to industrial reality*

The CarboZym technology is based on the hydrothermal carbonization, or more accurately the solvothermal carbonization, of sugar in the presence of phenolic compounds. Hydrothermal carbonization (HTC) is a thermochemical process that transforms organic matter into valuable carbon-based materials under subcritical conditions, i.e., at relatively high temperature and pressure [84]. HTC has demonstrated its efficacy at the laboratory scale and holds immense potential for sustainable material production [84,85]. However, translating this technology to industrial scale presents a unique set of challenges and opportunities that have been partially addressed in the literature for wet biomass wastes [86] and sewage sludges [87]. Several companies have developed HTC plants at pilot and industrial scales, such as C-Green (OxyPower HTC™ plant in Finland), Terra-Nova Energy, Ingelia, CarboREM (CarboREM C-700

Plant installed in Italy), and HTC-Cycle. Technical, economic, and environmental considerations are crucial for successfully scaling up HTC processes for porous carbon-based material production [84]. Even though CarboZym technology involves partially purified precursors that are soluble and therefore easier to process, the scale-up remains challenging and necessitates a meticulous approach to reactor design and operational parameters.

### 4.3.1. *Technical hurdles and engineering solutions*

**Reactor design and operation: navigating heat and pressure.** As reactor volume increases, the efficient transfer of heat becomes paramount. Maintaining uniform temperature distribution within the reaction medium is critical for consistent product quality and requires careful consideration of heating systems and mixing mechanisms. Efficient external jackets, internal heating elements, and robust mixing systems, such as impellers or recirculation loops, are essential for achieving homogeneous heating. In a recent industry perspective on zeolite manufacturing, Maurer and Parvulescu from BASF discussed heat distribution heterogeneities within high volume synthesis reactors (10–20 m$^3$) [88]. A computational fluid analysis showed that even for well-stirred and heated reactor gradients, mixing flows and temperature distributions could occur during the hydrothermal treatment [88].

Pressure management is another crucial aspect. HTC processes typically operate under autogenous pressure, ranging from 10 to 40 bar, demanding robust reactor construction materials capable of withstanding these conditions. Corrosion resistance is equally important, given the acidic nature of the reaction medium (pH is usually below 3 at the end of reaction). Selecting materials like stainless steel alloys or specialized corrosion-resistant coatings is vital for reactor longevity and safety. However, scaling up the synthesis of porous materials under these conditions is not insurmountable; the commercial scale production of zeolites [88,89], in particular Zeolite A (LTA), is a proof. Large-volume reactors of 10–20 m$^3$ have been reported for manufacturing zeolites at commercial scale using conventional batch technologies. Process intensification via continuous flow technology is currently developed by Arkema at pilot scale [90].

**Process control and monitoring: ensuring consistency and quality.** Maintaining consistent product quality at industrial scale requires sophisticated control systems. Continuous monitoring of key parameters, including temperature, pressure, residence time, and slurry concentration, is essential. Implementing in-line sensors and automated control systems allows for real-time adjustments, minimizing deviations from optimal operating conditions and ensuring product uniformity. Data acquisition and analysis can provide valuable insights into process performance, enabling continuous improvement and optimization.

**Feed handling, product recovery, washing and drying: streamlining the process.** Scaling up feed handling systems presents unique challenges. Solutions have been proposed for the continuous flow synthesis of zeolites with in-line mixing of the precursors and in-line seeding of the synthesis gel solution [90]. Efficient downstream processing is also essential. As mentioned above (Section 2.2), two crucial downstream processing steps are required to handle wet gels and slurries after HTC, e.g., solvent exchange through intensive washing, and drying. These steps will be inspired by downstream processing of hydrochar and zeolite slurries adopted in pilot plants, but also by other cryo- and aerogel technologies such as Starbon(R), a spin out from the University of York's Green Chemistry Centre of Excellence [91]. Besides, efficient solid–liquid separation techniques are essential for recovering the HTC-produced carbon-based material. Filtration methods, such as membrane filtration or pressure filtration, may be employed depending on the desired particle size and purity.

### 4.3.2. *Economic viability: balancing costs and returns*

The economic viability of scaled-up HTC processes hinges on several key factors.

**Raw material supply: securing a steady stream.** Securing a consistent supply of suitable biomass feedstock at competitive prices is paramount. The scale-up strategy must consider feedstock availability, transportation costs, and potential seasonal variations in supply. Diversifying feedstock sources and establishing strong partnerships with biomass suppliers can mitigate supply chain risks.

**Operating costs: optimizing efficiency and minimizing expenses.** Energy consumption, particularly for heating and potential activation processes, significantly impacts operating costs. Implementing heat recovery systems, optimizing process parameters, and exploring alternative energy sources, such as biomass-derived fuels, can contribute to improved energy efficiency and reduced operational costs.

**Capital investment: weighing the initial outlay.** The initial capital investment required for HTC facilities is substantial. Careful financial planning, thorough market analysis, and a robust business plan are essential for assessing the return on investment.

Modular design approaches, where production capacity can be incrementally increased, offer flexibility in adapting to changing market demands and minimizing initial capital requirements.

### 4.3.3. *Overcoming challenges: ensuring sustainability and consistency*

**Product consistency: maintaining quality at scale.** Maintaining consistent product quality across large production volumes is a key challenge. Implementing robust quality control systems, standardized operating procedures, and rigorous testing protocols are essential for ensuring that the HTC-produced carbon-based materials meet the required specifications.

**Environmental impact: minimizing the footprint.** Managing process emissions and wastewater treatment at industrial scale requires careful consideration. The development of closed-loop systems for water recycling and emission control becomes increasingly important. Implementing strategies for capturing and utilizing process emissions, such as carbon dioxide sequestration or biogas production, can further enhance the environmental sustainability of HTC processes.

### 4.3.4. *Future prospects: innovation driving advancement*

The future of HTC scale-up lies in continuous innovation and technological advancements.

**Advanced process control: harnessing the power of data.** The integration of artificial intelligence and machine learning can enable more sophisticated

process control and optimization, leading to improved product consistency, reduced operating costs, and enhanced process efficiency.

**Sustainable processing: embracing circular economy principles.** Integrating renewable energy sources, such as solar or wind power, can reduce the carbon footprint of HTC processes. Implementing circular economy principles, such as utilizing the HTC-derived soluble byproduct as biofuels or platform molecules for biorefinery schemes, can further enhance the sustainability and economic viability of HTC.

### 4.3.5. *Conclusion: a promising path forward*

Scaling up HTC for porous carbon-based material production presents a complex yet promising opportunity for industrial development. Success requires a multifaceted approach, addressing technical, economic, and environmental considerations. By embracing innovation, sustainability, and a commitment to responsible development, HTC has the potential to become a key technology for producing high-quality carbon-based materials, contributing to a more sustainable and resource-efficient future [84,85]. CarboZym has already reached key milestones, producing several hundred grams of support materials per week at laboratory scale with a high degree of homogeneity and reproducibility.

## 5. Conclusion

This report highlights the transformative potential of CarboZym technology through three compelling case studies. CarboZym's carbon-based, biomass-derived carriers offer a unique advantage in biomanufacturing by minimizing reliance on petrochemicals and aligning with the industry's growing demand for low-carbon solutions.

The simple immobilization procedure, demonstrated with industrially relevant enzymes (CALB, *Gs*OYE, and ω-TA B9L0N2), proved quick and highly effective, achieving 95–100% immobilization within approximately two hours. This success underscores the versatility of CarboZym's applicability in green chemistry and sustainable biocatalysis. Each immobilized enzyme exhibited distinct catalytic enhancements, showcasing the platform's adaptability to diverse enzymatic systems.

Immobilized CALB demonstrated exceptional stability and reusability, maintaining industrially relevant conversion rates over multiple cycles with minimal enzyme leaching. *Gs*OYE exhibited excellent efficiency and stability in both batch and continuous flow systems, achieving excellent turnover numbers in continuous mode. Immobilized ω-TA B9L0N2 achieved significant cost reductions through repeated use, retaining nearly full activity.

By combining high catalytic performance, low leaching, enhanced reusability, and a sustainable footprint, CarboZym's immobilization platform addresses key challenges facing biomanufacturing.

The broader implications of this technology extend far beyond individual applications. As the biomanufacturing industry strives for greater sustainability and efficiency, CarboZym emerges as a crucial enabler of this transition. Successful scale-up and adoption of CarboZym-based systems can significantly reduce costs, accelerating the shift towards greener, more circular industrial practices.

In conclusion, the CarboZym technology represents a transformative approach to enzyme immobilization, poised to reshape the future of sustainable biomanufacturing. By seamlessly integrating high-performance catalysis, operational robustness, and environmental responsibility, CarboZym paves the way for a more economically and ecologically viable industrial biotechnology landscape, unlocking new avenues for innovation and growth.

### Declaration of interests

JD, NB and CM are declared inventors on patents WO2024153593A1, WO2024153594A1 used by CarboZym. JD, NB and QH are cofounders of the CarboZym SAS.

### Funding

### Supplementary data

Supporting information for this article is available on the journal's website under https://doi.org/10.5802/crchim.397 or from the author.

# References

[1] R. A. Sheldon, A. Basso and D. Brady, "New frontiers in enzyme immobilisation: robust biocatalysts for a circular bio-based economy", *Chem. Soc. Rev.* **50** (2021), no. 10, pp. 5850–5862.

[2] J. M. Nelson and E. G. Griffin, "Adsorption of invertase", *J. Am. Chem. Soc.* **38** (1916), no. 5, pp. 1109–1115.

[3] C.-H. Kuo, H.-M. David Wang and C.-J. Shieh, "Enzymes in biomedical, cosmetic and food application", *Catalysts* **14** (2024), no. 3, article no. 162.

[4] A. Madhu and J. N. Chakraborty, "Developments in application of enzymes for textile processing", *J. Clean. Prod.* **145** (2017), pp. 114–133.

[5] P. Kalita, B. Basumatary, P. Saikia, B. Das and S. Basumatary, "Biodiesel as renewable biofuel produced via enzyme-based catalyzed transesterification", *Energy Nexus* **6** (2022), article no. 100087.

[6] Y.-F. Fan, Z.-B. Guo and G.-B. Ge, "Enzyme-based biosensors and their applications", *Biosensors* **13** (2023), no. 4, article no. 476.

[7] P. Bajpai, "Application of enzymes in the pulp and paper industry", *Biotechnol. Prog.* **15** (1999), no. 2, pp. 147–157.

[8] M. A. Valliere, T. P. Korman, M. A. Arbing and J. U. Bowie, "A bio-inspired cell-free system for cannabinoid production from inexpensive inputs", *Nat. Chem. Biol.* **16** (2020), no. 12, pp. 1427–1433.

[9] R. A. Sheldon, D. Brady and M. L. Bode, "The Hitchhiker's guide to biocatalysis: recent advances in the use of enzymes in organic synthesis", *Chem. Sci.* **11** (2020), no. 10, pp. 2587–2605.

[10] *Enzymes market, global industry size forecast [latest], Markets and Markets*. Online at https : / / www . marketsandmarkets . com / Market - Reports / enzyme - market-46202020.html (accessed on November 21, 2024).

[11] R. A. Sheldon and S. van Pelt, "Enzyme immobilisation in biocatalysis: why, what and how", *Chem. Soc. Rev.* **42** (2013), no. 15, pp. 6223–6235.

[12] R. DiCosimo, J. McAuliffe, A. J. Poulose and G. Bohlmann, "Industrial use of immobilized enzymes", *Chem. Soc. Rev.* **42** (2013), no. 15, pp. 6437–6474.

[13] J. Guisan, F.-L. Gloria, J. Rocha Martín and M. Daniel, "Enzyme Immobilization Strategies for the design of robust and efficient biocatalysts", *Curr. Opin. Green Sustain. Chem.* **35** (2022), article no. 100593.

[14] J. Britton, S. Majumdar and G. A. Weiss, "Continuous flow biocatalysis", *Chem. Soc. Rev.* **47** (2018), no. 15, pp. 5891–5918.

[15] M. P. Thompson, I. Peñafiel, S. C. Cosgrove and N. J. Turner, "Biocatalysis using immobilized enzymes in continuous flow for the synthesis of fine chemicals", *Org. Process Res. Dev.* **23** (2019), no. 1, pp. 9–18.

[16] J. Zdarta, A. S. Meyer, T. Jesionowski and M. Pinelo, "A general overview of support materials for enzyme immobilization: characteristics, properties, practical utility", *Catalysts* **8** (2018), no. 2, article no. 92.

[17] K. Xu, X. Chen, R. Zheng and Y. Zheng, "Immobilization of multi-enzymes on support materials for efficient biocatalysis", *Front. Bioeng. Biotechnol.* **8** (2020), article no. 660.

[18] A. M. Girelli, M. L. Astolfi and F. R. Scuto, "Agro-industrial wastes as potential carriers for enzyme immobilization: a review", *Chemosphere* **244** (2020), article no. 125368.

[19] N. A. Mohidem, M. Mohamad, M. U. Rashid, M. N. Norizan, F. Hamzah and H. bin Mat, "Recent advances in enzyme immobilisation strategies: an overview of techniques and composite carriers", *J. Compos. Sci.* **7** (2023), no. 12, article no. 488.

[20] N. R. Mohamad, N. H. Che Marzuki, N. A. Buang, F. Huyop and R. A. Wahab, "An overview of technologies for immobilization of enzymes and surface analysis techniques for immobilized enzymes", *Biotechnol. Biotechnol. Equip.* **29** (2015), no. 2, pp. 205–220.

[21] C. Ortiz, M. L. Ferreira, O. Barbosa, C. S. dos Santos J, R. C. Rodrigues, Á. Berenguer-Murcia, L. E. Briand and R. Fernandez-Lafuente, "Novozym 435: the 'perfect' lipase immobilized biocatalyst?", *Catal. Sci. Technol.* **9** (2019), no. 10, pp. 2380–2420.

[22] Y. R. Maghraby, R. M. El-Shabasy, A. H. Ibrahim and H. M. El-Said Azzazy, "Enzyme immobilization technologies and industrial applications", *ACS Omega* **8** (2023), no. 6, pp. 5184–5196.

[23] J. Drone, N. Brun and C. Mateos, Nouveau materiau carbone poreux comprenant une proteine immobilisee, son procede de preparation et ses utilisations, WO patent, WO2024153594A1, 2024.

[24] J. Drone, N. Brun and C. Mateos, Nouveau matériau carboné poreux, son procédé de préparation et ses utilisations, WO patent, WO2024153593A1, 2024.

[25] N. Brun, C. A. García-González, I. Smirnova and M. M. Titirici, "Hydrothermal synthesis of highly porous carbon monoliths from carbohydrates and phloroglucinol", *RSC Adv.* **3** (2013), no. 38, article no. 17088.

[26] N. Brun, S. A. Wohlgemuth, P. Osiceanu and M. M. Titirici, "Original design of nitrogen-doped carbon aerogels from sustainable precursors: application as metal-free oxygen reduction catalysts", *Green Chem.* **15** (2013), no. 9, pp. 2514–2524.

[27] N. Job, A. Théry, R. Pirard, J. Marien, L. Kocon, J.-N. Rouzaud, F. Béguin and J.-P. Pirard, "Carbon aerogels, cryogels and xerogels: Influence of the drying method on the textural properties of porous carbon materials", *Carbon* **43** (2005), no. 12, pp. 2481–2494.

[28] K. E. Cassimjee, M. Kadow, Y. Wikmark, M. S. Humble, M. L. Rothstein, D. M. Rothstein and J. E. Bäckvall, "A general protein purification and immobilization method on controlled porosity glass: biocatalytic applications", *Chem. Commun.* **65** (2014), pp. 9134–9137.

[29] M. P. Thompson, S. R. Derrington, R. S. Heath, J. L. Porter, J. Mangas-Sanchez, P. N. Devine, M. D. Truppo and N. J. Turner, "A generic platform for the immobilisation of engineered biocatalysts", *Tetrahedron* **75** (2019), no. 3, pp. 327–334.

[30] N. J. Baxter, T. H. Lilley, E. Haslam and M. P. Williamson, "Multiple interactions between polyphenols and a salivary proline-rich protein repeat result in complexation and precipitation", *Biochemistry* **36** (1997), no. 18, pp. 5566–5577.

[31] C. Le Bourvellec and C. M. G. C. Renard, "Interactions between polyphenols and macromolecules: quantification

methods and mechanisms", *Crit. Rev. Food Sci. Nutr.* **52** (2012), no. 3, pp. 213–248.

[32] A. Watrelot and E. Norton, "Chemistry and reactivity of tannins in vitis spp.: a review", *Molecules* **25** (2020), article no. 2110.

[33] A. Szczurek, G. Amaral-Labat, V. Fierro, A. Pizzi, E. Masson and A. Celzard, "The use of tannin to prepare carbon gels. Part I: carbon aerogels", *Carbon* **8** (2011), no. 49, pp. 2773–2784.

[34] Y. Shirmohammadli, D. Efhamisisi and A. Pizzi, "Tannins as a sustainable raw material for green chemistry: A review", *Ind. Crops Prod.* **126** (2018), pp. 316–332.

[35] R. D. Schmid and R. Verger, "Lipases: interfacial enzymes with attractive applications", *Angew. Chem. Int. Ed.* **37** (1998), no. 12, pp. 1608–1633.

[36] P. Adlercreutz, "Immobilisation and application of lipases in organic media", *Chem. Soc. Rev.* **42** (2013), no. 15, pp. 6406–6436.

[37] S. Lutz, "Engineering lipase B from *Candida antarctica*", *Tetrahedron Asymmetry* **15** (2004), no. 18, pp. 2743–2748. Integrating Biocatalysis into Organic Syntheses.

[38] C. José, R. D. Bonetto, L. A. Gambaro, M. d. P. Guauque Torres, M. L. Foresti, M. Ferreira and L. E. Briand, "Investigation of the causes of deactivation–degradation of the commercial biocatalyst Novozym® 435 in ethanol and ethanol–aqueous media", *J. Mol. Catal. B: Enzymatic* **71** (2011), no. 3, pp. 95–107.

[39] J. C. Lec and Arkema, "Biocatalysis for commodity & speciality chemistry [Oral presentation]", in *Enzynov'2 - Enzymatic Biocatalysis For Industry, October 26–27, 2023*, Adebiotech: Paris-Romainville, 2023.

[40] M. S. Robescu, M. Niero, M. Hall, L. Cendron and E. Bergantino, "Two new ene-reductases from photosynthetic extremophiles enlarge the panel of old yellow enzymes: CtOYE and GsOYE", *Appl. Microbiol. Biotechnol.* **104** (2020), no. 5, pp. 2051–2066.

[41] R. Stuermer, B. Hauer, M. Hall and K. Faber, "Asymmetric bioreduction of activated C=C bonds using enoate reductases from the old yellow enzyme family", *Curr. Opin. Chem. Biol.* **11** (2007), no. 2, pp. 203–213.

[42] G. Brown, T. S. Moody, M. Smyth and S. J. C. Taylor, "Almac: An Industrial Perspective of Ene Reductase (ERED) Biocatalysis", in *Biocatalysis: An Industrial Perspective* (G. de Gonzalo and P. Domínguez de María, eds.), The Royal Society of Chemistry: Cambridge, 2017, pp. 229–256.

[43] I. Slabu, J. L. Galman, R. C. Lloyd and N. J. Turner, "Discovery, engineering, and synthetic application of transaminase biocatalysts", *ACS Catal.* **7** (2017), no. 12, pp. 8263–8284.

[44] J. Rudat, B. R. Brucher and C. Syldatk, "Transaminases for the synthesis of enantiopure beta-amino acids", *AMB Express* **2** (2012), no. 1, article no. 11.

[45] H. Brundiek and M. Höhne, "Transaminases: A biosynthetic route for chiral amines", in *Applied Biocatalysis: From Fundamental Science to Industrial Applications*, 1st edition (G. Antranikian, ed.), Wiley-VCH: Weinheim, 2016, pp. 199–218.

[46] L. Gourbeyre, *Nouvelles transaminases et procédés multienzymatiques innovants pour la synthèse hautement*

*sélective d'amines et d'aminoalcools chiraux*, 2021. Chimie organique. Université Clermont-Auvergne, NNT : 2021UC-FAC113. tel-03888041.

[47] S. A. Kelly, S. Pohle, S. Wharry, S. Mix, C. C. R. Allen, T. S. Moody and B. F. Gilmore, "Application of $\omega$-transaminases in the pharmaceutical industry", *Chem. Rev.* **118** (2018), no. 1, pp. 349–367.

[48] F. López-Gallego, E. Jackson and L. Betancor, "Heterogeneous systems biocatalysis: the path to the fabrication of self-sufficient artificial metabolic cells", *Chem.–A Eur. J.* **23** (2017), no. 71, pp. 17841–17849.

[49] J. Santiago-Arcos, S. Velasco-Lozano and F. López-Gallego, "Multienzyme coimmobilization on triheterofunctional supports", *Biomacromolecules* **24** (2023), no. 2, pp. 929–942.

[50] D. L. Schmitt and S. An, "Spatial organization of metabolic enzyme complexes in cells", *Biochemistry* **56** (2017), no. 25, pp. 3184–3196.

[51] S. Ren, C. Li, X. Jiao, S. Jia, Y. Jiang, M. Bilal and J. Cui, "Recent progress in multienzymes co-immobilization and multienzyme system applications", *Chem. Eng. J.* **373** (2019), pp. 1254–1278.

[52] R. Siedentop, C. Claaßen, D. Rother, S. Lütz and K. Rosenthal, "Getting the most out of enzyme cascades: strategies to optimize in vitro multi-enzymatic reactions", *Catalysts* **11** (2021), no. 10, article no. 1183.

[53] H.-J. Federsel, T. S. Moody and S. J. C. Taylor, "Recent trends in enzyme immobilization—concepts for expanding the biocatalysis toolbox", *Molecules* **26** (2021), no. 9, article no. 2822.

[54] H. T. Imam, P. C. Marr and A. C. Marr, "Enzyme entrapment, biocatalyst immobilization without covalent attachment", *Green Chem.* **23** (2021), no. 14, pp. 4980–5005.

[55] S. Arana-Peña, D. Carballares, R. Morellon-Sterlling, Á. Berenguer-Murcia, A. R. Alcántara, R. C. Rodrigues and R. Fernandez-Lafuente, "Enzyme co-immobilization: Always the biocatalyst designers' choice... or not?", *Biotechnol. Adv. New Trends Ind. Biocatal.* **51** (2021), article no. 107584.

[56] Q. Ji, B. Wang, J. Tan, L. Zhu and L. Li, "Immobilized multienzymatic systems for catalysis of cascade reactions", *Process Biochem.* **9** (2016), no. 51, pp. 1193–1203.

[57] G. Rossino, M. S. Robescu, E. Licastro, et al., "Biocatalysis: A smart and green tool for the preparation of chiral drugs", *Chirality* **34** (2022), no. 11, pp. 1403–1418.

[58] S. M. Andler and J. M. Goddard, "Transforming food waste: how immobilized enzymes can valorize waste streams into revenue streams", *NPJ Sci. Food* **2** (2018), no. 1, article no. 19.

[59] I. O. Costa, J. R. Fernandes Morais, J. M. de Medeiros Dantas, L. R. Barros Gonçalves, E. S. Dos Santos and N. S. Rios, "Enzyme immobilization technology as a tool to innovate in the production of biofuels: a special review of the cross-linked enzyme aggregates (CLEAs) strategy", *Enzyme Microb. Technol.* **170** (2023), article no. 110300.

[60] F. Shakerian, J. Zhao and S.-P. Li, "Recent development in the application of immobilized oxidative enzymes for bioremediation of hazardous micropollutants—a review", *Chemosphere* **239** (2020), article no. 124716.

[61] J. Bié, B. Sepodes, P. C. B. Fernandes and M. H. L. Ribeiro, "Enzyme immobilization and co-immobilization: main framework, advances and some applications", *Processes* **10** (2022), no. 3, article no. 494.

[62] J. M. Bolivar, J. M. Woodley and R. Fernandez-Lafuente, "Is enzyme immobilization a mature discipline? Some critical considerations to capitalize on the benefits of immobilization", *Chem. Soc. Rev.* **51** (2022), no. 15, pp. 6251–6290.

[63] T. P. Korman, P. H. Opgenorth and J. U. Bowie, "A synthetic biochemistry platform for cell free production of monoterpenes from glucose", *Nat. Commun.* **8** (2017), no. 1, article no. 15526.

[64] R. Reshmy, E. Philip, R. Sirohi, et al., "Nanobiocatalysts: advancements and applications in enzyme technology", *Bioresour. Technol.* **337** (2021), article no. 125491.

[65] E. Orsi, L. S. von Borzyskowski, S. Noack, P. I. Nikel and S. N. Lindner, "Automated in vivo enzyme engineering accelerates biocatalyst optimization", *Nat. Commun.* **15** (2024), no. 1, article no. 3447.

[66] S. M. Mirsalami, M. Mirsalami and A. Ghodousian, "Techniques for immobilizing enzymes to create durable and effective biocatalysts", *Results Chem.* **7** (2024), article no. 101486.

[67] J. M. Clomburg, S. Qian, Z. Tan, S. Cheong and R. Gonzalez, "The isoprenoid alcohol pathway, a synthetic route for isoprenoid biosynthesis", *Proc. Nat. Acad. Sci. USA* **116** (2019), no. 26, pp. 12810–12815.

[68] S. Lund, R. Hall and G. J. Williams, "An artificial pathway for isoprenoid biosynthesis decoupled from native hemiterpene metabolism", *ACS Synth. Biol.* **8** (2019), no. 2, pp. 232–238.

[69] J. Couillaud, J. Rico, A. Rubini, et al., "Simplified in vitro and in vivo bioaccess to prenylated compounds", *ACS Omega* **4** (2019), no. 4, pp. 7838–7849.

[70] L. A. Johnson, A. Dunbabin, J. C. R. Benton, R. J. Mart and R. K. Allemann, "Modular chemoenzymatic synthesis of terpenes and their analogues", *Angew. Chem. Int. Ed.* **59** (2020), no. 22, pp. 8486–8490.

[71] S. Mordhorst and J. N. Andexer, "Round, round we go— strategies for enzymatic cofactor regeneration", *Nat. Prod. Rep.* **37** (2020), no. 10, pp. 1316–1333.

[72] K. Bachosz, J. Zdarta, M. Bilal, A. S. Meyer and T. Jesionowski, "Enzymatic cofactor regeneration systems: A new perspective on efficiency assessment", *Sci. Total Environ.* **868** (2023), article no. 161630.

[73] D. H. Williamson, P. Lund and H. A. Krebs, "The redox state of free nicotinamide-adenine dinucleotide in the cytoplasm and mitochondria of rat liver", *Biochem. J.* **103** (1967), no. 2, pp. 514–527.

[74] R. Wohlgemuth, A. Liese and W. Streit, "Biocatalytic phosphorylations of metabolites: past, present, and future", *Trends Biotechnol.* **35** (2017), no. 5, pp. 452–465.

[75] A. Weckbecker, H. Gröger and W. Hummel, "Regeneration of nicotinamide coenzymes: principles and applications for the synthesis of chiral compounds", *Adv. Biochem. Eng./Biotechnol.* **120** (2010), pp. 195–242.

[76] Q. Chen, Y. Wang and G. Luo, "Recycling of cofactors in crude enzyme hydrogels as co-immobilized heterogeneous biocatalysts for continuous-flow asymmetric reduc-

tion of ketones", *ChemSusChem* **16** (2023), no. 3, article no. e202201654.

[77] L. F. Bugada, M. R. Smith and F. Wen, "Engineering spatially organized multienzyme assemblies for complex chemical transformation", *ACS Catal.* **8** (2018), no. 9, pp. 7898–7906.

[78] B. Reus, M. Damian and F. G. Mutti, "Advances in cofactor immobilization for enhanced continuous-flow biocatalysis", *J. Flow Chem.* **14** (2024), no. 1, pp. 219–238.

[79] Y. Zou and C. B. Bailey, "Cofactor recycling strategies for secondary metabolite production in cell-free protein expression systems", *Biophys. Rev.* **16** (2024), pp. 591–603.

[80] K. Shortall, S. Arshi, S. Bendl, X. Xiao, S. Belochapkine, D. Demurtas, T. Soulimane and E. Magner, "Coupled immobilized bi-enzymatic flow reactor employing cofactor regeneration of NAD+ using a thermophilic aldehyde dehydrogenase and lactate dehydrogenase", *Green Chem.* **25** (2023), no. 1, pp. 4553–4564.

[81] C. E. Paul and F. Hollmann, "A survey of synthetic nicotinamide cofactors in enzymatic processes", *Appl. Microbiol. Biotechnol.* **100** (2016), no. 11, pp. 4773–4778.

[82] W. Kang, S. Gao, J. Bao, L. Yang, Y. Ma, P. Wang, C.-Y. Wang and C. Cui, "Synthetic nicotinamide cofactors as alternatives to NADPH in imine reductase-catalyzed reactions", *Org. Lett.* **26** (2024), no. 37, pp. 7817–7821.

[83] S. G. Kothalawala, J. Jiao, R. Speight, H. Song, Y. Yang and J. Zhang, "Pore architecture influences the enzyme immobilization performance of mesoporous silica nanospheres", *Microporous Mesoporous Mater.* **338** (2022), article no. 111963.

[84] S. Yu, J. He, Z. Zhang, et al., "Towards negative emissions: hydrothermal carbonization of biomass for sustainable carbon materials", *Adv. Mater.* **36** (2024), no. 18, article no. 2307412.

[85] Z. Xu, J. Wang, Z. Guo, et al., "The role of hydrothermal carbonization in sustainable sodium-ion battery anodes", *Adv. Energy Mater.* **12** (2022), no. 18, article no. 2200208.

[86] M. Owsianiak, M. W. Ryberg, M. Renz, M. Hitzl and M. Z. Hauschild, "Environmental performance of hydrothermal carbonization of four wet biomass waste streams at industry-relevant scales", *ACS Sustain. Chem. Eng.* **4** (2016), no. 12, pp. 6783–6791.

[87] M. Bagheri and E. Wetterlund, "Introducing hydrothermal carbonization to sewage sludge treatment systems— a way of improving energy recovery and economic performance?", *Waste Manage.* **170** (2023), pp. 131–143.

[88] A. N. Parvulescu and S. Maurer, "Toward sustainability in zeolite manufacturing: An industry perspective", *Front. Chem.* **10** (2022), article no. 1050363.

[89] Q. Wu, Y. Ma, S. Wang, X. Meng and F.-S. Xiao, "110th anniversary: sustainable synthesis of zeolites: from fundamental research to industrial production", *Ind. Eng. Chem. Res.* **58** (2019), no. 27, pp. 11653–11658.

[90] F. Grimaldi, H. Ramirez, C. Lutz and P. Lettieri, "Intensified production of zeolite A: Life cycle assessment of a continuous flow pilot plant and comparison with a conventional batch plant", *J. Ind. Ecol.* **25** (2021), no. 6, pp. 1617–1630.

[91] Starbons®, *Making separations simple with cutting-edge products, Starbons*. Online at https://www.starbons.com/ (accessed on November 21, 2024).

ACADÉMIE
DES SCIENCES
INSTITUT DE FRANCE

Review article

# Enzyme-membrane reactors: recent trends and applications for the production of fine chemicals and pharmaceutical building blocks

**Hippolyte Meersseman Arango** [a]**, Patricia Luis** [®, b]**, Tom Leyssens** [®, a] **and Damien P. Debecker** [®, *, a]

[a] Institute of Condensed Matter and Nanosciences (IMCN), Université catholique de Louvain (UCLouvain), Place Louis Pasteur, 1, 1348 Louvain-la-Neuve, Belgium

[b] Materials & Process Engineering (iMMC-IMAP), Université catholique de Louvain, Place Sainte Barbe 2, 1348 Louvain-la-Neuve, Belgium

*E-mail:* damien.debecker@uclouvain.be (D. P. Debecker)

**Abstract.** Biocatalysis has gained attention in recent decades as a green and efficient method for producing high-value chemicals. Enzymes, notably due to their high selectivity, offer significant advantages for organic synthesis. However, industrial implementation remains limited owing to challenges such as free enzyme instability, enzyme inhibition, and difficulties in catalyst recovery and reuse. The coupling of biocatalysis with membrane technology in enzyme-membrane reactors (EMRs) holds significant potential for process intensification, as it paves the way for continuous-flow synthesis concatenated with product purification and biocatalyst recovery. By allowing flow hybrid processes (i.e., simultaneous biocatalytic reactions and membrane operations via one-pot methods), EMRs have the potential to increase reaction yields and kinetics and reduce downstream processing requirements. This review explores recent trends and advancements in EMRs for the production of pharmaceutical building blocks and fine chemicals. We examine the combination of enzymes with both polymeric and ceramic membranes, highlighting their respective benefits and limitations. We cover both EMR processes where free enzymes are used separately from membrane devices and EMR processes employing membrane-immobilized enzymatic reactors. As enzyme immobilization in/on solid supports has emerged as an effective approach for enhancing enzyme stability and reusability, we argue that the development of such membrane-immobilized enzyme reactors is of prime importance for the pharmaceutical industry. These insights aim to provide a comprehensive overview of the role and recent applications of EMRs in advancing biocatalytic processes within the fine chemical and pharmaceutical industries.

**Keywords.** Biocatalysis, Membranes, Membrane processes, Intensification, Enzyme immobilization, Pharmaceutical industry.

*Manuscript received 2 November 2024, accepted 20 December 2024.*

## 1. Introduction—membranes as a practical tool to intensify biocatalytic processes

Over the past decades, biocatalysis has emerged as a promising and potentially greener approach to produce value-added molecules [1]. Owing to their unique characteristics, such as their high (enantio)selectivity and stereospecificity, non-toxicity (biodegradable), and their ability to operate under mild conditions (e.g., aqueous media, low temperatures), enzymes have attracted significant interest in organic synthesis and the pharmaceutical industry [2]. Hence, biocatalytic processes have the

potential to rapidly become a powerful synthetic tool for the industrial preparation of valuable compounds, such as pharmaceuticals and fine chemicals [3–5].

However, despite the multiple benefits and advantages they offer, their implementation at the industrial level in the pharmaceutical industry is not straightforward and remains limited [6] due to several challenges. These are generally related to the fact that enzymes are often used in their "free" form, functioning as soluble homogeneous biocatalysts that are difficult to reuse, restricted to batch reactors, and which typically exhibit limited stability [7]. Additionally, enzymes tend to suffer from substrate and/or product inhibition, and—in some cases—unfavorable thermodynamic equilibria for the targeted reactions. The quality of the final product can also be compromised by free enzyme deactivation, resulting in complex purification processes [8].

Some of these challenges can be mitigated by immobilizing enzymes on solid supports [9,10], which allows for their recovery and reuse and facilitates their implementation in continuous-flow processes [11]. Moreover, immobilization often results in enhancing enzyme stability and tolerance to organic solvents [12,13]. The transfer from batch to continuous-flow processing is of major industrial interest as it increases the productivity of (bio)catalytic transformations and the efficiency of subsequent/coupled unit operations (e.g., crystallization), thus improving the overall process's economic viability [1,14–23]. Enzymatic processes arguably pave the way for the development of intensified industrially relevant organic synthesis [24]. Enzyme immobilization can be performed in various ways and on a wide range of functional materials such as polymeric resins, inorganic powders, biopolymers, and membranes [12,25,26]. Ready-to-use synthetic resins are traditional ubiquitous carriers, allowing to run biocatalytic reactions in heterogeneous catalysis mode and to easily recover and reuse biocatalysts.

Enzyme immobilization on membranes is a particular case that deserves attention, as it additionally offers the possibility of performing biocatalytic reactions along with membrane separation by a one-pot approach. For example, the removal of a product can favorably shift the biocatalytic reaction equilibrium toward product formation and hence increase the reaction yield. Moreover, membranes can be used to introduce one of the reagents at a controlled rate to avoid enzyme inhibition. The coupling of biocatalytic reaction with membrane operation in so-called "enzyme-membrane reactors" (EMRs) has the potential to intensify biocatalytic processes. Typically, membrane separations require only a limited amount of energy with respect to other unit operations [27–29]. Furthermore, membrane reactors display relatively easy reactor operation and modulation as well as straightforward scale-up to large systems [8,30–32]. Thus, integrated hybrid processes allowing to simultaneously perform flow biocatalytic reactions and product separation (e.g., to drive the equilibrium) or controlled substrate addition are of particular interest for the pharmaceutical industry, as they can help reduce the need for additional downstream steps typically required to obtain pure active pharmaceutical ingredients (APIs) [33–35].

It must be noted that the concatenation of reaction and membrane separation on catalytically active membranes is already well established, and this has been reviewed extensively. For example, Zhang et al. [36] reviewed the applications of a wide range of polymeric catalytic membranes to intensify chemical processes. Furthermore, conventional enzyme immobilization methods and strategies have already been extensively and thoroughly reviewed [8,37–41]. These reports focus on the detailed preparation and/or functionalization of various supports—including membranes—for enzyme immobilization. In addition, some excellent reviews [8,34,36,39,42–44] cover the benefits of implementing EMR in organic synthesis by collecting scholarly examples and/or providing useful insights into industrial process considerations. For example, the tutorial reviews by Sitanggang et al. [44] and Dejonghe et al. [34] summarized the advantages of coupling enzymes (free or immobilized) with membrane reactors and exemplified their use in a selection of chemical processes.

In this review, we aim to discuss the recent trends (2010 or later) of EMR processes applied specifically for the production of valuable (chiral) building blocks for the pharmaceutical industry. We cover both ceramic and polymeric membrane applications. Polymeric membranes are most commonly employed as support to develop biocatalytic membrane reactors, and they present an array of advantages with respect

to their ceramic counterparts. For example, polymeric membranes tend to be generally cheaper and offer a wider range of manufacturing techniques, which have been developed to enable better control and tailoring of final membrane properties [2,36]. Yet, their organic nature often hampers their chemical stability, which could be an issue when such membranes are put in contact with organic solvents, and hence limit their applicability in multiphasic membrane reactors [45]. On the other hand, ceramic membranes are able to overcome these drawbacks thanks to their inherent outstanding chemical and thermal stability [45,46]; hence we consider it also important to cover their applications.

Overall, one of the key advantages of coupling biocatalysis with membrane technology is the ability to run biocatalytic reactions while simultaneously performing product/substrate separation from the enzymes and from the reaction medium. Furthermore, this allows operating the synthesis process in continuous-flow mode, which can enhance productivity and economic feasibility. Using multiple membranes in series with different molecular weight cutoffs (MWCOs) can also enhance product selectivity, and the final step of membrane separation allows the concentration of the non-permeable product. The selected membrane material must be stable under the conditions (temperature, pH, presence of organic solvent) that optimize the enzyme's catalytic activity. When being coupled with membrane reactors, enzymes can be used either separately from the membrane devices or as membrane-immobilized enzymatic reactors. This defines the two categories of hybrid processes that are discussed in this review. The coupling of enzymes with membrane reactors is exemplified in Section 2 while the use of membrane-immobilized enzymatic reactors is reviewed in detail in Section 3.

## 2. Main synthetic routes that can benefit from the synergistic use of enzymes and membranes

Chiral compounds are the most important building blocks in the chemical and pharmaceutical industry, as they are widely employed for the production of fine chemicals and drugs [47,48]. Moreover, it is increasingly important to synthesize enantiopure drugs for the pharmaceutical industry [49,50].

More precisely, enantiopure alcohols [51] and amines [1,3,52] are key examples of prime importance not only in the synthesis of pharmaceuticals but also in the flavor and fragrance industry. Small peptides and short oligosaccharides are other categories of functional molecules that can be accessed via biocatalytic synthesis processes.

The use of transaminases (Figure 1a) and alcohol dehydrogenases (Figure 1b) is a conventional biocatalytic strategy to produce chiral amines and alcohol, respectively [53–55]. Most industrially relevant transaminations suffer from unfavorable thermodynamics, and transaminases tend to be inhibited by their keto substrate (amino acceptor) and by-products. To achieve high transamination yields while avoiding transaminase inhibition, in situ (co)-product removal and/or controlled substrate addition can be performed using membrane technologies [56–58]. One possible strategy is the use of pervaporation to remove acetone (the most common co-product of transamination reactions). Pervaporation is especially attractive for temperature-sensitive processes because it can be operated at moderate temperatures. Dejonghe et al. [58] implemented hydrophobic pervaporation at the outlet of a transamination reactor (employing free enzymes) in order to remove the acetone by-product from the biocatalytic system. A polydimethylsiloxane (PDMS) membrane module was used as the pervaporation unit. Such transamination coupling with pervaporation resulted in a 13% increase in product yield after 9 h of reaction compared to the standard transamination process (where no pervaporation was performed). However, it was also observed that the effect of acetone removal by pervaporation is minimal at low acetone concentrations (in the biocatalytic system). This highlights the need to work at high substrate concentrations and possibly to couple pervaporation with another product separation technique (which would allow to primarily push transamination toward high product yields). The other product separation technique should target the amine product, and it may be also performed via membrane technology (e.g., via membrane extraction). Notably, Dejonghe et al. [59] conducted the flow asymmetric synthesis of 1-methyl-3-phenylpropylamine from benzyl acetone using free ATA-v2 mutant enzyme in organic solvent (n-heptane), and employed the polypropylene (PP) membrane contactor for in situ

amine product removal. An acidic aqueous solution (pH = 3) was used to efficiently extract the amine product via membrane-assisted extraction. In this study, the use of an organic solvent as the reaction medium was found beneficial in the sense that it allowed increasing the optimal keto-substrate concentration (by 2.5-fold with respect to its aqueous solubility) without triggering inhibition. This approach resulted in a significant increase in terms of the final product yield (99% yield) with respect to the standard transamination process (69% yield when run without membrane-assisted extraction). Additionally, by demonstrating the intensified asymmetric synthesis of the R-sitagliptin drug, Yang et al. [60] successfully expanded the applicability of such synergistic coupling between transamination and membrane-assisted product separation. In this case, transamination was conducted in aqueous medium (pH = 9) and PDMS was used as the membrane contactor for solvent extraction. In all these examples, the use of membrane operations offers avenues to intensify the synthesis process.

Other (chiral) molecules such as carboxylic acids or esters can lead to the formation of valuable compounds, including chiral intermediates [32,61–63]. To this end, lipases have gained much attention lately as they allow for the enantioselective hydrolysis/esterification (Figure 1c) and transesterification (Figure 1d) of poorly water-soluble compounds (i.e., in biphasic media or in organic solvents) [64,65]. Enzymatic esterification reactions are commonly conducted in non-aqueous solvents, as water accumulation in the reaction medium can promote side reactions (e.g., hydrolysis) and hamper final esterification yields [66,67]. Additionally, for an enzymatic process, it is well known that excess water should be avoided to preserve high lipase activity [68,69]. In lipase-catalyzed esterification, for example, the water by-product can be removed in situ from the reactor using membrane technologies. Pervaporation seems particularly suited for such purpose since it requires significantly lower energy consumption and operating costs with respect to distillation processes [70]. Notably, the pervaporation-aided enzymatic production of monoacylglycerols from lauric and caprylic acids with glycerol in solvent-free medium was demonstrated by Satyawali et al. [71] in 2021. Lipases immobilized on polymeric resins in a packed-bed reactor (3 kg scale) operating in recirculation mode

were coupled with two zeolite membranes (in series, 56.5 cm$^2$ total area) for pervaporation. Such a coupled esterification–pervaporation process not only allowed pushing the fatty acid conversion toward completion (>95% after 256 h) but also enabled increasing the relative monoacylglycerol content in the final product (with respect to di- and triacylglycerols). Such studies demonstrate the practical applicability of zeolite-based membranes to in situ water removal through hydrophilic pervaporation.

Various functional oligosaccharides, such as lactulose, galacto-oligosaccharides (GOSs) [72], cyclodextrins [73], and oligodextran (5–8 kDa) [74,75], are known to have potential applications in the fine chemical and pharmaceutical industries. β-galactosidase can catalyze the direct formation of GOS (Figure 1e) and lactulose from lactose via transgalactosylation reactions [72,76,77]. Lactose (a disaccharide composed of glucose and galactose) is generated in high content in the dairy by-product of many (bio)chemical processes [78], and it acts as renewable feedstock to produce such building blocks. Cyclodextrin glycosyltransferase and dextranase catalyze the conversion of starch into mixtures of (cyclo)dextrins and the hydrolysis of dextran into oligodextrans of various molecular weights, respectively. A severe limitation in transgalactosylation reactions is that the targeted products tend to spontaneously undergo undesired consecutive reactions (i.e., hydrolysis reactions to monosaccharides glucose and galactose) [79]. Besides, it has been observed that such monosaccharide formation inhibits β-galactosidase (i.e., inhibition of transgalactosylation reaction) [34], which further highlights the need of product separation in these processes. Finally, the selection of producing oligodextran of tailored molecular weight is also a complicated task. Hence, it clearly appears that in all these biocatalytic reactions, coupling with membrane technology is of particular interest since it would enable enhancing the selectivity of the process and the purity of the targeted product (i.e., desired molecular weight) by means of adequate size-exclusion membrane operations.

Peptides are another class of target compounds exhibiting biological activities (e.g., antihypertensive, antioxidative), which find nutritional, cosmetic, and pharmaceutical applications [34,80]. Peptidases catalyze their production through protein hydrolysis
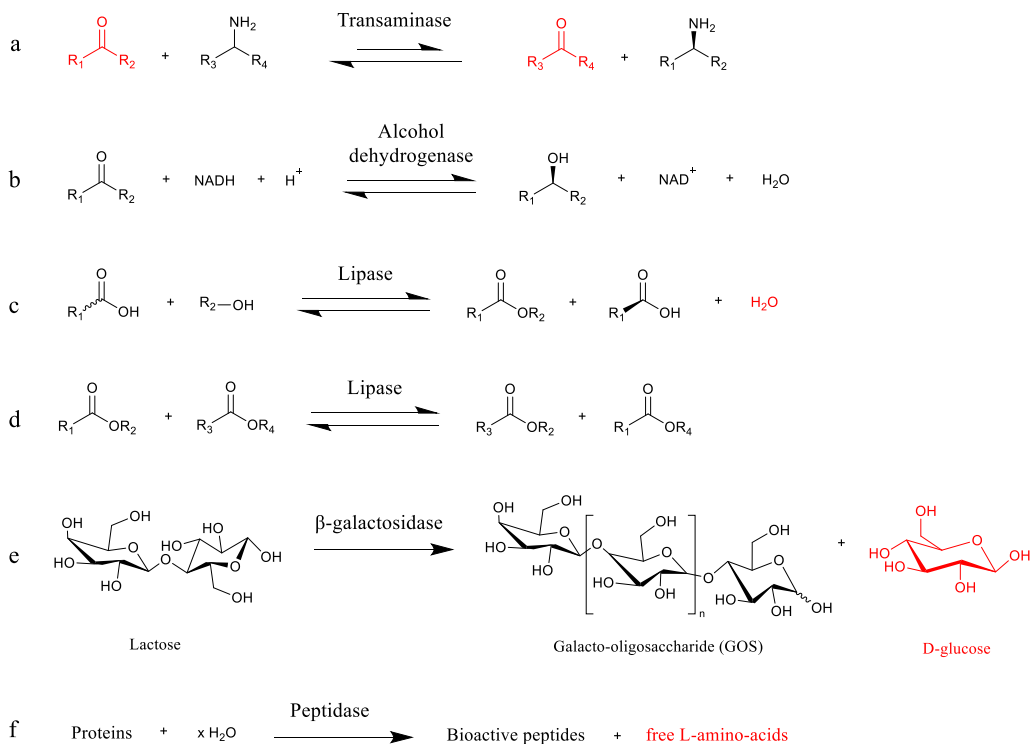
**Figure 1.** Main enzymatic transformations leading to pharmaceuticals and fine chemicals, and susceptible to be coupled with membrane reactors, studied in this work. Products highlighted in red are responsible for enzyme inhibition.

(Figure 1f). However, it is established that the efficiency of peptidases decreases upon accumulation of hydrolysis products (soluble peptides and amino acids) in the medium [34,81]. Here, conducting protein hydrolysis in continuous membrane reactors (through size-exclusion membrane operations) enables the separation of low-molecular-weight peptides from protein hydrolysates, thereby overcoming the drawbacks of batch reactions, such as product inhibition, low process productivity, and excessive hydrolyses (i.e., prevention of side reactions) [34]. Additionally, the continuous feeding of substrates (e.g., water in this case) to the reactor is advantageous as it allows improving the reaction kinetics and maintaining a constant volume in the reactor by compensating for the permeate flux. Such a beneficial substrate addition was demonstrated by Ma et al. [82], who conducted membrane-assisted enzymatic protein hydrolysis for the tailored production of antihypertensive peptides. First, the membrane ultrafiltration (UF) unit was implemented at the outlet

of the reactor tank, which allowed recycling free enzymes (retained in the retentate) and preventing undesired product inhibition (via product separation). When further coupling the enzymatic hydrolysis (performed in recirculating mode) with continuous feeding of water to the reactor, the yield and productivity were respectively enhanced by 62.7% and 22.1% when compared to the standard batch operation (i.e., run without membrane separation and substrate feeding). The continuous addition of the protein substrate (in addition to water feeding) enabled a further boost to peptide productivity.

As mentioned above in the reported examples, when working with free enzymes in solution, size-exclusion membrane operations are often chosen to separate the soluble biocatalyst [42] (retained in the retentate in cross-flow operations; see Figure 2) while isolating the product in the permeate [44]. In such size-exclusion operations, the membrane porosity—which defines its MWCO (in kDa)—has to be carefully chosen based on the molecular size of the enzyme

(if present in free form), substrate(s), and product(s). Given that enzyme molecular weights typically range from 10 to 150 kDa, UF membranes are commonly used in membrane reactor designs. The UF membrane pore size must ensure complete enzyme retention while ensuring unobstructed product transport. Nanofiltration (NF) membranes can also be employed in size-exclusion membrane operation design, especially for biocatalysts displaying small molecular weights (typically 0.2–10 kDa, such as, for example, some cysteine proteases [83]) [84,85]. Additionally, NF membranes are effective in concentrating target compounds as the secondary separation step [86]. As product purification is known to be a major driver of drug manufacturing cost, this is a crucial point.

Further than facilitating product separation, membrane-based operations are particularly helpful in displacing thermodynamic equilibrium and improving synthesis yields. Table 1 presents a list of membrane-induced equilibrium-shifting strategies that have already been applied in combination with soluble (or immobilized) enzymes in order to intensify biocatalyzed reactions (among the selected biocatalytic transformations listed in Figure 1). Here, soluble enzymes were typically employed separately from the membrane devices (i.e., membranes were at the boundary or at the effluent side of enzymatic reactors, acting as separation units) as represented in Figure 2 and not in a one-pot manner. Note that other membrane-intensified transaminations employing heterogeneous biocatalysts were also reported [56,57,87,88], yet these studies fall outside the scope of such reports as they involve whole cells (instead of enzymes) as biocatalysts. This list of examples shows the diversity of approaches and applications. We argue that the incorporation of enzyme into/onto membranes represents the next important step in the direction of intensification; as it is both more challenging and emerging, we discuss this in more detail in the following section.

## 3. Membrane-immobilized enzymatic reactors

The incentives for immobilizing enzymes to intensify biocatalytic processes are evident. Enzyme immobilization is a prerequisite to envisaging recovery and reuse. Immobilization usually tends to enhance enzyme stability and tolerance to organic solvents and to allow for the use of different reactor configurations [44], which are key features of industrial processes. It also paves the way for the integration of enzymes within heterogeneous catalysts, forming so-called hybrid chemoenzymatic catalysts that are excellent candidates to run intensified cascade reactions [114–119]. A potential downside of enzyme immobilization is that enzymatic activity may—in some cases—be decreased through the immobilization process (due to active site blockage, for example). Nevertheless, free enzymes can also experience activity reduction over time due to heat and mechanical stresses during extended biocatalytic processes [120].

Immobilization on membranes is going one step further in the direction of process intensification, as it implies fixing the enzyme on a material that is itself functional in the sense that it is able to perform tailored compound separation. As mentioned in the previous section, the membrane can be used to remove products during reaction, to inject reagents in a controlled way, and so on. In some cases, the membrane itself can also be chemocatalytically active. However, prior to enzyme immobilization on a membrane, the membrane surface often needs to be functionalized or chemically modified. Indeed, appropriate membrane materials that are directly amenable to enzyme immobilization are very rare [8]. A plethora of different surface functionalization techniques (e.g., wet chemical modification, plasma or UV exposure) have been reported in the literature [8,39,121,122], showing a variety of approaches depending on the substrate chemical nature. The implementation of such surface modifications depends on the type of enzyme immobilization (e.g., covalent grafting, electrostatic-assisted adsorption, site-specific immobilization through coordination) that is envisaged as well as the membrane operation that is targeted in the intensified biocatalytic process. Among the different existing strategies, silanization of inorganic membrane surface using (3-aminopropyl)triethoxysilane (APTES) and polydopamine (PDA) coating deposition on polymeric membranes have been employed in recent years [15,17,123–126] to confer amino groups at their surfaces, serving as anchoring points for grafting. In these cases, glutaraldehyde (GA) is most conventionally used as a coupling agent between

**Table 1.** Exhaustive list of recent (2010–2024) examples of enzyme combination with membrane technologies for the considered biocatalytic process intensification

| Reaction(s) | Substrate | Product | Enzyme | Immob. (carrier) | Membrane | Operation | Mode | Refs |
|---|---|---|---|---|---|---|---|---|
| Carboligation | Benzaldehyde + acetaldehyde | (S)-2-hydroxypropiophenone | Benzoylformate decarboxylase | /(free) | Polymeric (N.D., 10 kDa) | UF (dead end) | Flow | [89] |
| Cascade (De)hydrogenation | Octanone + D-glucose | R-octanol + D-gluconolactone | Alcohol dehydrogenase + glucose dehydrogenase | /(free) | N.D. (10 kDa) | UF (dead end) | Flow | [90] |
| Esterification | Fatty acids + glycerol | Monoacylglycerols | Lipase | Immob. (acrylic resin) | Ceramic (zeolite type T, N.D.) | Pervaporation | Recirculation | [71] |
| Esterification | Fatty acids + glycerol | Isopropyl esters | Lipase | Immob. (acrylic resin) | Ceramic (zeolite type T, N.D.) and polymeric (PVA, N.D) | Pervaporation | Recirculation | [91] |
| O-glycosylation | Resveratrol | Resveratrol O-glycosides | β-cyclodextrin–resveratrol | /(free) | Polymeric (N.D., 0.9 or 1.4 kDa) | NF | Recirculation | [92] |
| Transgalactosylation | Lactose | GOS | β-galactosidase | /(free) | Polymeric (cellulose, 50 kDa) | UF + NF | Flow | [93] |
| Transgalactosylation | Lactose | GOS | β-galactosidase | /(free) | Polymeric (PES, 10 kDa) | UF | Recirculation | [94] |
| Transgalactosylation | Lactose | GOS | β-galactosidase | /(free) | Ceramic (TiO$_2$, 20 kDa) | UF | Flow | [95] |
| Transgalactosylation | Lactose | GOS | β-galactosidase | /(free) | Ceramic (50 kDa) | UF | Recirculation | [96] |
| Transgalactosylation | Lactose | GOS | β-galactosidase | /(free) | Polymeric (cellulose acetate, N.D.) | UF | Recirculation | [97] |
| Transgalactosylation | Lactose | GOS | β-galactosidase | /(free) | Polymeric (PES, 10 kDa) | UF | Recirculation | [98] |
| Transgalactosylation | Lactose + fructose | Lactulose | β-galactosidase | /(free) | Polymeric (PES, PS, cellulose acetate, fluoropolymers; 10 kDa) | UF (dead end) | Flow | [99–101] |
| Hydrolysis | Phenylethanol + vinyl butyrate | Phenylethyl butyrate + acetaldehyde | Lipase (in water–oil emulsions) | /(free) | Polymeric (PES, 10 kDa) | UF (dead end) | Flow | [102] |
| Hydrolysis | Starches | Cyclodextrin | Cyclodextrin glycosyltransferase | /(free) | Polymeric (cellulose, 10 kDa) | UF | Flow | [103,104] |

**Table 1.** (continued)

| Reaction(s) | Substrate | Product | Enzyme | Immob. (carrier) | Membrane | Operation | Mode | Refs |
|---|---|---|---|---|---|---|---|---|
| Hydrolysis | BSA | Bioactive peptides | Peptidase | /(free) | Polymeric (PES, 3 or 10 kDa) or ceramic ($ZrO_2$/$TiO_2$, 15 kDa) | UF | Recirculation | [105] |
| Hydrolysis | *P. yezoensis* protein | Bioactive peptides | Peptidase | /(free) | N.D. (3 kDa) | UF | Flow | [82] |
| Hydrolysis | Egg white protein | Bioactive peptides | Peptidase | /(free) | Polymeric (PES, 10 kDa) | UF | Flow | [106] |
| Hydrolysis | Casein | Bioactive peptides | Peptidase | /(free) | Polymeric (PES, 1–10 kDa) | UF | Recirculation | [107] |
| Hydrolysis | Corn gluten meal | Bioactive peptides | Peptidase | /(free) | Polymeric (cellulose, 1–5 kDa) | UF | Flow | [108] |
| Hydrolysis | Casein | Bioactive peptides | Peptidase | /(free) | Polymeric (PES, 10 kDa) and ceramic ($Al_2O_3$, 10 kDa) | UF | Flow | [109] |
| Hydrolysis | Wheat gluten | Protein hydrolysate | Peptidase | /(free) | Ceramic (hollow fibers $Al_2O_3$, 5 or 10 kDa) | UF | Flow | [110] |
| Hydrolysis | Sesame seeds | Bioactive peptides | Peptidase | /(free) | Polymeric (PES, 5 kDa) | UF | Flow | [111] |
| Hydrolysis | Milk | Bioactive peptides | Peptidase | /(free) | Polymeric (cellulose, 5 kDa) | UF | Flow | [112] |
| Hydrolysis | Whey | Inhibitory peptides | Peptidase | /(free) | Polymeric (PES, 3 kDa) | UF | Flow | [113] |
| Transamination | Pro-sitagliptin ketone + isopropylamine | R-Sitagliptin + acetone | Transaminase | /(free) | Polymeric (PSF, 10 kDa ) + dense PDMS | UF (for enzyme retention) + solvent extraction | Recirculation | [60] |
| Transamination | Benzyl acetone + isopropylamine | R-1-methyl-3-phenylpropylamine + acetone | Transaminase | /(free) | Polymeric (PP, N.D.) | Solvent extraction | Recirculation | [59] |
| Transamination | Acetophenone + isopropylamine | R-MBA + acetone | Transaminase | /(free) | Dense PDMS | Pervaporation | Batch | [58] |

N.D.—non-specified; PES—polyethersulfone; PS—polystyrene; PSF—polysulfone; BSA—bovine serum albumin; MBA—methylbenzylamine; PDMS—polydimethylsiloxane; UF—ultrafiltration; NF—nanofiltration; GOS—galacto-oligosaccharide.
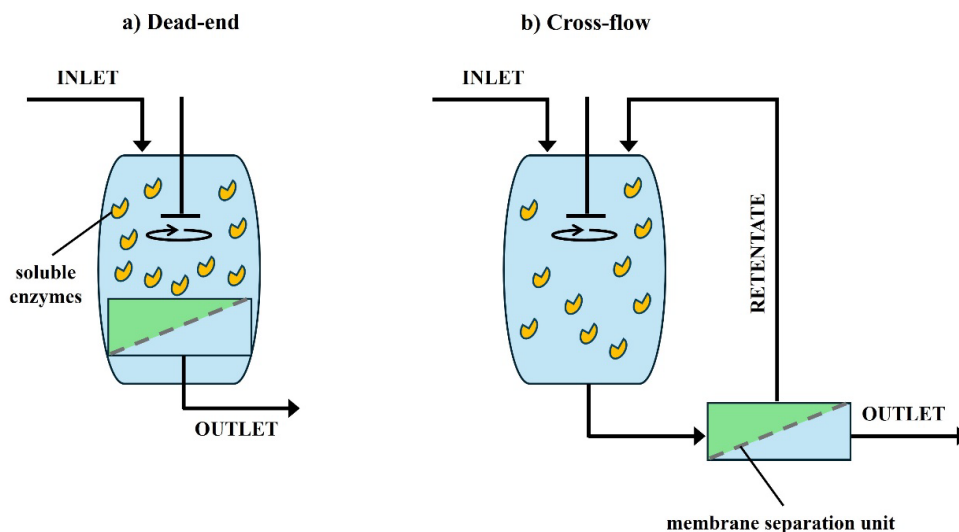
**Figure 2.** Schematic representation of biocatalytic processes involving free enzymes in combination with membrane separation units. In case (b), enzymes are recycled (retained) in the retentate through membrane separation. Reproduced from Sitanggang et al. [44] with permission.

the enzyme and the functionalized membrane. Another general trend is to try and stabilize the immobilized enzymes via electrostatic interactions; polyelectrolytes such as polyethyleneimine (PEI) are often employed with this aim.

Table 2 presents an exhaustive list of examples of membrane-immobilized enzymes exploited for the production of fine chemicals and pharmaceuticals from among the selected biocatalytic transformations listed in Figure 1. Enzymes are immobilized either in the membrane (i.e., entrapped in the membrane pores) or onto the membrane surface. In these examples, the membrane can either be employed as a mere solid support (i.e., not exploited to perform membrane operations) or as a functional support forming an EMR that acts as a combined reaction–separation unit (Figure 3).

Among the (recirculating) flow operations listed in Table 2, the dynamic kinetic resolution of ibuprofen ester is a prominent example of how the use of a lipase-membrane reactor can intensify a chemoenzymatic process and push such technology to the next level (Figure 4) [127,128]. In this example, a lipase was entrapped in the porosity of a polyacrylonitrile (PAN) membrane contactor. Such an EMR allowed simultaneously performing the continuous ibuprofen ester hydrolysis and

the resulting S-ibuprofen product separation (i.e., membrane-assisted extraction toward an aqueous phase). The unreacted R-ibuprofen ester was then recirculated into a chemocatalytic racemization unit (Amberlyst OH$^-$ coated resin) [127,128]. The resin is an excellent racemization catalyst due to its strong basicity and to its macroreticular network, which provides a high surface-to-volume ratio. Its large pores allow bulky molecules, such as (R)-ibuprofen ester, to diffuse effectively. This feature combined with its strong basic properties enables the rapid racemization of the ester through the ketol–enol tautomerism mechanism [158]. The racemized ibuprofen ester substrate is then recirculated to the organic tank and fed again to the enzyme-membrane module. Compartmentalization of the heterogeneous bio- and chemocatalysts allows protecting the lipase from the basic catalyst and from inhibition that would otherwise happen under the effect of unreacted substrate and by-product (2-ethoxyethanol, which is absorbed by the OH$^-$ resin).

Interestingly, the same kind of approach (membrane-assisted extraction) allowed achieving high product purity in the synthesis of oleuropein aglycone (an important antioxidant) through enzymatic hydrolysis in an EMR. To this end, β-glucosidase was covalently immobilized onto

**Table 2.** Exhaustive list of recent (2010–2024) examples of membrane-immobilized enzymes acting as simple heterogeneous membrane-immobilized biocatalysts (i.e., not performing membrane operations, operating in batch or in flow mode with or without recirculation) or as enzyme-membrane reactors (i.e., a reaction–separation unit) for the production of fine chemicals and pharmaceutical building blocks

| Reaction(s) | Substrate | Product | Enzyme(s) | Immob. (R. Sp. act) | Comments | Membrane | Separation | Mode | Refs |
|---|---|---|---|---|---|---|---|---|---|
| DKR | Ibuprofen ester | S-ibuprofen acid | Lipase | Entrapment (90%) | Retained 53% of initial sp. activity after 120 h of operation | Polymeric (PAN, 50 kDa) | Solvent extraction (interfacial; OP = isooctane) | Recirc. | [127,128] |
| Esterification (lipophilization) | Hesperidin + lauric acid | Hesperidin laurate | Lipase | Covalent grafting + cross-linking (≈900%) | / | Polymeric (PDA + GA-modified PES, 30 kDa) | / | Batch | [129] |
| Esterification | Stearic acid + lauryl alcohol | Lauryl stearate | Lipase | CLEAs + entrapment (142%) | / | Polymeric (CLEAs in PVA matrix, on PVA/PES dense layer) | Pervaporation | Recirc. | [68] |
| Esterification | Ethanol + lactic acid | Ethyl lactate | Lipase | Entrapment (≈100%) | Preserved 90% of sp. activity upon 6 cycles (36 h of operation) | Polymeric (sodium alginate network) | Pervaporation | Recirc. | [130] |
| Esterification | Valeric acid + ethanol | Ethyl valerate | Lipase | Covalent grafting (76%) | / | Polymeric (PPC, 150 kDa) | / | Batch | [131] |
| Transesterification | Rac-phenylethanol | S-phenylethanol + R-phenylacetate | Lipase | Covalent grafting (/) | / | Ceramic (ZrO$_2$, 300 kDa) | / | Recirc. | [132] |
| Transgalactosylation | Lactose | GOS | β-galactosidase | Covalent grafting (≈75%) | Retained 50% of its initial sp. activity after 30 days of storage | Polymeric (GA-modified PVDF) | Filtration | Recirc. | [133,134] |
| Transgalactosylation | Lactose | GOS | β-galactosidase | Covalent grafting + cross-linking (/) | / | Polymeric (PES, 5–50 kDa) and NF (0.4 kDa) | UF or NF | Flow | [135,136] |

164

**Table 2.** (continued)

| Reaction(s) | Substrate | Product | Enzyme(s) | Immob. (R. Sp. act) | Comments | Membrane | Separation | Mode | Refs |
|---|---|---|---|---|---|---|---|---|---|
| Transgalactosylation | Lactose | GOS | β-galactosidase | Covalent grafting (104%) | Maintained 54% of its initial sp. activity after 20 cycles | Polymeric (GO + APTES-modified electrospun PS nanofibers) | / | Batch | [137] |
| Transgalactosylation | Lactose | GOS | β-galactosidase | Adsorption (95%) | / | Mixed matrix (PSF + ZrO$_2$, 13.8 kDa) | / | Batch | [138] |
| Transgalactosylation | Lactose | GOS | β-galactosidase | Covalent grafting (/) | Maintained 91% of its sp. activity after 16 h of operation | Magnetic-responsive on polymeric membrane (PES, UF 50 kDa) | UF | Flow | [139] |
| Transgalactosylation | Lactose | GOS | β-galactosidase | Covalent grafting + cross-linking (140%) | / | Polymeric (PEI + GA-modified PSF, 10 kDa) | UF | Recirc. | [140] |
| Hydrolysis | Oleuropein | Oleuropein aglycone | β-glucosidase | Entrapment (≈100%) | Activity was unchanged after 30 h of continuous operation | Polymeric (PSF and cellulose, 30 kDa) | Solvent extraction of product (OP = limonene) | Flow | [141–144] |
| Hydrolysis | Oleuropein | Oleuropein aglycone | β-glucosidase | Covalent grafting (≈100%) | / | Ceramic (APTES + GA-modified Al$_2$O$_3$ capillary, 30 kDa) | Solvent extraction of product (OP = ethyl acetate) | Flow | [45] |
| Hydrolysis | Dextran | Oligodextran | Dextranase | Covalent grafting (/) | / | Polymeric (tannic Acid + APTES-modified PES (30 kDa) or cellulose (10 kDa)) | UF | Flow | [145] |
| Hydrolysis | Dextran | Oligodextran | Dextranase | Adsorption (/) | / | Polymeric (PES, 20 or 30 kDa) | UF | Flow | [75] |

**Table 2.** (continued)

| Reaction(s) | Substrate | Product | Enzyme(s) | Immob. (R. Sp. act) | Comments | Membrane | Separation | Mode | Refs |
|---|---|---|---|---|---|---|---|---|---|
| Hydrolysis | Wheat gluten | Protein hydrolysate | Peptidase | Entrapment (/) | / | Polymeric (UF) (PES, 10 kDa) | Filtration (dead end) | Flow | [146] |
| Hydrolysis | BSA | Bioactive peptides | Peptidase | Electrostatic interactions | / | Polymeric (PDA + PEI-modified PES, 50 kDa) | UF | Flow | [147] |
| Hydrolysis | BSA | Bioactive peptides | Peptidase | Covalent grafting (/) | 50% initial sp. activity retained after 6 cycles of 1 h | Polymeric (EDC/NHS-modified PVDF, nylon 6,6, chitosan composite) | / | Batch | [148] |
| Hydrolysis | Whey protein | Bioactive peptides | Peptidase | Electrostatic interactions (80%) | / | Polymeric (PDA + PEI-modified PES, 30 kDa) | / | Batch | [149] |
| Oligomerization | Rutin | Oligorutin | Laccase | Entrapment (/) | 90% of initial sp. activity after 3 cycles of 24 h | N.D. (10 kDa) | Filtration (dead end) of product | Batch | [150] |
| Oxidation | Tyrosine | L-DOPA | Tyrosinase | Entrapment (183%) | Unaltered initial sp. activity for 30 h of continuous operation | Polymeric (polyamide, 20 kDa) | UF | Flow | [151] |
| Oxidation | Tyrosine | L-DOPA | Tyrosinase | Covalent grafting (276%) | / | Ceramic (GA-modified NaY zeolite) | / | Recirc. | [152] |
| Oxidation | Tyrosine | L-DOPA | Tyrosinase | Covalent grafting (87%) | Unaltered initial sp. activity after 5 catalytic cycles ($\approx$24 h operation) | Polymeric (DAB + GA-modified PVDF) | / | Batch | [153] |
| Transamination (deamination) | S-MBA + pyruvate | Acetophenone + L-alanine | Transaminase | Coordination (His-tag) (23%) | Retained productivity after 5 days of continuous operation was 81% | Polymeric blend (Cu-functionalized fibers) | / | Flow | [154] |

Hippolyte Meersseman Arango *et al.*

**Table 2.** (continued)

| Reaction(s) | Substrate | Product | Enzyme(s) | Immob. (R. Sp. act) | Comments | Membrane | Separation | Mode | Refs |
|---|---|---|---|---|---|---|---|---|---|
| Transamination (deamination) | S-MBA + pyruvate | Acetophenone + L-alanine | Transaminase | Covalent grafting + His-tag driving (43.6%) | / | Polymeric blend (Co-derivatized PCADE/PVDF) | / | Batch | [155] |
| Cascade (transamination + (de)hydrogenation) | Cinnamaldehyde | Cinnamylamine | Transaminase + alanine dehydrogenase + formate dehydrogenase | EPC entrapment | / | N.D. (12 kDa dialysis membrane) | / | Batch | [156] |
| Transamination (kinetic resolution) | Rac-BMBA + pyruvate | S-BMBA + BAP + D-alanine | Transaminase | Covalent grafting (85%) | Unaltered initial sp. activity after 8 catalytic cycles ($\approx$16 h operation) | Polymeric (PDA + GDE + PEI-modified PP) | / | Batch | [157] |

R. Sp. act.—recovered specific activity (with respect to free enzymes); Recirc.—recirculation; N.D.—non-determined; DKR—dynamic kinetic resolution; OP—organic phase; PAN—polyacrylonitrile; PDA—polydopamine; GA—glutaraldehyde; PVA—polyvinyl alcohol; PVDF—polyvinylidene fluoride; CLEAs—cross-linked enzyme aggregates; PES—polyethersulfone; PSF—polysulfone; PS—polystyrene; GO—graphene oxide; PPC—polypropylene chloride; APTES—(3-aminopropyl)triethoxysilane; EDC/NHS—(1-ethyl-3-(3-dimethylaminopropyl)carbodiimide/$N$-hydroxysuccinimide); BSA—bovine serum albumin; PP—polypropylene; PEI—polyethyleneimine; DAB—1,4-diaminobutane; PCADE—polycarvone acrylate di-epoxide; Rac-BMBA—racemic bromo-$\alpha$-methylbenzylamine; BAP—bromoacetophenone; UF—ultrafiltration; NF—nanofiltration; GOS—galacto-oligosaccharide; EPC—enzyme-polyelectrolyte complex; GDE—glycerol diglycidyl ether.

Hippolyte Meersseman Arango *et al.*
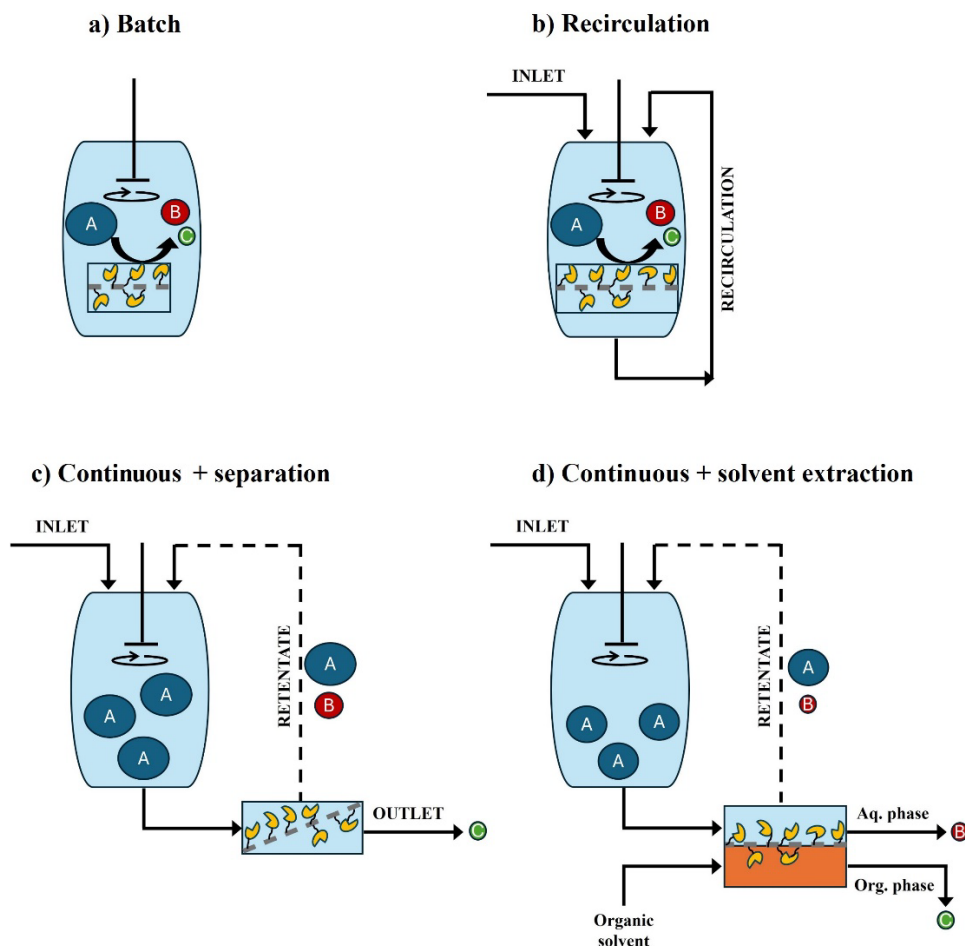


**Figure 3.** Schematic representation of membrane-immobilized enzymes acting as simple heterogeneous membrane-immobilized biocatalysts (i.e., not performing membrane operations) operating in (a) batch or (b) recirculating mode or as enzyme-membrane reactors (i.e., reaction–separation unit) in (c) compound separation (e.g., via size-exclusion, ion-exchange, etc.) or (d) solvent extraction operations. Note that when omitting the recirculations, (c) and (d) become continuous-flow operations.

ceramic membrane surfaces, and employed to hydrolyze oleuropein into oleuropein aglycone and glucose (in aqueous medium; see Figure 5) [45]. Given the differences in polarities between oleuropein aglycone and the other compounds involved in the process, membrane-assisted solvent extraction was chosen to intensify the process. The aglycone produced in the membrane contactor was continuously extracted with an organic solvent (ethyl acetate), which allowed its separation and purification from the reaction medium. An identical strategy was implemented with polymeric (polysulfone [PSF])

membranes containing entrapped β-glucosidase in its pores and using limonene as the organic solvent [141–143]. Yet, the use of such polymeric materials as aqueous–organic contactors for such solvent extraction processes might be less suitable than ceramic membranes given their limited chemical stability.

Another elegant example of membrane-immobilized enzyme reactor application is the in situ removal of water through pervaporation as in the intensified production of lauryl stearate (which is often used as an emollient and excipient in cosmetics
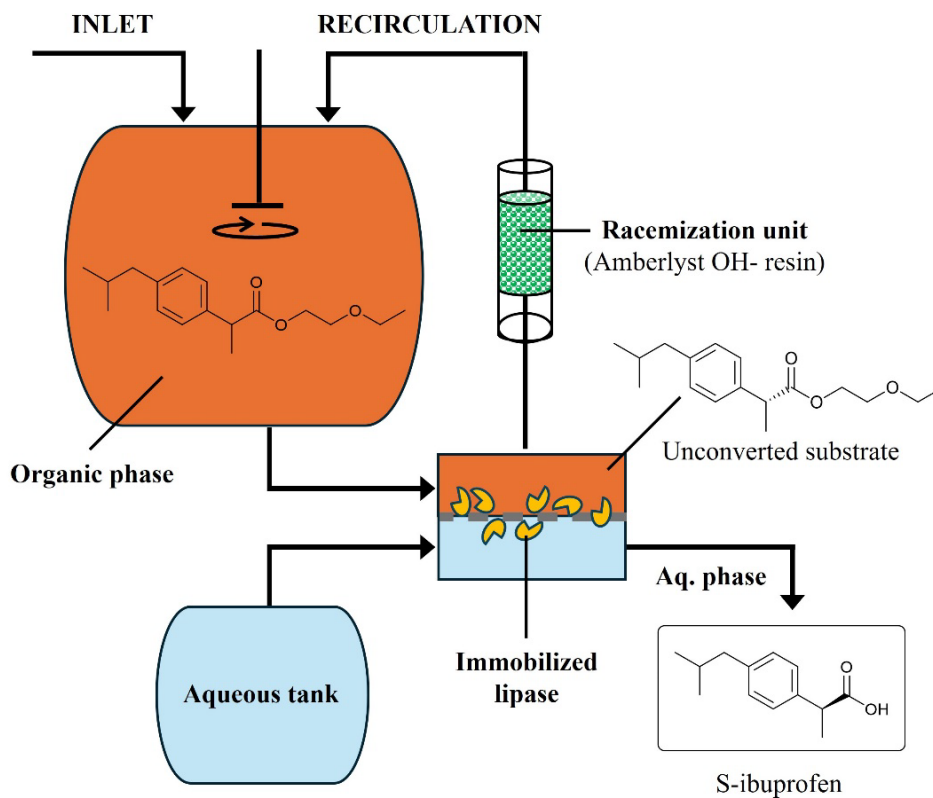
**Figure 4.** Schematic representation of the dynamic kinetic resolution of ibuprofen ester catalyzed by lipase-membrane reactor (Uzir et al., 2011) [127,128].

and pharmaceuticals [159]) [68]. In this work, a "sandwich-like" membrane structure, made of a porous lipase–polyvinyl alcohol (PVA) catalytic layer coated on a PVA/polyethersulfone (PES) matrix, was employed as an enzymatic-pervaporation reactor. Interestingly, the immobilized lipase exhibited enhanced specific activity and stability compared to the soluble enzyme. This improvement was attributed to the hydrophilic microenvironment created by the hydrophilic PVA carrier, which probably absorbs the water produced during the enzymatic esterification, thereby shielding the lipase from adverse effects like enzyme inactivation. The implementation of this catalytically active membrane in a pervaporation reactor resulted in a substantial increase in conversion (from 60% to 83%) compared to the equilibrium-limited esterification process (conducted without pervaporation). A similar strategy was applied for the synthesis of ethyl lactate (a pharmaceutical-grade excipient [160]) in which a lipase entrapped in a sodium alginate membrane was the enzymatic-pervaporation unit [130].

Immobilizing enzymes such as β-galactosidase, peptidase, and dextranase on membranes featuring adequate MWCO is also a practical tool to intensify the production of value-added compounds with tailored molecular weight via size-exclusion operations. For example, the production of GOSs from lactose is hindered by hydrolytic side reactions, and by enzyme inhibition caused by such monosaccharide formation and accumulation. To improve reaction yield and productivity, continuous coupled GOS purification and monosaccharide elimination from the reaction mixture is of particular interest. To this end, UF membranes are employed to simultaneously host the enzymes and perform product separation [133,134,139]. However, considering the molecular weight distribution of the carbohydrate mixture obtained after enzymatic reaction with lactose, NF also appears as an effective operation for
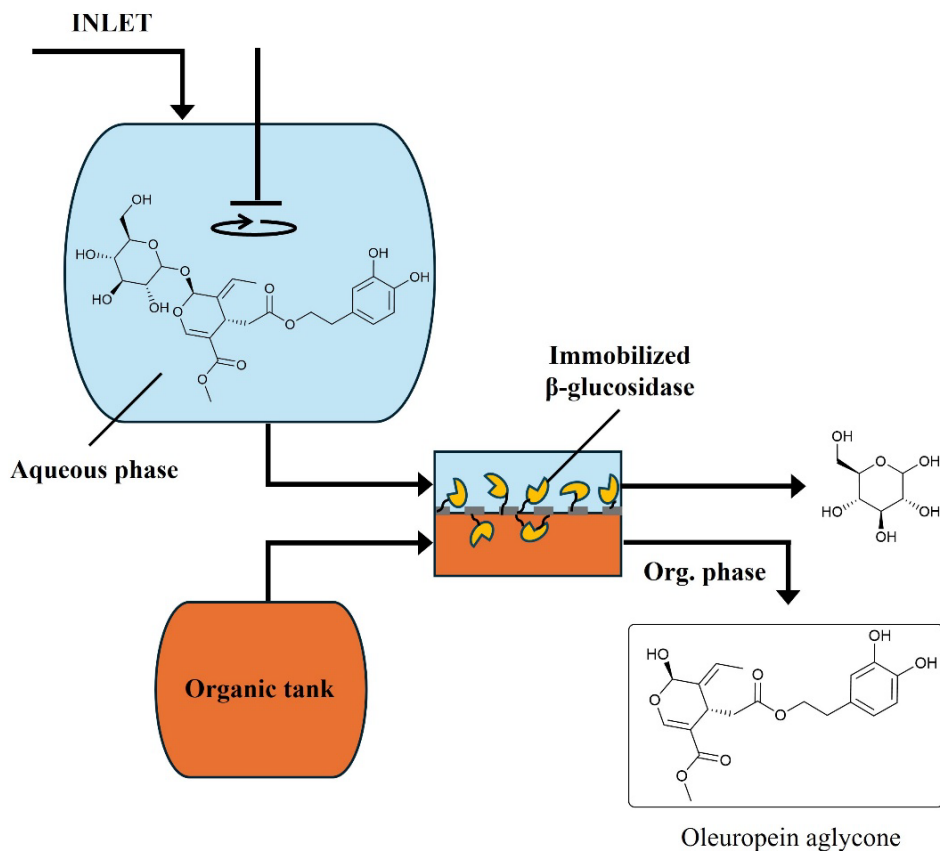
**Figure 5.** Schematic representation of oleuropein aglycone production through simultaneous hydrolysis and solvent extraction using an enzyme-membrane reactor (Giorno et al., 2018) [45].

GOS purification. Bhattacharjee et al. [135] immobilized β-galactosidase on NF (0.4 kDa) and UF (5–50 kDa) membranes via covalent grafting and compared their catalytic performance toward continuous membrane-assisted GOS production. A higher GOS yield was obtained when using the enzyme-loaded NF membrane, which aligns with the enhanced permeation of monosaccharides and improved retention of GOS observed with the NF membrane (compared to enzyme-immobilized UF membrane). Furthermore, the NF process resulted in substantial retention of the lactose substrate, providing extended residence time and greater interaction between the substrate and the immobilized enzyme, which contributed to increased GOS production. Similarly, Pinelo et al. [145] leveraged the use of membrane-immobilized dextranase in order to selectively permeate the produced oligodextran

featuring the desired molecular weight (5–8 kDa) and avoid overdegradation of products. In the latter study, the membrane unit consisted of a three-layer system, composed of polystyrene (PS) electrospun nanofibers placed between a pristine commercial membrane (PES, 30 kDa or cellulose, 10 kDa) and a macroporous support layer. To make them amenable to enzyme grafting, the PS nanofibers were functionalized with tannic acid and APTES prior to enzyme immobilization. This approach significantly improved the catalytic performance (i.e., constant productivity over time and controlled saccharide molecular weight in permeate) with respect to the EMR employing free enzymes (which showed rapid deactivation over time).

The use of an EMR in the enzymatic production of L-DOPA (which is a drug commonly used for the treatment of Parkinson's disease [161]) from tyrosine

offers numerous advantages. By continuously supplying L-tyrosine to the biocatalytic system at a controlled rate, the EMR helps prevent enzyme inhibition and maintain a constant substrate concentration. Additionally, it enables product separation, which is of particular interest as some by-products formed through L-DOPA spontaneous overoxidation (e.g., dopamine and dopaquinone) tend to polymerize and complicate purification. The EMR configuration facilitates the separation of these by-products via membrane filtration, ensuring continuous purification of L-DOPA on the permeate side. However, L-DOPA spontaneous oxidation remains problematic as it hampers the yields and productivity of such an enzymatic process. To address this, Donato et al. [151] attempted to continuously introduce ascorbic acid [162], a reducing agent, while simultaneously removing the biocatalytically produced L-DOPA. To this end, the authors immobilized tyrosinase on a polyamide tubular membrane sponge layer and implemented the EMR in crossflow configuration. The result was that the continuous removal of L-DOPA from the reaction environment along with the antioxidant effect of ascorbic acid further enhanced L-DOPA productivity, reaching 1.60 U·mg$^{-1}$, which is higher than that of other processes reported in the literature (where product separation and ascorbic acid addition were not applied).

## 4. Conclusion

Among the existing methods capable of intensifying biocatalytic processes in an efficient way, the coupling of enzymes with membrane technology in EMRs is emerging as a highly potential method. Such integrated systems, simultaneously combining biocatalytic reactions and membrane operations, allow for more productive flow processes displaying enhanced product yield (by increasing the conversion and/or the selectivity of the process, via, e.g., membrane-assisted product separation) and boosted enzyme kinetics (by preventing enzyme inhibition via controlled reagent introduction). Through this review, we aim at providing the recent trends and examples of the use of EMR for the intensified production of high-value chemicals and, in particular, APIs. Among the reviewed EMR configurations, we notably turn our attention toward

membrane-immobilized enzymatic reactors. We argue that the implementation of such novel hybrid reactors that simultaneously host the immobilized enzymes and perform in situ product separation will catalyze further advances in the field of green fine chemical and pharmaceutical manufacturing. Arguably, merging the fields of biocatalysis and organic synthesis on the one hand and process engineering on the other hand, resulting in EMRs, is crucial to both academic and industrial developments.

## Declaration of interests

The authors do not work for, advise, own shares in, or receive funds from any organization that could benefit from this article, and have declared no affiliations other than their research organizations.

## References

[1] H. Meersseman Arango, L. van den Biggelaar, P. Soumillion, P. Luis, T. Leyssens, F. Paradisi and D. P. Debecker, *React. Chem. Eng.* **8** (2023), pp. 1505–1544.

[2] S. Chakraborty, H. Rusli, A. Nath, J. Sikder, C. Bhattacharjee, S. Curcio and E. Drioli, *Crit. Rev. Biotechnol.* **36** (2016), pp. 43–58.

[3] D. Ghislieri and N. J. Turner, *Top. Catal.* **57** (2014), pp. 284–300.

[4] S. A. Kelly, S. Pohle, S. Wharry, S. Mix, C. C. R. Allen, T. S. Moody and B. F. Gilmore, *Chem. Rev.* **118** (2018), pp. 349–367.

[5] I. Slabu, J. L. Galman, R. C. Lloyd and N. J. Turner, *ACS Catal.* **7** (2017), pp. 8263–8284.

[6] M. D. Truppo, *ACS Med. Chem. Lett.* **8** (2017), pp. 476–480.

[7] F. Guo and P. Berglund, *Green Chem.* **19** (2017), pp. 333–360.

[8] P. Jochems, Y. Satyawali, L. Diels and W. Dejonghe, *Green Chem.* **13** (2011), pp. 1609–1623.

[9] R. A. Sheldon and S. van Pelt, *Chem. Soc. Rev.* **42** (2013), pp. 6223–6235.

[10] R. A. Sheldon, A. Basso and D. Brady, *Chem. Soc. Rev.* **50** (2021), pp. 5850–5862.

[11] M. P. Thompson, I. Peñafiel, S. C. Cosgrove and N. J. Turner, *Org. Process Res. Dev.* **23** (2019), pp. 9–18.

[12] A. I. Benítez-Mateos, M. L. Contente, D. R. Padrosa and F. Paradisi, *React. Chem. Eng.* **6** (2021), pp. 599–611.

[13] D. Remonatto, R. H. Miotti Jr., R. Monti, J. C. Bassan and A. V. de Paula, *Process Biochem.* **114** (2022), pp. 1–20.

[14] W. Khanam and N. C. Dubey, *Mater. Today Chem.* **24** (2022), article no. 100922.

[15] L. van den Biggelaar, P. Soumillion and D. P. Debecker, *RSC Adv.* **9** (2019), pp. 18538–18546.

[16] A. S. Dunn, V. Svoboda, J. Sefcik and J. H. ter Horst, *Org. Process Res. Dev.* **23** (2019), pp. 2031–2041.

[17] L. Van den Biggelaar, P. Soumillion and D. P. Debecker, *Catalysts* **7** (2017), article no. 54.

[18] P. D. Santis, L.-E. Meyer and S. Kara, *React. Chem. Eng.* **5** (2020), pp. 2155–2184.

[19] A. Hyer, D. Gregory, K. Kay, Q. Le, J. Turnage, F. Gupton and J. K. Ferri, *Adv. Synth. Catal.* **366** (2024), pp. 357–389.

[20] R. Gérardy, D. P. Debecker, J. Estager, P. Luis and J.-C. M. Monbaliu, *Chem. Rev.* **120** (2020), pp. 7219–7347.

[21] R. M. Lindeque and J. M. Woodley, *Catalysts* **9** (2019), article no. 262.

[22] L. Tamborini, P. Fernandes, F. Paradisi and F. Molinari, *Trends Biotechnol.* **36** (2018), pp. 73–88.

[23] L.-E. Meyer, M. Hobisch and S. Kara, *Curr. Opin. Biotechnol.* **78** (2022), article no. 102835.

[24] A. Adamo, R. L. Beingessner, M. Behnam, et al., *Science* **352** (2016), pp. 61–67.

[25] L. Cao, *Carrier-bound Immobilized Enzymes: Principles, Application and Design*, Wiley: Hoboken, 2005.

[26] J. M. Bolivar and F. López-Gallego, *Curr. Opin. Green Sustain. Chem.* **25** (2020), article no. 100349.

[27] P. Luis, *Fundamental Modeling of Membrane Systems*, 1st edition, Elsevier: Amsterdam, 2018.

[28] W. Li, J. Estager, J.-C. M. Monbaliu, D. P. Debecker and P. Luis, *J. Chem. Technol. Biotechnol.* **95** (2020), pp. 2311–2334.

[29] J. G. Crespo and K. W. Böddeker, *Membrane Processes in Separation and Purification*, Springer Science & Business Media: Dordrecht, 2013.

[30] S. B. Ameur, C. Luminiţa Gîjiu, M.-P. Belleville, J. Sanchez and D. Paolucci-Jeanjean, *J. Membr. Sci.* **455** (2014), pp. 330–340.

[31] M. Pinelo, G. Jonsson and A. S. Meyer, *Sep. Purif. Technol.* **70** (2009), pp. 1–11.

[32] J. L. Lopez and S. L. Matson, *J. Membr. Sci.* **125** (1997), pp. 189–211.

[33] J. Neuburger, F. Helmholz, S. Tiedemann, P. Lehmann, P. Süss, U. Menyes and J. von Langermann, *Chem. Eng. Process. - Process Intensif.* **168** (2021), article no. 108578.

[34] Y. Satyawali, K. Vanbroekhoven and W. Dejonghe, *Biochem. Eng. J.* **121** (2017), pp. 196–223.

[35] A. I. Benítez-Mateos and F. Paradisi, *J. Flow Chem.* **14** (2024), pp. 211–218.

[36] W. Qing, X. Li, S. Shao, X. Shi, J. Wang, Y. Feng, W. Zhang and W. Zhang, *J. Membr. Sci.* **583** (2019), pp. 118–138.

[37] D. Brady and J. Jordaan, *Biotechnol. Lett.* **31** (2009), pp. 1639–1650.

[38] U. T. Bornscheuer, G. W. Huisman, R. J. Kazlauskas, S. Lutz, J. C. Moore and K. Robins, *Nature* **485** (2012), pp. 185–194.

[39] Y.-K. Cen, Y.-X. Liu, Y.-P. Xue and Y.-G. Zheng, *Adv. Synth. Catal.* **361** (2019), pp. 5500–5515.

[40] J. Kujawa, M. Głodek, G. Li, S. Al-Gharabli, K. Knozowska and W. Kujawski, *Sci. Total Environ.* **801** (2021), article no. 149647.

[41] J. Luo, S. Song, H. Zhang, H. Zhang, J. Zhang and Y. Wan, *Eng. Life Sci.* **20** (2020), pp. 441–450.

[42] J. Agustian, A. H. Kamaruddin and S. Bhatia, *J. Chem. Technol. Biotechnol.* **86** (2011), pp. 1032–1048.

[43] L. Giorno, R. Mazzei and E. Drioli, *Membrane Operations*, Wiley-VCH: Weinheim, 2009, pp. 397–409.

[44] A. B. Sitanggang, A. Drews and M. Kraume, *Chem. Eng. Process. - Process Intensif.* **180** (2022), article no. 108729.

[45] G. Ranieri, R. Mazzei, T. Poerio, F. Bazzarelli, Z. Wu, K. Li and L. Giorno, *Chem. Eng. Sci.* **185** (2018), pp. 149–156.

[46] A. Kayvani Fard, G. McKay, A. Buekenhoudt, H. Al Sulaiti, F. Motmans, M. Khraisheh and M. Atieh, *Materials* **11** (2018), article no. 74.

[47] R. N. Patel, *Enzyme Microb. Technol.* **31** (2002), pp. 804–826.

[48] K. Goldberg, K. Schroer, S. Lütz and A. Liese, *Appl. Microbiol. Biotechnol.* **76** (2007), pp. 237–248.

[49] *Chirality*, **4** (1992), pp. 338–340.

[50] W. H. De Camp, *J. Pharm. Biomed. Anal.* **11** (1993), pp. 1167–1172.

[51] M. M. Musa, F. Hollmann and F. G. Mutti, *Catal. Sci. Technol.* **9** (2019), pp. 5487–5503.

[52] T. C. Nugent, in *Chiral Amine Synthesis. Methods, Developments and Applications* (T. C. Nugent, ed.), Wiley-VCH: Weinheim, 2010.

[53] A. Liese, T. Zelinski, M.-R. Kula, H. Kierkels, M. Karutz, U. Kragl and C. Wandrey, *J. Mol. Catal. B: Enzym.* **4** (1998), pp. 91–99.

[54] J. Haberland, W. Hummel, T. Daussmann and A. Liese, *Org. Process Res. Dev.* **6** (2002), pp. 458–462.

[55] C. K. Savile, J. M. Janey, E. C. Mundorff, et al., *Science* **329** (2010), pp. 305–309.

[56] G. Rehn, P. Adlercreutz and C. Grey, *J. Biotechnol.* **179** (2014), pp. 50–55.

[57] T. Börner, G. Rehn, C. Grey and P. Adlercreutz, *Org. Process Res. Dev.* **19** (2015), pp. 793–799.

[58] Y. Satyawali, D. F. Del Pozo, P. Vandezande, I. Nopens and W. Dejonghe, *Biotechnol. Prog.* **35** (2019), article no. e2731.

[59] Y. Satyawali, E. Ehimen, L. Cauwenberghs, M. Maesen, P. Vandezande and W. Dejonghe, *Biochem. Eng. J.* **117** (2017), pp. 97–104.

[60] J. Yang, A. Buekenhoudt, M. V. Dael, P. Luis, Y. Satyawali, R. Malina and S. Lizin, *Org. Process Res. Dev.* **26** (2022), pp. 2052–2066.

[61] R. Ciriminna and M. Pagliaro, *Org. Process Res. Dev.* **17** (2013), pp. 1479–1484.

[62] K. Sakaki, L. Giorno and E. Drioli, *J. Membr. Sci.* **184** (2001), pp. 27–38.

[63] E. Battistel, D. Bianchi, P. Cesti and C. Pina, *Biotechnol. Bioeng.* **38** (1991), pp. 659–664.

[64] M. B. Ansorge-Schumacher and O. Thum, *Chem. Soc. Rev.* **42** (2013), pp. 6475–6490.

[65] C.-S. Chen and C. J. Sih, *Angew. Chem. Int. Ed. Engl.* **28** (1989), pp. 695–707.

[66] K. Sakaki, A. Aoyama, T. Nakane, T. Ikegami, H. Negishi, K. Watanabe and H. Yanagishita, *Desalination* **193** (2006), pp. 260–266.

[67] Z. Findrik, Z. Németh, G. Ravcki, K. Bélafi-Bakó, K. Csanádi, Z. Gubicza and L. Gubicza, *Process Biochem.* **47** (2012), pp. 1715–1722.

[68] W. Zhang, W. Qing, Z. Ren, W. Li and J. Chen, *Bioresour. Technol.* **172** (2014), pp. 16–21.

[69] L. Gubicza, N. Nemestóthy, T. Fráter and K. Bélafi-Bakó, *Green Chem.* **5** (2003), pp. 236–239.

[70] A. Van der Padt, J. J. W. Sewalt and K. Van't Riet, *J. Membr. Sci.* **80** (1993), pp. 199–208.

[71] Y. Satyawali, L. Cauwenberghs, M. Maesen and W. Dejonghe, *Chem. Eng. Process. - Process Intensif.* **166** (2021), article no. 108475.

[72] V. Narisetty, P. Parhi, B. Mohan, et al., *Bioresour. Technol.* **346** (2022), article no. 126590.

[73] T. Loftsson and D. Duchêne, *Int. J. Pharm.* **329** (2007), pp. 1–11.

[74] D. Kim and D. F. Day, *Enzyme Microb. Technol.* **16** (1994), pp. 844–848.

[75] Z. Su, J. Luo, M. Pinelo and Y. Wan, *J. Membr. Sci.* **555** (2018), pp. 268–279.

[76] O. O. Ibrahim, *J. Food Chem. Nanotechnol.* **4** (2018), pp. 65–76.

[77] E. Zokaityte, D. Cernauskas, D. Klupsaite, et al., *Microorganisms* **8** (2020), article no. 1182.

[78] T. Sar, S. Harirchi, M. Ramezani, G. Bulkan, M. Y. Akbas, A. Pandey and M. J. Taherzadeh, *Sci. Total Environ.* **810** (2022), article no. 152253.

[79] S. Chockchaisawasdee, V. I. Athanasopoulos, K. Niranjan and R. A. Rastall, *Biotechnol. Bioeng.* **89** (2005), pp. 434–443.

[80] M. Akbarian, A. Khani, S. Eghbalpour and V. N. Uversky, *Int. J. Mol. Sci.* **23** (2022), article no. 1445.

[81] W. A. M. Mutilangi, D. Panyam and A. Kilara, *J. Food Sci.* **60** (1995), pp. 1104–1109.

[82] W. Qu, H. Ma, W. Li, Z. Pan, J. Owusu and C. Venkitasamy, *Process Biochem.* **50** (2015), pp. 245–252.

[83] M. Sajid and J. H. Mckerrow, *Mol. Biochem. Parasitol.* **120** (2002), pp. 1–21.

[84] B. Nidetzky, W. Neuhauser, D. Haltrich and K. D. Kulbe, *Biotechnol. Bioeng.* **52** (1996), pp. 387–396.

[85] MWCO. Online at https://www.lenntech.com/services/mwco.htm. (accessed 5 September 2024).

[86] J. Luo, R. T. Nordvang, S. T. Morthensen, B. Zeuner, A. S. Meyer, J. D. Mikkelsen and M. Pinelo, *Bioresour. Technol.* **166** (2014), pp. 9–16.

[87] D. Hülsewede, E. Temmel, P. Kumm and J. von Langermann, *Crystals* **10** (2020), article no. 345.

[88] J. S. Shin, B. G. Kim, A. Liese and C. Wandrey, *Biotechnol. Bioeng.* **73** (2001), pp. 179–187.

[89] D. Valinger, A. Vrsalović Presevcki, Ž. Kurtanjek, M. Pohl, Z. Findrik Blažević and D. Vasić-Ravcki, *J. Mol. Catal. B: Enzym.* **102** (2014), pp. 132–137.

[90] C. Kohlmann, S. Leuchs, L. Greiner and W. Leitner, *Green Chem.* **13** (2011), pp. 1430–1436.

[91] Y. Satyawali, W. Van Hecke, M. N. Khan, P. Vandezande, P. Van der Weeën and W. Dejonghe, *J. Clean. Prod.* **426** (2023), article no. 139050.

[92] I. Ioannou, E. Barboza, G. Willig, T. Marié, A. Texeira, P. Darme, J.-H. Renault and F. Allais, *Pharmaceuticals* **14** (2021), article no. 319.

[93] H. Ren, J. Fei, X. Shi, T. Zhao, H. Cheng, N. Zhao, Y. Chen and H. Ying, *Sep. Purif. Technol.* **144** (2015), pp. 70–79.

[94] K. Hofmann and C. Hamel, *Chem. Ing. Tech.* **95** (2023), pp. 767–772.

[95] M. Ebrahimi, L. Placido, L. Engel, K. S. Ashaghi and P. Czermak, *Desalination* **250** (2010), pp. 1105–1108.

[96] A. Córdova, C. Astudillo, C. Vera, C. Guerrero and A. Illanes, *J. Biotechnol.* **223** (2016), pp. 26–35.

[97] V. A. Botelho, M. Mateus, J. C. C. Petrus and M. N. de Pinho, *Membranes* **12** (2022), article no. 171.

[98] T. Cao, M. Pázmándi, I. Galambos and Z. Kovács, *Membranes* **10** (2020), article no. 203.

[99] A. B. Sitanggang, A. Drews and M. Kraume, *Bioresour. Technol.* **167** (2014), pp. 108–115.

[100] A. B. Sitanggang, A. Drews and M. Kraume, *Biochem. Eng. J.* **109** (2016), pp. 65–80.

[101] A. B. Sitanggang, A. Drews and M. Kraume, *J. Biotechnol.* **203** (2015), pp. 89–96.

[102] A. Heyse, C. Plikat, M. Ansorge-Schumacher and A. Drews, *Catal. Today* **331** (2019), pp. 60–67.

[103] J. A. Rodríguez Gastón, H. Costa and S. A. Ferrarotti, *Biotechnol. Prog.* **31** (2015), pp. 695–699.

[104] V. C. Fenelon, J. H. Miyoshi, C. S. Mangolim, A. S. Noce, L. N. Koga and G. Matioli, *Carbohydr. Polym.* **192** (2018), pp. 19–27.

[105] A. Trusek-Holownia, M. Lech and A. Noworyta, *Chem. Eng. J.* **305** (2016), pp. 61–68.

[106] S. Jakovetić, N. Ognjanovic Lukovic, B. Jugović, G. Milica, S. Grbavvcić, J. Jovanović and Z. Knežević-Jugović, *Food Bioprocess Technol.* **8** (2014), pp. 287–300.

[107] T. Eisele, T. Stressler, B. Kranz and L. Fischer, *Eur. Food Res. Technol.* **236** (2013), pp. 483–490.

[108] W.-H. Huang, J. Sun, H. He, H.-W. Dong and J.-T. Li, *Food Chem.* **128** (2011), pp. 968–973.

[109] J. Ewert, W. Claaßen, T. Stressler and L. Fischer, *Biochem. Eng. J.* **150** (2019), article no. 107261.

[110] M. Merz, T. Eisele, W. Claaßen, D. Appel, S. Rabe, T. Stressler and L. Fischer, *Biochem. Eng. J.* **99** (2015), pp. 114–123.

[111] R. Das, S. Ghosh and C. Bhattacharjee, *LWT* **47** (2012), pp. 238–245.

[112] S. Huang, Y. Gong, Y. Li, S. Ruan, S. M. Roknul Azam, Y. Duan, X. Ye and H. Ma, *Process Biochem.* **92** (2020), pp. 130–137.

[113] J. O'Halloran, M. O'Sullivan and E. Casey, *Food Bioprocess Technol.* **12** (2019), pp. 799–808.

[114] D. P. Debecker, V. Smeets, M. Van der Verren, H. Meersseman Arango, M. Kinnaer and F. Devred, *Curr. Opin. Green Sustain. Chem.* **28** (2021), article no. 100437.

[115] M. Van der Verren, V. Smeets, A. vander Straeten, C. Dupont-Gillain and D. P. Debecker, *Nanoscale Adv.* **3** (2021), pp. 1646–1655.

[116] V. Smeets, W. Baaziz, O. Ersen, E. M. Gaigneaux, C. Boissière, C. Sanchez and D. P. Debecker, *Chem. Sci.* **11** (2020), pp. 954–961.

[117] X. Li, Y. Cao, K. Luo, et al., *Nat. Catal.* **2** (2019), pp. 718–725.

[118] K. Engström, E. V. Johnston, O. Verho, K. P. J. Gustafson, M. Shakeri, C.-W. Tai and J.-E. Bäckvall, *Angew. Chem. Int. Ed. Engl.* **52** (2013), pp. 14006–14010.

[119] C. A. Ferraz, M. A. do Nascimento, R. F. O. Almeida, et al., *Mol. Catal.* **493** (2020), article no. 111106.

[120] C. R. Thomas and D. Geer, *Biotechnol. Lett.* **33** (2011), pp. 443–456.

[121] Z.-G. Wang, L.-S. Wan, Z.-M. Liu, X.-J. Huang and Z.-K. Xu, *J. Mol. Catal. B: Enzym.* **56** (2009), pp. 189–195.

[122] S. B. Sigurdardóttir, J. Lehmann, S. Ovtar, J.-C. Grivel, M. D. Negra, A. Kaiser and M. Pinelo, *Adv. Synth. Catal.* **360** (2018), pp. 2578–2607.

[123] H. Zhang, J. Luo, S. Li, Y. Wei and Y. Wan, *Langmuir* **34** (2018), pp. 2585–2594.

[124] J. Luo, A. S. Meyer, R. V. Mateiu, D. Kalyani and M. Pinelo, *ACS Appl. Mater. Interf.* **6** (2014), pp. 22894–22904.

[125] Z.-Y. Xi, Y.-Y. Xu, L.-P. Zhu, Y. Wang and B.-K. Zhu, *J. Membr. Sci.* **327** (2009), pp. 244–253.

[126] F. Marpani, J. Luo, R. V. Mateiu, A. S. Meyer and M. Pinelo, *ACS Appl. Mater. Interf.* **7** (2015), pp. 17682–17691.

[127] L. Sie Yon, F. N. Gonawan, A. H. Kamaruddin and M. H. Uzir, *Ind. Eng. Chem. Res.* **52** (2013), pp. 9441–9453.

[128] S. Y. Lau, F. N. Gonawan, S. Bhatia, A. H. Kamaruddin and M. H. Uzir, *Chem. Eng. J.* **166** (2011), pp. 726–737.

[129] S. Ming, S. Li, Z. Chen, et al., *Antioxidants* **11** (2022), article no. 1906.

[130] F. Ugur Nigiz and N. Durmaz Hilmioglu, *Int. J. Energy Res.* **40** (2016), pp. 71–80.

[131] G. Bayramoğlu, B. Hazer, B. Altıntaş and M. Y. Arıca, *Process Biochem.* **46** (2011), pp. 372–378.

[132] J. Kujawa, M. Głodek, I. Koter, B. Ośmiałowski, K. Knozowska, S. Al-Gharabli, L. F. Dumée and W. Kujawski, *Materials* **14** (2021), article no. 201.

[133] T. Palai, A. K. Singh and P. K. Bhattacharya, *Biochem. Eng. J.* **88** (2014), pp. 68–76.

[134] T. Palai and P. K. Bhattacharya, *J. Biosci. Bioeng.* **115** (2013), pp. 668–673.

[135] D. Sen, A. Sarkar, A. Gosling, et al., *J. Membr. Sci.* **378** (2011), pp. 471–478.

[136] D. Sen, A. Sarkar, S. Das, R. Chowdhury and C. Bhattacharjee, *Ind. Eng. Chem. Res.* **51** (2012), pp. 10671–10681.

[137] A. Chenafa, A. A. A. Abdo, A. A. Mahdi, et al., *Int. J. Biol. Macromol.* **270** (2024), article no. 132312.

[138] P. Jochems, Y. Satyawali, S. Van Roy, W. Doyen, L. Diels and W. Dejonghe, *Enzyme Microb. Technol.* **49** (2011), pp. 580–588.

[139] A. Córdova, C. Aburto, V. Carrasco, et al., *Process Saf. Environ. Prot.* **188** (2024), pp. 1081–1092.

[140] F. N. Gonawan, M. Z. A. Bakar, K. A. Karim and A. H. Kamaruddin, *RSC Adv.* **6** (2016), pp. 59865–59874.

[141] C. Conidi, R. Mazzei, A. Cassano and L. Giorno, *J. Membr. Sci.* **454** (2014), pp. 322–329.

[142] R. Mazzei, E. Drioli and L. Giorno, *J. Membr. Sci.* **390–391** (2012), pp. 121–129.

[143] R. Mazzei, E. Drioli and L. Giorno, *J. Membr. Sci.* **352** (2010), pp. 166–172.

[144] E. Piacentini, R. Mazzei, F. Bazzarelli, G. Ranieri, T. Poerio and L. Giorno, *Ind. Eng. Chem. Res.* **58** (2019), pp. 16813–16822.

[145] Z. Su, K. Jankowska, S. Björk Sigurdardóttir, W. A. Zhang, A. Kaiser, J. Luo and M. Pinelo, *Chem. Eng. Sci.* **283** (2024), article no. 119367.

[146] P. Berends, D. Appel, T. Eisele, S. Rabe and L. Fischer, *LWT - Food Sci. Technol.* **58** (2014), pp. 534–540.

[147] Z. Chen, Z. Sun, S. Ming, S. Li, Z. Zhu and W. Zhang, *Sep. Purif. Technol.* **259** (2021), article no. 118214.

[148] A. Vanangamudi, D. Saeki, L. F. Dumée, M. Duke, T. Vasiljevic, H. Matsuyama and X. Yang, *ACS Appl. Mater. Interf.* **10** (2018), pp. 27477–27487.

[149] Z. Chen, S. Zhu, H. Zhang, F. Wang, K. Marszałek and Z. Zhu, *Chem. Eng. J.* **453** (2023), article no. 139792.

[150] A. Muñiz-Mouro, B. Gullón, T. A. Lu-Chau and G. Eibes, *Food Bioprod. Process.* **124** (2020), pp. 434–444.

[151] C. Algieri, L. Donato, P. Bonacci and L. Giorno, *Biochem. Eng. J.* **66** (2012), pp. 14–19.

[152] L. Donato, C. Algieri, V. Miriello, R. Mazzei, G. Clarizia and L. Giorno, *J. Membr. Sci.* **407–408** (2012), pp. 86–92.

[153] C. Algieri, L. Donato and L. Giorno, *Biotechnol. Appl. Biochem.* **64** (2017), pp. 92–99.

[154] B. Šketa, J. L. Galman, N. J. Turner and P. Žnidaršivc-Plazl, *New Biotechnol.* **83** (2024), pp. 46–55.

[155] U. Montanari, D. Cocchi, T. M. Brugo, et al., *Polymers* **13** (2021), article no. 1804.

[156] D. Roura Padrosa, Z. Nisar and F. Paradisi, *Catalysts* **11** (2021), article no. 520.

[157] H. M. Arango, X. D. L. Nguyen, P. Luis, T. Leyssens, D. R. Padrosa, F. Paradisi and D. P. Debecker, *RSC Sustain.* **2** (2024), pp. 3139–3152.

[158] L. K. Thalén, D. Zhao, J.-B. Sortais, J. Paetzold, C. Hoben and J.-E. Bäckvall, *Chem. – Eur. J.* **15** (2009), pp. 3403–3410.

[159] D. Nakmode, V. Bhavana, P. Thakor, et al., *Pharmaceutics* **14** (2022), article no. 831.

[160] J. T. McConville, T. C. Carvalho, S. A. Kucera and E. Garza, *Pharm. Technol.* **33** (2009), pp. 74–80.

[161] S.-E. Soh, M. E. Morris and J. L. McGinley, *Parkinsonism Relat. Disord.* **17** (2011), pp. 1–9.

[162] P. Pialis, M. C. Jimenez Hamann and B. A. Saville, *Biotechnol. Bioeng.* **51** (1996), pp. 141–147.

ACADÉMIE
DES SCIENCES
INSTITUT DE FRANCE

Review article

# Biocatalysis in packed-bed reactors: immobilization as an enabling technology

**Cristina Lía Fernández Regueiro** [®],[a], **David Roura Padrosa** [®],[*],[a] **and**
**Francesca Paradisi** [®],[*],[b]

[a] inSEIT AG, Gesellschaftsstrasse 42, 3012 Bern, Switzerland

[b] Department of Chemistry, Biochemistry and Pharmaceutical Sciences, University of
Bern, Freiestrasse 3, 3012 Bern, Switzerland

*E-mails:* david.roura@inseit.ch (D. Roura Padrosa), francesca.paradisi@unibe.ch
(F. Paradisi)

**Abstract.** Biocatalysis and flow chemistry are two complementary technologies that can be used to
produce chemicals in a more efficient, sustainable, and safe manner. Enzyme immobilization is key
to enabling their combination. Various immobilization methods, including carrier-free and carrier-
based techniques, offer distinct advantages in terms of enzyme activity, stability, and productivity.
This review explores these immobilization strategies and their integration in packed-bed reactors,
highlighting their industrial applications and potential challenges.

**Keywords.** Biocatalysis, Enzyme immobilization, Flow biocatalysis, Packed-bed reactors.

*Manuscript received 11 November 2024, revised 14 February 2025, accepted 19 February 2025.*

## 1. Introduction

Enzymes, nature's catalysts, have evolved to facil-
itate biochemical reactions with remarkable speci-
ficity. Historically, they have been harnessed in fer-
mentation processes for food and beverage produc-
tion [1–4], and early industrial applications were pre-
dominantly focused on the use of naturally occurring
enzymes like xylose isomerase for high-fructose corn
syrup production [5], nitrile hydratase for acrylamide
synthesis [6,7], and penicillin amidase for semisyn-
thetic penicillins such as ampicillin [8]. Their high
selectivity avoided the need for complex protective
group strategies, thereby simplifying processes, re-
ducing waste, and aligning with the increasing de-
mand for sustainable industrial practices.

Despite these examples, natural enzymes often
exhibited limitations for industrial-scale applica-
tion. Their narrow substrate scope and suboptimal

operational stability in intensified conditions often
hindered broader industrial adoption [2]. Advance-
ments in directed evolution [9,10] and protein engi-
neering [11] have significantly mitigated these limi-
tations. There are examples of evolved enzymes with
enhanced solvent resistance [12], improved stability
under process conditions, optimized pH and tem-
perature ranges, and even more importantly, where
their reactivity is tailored to the substrate of interest
while maintaining excellent enantioselectivity [13].

In parallel to the growth of biocatalysis, flow
chemistry has become increasingly important over
the past few decades. Unlike traditional batch pro-
cesses, flow chemistry allows for more precise con-
trol of the reaction conditions (temperature, pres-
sure, contact time between substrate and catalyst),
resulting in higher yields, safer operations, and re-
duced waste [14–16]. Recently, the interest in flow
strategies has grown significantly in the fine chem-
ical industry [17–21]. Among the multiple reactor
types, packed-bed reactors (PBRs) allow the confine-
ment of the catalyst onto a column or similar reactor

---

*Corresponding authors

type. The confinement of the catalyst ensures a clean out-stream, facilitating downstream processing and product purification. Moreover, while scale-up is possible, PBRs also allow for the scale-out strategy— the use of parallel small-scale reactors to process larger volumes in shorter times. For this, PBRs hold exciting potential in the synthesis optimization of fine chemicals, while reducing costs and performing consistently, in a more sustainable manner, making flow chemistry essential for modern, sustainable chemical production.

Looking at the advantages of both technologies, it is only logical to combine them; this is the objective of flow biocatalysis. However, even engineered enzymes have a major downside for their integration into continuous manufacturing: their reusability. Enzymes are water-soluble and act in solution, and due to their complex structure, their recycling and reuse for multiple batches is extremely difficult— if not impossible—without modification. To solve this problem, enzyme immobilization is crucial to enabling enzymes in continuous reactors (Figure 1). Immobilization is a simple yet extremely powerful technique that involves confining enzymes within or onto solid materials, creating a heterogeneous biocatalyst that is no longer in solution. Immobilized enzymes allow for their reuse, and enhance the cost-efficiency of enzymatic processes [3,22]. Importantly, immobilized enzymes often exhibit enhanced stability due to the reduced flexibility upon immobilization and can retain activity over extended periods of time, even under conditions that normally would inactivate enzymes in solution [3,23]. Immobilized enzymes have been used in the pharmaceutical, fine chemical, and food industries, and yet only a few examples of their use in PBRs are available.

Several reviews have addressed the evolution of flow biocatalysis during the past 15 years [24–27]. In this concise review, we have focused on the applications of distinct enzyme immobilization techniques in the form of PBRs. We discuss the different immobilization methods and highlight their applications in industrially relevant transformation in continuous flow, discussing their advantages and the challenges encountered. By understanding these developments, we aim to highlight the potential for future innovations that can further integrate enzymatic processes into continuous manufacturing for industrial chemistry.

## 2. Immobilization techniques and their application in continuous-flow setups

Since the discovery of enzyme immobilization by Nelson and Griffith [28], many different approaches have been developed for the immobilization of enzymes. Finding a universal method has been proven challenging due to the complex nature of the enzymes and the multiple factors that play a role in the final activity and stability of the final biocatalyst. Thus, in most cases, the immobilization of choice is tailored to a specific enzyme for a desired application.

Immobilization methods are typically classified into reversible techniques (such as adsorption, encapsulation, and reversible covalent binding) and irreversible techniques (including cross-linking and irreversible covalent binding). However, for the purpose of this short overview, we classify immobilization methods based on the use (or not) of a solid support to immobilize the enzyme: carrier-based and carrier-free methods (Figure 2).

### 2.1. *Carrier-free immobilized enzymes*

Carrier-free immobilization of enzymes is carried out through their cross-linking to form insoluble supramolecular structures. Cross-linking involves the formation of covalent bonds between enzymes using bifunctional or multifunctional reagents like glutaraldehyde. These methods aim to maximize enzyme loading on the final biocatalyst by eliminating the need for carriers and maximizing the activity per unit of mass. However, they also present significant drawbacks that limit their applicability, especially, their mechanical stability and reusability [29,30].

There are different approaches to the creation of cross-linked (CL) biocatalysts. Enzymes can be cross-linked in different forms: as soluble enzymes (CLEs), lyophilized (CLELs), or in the form of enzyme aggregates (cross-linked enzyme aggregates [CLEAs]) and enzyme crystals (CLECs) [30]. Among these options, the most common strategies are CLEAs and CLECs, but only CLECs have been successfully incorporated into PBRs without further modification [31]. The application of CLEAs in flow biocatalysis has been challenging due to two main issues: the scalability in their production and their mechanical fragility [31–33]. Nonetheless, there are some examples such as

## Enzyme immobilization



- Reusability

- Increased stability

- Increased total turnover number

- Allows for the incorporation of biocatalysts into continuous systems

## Continuous manufacturing



- Higher automation

- Increased productivity (STY) vs batch

- Modularity

- Safety and sustainability through process intensification
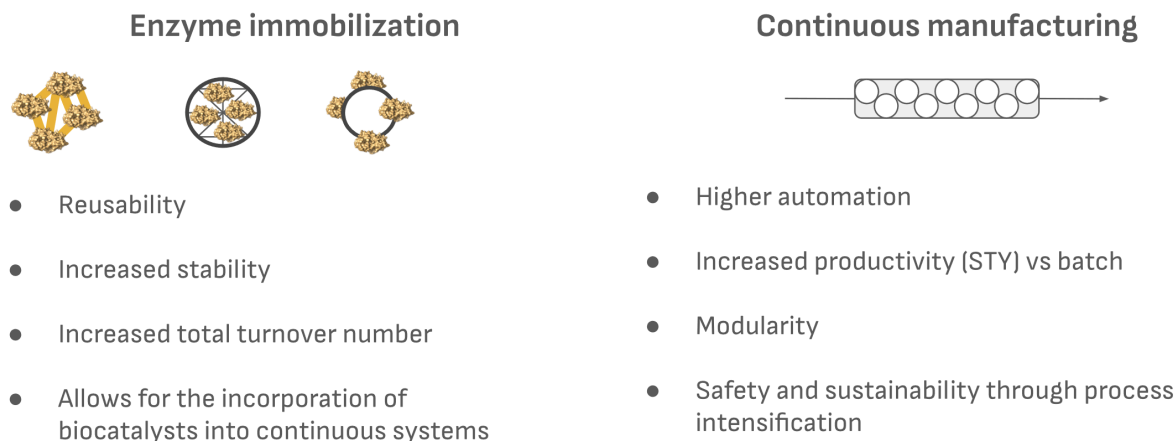
**Figure 1.** Main advantages of enzyme immobilization and continuous manufacturing.
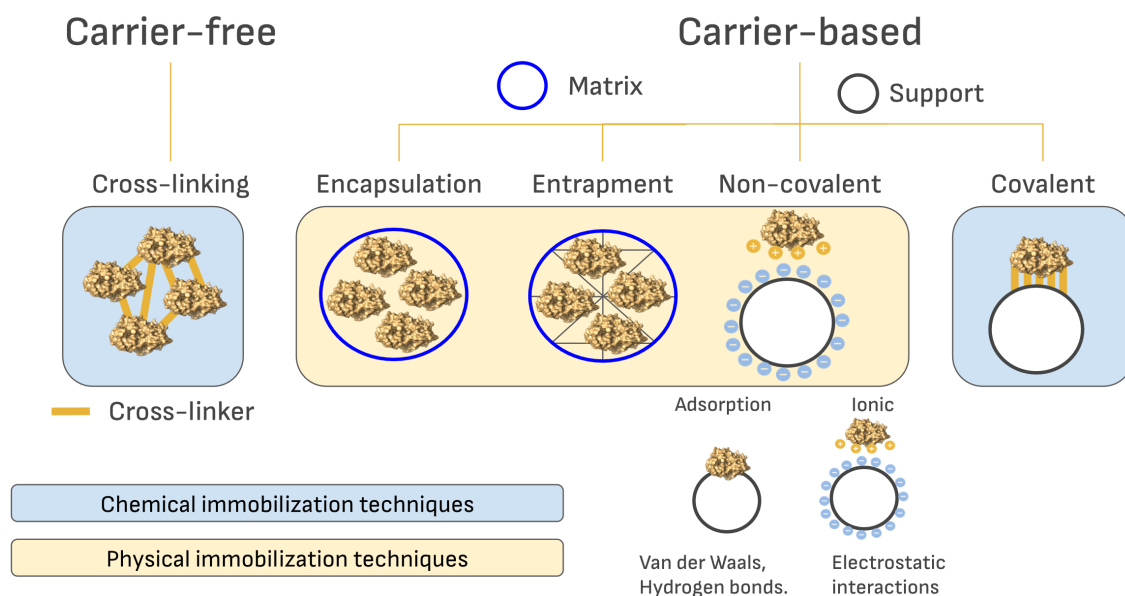


**Figure 2.** Schematic representation of the different methods of immobilization that have been used for continuous-flow biocatalysis.

the γ-lactamase CLEAs employed in a flow microreactor built from a capillary column [34,35].

On the other hand, CLECs show higher mechanical resistance and have been applied in different chemical reactor configurations [36,37]. Although only a few examples are available, their higher mechanical stability has allowed their successful use in PBRs (Figure 3). For example, glucoamylase CLECs have been used for the continuous production of glucose from starch and maltodextrin in PBRs [38]. In a more recent example, the preparation of differ-

ent β-substituted alcohols using halohydrin dehalogenase HheG CLECs has been successfully scaled up [32]. The production of HheG CLECs was performed using a stirred crystallization approach, enabling upscaling beyond 50 mL. The packing of these CLECs in a PBR facilitated the production of 2-azidocyclohexan-1-ol with an impressive space–time yield of 28.7 kg·L$^{-1}$·day$^{-1}$, demonstrating excellent operational stability and efficiency, which highlights their potential for industrial applications in continuous-flow processes.
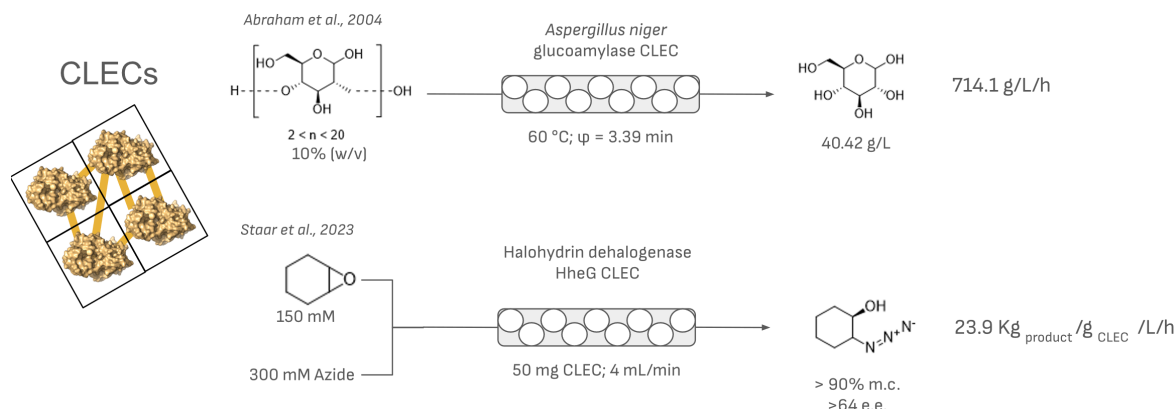
**Figure 3.** Selected examples of the use of CLECs in PBR systems.

## 2.2. *Carrier-based methods*

Carrier-based methods involve the use of a matrix or solid support that interacts with the enzymes and produces water-insoluble materials. The range of materials that have been already used is broad and expanding, including natural polymers, liposomes, petroleum-based polymers, inorganic materials, and more recently, metal-organic frameworks. The interaction of the enzyme with the carrier can be through physical confinement (entrapment and encapsulation), non-covalent interactions (adsorption, ionic interactions), or covalent bonding. Each of the strategies has its benefits and downsides. When using either entrapment or non-covalent interactions, the activity tends to be unaffected, but the reusability and stability of the resulting biocatalyst are generally low, except in specific enzyme types such as lipases, making its incorporation into continuous manufacturing processes challenging. On the other hand, with covalent methods, the reduced flexibility of the enzyme affects its activity but offers preparations with much higher stability and reusability.

### 2.2.1. *Entrapment and encapsulation methods*

Entrapment and encapsulation methods leverage a physical restriction of the enzymes or cells within a confined space or network using a carrier, in this case, a matrix. Several reviews focus on the techniques and discuss the applicability and limitations of these methods [39,40]. In general, entrapment provides a protective environment for the enzyme, but the presence of a surrounding extra layer causes

diffusional limitations. Moreover, if the pore size of the matrix is bigger than the enzyme size, potential leakage might happen during the reaction.

Probably the most common method of encapsulation of enzymes is alginate hydrogels [41,42]. Since the 1990s, a lot of research has focused on this method for its easy, cost-efficient, and mild conditions for preparation. Carefully controlling the conditions of polymerization, precursors, and modifiers allows for tailoring material porosity, which is especially important. Nonetheless, alginate encapsulation often suffers from low recyclability, a key aspect for applying biocatalysis in PBRs. Two different approaches have been taken to solve these problems: a post-entrapment treatment of the alginate beads and the entrapment of supramolecular enzyme structures (CLEAs, CLECs, and others).

One of the simplest post-modifications to alginate beads that has shown advantages is their drying. The so-called dried alginate-entrapped enzymes have been used in continuous flow for the production of fructo-oligosaccharides starting from sucrose (Figure 4). This strategy yielded a process with excellent productivity with a cheap and cost-effective immobilization method while keeping enzyme leakage minimal by selecting the appropriate process conditions (especially the control of water content in reaction to avoid rehydration) [43]. More recently, coating strategies with various polymers have also been tested to stabilize the alginate beads further, increase their reusability, and prevent the leaching of the enzyme. In some cases, the resulting preparations have been applied in PBRs, mostly as proof-of-concept re-
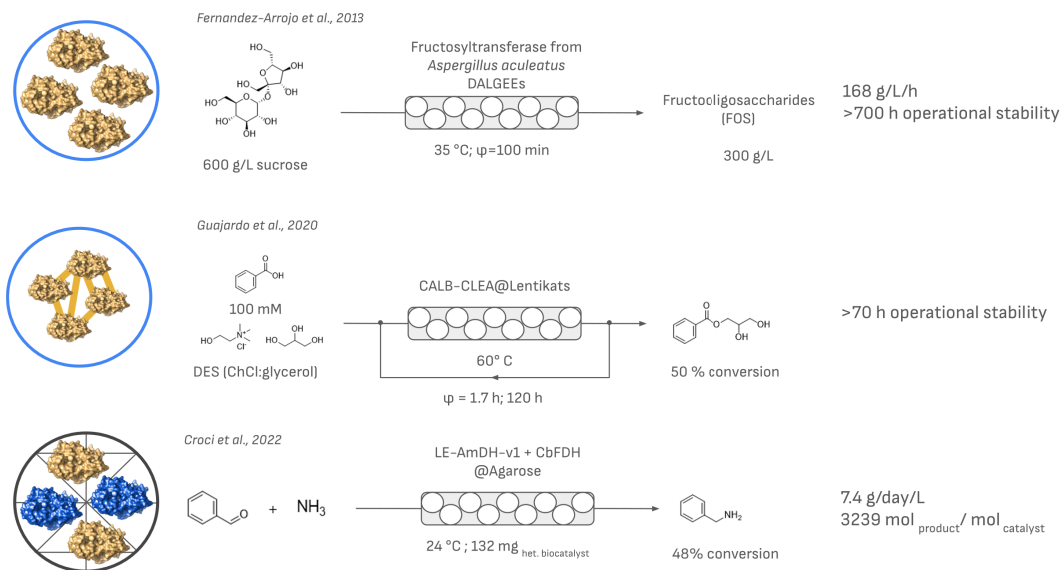
**Figure 4.** Selected examples of the use of entrapment and encapsulation methods in PBR systems. If specified in the original work, the contact time (φ) or the amount of biocatalyst used is indicated together with the space–time yield in g/L/h and either stability or productivity.

actions to show their applicability and advantages in terms of stability and reusability [44,45]. Although these strategies have been successful, the addition of a second layer hampers the free diffusion of the substrate and product from the bulk of the reaction to the biocatalyst. On the other hand, there are only a few examples of the use of supramolecular enzyme structures entrapped in alginate in PBRs [46,47].

Another interesting option for encapsulation is Lentikats®. Reported 20 years ago, Lentikats® mediated encapsulation relies on the formation of polyvinyl acetate hydrogels under mild conditions, harnessing the excellent mechanical stability that this polymer offers. Interestingly, the cross-linking of the enzyme is essential for entrapment to be efficient in Lentikats® as discussed even in the first reports [48]. Several samples have been incorporated into PBRs (Figure 4). Guajardo et al. [49] used a combination of CLEA and Lentikats® entrapment to allow for the use of a lipase (CALB) in deep eutectic solvents, which served both as the reaction media and cosubstrate. First, by preparing CLEA–CALB followed by encapsulation in Lentikats®, they created a biocatalyst that could be incorporated into a PBR and exhibited higher reusability (>65%) after six cycles of 24 h at 60 °C when compared to CLEA–CALB alone.

More recently, with the rise of additive manufacturing (3D printing) for biocatalysis [50], Rabe et al. investigated the use of entrapped enzymes in a 3D printed agarose matrix and their application in PBRs [51]. In their initial work, a keto-isovalerate decarboxylase mutant with enhanced thermal stability was printed in disks created with agarose. The resulting materials were stacked within a column reactor and used in the continuous production of isobutyraldehyde. The resulting entrapped enzyme retained 36% of the activity and could be used for over 5 h continuously with minimal elution of the enzyme (0.7%). The same technology was used by Croci et al. [52], but this time for the co-immobilization of an amine dehydrogenase (LE-AmDH-v1) and a cofactor regeneration partner (CbFDH). In their study, the authors compared different immobilization techniques highlighting the necessity to tailor the immobilization process to the enzymatic system. Entrapment within the agarose matrices was, in their case, the best solution to avoid enzyme inactivation upon immobilization and to maintain the stability of the immobilized preparation. When used in flow, it achieved up to $7.4 \text{ g·L}^{-1}\text{·day}^{-1}$ of productivity and a total turnover of $3239 \text{ mol}_{product}/\text{mol}_{enzyme}$.

### 2.2.2. *Carrier-bound immobilized enzymes for flow applications*

Carrier-binding methods involve the interaction of enzymes with water-insoluble materials, such as natural polymers and inorganic materials. This binding can be through physical adsorption, or covalent bonding.

**Physical adsorption.** Physical adsorption is one of the simplest and the earliest methods used for enzyme immobilization. It involves the attachment of enzymes onto carriers through weak forces such as van der Waals forces, ionic interactions, and/or hydrogen bonding. This method typically does not alter the native structure of the enzyme, preserving most of its catalytic activity [53]. This method was first described in 1916 when Nelson and Griffin demonstrated that an invertase physically adsorbed onto charcoal remained catalytically active [28]. However, the weak nature of these interactions also means that it is easy for the enzyme to leach, detaching from the support even under gentle conditions, and, in most cases, does not significantly improve enzyme stability [54].

Despite the limitations, enzyme adsorption has been widely used in industrial processes and enabled continuous production [53,55]. The most prominent example of this immobilization strategy is lipases [56], which have been extensively reviewed earlier [57,58]. These enzymes are mostly used in biodiesel production and enantioselective transesterification or hydrolysis of esters and amides.

One example of adsorption immobilization in industrial flow biocatalysis is Lipozyme® TL IM from Novozymes, a lipase from *Thermomyces lanuginosus* (Figure 5). The enzyme is immobilized by ionic adsorption onto silicate supports. Lipozyme® TL IM can be used in non-aqueous environments as PBRs, as the hydrophilic carrier retains the necessary water to maintain enzyme activity even in the presence of oils or organic solvents. It has been successfully applied in many industrial processes [59], including inter-esterification of sesame oil and fully hydrogenated soybean oil at 70 °C in continuous-flow PBRs, demonstrating the practical applicability of adsorbed biocatalysts [60]. Other lipases immobilized with similar strategies have also been applied successfully. Of importance is Novozym 435, which has been applied to a myriad of esterification and

hydrolysis reactions as a PBR [61,62]. Another industrial use of adsorption immobilization is the production of allulose in continuous flow using ketose-3-epimerase immobilized on an ion exchange resin and integrated in a PBR [63–65]. This method has led to significant cost reductions and even the commercialization of DOLCIA PRIMA® Allulose, a low-calorie sweetener.

Even multienzymatic systems have been immobilized using adsorption techniques (Figure 5). Co-immobilized lactate dehydrogenase and formate dehydrogenase on a carbon support facilitated ketone reduction with in situ cofactor recycling in a continuous-flow PBR. This system achieved a space–time yield of 11.2 $g \cdot L^{-1} \cdot h^{-1}$ in flow compared to 0.23 $g \cdot L^{-1} \cdot h^{-1}$ in batch processes, demonstrating the higher productivity achievable using low-flow reactor volumes (0.48 mL vs 24 mL in batch) [66].

Transaminases have also been immobilized through affinity adsorption using EziG™ materials. EziG™ is a hybrid controlled-pore glass coated with a functionalized polymer, engineered for selective metal-ion affinity immobilization of enzymes (Figure 5). It is designed for high loading of enzymes (up to 30% w/w). In a study performed by Böhmer et al., two stereoselective complementary $\omega$-transaminases were immobilized onto EziG™, achieving 20% w/w loading. These immobilized enzymes were then utilized in a multigram-scale continuous-flow PBR for the production of (S)-$\alpha$-MBA over 96 consecutive hours without any detectable loss of enzymatic activity [67,68].

**Covalent binding.** Covalent immobilization involves the formation of stable covalent bonds between enzyme functional groups—such as amino, carboxyl, and hydroxyl groups—and those on a suitable carrier (Figure 6). This method has become important due to the strong linkages it forms through multipoint attachment, which significantly reduces enzyme leaching and enhances stability compared to non-covalent adsorption-based methods [69]. The use of covalent binding in enzyme immobilization has been reported in numerous reviews [3,58,70,71].

An exemplary case of covalent immobilization in flow biocatalysis is the enzymatic synthesis of L-pipecolic acid using covalently immobilized lysine cyclodeaminase [72]. This study compared the reaction between a SpinChem® reactor and a PBR.

**Figure 5.** Examples of the application of non-covalently bound enzymes in a PBR system. If specified in the original work, the contact time (φ) or the amount of biocatalyst used is indicated together with the space–time yield in g/L/h and either stability or productivity.



**Figure 6.** Selected examples of covalently bound enzymes applied in PBR. The contact time (φ) is indicated together with the space–time yield in g/L/h and either stability or productivity.

Batch reactions with the enzyme in solution resulted in low conversion yields and significant enzyme deactivation over time. Conversely, when employing continuous-flow reactors, full conversion was achieved within 90 min while maintaining high operational stability. Additionally, the study compared different immobilization methods, including physical adsorption and covalent binding, revealing that covalent immobilization provided better reusability by preventing enzyme leaching.

Another example is the biocatalytic synthesis of (*R*)-sitagliptin in a recirculating PBR. In this case, a transaminase was co-immobilized with PLP inspired by the creation of a self-sufficient biocatalyst by Benítez-Mateos et al. [73]. This biocatalyst maintained yields and enantiomeric excess values above 90% and 99%, respectively, over 700 batch reactions without the use of additional PLP. An overall space–time yield of 40.0 g/L/h was obtained [74].

Additionally, the synthesis of (*S*)-nornicotine was enhanced through the covalent co-immobilization of IRED and NADP-dependent GDH on an epoxy resin within a PBR. This system maintained substrate conversion rates above 99% after 114 h of uninterrupted operation and attained a space–time yield of 211.47 g/L/h, which is 289.7 times higher than that of batch processes [75].

## 3. Current trends and outlook

The integration of enzymes into PBRs is highly dependent on developing novel materials and immobilization techniques. Due to the complexity of these immobilization methods as discussed in this review, it is challenging to determine in advance which immobilized biocatalyst will perform best in flow systems.

Consequently, immobilization strategies are approached on a case-by-case basis. Ideally, the search should focus on strategies that can (1) minimize enzyme desorption and deactivation, (2) enhance substrate and product diffusion to maximize conversion, and (3) simplify downstream processing. However, with current techniques, there is always a balance between biocatalyst activity and stability. It is true though that stability is often favored when applying enzymes in PBRs. Although immobilized enzyme activity might be lower than free enzyme activity, the high local concentration of enzymes within the

column allows for elevated substrate-to-catalyst ratios, resulting in higher conversion efficiency. Moreover, the precise control of reaction conditions within PBRs enables further process optimization. Adjustments such as increasing temperature, substrate loading, and implementing recirculation have been successfully employed to mitigate the lower activities observed in immobilized enzymes.

Innovation from material and chemical sides is still greatly needed in enzyme immobilization. Although immobilization has a long history, it remains predominantly based on interactions with charged amino acids, particularly the most reactive ones— almost exclusively cysteine and lysine or activated aspartic and glutamic acids. Therefore, developing new chemistry that can exploit other chemical handles is essential to ensure the process flexibility required for tailored immobilization strategies. Additionally, a deeper understanding of the interactions between enzymes and supports is important for optimizing these new immobilization techniques. Without this understanding, optimizing new immobilization strategies can be significantly hindered. Several key parameters of the support matrix are vital for maximizing the catalytic properties of immobilized enzymes. Consequently, investigations into novel formulations of bio-based polymers (such as lignocellulosic materials and innovative plastics), covalent- and metal-organic frameworks, and even solid materials previously regarded as waste are essential to enhance immobilization strategies [76–78].

Moreover, synergistically combining multiple immobilization techniques has shown promising results. Early examples included the combination of cross-linking and encapsulation. More recently, the integration of CLEAs with carrier-based immobilization has been employed to develop CLEANs (cross-linked enzyme-adhered nanoparticles), which have been applied to the synthesis of fragrances [79].

Adopting advanced screening technologies is crucial to identifying the most effective immobilization techniques. For example, López-Gallego and coworkers developed microtiter plate immobilization screening for high-throughput prototyping. This protocol tests 17 different carriers functionalized with various reactive groups in a 96-well plate format, simultaneously screening up to 21 immobilization protocols for up to 18 enzymes. By evaluating both activity and stability, this method enables the rapid

identification of optimal immobilization chemistry, significantly accelerating the development of efficient multienzyme systems [80]. Integrating computational tools like CapiPy, a Python-based GUI application, further enhances this workflow by rationalizing screening results and facilitating informed decision-making for immobilization strategies [81].

## Declaration of interests

Cristina Lía Fernández Regueiro and David Roura Padrosa are affiliated with inSEIT AG, and Francesca Paradisi is one of its founding members and its key scientific advisor.

## References

[1] C. M. Heckmann and F. Paradisi, "Looking back: A short history of the discovery of enzymes and how they became powerful chemical tools", *ChemCatChem* **12** (2020), pp. 6082–6102.

[2] H. E. Schoemaker, D. Mink and M. G. Wubbolts, "Dispelling the myths–biocatalysis in industrial synthesis", *Science* **299** (2003), pp. 1694–1697.

[3] R. DiCosimo, J. McAuliffe, A. J. Poulose and G. Bohlmann, "Industrial use of immobilized enzymes", *Chem. Soc. Rev.* **42** (2013), pp. 6437–6474.

[4] R. A. Sheldon, D. Brady and M. L. Bode, "The Hitchhiker's guide to biocatalysis: recent advances in the use of enzymes in organic synthesis", *Chem. Sci.* **11** (2020), pp. 2587–2605.

[5] K. H. Nam, "Glucose isomerase: functions, structures, and applications", *Appl. Sci.* **12** (2022), article no. 428.

[6] H. Yamada and M. Kobayashi, "Nitrile hydratase and its application to industrial production of acrylamide", *Biosci. Biotechnol. Biochem.* **60** (1996), pp. 1391–1400.

[7] S. Prasad and T. C. Bhalla, "Nitrile hydratases (NHases): at the interface of academia and industry", *Biotechnol. Adv.* **28** (2010), pp. 725–741.

[8] K. Buchholz, "A breakthrough in enzyme technology to fight penicillin resistance—industrial application of penicillin amidase", *Appl. Microbiol. Biotechnol.* **100** (2016), pp. 3825–3839.

[9] R. Buller, S. Lutz, R. J. Kazlauskas, R. Snajdrova, J. C. Moore and U. T. Bornscheuer, "From nature to industry: harnessing enzymes for biocatalysis", *Science* **382** (2023), article no. eadh8615.

[10] F. H. Arnold, "Directed evolution: bringing new chemistry to life", *Angew. Chem. Int. Ed.* **57** (2018), pp. 4143–4148.

[11] C. Li, R. Zhang, J. Wang, L. M. Wilson and Y. Yan, "Protein engineering for improving and diversifying natural product biosynthesis", *Trends Biotechnol.* **38** (2020), pp. 729–744.

[12] H. Cui, T. H. J. Stadtmüller, Q. Jiang, K.-E. Jaeger, U. Schwaneberg and M. D. Davari, "How to engineer organic solvent resistant enzymes: insights from combined molecular dynamics and directed evolution study", *ChemCatChem* **12** (2020), pp. 4073–4083.

[13] R. A. Rocha, R. E. Speight and C. Scott, "Engineering enzyme properties for improved biocatalytic processes in batch and continuous flow", *Org. Process Res. Dev.* **26** (2022), pp. 1914–1924.

[14] C. Wiles and P. Watts, "Continuous flow reactors: a perspective", *Green Chem.* **14** (2012), pp. 38–54.

[15] D. Dallinger and C. Oliver Kappe, "Why flow means green – evaluating the merits of continuous processing in the context of sustainability", *Curr. Opin. Green Sustain. Chem.* **7** (2017), pp. 6–12.

[16] B. Gutmann, D. Cantillo and C. Oliver Kappe, "Continuous-flow technology—a tool for the safe manufacturing of active pharmaceutical ingredients", *Angew. Chem. Int. Ed.* **54** (2015), pp. 6688–6728.

[17] S. Mascia, P. L. Heider, H. Zhang, et al., "End-to-end continuous manufacturing of pharmaceuticals: integrated synthesis, purification, and final dosage formation", *Angew. Chem. Int. Ed.* **52** (2013), pp. 12359–12363.

[18] G. Capellades, C. Neurohr, N. Briggs, K. Rapp, G. Hammersmith, D. Brancazio, B. Derksen and A. S. Myerson, "On-demand continuous manufacturing of ciprofloxacin in portable plug-and-play factories: implementation and in situ control of downstream production", *Org. Process Res. Dev.* **25** (2021), pp. 1534–1546.

[19] T. Bieringer, S. Buchholz and N. Kockmann, "Future production concepts in the chemical industry: modular—small-scale—continuous", *Chem. Eng. Technol.* **36** (2013), pp. 900–910.

[20] C. Badman, C. L. Cooney, A. Florence, K. Konstantinov, M. Krumme, S. Mascia, M. Nasr and B. L. Trout, "Why we need continuous pharmaceutical manufacturing and how to make it happen", *J. Pharm. Sci.* **108** (2019), pp. 3521–3523.

[21] J. K. Tom, M. M. Achmatowicz, M. G. Beaver, et al., "Implementing continuous manufacturing for the final methylation step in the AMG 397 process to deliver key quality attributes", *Org. Process Res. Dev.* **25** (2021), pp. 486–499.

[22] J. M. Bolivar, J. M. Woodley and R. Fernandez-Lafuente, "Is enzyme immobilization a mature discipline? Some critical considerations to capitalize on the benefits of immobilization", *Chem. Soc. Rev.* **51** (2022), pp. 6251–6290.

[23] A. A. Homaei, R. Sariri, F. Vianello and R. Stevanato, "Enzyme immobilization: an update", *J. Chem. Biol.* **6** (2013), pp. 185–205.

[24] A. I. Benítez-Mateos and F. Paradisi, "Perspectives on flow biocatalysis: the engine propelling enzymatic reactions", *J. Flow Chem.* **14** (2024), pp. 211–218.

[25] J. Britton, S. Majumdar and G. A. Weiss, "Continuous flow biocatalysis", *Chem. Soc. Rev.* **47** (2018), pp. 5891–5918.

[26] P. De Santis, L.-E. Meyer and S. Kara, "The rise of continuous flow biocatalysis—fundamentals, very recent developments and future perspectives", *React. Chem. Eng.* **5** (2020), pp. 2155–2184.

[27] M. Crotti, M. S. Robescu, J. M. Bolivar, D. Ubiali, L. Wilson and M. L. Contente, "Whats new in flow biocatalysis? a snapshot of 2020–2022", *Front. Catal.* **3** (2023), article no. 1154452.

[28] J. M. Nelson and E. G. Griffin, "Adsorption of invertase", *J. Am. Chem. Soc.* **38** (1916), pp. 1109–1115.

[29] L. Cao, L. van Langen and R. A. Sheldon, "Immobilised enzymes: carrier-bound or carrier-free?", *Curr. Opin. Biotechnol.* **14** (2003), pp. 387–394.

[30] V. Chauhan, D. Kaushal, V. K. Dhiman, S. S. Kanwar, D. Singh, V. K. Dhiman and H. Pandey, "An insight in developing carrier-free immobilized enzymes", *Front. Bioeng. Biotechnol.* **10** (2022), article no. 794411.

[31] U. Roessl, J. Nahálka and B. Nidetzky, "Carrier-free immobilized enzymes for biocatalysis", *Biotechnol. Lett.* **32** (2010), pp. 341–350.

[32] M. Staar and A. Schallmey, "Performance of cross-linked enzyme crystals of engineered halohydrin dehalogenase HheG in different chemical reactor systems", *Biotechnol. Bioeng.* **120** (2023), pp. 3210–3223.

[33] R. A. Sheldon, "Cross-linked enzyme aggregates as industrial biocatalysts", *Org. Process Res. Dev.* **15** (2011), pp. 213–223.

[34] A. M. Hickey, B. Ngamsom, C. Wiles, G. M. Greenway, P. Watts and J. A. Littlechild, "A microreactor for the study of biotransformations by a cross-linked γ-lactamase enzyme", *Biotechnol. J.* **4** (2009), pp. 510–516.

[35] A. M. Hickey, L. Marle, T. McCreedy, P. Watts, G. M. Greenway and J. A. Littlechild, "Immobilization of thermophilic enzymes in miniaturized flow reactors", *Biochem. Soc. Trans.* **35** (2007), pp. 1621–1623.

[36] T. S. Lee, M. K. Turner and G. J. Lye, "Mechanical stability of immobilized biocatalysts (CLECs) in dilute agitated suspensions", *Biotechnol. Progr.* **18** (2002), pp. 43–50.

[37] M. Conejero-Muriel, I. Rodríguez-Ruiz, S. Martínez-Rodríguez, A. Llobera and J. A. Gavira, "McCLEC, a robust and stable enzymatic based microreactor platform", *Lab on a Chip* **15** (2015), pp. 4083–4089.

[38] T. E. Abraham, J. R. Joseph, L. B. V. Bindhu and K. K. Jayakumar, "Crosslinked enzyme crystals of glucoamylase as a potent catalyst for biotransformations", *Carbohydr. Res.* **339** (2004), pp. 1099–1104.

[39] H. T. Imam, P. C. Marr and A. C. Marr, "Enzyme entrapment, biocatalyst immobilization without covalent attachment", *Green Chem.* **23** (2021), pp. 4980–5005.

[40] L. Betancor, F. López-Gallego, A. Hidalgo, M. Fuentes, O. Podrasky, G. Kuncova, J. M. Guisán and R. Fernández-Lafuente, "Advantages of the pre-immobilization of enzymes on porous supports for their entrapment in Sol-Gels", *Biomacromolecules* **6** (2005), pp. 1027–1030.

[41] O. Smidsrod and G. Skjakbrk, "Alginate as immobilization matrix for cells", *Trends Biotechnol.* **8** (1990), pp. 71–78.

[42] J. E. Fraser and G. F. Bickerstaff, "Entrapment in calcium alginate", in *Immobilization of Enzymes and Cells* (G. F. Bickerstaff, ed.), Humana Press: Totowa, NJ, 1997, pp. 61–66.

[43] L. Fernandez-Arrojo, B. Rodriguez-Colinas, P. Gutierrez-Alonso, M. Fernandez-Lobato, M. Alcalde, A. O. Ballesteros and F. J. Plou, "Dried alginate-entrapped enzymes (DALGEEs) and their application to the production of fructooligosaccharides", *Proc. Biochem.* **48** (2013), pp. 677–682.

[44] J. Pauly, H. Gröger and A. V. Patel, "Design, characterisation and application of alginate-based encapsulated pig liver esterase", *J. Biotechnol.* **280** (2018), pp. 42–48.

[45] P. Rehbein, N. Raguz and H. Schwalbe, "Evaluating mechanical properties of silica-coated alginate beads for immobilized biocatalysis", *Biochem. Eng. J.* **141** (2019), pp. 225–231.

[46] J. Moriyama and M. Yoshimoto, "Efficient entrapment of carbonic anhydrase in alginate hydrogels using liposomes for continuous-flow catalytic reactions", *ACS Omega* **6** (2021), pp. 6368–6378.

[47] F. Zhao, H. Li, X. Wang, et al., "CRGO/alginate microbeads: an enzyme immobilization system and its potential application for a continuous enzymatic reaction", *J. Mater. Chem. B* **3** (2015), pp. 9315–9322.

[48] M. Jekel, A. Buhr, T. Willke and K. D. Vorlop, "Immobilization of biocatalysts in Lentikats", *Chem. Eng. Technol.* **21** (1998), pp. 275–279.

[49] N. Guajardo, K. Ahumada and P. D. De María, "Immobilized lipase-CLEA aggregates encapsulated in Lentikats® as robust biocatalysts for continuous processes in deep eutectic solvents", *J. Biotechnol.* **310** (2020), pp. 97–102.

[50] E. Gkantzou, M. Weinhart and S. Kara, "3D printing for flow biocatalysis", *RSC Sustain.* **1** (2023), pp. 1672–1685.

[51] M. Maier, C. P. Radtke, J. Hubbuch, C. M. Niemeyer and K. S. Rabe, "On-demand production of flow-reactor cartridges by 3D printing of thermostable enzymes", *Angew. Chem. Int. Ed.* **57** (2018), pp. 5539–5543.

[52] F. Croci, J. Vilím, T. Adamopoulou, V. Tseliou, P. J. Schoenmakers, T. Knaus and F. G. Mutti, "Continuous flow biocatalytic reductive amination by co-entrapping dehydrogenases with agarose gel in a 3D-printed mould reactor", *ChemBioChem* **23** (2022), article no. e202200549.

[53] T. Jesionowski, J. Zdarta and B. Krajewska, "Enzyme immobilization by adsorption: a review", *Adsorption* **20** (2014), pp. 801–821.

[54] D. Brady and J. Jordaan, "Advances in enzyme immobilisation", *Biotechnol. Lett.* **31** (2009), pp. 1639–1650.

[55] A. Basso and S. Serban, "Industrial applications of immobilized enzymes—a review", *Mol. Catal.* **479** (2019), article no. 110607.

[56] R. Fernandez-Lafuente, P. Armisén, P. Sabuquillo, G. Fernández-Lorente and J. M. Guisán, "Immobilization of lipases by selective adsorption on hydrophobic supports", *Chem. Phys. Lipids* **93** (1998), pp. 185–197.

[57] A. Letícia Silva Coelho and R. Casarotti Orlandelli, "Immobilized microbial lipases in the food industry: a systematic literature review", *Crit. Rev. Food Sci. Nutr.* **61** (2021), pp. 1689–1703.

[58] D. Remonatto, R. H. Miotti Jr, R. Monti, J. C. Bassan and A. V. de Paula, "Applications of immobilized lipases in enzymatic reactors: a review", *Proc. Biochem.* **114** (2022), pp. 1–20.

[59] R. Fernandez-Lafuente, "Lipase from thermomyces lanuginosus: uses and prospects as an industrial biocatalyst", *J. Mol. Catal. B: Enzym.* **62** (2010), pp. 197–212.

[60] A. Lopez-Hernandez, C. Otero, E. Hernández-Martín, H. S. Garcia and C. G. Hill Jr, "Interesterification of sesame oil and a fully hydrogenated fat using an immobilized lipase catalyst in both batch and continuous-flow processes", *Eur. J. Lipid Sci. Technol.* **109** (2007), pp. 1147–1159.

[61] C. Ortiz, M. Luján Ferreira, O. Barbosa, J. C. S. dos Santos, R. C. Rodrigues, Á. Berenguer-Murcia, L. E. Briand and R. Fernandez-Lafuente, "Novozym 435: the "perfect" lipase immobilized biocatalyst?", *Catal. Sci. Technol.* **9** (2019), pp. 2380–2420.

[62] A. Khan, S. K. Sharma, A. Kumar, A. C. Watterson, J. Kumar and V. S. Parmar, "Novozym 435-catalyzed syntheses of polyesters and polyamides of medicinal and industrial relevance", *ChemSusChem* **7** (2014), pp. 379–390.

[63] R. D. Woodyer and R. W. Armentrout, 3-epimerase, WO patent, WO2014049373A1, 2014.

[64] R. D. Woodyer, J. C. Cohen and J. R. Bridges, Sweetener, US patent, US9635879B2, 2017.

[65] B.-C. Lim, H.-J. Kim and D.-K. Oh, "A stable immobilized d-psicose 3-epimerase for the production of d-psicose in the presence of borate", *Proc. Biochem.* **44** (2009), pp. 822–828.

[66] B. Poznansky, L. A. Thompson, S. A. Warren, H. A. Reeve and K. A. Vincent, "Carbon as a simple support for redox biocatalysis in continuous flow", *Org. Process Res. Dev.* **24** (2020), pp. 2281–2287.

[67] W. Böhmer, T. Knaus, A. Volkov, T. K. Slot, N. Raveendran Shiju, K. Engelmark Cassimjee and F. G. Mutti, "Highly efficient production of chiral amines in batch and continuous flow by immobilized ω-transaminases on controlled porosity glass metal-ion affinity carrier", *J. Biotechnol.* **291** (2019), pp. 52–60.

[68] W. Böhmer, A. Volkov, K. Engelmark Cassimjee and F. G. Mutti, "Continuous flow bioamination of ketones in organic solvents at controlled water activity using immobilized ω-transaminases", *Adv. Synt. Catal.* **362** (2020), pp. 1858–1867.

[69] C. Linqiu, *Carrier-bound Immobilized Enzymes: Principles, Application and Design*, John Wiley & Sons, Willey-VCH: New Jersey, 2006.

[70] A. Schmid, J. S. Dordick, B. Hauer, A. Kiener, M. Wubbolts and B. Witholt, "Industrial biocatalysis today and tomorrow", *Nature* **409** (2001), pp. 258–268.

[71] A. Liese and L. Hilterhaus, "Evaluation of immobilized enzymes for industrial applications", *Chem. Soc. Rev.* **42** (2013), pp. 6236–6249.

[72] K. Stalder, A. I. Benitez-Mateos and F. Paradisi, "Biocatalytic synthesis of L-pipecolic acid by a lysine cyclodeaminase: batch and flow reactors", *ChemCatChem* **16**, article no. e202301671.

[73] A. I. Benítez-Mateos, M. L. Contente, S. Velasco-Lozano, F. Paradisi and F. López-Gallego, "Self-sufficient flow-biocatalysis by coimmobilization of pyridoxal 5′-phosphate and ω-transaminases onto porous carriers", *ACS Sustain. Chem. Eng.* **6** (2018), pp. 13151–13159.

[74] X.-J. Zhang, H.-H. Fan, N. Liu, X.-X. Wang, F. Cheng, Z.-Q. Liu and Y.-G. Zheng, "A novel self-sufficient biocatalyst based on transaminase and pyridoxal 5′-phosphate covalent co-immobilization and its application in continuous biosynthesis of sitagliptin", *Enzyme Microb. Technol.* **130** (2019), article no. 109362.

[75] S. Guan, W. Zhou, Y. Yue, S. Wang, B. Chen and H. Yang, "Efficient synthesis of (S)-nornicotine using co-immobilized IRED and GDH in batch and continuous flow reaction systems", *Org. Process Res. Dev.* **28** (2024), pp. 2050–2060.

[76] S. Liu, M. Bilal, K. Rizwan, I. Gul, T. Rasheed and H. M. N. Iqbal, "Smart chemistry of enzyme immobilization using various support matrices—a review", *Int. J. Biol. Macromol.* **190** (2021), pp. 396–408.

[77] F. T. T. Cavalcante, A. L. G. Cavalcante, I. G. de Sousa, F. S. Neto and J. C. S. dos Santos, "Current status and future perspectives of supports and protocols for enzyme immobilization", *Catalysts* **11** (2021), article no. 1222.

[78] M. N. Morshed, N. Behary, N. Bouazizi, J. Guan and V. A. Nierstrasz, "An overview on biocatalysts immobilization on textiles: preparation, progress and application in wastewater treatment", *Chemosphere* **279** (2021), article no. 130481.

[79] F. Nagy, E. Sánta-Bell, M. Jipa, et al., "Cross-linked enzyme-adhered nanoparticles (CLEANs) for continuous-flow bioproduction", *ChemSusChem* **15** (2022), article no. e202102284.

[80] I. L. López, M. Sánchez-Costa, A. H. Orrego, N. Zeballos, D. Roura Padrosa and F. López-Gallego, "Microtiter plate immobilization screening for prototyping heterogeneous enzyme cascades", *Angew. Chem. Int. Ed.* **63** (2024), article no. e202407411.

[81] D. Roura Padrosa, V. Marchini and F. Paradisi, "CapiPy: python-based GUI-application to assist in protein immobilization", *Bioinformatics* **37** (2021), pp. 2761–2762.

Account

# Accelerating the implementation of biocatalysis in pharmaceutical research and development portfolio

**Alain Rabion** [*, a], **Davide Panigada** [ⓘ, a], **Sebastien Roy** [a], **Antony Bigot** [ⓘ, a] and
**Jason S. Tedrow** [ⓘ, b]

[a] Sanofi's Chemistry, Manufacturing and Control, 1 impasse des ateliers, 94400 Vitry-sur-Seine, France

[b] Sanofi's Chemistry, Manufacturing and Control, 350 Water St, Cambridge (U.S.) Massachusetts 02141, USA

*E-mails:* alain.rabion@sanofi.com (A. Rabion), davide.panigada@sanofi.com (D. Panigada), sebastien.roy@sanofi.com (S. Roy), antony.bigot@sanofi.com (A. Bigot), jason.tedrow@sanofi.com (J. S. Tedrow)

**Abstract.** Biocatalysis is widely regarded as a sustainable technology to innovate Active Pharmaceutical Ingredient (API) synthesis. Biotransformation is considered a unique technology in the drug manufacturing world to unlock synthetic routes to complex chiral motifs. Sanofi is accelerating the development of strong mindset and efficient capabilities in biocatalysis to foster API delivery and promote greener solutions for its synthetic processes.

In this article, we will describe how Sanofi is building its internal biocatalytic capabilities in order to address new challenges related to sustainability and the growing complexity of its portfolio. The outcomes of recent studies will be presented demonstrating the successful implementation of the biocatalysis technology across early and late-stage development of our pipeline assets.

## 1. Introduction

In the past decade, advances in protein engineering, genomic database mining, and computational methods associated with high-throughput screening tools and DNA library synthesis have enabled a step change in biocatalysis. As a consequence, the nature of biocatalytic transformations can be nearly infinitely tunable and optimizable with billions of combinations of alterations to tailor specific reactivity and selectivity [1]. Due to modern directed evolution techniques [2,3], advanced artificial intelligence (AI) [4], machine learning (ML) techniques [5,6], the introduction of non-natural amino acids and new reactivity [1], the potential of biocatalysis to transform modern drug manufacturing has been expanded. The field has moved beyond traditional like-for-like enzyme replacements to wholly new routes designed around system biocatalysis [7,8]. Sanofi, among others, has identified biotransformations as one of the most transformative technologies to date in the synthesis of today's complex new drug candidates. In this article, we describe how Sanofi is accelerating the implementation of biocatalysis in its pharmaceutical research and development portfolio. For details, original publications and patents are referenced.

[*]Corresponding author
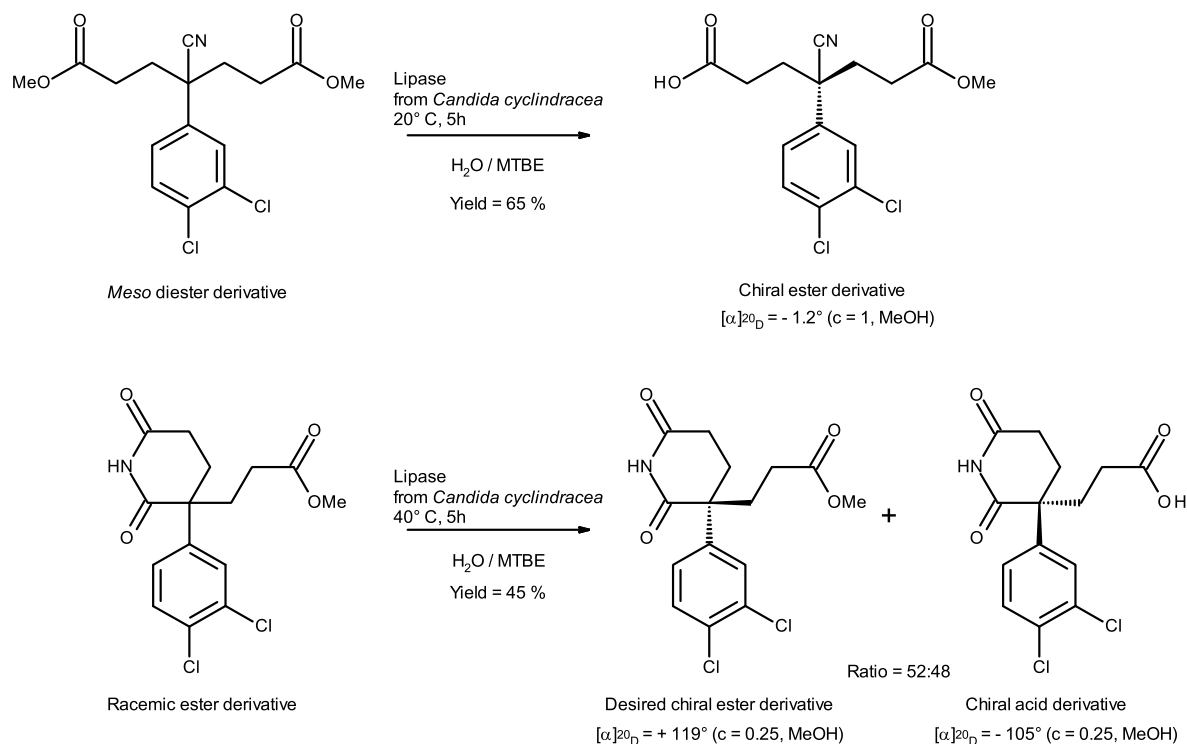
**Scheme 1.** Examples of biocatalytic transformation at Sanofi [9].

## 2. History of Sanofi use and production of enzymes

Sanofi has extensive experience in the synthesis of molecules of interest, including small molecules and recombinant enzymes, through fermentation processes.

Sanofi also used enzyme technologies to produce small molecules at various stages of their development. Discovery capabilities were developed to produce drug metabolites for quantification and profiling of in-vivo generated compounds. The CYP450 enzymes of microorganisms are well described for their metabolizing ability, as "the microbial model for drug metabolism". This type of technology was developed internally, and the use of such enzymes has been proven to be an efficient way to produce either Phase I or Phase II metabolites [10] in their labeled [11,12] or non-labeled form. Another class of enzyme used for the synthesis of Carbon-14-radiolabeled metabolite is nitrilase. We showed that radiolabeled nitrile derivatives can be hydrolyzed

to get the corresponding radiolabeled acid, using mild enzymatic conditions [13,14]. In addition to the use of biocatalysis for small-scale pharmaceutical metabolite synthesis, implementation of enzyme technologies for the scalable synthesis of pharmaceutical advanced intermediates was also developed. Castro et al. [9] identified commercial lipase for the enantioselective hydrolysis of racemic carboxylic ester and for the desymmetrization of a symmetrical diester to achieve a chiral monoacid ester product (Scheme 1).

By taking advantage of internal history in using enzymes for synthesizing optically molecules, and in fermentation processes, Sanofi decided in early 2020, to build a fully integrated end-to-end biocatalysis platform within the Process Chemistry department belonging to the R&D organization. This platform aims to provide chemists with efficient tools for improving the environmental impact of API synthesis and addressing the challenges associated with the growing complexity of molecules entering development.

**Figure 1.** Sanofi charter on Planet Care environmental sustainability program.

## 3. Biosynthesis technology to address new challenges from the R&D portfolio

Sanofi has a strong ambition to build a sustainable environment with a global approach to minimizing impacts. Three main axes have been defined and are described in Figure 1. A key pillar toward achieving these environmental commitments revolves around reducing the environmental footprint of manufacturing processes through an ecodesign approach. This includes reduced water and solvent use, eliminating toxic metals, reagents and solvents, and lowering energy requirements. To meet our long-term environmental sustainability commitment, technological innovations such as biocatalysis, are required.

### 3.1. *Molecular complexity of next generation small molecule APIs*

A general trend at Sanofi, and elsewhere, is that new molecular entities entering development are increasing in complexity (Figure 2) [15]. The trend is moving away from traditional activators/inhibitors toward a next-generation approach of stabilizing or disrupting complex protein–protein interactions (next-generation small molecules) to obtain the desired effects. Additionally, the introduction of bispecific small molecule degraders has also increased the overall complexity and size of the synthetic targets. With increased complexity comes chemistry manufacturing and control (CMC) risks to supply,

**Figure 2.** Evolution of the structural complexity in Sanofi's small molecule portfolio.

resources, time to clinic and/or cost manufacture. The utilization of biotransformation is a key lever to help us manage the increase in synthetic complexity.

## 4. How we proceed to accelerate the implementation of biocatalysis in the Sanofi Pharmaceutical R&D Portfolio

Sanofi's strategy is based on three pillars.

### 4.1. *Development of a route-scouting mindset for an innovative route design approach*

We consider that organic chemists and biochemists need to work together to design routes integrating a biocatalytic retrosynthesis approach, supported by a strong network of external experts and partners (Figure 3). The biosynthetic technologies team is integrated into the global Process Chemistry organization which favors scientific exchange through brainstorming sessions on innovative chemical route design. Furthermore, enzymatic transformations can be considered for the design of clinical and commercial routes thanks to new enzyme engineering techniques that can quickly deliver an effective biocatalyst in a short time.

### 4.2. *Contribution all along value chain (Figure 4)*

At the research stage, the main input from biocatalysis is either to produce metabolites or to generate diversity through late-stage functionalization (LSF) for accelerating compound discovery [16]. Currently, we are using biotransformation early in discovery as a diversity engine to aid candidate generation.

Starting in preclinical development, a first generation of synthetic routes is used for delivering preclinical and clinical batches with a focus on speed to the clinic. A retrosynthetic strategy integrating biotransformation from the beginning has proven to be of great interest. Accelerating pressure on clinical timelines is squeezing development timelines and shifting our strategy toward fewer cycles of route selection and development. In some cases, this can mean keeping the same disconnection strategy throughout the product's life cycle, but optimizing, concatenating and replacing less sustainable technologies with highly selective and efficient technologies. This could involve using an off-the-shelf enzyme, readily accessible at scale, that may not be optimal for the system but can sustain projects within a short timeframe (see example in Section 5). Another option is to utilize a non-enzymatic strategy that could

**Figure 3.** Route design workflow.
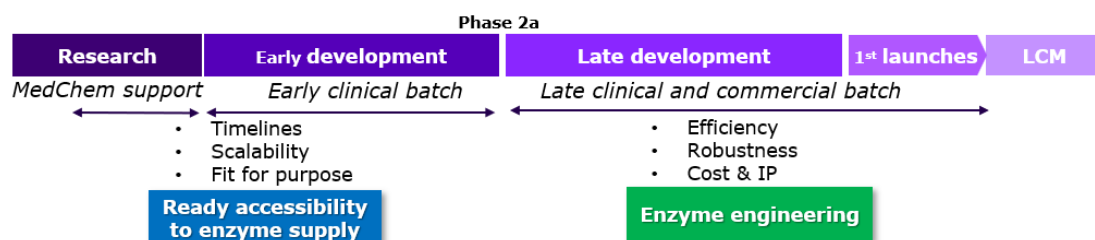


**Figure 4.** Implementation of biocatalysis all along the value chain.

be replaced by a more sustainable biocatalyzed sequence later in the development phase. An illustrative example from our R&D portfolio of such chemical transformation is the asymmetric hydrogenation catalyzed by a very expensive chiral ruthenium catalyst (Scheme 2) [17].

In addition to the costly precious ruthenium catalyst, the diastereoisomeric ratio obtained after the chemo selective reduction step was moderate (84:16), negatively impacting the process efficiency, manufacturing costs, and waste generation. To anticipate potential constraints regarding large-scale drug supply, we initiated a study on biocatalytic transformation using ketoreductase (KRED) enzymes [18].

One enzyme was found to be highly selective toward the desired *cis* alcohol product **B** (*cis*/*trans* = 99:1 and enantiomeric excess ~90%). Our results demonstrate that the KRED enzyme is an alternative to the ruthenium catalyst for the reduction of the very bulky ketone substrate **A** to the chiral alcohol product **B**.

Once the project has moved into late clinical development and, drug supply has been taken out of the critical path, the time and resources needed to find the most ideal way to utilize biotransformation was investigated. At that stage, the chemical route for launch is selected and we can introduce the fully engineered enzyme as if we can replace one catalyst by another one. The objective at this point is to meet the prerequisites of an industrial process, including pro-

ductivity, yield, turnover number, robustness, cost. Finally, the incorporation of the biocatalytic strategy early in development, when possible, allows us to focus our efforts on enzyme engineering and optimization instead of compressing enzyme development on top of additional route selection activities.

### 4.3. *Building efficient capacity*

A biosynthetic technologies team was created, designed for end-to-end biocatalyst development and deployment, able to take in charge the different studies related to biocatalysis involved at early and late development phases.

A global workflow has been established and related capacities and expertise have been developed internally with the support of key partners to rapidly implement biocatalytic process:

- Molecular biology platform including expertise in enzyme discovery and in the design of new enzyme through protein engineering approaches such as directed evolution or more rational engineering. This is supported by internal protein physical modeling. Regarding the large computational power needed for the enzyme searches and multimodal modifications we have implemented strategic partnerships in order to enhance our in-house capabilities.

Initial ruthenium-catalyzed hydrogenation
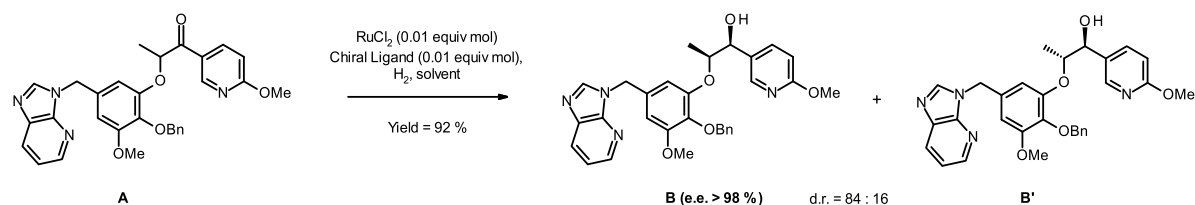


Alternative KRED catalyzed reduction
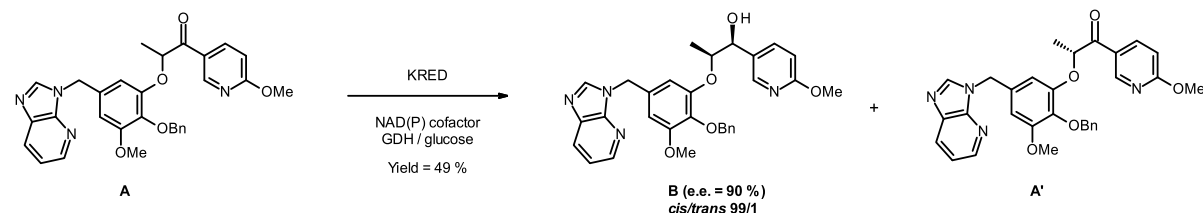


**Scheme 2.** Initial ruthenium-catalyzed hydrogenation [17] and KRED-mediated biocatalytic reaction [18] affording chiral hydroxy intermediate **B**.

- Reaction engineering capacities including medium- and high-throughput equipment and homothetic vessels for the development and the optimization studies of biocatalytic reaction.
- Enzyme production platform including various host fermentation and formulation techniques for biocatalysts production.
- Pilot capacities for the upscaling of biocatalytic processes and the production of enzymes at medium scale by fermentation.
- Analytical platform capable of developing analytical methods for reaction monitoring, conducting structural analyses for product and impurity identification, and characterizing biocatalytic enzyme.

## 5. Recent examples of enzyme use in the manufacture of APIs across early- and late-stage development

One of the first projects, using biocatalysts in manufacturing and studied in the newly created biosynthesis technology platform, was the new route toward a potent and selective LRRK2 inhibitor via chiral intermediate **1** [18–22]. One key intermediate of the route, for the early preclinical batches, was the chiral 3-hydroxy 4-methyl tetrahydrofuran **4**, which could be prepared by an enantio- and diasteroselective reduction of ketone **5** (Scheme 3) [19,23].

Access to the challenging fragment **4** for early clinical deliveries was first achieved through the enabling route presented in Scheme 4.

In this first-generation route, it should be noted that to increase the enantiomeric excess of **4**, a lipase-catalyzed kinetic resolution (esterification) was performed, using Lipase Amano AK [24] from *Pseudomonas fluorescens* (commercially available from Sigma-Aldrich) in the presence of vinyl acetate. This resulted in an isolated enantio-enriched (ee = 94%) O-acetylated intermediate **8** which was then deprotected to generate enantio-enriched secondary alcohol **4** (ee = 94%). However, this suboptimal enantiomeric excess necessitates performing a chiral SFC later in the synthesis, as requested by the project.

This synthetic route faced CMC risks related to the supply of 50 kg of intermediate **4**, resources, time to clinic and cost of manufacture. Therefore, alternate chemistry was quickly required to advance the program.

Having solved the challenge associated with the preparation of **5** through a safe process [19], we then turned our attention to the challenging task of improving both the yield and the enantiomeric excess of compound **4**, while diminishing the number of steps.
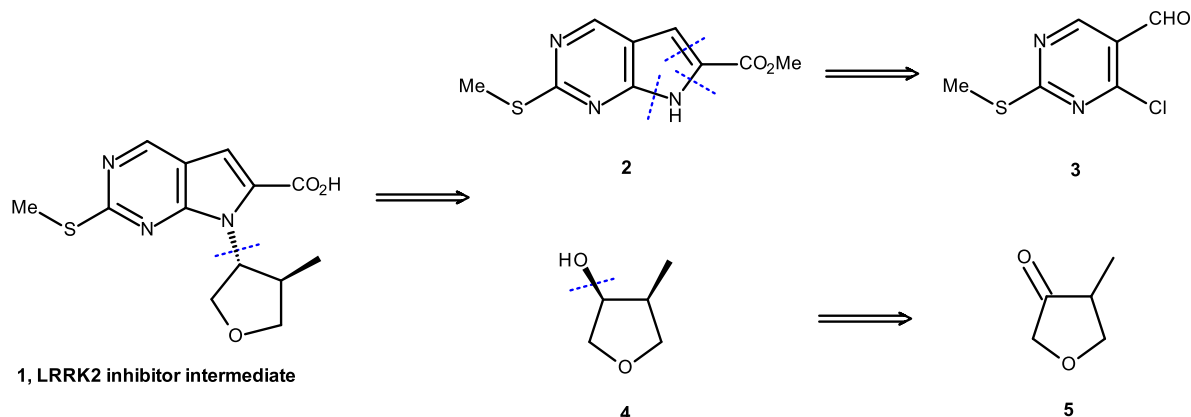
**Scheme 3.** Disconnection of **1** toward simpler fragments.
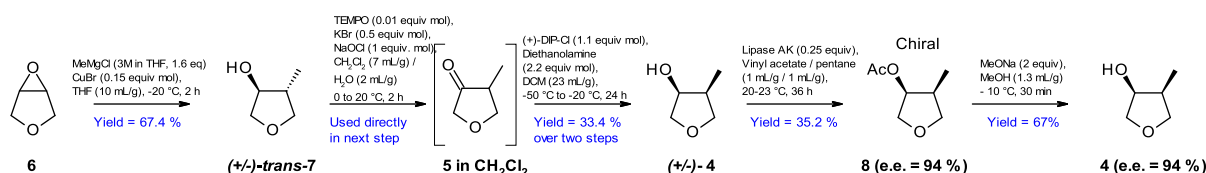


**Scheme 4.** Enabling route to chiral tetrahydrofuran derivative **4**.

Starting from methyl ketone **5**, we explored the synthesis of **4** through asymmetric reduction with KRED enzymes (Scheme 5) which are known to catalyze the reduction of sterically hindered ketones into the corresponding chiral alcohol [25,26]. Due to short project timelines, we went for commercial or readily available enzymes for first deliveries while postponing the expensive and time-consuming enzyme evolution studies until later. Following an internal screening of KRED enzymes from commercially available kits, a very selective and active enzyme was found and selected for further process development.

Interestingly, the complete conversion of the two enantiomers of the ketone into one main diastereoisomer of the hydroxy methyl tetrahydrofuran, **4** demonstrated that a dynamic kinetic resolution is occurring under the reaction conditions (Scheme 6).

The optimized laboratory process was further refined to fit the scale and was successfully scaled in the pilot plant to 40 kg of ketone **5** per batch (Table 1). Yield and enantiomeric excess like those observed at laboratory scale were obtained, demonstrating the robustness of the biocatalytic process.

A qualitative comparison between the enabling route (3 steps from ketone **5**) and the biocatalytic
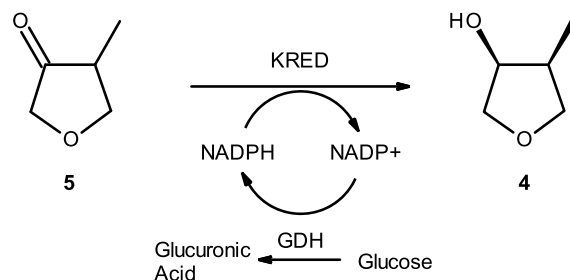


**Scheme 5.** Synthesis of **4** via KRED reaction: global reaction scheme principle.

alternative (1 step from ketone **5**) is shown in Table 2 [19].

The one step enzymatic process outperforms the three steps chemical reactions in terms of yield, waste generated, scalability, and timelines. Ultimately, the enzymatic route was the only viable alternative for large scale clinical batch manufacturing to meet timelines and quality.

After unlocking the production of preclinical and clinical batches with the implementation of the ketoreductase process to produce the chiral hydroxy methyl tetrahydrofuran derivative, we looked for
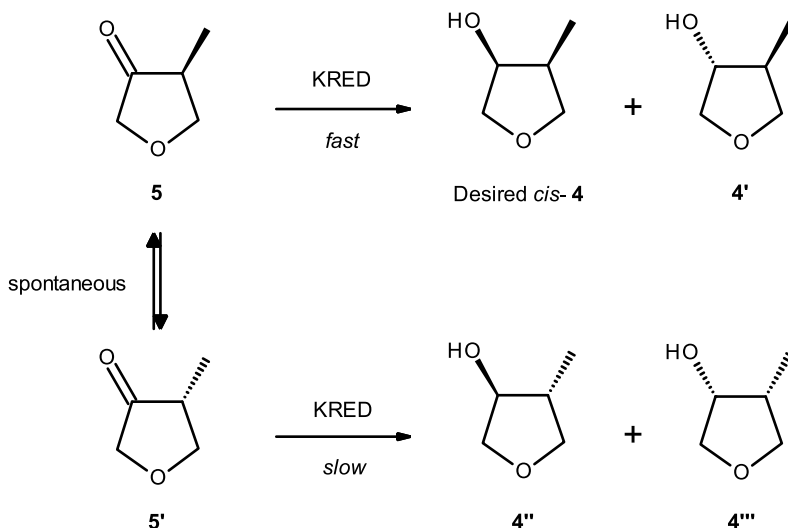
**Scheme 6.** Kinetic resolution (KR) and dynamic reductive kinetic resolution (DRKD) based on ketoreductase-catalyzed reduction.

**Table 1.** Scale up results for preparation of alcohol 4

| Batch type | Starting material | Product | ee (%)[a] | *cis*/*trans* Ratio[a] | Yield (%)[*] |
|---|---|---|---|---|---|
| Demo batch | 1.155 kg | 0.86 kg | >99.9 | 16.7 | 73.2 |
| Pilot plant #1 | 39.95 kg | 31.7 kg | >99.9 | 13.4 | 78.0 |
| Pilot Plant #2 | 33.75 kg | 25.6 kg | >99.9 | 14.9 | 75.0 |

[*]Assay yield. [a]Calculation: Ratio *cis*/*trans*: $R = \sum[cis(S,S) + cis(R,R)]/\sum[trans(R,S) + trans(S,R)]$. Enantiomeric excess: ee (%) = $100 \times [cis(S,S) - cis(R,R)]/\sum[cis(S,S) + cis(R,R)]$.

**Table 2.** Qualitative comparison between enabling and biochemical processes from ketone 5 to alcohol 4

| Route | Number of steps | Work up Chromato. | Operating temp | Solvent with constraints | Isolated yield (%) | *cis*/*trans* ratio | ee (%) | PMI (kg/kg) |
|---|---|---|---|---|---|---|---|---|
| Enabling[a] | 3 | 1 | −65 °C | $CH_2Cl_2$ | 8 | >30 | 93.0 | 1142 |
| Enzymatic[b] | 1 | 0 | 30 °C | None | 75 | 14.9 | >99.9 | 151 |

[a]Kilolab campaign, [b]Pilot plant campaign #2.

an optimal synthesis route in anticipation of the commercial launch (Scheme 7)[1].

The preclinical route based on the chiral hydroxy methyl tetrahydrofuran derivative intermediate **4** was first assessed [19]. The enantiomerically pure compound **4** obtained from KRED-mediated reduction was introduced at the next step of synthesis under Mitsunobu conditions. It quickly became apparent that this transformation was not efficient enough due to the formation of by-products such as triphenylphosphine oxide as well as reduced form of

Preclinical route
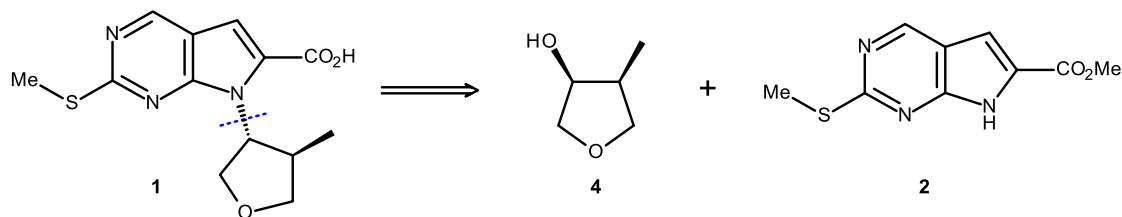


Alternative route
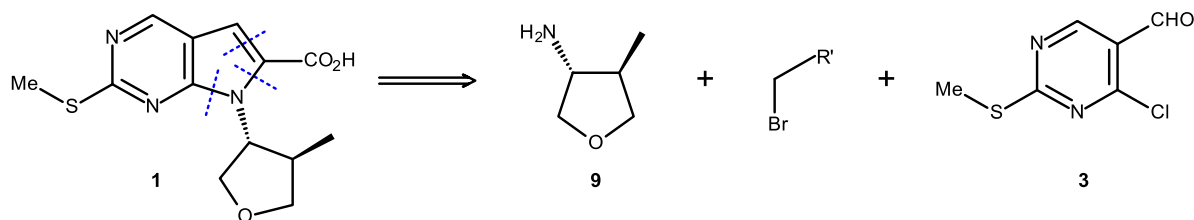


**Scheme 7.** Disconnections integrating hydroxy methyl tetrahydrofuran **4** and amino methyl tetrahydrofuran **9**.

DIAD used in the Mitsunobu reaction. Additionally, an excess of compound **4** (3 equiv) was necessary, likely due to decomposition under the reaction conditions [27].

To install the chiral fragment into the molecule, the *trans*-(3*R*,4*R*)-amino methyl tetrahydrofuran derivative **9** was identified as a potential intermediate. It was demonstrated that it could be introduced into the global synthesis through an efficient nucleophilic substitution reaction without degrading the diastereoselectivity. Having solved the challenge associated with the introduction of the chiral fragment onto the molecule, we then turned our attention to the challenging task of preparing the chiral amino methyl tetrahydrofuran derivative **9**.

Two alternative routes have been evaluated in parallel, namely alternative 1 (chemical pathway) and alternative 2 (enzymatic pathway) starting from the same methyl ketone intermediate **5** (Scheme 8). The chemical route initially studied produced the first grams of the chiral (3*R*,4*R*)-amino methyl tetrahydrofuran derivative **9**, which allowed validation of the end of the synthesis. It should be noted that diastereo- and enantioselectivity were improved through (*S*)-mandelate salt formation but remained moderate (*trans*/*cis* = 88:12 and ee ~ 93%). The over-

all yield of this four-step synthesis was low (~15%) and generated high quantities of waste. This chemical route was not suitable for commercial batch manufacturing, and it was decided to investigate enzymatic approaches.

Starting from methyl ketone **5**, we explored the synthesis of the amino methyl tetrahydrofuran derivative **9** through asymmetric *trans* amination with transaminase enzymes (see footnote 1) [28,29].

At first, commercial enzymes were used for the proof-of-concept. Following an internal screening of 83 transaminase enzymes from commercially available kits, 19 enzymes demonstrated good biocatalytic activity (assay yield > 50%). We identified one enzyme (transaminase ATA-047) that was able to deliver the amino methyl tetrahydrofuran derivative **9** with high selectivity toward the desired *trans* (3*R*,4*R*)-diastereoisomer (assay yield ~ 99% after 24 h reaction, ee > 99%, *trans*/*cis* > 30) under screening conditions. Interestingly, the reaction occurred under dynamic kinetic resolution and only the *trans* (3*R*,4*R*)-diastereoisomer **9** was produced starting from the racemic ketone **5**. To demonstrate the potential of the transaminase approach, a scale trial in 100 mL thermostated glass reactor with overhead stirring containing was performed. Applying
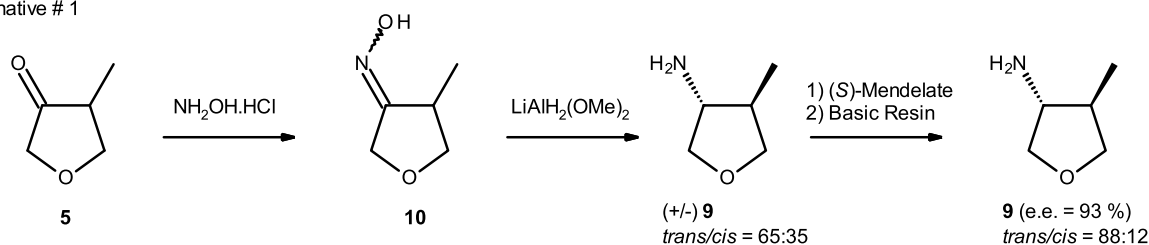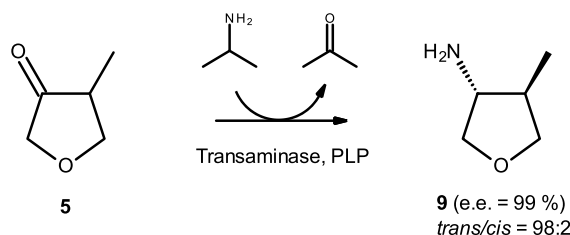
**Scheme 8.** Chemical pathway and enzymatic transamination pathway toward the synthesis of trans amino methyl tetrahydrofuran **9**.

a low enzyme/substrate ratio (1:10), a high conversion rate (assay yield **9** = 92.7%) was observed after 48 h reaction with excellent stereoselectivity (Figure 5).

Conditions: transaminase ATA47 1 mg/mL; ketone **5** = 100 mM; isopropylamine = 0.9 M; PLP = 10 mM; sodium phosphate buffer 100 mM, pH 9; temperature = 30 °C; volume = 100 mL. See footnote for calculation[2].

Although the commercial enzyme performed well, industrial objectives required a more efficient biocatalyst with better stability and higher substrate loading compatibility. Thus, in parallel with the testing of commercial kits, we carried out a genome mining approach through literature search and database in-silico screening. Fifty wild-type transaminases were selected for cloning and screening assays. Two enzymes were found to be very active in the formation of the amino methyl tetrahydrofuran derivative **9** (screening conditions), e.g., transaminase from *Chromobacterium violaceum* (assay yield amino

methyl tetrahydrofuran ∼ 90%), providing mainly the *trans*-(3*R*,4*R*)-diastereoisomer and *Arthrobacter sp* (assay yield amino methyl tetrahydrofuran ∼ 50%) providing mainly the *cis*-diastereoisomers. Enantioselectivity could be reversed during enzyme evolution. Thus, with such results in hand, we considered these two enzymes to be good hits to start an enzyme evolution campaign to achieve the industrial goal of an efficient biocatalyst.

The third example deals with the optimization of a sulfotransferase enzyme for the synthesis of one of our late-stage assets [30]. The biocatalytic process used 3′-phosphoadenosine-5′-phosphosulfate (PAPS) as a donor of the $SO_3$ group and was viewed as unsustainable and a significant cost driver. As an alternative to reduce the process cost, a PAPS recycling system was envisaged. We demonstrated how it was possible to rapidly increase the activity of an enzyme for a non-natural reaction in a few optimization rounds through enzyme evolution campaign. In the literature, it is known that the enzyme Aryl sulfotransferase IV (AST-IV) from rat can produce the PAPS from a $SO_3$ donor much cheaper, the *p*-nitrophenyl sulfate (*p*-NPS) (Scheme 9).

However, this is the reverse reaction of this enzyme since its natural function is the sulfation of *p*-NP starting from PAPS. Therefore, the challenge was

---

[2]Calculation : ee = [*trans*(3*R*,4*R*) − *trans*(3*S*,4*S*)]/[*trans*(3*R*,4*R*) + *trans*(3*S*,4*S*)]; conversion *cis* (%) = [*cis*(3*R*,4*S*) + *cis*(3*S*,4*S*)]/ [*cis*(3*R*,4*S*) + *cis*(3*S*,4*R*) + *trans*(3*R*,4*R*) + *trans*(3*S*,4*S*) + Ketone]; conversion *trans* (%) = [*trans*(3*R*,4*R*) + *trans*(3*S*,4*S*)]/[*cis*(3*R*,4*S*) + *cis*(3*S*,4*R*) + *trans*(3*R*,4*R*) + *trans*(3*S*,4*S*) + Ketone].
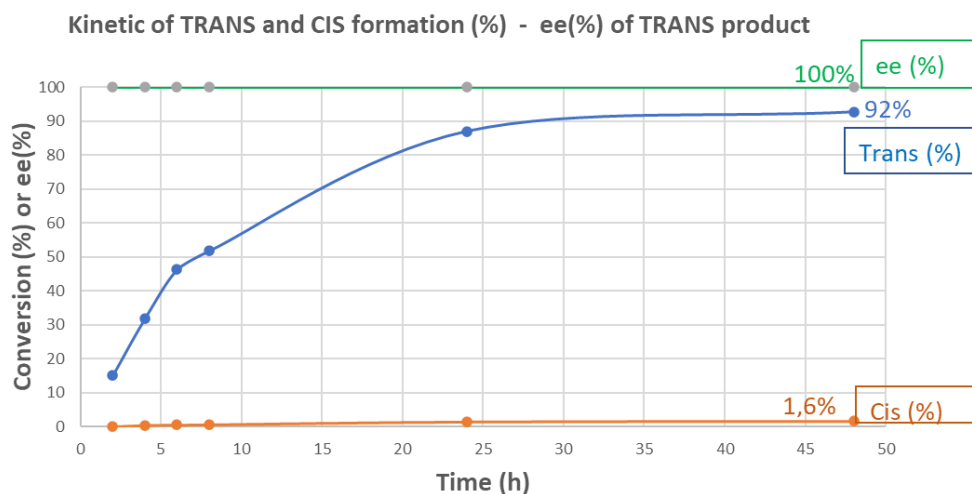
**Figure 5.** Time course of transamination reaction of **5** with ATA-047 at 100 mL scale.
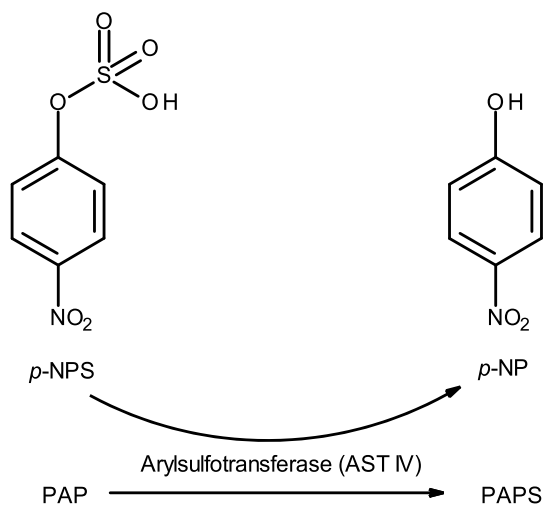


**Scheme 9.** PAPS regeneration system. AST-IV catalyzes the transfer of the sulfo group from the less expensive donor, *p*-NPS.

to force an enzyme to be efficient against its natural reaction equilibrium.

An optimization program was started with a directed evolution approach by recombination of homologues. This method consists of taking advantage of some homologues of the starting gene and recombining them randomly to produce new sequences among which we might find some improved versions of the enzyme. In this first round, 12,000 clones were screened, and we achieved a twofold activity increase in PAPS production. Even though we found more efficient variants, this method did not lead to an enzyme active enough to reach the goal, and we decided to use a more structure-guided rational design approach.

By using computational tools and molecular modeling, it is possible to predict mutations that might enhance the enzyme performance. Thanks to the 3D modelling tools, we were able to reconstitute the structure of the protein and identify the binding region for the substrates and products (PAP/*p*-NPS and PAPS/*p*-NP) in the catalytic site. The challenge was then to find how to increase PAPS formation. We decided to create variants to destabilize the binding between the enzyme and the *p*-NP in order to favor the binding of *p*-NPS as a substrate. In this case we found one mutant able to increase the activity of the enzyme sevenfold (Figure 6).

After this first positive result we decided to launch a more in-depth study. We tested a list of other ~100 variants targeting both the binding site (to directly increase the activity) and the entire protein with the idea of stabilizing the activity of the enzyme during the reaction. After this additional round, we identified 10 mutations that, in combination, were able to increase the activity of the protein more than 10-fold, maintaining a high level of activity throughout the reaction.
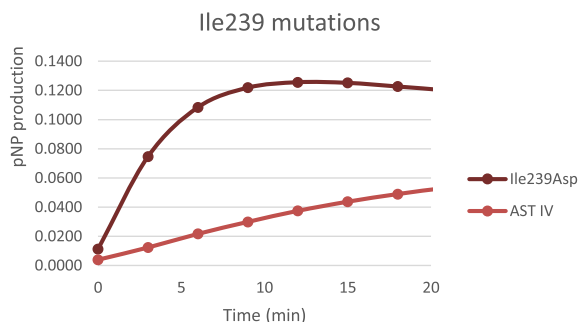
**Figure 6.** *p*-NP production achieved by Isoleucine 239 mutant compared to wild type enzyme.
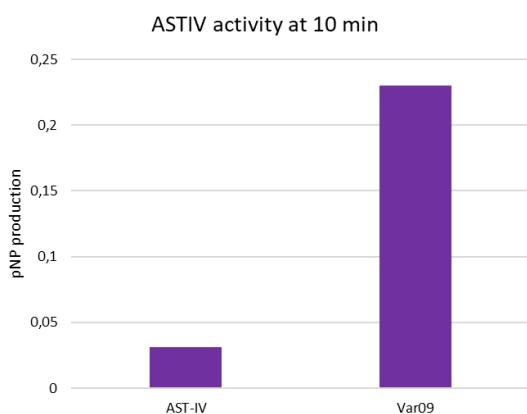


**Figure 7.** Activity of final variant (Var09) of AST-IV.

This final variant of the enzyme can sustain the recycling of PAPS and allow an efficient sulfonation of the target, reducing the manufacture cost of the process (Figure 7).

## 6. Outlook and opportunities

Environmental considerations drive our processes all along development and industrial phases. This is a key factor in accelerating the implementation of our internal Biosynthetic Technologies platform. A key success factor for the implementation of biocatalysis is the collaboration between organic chemists and biochemists to design new and more efficient chemical routes enabled by biocatalysis.

The examples described in this article show that the implementation of enzymatic transformations in the synthesis of complex molecules of our R&D portfolio has a positive impact on environmental footprint and can be in some cases the only viable alternative for large scale clinical batch manufacturing to meet timelines and quality.

We have built a very efficient toolbox to investigate common biocatalytic transformations using well-developed classes of enzymes (such as imine reductase (IRED), transaminase, ketoreductase (KRED), ene-reductase or nitrilase). However, the molecules entering our R&D portfolio are becoming increasingly complex. Innovative retrosynthetic pathway integrating biocatalytic step will be of great interest to overcome associated CMC risks. Diversification of our toolbox with less well-investigated classes is needed to enlarge the investigation in the repertoire of biocatalytic reaction on non-natural substrates. Currently, certain gaps in the toolbox remain. The biocatalysis community (academics and industrials) is addressing these challenges and new enzymatic platforms for industrial chemistry should arise in the near future [1].

Protein engineering is of great importance for developing enzymes for biocatalytic transformations at an industrial scale. We decided to build an in-house molecular biology platform (expertise and capabilities) that allows us to tailor enzyme performance to meet demanding industrial requirements. A proof-of-concept was achieved through the development of an efficient AST-IV enzyme. Looking to the future, the ability in expanding the field of computational methods, such as artificial intelligence, machine learning or data management will support our internal strategy toward designing highly efficient enzyme for non-natural substrates within reduced cycles time. This will be possible thanks to: (1) the better identification of suitable enzymes from protein sequence information accessible in databanks (genomic database mining); (2) smarter mutant libraries design.

## Abbreviations

CMC, chemistry, manufacturing and control; DIAD, diisopropyl azodicarboxylate; DKR, dynamic kinetic resolution; DNA, deoxyribonucleic acid; IPA, isopropyl alcohol; IRED, imine reductase; KRED, ketoreductase; PMI, process mass intensity; PLP: pyridoxal 5′-phosphate; R&D, research and development; SFC, supercritical fluid chromatography.

## Declaration of interests

## Author contributions

The manuscript was written through contributions of all authors. All authors have given approval to the final version of the manuscript.

## Acknowledgments

## References

[1] J. C. Reisenbauer, K. M. Sicinski and F. H. Arnold, "Catalyzing the future: recent advances in chemical synthesis using enzymes", *Curr. Opin. Chem. Biol.* **83** (2024), article no. 102536.

[2] F. H. Arnold, "Directed evolution: bringing new chemistry to life", *Angew. Chem. Int. Ed.* **57** (2018), article no. 4143.

[3] M. T. Reetz, *Directed Evolution of Selective Enzymes: Catalysts for Organic Chemistry and Biotechnology*, 1 edition, Wiley VCH: Germany, 2016.

[4] A. Holzinger, K. Keiblinger, P. Holub, K. Zatloukal and H. Müller, "AI for life: Trends in artificial intelligence for biotechnology", *New Biotechnol.* **74** (2023), pp. 16–24.

[5] P. Kouba, P. Kohout, F. Haddadi, et al., "Machine learning-guided protein engineering", *ACS Catal.* **13** (2023), pp. 13863–13895.

[6] P. S. Sampaio and P. Fernandes, "Machine learning: a suitable method for biocatalysis", *Catalysts* **13** (2023), article no. 961.

[7] M. A. Huffman, A. Fryszkowska, O. Alvizo, et al., "Design of an *in vitro* biocatalytic cascade for the manufacture of islatravir", *Science* **366** (2019), pp. 1255–1259.

[8] J. A. McIntosh, Z. Liu, B. M. Andresen, et al., "A kinase-cGAS cascade to synthesize a therapeutic STING activator", *Nature* **603** (2022), pp. 439–444.

[9] B. Castro, J.-R. Dormoy and A. Rabion, Alkyl esters of 3-(3,4-dihalophenyl) -2,6-dioxopoperidine-3-propionic acid of use as intermediates, WO patent, WO2000037445, June 23, 2000.

[10] C. Marvalin, M. Denoux, S. Pérard, S. Roy and R. Azerad, *Xenobiotica* **42** (2012), pp. 285–293.

[11] S. Roy, "Metabolism of a glycine transporter 1 inhibitor: identification of metabolite structures, a case study", *Label Compd. Radiopharm.* **56** (2013), pp. 399–407. Oral Communication International Isotope Society: Heidelberg, 2012.

[12] J. Atzrodt, J. Blankenstein, D. Brasseur, et al., "Synthesis of stable isotope labelled internal standards for drug-drug interaction (DDI) studies", *Bioorg. Med. Chem.* **20** (2012), pp. 5658–5667.

[13] J. Allen, D. Brasseur, B. De Bruin, M. Denoux, S. Pérard, N. Philippe and S. Roy, "The use of biocatalysis in the synthesis of labelled compounds", *J. Labell. Compd. Radiopharm.* **50** (2007), pp. 342–346.

[14] J. Allen, M. Denoux, N. Philippe, R. Luc and S. Roy, "Chemoselective hydrolysis of a radiolabelled nitrile using nitrilases", *J. Labell. Compd. Radiopharm.* **50** (2007), pp. 624–626.

[15] S. Caille, S. Cui, M. M. Faul, S. M. Mennen, J. S. Tedrow and S. D. Walker, "Molecular complexity as a driver for chemical process innovation in the pharmaceutical industry", *J. Org. Chem.* **84** (2019), no. 8, pp. 4583–4603.

[16] J. Boström, D. G. Brown, R. J. Young and G. M. Keserü, "Expanding the medicinal chemistry synthetic toolbox", *Nat. Rev. Drug Discov.* **17** (2018), pp. 709–727.

[17] P. Demontigny, C. S. Siegel and D. Yang, Solid forms of deuterated colony stimulating factor-1 receptor CSF-1R inhibitors, WO patent, WO2023249989, 2023.

[18] A. Rabion, "Accelerating the implementation of Biocalysis in API synthesis: contribution to Sanofi eco-design commitment", in *Oral Communication Biotrans 2023 16th International Symposium on Biocatalysis & Biotransformations, June 25–29, 2023, La Rochelle, France*. Online at https://biotrans2023.livescience.io/book-of-abstracts.html, 20, 86, 0, 0, 0 (accessed on April 28, 2025). Book of abstract online #581.

[19] A. Bigot, A. Rabion, J.-B. Landier, et al., "Chemical & biochemical approaches to enantiomerically pure 3,4 disubstituted tetrahydrofuran derivative at multi-kilogram scale: the power of KRED", *Org. Process Res. Dev.* **28** (2024), no. 12, pp. 4467–4476.

[20] A. J. Lees, J. Hardy and T. Revesz, "Parkinson's disease", *Lancet* **373** (2009), no. 9680, pp. 2055–2066.

[21] K.-L. Lim and C.-W. Zhang, "Molecular events underlying Parkinson's disease — an interwoven tapestry", *Front. Neurol.* **4** (2013), article no. 33.

[22] P. Martinez-Martin and M. M. Kurtis, "Health-related quality of life as an outcome variable in Parkinson's disease", *Ther. Adv. Neurol. Disord.* **5** (2012), no. 2, pp. 105–117.

[23] P. Bernardelli, S. Deprets, L. Dubois, J. Macor, F. Petit, C. Terrier and M. Bianciotto, Substituted pyrrolo[2,3-d]pyrimidines, their preparation and their therapeutic application, WO patent, WO2022263472A1, 2022.

[24] N. Saraiva Rios, B. Bandeira Pinheiro, M. Pessoa Pinheiro, R. Mendes Bezerra, J. C. Sousa dos Santos and L. Rocha Barros Gonçalves, "Biotechnological potential of lipases from *Pseudomonas*: Sources, properties and applications", *Process. Biochem.* **75** (2018), pp. 99–120.

[25] M. Y. Raynbird, J. B. Sampson, D. A. Smith, S. M. Forsyth, J. D. Moseley and A. S. Wells, "Ketone reductase biocataly-

sis in the synthesis of chiral intermediates toward generic active pharmaceutical ingredients", *Org. Process Res. Dev.* **24** (2020), no. 6, pp. 1131–1140.

[26]  R. L. Hanson, Z. Guo, F. González-Bobes, M. D. B. Fenster and A. Goswami, "Enzymatic reduction of $\alpha$-substitutes Ketones with concomitant dynamic kinetic resolution", *J. Mol. Catal. B Enzym.* **133** (2016), pp. 20–26.

[27]  P. Tapolcsányi, J. Wélfling, E. Mernyák and G. Schneider, "The mitsunobu inversion reaction of sterically hindered 17-hydroxy steroids", *Monatsh. Chem.* **135** (2004), pp. 1129–1136.

[28]  S. Duan, D. W. Widlicka, M. P. Burns, et al., "Application of biocatalytic reductive amination for the synthesis of a key intermediate to a CDK 2/4/6 inhibitor", *Org. Process Res. Dev.* **26** (2022), no. 3, pp. 879–890.

[29]  J. Limanto, E. R. Ashley, J. Yin, G. L. Beutner, B. T. Grau, A. M. Kassim, M. M. Strotman and M. D. Truppo, "A highly efficient asymmetric synthesis of vernakalant", *Org. Lett.* **16** (2014), pp. 2716–2719.

[30]  A. Deplace, E. Monza, D. Panigada and A. Steinmetz, Uses and methods for sulfating a substrate with a mutated aryl-sulfotransferase, WO patent, WO2023052490, 2023.

Review article

# Practical examples of biocatalysis in industry

**Amelia K. Gilio** [®],[*a*]**, Miguel A. Abdo** [*a*]**, Carlos A. Martinez** [*a*]**, Andrew T. Palaia** [*a*] **and Jovan Livada** [*,*a]

[*a*] Pfizer Global Research and Development, Groton, CT, 06340, USA

*E-mail:* jovan.livada@pfizer.com (J. Livada)

**Abstract.** Biocatalysis has been used in industrial settings, especially in the pharmaceutical industry, for decades. In this review, we showcase the six most prominent enzyme classes in industrial biocatalysis: keto-reductases, ene-reductases, imine-reductases, transaminases, oxygenases, and hydrolases. For each class, several examples are presented that highlight the substrate scope and enantioselectivity of these biotransformations from milligram to multikilogram scale.

**Keywords.** Enzyme, Biocatalysis, Hydrolase, Ketoreductase, Imine-reductase, Ene-reductase, Transaminase.

## 1. Introduction

Biocatalytic reactions are characterized by exceptional chemo-, regio-, and enantioselectivity, making biocatalysis a key enabling technology in asymmetric synthesis. In this review, we highlight the most prominent enzyme classes, and more importantly, dozens of successfully implemented examples. We provide relevant conditions for successful biocatalytic reaction execution, including buffers, pH, temperature, and cofactor recycling systems when applicable. A significant number of enzymes are readily accessible through commercial suppliers or through preparation via fermentation of recombinant microorganisms. Crude lyophilized enzyme formulations have facilitated widespread distribution of biocatalysts, while genetic engineering has advanced contemporary enzymatic processes by improving reaction selectivity and productivity. These processes are performed under a diverse array of conditions and in many cases at concentrations comparable to those achieved in traditional synthetic chemistry methods [1].

## 2. Ketoreductases (KREDs)

Enzymatic reduction of ketones and aldehydes are well-established methods for the synthesis of chiral alcohols. These transformations are catalyzed by a diverse array of enzyme families, including alcohol dehydrogenases (ADHs) and aldo-keto reductases (AKRs), collectively referred to as ketoreductases (KREDs) or carbonyl reductases (CREDs). In their active sites, these enzymes bind NAD(P)H, which delivers a hydride to the carbonyl of interest, producing the chiral alcohol [2].

Most examples utilize a second enzyme for NAD(P)H cofactor recycling. Others employ a single enzyme for both ketone reduction and cosubstrate oxidation of propan-2-ol to acetone [3]. Generally, KREDs exhibit broad substrate specificity, although the reduction of ketones with bulky substituents is lacking. For instance, an intermediate for an investigational $\gamma$-secretase inhibitor for Alzheimer's Disease treatment (Scheme 1), 1,1-dimethylethyl ($R$)-2-hydroxypentanoate **2**, was synthesized via enzymatic reduction of a ketoester [4]. The reaction, conducted with 35 kg of ketoester in phosphate buffer and glycerol, utilized low enzyme loadings of ADH-108L and glucose dehydrogenase (GDH), with efficient NAD$^+$ recycling by GDH and glucose.

---

[*]Corresponding author
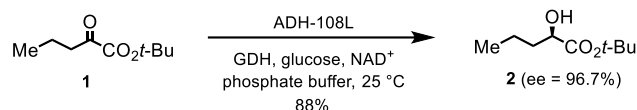
**Scheme 1.** KRED-catalyzed reduction toward a γ-secretase inhibitor.
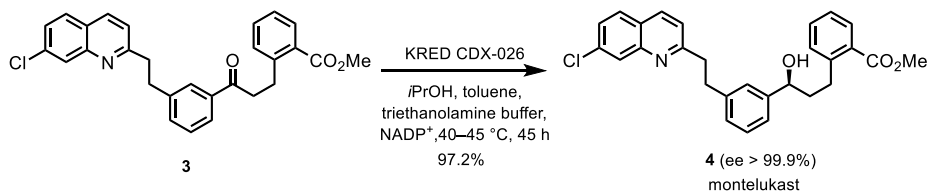


**Scheme 2.** KRED-catalyzed reduction toward montelukast.
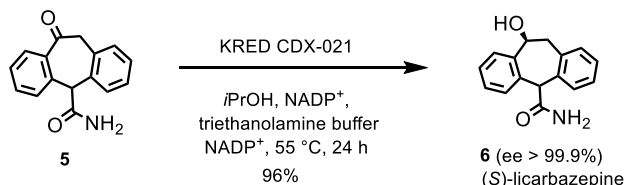


**Scheme 3.** KRED-catalyzed reduction toward (*S*)-licarbazepine.
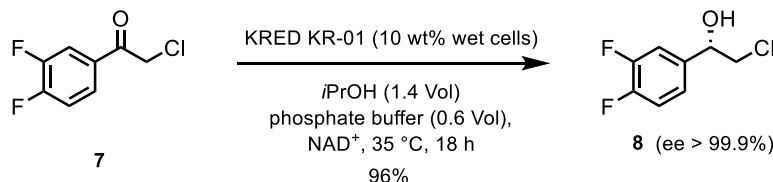


**Scheme 4.** KRED-catalyzed reduction toward ticagrelor.

Another example employed an engineered KRED, CDX-026, in the synthesis of an intermediate for montelukast, the active ingredient in Singulair® from Merck (Scheme 2) [1]. The reaction, performed on 230 kg of ketone **3** in a mixture of propan-2-ol, toluene, and triethanolamine buffer, achieved a 97% yield. Crystallization of the alcohol as monohydrate drove the reaction to high conversion without acetone removal, with CDX-026 recycling NADP⁺ by oxidizing propan-2-ol.

Additionally, an engineered KRED facilitated the scalable synthesis of (*S*)-licarbazepine, an anticonvulsant [5]. After four rounds of engineering and a design of experiments (DoE) made up of 32 experiments, the process was conducted on a 500 mL scale, 50 g of ketone, and 1% w/w of KRED CDX-021. This

produced (*S*)-licarbazepine **6** in 96% yield after distillation and filtration (Scheme 3). KRED CDX-021 recycled NADP⁺ by oxidizing propan-2-ol, with a nitrogen sweep removing acetone to drive the reaction forward.

A wild-type KRED from *Leifsonia* sp. S749 was used to synthesize (*S*)-2-chloro-1-(3,4-difluorophenyl)ethanol **8**, an intermediate for ticagrelor, a treatment for acute coronary syndromes [6]. The enzyme, overexpressed in recombinant *E. coli*, was used in concentrated conditions with propan-2-ol and phosphate buffer, recycling NAD⁺ by oxidizing isopropanol (Scheme 4). The reaction was optimized to substrate loadings of 500 g/L and resulted in space time yields of 145.8 mmol/L/h. The same enzyme also converted a different substrate,
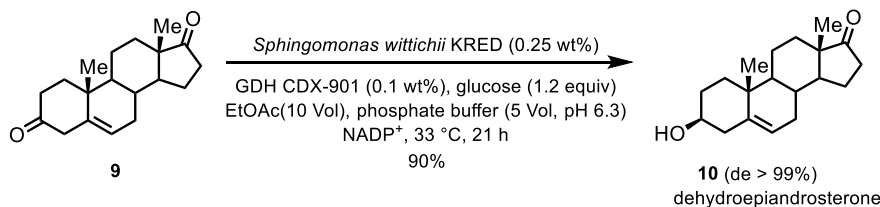
**Scheme 5.** KRED-catalyzed reduction that produces dehydroepiandrosterone.
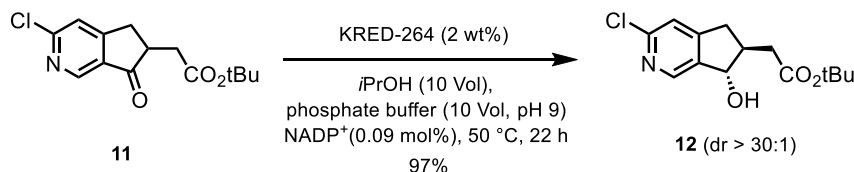


**Scheme 6.** KRED-catalyzed dynamic kinetic resolution towards a GPR40 partial agonist.
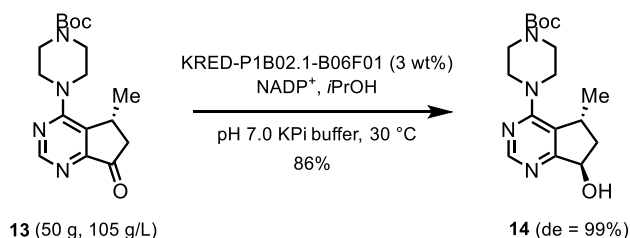


**Scheme 7.** KRED-catalyzed reduction toward ipatasertib.

($R$)-1-(3,5-bis(trifluoromethyl)-phenyl)ethanol, also at 500 g/L substrate loading with high yield and high stereoselectivity.

An example of a bulky substrate involved a wild-type KRED from *Sphingomonas wittichii* for the reduction of 5-androstene-3,17-dione **9** to dehydroepiandrosterone (DHEA) **10**, a precursor for steroidal drugs (Scheme 5) [7]. This KRED was identified by a colorimetric screen in the reverse oxidative direction, to streamline the identification of enzymes which acted on the desired regio- and stereoisomer. The resulting highly stereo- and regioselective reaction produced DHEA with minimal by-products and up to 150 g/L substrate loadings under biphasic reaction conditions.

Merck reported a KRED process that involved a dynamic kinetic resolution for the synthesis of an intermediate for a GPR40 partial agonist [8]. Following assessments of the kinetic and free energy profiles of the KRED reaction, and by performing six rounds of enzyme engineering, KRED-264 provided the desired *trans* diastereomer in high yield and diastereomeric ratio (Scheme 6).

Diastereoselectivity was also a beneficial characteristic of the KRED employed in Roche's synthesis of investigational cancer therapeutic ipatasertib. The process offered higher yields and diastereomeric ratios than those obtained by the ruthenium- or palladium-catalyzed processes explored in parallel. A commercially available KRED was therefore applied to this route and achieved highly diastereoselective reduction and NADPH regeneration via propan-2-ol oxidation. The overall chemoenzymatic synthesis of ipatasertib has been performed on a hundred-kilogram scale (Scheme 7) [9].

Another report from Roche detailed the synthesis of an intermediate for the indoleamine 2,3-dioxygenase inhibitor navoximod. Both ketone moieties of the diketone intermediate were initially targeted for biocatalytic reductions with a screen of 500 KREDs performed; however, a metal hydride reduction was ultimately favored for the central ketone.
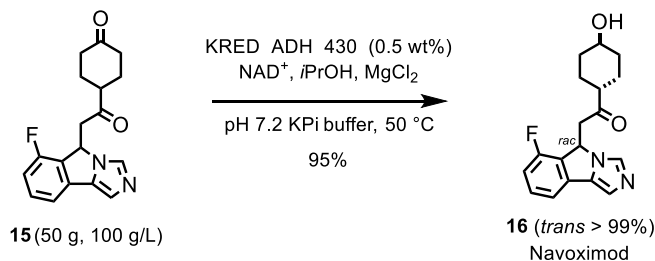
**Scheme 8.** KRED-catalyzed reduction toward navoximod.

Their KRED panel was successfully screened resulting in a process scaled up to 50 g scale, achieving high yield and selectivity with low enzyme loading (Scheme 8) [10].

## 3. Ene-reductases (EREDs)

Ene-reductases (EREDs), a subset of the oxidoreductase enzyme family, are known for their ability to facilitate the asymmetric reduction of electron-deficient alkenes [11]. Distinct from KREDs and imine-reductases (IREDs), which directly utilize NAD(P)H, EREDs operate through a unique mechanism involving hydride transfer from a non-covalently associated, reduced flavin mononucleotide ($FMNH_2$) cofactor to the substrate alkene [12,13]. The subsequent reduction process of FMN is mediated by NAD(P)H [14].

The classification of ene-reductases encompasses five distinct classes, with the Old Yellow Enzyme representing the most extensively researched category [15]. The initial demonstration of ene-reductase activity dates back to 1932, as documented by Warburg and Christian [16]. It was not until 1995 that EREDs were employed in the synthesis of chiral intermediates. After this pivotal development, numerous instances of ERED applications in biocatalysis have been documented.

A recent scholarly article detailed the characterization of a novel ERED derived from *Pichia angusta* (*Pa*ER), which exhibited remarkable stereoselectivity in the reduction of ketoisophorone **17** to (*R*)-levodione **18** as depicted in Scheme 9 [17]. The reaction was conducted with an impressive substrate concentration of 154 g/L, utilizing whole *E. coli* cells that housed both the ERED and the GDH cofactor recycling enzyme.

Another example characterized by almost perfect stereoselectivity involves an ERED isolated from *Lactobacillus casei* (*Lac*ER). This ene-reductase was used to catalyze the reduction of (5*R*)-carvone **19**, yielding (2*R*, 5*R*)-dihydrocarvone **20** as illustrated in Scheme 10 [18]. The enzyme facilitated the production of this compound with a diastereomeric excess (de) of 99%. Additionally, this ERED demonstrated versatility by functioning in a one-pot cascade reaction alongside a KRED, culminating in the synthesis of (1*S*, 2*R*, 5*R*)-dihydrocarveol.

In instances where the catalytic characteristics of ERED catalysts are deemed suboptimal, enzyme-engineering techniques can be harnessed to enhance the enzymatic properties. A 2015 study demonstrated that enzyme engineering could modify the enantioselectivity of OYE 1 from *S. pastorianus* through the introduction of a singular W116V mutation [19]. In a separate investigation, a consensus mutagenesis approach was applied to the 12-oxophytodienoate reductase from *L. esculentum* (tomato) applied to cyclohex-2-en-1-one-based substrates, resulting in an improved enantioselectivity exceeding 99% ee [20]. Furthermore, a rational design strategy was employed to truncate the flexible loops of the nicotinamide-dependent cyclohexenone reductase (NCR), thereby augmenting both the thermal stability and solvent resistance of the ERED [21].

The NCR ERED has also been documented to function effectively at elevated substrate concentrations. For instance, a study focusing on the reduction of 1-(cyclohex-1-en-1-yl)ethan-1-one **21** to 1-cyclohexylethan-1-one **22** reported a substrate loading capacity of 100 g/L, achieving a 99% conversion over a span of 110 h (Scheme 11) [22].

EREDs have been employed in the synthesis of pharmaceutical intermediates, notably in the

**17** (3 g, 20 mmol)

10 g/L *Pa*ER and *Bm*GDH
coexpressed in whole cell *E. coli*
0.2 mM NADP$^+$

1.05 M glucose
20 mL 100 mM PBS buffer
pH 7.5
40 °C, 24 h
100%

**18** (ee = 99%)
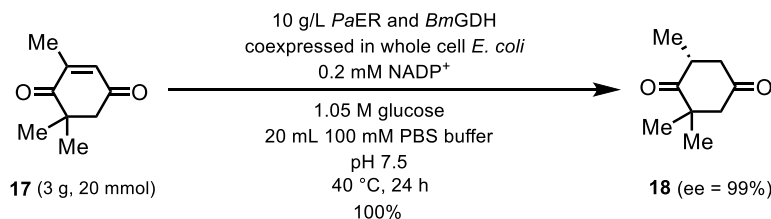
**Scheme 9.** Preparative-scale reduction of ketoisophorone.

**19** (450 mg, 3 mmol)

2 g/L purified *Lac*ER
2 g/L GDH
1 g/L NADP$^+$

12 g/L glucose
1 mL 100 mM potassium phosphate buffer
pH 8.0
37 °C, 4 h
99%

**20** (de > 99%)
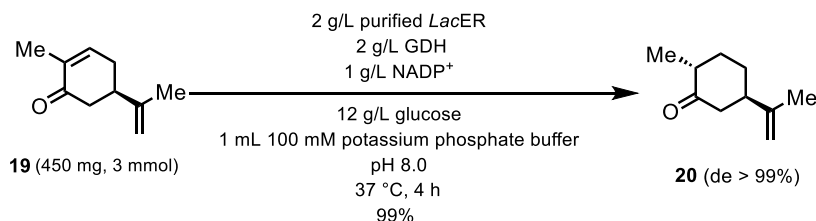
**Scheme 10.** Analytical-scale reduction of (5*R*)-carvone.

**21** (3 g, 24.2 mmol)

20 g/L NCR lysate
2 g/L GDH CDX901
2 g/L NADP$^+$

200 g/L glucose
30 mM phosphate buffer
10% PEG, 20% cyclohexane
pH 7.2
RT, 110 h
99%

**22**
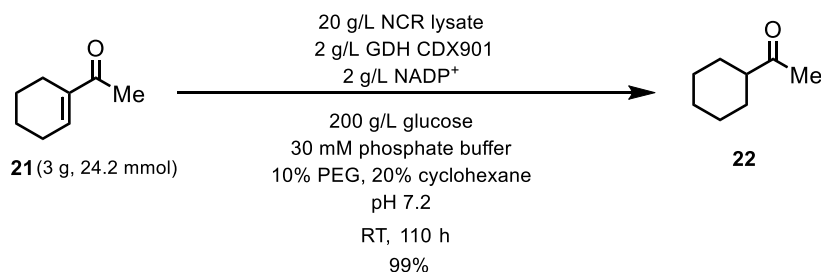
**Scheme 11.** Reduction of 1-(cyclohex-1-en-1-yl)ethanone via NCR.

**23** (1.8 mg, 19 umol)

0.1 g/L purified OPR1, H245D variant
15 mM NADH

50 mM Tris-HCl buffer
pH 7.5
30 °C, 24 h
24%

**24** (ee > 99%)
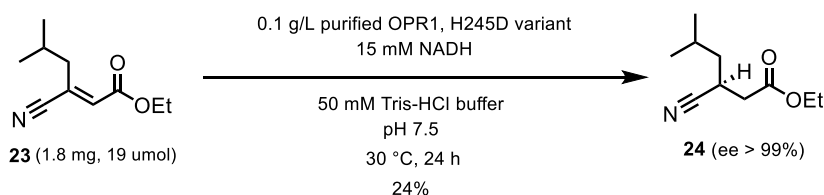
**Scheme 12.** Analytical-scale reduction of a potential intermediate in pregabalin synthesis.

production of pregabalin, a medication with anti-convulsant, analgesic, and anxiolytic properties for treating neurological conditions. Ethyl (*E*)-3-cyano-5-methylhex-2-enoate **23** underwent reduction by 12-oxophytodienoate reductase (OPR1) to yield ethyl (*S*)-3-cyano-5-methylhexanoate **24**, as depicted in Scheme 12 [23].

EREDs have also been utilized in the synthesis of intermediates for pharmaceuticals, exemplified by tesaglitazar, a drug under investigation for the treatment of type 2 diabetes [24]. The specific reaction involves the reduction of (*Z*)-2-ethoxy-3-(4-methoxyphenyl)acrylaldehyde **25** to (*S*)-2-ethoxy-3-(4-methoxyphenyl)propanoic acid **26**, executed with
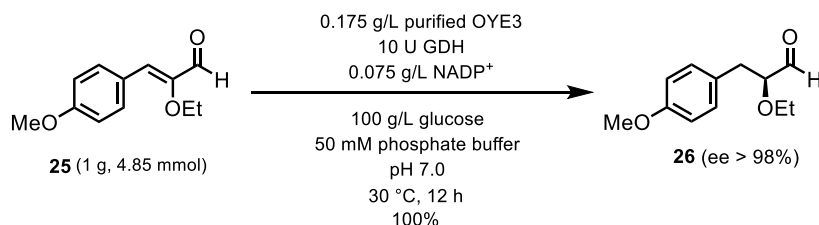
**Scheme 13.** Analytical-scale reduction of a potential intermediate in tesaglitazar synthesis.
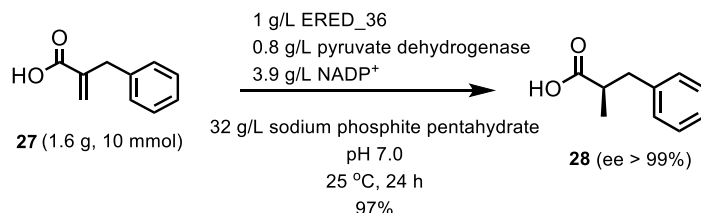


**Scheme 14.** Demonstrated ERED reduction of a carboxylic acid substrate.
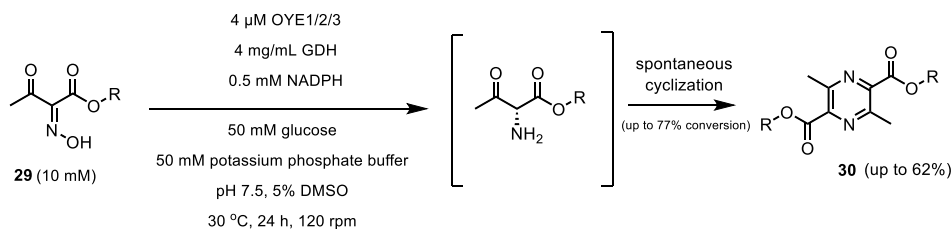


**Scheme 15.** ERED reduction of C=N bonds in oximes.

high efficiency and selectivity (100% conversion; 98% ee), employing Old Yellow Enzyme 3 (OYE3) as the biocatalyst (Scheme 13).

Ene-reductases have also been shown to catalyze reactions that are not limited only to activated olefins. Two recent reports have shown the expansion of the ERED substrate scope. The first report demonstrated that EREDs can reduce several carboxylic acid substrates [25], of which the most successful example involved the stereoselective reduction of 2-benzylacrylic acid **27** (Scheme 14).

The second report showed a novel feature of EREDs, the reduction of C=N in oximes (Scheme 15) [26]. Several enzymes exhibited this activity with the most notable members being OYEs 1, 2 and 3. In addition, for seven out of the eight oxime substrates tested, EREDs have demonstrated catalysis characterized by an isolated yield greater than 50%, at 10 mM substrate loading.

Therefore, in recent years, the type of activities that EREDs exhibit have been significantly expanded. We do not see this trend slowing down soon.

## 4. Imine-reductases (IREDs)

Imine reductases (IREDs) are a class of enzymes commonly used for the formation of secondary and tertiary amines, and less frequently primary amines. As the name suggests, these enzymes catalyze the reduction of imine C=N bonds with a NADPH cofactor. This activity was first shown by Nagasawa and coworkers in 2009 with two enzymes from strains of *Streptomyces* reducing 2-methyl-1-pyrroline to (*R*)- or (*S*)-2-methylpyrrolidine [27]. Further research expanded the panel of known IREDs and showed that these enzymes work well with a range of ketones and imines including cyclic and acyclic, aromatic, and aliphatic ketones [28]. For the amine partner,
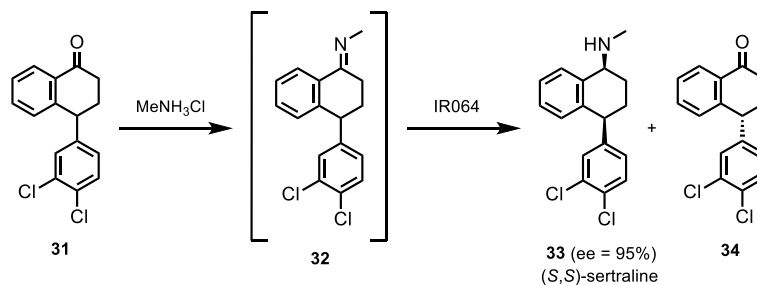
**Scheme 16.** Telescoped condensation and reduction toward the synthesis of (*S*,*S*)-sertraline.

IREDs prefer smaller amines such as methyl, allyl, and cyclopropyl amines. Couplings with ammonia, however, can be difficult. Regardless, larger amines like benzylamine and isoindoline [29] have been reported to be accepted. A recent report even showed a successful coupling of an aldehyde with α-(1-aminoethyl)naphthalene [30].

Being NADPH-dependent, IREDs are typically used in tandem with an NADPH recycling system. Many of these are the same systems used in KRED reactions. The most used system is the glucose-dehydrogenase (GDH)-catalyzed oxidation of glucose to gluconic acid. As the glucose oxidation step is non-reversible, this imparts a driving force on the imine reduction step. Other recycling systems have been reported such as alcohol dehydrogenase (ADH) oxidation of alcohols to carbonyls (typically propan-2-ol to acetone) [31,32], soluble hydrogenase (SH) reduction of NADP$^+$ with hydrogen gas [33], phosphite dehydrogenase (PTDH) oxidation of phosphite to phosphate [34], and formate dehydrogenase (FDH) oxidation of formic acid to carbon dioxide [35]. While these systems are very attractive from an atom economy standpoint, glucose oxidation remains the most commonly used in industry.

In 2017, Pfizer gave a brief report of an IRED-catalyzed reduction to synthesize (*S*,*S*)-sertraline [36]. Since the aryl ketimine **32** did not form spontaneously, the team synthesized the imine by chemical means and fed it into the IRED reduction. Via this route, IR064 from *Myxococcus fulvus* was identified as a hit for the reduction with the desired selectivity at both chiral centers and 95% ee (Scheme 16). Enzyme engineering efforts focused on IR064 allowed the team to identify variants with improved activity and selectivity. One variant with 5 mutations gave a 2.3-fold improvement in activity with 95% ee [36].

In the same year, Aleku and coworkers reported a new IRED from *Aspergillus oryzae* which, in addition to reducing imines, also catalyzed the condensation of a ketone and amine to form the imine for reduction [37]. This subset of IREDs has been dubbed reductive aminases or RedAms, and following their discovery, a mechanism of enzymatic reductive amination was proposed [38]. Since then, several articles reporting the use of RedAms to produce various amines have been published, and additional IREDs that show this activity have been discovered.

The first of these reports came in 2019 from GSK showing the use of an IRED from *Saccharothrix espanaensis* (IR-46) to resolve *trans*-phenylcyclopropylamine **35** and use it in the reductive amination of an aldehyde (Scheme 17) [39]. After three rounds of enzyme engineering, Schober and coworkers reported that they were able to run the reaction at 20.1 g/L aldehyde **35** with 1.2 wt% enzyme loading to reach 84% isolated yield of the desired product amine obtained with 99.7% ee. They noted that, although IREDs are typically most active at neutral to slightly basic pH, a slightly acidic pH was needed for product and substrate stability, and product solubility.

A few years later, Pfizer reported using an IRED from *Streptomyces purpureus* (*Sp*RedAm) to couple isopropyl 3-ketocyclobutylcarboxylate **38** with methylamine for the production of an intermediate in the synthesis of abrocitinib [40]. The wild-type enzyme (40 wt%) was able to convert 20 g/L of ketone with 2 equiv of methylamine to give the desired product in 27% isolated yield. The engineered enzyme (*Sp*RedAm-R3-V6) was used in this reaction at 230 kg scale with 125 g/L ketone and 1.5 wt% enzyme. Reaction performance under these conditions
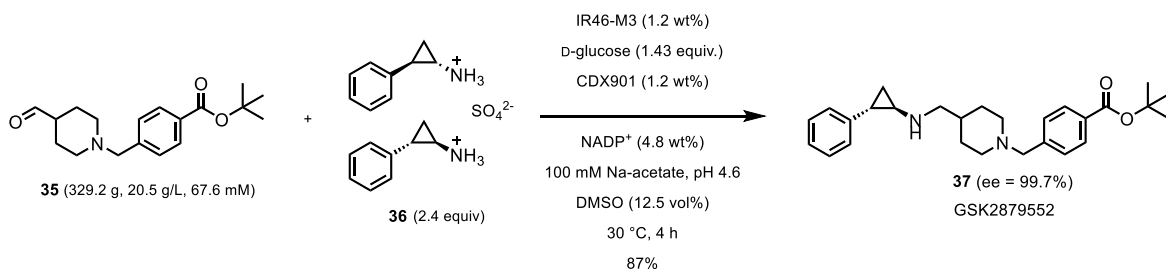
**Scheme 17.** Pilot-scale reductive amination toward the synthesis of GSK2879552.
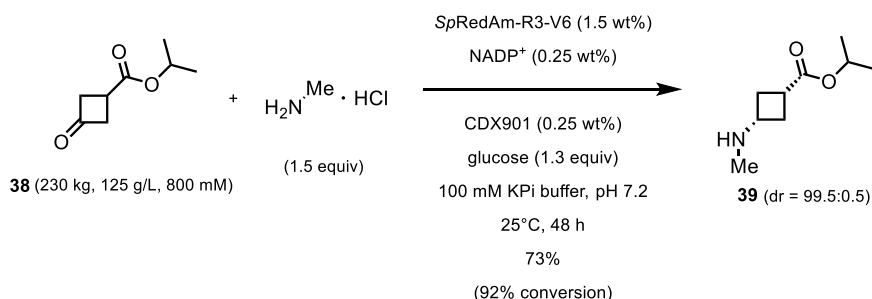


**Scheme 18.** Preparative-scale reductive amination toward the synthesis of abrocitinib.
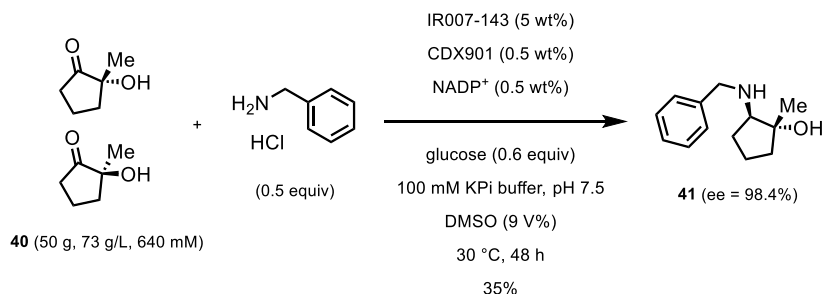


**Scheme 19.** Preparative-scale reductive amination with IR007-143.

improved to 92% assay yield with 73% isolated yield and 99.5:0.5 dr (Scheme 18).

Another report from Pfizer showed the use of a larger amine in a resolution and reductive amination of hydroxyketone **40** [41]. As part of a synthesis toward an investigatory CDK2/4/6 inhibitor, the team identified an IRED from *Amycolatopsis azurea*, dubbed IR007, which resolved the racemic hydroxyketone via reductive amination with benzylamine as the donor to produce the desired amine as a single stereoisomer. After engineering IR007 for improved activity and stability, variant IR007-143 was identified, which resolved the ketone with only 2.5 wt%

catalyst loading to give 35% isolated yield and 98.4% ee after 48 h (Scheme 19). This process was developed as an alternative to a transaminase-catalyzed reaction discussed in a later section of this review. With higher chiral purity and easier product isolation, this IRED approach was selected to move forward.

Most recently, Thorpe and coworkers have reported a new type of activity from IREDs. In 2022, the group showed the use of an IRED with $\alpha, \beta$-unsaturated imines to reduce not only the C=N bond but also the C=C bond [42]. From a screen of 389 IREDs, 44 enzymes were identified which reduced
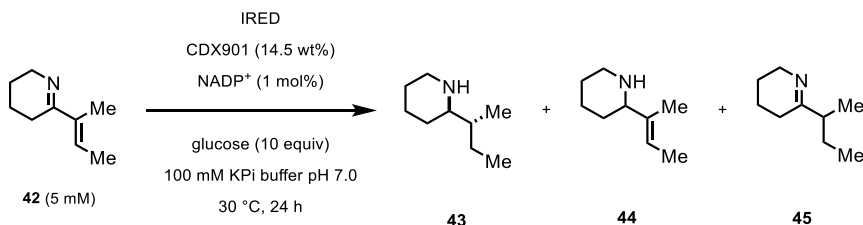
**Scheme 20.** Analytical-scale screening for Ene-IRED reactivity.
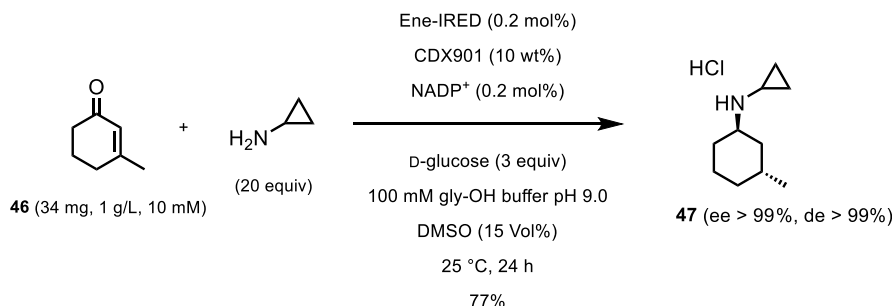


**Scheme 21.** Analytical-scale screening for Ene-IRED reactivity.

the ene–imine to the fully saturated piperidine **43** (Scheme 20).

An additional 12 IREDs were identified that gave the reduction of only the C=C double bond resulting in **45**. The enzyme with the highest activity for the full reduction was dubbed EneIRED and was selected for further study. After reaction optimization, EneIRED was able to catalyze the condensation and reduction of methylcyclohexenone **46** and cyclopropylamine to 61% conversion with only 1.1 equiv of amine (Scheme 21). When the reaction was performed with 20 equiv, the final product was isolated as the chlorhydrate salt in 69% yield. To test the scalability of the new reaction, the condensation/reduction of 3-methylcyclohex-2-en-1-one and cyclopropylamine was run at mmol scale with 50 mM enone and 5 equiv of amine. The desired product of this reaction was isolated in 77% yield.

## 5. Transaminases

Another class of enzymes for amination are transaminases. These enzymes are used to synthesize primary amines from a ketone or aldehyde using a pyridoxal phosphate (PLP) cofactor and a sacrificial amine donor such as isopropylamine. This is

achieved via a two-step mechanism where the amine donor is deaminated by the PLP cofactor to form a ketone and pyridoxamine (PMP). An amination step then transfers the amine group on to the target carbonyl, reforming PLP in the process. During this reaction, the enzyme can preferentially form one epimer of the amino compound. In cases where the starting carbonyl compound has additional stereogenic centers, the transaminase may also show preference for one of the starting material stereoisomers and set both chiral centers of the product in a single reaction. $\alpha$-Transaminases are limited to the formation of $\alpha$-amino and $\alpha$-keto acids whilst $\omega$-transaminases exhibit a much wider substrate scope and are employed much more widely for biocatalysis.

In 2019, the biocatalysis team at Merck reported the use of a transaminase for the synthesis of an intermediate for a CGRP receptor antagonist, 4-amino-*N*-Boc-3-fluoropiperidine **49** [43]. Starting from the racemic fluoroketone **48** and screening at pH 10.5 to promote epimerization of the chiral fluoride center, the team identified ATA-303 from Codexis as a hit for the desired product stereoisomer. Under initial screening conditions, the ATA-303 gave the desired isomer with 79% ee and 16:1 dr (Scheme 22). Without
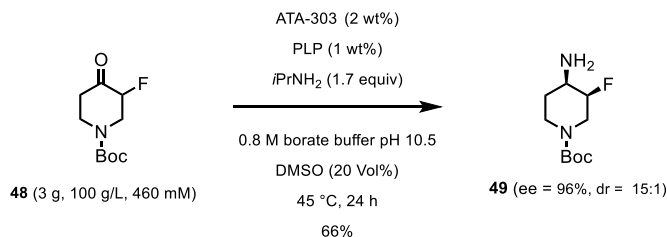
**Scheme 22.** Preparative-scale synthesis of a chiral building block.
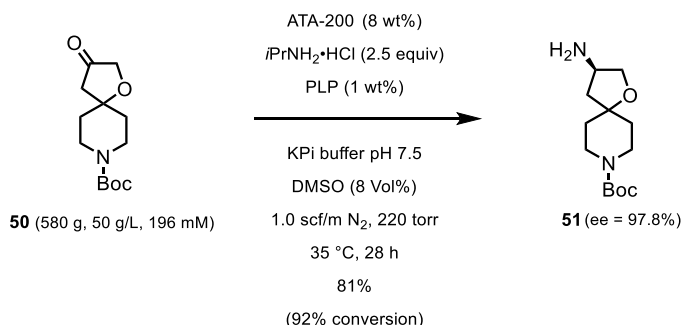


**Scheme 23.** Pilot-scale synthesis of chiral amine.

any enzyme engineering, the process was intensified to 100 g/L ketone and 2 wt% enzyme. This process resulted in 66% isolated yield, with 94% ee and 15:1 dr.

One obstacle commonly encountered with transaminases is the fact that these reactions are controlled by the reaction equilibrium and require a large excess of amine donor to push the reaction forward. Fortunately, several methods have been developed to introduce a thermodynamic or entropic driving force into the reaction. With isopropylamine as the amine donor, the reaction can be pushed to completion by removing the acetone by-product with a constant nitrogen sweep, or by applying a slight vacuum. A report from Pfizer in 2021 showed the use of another commercial transaminase (ATA-200) in the synthesis of 3-amino-4′-Boc-spiro[oxolane-2,4′-piperidine] **51** [44]. In this process, the spiroketone was converted to the amine using 2.5 equiv of IPA and applying a constant nitrogen sweep with periodic vacuum at 220 torr. As in the previous example, no enzyme engineering was needed, and the process was successfully implemented at 50 g/L ketone and 8 wt% enzyme. The optimized conditions resulted in the reaction where the desired amine was isolated with 82% yield and 98% ee (Scheme 23).

Additionally, the enzymatic synthesis enabled the formation of **51** as a single enantiomer, avoiding the use of hazardous reagents such as bromine, sodium azide, and triphenylphosphine.

Alternatively, when methylbenzylamine (MBA) is used as the amine donor, evaporation of the by-product can be replaced by removal extraction. In 2022 [41], a report showcased this in a transamination/resolution of hydroxyketone **52** (Scheme 24). In this report, the authors explain that while isopropylamine was initially used for development, it led to an unfavorable reaction equilibrium causing the reaction to stall at low conversion. Applying the nitrogen sweep helped increase conversion but also caused significant solvent loss and deactivation of the enzyme. To remedy this, the team used (*R*)-MBA instead, as using this donor imparted a more favorable equilibrium. One caveat to this is that the formation of acetophenone can be detrimental to the enzyme at higher concentrations. To account for this phenomenon, the reaction was run as a biphasic mixture with 25 vol% toluene to remove the acetophenone as it is formed. These conditions allowed the reaction of 50 g/L ketone and 16 wt% enzyme load to reach 40% yield over 3 steps with a very favorable 97% ee.
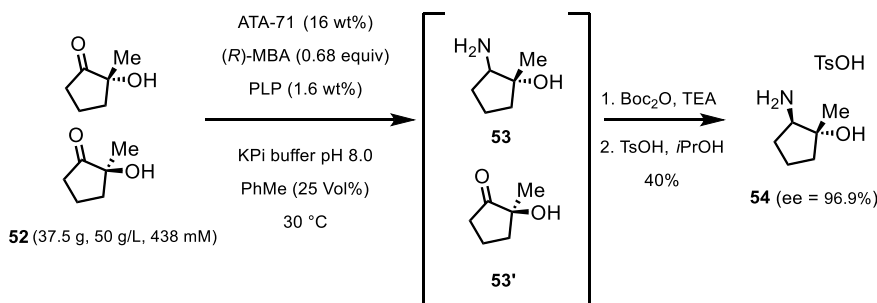
**Scheme 24.** Preparative-scale transamination with ATA-71 and (*R*)-MBA.
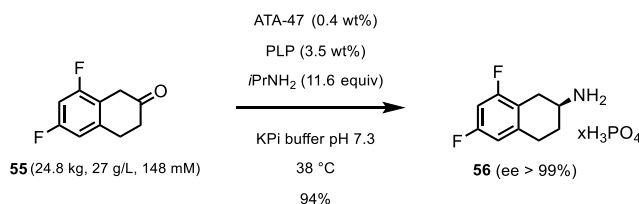


**Scheme 25.** Industrial-scale transamination with ATA-47.

It should be noted that when using a chiral amine donor (e.g., methylbenzylamine, alanine, etc.) it is important to use the correct enantiomer. Typically, this is the isomer with the same chirality as the desired product (e.g., (*R*)-MBA was used in this example to generate the (*R*)-amine).

A less common method of driving the transaminase equilibrium forward is by removing the desired product from the reaction mixture as it is formed. A 2017 report showcases the synthesis of 2-amino-6,8-difluorotetralin **56** [45]. The Pfizer biocatalysis group showed that using ATA-47 from c-LEcta GmbH enabled the conversion of 6,8-difluoro-beta-tetralone **55** to the desired (*S*)-amine in 94% yield (Scheme 25). More importantly, they reported that due to low solubility of starting material and product, the product precipitated in the form of phosphoric acid salt as it was formed.

Other transaminase reactions involve the removal of pyruvate (formed from alanine) that can be achieved using lactate dehydrogenase (LDH) or pyruvate decarboxylase (PDC). A downside to using LDH is that it requires a NADPH recycling system to continue removing pyruvate. On the other hand, PDC yields acetaldehyde and carbon dioxide that can be removed by vacuum or a nitrogen stream due to their volatility [46].

Another obstacle with transaminase processes is that they are typically limited to aldehydes or small ketones (e.g., methylo, cyclic ketones). However, a large area of transaminase research has focused on expanding the binding pocket of transaminases to accommodate larger substrates. Several groups have reported successfully expanding the active site of a transaminase to accommodate carbonyls as large as phenyl tert-butyl ketone [47]. In fact, in 2010, Codexis and Merck reported a transaminase that after only one round of engineering, was able to transaminate pro-sitagliptin ketone **57** (Scheme 26) [48]. This variant achieved less than 1% conversion with high enzyme load; however, this was a huge improvement considering the lack of any hits in the initial screen. After several additional rounds of enzyme and process engineering, the team was able to develop an enzyme which converted the target ketone in 88% assay yield at 134 g/L with only 4 wt% enzyme.

## 6. Cytochrome P450

Cytochrome P450 monooxygenases (P450s or CYPs) are heme enzymes which perform oxidations with molecular oxygen and often with the aid of NADPH cofactor and a redox partner protein [49,50]. P450s
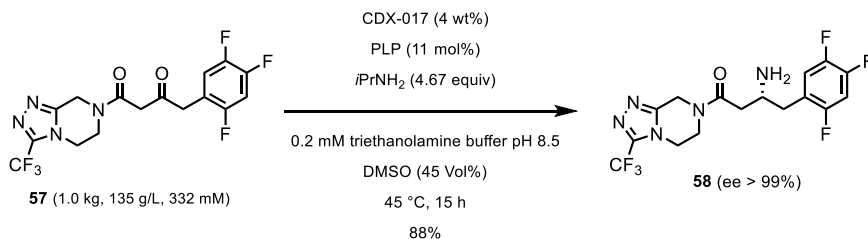
**Scheme 26.** Transamination of the bulky pro-sitagliptin ketone.
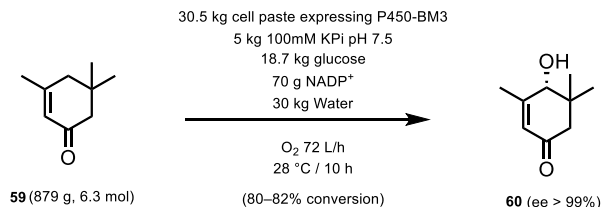


**Scheme 27.** 100 kg scale hydroxylation of a-isophorone by P450-BM3.

perform a diverse range of functionalizations from oxidation of heteroatoms, to C–C bond formation or cleavage, to aromatic hydroxylation of aromatic compounds. However, they are most often used to achieve the hydroxylation of sp$^3$ C–H bonds. The ability to stereo- and regioselectively activate a previously inactivated C–H has been captivating due to the ability of P450s to eliminate the need for multistep synthetic processes. P450s do come with many limitations such as low stability, limited substrate scope and low activity, which have prevented them from replacing these synthetic steps on a larger scale. Engineering has been applied to combat these limitations, often with P450-BM3 from *Bacillus megaterium* as the starting point for these enzyme-modifying methods [51].

An example of P450-BM3 reaching a kilogram scale production was demonstrated by Kaluzna et al. [52] where they synthesized 4-hydroxy-$\alpha$-isophorone **60** from $\alpha$-isophorone **59**. At a 1 L scale, Kaluzna et al. were able to obtain unprecedented product concentration of 10 g/L and a space time yield of 1.5 g/L/h (Scheme 27). Upon extensive reaction engineering, the process was scaled up to a 100 L scale, however the authors noted that at this scale, the reaction was restricted by the oxygen transfer rate (OTR) and by self-deactivation of the enzyme.

To overcome some of the restrictions of P450s, fusion enzymes have been designed. Many families of P450s require a reductase partner enzyme for NADPH binding. An electron is transferred from the reductase partner to the P450 heme domain, allowing the desired oxidation reaction to proceed with the target substrate. In a so-called self-sufficient P450, the reductase domain is already fused to the heme domain, however nonnatural self-sufficient P450s have also been developed to improve the catalytic efficiency [53].

This has also been taken a step further, by Kokorin et al. [54], where a dehydrogenase enzyme has been fused to a self-sufficient P450 to eliminate the need for a separate cofactor recycling enzyme, resulting in an increase of activity and catalytic efficiency. Kokorin and Urlacher [55] then expanded on this work by applying a fusion enzyme to the two-step oxidation of the insecticide and food additive (+)-nootkatone **62** from (+)-valencene **61** with 1.5 times increase in activity compared to the individual enzymes (Scheme 28).

Although P450s are often considered to have narrow substrate scopes, Zhang et al. [56] have demonstrated that hydroxylation at a tertiary carbon position is possible with P450s. Tertiary hydroxylation is synthetically often difficult to achieve on inactivated C–H bonds and even more difficult to achieve in high enantiomeric excess. Zhang et al. engineered P450-BM3 variant P450$_{PL2}$ to reach up to 99% ee and 32% yield upon $\alpha$-hydroxylation of a benzylic
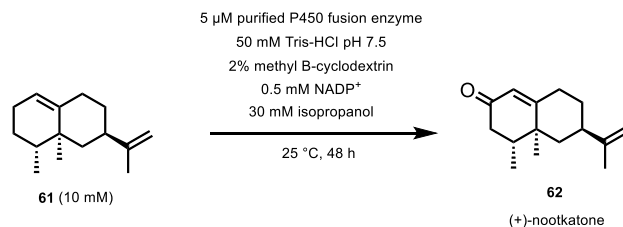
**Scheme 28.** Two-step oxidation of (+)-valencene to (+)-nootkatone.
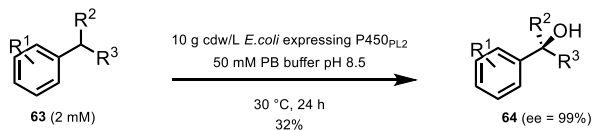


**Scheme 29.** Tertiary hydroxylation of benzylic CH by P450-BM3 variant P450$_{PL2}$.
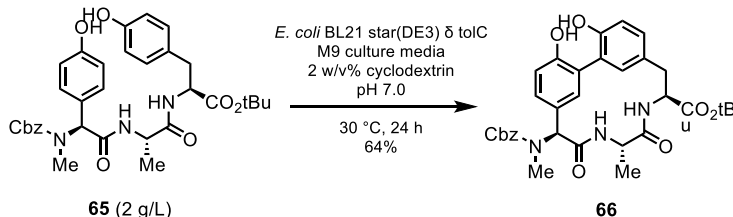


**Scheme 30.** P450-catalyzed biaryl coupling of arylomycin.

C–H bond with a range of substituted substrates (Scheme 29).

Aside from hydroxylations, alternative functionalizations by P450s are being explored on process scales. A recent report by Genentech has demonstrated that engineered P450s are a viable replacement for Suzuki–Miyaura couplings on a gram scale by performing an oxidative biaryl macrocyclization to produce an arylomycin antibiotic core **66**. Molinaro et al. [57] obtained 1.3 g of product in 64% yield from a 3 L fermentation process after purification (Scheme 30).

Bond connections that do not occur in natural biological processes have also been performed by P450s. Inspired by P450's non-natural carbene transfers with N–H and S–H insertions to form C–N or C–S bonds [58,59], Kan et al. [60] proposed that a similar method could be achieved with Si–H insertions to form carbon–silicon bonds. As C–Si bonds are present in a diversity of compounds which include materials and pharmaceutical compounds, upon

engineering cytochrome c from *Rhodothermus marinus* (*Rma* cyt c), Kan et al. were able to stereoselectively insert a C–Si bond into 4-(dimethylsilyl)aniline **67**. Moreover, *Rma* cyt c was engineered to chemoselectively form the C–Si bond despite the presence of a competing nitrogen atom in the molecule. Preparative-scale reactions with whole cells resulted in over 95% conversion and a 70% isolated yield with 98% ee and a total turnover number (TTN) of 3410 (Scheme 31).

## 7. Iron/α-ketoglutarate-dependent oxygenases

Like P450s, iron/α-ketoglutarate-dependent oxygenases or iron/2-oxoglutarate-dependent oxygenases (Fe/αKGs or 2ODs) are iron-coordinating enzymes which perform oxidations with molecular oxygen. However, unlike P450s, Fe/αKGs are non-heme iron-binding enzymes and instead recruit an α-ketoglutarate (αKG) cofactor which coordinates to
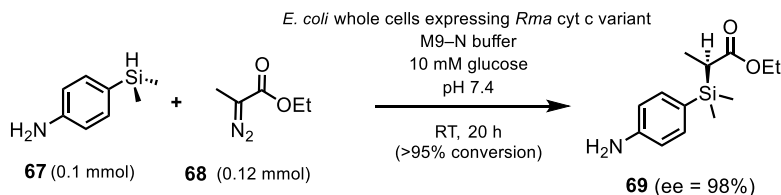
**Scheme 31.** Chemo- and stereoselective carbene Si–H insertion of to 4-(dimethylsilyl)aniline.
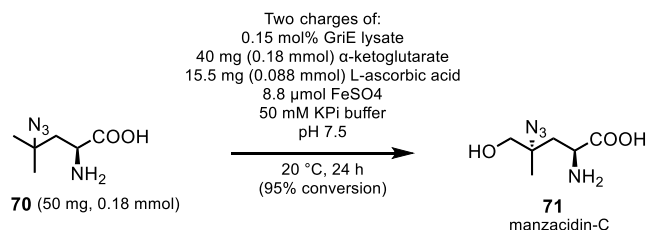


**Scheme 32.** Hydroxylation by GriE of an intermediate in the chemoenzymatic synthesis of manzacidin-C.

the iron via a catalytic triad and assists in electron transfer to the substrate of interest. Fe/αKGs, first discovered in the 1960s [61], have many important roles in biological processes, both in humans and many other organisms [62]. As such, Fe/αKGs can perform a diverse range of C–H functionalizations, but biocatalytic applications are often focused on their halogenation or hydroxylation capabilities.

One such enzyme, is the putative leucine hydroxylase GriE, which performs sequential oxidations at the delta position of L-leucine, forming 4-methylproline by cyclization via a spontaneous reductive amination in the biosynthesis of griselimycin [63]. Zwick and Renata [64,65], report a proof of concept where they employ GriE as the first Fe/αKG to be used in a natural product synthesis. They share that GriE can produce an array of substituted pyrrolidine building blocks and also demonstrate the utility of the enzymes in natural product synthesis by performing the chemoenzymatic preparation of manzacidin-C (Scheme 32), a bromopyrrole alkaloid first isolated from sea sponge *Hymeniacidon* sp. [66] Zwick and Renata reported a photocatalytic azidation to L-leucine which is followed by a single Δ hydroxylation by GriE, creating the hydroxylated product intermediate with a yield of 95% on a 130 mg scale.

Most recently, the industrial potential of Fe/αKG hydroxylases has been used by scientists at Merck who have incorporated an Fe/αKG into the synthesis of the oncology treatment belzutifan, by performing a stereoselective hydroxylation on a non-native fluoroindanone intermediate **72** [67–69]. This biocatalytic step replaced five chemical synthesis steps reducing the process mass intensity (PMI) by 43%, again illustrating the environmental advantages to employing biocatalysts in industry. Cheung-Lee et al. [67] reported that, despite a P450 reaching higher conversions in their initial screens, a Fe/αKG hydroxylase, FoPip4H from *Fusarium oxysporum*, was selected for further development in this process due to the resulting economic and time benefits. After 15 rounds of directed evolution, FoPip4H Rd16BB showed a 3000-fold improvement in catalytic efficiency over the wild type. Furthermore, DiRocco et al. [68] stated that an overall improvement of more than 400,000-fold was observed in comparison to the wild type when enzyme loading, reaction concentration, yield, and enantioselectivity were achieved. At kilogram scale, the final variant exhibited yields and ee of more than 90% and than 99%, respectively (Scheme 33).

Another scaled up application of Fe/αKGs was demonstrated by Hara et al. [70]. They reported the preparative-scale synthesis of (2*S*,3*S*)-3-hydroxylysine **75**, among other hydroxylysines, which can be an intermediate in the synthesis of (−)-balanol, a protein kinase C inhibitor. The lysine
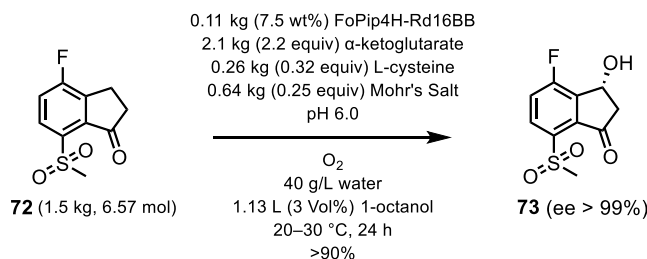
**Scheme 33.** Hydroxylation of a fluoroindanone intermediate in the synthesis of belzutifan.
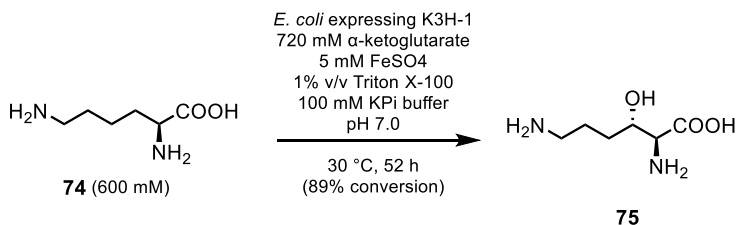


**Scheme 34.** Preparative-scale hydroxylation of lysine by K3H-1.

hydroxylases tested in this study were identified by sequence analysis of the clavaminic acid synthase superfamily with K3H-1 showing the greatest productivity. High substrate loadings were achieved of up to 600 mM lysine, and after 52 h, a 40 mL reaction yielded 531 mM (86.1 g/L) of (2*S*,3*S*)-3-hydroxylysine, with 89% molar conversion from whole cells expressing K3H-1 (Scheme 34). The authors did not report the diastereoselectivity of the enzyme.

Aside from hydroxylations, halogenations with Fe/αKG enzymes are being reported more frequently in the literature. In 2005 the first Fe/αKG halogenase, SyrB2, was discovered to perform monochlorination of a L-threonine substrate covalently tethered to carrier protein, SyrB1 [71]. The requirement of a carrier protein limited the biocatalytic applicability of these enzymes. However, in 2014, WelO5, isolated from *Fischerella ambigua* and *Hapalosiphon welwitschia*, was identified as the first Fe/αKG halogenase to work on a freestanding small molecule. WelO5 performed a stereoselective monochlorination of an aliphatic carbon in the native substrates 12-*epi*-fischerindole U and 12-*epi*-hapalindole C [72], and has subsequently been engineered for biocatalytic applications. Mutagenesis studies on these halogenases were performed by Novartis and the Buller team in Switzerland [73,74], using a homolog of WelO5

called WelO5* with 95% sequence identity from *Hapalosiphon welwitschia*. This was the first study to evolve a Fe/αKG halogenase for a substrate other than the native indole-alkaloids. Hayashi et al. were able to evolve WelO5* to halogenate fragments of a substrate analog of martinelline **76**, a bradykinin receptor agonist. After two rounds of mutagenesis, the final variant was able to perform both chlorination and bromination to the martinelline core analog reaching 95% conversion at 10 mM substrate loadings (Scheme 35). It was noted that this mutant reduced the formation of unwanted side products, exhibiting 290- and 400-fold increases in TTN and catalytic efficiency, respectively, over the wild-type enzyme. No diastereoselectivity of the catalyst was reported in the work of Hayashi et al.

The Fe/αKG halogenases act on natural products. However, Fe/αKG amino acid halogenases and Fe/αKG nucleotide halogenases have also recently been discovered. BesD catalyzes the chlorination, bromination and azidation of aliphatic carbons in amino acids [75]. In 2020, an Fe/αKG nucleotide halogenase called AdeV was the first Fe/αKG to perform halogenations of nucleotides by carrying out a C2′-chlorination to 2′-deoxyadenosine-5′-monophosphate (dAMP) **78** (Scheme 36) [76]. Despite the narrow substrate scope of AdeV, these nucleotide halogenases have the potential to catalyze
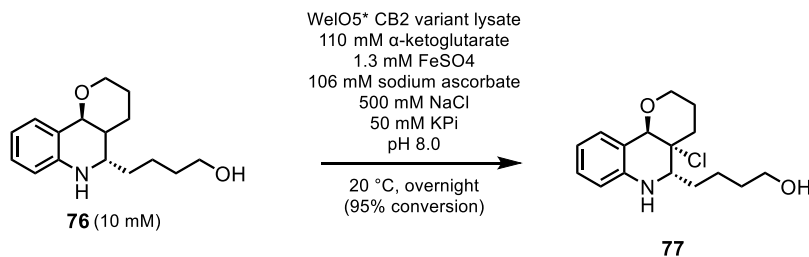
**Scheme 35.** Halogenation of a martinelline core analog.
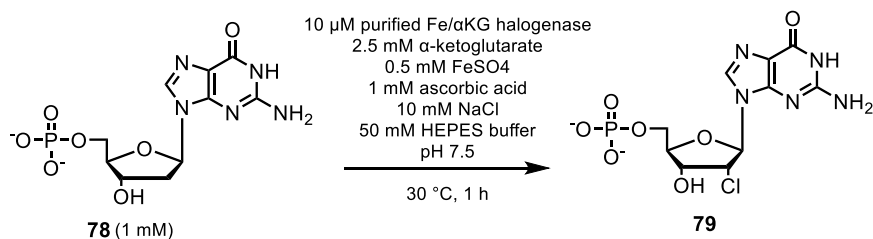


**Scheme 36.** Halogenation of a dGMP.

the halogenation of nucleotide analogs for thera-peutic purposes such as anticancer medicine like clofaribine or antiviral drugs such as uprifosbuvir. Recent developments in nucleotide halogenases have been made by Ni et al. [77] who have identified enzymes VaNTH and CtNTH which can carry out chlorinations, brominations and azidations at the C2′ position of 2′-deoxyguanosine monophosphate (dGMP) and exhibit a more than 43-fold improve-ment in catalytic efficiency when compared with AdeV acting on dAMP. Furthermore Ni et al. demon-strated that the activity and nucleotide specificity can be modulated with engineering, demonstrating the potential that these enzymes hold for nucleotide modifications.

## 8. Monoamine oxidases

Monoamine Oxidases (MAOs) selectively oxidize amines to form imines with the aid of molecular oxygen and a flavin adenine dinucleotide (FAD) co-factor, producing hydrogen peroxide as a byproduct. A monoamine oxidase from *Aspergillus niger* (MAO-N) was first discovered by Schilling and Lerch [78] and exhibits high *S*-stereoselectivity for amines at the α-carbon position. This can be exploited in ki-netic resolutions and deracemizations to access a

single (*R*)-enantiomer of an amine starting mate-rial when combined with a chemical reducing agent such as $BH_3NH_3$. Wild type MAO-N exhibits a nar-row substrate scope of alkylamines but this has been substantially broadened by engineering, with three key variants D5, D9 and D11 often employed [79].

The pharmaceutical applicability of these MAO-N variants was demonstrated by the analytical-scale syntheses of solifenacin and levocetirizine. Their utility outside of deracemizations was also demon-strated by two approaches with the MAO-N D9 vari-ant via the synthesis of (*R*)-harmicine **81**, an alka-loid which shows anti-leishmania activity [79]. The first approach to synthesizing this active pharmaceu-tical ingredient (API) involved a deracemization step to afford the final product in more than 99% ee and 95% yield. The second approach reduced the overall syntheses to two synthetic steps by using an oxida-tive asymmetric Pictet–Spengler reaction resulting in more than 99% ee and 83% conversion (Scheme 37).

Recently, it has been demonstrated that MAOs can oxidize 1,2,3,4-tetrahydroquinolines (THQs) into quinolines and 2-quinolones [80] which are preva-lent scaffolds in many APIs. Biotransformations were successful with unsubstituted or electron-donating substituents to THQ, with the ethoxy-substituted THQ affording 84% conversion (Scheme 38).
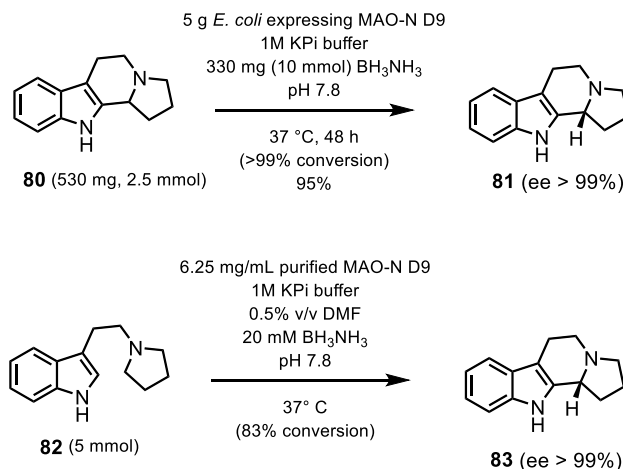
**Scheme 37.** Two routes to (*R*)-harmicine with MAO-N D9.
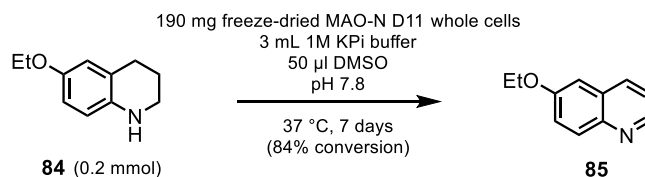


**Scheme 38.** Synthesis of a quinoline heterocycle by MAO-N D11 variant.

However, bulkier or electron-withdrawing substituents performed poorly. In-silico studies did note that steric and binding constraints may be hindering the activity with bulkier substituted substrates. To overcome this, Xiang et al. also employed a horseradish peroxidase.

This focus on THQ-like molecules was taken even further by the Turner group. They introduced a chemoenzymatic cascade where they employed MAO-N and R-IRED enzymes alongside a chemical allylation resulting in C–C bond formation at the C1 position of tetrathydroisoquinoline (THIQ) **86** [81]. Sangster et al. noted that there have been few reports of enantioselective allylation of cyclic imines despite their prevalence in many pharmaceutical scaffolds. Here they demonstrated that the scaffolds can be synthesized on a preparative scale at high enantioselectivity of up to 98% ee and purified yields of 64% (Scheme 39). Furthermore, on analytical scales, a range of substituents both on the aryl ring and boryl–allyl partner were accepted with good conversions, albeit lower ee values, demonstrating the broad substrate scope that can be reached by this cascade.

However, MAOs have not only been used to synthesize APIs on an analytical scale. Merck and Codexis employed a MAO for the synthesis of protease inhibitor boceprevir, used in the treatment of chronic hepatitis C infections [82]. MAO-N was evolved through 4 engineering rounds into MAON401, which replaced a synthetic resolution step in the synthesis of the P2 moiety of boceprevir **90**. By replacing this synthetic step, Merck increased the product yield by 150% and reduced overall process waste (E-factor) by 63.1%, demonstrating the environmental advantages of employing biocatalytic steps in industrial processes (Scheme 40). The stereoselectivity of this MAO-N-catalyzed step was not reported.

Aside from MAO-N, other *S*-selective FAD-dependent monoamine oxidases have been identified including human monoamine oxidases MAO-A [83], MAO-B [84], and cyclohexylamine oxidase from *Brevibacterium oxydans* [85,86]. Only one *R*-selective MAO is reported in the literature by Heath et al. [87] 6-hydroxy-D-nicotine oxidase (6-HDNO) has been shown to isolate secondary and tertiary
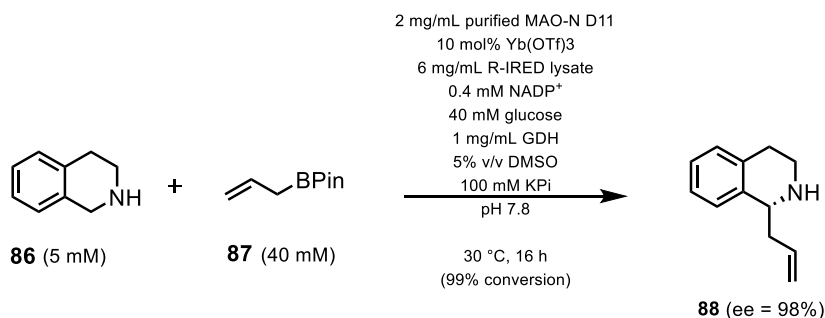
**Scheme 39.** Enzymatic cascade using MAO-N D11 and an R-IRED for the allylation of tetrahydroiso-quinolines.
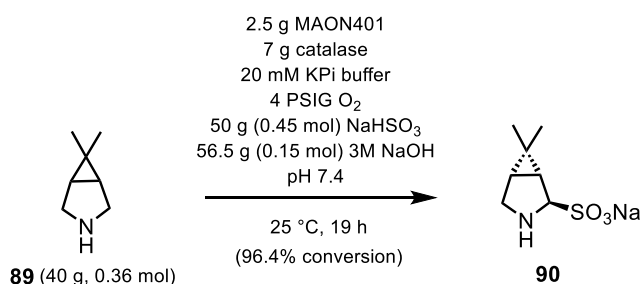


**Scheme 40.** MAO synthetic step in the synthesis of the P2 moiety of boceprivir.
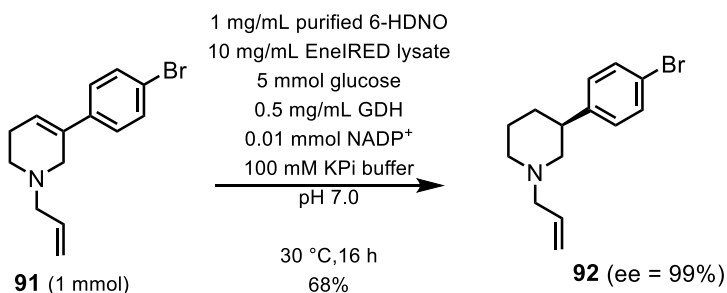


**Scheme 41.** Enzymatic cascade using 6-HDNO and an eneIRED for the synthesis of a Niraparib intermediate.

*S*-amines upon enzyme engineering. 6-HDNO has been included in cascades alongside IREDS [88]. Such a cascade reported by Harawa et al. [89] employs 6-HDNO and an EneIRED for the synthesis of 3-substituted and 3,4-disubstituted piperidines as intermediates in the synthesis of ovarian cancer drug Niraparib. 6-HDNO oxidizes a tetrahydropyridinium (THP) to form a dihydropyridinium (DHP) which is then enantioselectively reduced by an EneIRED to form the 3-substituted piperidine, which was obtained in 68% yield (Scheme 41).

## 9. Hydrolases

Hydrolases are a well-established enzymatic class in biocatalysis, represented by a broad range of enzymes, operating on esters and amides (hydrolysis catalyzed by proteases, esterases, and lipases); alcohols and amines (in lipase-catalyzed acylations); and nitriles and epoxides (hydrolysis catalyzed by nitrilases and epoxide hydrolases, respectively). Their mechanisms involve a catalytic triad to enable catalysis [90]. Lipases are hydrolases that can operate in
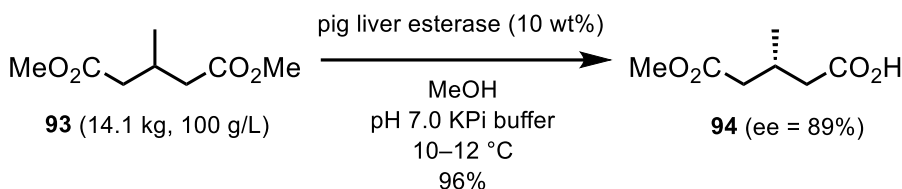
**Scheme 42.** Esterase desymmetrization in the synthetic process of CGRP receptor antagonist (VIII).
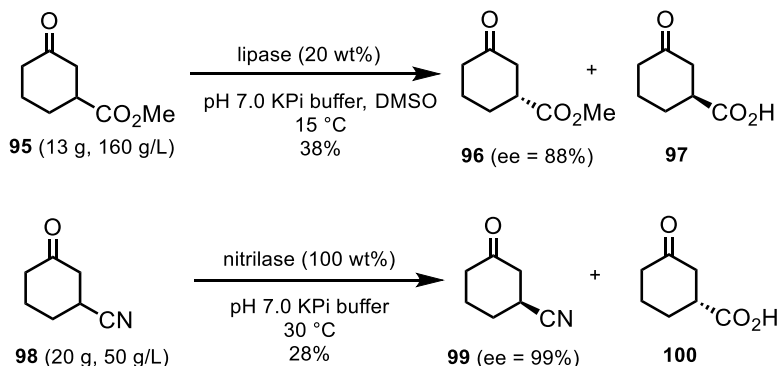


**Scheme 43.** Lipase and nitrilase approaches to synthesize chiral 3-substituted cyclohexanone building blocks.
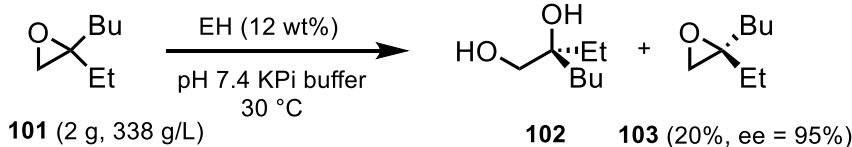


**Scheme 44.** Epoxide hydrolase resolution involved in the synthetic process of an acid transport (iBAT) inhibitor GSK2330672.

the presence of organic solvents, including biphasic systems and without a strict immobilization requirement [91]. The following examples, highlight various substrates and typical conditions employed for preparative-scale applications.

A biocatalytic desymmetrization was employed in the synthesis of the chiral lactam motif of the CGRP receptor antagonist (VIII). Researchers at Merck developed an esterase-catalyzed hydrolysis of the symmetrical diester **93** to achieve the chiral monoacid **94** in high yield (96%) (Scheme 42) [43]. Commercially available pig liver esterase was used for this transformation which was successfully scaled to multikilogram scale at high substrate loading (100 g/L). Only a modest ee of 89% was obtained from this enzymatic process, which could however be efficiently in-

creased to 99% by a chiral salt resolution in a subsequent synthetic step.

Researchers at GSK developed hydrolase resolutions to the enantiocomplementary compounds **97** and **100** (Scheme 43) [92]. A commercial lipase and a wild-type nitrilase were selected from screening for rapid process enablement to deliver multigram quantities of each material.

An epoxide hydrolase (EH) process was developed by GSK to resolve racemic epoxide **101**, a key intermediate used to access the ileal bile acid transport (iBAT) inhibitor GSK2330672 (XVII) for type 2 diabetes and cholestatic pruritus (Scheme 44) [93]. The wild-type enzyme used for this reaction was identified from a panel comprised of literature and metagenomically sourced biocatalysts. This enzyme
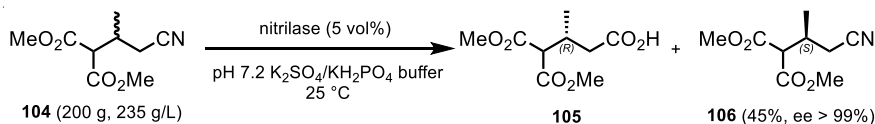
**Scheme 45.** Nitrilase resolution process to access an enantiopure nitrile building block for ipatasertib.
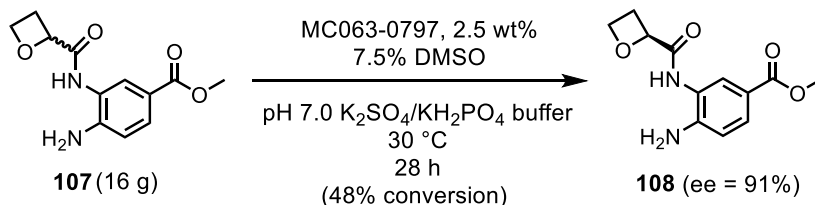


**Scheme 46.** A hydrolase resolution used to synthesize a key chiral intermediate in the synthetic process of a glucagon-like peptide-1 receptor agonist (GLP-1-RA).

had sufficient activity and substrate tolerance to enable a 22 g scale-up with very high substrate loading (338 g/L). It was noted that enzyme engineering may be able to improve the selectivity of the enzyme to increase the yield of **103** while maintaining high enantioselectivity.

Genentech and Roche utilized a nitrilase to access an enantiopure nitrile building block for ipatasertib (Scheme 45) [94]. As part of their efforts to develop a long-term manufacturing synthesis of this API, a nitrile resolution process was developed in which the (*R*)-enantiomer of racemic nitrile **104** was selectively hydrolyzed to the corresponding acid **105**, leaving the desired (*S*)-enantiomer **106** unreacted. A commercial enzyme from c-LEcta GmbH was employed in this transformation as a liquid preparation. It was found that high concentrations of sulfate and phosphate ions enhanced the enzyme activity and polar organic cosolvents had a detrimental effect on the enzyme performance. This led to a process being implemented on 200 g scale at very high substrate loading (235 g/L) without organic cosolvents (Scheme 45).

Another example of a successfully implemented hydrolase into a biocatalytic process involved an engineered variant of MC064, MC064-0797. This hydrolase was responsible for resolving a key racemic amide **107** in the synthetic process of an oral late-stage glucagon-like peptide-1 receptor agonist (GLP-1-RA) used in the treatment of type 2 diabetes mellitus (T2DM) and for weight loss [95,96]. Two rounds of enzyme engineering improved the

wild-type enzyme to support a 16 g reaction at low enzyme loads of 2.5 wt% (Scheme 46). The reaction yielded a close to perfect resolution of 48% conversion and **108** with an ee of 91%. The ee of the resulting product could be improved by using a chiral salt crystallization as a subsequent step.

A nitrilase was also employed by Gilead and Almac for the enantioselective, dynamic kinetic resolution of (*R*)-2-methoxymandelic acid **111** [97]. A one-pot process was devised to exploit the reversible nature of the cyanohydrin formation step by performing a dynamic kinetic resolution with nitrilase BCJ2315 isolated from *Burkholderia cenocepacia* J2315. A multipronged approach was developed to improve the reaction performance and reduce enzyme deactivation by carrying out process development alongside in-silico-guided enzyme engineering. A scaled-up process at 10 g/L substrate loadings with the M100 mutant resulted in 70% isolated yield and 97% ee in **111** (Scheme 47).

Ghosh and Nyalapatla presented a total synthesis of (+)-amphirionin-4 which exhibits proliferation-promoting activity in ST-2 cells [98]. This synthetic route includes a lipase resolution step to isolate an acetate intermediate **113** with readily available *Burkholderia cepacia* lipase (Amano PS-30). Using lipases in biocatalytic reactions is beneficial in this process since it requires a high solvent content. The resilience of this lipase to nonaqueous environments is demonstrated in the following example where approximately 50% of the reaction solution was THF (Scheme 48).
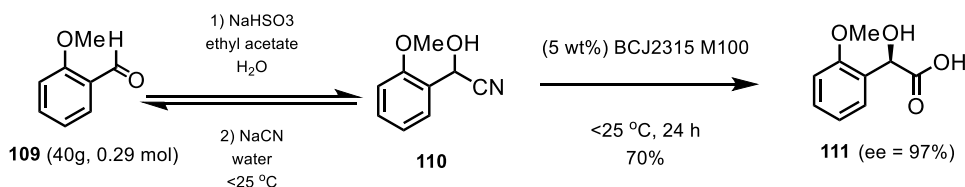
**Scheme 47.** One-pot preparation of (*R*)-2-methoxymandelic acid.
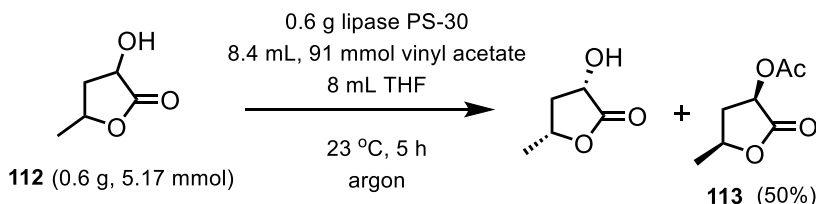


**Scheme 48.** Lipase PS-30 catalyzes lactone resolution.

## 10. Enzyme and process engineering considerations

Enzyme engineering has proven to be a key enabler to developing biocatalytic processes in the pharmaceutical sector [99,100]. However, the rapid engineering of enzymes for complex and insoluble substrates remains a bottleneck. The use of computational tools to design and accelerate enzyme engineering is proving to be of vital importance in the development of robust enzyme catalysts [101–103]. Among those, machine-learning-assisted enzyme engineering and ancestral sequence reconstruction (ASR) have the potential to accelerate enzyme engineering [104–109]. High-throughput platforms include microfluidics with enhanced capabilities to acquire enzyme kinetic data. These novel methods have the potential to make game changing leaps in how biocatalysis development is performed, particularly by enabling the screening of more complex multisite recombination libraries [110–113].

From a process chemistry implementation perspective, the solubility and complexity of substrates, and the need to run processes at high substrate loadings, often lead to processes operating as slurries. Efficient protein removal remains a challenge which is especially heightened in cascade processes when there are many enzymes present in the system. Ultimately, enzymes engineered for high specific activity and stability, enabling high utilization factors (ratio of substrate load to enzyme load), are required to minimize challenges in downstream processing. A strong control strategy demands fate and purge studies of enzymes, and monitoring using gel electrophoresis and MS techniques has become essential. Moreover, well-defined process acceptable ranges (PARs), ensuring robustness and easily defined normal operating ranges (NORs) for enzyme steps, minimizes failures at manufacturing scale. Although there is great promise for the successful combination of flow chemistry and biocatalysis, the vast majority of biocatalysis processes are still run in batch mode, mainly due to substrate insolubility in aqueous solutions. The scientific literature is dominated by examples of immobilized enzymes operated in packed bed reactors, however, there is huge potential for growth in the flow biocatalysis area on alternative systems [114–116]. Photobiocatalysis is an emerging area in the field of biocatalysis; during the past few years, it has been used to generate new reaction pathways for asymmetric synthesis, resulting in new-to-nature transformations enabled by photo-bio-redox systems, in situ production of hydrogen peroxide, as well as cascade reactions [117,118].

## 11. Final remarks

As demonstrated by the examples mentioned in this review, biocatalysis continues to be highly impactful for key synthetic challenges in the pharmaceutical industry. Well-established enzyme classes such as ketoreductases and transaminases have become

646      Amelia K. Gilio *et al.*

the go-to methods for the synthesis of chiral alcohols or amines, respectively, as well as hydrolases for desymmetrizations or resolution processes. In addition, imine-reductase, reductive aminases and ene-reductases have increasingly joined the top tier of enzymes enabling highly feasible transformations [92].

Looking ahead to the continued growth of biocatalysis implementation in the pharmaceutical industry, certain gaps in the biocatalytic toolbox remain. Amide bond synthesis, present in many pharmaceutical drugs is still a challenge, despite advances being made in the use of ligases for these transformations [119–121]. Functional group interconversions starting from carboxylic acids are still underexploited, and carboxylic acid reductases (CARs) offer great potential to bridge the gap and enable amine and alcohol synthesis from acid derivatives [122]. Continued development that involves engineering and efficient enzyme expression of these complex ATP-dependent reactions is anticipated in the coming years. Enzymatic halogenations have great potential for pharmaceutical synthesis due to the ubiquitous presence of halogens in pharmaceutical route scouting. Implementable enzymatic solutions remain elusive primarily due to low catalytic activities and very limited substrate specificity [123,124]. Applications of underutilized biocatalysts for the synthesis of chiral amines, sulfoxides, carboxylic acids, and amino acid analogs is mainly associated to low activities and limited substrate scope [125]. Finally, there are still limited options for general C–C bond forming in biocatalytic transformations; despite lyase-catalyzed C–C bond formation being represented in scattered examples over the past two decades, there is a need for the discovery of novel and broad scope enzymes to perform enzymatic carboligations [126,127]. The repertoire of reactions available to synthetic chemists is rapidly growing, aided by the emergence of sophisticated computational tools to sort through ever-expanding public and private enzyme databases [128–130].

## Declaration of interests

The authors do not work for, advise, own shares in, or receive funds from any organization that could benefit from this article, and have declared no affiliations other than their research organizations.

## References

[1] G. W. Huisman, J. Liang and A. Krebber, "Practical chiral alcohol manufacture using ketoreductases", *Curr. Opin. Chem. Biol.* **14** (2010), no. 2, pp. 122–129.

[2] T. M. Penning, "The aldo-keto reductases (AKRs): Overview", *Chem.-Biol. Interact.* **234** (2015), pp. 236–246.

[3] M. D. Truppo, "Biocatalysis in the pharmaceutical industry: The need for speed", *ACS Med. Chem. Lett.* **8** (2017), no. 5, pp. 476–480. From NLM PubMed-not-MEDLINE.

[4] M. Burns, C. A. Martinez, B. Vanderplas, R. Wisdom, S. Yu and R. A. Singer, "A chemoenzymatic route to chiral intermediates used in the multikilogram synthesis of a gamma secretase inhibitor", *Org. Process Res. Dev.* **21** (2017), pp. 871–877.

[5] N. K. Modukuru, J. Sukumaran, S. J. Collier, et al., "Development of a practical, biocatalytic reduction for the manufacture of (S)-licarbazepine using an evolved ketoreductase", *Org. Process Res. Dev.* **18** (2014), no. 6, pp. 810–815.

[6] X. Guo, J.-W. Tang, J.-T. Yang, G.-W. Ni, F.-L. Zhang and S.-X. Chen, "Development of a practical enzymatic process for preparation of (S)-2-chloro-1-(3, 4-difluorophenyl) ethanol", *Org. Process Res. Dev.* **21** (2017), pp. 1595–1601.

[7] A. Fryszkowska, J. Peterson, N. L. Davies, et al., "Development of a chemoenzymatic process for dehydroepiandrosterone acetate synthesis", *Org. Process Res. Dev.* **20** (2016), no. 8, pp. 1520–1528.

[8] A. M. Hyde, Z. Liu, B. Kosjek, et al., "Synthesis of the GPR40 partial agonist MK-8666 through a kinetically controlled dynamic enzymatic ketone reduction", *Org. Lett.* **18** (2016), no. 22, pp. 5888–5891.

[9] C. Han, S. Savage, M. Al-Sayah, et al., "Asymmetric synthesis of Akt kinase inhibitor ipatasertib", *Org. Lett.* **19** (2017), no. 18, pp. 4806–4809. From NLM PubMed-not-MEDLINE.

[10] F. St-Jean, R. Angelaud, S. Bachmann, et al., "Stereoselective synthesis of the IDO inhibitor navoximod", *J. Org. Chem.* **87** (2022), no. 7, pp. 4955–4960. From NLM Medline.

[11] H. S. Toogood, D. Mansell, J. M. Gardiner and N. S. Scrutton, *Enantioselective Bioreduction of Carbon–Carbon Double Bonds*, Elsevier Science: Amsterdam, 2011.

[12] K. Durchschein, M. Hall and K. Faber, "Unusual reactions mediated by FMN-dependent ene- and nitroreductases", *Green Chem.* **15** (2013), no. 7, pp. 1764–1772.

[13] C. K. Winkler, G. Tasnadi, D. Clay, M. Hall and K. Faber, "Asymmetric bioreduction of activated alkenes to industrially relevant optically active compounds", *J. Biotechnol.* **162** (2012), no. 4, pp. 381–389.

[14] H. S. Toogood and N. S. Scrutton, "Discovery, characterisation, engineering and applications of ene reductases for industrial biocatalysis", *ACS Catal.* **8** (2019), no. 4, pp. 3532–3549.

[15] M. S. Robescu, M. Niero, G. Loprete, L. Cendron and E. Bergantino, "A new thermophilic ene-reductase from the filamentous anoxygenic phototrophic bacterium chloroflexus aggregans", *Microorganisms* **9** (2021), no. 5, pp. 953–967.

[16] O. Warburg and C. Walter, "Ein zweites sauerstoffüber-tragendes Ferment und sein Absorptionsspektrum", *Die Naturwissenschaften* **20** (1932), no. 37, pp. 688–688.

[17] B. Zhang, J. Sun, Y. Zheng, X. Mao, J. Lin and D. Wei, "Identification of a novel ene reductase from Pichia angusta with potential application in (R)-levodione production", *RSC Adv.* **12** (2022), no. 22, pp. 13924–13931.

[18] X. Chen, X. Gao, Q. Wu and D. Zhu, "Synthesis of optically active dihydrocarveol via a stepwise or one-pot enzymatic reduction of (R)- and (S)-carvone", *Tetrahedron: Asymmetry* **23** (2012), no. 10, pp. 734–738.

[19] A. B. Daugherty, J. R. Horton, X. Cheng and S. Lutz, "Structural and functional consequences of circular permutation on the active site of old yellow enzyme", *ACS Catal.* **5** (2015), no. 2, pp. 892–899.

[20] A. B. Daugherty, S. Govindarajan and S. Lutz, "Improved biocatalysts from a synthetic circular permutation library of the flavin-dependent oxidoreductase old yellow enzyme", *J. Am. Chem. Soc.* **135** (2013), no. 38, pp. 14425–14432.

[21] S. Reich, N. Kress, B. M. Nestl and B. Hauer, "Variations in the stability of NCR ene reductase by rational enzyme loop modulation", *J. Struct. Biol.* **185** (2014), no. 2, pp. 228–233.

[22] T. Reß, W. Hummel, S. P. Hanlon, H. Iding and H. Gröger, "The organic-synthetic potential of recombinant ene reductases: Substrate-scope evaluation and process optimization", *ChemCatChem* **7** (2015), no. 8, pp. 1302–1311.

[23] C. K. Winkler, D. Clay, S. Davies, et al., "Chemoenzymatic asymmetric synthesis of pregabalin precursors via asymmetric bioreduction of beta-cyanoacrylate esters using ene-reductases", *J. Org. Chem.* **78** (2013), no. 4, pp. 1525–1533.

[24] M. Bechtold, E. Brenna, C. Femmer, F. G. Gatti, S. Panke, F. Parmeggiani and A. Sacchetti, "Biotechnological development of a practical synthesis of ethyl (S)-2-Ethoxy-3-(p-methoxyphenyl)propanoate (EEHP): Over 100-fold productivity increase from yeast whole cells to recombinant isolated enzymes", *Org. Process Res. Dev.* **16** (2011), no. 2, pp. 269–276.

[25] C. H. An, M. H. Shaw, A. Tharp, D. Verma, H. M. Li, H. Wang and X. Wang, "Enantioselective enzymatic reduction of acrylic acids", *Org. Lett.* **22** (2020), no. 21, pp. 8320–8325.

[26] S. Velikogne, W. B. Breukelaar, F. Hamm, R. A. Glabonjat and W. Kroutil, "C=C-Ene-reductases reduce the C=N bond of oximes", *ACS Catal.* **10** (2020), no. 22, pp. 13377–13382.

[27] K. Mitsukura, M. Suzuki, K. Tada, T. Yoshida and T. Nagasawa, "Asymmetric synthesis of chiral cyclic amine from cyclic imine by bacterial whole-cell catalyst of enantioselective imine reductase", *Org. Biomol. Chem.* **8** (2010), no. 20, pp. 4533–4535.

[28] S. P. France, R. M. Howard, J. Steflik, et al., "Identification of novel bacterial members of the imine reductase enzyme family that perform reductive amination", *ChemCatChem* **10** (2018), no. 3, pp. 510–514.

[29] A. K. Gilio, T. W. Thorpe, A. Heyam, et al., "A reductive aminase switches to imine reductase mode for a bulky amine substrate", *Acs Catal.* **13** (2023), no. 3, pp. 1669–1677.

[30] F. F. Chen, X. F. He, X. X. Zhu, et al., "Discovery of an imine reductase for reductive amination of carbonyl compounds with sterically challenging amines", *J. Am. Chem. Soc.* **145** (2023), pp. 4015–4025.

[31] Z. X. Liu, Y. D. Gao and L. C. Yang, "Biocatalytic hydrogen-borrowing cascade in organic synthesis", *Jacs Au* **4** (2024), no. 3, pp. 877–892.

[32] S. L. Montgomery, J. Mangas-Sanchez, M. P. Thompson, G. A. Aleku, B. Dominguez and N. J. Turner, "Direct alkylation of amines with primary and secondary alcohols through biocatalytic hydrogen borrowing", *Angew. Chem. Int. Ed.* **56** (2017), no. 35, pp. 10491–10494.

[33] J. Preissler, H. A. Reeve, T. Z. Zhu, et al., "Dihydrogen-driven NADPH recycling in imine reduction and P450-catalyzed oxidations mediated by an engineered O2-tolerant hydrogenase", *ChemCatChem* **12** (2020), no. 19, pp. 4853–4861.

[34] H. A. Relyea and W. A. van der Donk, "Mechanism and applications of phosphite dehydrogenase", *Bioorg. Chem.* **33** (2005), no. 3, pp. 171–189.

[35] Z. Shaked and G. M. Whitesides, "Enzyme-catalyzed organic-synthesis—NADH regeneration by using formate dehydrogenase", *J. Am. Chem. Soc.* **102** (1980), no. 23, pp. 7104–7105.

[36] IP.com Prior Art Database, Imine reductase mediated synthesis of (S,S)-sertraline, 2017. Online at https : / / priorart.ip.com / IPCOM / 000251929. 12B, 1-3. IP.com Disclosure Number IPCOM000251929D.

[37] G. A. Aleku, S. P. France, H. Man, et al., "A reductive aminase from Aspergillus oryzae", *Nat. Chem.* **2017** (9), no. 10, pp. 961–969.

[38] M. Sharma, J. Mangas-Sanchez, S. P. France, G. A. Aleku, S. L. Montgomery, J. I. Ramsden, N. J. Turner and G. Grogan, "A mechanism for reductive amination catalyzed by fungal reductive aminases", *ACS Catal.* **8** (2018), no. 12, pp. 11534–11541.

[39] M. Schober, C. MacDermaid, A. A. Ollis, et al., "Chiral synthesis of LSD1 inhibitor GSK2879552 enabled by directed evolution of an imine reductase", *Nat. Catal.* **2** (2019), no. 10, pp. 909–915.

[40] R. Kumar, M. J. Karmilowicz, D. Burke, et al., "Biocatalytic reductive amination from discovery to commercial manufacturing applied to abrocitinib JAK1 inhibitor", *Nat. Catal.* **4** (2021), no. 9, pp. 775–782.

[41] S. Q. Duan, D. W. Widlicka, M. P. Burns, et al., "Application of biocatalytic reductive amination for the synthesis of a key intermediate to a CDK 2/4/6 inhibitor", *Org. Process. Res. Dev.* **26** (2022), no. 3, pp. 879–890.

[42] T. W. Thorpe, J. R. Marshall, V. Harawa, et al., "Multifunctional biocatalyst for conjugate reduction and reductive amination", *Nature* **604** (2022), no. 7904, pp. 86–91.

[43] C. Molinaro, E. M. Phillips, B. P. Xiang, et al., "Synthesis of a CGRP receptor antagonist via an asymmetric synthesis of 3-fluoro-4-aminopiperidine", *J. Org. Chem.* **84** (2019), no. 12, pp. 8006–8018.

[44] J. T. Kohrt, P. H. Dorff, M. Burns, et al., "Application of flow and biocatalytic transaminase technology for

the synthesis of a 1-Oxa-8-azaspiro[4.5]decan-3-amine", *Org. Process Res. Dev.* **26** (2022), no. 3, pp. 616–623.

[45] M. Burns, C. A. Martinez, B. Vanderplas, R. Wisdom, S. Yu and R. A. Singer, "A chemoenzymatic route to chiral intermediates used in the multikilogram synthesis of a gamma secretase inhibitor", *Org. Process Res. Dev.* **21** (2017), no. 6, pp. 871–877.

[46] M. Höhne, S. Kühl, R. Karen and U. T. Bornscheuer, "Efficient asymmetric synthesis of chiral Amines by combining transaminase and pyruvate decarboxylase", *ChemBioChem* **9** (2008), no. 3, pp. 363–365.

[47] M. Genz, O. Melse, S. Schmidt, C. Vickers, M. Dörr, T. van den Bergh, H. J. Joosten and U. T. Bornscheuer, "Engineering the amine transaminase from vibrio fluvialis towards branched-chain substrates", *ChemCatChem* **8** (2016), no. 20, pp. 3199–3202.

[48] C. K. Savile, J. M. Janey, E. C. Mundorff, et al., "Biocatalytic asymmetric synthesis of chiral amines from ketones applied to sitagliptin manufacture", *Science* **329** (2010), no. 5989, pp. 305–309.

[49] I. G. Denisov, T. M. Makris, S. G. Sligar and I. Schlichting, "Structure and chemistry of cytochrome P450", *Chem. Rev.* **105** (2005), no. 6, pp. 2253–2278.

[50] R. Fasan, "Tuning P450 enzymes as oxidation catalysts", *ACS Catal.* **2** (2012), no. 4, pp. 647–666.

[51] D. J. Fansher, J. N. Besna, A. Fendri and J. N. Pelletier, "Choose your own adventure: A comprehensive database of reactions catalyzed by cytochrome P450 BM3 variants", *ACS Catal.* **14** (2024), no. 8, pp. 5560–5592.

[52] I. Kaluzna, T. Schmitges, H. Straatman, D. Van Tegelen, M. Müller, M. Schürmann and D. Mink, "Enabling selective and sustainable P450 oxygenation technology. Production of 4-hydroxy-$\alpha$-isophorone on kilogram scale", *Org. Process Res. Dev.* **20** (2016), no. 4, pp. 814–819.

[53] F. Hannemann, A. Bichet, K. M. Ewen and R. Bernhardt, "Cytochrome P450 systems—biological variations of electron transport chains", *Biochim. Biophys Acta (BBA) - Gen. Sub.* **1770** (2007), no. 3, pp. 330–344.

[54] A. Kokorin, P. D. Parshin, P. J. Bakkes, A. A. Pometun, V. I. Tishkov and V. B. Urlacher, "Genetic fusion of P450 BM3 and formate dehydrogenase towards self-sufficient biocatalysts with enhanced activity", *Sci. Rep.* **11** (2021), no. 1, article no. 21706.

[55] A. Kokorin and V. B. Urlacher, "Artificial fusions between P450 BM3 and an alcohol dehydrogenase for efficient (+)-nootkatone production", *ChemBioChem* **23** (2022), no. 12, article no. e202200065.

[56] R.-Y. Zhang, T. Ma, D. Liu, Y.-L. Yang, L. Gao, H.-B. Cui, Z.-Q. Wang and Y.-Z. Chen, "Biocatalytic hydroxylation tertiary C–H bonds for synthesis of chiral tertiary alcohols by cytochrome P450", *Mol. Catal.* **553** (2024), article no. 113791.

[57] C. Molinaro, Y. Kawasaki, G. Wanyoike, T. Nishioka, T. Yamamoto, B. Snedecor, S. J. Robinson and F. Gosselin, "Engineered cytochrome P450-catalyzed oxidative biaryl coupling reaction provides a scalable entry into arylomycin antibiotics", *J. Am. Chem. Soc.* **144** (2022), no. 32, pp. 14838–14845.

[58] Z. J. Wang, N. E. Peck, H. Renata and F. H. Arnold, "Cytochrome P450-catalyzed insertion of carbenoids into N–H bonds", *Chem. Sci.* **5** (2014), no. 2, pp. 598–601.

[59] V. Tyagi, R. B. Bonn and R. Fasan, "Intermolecular carbene S–H insertion catalysed by engineered myoglobin-based catalysts", *Chem. Sci.* **6** (2015), no. 4, pp. 2488–2494.

[60] S. B. J. Kan, R. D. Lewis, K. Chen and F. H. Arnold, "Directed evolution of cytochrome c for carbon–silicon bond formation: Bringing silicon to life", *Science* **354** (2016), no. 6315, pp. 1048–1051.

[61] D. J. Prockop and K. Juva, "Synthesis of hydroxyproline in vitro by the hydroxylation of proline in a precursor of collagen", *Proc. Natl. Acad. Sci. USA* **53** (1965), no. 3, pp. 661–668.

[62] C. Loenarz and C. J. Schofield, "Expanding chemical biology of 2-oxoglutarate oxygenases", *Nat. Chem. Biol.* **4** (2008), no. 3, pp. 152–156.

[63] P. Lukat, Y. Katsuyama, S. Wenzel, T. Binz, C. König, W. Blankenfeldt, M. Brönstrup and R. Müller, "Biosynthesis of methyl-proline containing griselimycins, natural products with anti-tuberculosis activity", *Chem. Sci.* **8** (2017), no. 11, pp. 7521–7527.

[64] C. R. Zwick and H. Renata, "Evolution of biocatalytic and chemocatalytic C–H functionalization strategy in the synthesis of manzacidin C", *J. Org. Chem.* **83** (2018), no. 14, pp. 7407–7415.

[65] C. R. Zwick III and H. Renata, "Remote C–H hydroxylation by an $\alpha$-ketoglutarate-dependent dioxygenase enables efficient chemoenzymatic synthesis of manzacidin C and proline analogs", *J. Am. Chem. Soc.* **140** (2018), no. 3, pp. 1165–1169.

[66] J. Kobayashi, F. Kanda, M. Ishibashi and H. Shigemori, "Manzacidins A-C, novel tetrahydropyrimidine alkaloids from the Okinawan marine sponge Hymeniacidon sp", *J. Org. Chem.* **56** (1991), no. 14, pp. 4574–4576.

[67] W. L. Cheung-Lee, J. N. Kolev, J. A. McIntosh, et al., "Engineering hydroxylase activity, selectivity, and stability for a scalable concise synthesis of a key intermediate to belzutifan", *Angew. Chem. Int. Ed.* **63** (2024), article no. e202316133.

[68] D. A. DiRocco, Y.-L. Zhong, D. N. Le, et al., "Evolution of a green and sustainable manufacturing process for belzutifan: Part 1—Process history and development strategy", *Org. Process Res. Dev.* **2024** (28), no. 2, pp. 404–412.

[69] J. Kim, V. Zhang, K. Abe, et al., "Evolution of a green and sustainable manufacturing process for belzutifan: Part 3—Development of a scalable enzymatic oxidation process", *Org. Process Res. Dev.* **28** (2024), no. 2, pp. 422–431.

[70] R. Hara, K. Yamagata, R. Miyake, H. Kawabata, H. Uehara and K. Kino, "Discovery of lysine hydroxylases in the clavaminic acid synthase-like superfamily for efficient hydroxylysine bioproduction", *Appl. Environ. Microbiol.* **83** (2017), no. 17, e00693–e00617.

[71] F. H. Vaillancourt, J. Yin and C. T. Walsh, "SyrB2 in syringomycin E biosynthesis is a nonheme Fe$^{II}$ $\alpha$-ketoglutarate- and O$_2$-dependent halogenase", *Proc. Natl. Acad. Sci. USA* **102** (2005), no. 29, pp. 10111–10116.

[72]  M. L. Hillwig and X. Liu, "A new family of iron-dependent halogenases acts on freestanding substrates", *Nat. Chem. Biol.* **10** (2014), no. 11, pp. 921–923.

[73]  T. Hayashi, M. Ligibel, E. Sager, M. Voss, J. Hunziker, K. Schroer, R. Snajdrova and R. Buller, "Evolved aliphatic halogenases enable regiocomplementary C–H function-alization of a pharmaceutically relevant compound", *Angew. Chem. Int. Ed.* **58** (2019), no. 51, pp. 18535–18539.

[74]  M. Voss, S. Hüppi, D. Schaub, et al., "Enzyme engineering enables inversion of substrate stereopreference of the halogenase WelO5*", *ChemCatChem* **14** (2022), no. 24, article no. e202201115.

[75]  M. E. Neugebauer, K. H. Sumida, J. G. Pelton, J. L. Mc-Murry, J. A. Marchand and M. C. Y. Chang, "A fam-ily of radical halogenases for the engineering of amino-acid-based products", *Nat. Chem. Biol.* **15** (2019), no. 10, pp. 1009–1016.

[76]  C. Zhao, S. Yan, Q. Li, H. Zhu, Z. Zhong, Y. Ye, Z. Deng and Y. Zhang, "An $Fe^{2+}$- and $\alpha$-ketoglutarate-dependent halogenase acts on nucleotide substrates", *Angew. Chem. Int. Ed.* **59** (2020), no. 24, pp. 9478–9484.

[77]  J. Ni, J. Zhuang, Y. Shi, Y.-C. Chiang and G.-J. Cheng, "Discovery and substrate specificity engineering of nu-cleotide halogenases", *Nat. Commun.* **15** (2024), no. 1, ar-ticle no. 5254.

[78]  B. Schilling and K. Lerch, "Amine oxidases from As-pergillus niger: identification of a novel flavin-dependent enzyme", *Biochim. Biophys. Acta (BBA) - Gen. Sub.* **1243** (1995), no. 3, pp. 529–537.

[79]  D. Ghislieri, A. P. Green, M. Pontini, S. C. Willies, I. Rowles, A. Frank, G. Grogan and N. J. Turner, "Engineering an enantioselective amine oxidase for the synthesis of phar-maceutical building blocks and alkaloid natural prod-ucts", *J. Am. Chem. Soc.* **135** (2013), no. 29, pp. 10863–10869.

[80]  H. Xiang, S. Ferla, C. Varricchio, A. Brancale, N. L. Brown, G. W. Black, N. J. Turner and D. Castagnolo, "Bio-catalytic and chemo-enzymatic synthesis of quinolines and 2-quinolones by monoamine oxidase (MAO-N) and horseradish peroxidase (HRP) biocatalysts", *ACS Catal.* **13** (2023), no. 5, pp. 3370–3378.

[81]  J. J. Sangster, R. E. Ruscoe, S. C. Cosgrove, J. Mangas-Sánchez and N. J. Turner, "One-pot chemoenzymatic cascade for the enantioselective C(1)-allylation of tetrahydroisoquinolines", *J. Am. Chem. Soc.* **145** (2023), no. 8, pp. 4431–4437.

[82]  T. Li, J. Liang, A. Ambrogelly, et al., "Efficient, chemoenzy-matic process for manufacture of the boceprevir bicyclic [3.1.0]proline intermediate based on amine oxidase-catalyzed desymmetrization", *J. Am. Chem. Soc.* **134** (2012), no. 14, pp. 6467–6472.

[83]  L. De Colibus, M. Li, C. Binda, A. Lustig, D. E. Edmondson and A. Mattevi, "Three-dimensional structure of human monoamine oxidase A (MAO A): Relation to the struc-tures of rat MAO A and human MAO B", *Proc. Natl. Acad. Sci. USA* **102** (2005), no. 36, pp. 12684–12689.

[84]  C. Binda, F. Hubálek, M. Li, D. E. Edmondson and A. Mat-tevi, "Crystal structure of human monoamine oxidase B, a drug target enzyme monotopically inserted into the

mitochondrial outer membrane", *FEBS Lett.* **564** (2004), no. 3, pp. 225–228.

[85]  H. Leisch, S. Grosse, H. Iwaki, Y. Hasegawa and P. C. K. Lau, "Cyclohexylamine oxidase as a useful biocatalyst for the kinetic resolution and dereacemization of amines", *Canad. J. Chem.* **90** (2012), no. 1, pp. 39–45.

[86]  H. Iwaki, M. Shimizu, T. Tokuyama and Y. Hasegawa, "Biodegradation of cyclohexylamine by *Brevibacterium oxydans* IH-35A", *Appl. Environ. Microbiol.* **65** (1999), no. 5, pp. 2232–2234.

[87]  R. S. Heath, M. Pontini, B. Bechi and N. J. Turner, "De-velopment of an *R*-selective amine oxidase with broad substrate specificity and high enantioselectivity", *Chem-CatChem* **6** (2014), no. 4, pp. 996–1002.

[88]  R. S. Heath, M. Pontini, S. Hussain and N. J. Turner, "Combined imine reductase and amine oxidase cat-alyzed deracemization of nitrogen heterocycles", *Chem-CatChem* **8** (2016), no. 1, pp. 117–120.

[89]  V. Harawa, T. W. Thorpe, J. R. Marshall, et al., "Synthe-sis of stereoenriched piperidines via chemo-enzymatic dearomatization of activated pyridines", *J. Am. Chem. Soc.* **144** (2022), no. 46, pp. 21088–21095.

[90]  G. Dodson and A. Wlodawer, "Catalytic triads and their relatives", *Trends Biochem. Sci.* **23** (1998), no. 9, pp. 347–352.

[91]  A. Kumar, K. Dhar, S. S. Kanwar and P. K. Arora, "Li-pase catalysis in organic solvents: advantages and appli-cations", *Biol. Proced. Online* **18** (2016), article no. 2.

[92]  S. P. France, R. D. Lewis and C. A. Martinez, "The evolving nature of biocatalysis in pharmaceutical research and development", *Jacs Au* **3** (2023), no. 3, pp. 715–735.

[93]  G. D. Roiban, P. W. Sutton, R. Splain, et al., "Development of an enzymatic process for the production of ( )-2-butyl-2-ethyloxirane", *Org. Process Res. Dev.* **21** (2017), no. 9, pp. 1302–1310.

[94]  C. Han, S. Savage, M. Al-Sayah, et al., "Asymmetric syn-thesis of Akt kinase inhibitor ipatasertib", *Org. Lett.* **19** (2017), no. 18, pp. 4806–4809.

[95]  M. S. Brown, J. Buck, D. J. Critcher, et al., "Development of the synthetic route to PF-06878031 Part 2: Amide re-duction route", *Org. Process Res. Dev.* **28** (2024), no. 7, pp. 2446–2461.

[96]  O. Brea, J. Buck, N. Carson, et al., "Development of the synthetic route to PF-06878031 Part 1: Selective alky-lation route", *Org. Process Res. Dev.* **28** (2024), no. 7, pp. 2433–2445.

[97]  M. E. Scott, X. T. Wang, L. D. Humphreys, et al., "En-zyme optimization and process development for a scal-able synthesis of (*R*)-2-methoxymandelic acid", *Org. Pro-cess Res. Dev.* **26** (2022), no. 3, pp. 849–858.

[98]  A. K. Ghosh and P. R. Nyalapatla, "Enantioselective to-tal synthesis of (+)-amphirionin-4", *Org. Lett.* **18** (2016), no. 9, pp. 2296–2299.

[99]  M. T. Reetz, G. Qu and Z. Sun, "Engineered enzymes for the synthesis of pharmaceuticals and other high-value products", *Nat. Synth.* **3** (2024), no. 1, pp. 19–32.

[100]  J. Nazor, J. Liu and G. Huisman, "Enzyme evolution for industrial biocatalytic cascades", *Curr. Opin. Biotechnol.* **69** (2021), pp. 182–190.

[101] S. M. Marques, J. Planas-Iglesias and J. Damborsky, "Web-based tools for computational enzyme design", *Curr. Opin. Struct. Biol.* **69** (2021), pp. 19–34.

[102] S. Osuna, "The challenge of predicting distal active site mutations in computational enzyme design", *WIREs Comput. Mol. Sci.* **11** (2021), no. 3, article no. e1502.

[103] Y. Cui, J. Sun and B. Wu, "Computational enzyme re-design: large jumps in function", *Trends Chem.* **4** (2022), no. 5, pp. 409–419.

[104] S. Goldman, R. Das, K. K. Yang and C. W. Coley, "Machine learning modeling of family wide enzyme-substrate specificity screens", *PLoS Comput. Biol.* **18** (2022), no. 2, article no. e1009853.

[105] J. Yang, F.-Z. Li and F. H. Arnold, "Opportunities and challenges for machine learning-assisted enzyme engineering", *ACS Central Sci.* **10** (2024), no. 2, pp. 226–241.

[106] M. Hegde, *Unlocking the Secrets of Life: AI Protein Models Demystified*, 2023. Online at https : / / www . ml6 . eu / blogpost / unlocking - the - secrets - of - life - ai - protein - models- demystified (accessed on November 12, 2024).

[107] B. Markus, K. Andreas, K. Arkadij, L. Stefan, O. Gustav, S. Elina and S. Radka, "Accelerating biocatalysis discovery with machine learning: a paradigm shift in enzyme engineering, discovery, and design", *ACS Catal.* **13** (2023), no. 21, pp. 14454–14469.

[108] J. Livada, A. M. Vargas, C. A. Martinez and R. D. Lewis, "Ancestral sequence reconstruction enhances gene mining efforts for industrial ene reductases by expanding enzyme panels with thermostable catalysts", *ACS Catal.* **13** (2023), no. 4, pp. 2576–2585.

[109] P. Kouba, P. Kohout, F. Haddadi, et al., "Machine learning-guided protein engineering", *ACS Catal.* **13** (2023), no. 21, pp. 13863–13895.

[110] C. Markin, D. Mokhtari, F. Sunden, et al., "Revealing enzyme functional architecture via high-throughput microfluidic enzyme kinetics", *Science* **373** (2021), no. 6553, article no. eabf8761.

[111] R. Vanella, G. Kovacevic, V. Doffini, J. F. de Santaella and M. A. Nash, "High-throughput screening, next generation sequencing and machine learning: advanced methods in enzyme engineering", *Chem. Commun.* **58** (2022), no. 15, pp. 2455–2467.

[112] A. Stucki, J. Vallapurackal, T. R. Ward and P. S. Dittrich, "Droplet microfluidics and directed evolution of enzymes: an intertwined journey", *Angew. Chem. Int. Ed.* **60** (2021), no. 46, pp. 24368–24387.

[113] M. Gantz, S. Neun, E. J. Medcalf, L. D. van Vliet and F. Hollfelder, "Ultrahigh-throughput enzyme engineering and discovery in in vitro compartments", *Chem. Rev.* **123** (2023), no. 9, pp. 5571–5611.

[114] A. I. Benítez-Mateos, M. L. Contente, D. Roura Padrosa and F. Paradisi, "Flow biocatalysis 101: design, development and applications", *React. Chem. Eng.* **6** (2021), no. 4, pp. 599–611.

[115] Y.-J. Hu, J. Chen, Y.-Q. Wang, N. Zhu, Z. Fang, J.-H. Xu and K. Guo, "Biocatalysts used for multi-step reactions in continuous flow", *Chem. Eng. J.* **437** (2022), article no. 135400.

[116] M. P. Thompson, I. Peñafiel, S. C. Cosgrove and N. J. Turner, "Biocatalysis using immobilized enzymes in continuous flow for the synthesis of fine chemicals", *Org. Process Res. Dev.* **23** (2019), no. 1, pp. 9–18.

[117] Y. Peng, Z. Chen, J. Xu and Q. Wu, "Recent advances in photobiocatalysis for selective organic synthesis", *Org. Process Res. Dev.* **26** (2022), no. 7, pp. 1900–1913.

[118] H. Fu and T. K. Hyster, "From ground-state to excited-state activation modes: Flavin-dependent "ene"-reductases catalyzed non-natural radical reactions", *Acc. Chem. Res.* **57** (2024), no. 9, pp. 1446–1457.

[119] M. Lubberink, W. Finnigan and S. L. Flitsch, "Biocatalytic amide bond formation", *Green Chem.* **25** (2023), no. 8, pp. 2958–2970.

[120] Q. Tang, M. Petchey, B. Rowlinson, T. J. Burden, I. J. Fairlamb and G. Grogan, "Broad spectrum enantioselective amide bond synthetase from streptoalloteichus hindustanus", *ACS Catal.* **14** (2024), no. 2, pp. 1021–1029.

[121] H. K. Philpott, P. J. Thomas, D. Tew, D. E. Fuerst and S. L. Lovelock, "A versatile biosynthetic approach to amide bond formation", *Green Chem.* **20** (2018), no. 15, pp. 3426–3431.

[122] S. R. Derrington, N. J. Turner and S. P. France, "Carboxylic acid reductases (CARs): An industrial perspective", *J. Biotechnol.* **304** (2019), pp. 78–88.

[123] J. C. Lewis, "Identifying and engineering flavin dependent halogenases for selective biocatalysis", *Acc. Chem. Res.* **57** (2024), no. 15, pp. 2067–2079.

[124] E. Hegarty, J. Büchler and R. M. Buller, "Halogenases for the synthesis of small molecules", *Curr. Opin. Green Sustain. Chem.* **41** (2023), article no. 100784.

[125] R. M. Phelan, M. J. Abrahamson, J. T. C. Brown, R. K. Zhang and C. R. Zwick III, "Development of scalable processes with underutilized biocatalyst classes", *Org. Process Res. Dev.* **26** (2022), no. 7, pp. 1944–1959.

[126] D. Gamenara and G. A. Seoane, "Chapter 8 – Biocatalyzed Carbon–Carbon bond formation in enantioselective synthesis", in *Biocatalysis in Asymmetric Synthesis* (G. D. Gonzalo and A. R. Alcántara, eds.), Academic Press: Cambridge, MA, 2024, pp. 237–296.

[127] M. Liu, D. Wei, Z. Wen and J.-b. Wang, "Progress in stereoselective construction of C–C bonds enabled by aldolases and hydroxynitrile lyases", *Front. Bioeng. Biotechnol.* **9** (2021), article no. 653682.

[128] H. J. Atkinson, J. H. Morris, T. E. Ferrin and P. C. Babbitt, "Using sequence similarity networks for visualization of relationships across diverse protein superfamilies", *PLoS One* **4** (2009), no. 2, article no. e4345.

[129] W. Bort, I. I. Baskin, T. Gimadiev, et al., "Discovery of novel chemical reactions by deep generative recurrent neural network", *Sci. Rep.* **11** (2021), no. 1, article no. 3178.

[130] E. L. Bell, A. E. Hutton, A. J. Burke, A. O'Connell, A. Barry, E. O'Reilly and A. P. Green, "Strategies for designing biocatalysts with new functions", *Chem. Soc. Rev.* **53** (2024), no. 6, pp. 2851–2862.

**Objectif de la revue**

Les *Comptes Rendus Chimie* sont une revue électronique évaluée par les pairs de niveau international, qui couvre l'ensemble des domaines des sciences chimiques.

Ils publient des numéros thématiques, des articles originaux de recherche, des articles de synthèse, des mises au point, des mises en perspective historiques, des textes à visée pédagogique, ou encore des actes de colloque, en anglais ou en français, sans limite de longueur et dans un format aussi souple que possible (figures, données associées, etc.).

Depuis 2020, les *Comptes Rendus Chimie* sont publiés avec le centre Mersenne pour l'édition scientifique ouverte, selon une politique vertueuse de libre accès diamant, gratuit pour les auteurs (pas de frais de publication) comme pour les lecteurs (accès libre, immédiat et pérenne).

**À propos de la revue**

Les *Comptes Rendus Chimie* sont exclusivement publiés au format électronique.

Toutes les informations sur la revue, ainsi que le texte intégral de l'ensemble des articles, sont disponibles sur son site internet, à l'adresse https://comptes-rendus.academie-sciences.fr/chimie/.

**Informations pour les auteurs**

Pour toute question relative à la soumission d'un manuscrit, merci de consulter le site internet de la revue : https://comptes-rendus.academie-sciences.fr/chimie/.

# Contents / *Sommaire*

*Page numbers below refer to the top-of-the-page pagination in this document
which compiles articles published individually with a different pagination
(retained on the top left and top right of each article).*